



[International Virtual Conference on Industry](#)

IVCI 2021: **International Virtual Conference on Industry 4.0** pp 211–220

[Home](#) > [International Virtual Conference on Industry 4.0](#) > Conference paper

Elevated CNN Based Secured Sensor Image Data Communication for HAR: IIOT

[P. Alli](#)  & [J. Dinesh Peter](#)

Conference paper | [First Online: 01 April 2023](#)

38 Accesses

Part of the [Lecture Notes in Electrical Engineering](#) book series
(LNEE, volume 1003)

Abstract

The Industrial Internet of Things (IIOT) is constituted by the development of the Internet of Things into the fields of manufacturing, monitoring, and management. It enables industries to make use of data communication and control by leveraging the capabilities of smart machines and real-time analysis. Our proposed work concentrates on the application of IIOT along with two contributions: the first one is to secure sensor based image, video and audio communication and the other one is the detection of human activity. Initially, the human activities data are captured by the camera sensors which is attached in the employee ID card that sensor monitors the employee activities as a motion image along with vibrations and sound signals. All this information is securely communicated to the smart office dashboard with the help of an efficient encryption algorithm namely Software Defined Network along with Stochastic Honey Overlapping Based Dual Helix Scan (SDN-SHODHS), that secures the communication in the access network. In the second phase to detect employee activity, we propose an

efficient Elevated Deep Convolutional Neural Network that gives the best efficient result compared to all other existing works. Our proposed framework achieves secure sensor data image, audio and video communication and accurate human activity recognition in terms of encryption and decryption time, precision, recall and F-measure.

Keywords

Industrial internet of things Sensors

Secured image communication

SDN- stochastic AES overlapping based dual helix scan

Human activity recognition Smart office monitoring

This is a preview of subscription content, [access via your institution](#).

<div>▼ Chapter</div> <div>EUR 29.95</div> <div>Price includes VAT (India)</div> <div><ul style="list-style-type: none">• Available as PDF• Read on any device• Instant download• Own it forever</div> <div>Buy Chapter</div>	<div>▼ eBook</div> <div>EUR 213.99</div> <div>Price includes VAT (India)</div> <div><ul style="list-style-type: none">• Available as EPUB and PDF• Read on any device• Instant download• Own it forever</div> <div>Buy eBook</div>
<div>▼ Hardcover Book</div> <div>EUR 249.99</div> <div>Price excludes VAT (India)</div> <div><ul style="list-style-type: none">• Durable hardcover edition• Dispatched in 3 to 5 business days• Free shipping worldwide - see info</div> <div>Buy Hardcover Book</div>	

Tax calculation will be finalised at checkout

Purchases are for personal use only
[Learn about institutional subscriptions](#)

References

1. Vermesan O, Friess P (eds) (2013) Internet of things: converging technologies for smart environments and

2. Bhide VH, Wagh S (2015) I-learning IoT: an intelligent self learning system for home automation using IoT. In: 2015 International conference on communications and signal processing (ICCSP). pp 1763–1767
3. Nagy J, Oláh J, Erdei E, Máté D, Popp J (2018) The role and impact of Industry 4.0 and the internet of things on the business strategy of the value chain—the case of Hungary. *Sustainability* 10(10):3491
4. Ronao CA, Cho SB (2016) Human activity recognition with smartphone sensors using deep learning neural networks. *Expert Syst Appl* 59:235–244
5. Lin J, Yu W, Zhang N, Yang X, Zhang H, Zhao W (2017) A survey on internet of things: architecture, enabling technologies, security and privacy, and applications. *IEEE Internet Things J* 4(5):1125–1142
6. Wang X, Ong SK, Nee AY (2018) A comprehensive survey of ubiquitous manufacturing research. *Int J Prod Res* 56(1–2):604–628
7. Jain S, Chandrasekaran K (2020) Industrial automation using Internet of Things. In: *Security and privacy issues in sensor networks and IoT*. IGI Global, pp 28–64
8. Castro D, Coral W, Rodriguez C, Cabra J, Colorado J (2017) Wearable-based human activity recognition using an iot approach. *J Sens Actuator Netw* 6(4):28
9. Zhang H, Xiao Z, Wang J, Li F, Szczerbicki E (2019) A novel IoT-perceptive human activity recognition (HAR) approach using

multihead convolutional attention. IEEE Internet Things J
7(2):1072–1080

10. Hassan MM, Uddin MZ, Mohamed A, Almogren A (2018) A robust human activity recognition system using smartphone sensors and deep learning. Futur Gener Comput Syst 81:307–313

11. Jain A, Kanhangad V (2017) Human activity classification in smartphones using accelerometer and gyroscope sensors. IEEE Sens J 18(3):1169–1177

12. Khan PW, Byun Y (2020) A blockchain-based secure image encryption scheme for the industrial Internet of Things. Entropy 22(2):175

Author information

Authors and Affiliations

Velammal College of Engineering and Technology, Madurai, India

P. Alli

Karunya Institute of Technology and Sciences, Coimbatore, India

J. Dinesh Peter

Corresponding author

Correspondence to [P. Alli](#).

Editor information

Editors and Affiliations

School of Computer Science and Engineering, Vellore Institute of Technology, Chennai, India

R. Jagadeesh Kannan

School of Computer Science and Engineering, Vellore Institute of Technology, Chennai, India

S. Geetha

Department of Science and Engineering, Manchester

Metropolitan University, Manchester, UK

Sravanthi Sashikumar

Academic Lead Industry 4.0, Manchester Metropolitan

University, Manchester, UK

Carl Diver

Rights and permissions

[Reprints and Permissions](#)

Copyright information

© 2023 The Author(s), under exclusive license to Springer Nature Singapore Pte Ltd.

About this paper

Cite this paper

Alli, P., Dinesh Peter, J. (2023). Elevated CNN Based Secured Sensor Image Data Communication for HAR: IIOT. In: Kannan, R.J., Geetha, S., Sashikumar, S., Diver, C. (eds) International Virtual Conference on Industry 4.0. IVCI 2021. Lecture Notes in Electrical Engineering, vol 1003. Springer, Singapore. https://doi.org/10.1007/978-981-19-9989-5_18

[.RIS](#) [↓](#) [.ENW](#) [↓](#) [.BIB](#) [↓](#)

DOI	Published	Publisher Name
https://doi.org/10.1007/978-981-19-9989-5_18	01 April 2023	Springer, Singapore

Print ISBN	Online ISBN	eBook Packages
978-981-19-9988-8	978-981-19-9989-5	Engineering Engineering_(RO)

THREE TIER FRAMEWORK IRIS AUTHENTICATION FOR SECURE IMAGE STORAGE AND COMMUNICATION

P. ALLI¹, J. DINESH PETER²

¹Department of Computer Science and Engineering, Velammal College of Engineering and Technology, Madurai, India.

²Department of computer science and Engineering Karunya Institute of Technology and science Coimbatore

¹E-mail: alli rajus@yahoo.com

ABSTRACT

Due to the increasing popularity of multimedia technology, the need for secure image storage and communication has become more critical, because strangers try to access these data for illegal uses. Most researchers try to provide secure image communication and security frameworks, however, they have some limitations like high cost, minimum level of security, authentication issues, etc. To overcome that issues, our proposed work provides a three-tier architecture with secure iris authentication, secure data storage, and communication. Tier 1 includes user authentication with multifactor, authentication factors are username, password, mobile number OTP and iris authentication. Tier 2 has image encryption technology through a two-fold map concept known as the Twofold Logistic Chaotic Map, here the keys are generated using a pseudo-random number (PSNR) generator for randomness. Tier 3 has the communication phase, if two parties need to communicate between them, quantum key distribution along with PSNR is implemented to ensure secure communication. Finally, the proposed method was subjected to various experiments for performance analysis, including a histogram, an entropy rate, a number of pixels change ratio, and a correlation coefficient, through the analysis of the key space, the method can improve the security and reliability.

Keywords: *Quantum Key Distribution, Image Communication, Logistic Chaotic Map, and Pseudo-Random Number*

1. INTRODUCTION

The rise of the Internet has brought about a new era of convenience and information access for people. Through the Internet, individuals can now connect and store and retrieve vast amounts of data. Images have become more informative compared to text information. They contain more details and are easier to understand. As images become the main source of information, people must be vigilant about the risks associated with information leakage. In 2013, former CIA employee Edward Snowden revealed details of the agency's surveillance program known as the Program for the Evaluation of Strategic Materials, or the PRISM Project [1]. This program allowed the US government to monitor the activities of the public. During the 2018 Winter Olympics in South Korea, the personal information of spectators and athletes was stolen by hackers. This incident caused various negative effects. Due to the increasing number of sensitive information being

stored on the Internet, people must take measures to safeguard their data. Traditional encryption methods such as DES and RSA can be used to protect sensitive information. Unfortunately, the applications of these methods are not sufficient to meet the security requirements of image encryption [2]. The field of research mainly focuses on the protection of these images from various threats. Various digital image encryption techniques are used in digital image processing. Some of these include chaos encryption, pixel transformation, random sequence, and image compression coding [3]. The complexity of the chaos technology makes it hard to crack and randomize digital image encryption. Chaos encryption is a new type of digital image encryption that can be more secure and reliable.

Aside from having high data capacity and bulk data capacity, color image encryption also has certain characteristics that make it different from standard text encryption. Although many security

considerations have been discussed in terms of image encryption, many of these schemes are still not high enough. The short cycle length of keystream generators is one of the main factors that make it possible to transmit various attacks. To achieve a pseudo-random sequence, some chaotic stream ciphers have dual chaotic systems. However, when used with random map selection, the result is not secure enough [4]. The concept of confusion and diffused cryptography proposed by Shannon [5] is commonly used in encryption. It involves changing the pixel positions to reduce the complexity of input image data. The goal is to minimize the complexity of the input image by changing the pixel positions. This chaotic system has a weakness; it can only generate iterations that are less than 1000 times faster than the previous versions [6]. A good chaotic generator can help a cryptographic system achieve desirable statistical properties. For instance, a system that has a dense set of periodic windows can benefit from the existence of desirable statistical properties. Although many image encryption schemes can be used in chaotic cryptography, they are not ideal for practical applications [7]. Due to the nature of chaotic cryptography, it is not possible to implement image encryption schemes with good random sources. The author [8] presents an algorithm based on a simple Perceptron procedure. It combines the high-dimensional chaotic system with three sets of pseudorandom categorizations. A nonlinear approach is then used to produce the weight of Perceptron. The strategy is then used to dynamically adjust the chaotic system's parameters to resolve its cycle state issues.

The encryption issue is solved by employing a chaotic system; however, the security does not fulfill without secure authentication. For the secure authentication, we utilized a multifactor: username, password, mobile OTP, and biometric iris. A username is for the identification of a user by a name, password, and mobile OTP are the support factors of authentication. Biometrics is a type of secure authentication that can be used to uniquely identify a person. They can be stored in a secure environment, and they cannot be lost or stolen. This makes them ideal for addressing the security weakness of cryptography. The use of iris, which is considered to be the most reliable and secure biometric, has been widely used to identify people. Captured iris's features are extracted with a fuzzy extractor and the feature vectors are matched for identification. The resulting feature vectors are matched and generated according to a process.

One-time passwords are very secure, but it is not always feasible to share a long-term key between two parties using a communication channel [9]. A quantum key distribution method can provide high-security but it can also lead to issues due to its high cost and lower generation efficiency. If the two parties have a lot of data, then the issue with QKD might become more critical [10]. A pseudo-random algorithm can generate a sequence of random numbers with a fast and stable rate [11]. This type of algorithm guarantees the statistical characteristics of the sequence. PRNG is commonly used in various applications such as statistical sampling, numerical simulation, and gaming. It has a high generation efficiency and is simple to implement [12]. The PRNG algorithm is public, which means its security is completely dependent on the seed's confidentiality. This type of algorithm also ensures that the sequence's random number is always correlated with the seed's random number. To achieve high-efficiency random numbers in communication, a PRNG algorithm is proposed that generates a sequence of pseudo-random numbers at a low key generation rate and a high level of security. The paper shows that this method can be used to solve the issues related to QKD technology and reduce the cost of production. The proposed PRNG algorithm uses a method that allows QKD to share a seed key with the other party in a communication. After the two parties exchange a seed, the resulting algorithm will generate a pseudo-random number. The two parties then share a single pseudo-random number as a one-time pad secret key. This method is significantly different from the traditional QKD protocol, as it uses the security and randomization of QKD to solve the issues related to its generation rate and cost.

The main contributions of this paper are secure authentication, secure image data storage, and secure communication. These three contributions are provided in a three-tier structure.

- Tier 1: Secure authentication with multi factors: Username, password, Mobile number OTP, biometric iris (feature extraction and feature vector matching with fuzzy extractor).
- Tier 2: Secure image data storage: Twofold logistic chaotic map encryption and Pseudo-Random Number (PSNR) for random encryption key generation.
- Tier 3: Secure image data communication: Quantum key distribution with PSNR.

2. RELATED WORKS

Ghazanfaripour, H et al [13] - Using the 3D chaotic map, this study proposes a method for encrypting grey-level images. The method achieves many advantages over current techniques. Among these were: it can meet the security requirements of image cryptography and it can resist various attacks. It can also be executed randomly. In this paper, the main goal was to provide a method that applies to various image encryption methods. Although it was mainly focused on gray-level encryption, this approach may be used to encrypt a variety of different color images. This study proposes that the Galois Fields overcome the issues. The restriction of this study was choosing a prime number for a 3D modular chaotic map, it can increase the computation time and lag in security requirements.

Deng et al [14] use a chaotic map to protect images. It has a sensitive key and a huge key space, comparable to a sensitive key. The algorithm is flawed since it does not take into account the encryption attack of choice. Instead, it uses image scramble to achieve encryption. The results of the test show that an algorithm can effectively resist a variety of attacks, and it's sensitive to even little changes in plaintext. The main drawback of this study was that it fails to consider the different types of attack effectivity when choosing a plaintext attack.

Huang et al [15] - constructed a quantum logistic map with a discrete cosine transform (DCT) (QML) structure, which is utilized to convert a frequency domain object. The former provides the security properties of confusion, while the latter makes it fast and secure. The proposed scheme was subjected to various statistical experiments and security assessments. The results of the analysis revealed that the proposed scheme was able to successfully deal with the image of a man in a middle attack, which had been rendered in color and grayscale.. The drawback here is the outweighed computational complexity.

Alli et al [16]- presented a framework that combines the properties of DNA encoding and the mappings of the sequence to create an auto-encoder-induced DNA sequence. It can effectively handle the data losses caused by various attacks, such as those caused by statistical attacks and

chosen-plaintext attacks. The proposed framework generates a permuted image with less noise and complexity by activating the auto-encoder. After a secret key is obtained, it is decrypted using SHA-256. The output of the image is then sent via a digital network. Its efficiency is evaluated by taking account of the various metrics. Compared to the current frameworks, the proposed one is faster and more secure. However, it is still vulnerable to exploitation due to its weak encryption performance in terms of randomness.

Man et al [17]- a convolutional neural network algorithm was presented to implement a 2-dimensional encryption algorithm with chaotic sequence. It can resist known-plaintext attacks. A new image fusion method combined the various bits of information in two fused images. It achieves this by taking advantage of the varying characteristics of the binary bits. This study demonstrated the efficacy and security of a two-image fusion-based encryption system. It may be used to encrypt many images and is not restricted to just two. This method only protected two images. In contrast, image fusion can achieve a more secure encryption algorithm by combining the bits containing different information. This method can be used to protect multiple images.

3. PROPOSED THREE-TIER FRAMEWORK FOR DIGITAL IMAGE SECURITY AND COMMUNICATION

The rise of digital communication has made it easy for people to access and share information. Therefore, it is important to protect data from unauthorized access and sharing. There are three measures to be considered when it comes to protecting the data: Authentication, storage, and communication. Our proposed three-tier architecture is based on these considerations, figure 1 displays the three-tier architecture of our proposed framework.

- Tier 1: Secure authentication with multi factors: Username, password, Mobile number OTP, biometric iris (feature extraction and feature vector matching with fuzzy extractor).
- Tier 2: Secure image data storage: Twofold logistic chaotic map encryption and Pseudo-Random Number (PSNR) for random encryption key generation.

- Tier 3: Secure image data communication:
Quantum key distribution with PSNR.

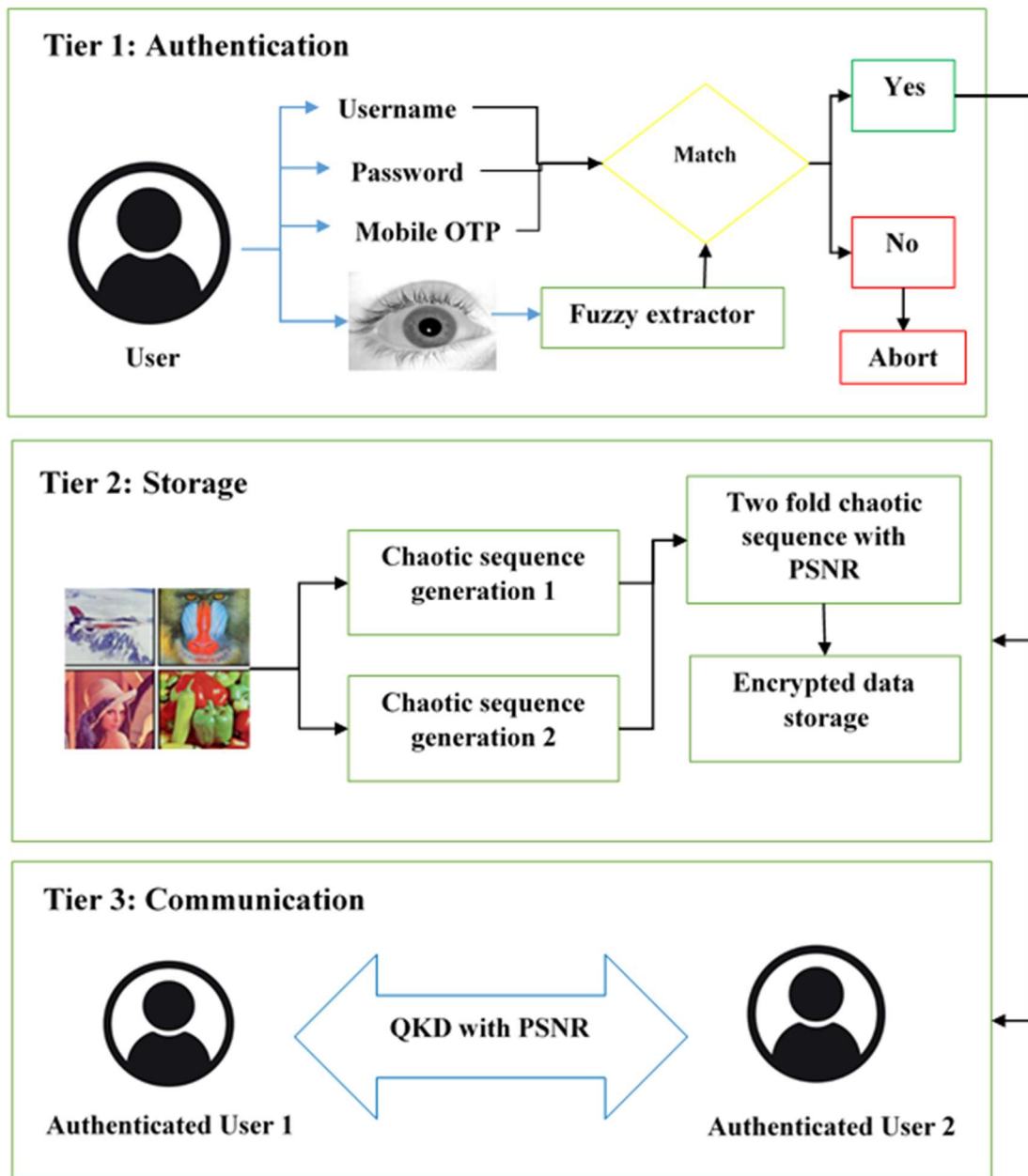


Figure 1: Three-Tier Architecture for Digital Image Security and Communication

3.1 Authentication Phase

In the authentication phase, the user must provide the factors such as Username, password, Mobile number OTP, and biometric iris. The username and password were matched with the stored credentials, the mobile number OTP is

randomly generated and it is verified for the corresponding mobile number. Biometric iris features are extracted using a fuzzy extractor and the extracted feature vectors are matched with the iris templates for accurate identification.

3.2 Twofold Logistic Chaotic Map For Secure Image Storage:

Various research on the subject of image communication has been undertaken to increase the security of digital media. Chaotic maps are often used in encryption to achieve tasks like key generation and pixel substitution. The complexity of a system can affect the security of an encrypted key. This paper presents a method that uses the double-logistical chaotic map to generate pseudorandom sequences for digital image encryption. The key is computed using the first and second level chaotic maps. The results of the study indicate that the various parameters of an image, such as its histogram, key size, information entropy, and space size, can be efficiently performed in the decryption process.

3.2.1. Theory of chaotic map

The concept of the chaotic theory is a non-deterministic theory that relates to the random state of systems.

1) The retro of $f(x)$ does not have a definite upper bound;

2) Occupancy S be a countless subsection of I , then the next state of interactions is true:

$$\forall_{x,y} \in S, x \neq y, \lim_{n \rightarrow \infty} \sup |f^n(x) - f^n(y)| > 0 \quad (1)$$

$$\forall_{x,y} \in S, \lim_{n \rightarrow \infty} \inf |f^n(x) - f^n(y)| = 0 \quad (2)$$

$$\forall_{x,y} \in S, \lim_{n \rightarrow \infty} \sup |f^n(x) - f^n(y)| > 0 \quad (3)$$

(Any intermittent point of $f(x)$ is denoted by Y .)

The $f(x)$ is the chaotic system that satisfies the limit points on S , which are distributed and concentrated. It does not correlate with all subsets. Chaotic systems have many characteristics. Some of these include boundedness, ergodically, and internal randomness. The concept of a chaotic system is not connected to all subsets. In chaotic systems, a linearized iterative equation shows the relationship between an insect population and a system. Logistic mapping can be used to evaluate the quantitative breeding models of flies. In the refinement progression, The number of children is greater than the number of parents. This means that if neither parent is present, the number of

children can be ignored and the chaotic sequence will appear different depending on the parameter. It will be generated if the condition satisfies the parameter (3, 4). It is similar to the white noise characteristic of sound. Before H. this approach was used to encrypt digital images.

The chaotic system's key sensitivity to the beginning value may be determined using its properties. This indicates that the encryption algorithm will change if the key changes that will have a better encryption effect. The existence of the key can be obtained through a chaotic system. This concept can be used to implement an encryption system that is based on the initial value.

Chaotic systems are used in two forms of encryption. The first is called chaotic synchronization, and the second type is the homogeneous group key. The chaotic system can be used for distinguishing the key sensitive demand and the pseudo-randomness of an encryption process. The different phases in the encryption process may be described as chaotic systems. A mapping algorithm is used for carrying out chaotic mapping operations. It can also be compared with the pseudo-randomness of the encryption system. Chaotic mapping is a process that uses a chaotic representation of a digital object to protect it. This method uses the chaotic sequence to create a pseudorandom number. It avoids using computer software to generate the same result. The image chaotic encryption system is an algorithm that can generate pseudorandom number sequences using an image pixel set and chaotic system. The chaotic system can generate an image pixel set and chaos, which can be used to achieve the opposite process (decryption).

3.2.2 Twofold digital image encryption method

An encryption system is very important to modern cryptography. It involves the transformation of the old keys into new ones, and the target of the encryption is the plaintext space. The decryption key is the one that's used to decrypt the encoded data.. For a framework, the C and P values of the original digital image are used to identify the image pixel that needs to be decrypted after encryption. The spaces obtained by encryption are obtained in an insecure channel. This feature allows the key to be used for various encryption methods. The control of an encryption algorithm is carried out in the key space K . This space contains the basic information that's required to perform the encryption.

The current cryptosystem comprises the key and encryption key operations. The component is the encryption key that is used to transform the encryption space P into the ciphertext space. The space C corresponds to the key that is used to secure the encryption. It can be obtained by sending the plaintext P to an anxious network. The key K is part of an encryption algorithm that can be used to perform various encryption operations. It can also be used to carry out a cryptographic transformation. The chaotic sequence generators are also responsible for the algorithm's development. A chaotic map is composed of two maps. These two maps are used to implement the modules that have to do with digital image encryption.

The pseudorandom sequence formed by the chaotic mapping is not random since the random number generator technique cannot guarantee complete unpredictability. The algorithm used for the random sequence generator is known as the logistic mapping method. The logistic pseudorandom sequence generator is commonly used to generate a pseudorandom order. It is formulated by way of follows.

$$\rho(x) = \begin{cases} \left(\pi \sqrt{1-x^2}\right)^{-1} & x \in (0,1) \\ 0 & x \notin (0,1) \end{cases} \quad (4)$$

The following two logistic maps are used for the compeers of pseudorandom orders. The first one is used for the first level and the second one for the second level. The following random number sequence is computed when the value is set. It is used for stream encryption. PRNGs are frequently used to produce a broad range of numbers which are typically used for generating number plots, rounding, linear, and nonlinear congruence. For producing pseudo-random numbers, the linear congruence approach is a simple and reliable method. It may be used to generate random sequences with high-quality random sequences. It uses a linear operation to get the next number.

$$x_{n+1} = (ax_n + c) \bmod m \quad (5)$$

a is a multiplier, c is an increment, m is a modulus in the formula, and x_n is a random number. The Q-base and P-base are two kinds of measurement bases, respectively.

$$|+\rangle = \frac{1}{\sqrt{2}}(|0\rangle + |1\rangle), \quad |-\rangle = \frac{1}{\sqrt{2}}(|0\rangle - |1\rangle) \quad (6)$$

$$|0\rangle = \frac{1}{\sqrt{2}}(|+\rangle + |-\rangle), \quad |1\rangle = \frac{1}{\sqrt{2}}(|+\rangle - |-\rangle) \quad (7)$$

Table 1 shows the four distinct states that were assessed using the two different measurement bases.

Table 1. Measurement Results Of Different States.

	$ 0\rangle$	$ 1\rangle$	+	-
Q-basis	$ 0\rangle$	$ 1\rangle$	50% $ 0\rangle$ or 50% $ 1\rangle$	50% $ 0\rangle$ or 50% $ 1\rangle$
P-basis	50% $ +\rangle$ or 50% $ -\rangle$	50% $ +\rangle$ or 50% $ -\rangle$	$ 0\rangle$	$ 1\rangle$

3.3 QKD With Pseudo-Random Number Generation Algorithm For Secure Communication

This research suggests a PRNG scheme that enables two parties to share arbitrary numbers without increasing the complexity or cost of QKD technology. The project's goal is to develop a secure QKD-based system with a high level of randomness. The project proposes a QKD-based system that uses a seed key to share a binary bit with two parties. The algorithm used for the PRNG will be the same as the one used for the arbitrary digit producer. The key will then be used to generate a PRNG with the same algorithm. This scheme uses the same pseudo-random number as a key that is used as a secret key. It avoids the high cost and slow generation of QKD. This scheme uses the unconditional security of true randomness to prevent the exploitation of pseudo-random numbers.

Step 1: For the open channel, both sides (sender and receiver) use a linear random number-generating technique.

Step 2: S1 is sent to a receiver after constructing a quantum sequence containing 4n single photons.

Step 3: After receiving S1, the receiver measures S1 at random using the Q-basis or P-basis.

Step 4: Following the preparation of S1's base sequence, the receiver must recreate S2's base sequence. By rejecting the single photon state of the same base, the quantum sequence S2 should be created.

Step 5: The receiver chooses a portion of the single photon and indicates if it is ready.

Step 6: The protocol is stopped if the bit error rate exceeds the threshold.

Step 7: To inspect the photons, both the receiver and the emitter must round them off. After that, the leftover particles form the quantum sequence

S3.

Step 8: The receiver delivers k_1 as a seed to a linear congruence algorithm, which returns K_2 .

This paper shows how to generate a random sequence using two logistic maps. The generated sequence is used for encrypted communication.

The image encryption process begins with two steps: confusing processing and scrambling. The confusing processing takes place when the encryption key is confused.

- 1) To calculate the Qkd model, set design parameter 1 to the pseudorandom sequence number X .
- 2) The pseudorandom sequence number will be converted to binary using this approach.
- 3) Encrypt the grey or color component code of the digital image.
- 4) The XOR for the first element in G is calculated using the X'_{gi} formula.

$$I'(k) = X^{(k)} \oplus \{ [X^{(k)} + g_k] \bmod N \} \oplus I'(K + 1)$$

(8)

The k pixel in the image is represented by k .

5) After the fourth step, the sequence of pixels is reversed and the original components are repositioned to the first and second locations according to formula 8.

4. RESULT AND DISCUSSION

4.1 Simulation Environment

The numerical simulations are carried out using the MATLAB program in a classical computer. We take into account the various plain images such as Baboon, Lena, and Airplane. Due to the complexity of the algorithm and the need for high-end computing hardware, our proposed method was simulated using a classical computer with an Intel(R) Core i7-4760U. The R2015a is equipped with a 64-bit CPU and 8GB of RAM.

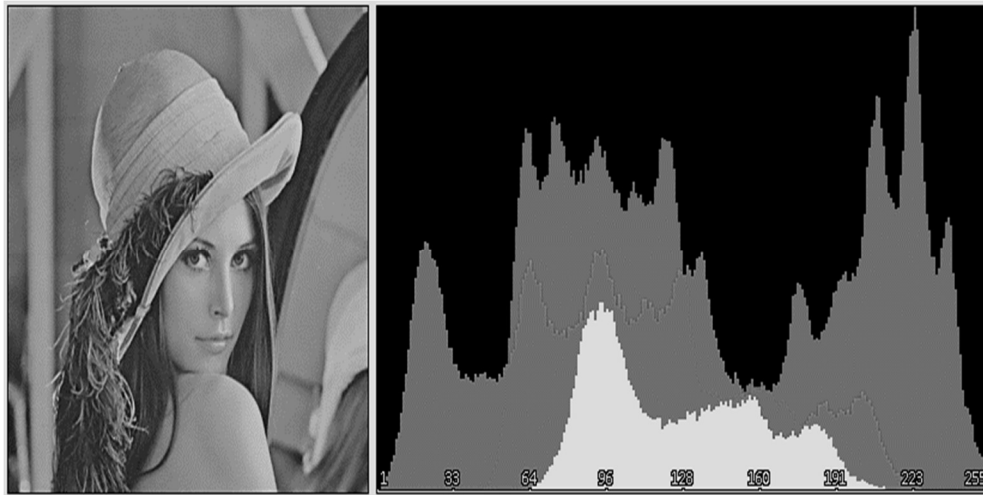


Figure 2: Original Lena Image And 3D Histogram

The original image presented in Figure 2 is kept in a $256 * 256 * 3$ matrix. It must be grayscale to obtain greater digital encryption. Figure 2 shows Lena's original image, which is a three-dimensional array. It's stored as a matrix $490 \times 490 \times 3$. To achieve better encryption, the image should be rendered in grayscale.

4.2 The Histogram Analysis

A distributed histogram is a representation of the quality and reliability of an encryption system. It displays the intensity of an image's colors using the x- and y-axis. The values are represented by the y- and the x-axis of the

image. Having a flat image histogram helps in the discovery of more diffused colors in an image since it avoids generating random distributions.

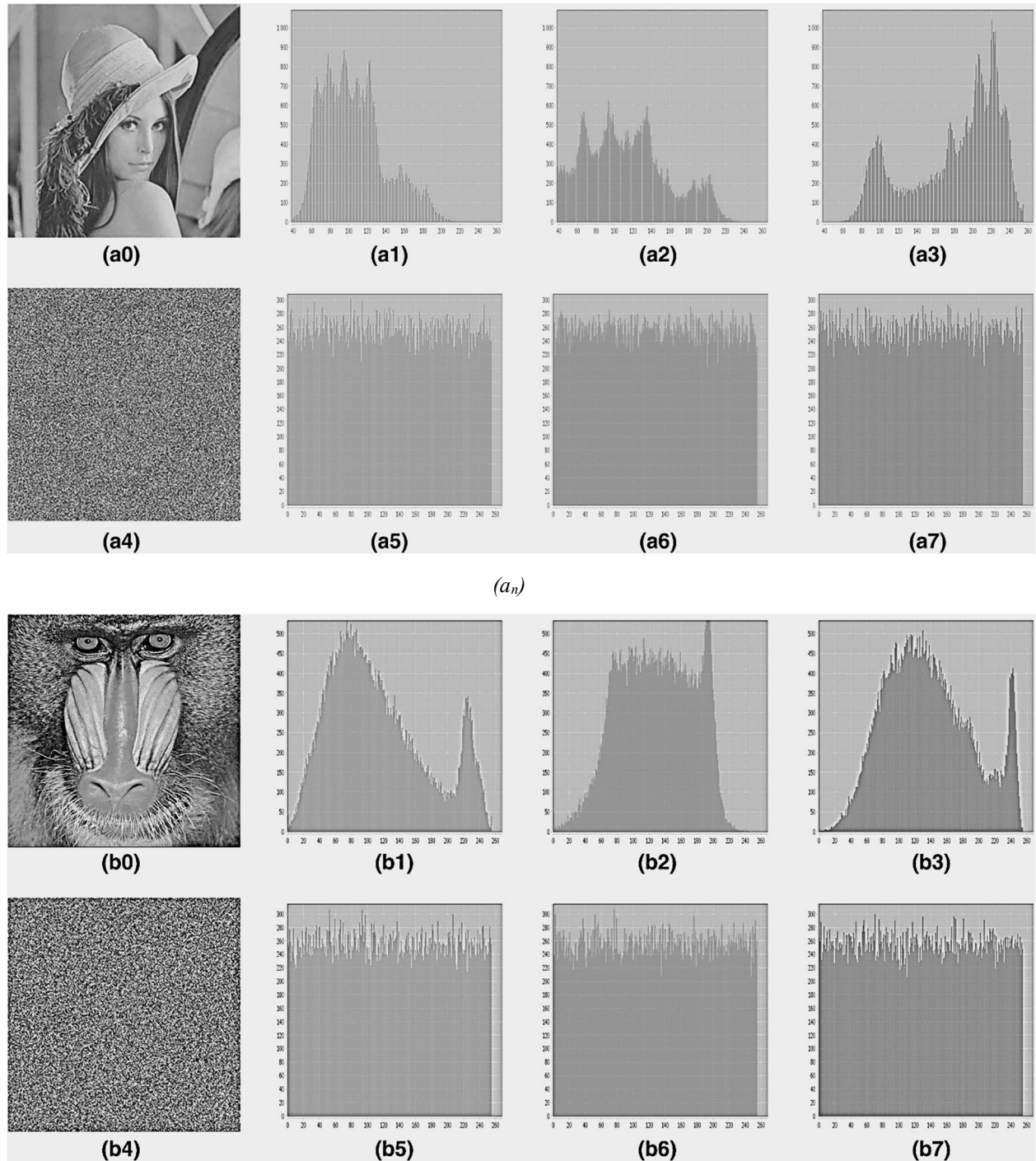
For each key, we use the principles of variances to evaluate the uniformity of ciphered images. We also calculate the differences between the encryption keys used for different ciphered images. The values of these factors are then computed to determine the variances of the encoded images. The appearance of encrypted images is determined by the relative values of histograms. The closer the values get, the more

uniform the encrypted images are presented as follows:

$$\text{var}(Z) = \frac{1}{n^2} \sum_{i=1}^n \sum_{j=1}^n \frac{1}{2} (z_i - z_j)^2, \quad (9)$$

Where Z is the vector of the values z_1, z_2, \dots, z_{256} , the numbers of pixels are equal to i and j respectively. In experiments, we show how to

simulate two ciphered images with different secret keys. In this study, we show how two sets of histograms could be obtained from an image with different secret keys. The encryption algorithm used for this test only changes one parameter of the secret key. The image of Airplane, Lena, and Baboon is tested for encryption and the histogram analysis is presented in Figure 3.



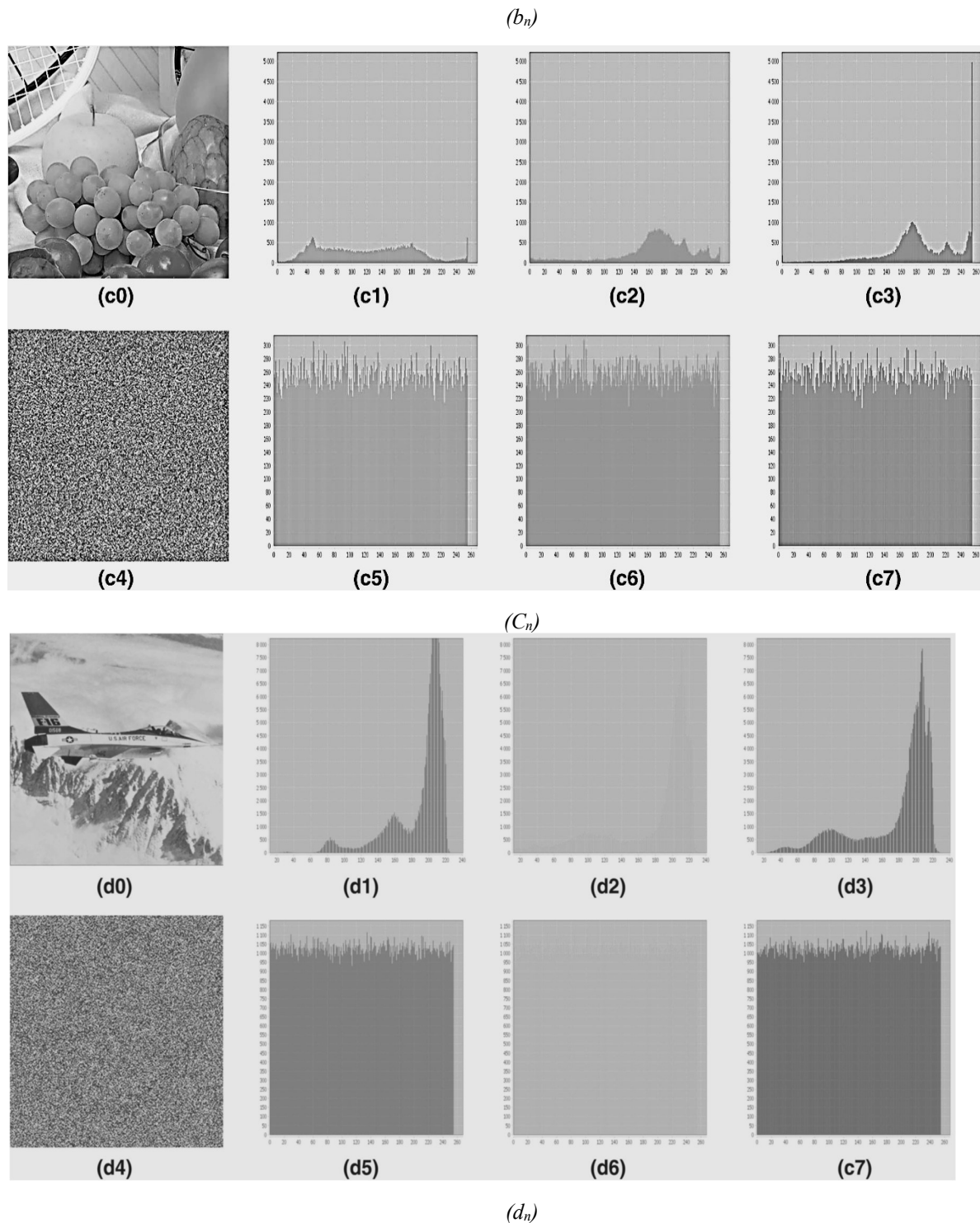


Figure 3: A) Lena, B) Baboon C) Fruits, And D) Airplane Image And Histogram Image Of RGB

4.2.1. Histogram statistics

The standard deviation and variance metrics are used to measure the dispersion of data in graphic histograms. A set of values with the

same average size can have the same elements, but their variation can be significant. Squared-point computation is a process that takes the central point and measures its variance. This process is

used to minimize the effects of distributed data and increase the variance of non-standard ones.

$$\alpha = \frac{1}{256} \sum_{i=1}^{256} (x_i - \bar{x})^2 \quad (10)$$

Where,

$$\bar{x} = \frac{M \times N}{256} \quad (11)$$

x_i is the frequency for the intensity value of the histogram is 0 to 255, and the mean is the sum of the histogram's variance.

4.2.2. Histogram uniformity

The ideal uniform histogram should have the same pixel frequencies across all 256 values. The histogram should have 256 standard deviations ranging from 0 to 255. The histogram uniformity percentage is a function that measures the consistency of the intensities across all 256 levels.

$$HUP(\%) = \frac{1}{256} \sum_{i=1}^{256} \rho(i) \quad (12)$$

Where:

$$\rho(i) = \begin{cases} 1 & \text{if } \rho \geq \bar{x} - \beta \text{ and } \rho \leq \bar{x} + \beta \\ 0 & \text{otherwise} \end{cases} \quad (13)$$

The acceptable range 'p' can be determined by taking into account the variance in the standard deviation 'β' and the mean 'x̄', while the mean can be derived from the data. For instance, the values of the HUP of the images Lena's and Baboon's encrypted images are 85.01% and 85.54%, respectively,

In experiments, we compare the sensitivity of various secret keys. The results of the tests reveal that changing one parameter can significantly affect the sensitivity of the secret key. Table 2 compares the proportion of histograms variances for all secret keys. The first and next columns' variances are obtained by changing the secret key l's parameters k1, l, e, g, and c[0]. The number of rows with the lowest and highest variance is computed by dividing the gray value by the number of pixels. The number of rows with the highest and lowest variance is 5000. The calculation of the variance value is performed by taking the sum of the gray value and the plaintext image's variability. The most common way to

determine a 10% fluctuation is by changing the K1 key to a secret key.

Table 2: Compares The Percentage Of Variances Difference Of Histograms For All Secret Keys

Ciphered image	K1 (%)	l (%)	e (%)	g (%)	c[0] (%)
Lena	9.8	1.57	1.19	2.22	5.2
Baboon	11.30	3.53	9.96	3.18	1.0
Fruits	8.96	6.59	5.49	2.36	1.42
Airplane	10.56	5.32	3.78	3.63	4.83
Average	10.155	4.2525	5.105	2.8475	3.1125

4.3. Encryption Quality

The various techniques used in validating the encryption of images are discussed in this section. One of the methods that can be used to calculate the signal-to-noise ratio is the mean-square error method. The peak signal-to-noise ratio is the most common component of this

$$\text{equation. } MSE = \frac{1}{M \times N} \sum_{i=1}^M \sum_{j=1}^N [P(i, j) - E(i, j)]^2 \quad (14)$$

Where, MXN- image size

P- Plain image

E- Encrypted image

The size and encryption quality of an image is two key factors that are used to consider when choosing one. The MSE analysis is a tool that can be used to test the operation of an encrypted color image and the RGB plain image. The PSNR is a function that shows the ratio between the signal's maximum power and the distortion that affects the quality.

$$PSNR = 20 \log_{10} \left(\frac{255}{\sqrt{MSE}} \right) \quad (15)$$

Due to the high MSE of encryption algorithms, the PSNR of encrypted images is expected to be less than 10 dB. Table 3 presents the Comparison of MSE and PSNR (dB) in terms of encrypted images.

Table 3: Comparison Of MSE And PSNR (Db) In Terms Of Encrypted Images

Encrypted Images	MSE			PSNR (dB)		
	R	G	B	R	G	B
Lena	23296	21267	25685	8.3	9.17	7.50
Baboon	9452	8015	9648	8.37	9.09	8.28
Fruits	10677	9105	7200	7.87	8.60	9.68
Airplane	7825	6589	8956	7.56	8.69	8.96

4.4. The Correlation Coefficient

The correlation factor is a statistical measure that shows how similar two variables are to each other. It's commonly used to measure the quality of an encryption scheme. The strength and usefulness of an encryption technique are measured by how it can conceal all of the original data's attributes and produce an uncorrelated encrypted version. In image processing, the correlation between the image's adjacent pixels and the original image is usually very high. On the other hand, if the correlation between the two is very low, then an encryption scheme is very effective. An efficient algorithm should reduce the correlation coefficient as much as possible to zero.

The correlation coefficient is a function that measures the number of pixels in an image. The number of pixels in an image is computed by dividing the distance between the objects by the number of digits. The algorithm used to determine the correlation coefficient is the most

advantageous one for achieving the most favorable result in the computed correlation. The Correlation Coefficient rates are computed by taking the coordinate coordinates of three vertical and horizontal coordinate coordinates. They were computed using the MATLAB environment's predefined functions.

$$r_{x,y} = \frac{E((x - E(x))(y - E(y)))}{\sqrt{D(x)D(y)}} \quad (16)$$

$$E(x) = \frac{1}{N} \sum_{i=1}^N x_i \quad (17)$$

$$D(x) = \frac{1}{N} \sum_{i=1}^N (x_i - E(x))^2 \quad (18)$$

The number of pixels that were chosen for the image is expressed in the gray area of the two adjacent pixels.

4.5. Differential Attack Analysis

The following equations 19 and 20 are used to analyze the performance of an encryption framework.

$$NPCR = \frac{\sum_{i,j} D(i,j)}{W \times H} \times 100\% \quad (19)$$

$$UACI = \frac{1}{W \times H} \left[\sum_{i,j} \frac{|C_1(i,j) - C_2(i,j)|}{255} \right] \times 100\% \quad (20)$$

The height and width of the image are respectively indicated by the cipher image before and after it has been changed.

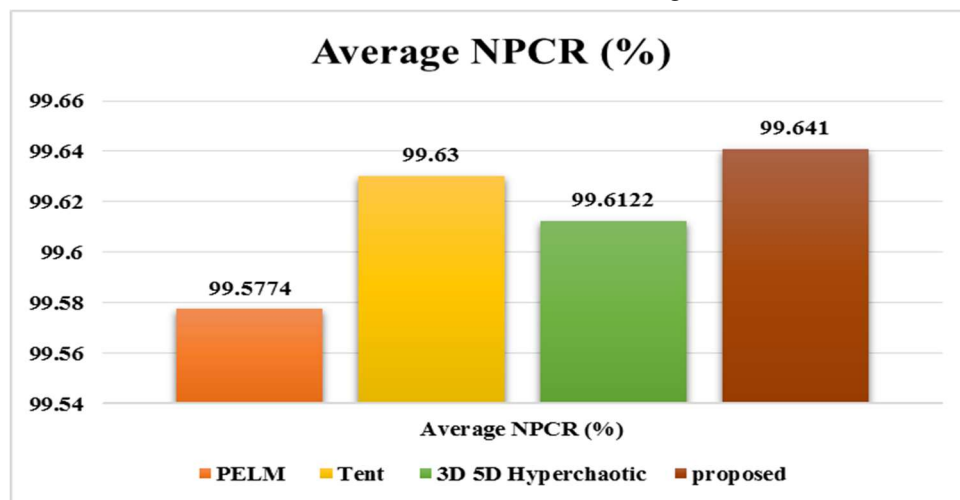


Figure 4: Comparison Of Average NPCR With Existing Methodology

From figure 4, the two-dimensional logistic map with QKD was able to pass the critical values test in the number of pixel change rates (NPCR) analysis. It also exhibited similar results to those obtained from other works [18].

4.6 Robustness evaluation

An excellent encryption system depends on the image's ability to resist the effects of noise and clip attacks.

- 1 **Clipping attacks:** The quality of an image reconstructed after it has been

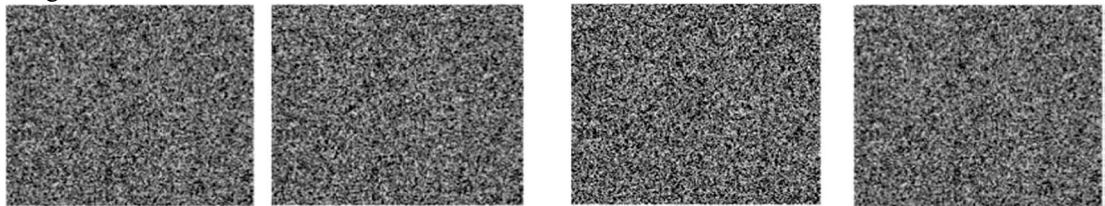


Figure 5: Encrypted Images Of Lena With 1–25 % Of Noise And Their Decrypted Images

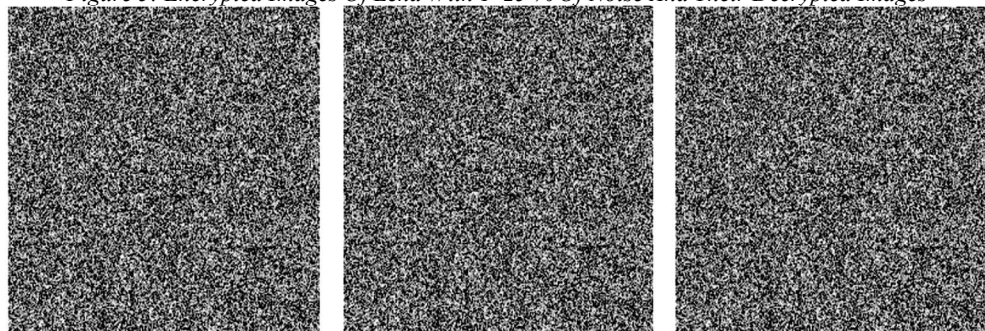


Figure 6: The Encrypted Images Of Lena With Gaussian Noise And The Decrypted Images

encrypted will decrease if it is attacked by pixel clipping.

- 2 **Noise attack:** Existing cryptosystems are prone to noise, especially if a small distortion appears in the cipher text. This issue can render the decrypted image unusable. Figure 5 reveals the images of Lena that have varying amounts of noise, while those with Gaussian noise are shown in Figure 6. This paper proposes a novel algorithm that can effectively suppress noise attacks.

Table 4: NIST Test Results For Lena Cipher Image

Test name		p values for encrypted image		
	Red	Green	Blue	
Frequency		0.4934	0.9773	0.59773
Block-frequency		0.95857	0.30998	0.7952
Runs (M = 10,000)		0.33534	0.4262	0.3375
Long runs of one		0.1468	0.1468	0.1486
Rank		0.3020	0.3020	0.3020
Spectral DFT		0.57927	0.77447	0.88278
No overlapping templates		0.93396	0.98892	1
Overlapping templates		0.96099	0.96099	0.96999
Universal		0.99550	0.98863	0.98284
Serial	<i>p values 1</i>	0.06751	0.4900	0.38419
Serial	<i>p values 2</i>	0.22893	0.64973	0.61688
Approximate entropy		0.32616	0.52073	0.29336
Cumulative sums forward		0.45878	0.38780	0.35722
Cumulative sums reverse		0.79386	0.4193	0.39884
Random excursions	$X = -4$	0.88486	0.121568	0.65737
	$X = -3$	0.5800	0.157192	0.88090
	$X = -2$	0.61416	0.93205	0.61759
	$X = -1$	0.64453	0.71386	0.8238
	$X = 1$	0.31163	0.94425	0.47204
	$X = 2$	0.129964	0.44806	0.36073
	$X = 3$	0.1141647	0.63529	0.3365
	$X = 4$	0.1183702	0.066905	0.98603
Random excursions	$X = -4$	0.81829	0.60299	60.92218
variants	$X = -3$	0.69707	1	0.99865
	$X = -2$	0.59410	1	0.8920
	$X = -1$	0.43139	0.93837	0.37949
	$X = 1$	0.37057	0.34117	0.19200
	$X = 2$	0.95027	0.52394	0.21146
	$X = 3$	0.45918	0.50532	0.176001
	$X = 4$	0.36087	0.28466	0.142555

Table 4 shows the NIST test results, and the suite of statistical tests provided by NIST is used to evaluate the proposed method. The value of the tests is compared with their significance level, which is 0.001. If the test's value exceeds the threshold, the method is considered to be passed. The results show that the proposed approach can achieve a high level of security.

The proposed algorithm is subjected to four image processing attacks to evaluate its robustness. The results show that the design is associated with higher reliability and higher normalized correlation. The results show that the proposed algorithm does not affect image decryption and encryption. In addition, the proposed method's robustness is strengthened by the higher normalized correlation. These are the histograms for encrypted images, which are almost flat and uniform compared to the plain ones. The improved scheme can prevent unauthorized access to an image's data through statistical attacks. Due to the nature of electronic transmission, image transmission can get infected with noise. This is a serious issue that affects the reliability of cryptosystems. A good encryption algorithm should be able to prevent this issue by protecting the data from getting distorted due to a minor change in the encryption algorithm. This could prevent the recovery of the image after an error in one pixel. A good encryption scheme should also consider the robustness of its algorithm against noise. This ensures that the data is not distorted due to propagation errors.

4.7 Image Entropy

Global information entropy is a measure of signal randomization. It should be around 8 bits for a grayscale. Image entropy is a measure of how much information can be presented in a given image. It can be computed by analyzing the color intensity of individual pixels. If the pixel's color intensity is the same across all the images in the same frame, then the resulting image with the minimal entropy value will have the same color. If the computed image entropy value is less than 8, then an image scramble procedure is a good idea. Table 5 shows the entropy values of our proposed method.

Table 5: The Calculated Entropy Values In Our Simulation

Image	The entropy value(original image)	The entropy value
Airplane	7.7047	7.9236
Baboon	7.7033	7.9949
Lena	7.7322	7.9742
fruits	7.7249	7.9743

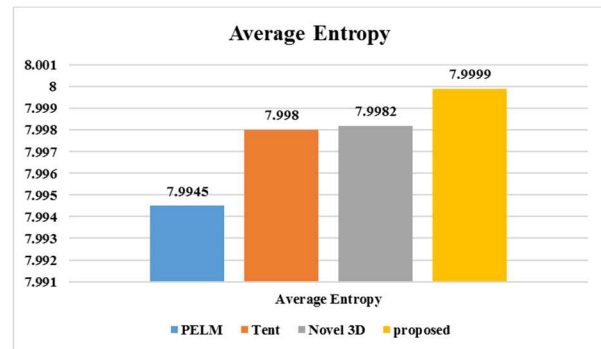


Figure 7: Comparison Of Average Entropy With Different Methodologies

Ideally, digital images with an entropy of 8 should be encrypted. For cryptographic systems, this threshold is maintained to prevent their security from being threatened [19-21]. For the proposed method, the two logistic chaotic maps with QKD and the Lena RGB image are used. For comparison, the results of the same work can be obtained by comparing them to works that use the same image and 8-bit RGB format. In this case, the proposed method shows better results than most of the works. To prevent unauthorized access to the contents of a given ciphertext image, the proposed scheme uses an information entropy attack. This prevents an attacker from extracting information from the image.

4.8 Security Analysis

The algorithm that generates a quantum encryption algorithm is known as a cryptographic algorithm. The security of the quantum encryption algorithm is dependent on the details of its generation process. The length of the key stream and the size of the image are also known to affect the gray value. The length of the key stream is generally determined by the size of the key space. The key must have sensitive bit changes to decipher the image. The number of bit changes

(NBCR) of an image is also known as the key sensitivity.

$$NBCR(B_1, B_2) = \frac{ham(B_1, B_2)}{T_b} \quad (23)$$

If the number of bits from B1 to B2 is less than 50%, then the distance between them is equal to the overall distance between them.

A cryptographic system's total number of secret keys is known as key space. The secret keys are generated using a linear key distribution algorithm. The algorithm generates the secret keys by taking a pseudo-random sequence of digits k2. The seed number k1, which is the pseudo-random sequence k2, is used to input the linear algorithm are shown in Table 6.

Table 6: The Value Of K1 And K2.

Key	The value
K1	01011110001010101010
K2	46547632875934570297382675465947604 85937482612`136r26583745640968349568 32571536426543876594878467357126143 62154732658932759847598236583276472 15327186487236498365837644712648716 983562837657467286735763

4.9 Encryption And Decryption Speed

The main functions of decryption and encryption are similar. They are computed by comparing the length and size of the secret message and the secret key. The time it takes to decrypt or encrypt a message depends on the condition of the secret key and its size. Figure 8 depicts the Encryption/decryption time for different image sizes and secret key lengths

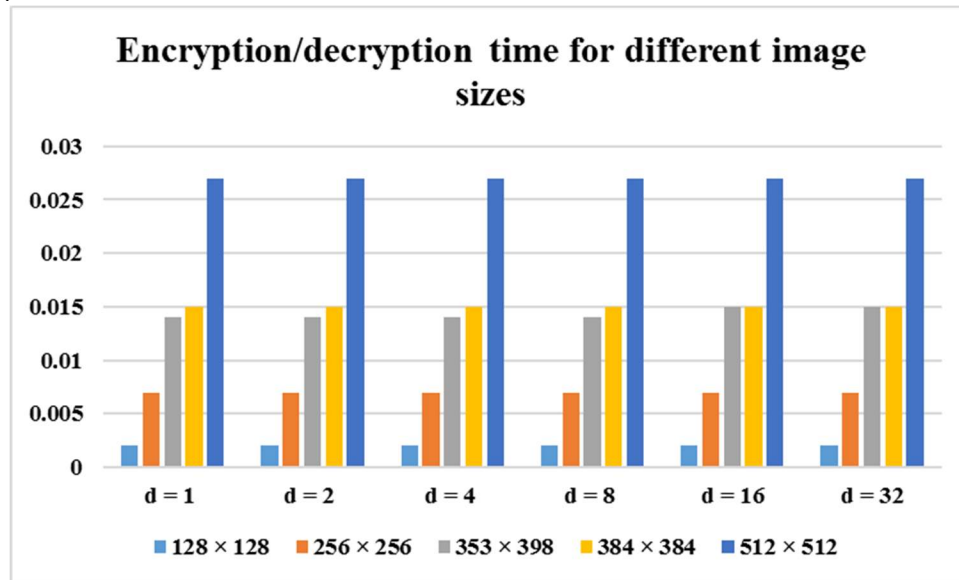


Figure 8: Encryption/Decryption Time For Different Image Sizes And Secret Key Lengths

Table 7 shows the computational cost calculation for cost efficiency; where Te represents the time for one exponential operation, Tb represents the time for one bilinear operation.

Table 7: Computational Cost

Scheme	Encoding Cost **	Decoding Cost **
CP-ABE + Hidden Access policy [22]	3Te	3Tb

CP-ABE + Hidden Access policy [23]	4Te	3Tb
CP-ABE + Partially Hidden Access policy [24]	4Te	3Tb + Te
CP-ABE + Hidden Access policy [25]	3Te	3Tb + Te

CP-ABE + Hidden Access policy [26]	3Te	2Tb + Te
Proposed	3Te	2Tb + 2Te

4.9.1. Effectiveness key sensitivity analysis of the scheme

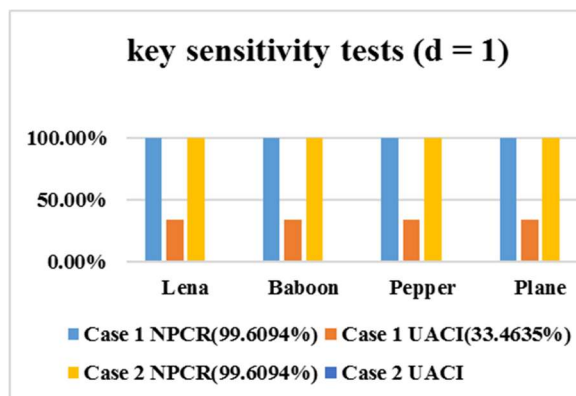
The generation time of k_1 is t_1 , and $t_1 = 0.00256s$.
The generation time of k_2 is t_2 and $t_2 = 0.00047s$.

The key generation efficiency is η_1 , $\eta_1 = 7799.54b / s$, and the pseudo-random number generation efficiency obtained by the linear congruence algorithm is η_2 ,

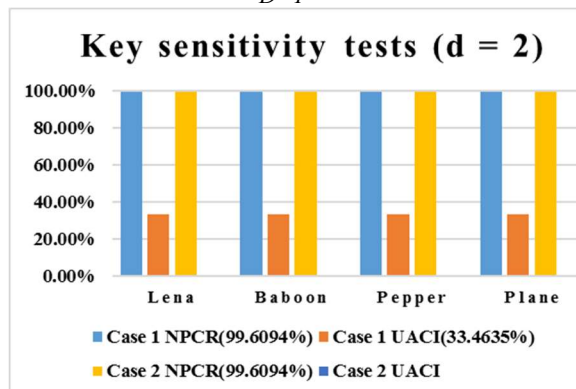
$$\eta_2 = 600bit / (t_1 + t_2) = 600bit / (0.00256s + 0.00047s) = 198216.06b / s \quad (14)$$

In the research, the ratio of generation efficiency to quantum random key efficiency is p ,

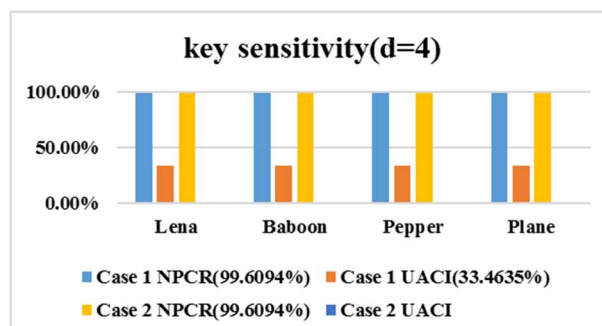
$$p = \eta_2 / \eta_1 = 198216.06 / 7799.54 = 25.42 \quad (15)$$



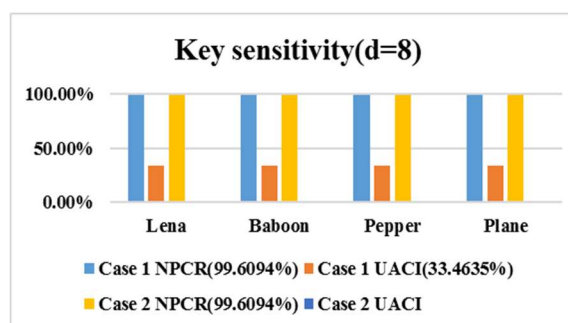
$D=1$



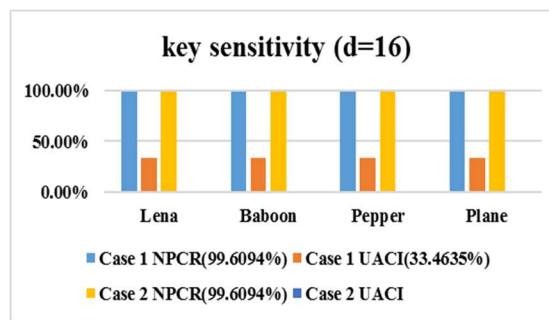
$D=2$



$(D = 4)$



$(D = 8)$



$(D = 16)$

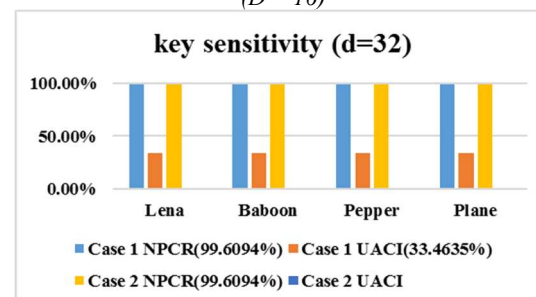


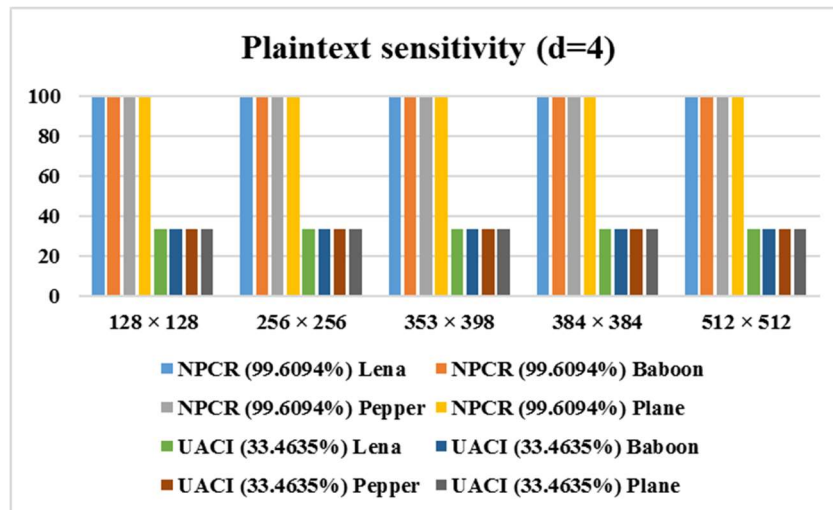
Figure 9: Results Of Key Sensitivity Tests ($D = 1, 2, 4, 8, 16$ And 32)

The results of the key sensitivity test are shown in Figure 9. As the number of keys increases, the pseudo-random number's efficiency will improve, which will make it more useful in generation of keys. The ratio of the pseudo-

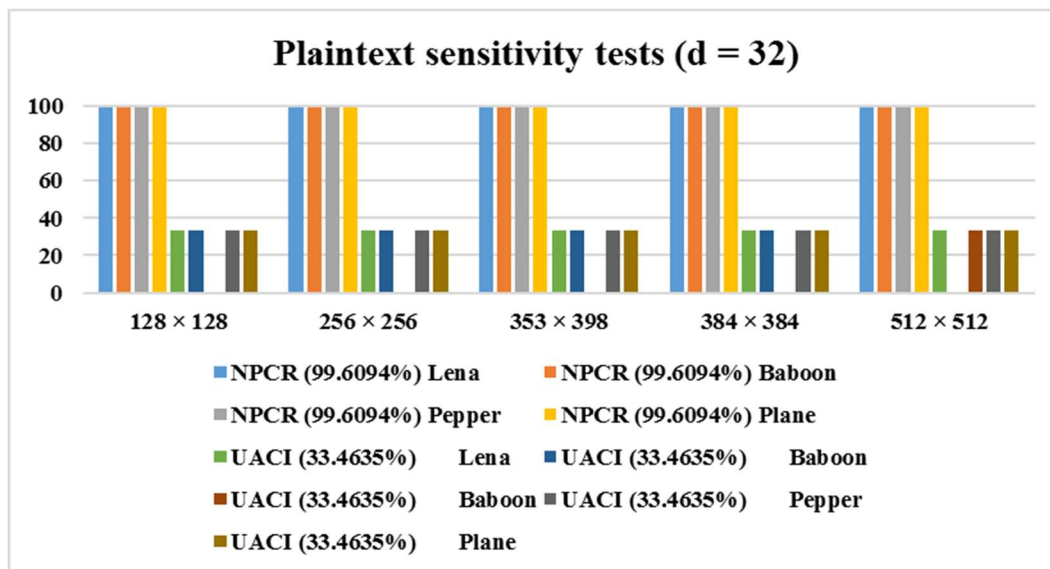
random to the quantum random key will also increase, which shows that the former is more efficient. Likewise, figure 10 shows the Results of plaintext sensitivity tests. A typical attacker makes a small change in the plain image and then observes the changes in the cipher image. This method can break the encryption process if the

change is small. On the other hand, differential analysis is useless when the attacker discovers the relationship between the two. Plain text sensitivity can be computed by comparing the NPCR and the Unified Average Change Intensity (UACI). For instance, if an input is changed slightly, the output changes significantly.

($d = 32$)



$d=4$



$d=32$

Figure 10: Results Of Plaintext Sensitivity Tests ($D = 4$ And 32)

4.10. Running Efficiency Analysis

For our proposed encryption algorithm, we consider the efficiency of its transmission. In this paper, we introduce 3 groups with different

sizes. For tests, we only selected groups with 256×256 . In this paper, we introduce the concept of group images, which are composed of three

images. The test results revealed that the proposed algorithm achieves good transmission efficiency.

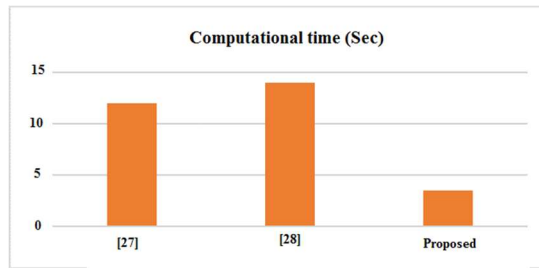


Figure 11: Computation Time With Different Related Works

In addition to the security aspect, the running speed is also an important factor that can be used to measure the image encryption scheme. Figure 11 shows that the time complexity of computation is also significantly reduced compared to that of the existing methodologies.

5. CONCLUSION

Due to the increasing number of applications of communication and networking technology, encryption has become an effective method for protecting the secure transmission of data. This paper shows the three-tier framework for secure image storage, authentication, and communication. An image scrambling procedure has been investigated on two levels. The procedure was performed on various images to evaluate their performance. By calculating the NCAR, entropy, and histogram graphs, where the requirements have been confirmed. Our proposed method surpasses a previous approach in terms of security, key generation efficiency, and cost efficiency. In the future, there will be another phase before the encryption key is applied to a particular site. This will make the confusion on the site even worse. An additional phase will allow developers to create more complex encryption methods.

REFERENCES:

- [1] Pan, H., Lei, Y. and Jian, C., 2018. Research on digital image encryption algorithm based on double logistic chaotic map. *EURASIP Journal on Image and Video Processing*, 2018(1), pp.1-10.
- [2] Dupont, B., 2004. Security in the age of networks. *Policing and society*, 14(1), pp.76-91.
- [3] Niu, Y., Zhou, Z. and Zhang, X., 2020. An image encryption approach based on chaotic maps and genetic operations. *Multimedia Tools and Applications*, 79(35), pp.25613-25633.
- [4] Liu, H. and Wang, X., 2010. Color image encryption based on one-time keys and robust chaotic maps. *Computers & Mathematics with Applications*, 59(10), pp.3320-3327.
- [5] C.E. Shannon, Bell System Technical Journal 28 (4) (1949) 656.
- [6] Liu, H. and Wang, X., 2011. Color image encryption using spatial bit-level permutation and high-dimension chaotic system. *Optics Communications*, 284(16-17), pp.3895-3903.
- [7] Liu, H. and Wang, X., 2012. Image encryption using DNA complementary rule and chaotic maps. *Applied Soft Computing*, 12(5), pp.1457-1466.
- [8] Wang, X.Y., Yang, L., Liu, R. and Kadir, A., 2010. A chaotic image encryption algorithm based on perceptron model. *Nonlinear Dynamics*, 62(3), pp.615-621.
- [9] Jiang, Y., Liu, B., Guo, C. and Zhao, J., 2021, August. A quantum pseudo-random number generation scheme. In *Journal of Physics: Conference Series* (Vol. 2004, No. 1, p. 012001). IOP Publishing.
- [10] Mi, S., Wang, T.J., Jin, G.S. and Wang, C., 2015. High-capacity quantum secure direct communication with orbital angular momentum of photons. *IEEE Photonics Journal*, 7(5), pp.1-8.
- [11] Hadfield, R.H., 2009. Single-photon detectors for optical quantum information applications. *Nature photonics*, 3(12), pp.696-705.
- [12] Tchoffo, M. and Tene, A.G., 2021. Security and communication distance improvement in decoy states based quantum key distribution using pseudo-random bases choice for photon polarization measurement. *Optical and Quantum Electronics*, 53(8), pp.1-24.
- [13] Ghazanfaripour, H. and Broumandnia, A., 2020. Designing a digital image encryption scheme using chaotic maps with prime modular. *Optics & Laser Technology*, 131, p.106339.
- [14] Deng, Z. and Zhong, S., 2019. A digital image encryption algorithm based on chaotic mapping. *Journal of Algorithms & Computational Technology*, 13, p.1748302619853470.
- [15] Ye, G., Jiao, K., Huang, X., Goi, B.M. and Yap, W.S., 2020. An image encryption

- scheme based on public key cryptosystem and quantum logistic map. *Scientific Reports*, 10(1), pp.1-19.
- [16] Alli, P. and Dinesh Peter, J., A novel auto-encoder induced chaos based image encryption framework aiding DNA computing sequence. *Journal of Intelligent & Fuzzy Systems*, (Preprint), pp.1-17.
- [17] Man, Z., Li, J., Di, X., Sheng, Y. and Liu, Z., 2021. Double image encryption algorithm based on neural network and chaos. *Chaos, Solitons & Fractals*, 152, p.111318.
- [18] Wu, Y.; Noonan, J.P.; Agaian, S. NPCR and UACI randomness tests for image encryption. *Cyber J.* **2011**, 1, 31–38.
- [19] Murillo-Escobar, M.A.; Cruz-Hernández, C.; Cardoza-Avendaño, L.; Méndez-Ramírez, R. A novel pseudorandom number generator based on pseudorandomly enhanced logistic map. *Nonlinear Dyn.* 2017, 87, 407–425.
- [20] Palacios-Luengas, L.; Pichardo-Méndez, J.L.; Díaz-Méndez, J.A.; Rodríguez-Santos, F.; Vázquez-Medina, R. PRNG Based on Skew Tent Map. *Arabian J. Sci. Eng.* 2018, 1–14.
- [21] Sahari, M.L.; Boukemara, I. A Pseudo-Random Numbers Generator Based on A Novel 3D Chaotic Map with An Application to Color Image Encryption. *Nonlinear Dyn.* 2018, 94, 723–744.
- [22] Helil, N.; Rahman, K. CP-ABE Access Control Scheme for Sensitive Data Set Constraint with Hidden Access Policy and Constraint Policy. *Secur. Commun. Netw.* 2017, 2017, 2713595.
- [23] Sabitha, S.; Rajasree, M.S. Access control based privacy preserving secure data sharing with hidden access policies in cloud. *J. Syst. Archit.* 2017, 75, 50–58.
- [24] Liu, L.; Lai, J.; Deng, R.H.; Li, Y. Ciphertext-policy attribute-based encryption with partially hidden access structure and its application to privacy-preserving electronic medical record system in cloud environment. *Secur. Commun. Netw.* 2016, 9, 4897–4913.
- [25] Wu, A.; Zheng, D.; Zhang, Y.; Yang, M. Hidden Policy Attribute-Based Data Sharing with Direct Revocation and Keyword Search in Cloud Computing. *Sensors* 2018, 18, 2158.
- [26] Odelu, V.; Das, A.K.; Khan, M.K.; Choo, K.R.; Jo, M. Expressive CP-ABE Scheme for Mobile Devices in IoT Satisfying Constant-Size Keys and Ciphertexts. *IEEE Access* 2017, 5, 3273–3283.
- [27] Yeoh, W.; Teh, J.; Chern, H. A Parallelizable Chaos-Based True Random Number Generator Based on Mobile Device Cameras for the Android Platform. *Multimed. Tools Appl.* 2018, 1–21.
- [28] Belazi M, E-Latif AAA, Belghith S (2017) Khan efficient cryptosystem approaches: S-boxes and permutation-substitution-based encryption. *Wirel Pers Commun* 87(1):337–361.

Enhanced Image Colorization in Medical Image Analysis using Deep Learning Model

K. Indira

Thiagarajar College of Engineering, Madurai, Tamil Nadu, India

C. V. Nisha Angeline

Thiagarajar College of Engineering, Madurai, Tamil Nadu, India

S. Karthiga

Thiagarajar College of Engineering, Madurai, Tamil Nadu, India

C. Santhiya

Thiagarajar College of Engineering, Madurai, Tamil Nadu, India

RajaLavanya

Thiagarajar College of Engineering, Madurai, Tamil Nadu, India

G. Vinoth Chakkaravarthy

Velammal College of Engineering and Technology, Madurai, Tamil Nadu, India

Abstract

Grayscale images are images that contain only intensity values. We use a process where we capture a grayscale image and give an image that is in semantic colours and tones of the input. This process is known as Image colouring (for example, the model colours it to hot pink). Image colouring can be used in many areas, including old black-and-white photography, old film, medical and scientific image colouring. Colouring is very important, but rewarding, because a colour image that looks natural must be taken from every grayscale input. Existing approaches to colouring black-and-white images rely on manual human annotation. This often leads to incredibly desaturated results as true colouring. With less degree, the colour is more subdued (more black or white is added). Unlike traditional old-fashioned techniques, neural network-based colouring techniques are fully automated that do not require human assistance. From a variety of colouring techniques such as automatic colouring, semi-automatic colouring and hand colouring, convolutional neural networks and deep neural networks are chosen because they can process image classification and recognition datasets with high precision. In this paper, we are going to use the Convolutional Neural Network (CNN), a deep learning algorithm which is mostly used to analyse an image visually and Autoencoders, which reduces dimensionality of the input.

Keywords: *Deep Learning, CNN, Autoencoders, Image Colourization.*

I. Introduction

Although classic image grouping methods are widely used in pragmatic situations, significant issues with their implementation arise, such as disappointing impacts, low classification accuracy, and poor adaptable capacity. For classification, this approach divides picture feature extraction and categorization into two parts. The deep learning model has a strong learning ability, allowing it to combine the feature extraction and classification processes to complete the image classification test and so enhance image classification accuracy. The process of taking a gray scaled image as an input and resulting in a colourized image that is constituted by semantic colours and tones is generalised as Image colourization. Use image colouring technology to highlight old grayscale photos and restore old memories with the most appropriate skin tones and textures.

The goal is to remove colours from colour pictures at the transmitter while maintaining colour information so that the image may be recoloured at the receiver. The reason behind this methodology is to exploit the smaller size of gray images. On the receiving side, the colours are restored and the colours in the image are changed. This method of encoding is called Image De-colourization. The convolutional layers' objective is to use convolution filtering to extract possible features. The intricate layers will usually get the input (for example, a 2D picture) and keep a specific form of kernel over it. The features that we wish to find are represented by the kernel. At each step, the kernel values multiply the input, and then the output is subjected to a non-linear activation function. The actual image entered as an input is turned to a filter map in this manner. Multiple levels of abstraction can be created by stacking intricate and aggregating (pooling) layers over each other. Many well-known image classification architectures such as AlexNet, VGG16, and ResNeta are created in a similar way. I merged

CNNs with auto encoders for the capstone project, resulting in a family of architectures which is known as intricate auto encoders. The grayscale image is the input for such a network (1channel), with the outputs being the two colour layers (a/b layers of the Lab representation).

II. LITERATURE SURVEY

o A. Overview of image colourization and its applications

Authors: Hao Wang, Xue Dong Lin (2021).

“This publication outlines an approach to image colouring. In addition, we classify image colouring approaches into three groups, describing common methods and applications, and evaluate their strengths and weaknesses with respect to future development trends. In terms of image quality and real-time performance, the results show that model-based colouring has a better colouring effect than other methods”[1]

o B. Deep learning for automatic colourization of legacy grayscale aerial photographs

Authors: Quentin Poterek, Pierre-Alexis, Herrault, David shreeren (2020)

“This article introduces a deep learning model called a conditional generative hostile network that enriches older images by forecasting the colour channels of the grayscale image which is taken as an input. Two ortho photographs (captured in 1956 and 1978) covering the entire Eurométropole de Strasbourg were coloured using this technique. To evaluate the performance of the model, two strategies were proposed. In the first one, the evaluation of colour photographs are done using metrics like peak signal-to-noise ratio (PSNR) and the structural similarity index (SSIM). Next, grayscale and colour photographs were subjected to random forest classification to extract land cover classes. The results showed

that the mapping between grayscale images and colour images are learnt by the model over a huge area with PSNR = 25.562.20 and SSIM = 0.93 0.06. In addition, the 1956 and 1978 colour data-based land cover classifications showed a significant increase over grayscale images, with improvements of + 6% and + 17%, respectively. Finally, we have visually evaluated the reliability of the generated image. In conclusion, the deep learning model is generalised as a potent tool for improving the radiation characteristics of past aerial gray levels. It is also believed that the proposed method may serve as the foundation for future work 13 aimed at facilitating the use of aerial archives for landscape reformation.”[2]

o C. Unpaired Image-to-Image Translation Using Cycle-Consistent Adversarial Networks

o Authors: J. -Y. Zhu, T. Park, P. Isola and A. A. Efros(2020).

“Using a training set of image pairs that are aligned in order to understand mapping between input and output images is the sole purpose of image-to-image conversion, a class of visual and graphics tasks. However, matching training data is not available for many issues. If we don't have an instance of the pair, it provides a way to learn the conversion of image from X (source domain) to Y (target domain). Using hostile loss, we train the map $G: X \rightarrow Y$ so that the distribution of the image of $G(X)$ from the distribution Y is indistinguishable. Associate this with the reverse map $F: Y \rightarrow X$, which is so unconstrained(and vice versa) that the cycle is inconsistent due to pushing $F(G(X)) \neq X$. For many tasks for which matching training data is not available, qualitative results are reported, such as B. collection-style forwarding, object deformation, seasonal forwarding, and photo highlighting. Quantitative comparisons with many previous methods show that our approach is superior.”[3]

o D. Single image colourization via modified cycle GANAuthors: Y. Xiao, A. Jiang, C. Liu and M. Wang

“The necessity of this work is without personal intervention, we have to colour a single grayscale image. Most existing approaches attempted to reliably restore unknown groundtruth colours and required paired training data to optimise the model. Our performance was limited by ideal repair goals and strict training limits. We formulate colouring as an image-to-image conversion and provide a CycleGAN- inspired colour CycleGANsolution. It has also been proposed that the loss of semantic identity is high and the loss of colour is low due to model optimization. Using RGB colour space, training and direct prediction both are enabled using this method. This makes data collection for training much more simple and common. Our model is trained with randomly selected images from PASCAL VOC 2007. Grayscale SUN is used to study all loss function ablation and compare it with state-of-the-art technology. Experimental results show that reducing training losses can increase content consistency, reduce artifacts, and create more realistic colours. Also, because our model is bidirectional, the proposed approach creates a by-product that provides an ideal alternative solution for graying colour images”[4]

o E. Learning from paired and unpaired data: alternately trained cycleGAN for near infrared image colourization

Authors: Z. Yang and Z. Chen

“At the Grand Challenges presented by the IEEE International Conference on Visual Communications and Picture Processing 2020, this presentation features innovative Near Infrared (NIR) Image colouring Technology (VCIP). A CycleConsistent Generative Adversarial Network (CycleGAN) with a tight cross-scale connection is set up to understand colour conversions from NIR to RGB domains that are done based on paired as

well as unpaired data. Due to the limited number of NIR and RGB images paired, we use data expansion techniques such as cropping, scaling, contrast, and mirroring to extend the variability of the NIR domains. CycleGAN was developed to learn explicit pixel-level mapping from paired NIR RGB data and implicit domain mapping from pairless data using alternating training techniques. The technique was tested and validation data (AE) was used to compare the structural similarity (SSIM), peak signal-to-noise ratio (PSNR), and angular error with the traditional CycleGAN method. The results of the experiment support the actual proposed colour scheme.”[5]

III. PROPOSED ARCHITECTURE

A. Modules

Module 1: BUILDING DATA

- We can get a grayscale channel from any coloured image, thus colourization of data is available everywhere.
- We will be using the Image Colourization dataset that is available in kaggle for this paper.
- The dataset used from kaggle will possess 25,000 224x224 grayscale as well as normal images.

Module 2: DATA PREPARATION

- Rather than selecting individual grayscale photographs, we iterated through the available dataset images and transformed them to lab space (gray-scale) images.
- We cropped all of the photographs to 224x224 pixels to keep the modifications to a minimum, since this is the size that has been used in that architecture.
- We used Lab colour space to convert the RGB input image into two images: the grayscale input of 224x224 pixels and the output, a/b layers (shape: [2, 224, 224]).

- After the conversion of pictures to Lab, we normalised the layers in the same way we did before. We multiplied the grayscale channel by 100, resulting in values in the range [0,1]. Then we multiplied the a/b channel values by 128, yielding a range of [-1, 1], that is appropriate for the last activation of the network, i.e, tanh activation function.

Module 3: MODEL AND TRAINING

- It is preferable to convert the photos to float for the model to learn rapidly. We also need to normalise the picture channel values so that they fall between 0 and 1, else the gradients will go out of control.
- The encoder is made up of three Convolutional Layers with increasing numbers of filters, followed by a 256-unit Dense Layer for generating latent vectors.
- The Autoencoder's decoder part tries to decompress the latent vector in order to match it to the input. The input to the Decoder in our scenario is a form layer (None, 256). It's followed by a stack of three De Convolutional layers, each with a decreasing filter number. In this scenario, we ensure that the final layer is in good form (None, 32, 32, 3).

Finally, we fit the model, which takes an input and then returns an output.

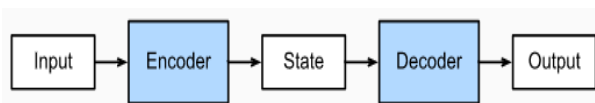
Module 4: EVALUATION

- Choosing a decent evaluation criteria is difficult because colouring is subjective to a large extent, in addition to this different variants can be judged acceptable.
- The MSE loss function has some drawbacks because of the multimodal nature of the colourization problem – a single grayscale image can correlate to a variety of acceptable colour images. As a result, the model prefers de-saturated hues over bright, vibrant colours because they are less likely to be incorrect (and so incur a high MSE penalty).

B. ALGORITHMS/TECHNIQUES USED

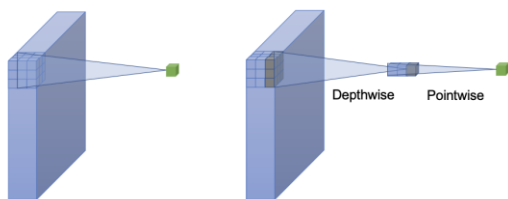
The algorithm that we have used here is Autoencoders. The Encoder is the First component which takes variable sequence length as Input and converts it to fixed-shape state. The state is also called bottleneck, which is where the maximum information of the input image is stored in a compressed manner. It enables only the most important information to flow through to the decoder. The decoder is the last part, which transfers the encoded state to a variable-length sequence. This is known as an encoder-decoder architecture, which is illustrated in the below diagram.[6]

FIGURE 1. Architecture of Encoder and Decoder.



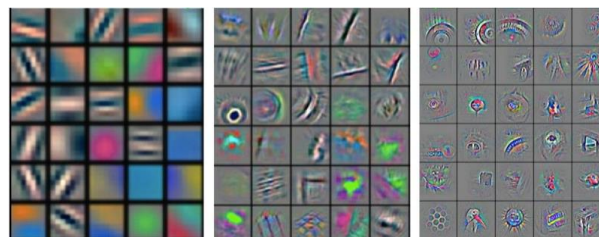
Convolutional neural networks(CNN), used for visualisation of the image after it is through the decoder component in Autoencoders. First step is sliding over the image spatially by computing the dots, but keeping the full depth of the input volume and for each filter we' ll get an activation map. Number of filter is chosen in $2n$, where $n \in \mathbb{Z}^+$.

FIGURE 2. Convolutional filter.



Each filter stacks upon itself with different depth of input resulting in a feature hierarchy of activation map. These activation maps generated by the filters are then stacked up in depth and fed into the next convolutional layer.

FIGURE 3. Different levels of filter stacked upon resulting in activation map.



IV. METHODOLOGY

Autoencoders said to have a unique feature exhibiting their input is more or less equal to its output by devising feed forwarding networks. Autoencoder changes the input into compressed data also called as latent space representation, which forms a low dimensional code and soon retraces the input to form the desired output with the help of CNN, after stacking layers of activation map for the respective image in volume representation in columns. After the convolutional layering, the dataset will be trained for the image colourisation. In a nutshell, the primary objective is to minimise distortion in between circuits and colourise the image that was an input from the dataset which was taken from kaggle.

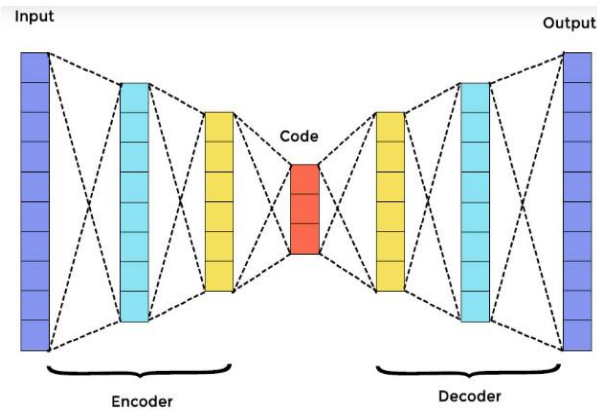
A. COMPONENTS

Autoencoders are composed of three major components, that are Encoder, Decoder and Code. Feed forwarding mesh is formed when the encoder and decoder are fully coupled. The code will be acting as a single layer with its own self dimensions. We must set a hyperparameter and the core layer constitution to construct an Autoencoder. In a more sophisticated fashion, the output network of the decoder mirrors the input encoder. Only with the assistance of the coding layer, the decoder can produce the desired result.[7]

As certain, the encoder and decoder have identical dimensional values. Size of the code, number of layers, and total number of nodes in

each layer are crucial parameters to establish when using an autoencoder.

FIGURE 4. Simplified Illustration of Autoencoders



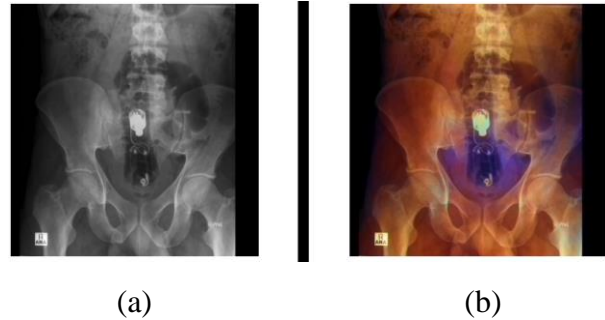
All the nodes in the middle layer determine the code size. The modest size of a middle layer is recommended for optimal compression. The autoencoder's layers can be as deep or as shallow as you like. In both the encoder and decoder, the number of nodes in the autoencoder must be the same. The decoder and encoder layers must be symmetric. In a stacked autoencoder, both the encoder and the decoder have one invisible layer. It is made up of handwritten pictures that are 28*28 inches in size. You can now create an autoencoder in the invisible layer with 128 nodes and a code size of 32. Use this function to add a large number of layers.

```
" model.add(Dense(16, activation='relu'))
```

```
model.add(Dense(8, activation='relu')) "
```

Now the input of the next layer is the added sum of output of these layers. In this dense method, this is the callable layer. The decoder performs this function which uses the sigmoid method to get output in range of 0 and 1. Since the input lies in between 0 and 1.

FIGURE 5. (a) Gray Image (b) Coloured Image



This method uses prediction to reconstruct input from an Autoencoder. The individual image test is then performed, with the output being similar but not identical to the input. The autoencoder can be made more efficient than this by adding numerous layers and multiple nodes to layers which results in overcoming these challenges. Making it more powerful, on the other hand, results in a replica of the data that is similar to input. However, this is not the expected outcome.

V. RESULTS AND DISCUSSIONS

A. Expected Outcomes

Since we are using a model, we will be getting the outcome in the console.

The expected outcome is that the web app is running to colourize the black and white image uploaded by the user.

B. Performance Evaluation

Here we have dealt with execution time, epochs, accuracy and loss. We have tried with different epochs and we could find that by increasing epochs, the results can be obtained with high accuracy and less loss. Increasing epochs can provide good colour to the black and white image.

FIGURE 6. Accuracy can be increased by increased epochs.

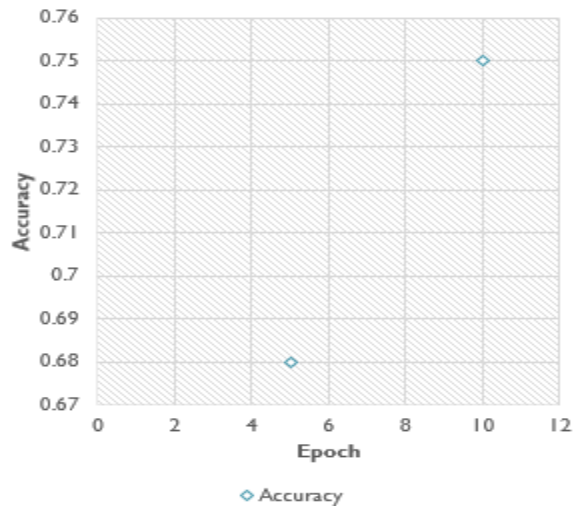
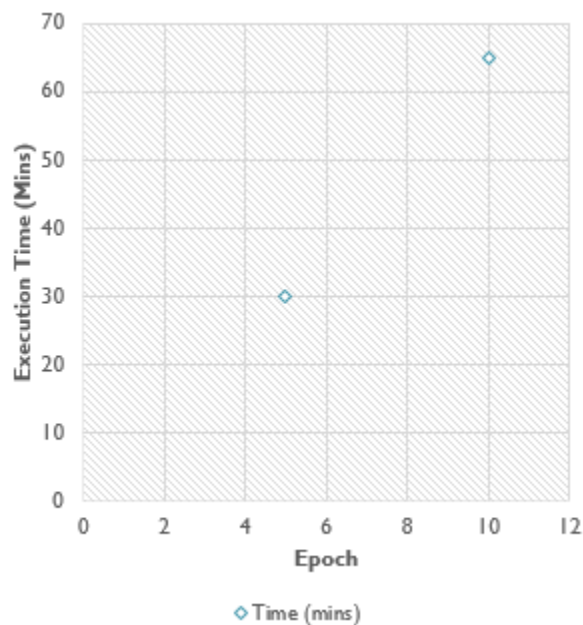


FIGURE 7. Increased epochs will lead to increased execution time.



C. Comparison with Existing Systems

Based on the analysis we found 2 results. They are as follows

Result 1: Based on this finding, every system uses a pre-trained model to train their system, which includes the caffemodel (ML model) and prototxt (a text file that holds metadata of the neural network).

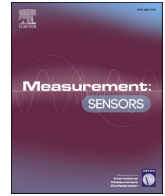
Result 2: Every system in this criteria follows a pattern of displaying the intended output in the user-specified colour, making it a colourization tool that responds to the user's request.

We used several techniques, such as auto encoders, openCV, and CNN, to train the dataset and obtain the desired output, which colourizes the input image without prompting.

References

- Nazeri, Kamyar, Eric Ng, and Mehran Ebrahimi. "Image colourization using generative adversarial networks." In International conference on articulated motion and deformable objects, pp. 85-94. Springer, Cham, 1-6 (2018).
- Hwang, Jeff, and You Zhou. "Image colorization with deep convolutional neural networks." In Stanford University, Tech. Rep.3-5 (2016).
- An, Jiancheng, Koffi Gagnon Kpeyton, and Qingnan Shi. "Grayscale images colorization with convolutional neural networks." *Soft Computing* 24, no. 7, 4751-4758 (2020)
- Abhishek Pandey, Rohit Sahay, C. Jayavardhini."Automatic Image colourization using Deep Learning",Volume-8 Issue-6, 1592-1595 (2020)
- Shankar, R. Shiva, G. Mahesh, K. V. S. S. Murthy, and D. Ravibabu. "A Novel approach for Gray Scale Image colourization using Convolutional Neural Networks." In 2020 International Conference on System, Computation, Automation and Networking (ICSCAN), pp. 1-8. IEEE, (2020).
- Simonyan, Karen, and Andrew Zisserman. "Very deep convolutional networks for large-scale image recognition." arXiv

- preprint arXiv:1409.1556 (2014).
- Levin, Anat, Dani Lischinski, and Yair Weiss. "colourization using optimization." In ACM SIGGRAPH 2004 Papers, pp. 689-694. 2004.
- Sarmai, Arshiya, and Apratim Sadhu. "Image colourization using Convolutional Autoencoders and Generative Adversarial Networks." IARJSET 9: 86-99 (2022).
- Pandey, Abhishek Thakur Sumit, and Priyanka Dusane Nidhi Sharma. "Image colourization using deep learning." Int J Scientif Res Eng Trends 5.6, 2258-2260 (2019)
- Zhang, Richard, Phillip Isola, and Alexei A. Efros. "colourful image colourization." In European conference on computer vision, pp. 649-666. Springer, Cham (2016)
- Anwar, Saeed, Muhammad Tahir, Chongyi Li, Ajmal Mian, Fahad Shahbaz Khan, and Abdul Wahab Muzaffar. "Image colourization: A survey and dataset." arXiv preprint arXiv:2008.10774 (2020).
- Zhang, Zexu, Huiyan Jiang, Jiaji Liu, and Tianyu Shi. "Improving the fidelity of CT image colourization based on pseudo-intensity model and tumour metabolism enhancement." Computers in Biology and Medicine 138 (2021): 104885.
- Litjens, Geert, Thijs Kooi, Babak Ehteshami Bejnordi, Arnaud Arindra Adiyoso Setio, Francesco Ciompi, Mohsen Ghafoorian, Jeroen Awm Van Der Laak, Bram Van Ginneken, and Clara I. Sánchez. "A survey on deep learning in medical image analysis." Medical image analysis 42, 60-88 (2017)
- Pahal, S., Sehrawat, P. Image colourization with Deep Convolutional Neural Networks. In: Hura, G., Singh, A., Siong Hoe, L. (eds) "Advances in Communication and Computational Technology". Lecture Notes in Electrical Engineering, vol 668. Springer, Singapore (2021).
- Huang, Shanshan, Xin Jin, Qian Jiang, and Li Liu. "Deep learning for image colourization: Current and future prospects." Engineering Applications of Artificial Intelligence 114 (2022): 105006.



Blink talk: A machine learning-based method for women safety using EEG and eye blink signals

K. Shanmuga Priya^{a,*}, S. Vasanthi^a, Nithyanandhan R^b, Vinoth Chakkaravarthy G^c, Golda Jeyasheeli P^d, Karthiga M^e, Pandi C^f

^a Department of EEE, University College of Engineering, Dindigul, 624709, Tamilnadu, India

^b Department of CSE, S.A Engineering College, Thiruverkadu, Chennai, 600077, Tamilnadu, India

^c Department of CSE, Velammal College of Engineering and Technology, Madurai, 625009, Tamilnadu, India

^d Department of Computer Science and Engineering, Mepco Schlenk Engineering College, Sivakasi, 626005, Tamilnadu, India

^e Department of Electronics and Communication Engineering, Bannari Amman Institute of Technology, Erode, 638401, Tamilnadu, India

^f Department of Computer Science and Engineering, Veltech MultiTech Dr.Rangarajan Dr.Sakunthala Engineering College, Avadi, 600062, Chennai, India

ARTICLE INFO

Keywords:

Women safety
Machine learning
Stacked denoising autoencoder (SDAE)
Multiclass support vector machine (MSVM)
EEG
Discrete wavelet transform

ABSTRACT

Women's safety is currently thought to be a big issue in both urban and rural settings. A variety of smart gadgets and software were created to provide women with security. There are a lot of smart gadgets and applications on the market, but they don't offer a good answer and are too expensive. In this research, a novel machine learning-based Blink Talk method has been proposed for women safety. EEG based on some blink talk algorithms for eye blink detection. Initially, the EEG and eye blink signals are pre-processed using Discrete wavelet transform (DWT). The pre-processed signals are fed into Stacked Denoising autoencoder (SDAE) for extracting the features. In the next phase, the extracted features are used to classify the emotions of women through Multiclass Support vector machine (MSVM). The classification results are sad, happy, normal, and fear; finally, fear emotion is converted into text using GSM to the saved contacts and nearby police station and GPS scan the near radius surrounding people to send the alert and help request message for the help needed person. The experimental results reveal that the suggested approach provides high accuracy range of 98.04%. then the traditional machine learning techniques.

1. Introduction

Women's safety is in danger in today's globe, particularly in India. In the twenty-first century, women have made significant contributions to society and have joined males in a variety of industries [1]. Women's crimes, such as harassment, molestation, eve-teasing, rape, kidnapping, and domestic abuse, are not decreasing, but rather increasing [2]. The government has taken many pre-emptive measures to prevent these misbehaving acts, but nothing has changed the number of crimes and they remain untouched. Currently, there are more crimes committed against women than ever before. Harassment of women occurs not only at night or during the evening, but also during the day at home, at work, and even while shopping. Women are often scared of strangers and worried about their safety. About 80% of our country's women are concerned about their safety [3].

According to survey findings, more than 370,000 incidences of

women's crime were reported in 2020, and women's crime is gradually increasing. Uttar Pradesh has 49,385 such incidents, followed by West Bengal (36,439), Rajasthan (34,535), Maharashtra (31,954), and Madhya Pradesh (31,954). (31,954). (25,640) [4]. The majority of crimes against women (30.2%) were committed by a husband or his family, followed by attacks on women with the goal of disturbing modesty (19.7%), kidnapped and abducted of women (19.0%), and rape (15.0%). (7.2%)

An electroencephalogram (EEG) is a method of measuring neuronal activity using non-stationary electric potential signals from the scalp of the brain [5]. A wide range of research has been conducted on brain-computer interfaces (BCIs) based on electroencephalograms (EEGs) for the purpose of women safety [6]. In EEG applications, efficient algorithms are becoming increasingly important for detecting and rejecting artifacts [7]. During an EEG, electrodes are put to the scalp to record the electrical activity of the brain. This approach provides high

* Corresponding author.

E-mail address: shanmuga86819481@gmail.com (K.S. Priya).

<https://doi.org/10.1016/j.measen.2023.100810>

Received 29 September 2022; Received in revised form 10 March 2023; Accepted 20 May 2023

Available online 22 May 2023

2665-9174/© 2023 Published by Elsevier Ltd. This is an open access article under the CC BY-NC-ND license (<http://creativecommons.org/licenses/by-nc-nd/4.0/>).

temporal resolution and is safe, simple, and inexpensive to employ [8]. EEG data are frequently recorded and connected to physiological and cognitive activities to better understand these processes. Wearable EEG headsets are growing in popularity among those who want to analyze their statistics on mental health, meditation, mindfulness, and sleep [9, 20].

Electrical field disturbances are very dangerous to EEG signals. Eye blinks, in particular, drastically reduce the signal-to-noise ratio (SNR) of recorded EEG readings by generating electric impulses when the retina and cornea, or the eyes and eyelids, create an electric dipole. EEG interpretations become unclear or may even be inaccurate due to eye-blink artifacts in the EEG output. Therefore, it may be helpful to identify and eliminate eye-blink components from any EEG investigation [10]. The EEG may be utilized to get physiological data such as consciousness levels, sleep phases, or simple eye blinks. The two types of Eye Blinks are reflexive Eye Blinks and deliberate Eye Blinks. The simplest response is the reflexive eye blink because it doesn't involve any cerebral structures. Intentional eye blinking, on the other hand, includes various parts of the cerebral cortex [11,12].

In the current circumstances, Women want to work and be outside, yet there is a lack of safety; many schemes, devices and techniques have been established for women safety still it has some limitations such as low-frequency noise removal, this is because of the chances of loss of data inherent in the EEG signal. So, this paper proposes ML-based methods in eye blink and EEG artifact detection for providing solutions to the women safety. When an eye blink is detected, the suggested method will activate and send the victim's information and location to the closest police station. The main contribution of our proposed technique,

- The main purpose of this study is to detect the need of paralyzed people using blink talk.
- In pre-processing stage, DWT (Discrete Wavelet Transform) is used for filtering the eye blinks in EEG signals to avoid an erroneous brain activity analysis.
- In feature extraction stage, Stack Denoising autoencoder is used to extract the reflexive Eye Blink and the intentional Eye Blink features.
- The Multiclass classification is performed by Multiclass Support Vector Machine (MSVM) for classifying the signals extracted from the features.
- The classified brain waves are converted into text and the text message is sent to the nearby police station via the GSM module.
- The proposed Machine learning-based Blink Talk method is evaluated based on its specificity, and accuracy.

The remainder of this study was organized into five sections as follows. Section 2 outlines the literature survey, Section 3 includes the proposed method named Blink talk, Section 4 comprises results and discussion and finally, Section 5 encloses with the conclusion and future enhancement.

2. Literature survey

In recent days several tools and methods were introduced by the investigators mostly to progress the women safety with EEG signal. Some of those methods are deliberate briefly in this section.

In 2018, Singh, H., Singh, J. et al. [13] presented a real-time eye blink detection method. In the experiment, blinking is detected in both controlled and natural environments. Blinks (both eyes blinking simultaneously), and left and right winks are detected by the blink detector. Eye blinks left winks, and right winks were detected with 96, 92, and 88% accuracy in this study.

Yasoda, K. et al. [14] presented a fuzzy kernel support vector machine to automatically classify WICA artifacts in 2020. The suggested technique removes EEG signal artifacts from the raw dataset automatically. The proposed technique constantly improves artifact component

detection and achieves a classification accuracy of 86.1%.

In 2021 Sivachitra, M. et al. [15] proposed Women Safety Patrolling Robotic system to ensure the women's safety. In order to patrol in its designated region with the least amount of human interaction, the suggested technique makes the best use of its characteristics, including sound sensors, ultrasonic sensors, ESP cameras, and IoT. This means that the community of women will benefit more from the proposed night patrolling robot.

In 2021 Nivedetha, B. [16], suggested approach makes the best use of its capabilities, including sound sensors, ultrasonic sensors, ESP cameras, and IoT, to patrol in its designated region with the least amount of human involvement. This means that the community of women will benefit more from the proposed night patrolling robot. The suggested system aims to protect women in society by giving them wearable technology, encouraging them to be brave in any circumstance, and leveraging the Internet of Things to convey the appropriate message in an encrypted format.

In 2021 Tayal, S. et al. [17] proposed a simple and cost-effective women's safety device design and hardware implementation using GSM, NodeMCU, and GPS modules are suggested. A push button on this safety device must be pressed by a woman in the event that she detects any risk. In this situation, GPS locates the women fast, and a GSM module sends an emergency message to contacts who have been saved, as well as to a nearby police control room. Additionally, the buzzer signals passersby to assist the women. As a result, comprehensive protection for women is guaranteed.

In 2021 Hariharan, K. et al. [18] proposed an application with a machine learning mechanism for warning and protecting female cab passengers. The software also has extra features like real-time location monitoring and incorrect route prediction. The advantage of this application is that it has an auto mode for use in emergency scenarios. Three machine learning models have also been tried, and the SVM classifier performs the best with our dataset, with an accuracy of 89.5%.

In 2021 Gomathy, C.K. and Geetha, M.S [19] have proposed an Arduino-powered wearable safety gadget for women. This device is meant to protect ladies in case they encounter any threat. To communicate with other devices and provide alerts to them, the device employs wireless sensor networks. The user's location is shared immediately with the appropriate authorities and stored contacts via GPS and GSM. The proposed method enables many users to manage device functionality, and the switch's built-in authentication feature speeds up fault detection and correction.

Various technologies and techniques were focused on women's safety with EEG signals according to the research review. Our proposed machine learning-based Blink Talk method improves accuracy and reduces the computational cost.

3. Proposed methodology

The proposed machine learning-based Blink talk method aims to bring out a solution for Women's safety without any outward or internal harm to their bodies Due to the fact that none of the components come into close contact with the women, the proposed blink talk model is significantly safer and costs less than earlier models shown in Fig. 1.

3.1. Data acquisition

A peaceful setting, ten participants between the ages of 21 and 31 provided the raw EEG data and eye blinks. During one session, 6 to 8 trials of 20 s each of EEG signals were recorded. The volunteer was required to blink 8 to 12 times during each trial. recorded the EEG signals of women in two sessions separated by more than two weeks, whereas the signals of the other women were recorded in one session. MATLAB was used to process the EEG data from the Neurosky headgear.

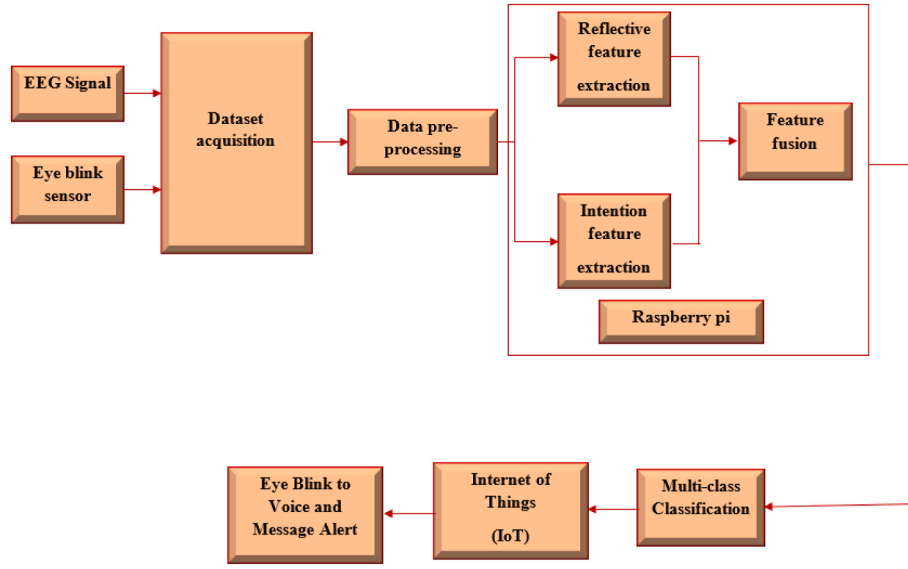


Fig. 1. The overall workflow of the proposed Blink Talk method.

3.2. Data pre-processing

For time-frequency analysis, wavelet transforms are employed. It is a technique for data transformation that divides the data into several frequency components and analyses each component according to its resolution at that scale. Non-stationary signals include EEG signals. In the study, DWT was used to split the collected EEG signals into their frequency components, and properties of the frequency bands at the decomposition levels were retrieved. The discrete values of dilation and translation are represented by the parameters A and B in the discrete wavelet transform. It is usual to practice discretizing the dilation factor A using a logarithmic scale in order to link it to B by making B proportional to A. Therefore, the normalized wavelet function can be discretized as follows,

$$\varphi(x, y) = \frac{1}{A_0^x} \varphi\left(\frac{T - yB_0A_0^x}{A_0^x}\right) \quad (1)$$

which is the result by taking $A = A_0^x$, and $B = yB_0A_0^x$, respectively, the

integers x, y translation, regulate dilation, respectively. A_0 is the fixed dilation phase that is larger than 1. B_0 is the location parameter that is larger than 0.

3.3. Feature extraction

The pre-processed signals' redundant and irrelevant data are removed at the crucial phase of feature extraction. The stacked autoencoder is a multi-autoencoder ANN design that is taught using a greedy layer-wise training technique. Each autoencoder is made up of a middle layer, an output layer, and an input layer. The following autoencoder of the layered autoencoder shown in Fig. 2 receives input from a middle layer output.

The stacking autoencoder is extended by the SDAE. SDAE's input signals are tainted by noise. To decode and recover the blurred original input $G P = \{p_1, p_2, \dots, p_n\}$. These distorted input signals are transferred using a sigmoid function to a hidden layer with units as,

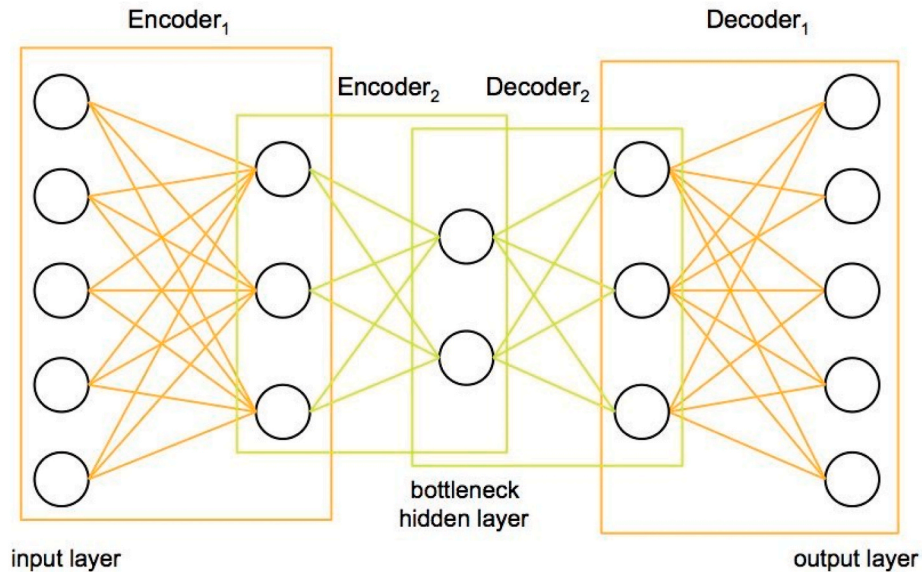


Fig. 2. Structure of stacked denoising autoencoder (SDAE).

$$S = f_{1,\theta}(P_1) = z(WP_1 + b) \quad (2)$$

$$p(u) = \frac{1}{1 + e^{-u^2}} \quad (3)$$

where W , q , and f represent the weight matrices, bias, and activation function of the encoder on the first autoencoder, and S represents the signal on the middle layer of the first autoencoder, respectively. The weight and bias matrices are chosen at random during initialization. The uncorrupted input $Q = \{q_1, q_2, \dots, q_n\}$ the estimation of P , can be reconstructed by the decoder of the first autoencoder as,

$$Y = g_{2,\theta}(Z_1) = z(S'Q_1 + b') \quad (4)$$

where S' , b' , and g are the weight matrices, bias, and nonlinear function of the decoder for the first autoencoder, respectively. To make the feature vectors of the signals produced by the autoencoder smaller, statistical characteristics are added to the set of wavelet coefficients.

3.4. Feature fusion

Feature concatenation is a crucial step in the domain of eye blink pattern recognition. The various feature vectors are sequentially fused to build a finalized feature vector for eye blink detection. The main rationale for conducting this step is to consolidate all descriptor data into a single feature vectors column, which can be effective in reducing the error rates. The structural and geometric features are extracted by the SDAE by eliminating the irrelevant features of the input image as feature set 1 and 2. Then the fusion selection method selects the relevant or particular features from extracted features and these features are fused for the classification process.

3.5. Multi-class classification

A support vector machine (SVM) is an important supervised learning approach and a useful technique for data classification. SVM identifies binary classes by locating and employing a hyperplane class border that maximizes the margin in the training dataset. The support vectors are the training data samples that flow along hyper planes at the class border, and the margins are the gap between both the support vectors and the class border hyperplanes. Binary classification is done by SVM, which can distinguish between two classes. Multiclass classification is not natively supported by SVM. It makes binary categorization and dividing data points into two classes easier. The similar approach is used for multiclass classification after breaking the issue down into several binary classification problems.

3.6. Eye blink to voice and message alert

The research study's final module is this one. One of Python's modules, "imutils," has a dictionary of face landmarks. contains points for the right and left eyes, respectively, which can be used to access the eyes. The eye aspect ratio (EAR) value has been utilized to identify blinks in real time. Calculating and averaging the EAR of each eye's blinking results in the EAR of both eyes blinking. When the eye is shut, the EAR value steadily approaches 0. The face is detected and the blink detection system records the eye blinking.

Algorithm. Eye Blink Detection Algorithm

1. Point feature extraction.
2. Eye aspect ratio (EAR) calculation.
3. Calculation of time duration.
4. Based on the duration of eye blink the input is considered as dot or dash.
5. Dot-Dash sequence measure code is converted into normal text.
6. Dot - Dash sequence is stored in an array.
7. This sequence is converted into the respective letter.

The eye blinks are recognized using the EAR formula following the eye detection from the face. Now, the voice will be created from the eye blink. Blinks from that initial eye must be noticed. When the eyes are open, the EAR is constant; when they close, it becomes 0. Therefore, the colour red is used to represent an open eye, while the colour green is used to represent a closed eye. The eye-aspect ratio is,

$$EAR = \frac{||v_2 - v_6|| + ||v_3 - v_5||}{2||v_1 - v_4||} \quad (5)$$

Where v_1, v_2, v_3, v_4, v_5 and v_6 landmarks on eye with (x,y) coordinates. Each number on the virtual keys represents a specific requirement for the people who are paralyzed. Durations of single and double eye blinks are not constrained. Like when using the Morse Alphabet, respondents were requested to leave a little waiting period at the end of each letter as they entered words using their eyes only. In-letter space is the term for this brief pause in the letters. On the other hand, individuals chose for themselves the length of time between a single and double eye blink. However, this period's length must be shorter than the one that follows each letter. The system's only constraint during data entering is this.

In order to take Fig. 3's blink detection action, the woman must keep her eyes closed for a duration of between one and 5 s. Eye aspect ratio is estimated based on which voluntary and involuntary blinks are differentiated. If any voluntary blinks are detected, count of the blinks is used to identify the emotions. Then, the fear emotion is converted into via voice call and text message is sent by the GSM module about task given for particular count of blinks. To turn the blink into voice, a GMS module included from the dlib library converts the speech into a text message and sends it to the nearby police station.

4. Results and discussions

The experimental design for the research was put into practise using the machine learning toolkit MATLAB 2019b. In this result analysis, the EEG signals were used for detecting eye blinking for classifying the emotions of women.

4.1. Performance analysis

In this research the performance evaluation of the proposed Blink talk based on machine learning is calculated based on specificity, accuracy and sensitivity.

$$spe = \frac{tn}{tn + fp} \quad (6)$$

$$sen = \frac{tp}{tp + fn} \quad (7)$$

$$acc = \frac{tp + tn}{total\ no.of\ samples} \quad (8)$$

False positives and negatives are referred to as fp and fn, respectively, in place of true positives and true negatives of the samples, tp and tn, respectively.

In this proposed study, a testing methodology is used to classify the emotions of the women for their safety. From Table 1, it is clear that the

















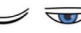
























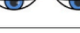












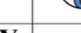
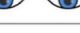


























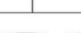










Eye's blink < 0.6 sec. = Dot = .		Eye's blink > 0.6 sec. = Dash = -	
			
A	 	N	 
B	   	O	   
C	   	P	   
D	  	Q	   
E		R	  
F	   	S	  
H	   	T	
I	 	U	  
J	   	V	   
K	  	W	  
L	   	X	   
M	 	Y	   
Z	   	.	    
Space			     

Fig. 3. Morse code of eye blink.

Table 1
Performance analysis of MSVM with SVM.

Models	SVM	MSVM
Testing accuracy	92.58	98.04
Training accuracy	94.29	97.85

suggested MSVM classifiers performs better than the traditional SVM. Utilizing the metrics of specificity, sensitivity, and accuracy, the effectiveness of the suggested model was assessed. The testing accuracy is determined based on the raw dataset and testing accuracy is taken from the real time signals as input is given in Fig. 4. Further, training and testing loss is also evaluated based on the epochs is shown in Fig. 5 for

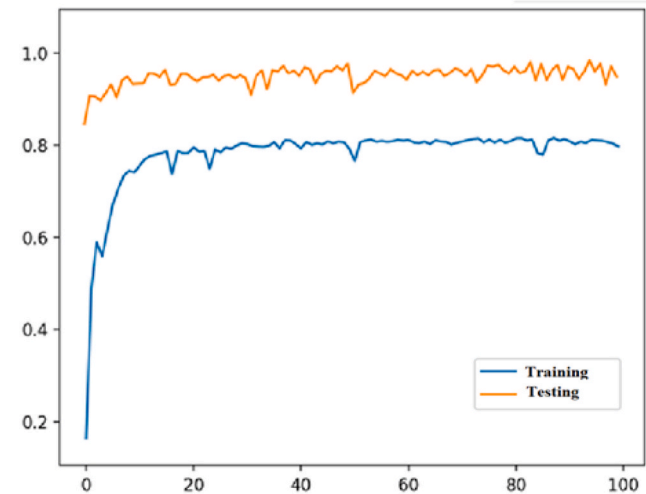


Fig. 4. Training and testing accuracy of the proposed method.

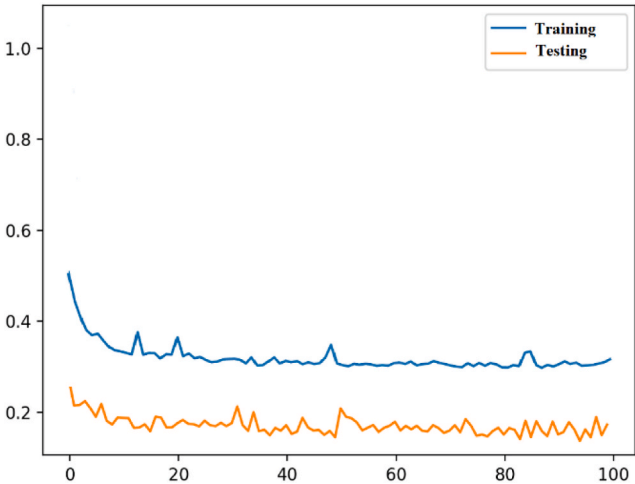


Fig. 5. Training and testing loss of the proposed method.

multiclass SVM. This lower loss rate could lead to a higher accuracy.

4.2. Comparative analysis

Each ML classifier's performance was evaluated to demonstrate how much more effective the outcome of the suggested method is. The sensitivity, specificity, and accuracy of each classifier are used to determine the classification, and the MSVM classifier achieved an accuracy of 98.04%. The Stacked Denoising Auto-encoder and Multi-class SVM classifier integration produces a classification accuracy rate that is higher than that of the existing models. The four conventional machine learning classifiers, including SVM, RF, NB, and KNN's suggested MSVM model, are compared.

Table 2 shows the comparative performance of each classifier, and

Table 2
Comparative analysis of ML classifiers.

Classifiers	Accuracy	Sensitivity	Specificity
KNN	85.25	83.69	84.28
NB	91.23	92.54	93.25
RF	92.59	90.25	89.63
SVM	94.29	91.85	90.65
MSVM	98.04	96.25	96.48

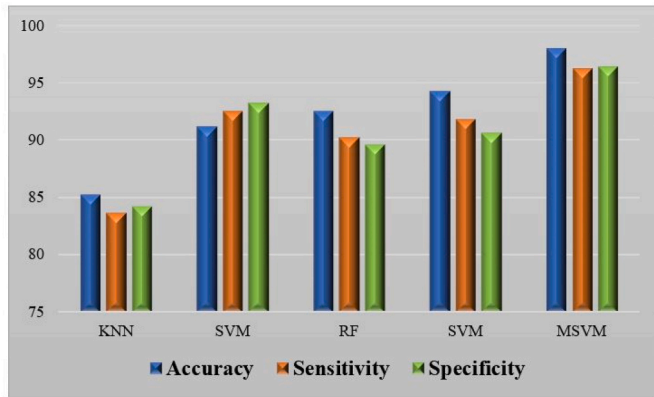


Fig. 6. Graphical comparison of machine learning classifiers.

Fig. 6 shows a graphical comparison. Table 3 shows the relative effectiveness of each ML technique, and Fig. 7 shows a graphical comparison.

Table 2 displays the results of a comparison between the proposed SDAE model and the four conventional ML feature extraction techniques (PCA, LDA, GLCM, and AE). From the above comparison the SDAE yields higher accuracy than the existing models.

5. Conclusion

In this research, a novel ML based Blink Talk technique has been proposed for women safety. EEG based on some blink talk algorithms for eye blink detection. Initially, the EEG and eye blink signals are pre-processed using Discrete wavelet transform (DWT). The pre-processed signals are fed into Stacked Denoising autoencoder (SDAE) for extracting the features. The next stage uses the extracted features to categorize the emotions of women using a multiclass SVM. The classification results are sad, happy, normal, and fear; finally, fear emotion is converted into text using GSM to the saved contacts and nearby police station and GPS scan the near radius surrounding people send the alert and help request message for the help needed person. The experimental findings show that the suggested approach offers high accuracy within a 98.04% range than the traditional machine learning techniques. The suggested classification model will be built to accurately anticipate the different emotions in the future using deep learning techniques.

CRediT authorship contribution statement

K. Shanmuga Priya: Conception and design of study, Drafting the manuscript, Approval of the version of the manuscript to be published. **S. Vasanthi:** Acquisition of data, Revising the manuscript critically for important intellectual content, Approval of the version of the manuscript to be published. **Nithyanandhan R:** Formal analysis, Analysis and/or interpretation of data, Approval of the version of the manuscript to be published. **Vinoth Chakkaravarthy G:** Formal analysis, Analysis and/or interpretation of data, Approval of the version of the manuscript to be published. **Golda Jeyasheeli P:** Approval of the version of the manuscript to be published. **Karthiga M:** Drafting the manuscript, Approval of the version of the manuscript to be published. **Pandi C:**

Table 3
Comparative analysis of ML feature extractors.

Models	Accuracy	Sensitivity	Specificity
PCA	84.53	83.89	80.77
LDA	92.05	90.25	91.68
GLCM	93.85	89.32	91.89
AE	95.06	92.52	93.26
SDAE	98.04	95.28	95.45

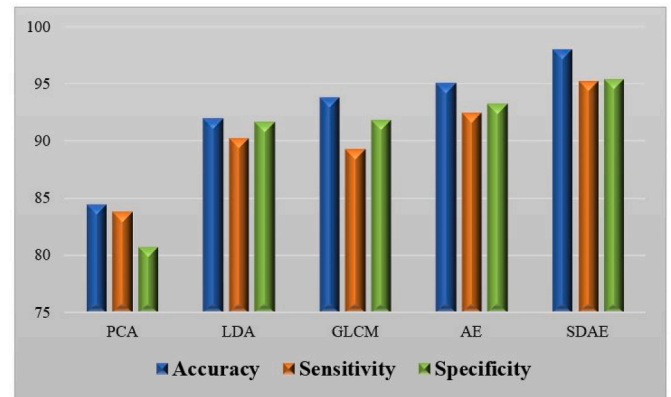


Fig. 7. Graphical comparison of machine learning techniques.

Revising the manuscript critically for important intellectual content, Approval of the version of the manuscript to be published.

Declaration of competing interest

No conflict of interest exists between authors to publish this paper.

Data availability

The data that has been used is confidential.

References

- [1] B. Sathyasri, U.J. Vidhya, G.J. Sree, T. Pratheeba, K. Ragapriya, Design and implementation of women safety system based on Iot technology, *Int. J. Recent Technol. Eng.* 7 (6S3) (2019).
- [2] B.S. Bala, M. Swetha, M. Tamilarasi, D. Vinodha, Survey on women safety using IOT, *International Journal of Computer Engineering in Research Trends* 5 (2) (2018) 16–24.
- [3] A. Mojahed, N. Alaidarous, H. Shabta, J. Hegewald, S. Garthus-Niegel, Intimate partner violence against women in the Arab countries: a systematic review of risk factors, *Trauma Violence Abuse* 23 (2) (2022) 390–407.
- [4] D.K. Tran, T.H. Nguyen, T.N. Nguyen, Detection of EEG-based eye-blinks using a thresholding algorithm, *European Journal of Engineering and Technology Research* 6 (4) (2021) 6–12.
- [5] A. Palumbo, N. Ielpo, B. Calabrese, An FPGA-embedded brain-computer interface system to support individual autonomy in locked-in individuals, *Sensors* 22 (1) (2022) 318.
- [6] S. Zhu, T. Yu, T. Xu, H. Chen, S. Dustdar, S. Gigan, D. Gunduz, E. Hossain, Y. Jin, F. Lin, B. Liu, Intelligent Computing: the Latest Advances, Challenges and Future, 2022 arXiv preprint arXiv:2211.11281.
- [7] J. Cao, L. Chen, D. Hu, F. Dong, T. Jiang, W. Gao, F. Gao, Unsupervised eye blink artifact detection from EEG with Gaussian mixture model, *IEEE Journal of Biomedical and Health Informatics* 25 (8) (2021) 2895–2905.
- [8] M. Agarwal, R. Sivakumar, Blink: a fully automated unsupervised algorithm for eye-blink detection in eeg signals, in: 2019 57th Annual Allerton Conference on Communication, Control, and Computing (Allerton), IEEE, 2019, September, pp. 1113–1121.
- [9] D. Hu, J. Cao, X. Lai, J. Liu, S. Wang, Y. Ding, Epileptic signal classification based on synthetic minority oversampling and blending algorithm, *IEEE Transactions on Cognitive and Developmental Systems* 13 (2) (2020) 368–382.
- [10] C.R. Rashmi, C.P. Shantala, EEG artifacts detection and removal techniques for brain computer interface applications: a systematic review, *International Journal of Advanced Technology and Engineering Exploration* 9 (88) (2022) 354.
- [11] R. Akhter, F. Ahmad, F.R. Beyette, Automated detection of ERP artifacts of auditory oddball paradigm by unsupervised machine learning algorithm, in: 2022 IEEE

- Conference on Computational Intelligence in Bioinformatics and Computational Biology (CIBCB), IEEE, 2022, August, pp. 1–8.
- [12] A. Boudaya, S. Chaabene, B. Bouaziz, H. Batatia, H. Zouari, S.B. Jemea, L. Chaari, A convolutional neural network for artifacts detection in EEG data, in: Proceedings of International Conference on Information Technology and Applications, Springer, Singapore, 2022, pp. 3–13.
- [13] H. Singh, J. Singh, Real-time eye blink and wink detection for object selection in HCI systems, *Journal on Multimodal User Interfaces* 12 (1) (2018) 55–65.
- [14] K. Yasoda, R.S. Ponmagal, K.S. Bhuvaneshwari, K. Venkatachalam, Automatic detection and classification of EEG artifacts using fuzzy kernel SVM and wavelet ICA (WICA), *Soft Comput.* 24 (21) (2020) 16011–16019.
- [15] M. Sivachitra, T. NaveenRaj, V.G. Rekhasri, N. Sowmiyaa, Women safety night patrolling robot, *Annals of the Romanian Society for Cell Biology* (2021) 15706–15714.
- [16] B. Nivedetha, Wearable device for women safety using IOT, *JAC (J. Antimicrob. Chemother.): A Journal of Composition Theory* 14 (6) (2021) 94–97.
- [17] S. Tayal, H.P.G. Rao, A. Gupta, A. Choudhary, Women safety system design and hardware implementation, in: 2021 9th International Conference on Reliability, Infocom Technologies And Optimization (Trends And Future Directions) (ICRITO), IEEE, 2021, September, pp. 1–3.
- [18] K. Hariharan, R.R. Jain, A. Prasad, M. Sharma, P. Yadav, S.S. Poorna, K. Anuraj, A comprehensive study toward women safety using machine learning along with android app development, in: Sustainable Communication Networks and Application, Springer, Singapore, 2021, pp. 321–330.
- [19] C.K. Gomathy, M.S. Geetha, Women safety device using Iot, *International Journal of Scientific Research in Engineering and Management (IJSREM)* 5 (10) (2021) 1–9.
- [20] M. Wang, J. Wang, X. Cui, T. Wang, T. Jiang, F. Gao, J. Cao, Multidimensional feature optimization based eye blink detection under epileptiform discharges, *IEEE Trans. Neural Syst. Rehabil. Eng.* 30 (2022) 905–914.

An Enhanced Routing and Lifetime Performance for Industrial Wireless Sensor Networks

J. V. Anchitalagammai^{1,*}, K. Muthumayil², D. Kamalraj Subramaniam³, Rajesh Verma⁴,
P. Muralikrishnan⁵ and G. Visalaxi⁶

¹Department of Computer Science and Engineering, Velammal College Engineering and Technology, Madurai, 625009, India

²Department of IT, PSNA College of Engineering and Technology, Dindigul, 624622, India

³Department of ECE, Karpagam Academy of Higher Education, Coimbatore, India

⁴Electrical Engineering Department, King Khalid University, Abha, 62529, Saudi Arabia

⁵Department of ECE, K.Ramakrishnan College of Engineering, Tiruchirappalli, 621112, India

⁶Department of Computer Science and Engineering, Bharath Institute of Higher Education and Research, Chennai, 600073

*Corresponding Author: J. V. Anchitalagammai. Email: anchitalagammaiphd@gmail.com

Received: 15 June 2021; Accepted: 16 July 2021

Abstract: Industrial Wireless Sensor Networks (IWSNs), especially energy resources, are scarce. Since sensor nodes are usually very dense, and the data sampled by the sensor nodes have high redundancy, data aggregation saves energy, reduces the number of transmissions, and eliminates redundancy. Many applications can be used in IWSNs, and a new technique is introduced to detect multiple sensors embedded in different sensor nodes. Packets created by different applications have different properties. Sensors are resource-constrained devices because it is necessary to find effective reaction analysis methods and transfer sensed data to base stations. Since sensors are resource-constrained devices, efficient topologies require data distribution from base stations for management, aggregation, and cloud services in the business tier. To propose a Distributed time series Convergence Routing Protocol (DTSCR) is introduced to detect the correct relay node from the source sensors and transmit the data with the data aggregation node help of the eDCP (Edge Data Collection Protocol). The node will send data to the target source only when those in the process transmit the data, and the cutting edge of the terminal generates a trusted merger. This method can provide a reliable and efficient routing path scheme for information collection and dissemination with maximized packets exchanged between nodes and their Neighbor. Recognizes a specific set of sensor network applications to be flexible to this measurable range. We are also improving the DTSCR roaming with both network size and node density.

Keywords: Distributed time series routing protocol; edge data collection protocol; industrial WSN

1 Introduction

Wireless sensor networks are used in a variety of fields, from environmental monitoring to sniper localization. Wireless components' easy installation and reduced installation costs are the main reasons to



This work is licensed under a Creative Commons Attribution 4.0 International License, which permits unrestricted use, distribution, and reproduction in any medium, provided the original work is properly cited.

consider wireless solutions for industrial applications. This has led to the increased popularity in the industry, especially for companies interested in automating industrial processes. Wireless Sensor Network (WSN) is a low-power wireless fine dust deep, low-power wireless dust detection with high-resolution CPU and memory, and networking system with environment and major partner network strategies. The advantage of wireless sensor networks is their flexibility and scalability. It is self-contained, and the wireless communication capacity characteristics allow sensor nodes to be deployed in WSN mode without the existing infrastructure in remote and hazardous locations. Wireless sensor nodes communicate directly with other nodes in their vicinity and reach remote nodes *via* multi-hop communication. It has very limited resources with limited power, bandwidth, processing power, storage, and computing power. Therefore, when a fault occurs, the sensor node is mainly inoperable and irreplaceable due to energy consumption. Improving the sustainable development and longevity of the network is a key issue in modern research sensors. Power consumption is usually dominated by advanced wireless transmission. The exhaustion of radio communication energy is directly related to any transmission on the network. Reduce wireless transmission and increase the number of life-cycle clustering technologies for sensor networks. As a result, the technology effectively coordinated pots, various sensor applications, robot control, environmental control, offices, smart homes, the production environment, the human body communication, and sensor networks are added, such as underwater lived. The main source of energy use is data communication modules. Transmission and acquisition controls that devote part of the information consumption measure more energy. Power usage measurement is mainly two basic parameters; the amount of information sent, the communication range is used for the transmission. Conversely, suppose the increase in the amount of information is an additional increment over the cost of transmitting the information. It is used for communication to minimize the information, so the communication cost is also reduced. In the rest of the paper, Section 2 describes the related work, Section 3 describes the proposed Equations and Mathematical Expressions, Section 4 describes the result and discussion. Finally, Section 5 describes the conclusion.

2 Related Work

Wireless sensor networks to detect indoor and industrial environments, avoid obstacles with obstacles and include three-dimensional rangefinders for moving static and dynamic obstacle micro-flying robots. It is only necessary to track the controller of the micro-flying robot. There are no complicated calculations for micro-flying robots in the path [1]. But for industrial wireless sensor networks, it can guarantee the reliability, so it is a useful task in low-power communication and harsh wireless environments. The first QoS framework [2] provides a hybrid wired/wireless network that guarantees that any waiting time can be combined and target reliability for each application.

The central fusion method requires communication and high-bandwidth computing of the processor fast and is not robust due to a single failure point. The identification in this document is to estimate the parameters of the space-time Volterra model in the network using the data distribution system to remove these limitations. A large amount of data can be processed by assigning FC processing tasks to wireless sensor network nodes [3]. Prototypes made from industrial production workshops provide high-reliability and reliable wireless sensing with low application failure rates for measurement, thus providing more confidence for industrial automation to realize what you can do during operation [4]. Based on these characteristics, the risk analysis of industrial activities is based on real-time algorithms, and a large amount of data is collected from within the wireless sensor network. The algorithm allows the sensor node to the screen to receive signal strength indications and remaining energy information based on the established risk analysis in this clustering data transmission structure based on the data collected by the environment or equipment [5].

An optimal delay control scheme based on the channel's transfer delay can reduce the total time spent on the sensor nodes by solving the common wireless channel function. Specifically, channel degradation has been described by examining the probability density function of the received signal level across the speed of the first industrial radio environment [6]. The key hybrid industrial system presents a comprehensive demand/supply function analysis based on its first organizational method. Also, consider routing and routing graphical signal sources. If the system is in low critical mode, first, the source route considers each flow schedule in [7]. Clustering and routing are then grouped for a detailed analysis of the relationship between large wireless sensor networks used for routing protocols for reliable and efficient data collection. The node is connected to the maximum transmission distance constraint [8] and uses a route backoff timer and gradient to produce an effective inter-cluster topology. However, the formation of clusters is the overhead of the cluster head in this algorithm's process. To solve this problem, wireless sensor networks, many researchers have come up with the idea to make decisions using fuzzy logic. These guidelines [9] can improve the network lifetime, and to balance the load on the sensor nodes can be adaptively CH flexible.

An improved hierarchical clustering method has been proposed to achieve wireless sensor networks' energy efficiency using overlapping and adjacent nodes in the sleep-wake mechanism. This minimizes data redundancy, which in turn maximizes network life. Compared to previous hierarchical routing protocols, which require all nodes to collect and send data, this method only occurs when the energy consumption WSN critically performs these tasks [10]. The priority table is formed by prioritizing the two shortest paths to CH or sink according to some simple and efficient rules. The rule is to use some routing metrics, such as range/power and remaining energy. Simulation results show that the proposed routing protocol can also be integrated with more WSN [11] clustering algorithms. The cluster head (CH) is selected based on energy, reliability, signal-to-interference plus noise ratio, and load residual parameters. Intra-cluster routing is then done using a probabilistic routing method based on network coding. A fuzzy-based clustering protocol helps determine the participating cooperative nodes (CNs) in a cluster [12]. The condition for the cluster formation is that d-CPCCA does not fail to address the main components in any cluster. SODCC is extensible and has the same or more complexity than other well-known SOA (Self-organizing algorithms) information [13].

A new method for analyzing regional energy awareness clustering using individual nodes and regional energy awareness clustering is wireless network energy. The head of the cluster is selected based on weights. The weight is determined based on each sensor's remaining energy and the average energy of all sensors in each group. Improperly designed distributed pool algorithms will continue to separate nodes from the channel. Such separated nodes communicate through excessive power consumption [14] sinks. The attenuation model and the chamber model describe changes in the signal power from the propagation distance and the opportunity. To minimize energy consumption, the Taylor series expansion in the compartment model [15] is used to calculate the optimal number of clusters for different orders.

3 Equations and Mathematical Expressions

The proposed Distributed Time Series Convergence Routing Protocol (DTSCR) low packet transmission, while establishing the connection will be provided with the effective data collection is implemented with the intention of WSN. This industrial wireless sensor network collects sensing data to send to base stations from the industrial environment with sink nodes' help. Trust the collected sensor node data to send Edge Data Collection Protocol (EDCP) help. This proposal is made at WSN by improving the aggregation rate by forming an intra-network, efficient data delivery to DTSCR. The proposed implementation of link quality is based on low packet loss, transmission speed, throughput performance.

The proposed method block diagram is shown in Fig. 1. The problem associated with the maximum number of shortest paths has not been considered to solve the network by using Bidirectional Topological Sort (DTS) to improve the throughput and reduce the energy consumption of data collection, and the network improves the life.

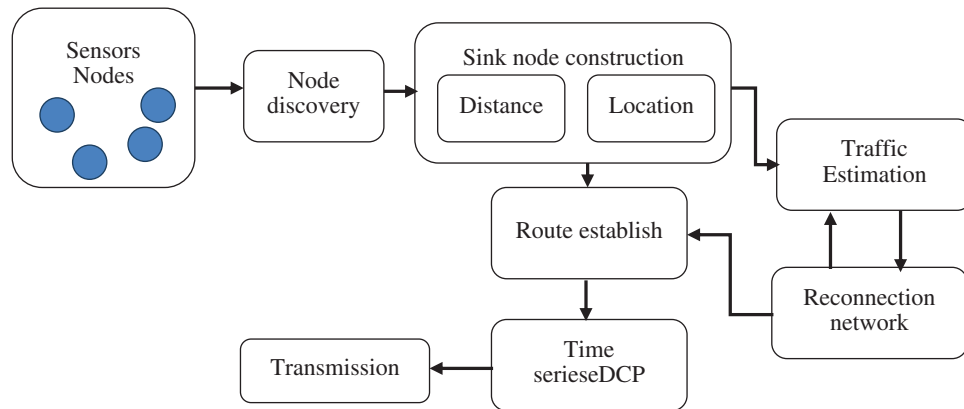


Figure 1: Proposed method block diagram

3.1 Edge Sink Node Construction

When the sensor collects data from different corners of the tank is to WSN. Only energy resources decreased absorption path length. Therefore, it isn't easy to gain access to the network to reach all the sensor nodes. The mobile receiving systems search to meet the navigator's controls in a specific way and create an environment with the maximum number of nodes at the entrance edge. A collection point (CP) is considered to be each cluster at any physical location within it. The central point of each sink in DEPC is assumed to be the CP of the sink node. After this, data collection will be completed through this CPS to improve the network's life cycle.

Algorithm steps

Step 1: Topological sort (Vertex l , node n) and graph g

Location $n(x, y)$ where the node positions x as a vertical and y is horizontal in the network.

Step 2: identify the node edge point add it to the routing table as

For ($i = l.start()$; $i \neq l.end$; $l++$)

If ($l.visit[n(i)]$)

Add (l, g), stack(l).

End

For ($i = 0$; $i < l$; $i++$)

If ($visit(n) == false$)

$r.add(n(i))$

End

Step 3: Finally, unitized silk node and sorted node in network added to the routing table.

After this, the sensor node responds with the requested data along the original path. In this process, to achieve in eDCP using a bidirectional Topological Sort algorithm to find the best path and collect the data each sink in an industrial network.

3.2 Traffic and Reconnection

The proposed TRSP method is suitable for reconnecting network structures separated from their larger sensor element groups. By using this network structure to connect, efficient data collection is completed from the sensor network. The data collection process is shown in Fig. 2. It is placed at the separation node's exact location to realize the reconfiguration process of the transportation network structure. In this method, the distance measurement of the sink node and the center average point analysis method are split into two parts, as shown in Fig. 3. First, the gap of affected nodes in transportation networks was measured using time-based traffic estimation. Let us consider the edge of the sensor network as 'I' and node position vertex as 'the integers value points are 'X' and 'Y'.

$$\text{Sink node position} = \sum_{i=1}^e \text{Dir}(v(i)) \quad (1)$$

Algorithm steps

Step 1 initialize the network node vertex as v and node as n and variable x, y.

Step 2: identify the node position in the network area using Eq. (1).

Step 3: compute the distance point into the sink node

$$\text{distances} = \sum_{i=1, j=i+1}^n \text{dis}(\text{root}, n(i, j)) \quad (2)$$

Step 4: participate node list add to the routing table following Edge sink node construction algorithm steps.

Step 5: establish the center point on the network and route between the two nodes.

The sensor network is separated from the network by multiple sensor nodes whose nodes do not participate in the network operation partition. Where Eq. (1) estimates the sink node direction and position in the network.

3.3 Time Series Edge Data Collection

The sensors in a particular cluster node are time series adhesives. Therefore, it is very likely that collecting and sharing data about one's own future commemorative events are the same. Spatially correlated observation measurements are used to provide WSN time-series data at intervals between sensor nodes. Let us consider the nodes, N1, N2, N3, where the sensor records similar time-series observations in the past.

$$b \rightarrow \text{collection}(\text{time}(n1, n2, n3)) \quad (3)$$

The data collection process is shown in Fig. 4 from Eq. (3), the sensors are N1 and N2, and the observation (b) is based on N3, the nodes observed in the same time series.

Algorithm steps

Begin initialize the network nodes and sink node sn

For each n to sn

Estimate the collection observation time using Eq. (3).

The observation data transmit to the Access point of the base station.

The actives are store in the routing table.

End

In this method group, a dynamic sensor node uses this time correlation. A node in the sensor's immersion step also has a strong chronological correlation similar to observations.

4 Result and Discussion

The purpose of our simulation is to observe the appearance of wireless networks. The iterative environment is designed using NS-2 (C++ language algorithm) and is used as a semantic tool for command languages. It leads the allowance for the Advanced Tools Command Language (TCL). The proposed method is performed using a simulation of all networks, after which all code is written into a TCL script. According to the simulation result, the given output simulation result is taken.

Table 1: Simulation parameters of the proposed method

Parameter	Value
Number of nodes	100
Packet size	512 kb
Data size	40 mb
Number of packets	80
Routing protocol	DTSCR, AODV

Above [Tab. 1](#) this shows that it is an IoT cloud performance evaluation using the simulation parameters of the proposed method. This section analyzes the routing performance, throughput analysis and time complexity of data packets, which we are discussing.

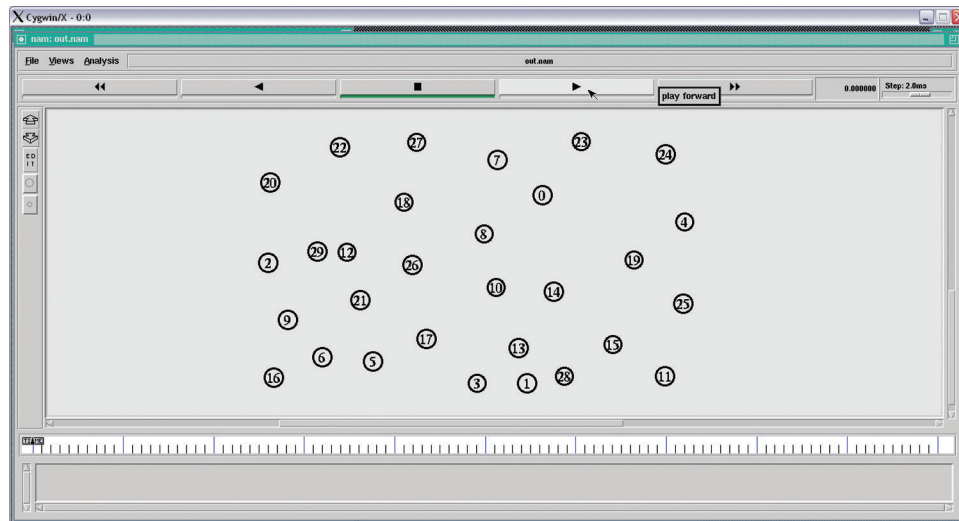


Figure 2: Network initialization process

These industrial sensor node points are shown in [Fig. 3](#) for the process with the network. It node is created in windows with the help of geometrical x and y-axis points.

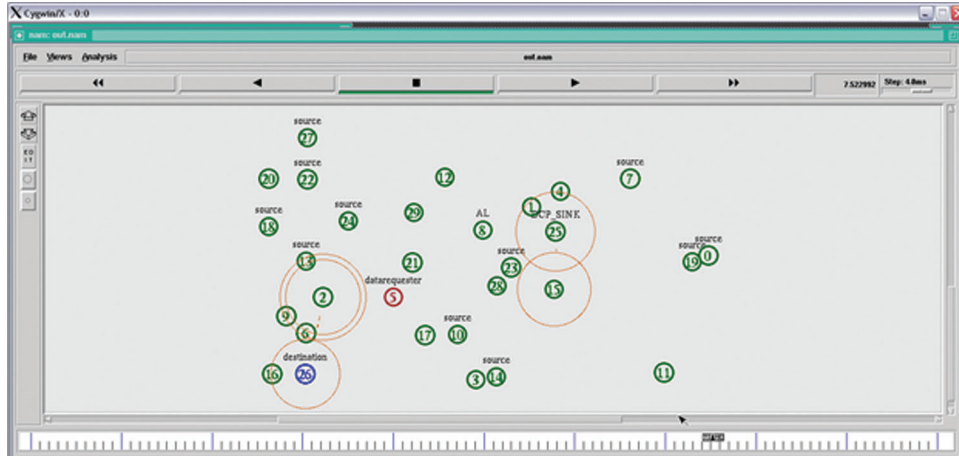


Figure 3: Data collection process

Fig. 3 shows the collecting of the data from sink nodes with the help of DCP sinks. The proposed method Distributed time series Convergence Routing Protocol (DTSCR) compare to the existing method Distributed Graph Routing Algorithm (DGR) and Q-learning reliable routing (QLRR) are analyzed.

$$\text{packet delivery ratio} = \frac{\text{number of the packet received}}{\text{several packet send}} \quad (4)$$

According to the analysis in Fig. 4, the proposed method DTSCR is compared with the existing method QLRR and the data packet transfer ratio DGR. The results show that compared with the existing method DGR, this method has a 93.4% higher data packet transfer rate than 85.7%. Data packet delivery. Provide 91.2%.

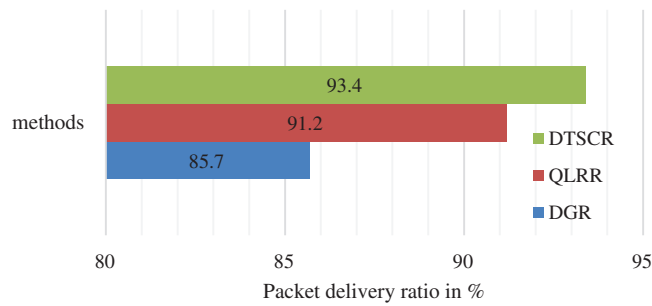


Figure 4: Average packet delivery ratio

This is to obtain the total amount of data received in the last packet, defined as the source from the destination packet divided by 1000. Throughput is the number of bits transferred per second.

$$\text{Throughput} = \text{packet size} * \text{recv.packet} * 8.0 / 1000 \quad (5)$$

Fig. 5 shows the experimental results of the comparison of Throughput Analysis of existing method DGR, QLRR, proposed method DTSCR, against the 1800 kbps of 200 s. Similarly, the existing method, DGR, QLRR method, has 845 kbps, 934 kbps for 200 s.

$$\text{End to End Delay} = \frac{\text{Arrival time} - \text{Sent time}}{\text{Total number of connections}} \quad (6)$$

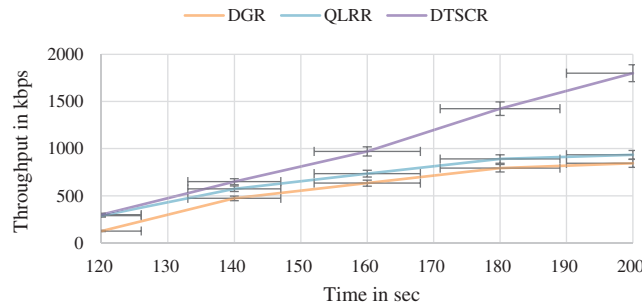


Figure 5: Comparison of throughput analysis

Fig. 6 shows the comparison of the proposed method and the existing method of time complexity taken different nodes like 30, 60, 100 nodes. The proposed method provides less time complexity compared to other existing methods. The proposed method DTSCR has 224ms of less time complexity compared to the existing method QLRR and DGR.

$$\text{Routing packet} = \frac{\text{total number of data packets received}}{\text{the total number of routing packets received}} * 100 \quad (7)$$

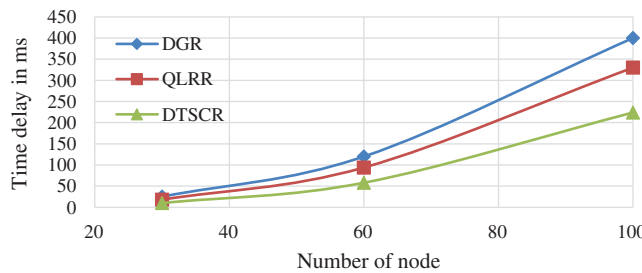


Figure 6: Comparison of End to the End time delay

In this comparison of the proposed method DTSCR and the existing method, QLRR and DGR routing packets are shown Fig. 7. In this analysis of the proposed DTSCR method, results provide 92% for 200 s, and the existing method has 71%, 64%, and 30% for 200, 180, and 160 s of rate.

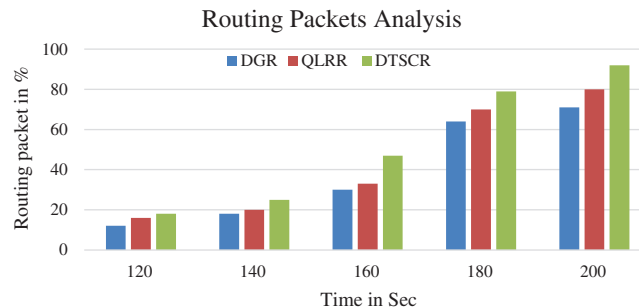


Figure 7: Comparison analysis of routing packets

5 Conclusion

This research aims to the transmission time of each sensor deployed in the network to find the time-consuming selection of the appropriate sensor nodes to improve the life cycle of the sensor network. Within the surveillance area, scatter sensors have two ways to send observations to a receiver, either single or multi-hop. When multi-hop communication is adopted, the nearest sink node is ejected early. There can be holes near the sink node for heavy traffic because its packet demand is higher than other nodes—this issue overcome to use the DTSCR method to reduce data communication and higher routing packet. The eDCP performs collected data on each edge node. It reduces time delay communication between the nodes if any path or new node enters the network, the re-establish network using Topological Sort (DTS) algorithm. The proposed method DTSCR 93.4% of packet delivery ratio, 92% of routing packets, and 224ms time delay compared to the existing method. The proposed algorithm provides higher efficiency of throughput performance, lower packet loss, end-to-end time delay, and packet delivery rate than previous methods.

Funding Statement: The authors extend their appreciation to the Deanship of Scientific Research at King Khalid University, Kingdom of Saudi Arabia for funding this work through General Research Project under the Grant Number (RGP. 1/262/42).

Conflicts of Interest: The authors declare they have no known competing financial interests or personal relationships that could influence the work reported in this paper.

References

- [1] H. Li and A. V. Savkin, "Wireless sensor network-based navigation of micro flying robots in the industrial internet of things," *IEEE Transactions on Industrial Informatics*, vol. 14, no. 8, pp. 3524–3533, 2018.
- [2] S. Zoppi, A. Van Bemten, H. M. Gursu, M. Vilgelm, J. Guck *et al.*, "Achieving hybrid wired/wireless industrial networks with wDetServ: Reliability-based scheduling for delay guarantees," *IEEE Transactions on Industrial Informatics*, vol. 14, no. 5, pp. 2307–2319, 2018.
- [3] S. Gupta, A. K. Sahoo and U. K. Sahoo, "Wireless sensor network-based distributed approach to identify Spatio-temporal volterra model for industrial distributed parameter systems," *IEEE Transactions on Industrial Informatics*, vol. 16, no. 12, pp. 7671–7681, 2020.
- [4] K. Yu, M. Gidlund, J. Akerberg and M. Bjorkman, "Performance evaluations and measurements of the realflow routing protocol in industrial wireless networks," *IEEE Transactions on Industrial Informatics*, vol. 13, no. 3, pp. 1410–1420, 2017.
- [5] X. Ding, X. Tian and Y. Yu, "A real-time big data gathering algorithm based on indoor wireless sensor networks for risk analysis of industrial operations," *IEEE Transactions on Industrial Informatics*, vol. 12, no. 3, pp. 1232–1242, 2016.
- [6] Q. Li, N. Zhang, M. Cheffena and X. Sherman, "Channel-based optimal backoff delay control in delay-constrained industrial wsns," *IEEE Transactions on Wireless Communications*, vol. 17, no. 12, pp. 1–15, 2019.
- [7] C. Xia, X. Jin, L. Kong and P. Zeng, "Bounding the demand for mixed-criticality industrial wireless sensor networks," *IEEE Access*, vol. 5, pp. 7505–7516, 2017.
- [8] H. Haifeng, W. Xiaodong, Y. Zhen and Z. Baoyu, "A spectral clustering approach to identifying cuts in wireless sensor networks," *IEEE Sensors Journal*, vol. 15, no. 3, pp. 1838–1848, 2015.
- [9] X. Zhezhuang, C. Liquan, C. Cailian and G. Xinping, "Joint clustering and routing design for reliable and efficient data collection in large-scale wireless sensor networks," *IEEE Internet of Things Journal*, vol. 3, no. 4, pp. 520–532, 2016.
- [10] S. M. Hosseini and M. H. Kahaei, "Target detection in cluster-based WSN with massive MIMO systems," *Electronics Letters*, vol. 53, no. 1, pp. 50–52, 2017.
- [11] E. Vishnupriya, T. Jayasankar and P. MaheswaraVenkatesh, "SDAOR: Secure Data Transmission of Optimum Routing protocol in wireless sensor networks for surveillance applications," *ARPJ Journal of Engineering and Applied Sciences*, vol. 10, no. 16, pp. 6917–6931, 2015.

- [12] M. Farsi, M. Badawy, M. Moustafa, H. Arafat Ali and Y. Abdulazeem, "A congestion-aware clustering and routing (CCR) protocol for mitigating congestion in WSN," *IEEE Access*, vol. 7, pp. 105402–105419, 2019.
- [13] S. Lata, S. Mehfuz, S. Urooj and F. Alrowais, "Fuzzy clustering algorithm for enhancing reliability and network lifetime of wireless sensor networks," *IEEE Access*, vol. 8, no. 3, pp. 66013– 66024, 2020.
- [14] P. Neamatollahi, M. Naghibzadeh, S. Abrishami and M. Yaghmaee, "Distributed clustering-task scheduling for wireless sensor networks using dynamic, hyper round policy," *IEEE Transactions on Mobile Computing*, vol. 17, no. 2, pp. 334–347, 2018.
- [15] J. Qiao and X. Zhang, "Compressive data gathering based on even clustering for wireless sensor networks," *IEEE Access*, vol. 6, pp. 24391–24410, 2018.

Fuzzy Based Reliable Load Balanced Routing Approach for Ad hoc Sensor Networks

J. V. Anchitaalagammai^{1,*}, Rajesh Verma², M. Kavitha³, A. R. Revathi⁴, S. R. Preethi⁵ and Kiranmai Bellam⁶

¹Department of Computer Science and Engineering, Velammal College of Engineering and Technology, Madurai, 625009, TamilNadu, India

²Department of Electrical Engineering, King Khalid University, Abha, 62529, Saudi Arabia

³Department of Electronics and Communication Engineering, K. Ramakrishnan College of Technology, Tiruchirappalli, 621112, Tamil Nadu, India

⁴Department of Information Technology, SRM Valliammai Engineering College, Chennai, 603203, Tamil Nadu, India

⁵Department of Electronics and Communication Engineering, SRM Valliammai Engineering College, Chennai, 603203, Tamil Nadu, India

⁶Department of Computer Science, Prairie View A & M University, Prairie View, TX, United States

*Corresponding Author: J. V. Anchitaalagammai. Email: anchitaalagammailphd@gmail.com

Received: 21 June 2021; Accepted: 23 July 2021

Abstract: Energy management and packet delivery rate are the important factors in ad hoc networks. It is the major network where nodes share the information without administration. Due to the mobility of nodes, maximum energy is spent on transmission of packets. Mostly energy is wasted on packet dropping and false route discovery. In this research work, Fuzzy Based Reliable Load Balanced Routing Approach (RLRA) is proposed to provide high energy efficiency and more network lifetime using optimal multicast route discovery mechanism. It contains three phases. In first phase, optimal multicast route discovery is initiated to resolve the link failures. In second phase, the link quality is estimated and set to threshold value to meet the requirements of high energy efficiency. In third phase, energy model is shown to obtain total energy of network after transmission of packets. A multicast routing is established Based on path reliability and fault tolerant calculation is done and integrated with multicast routing. The routes can withstand the malicious issues. Fuzzy decision model is integrated with propose protocol to decide the performance of network lifetime. The network simulation tool is used for evaluating the RLRA with existing schemes and performance of RLRA is good compared to others.

Keywords: Fuzzy model; link quality; multicast route; energy model; cluster group; node lifetime

1 Introduction

MANET is one of the modes popular networks and important model for delay tolerant networks where the nodes are communicating without the need of infrastructure and discontinued path exists between source



This work is licensed under a Creative Commons Attribution 4.0 International License, which permits unrestricted use, distribution, and reproduction in any medium, provided the original work is properly cited.

and destination nodes. The information exchange among group of users was supported by the multicast delivery mechanism where source node is linked to group of sink nodes. It can be illustrated in battlefield where the commander sends message to group of soldiers without access point. In social networks and applications, single user can share audio, video, picture, and messages to group of his neighbors or friends. The packet delivery rate and energy efficiency can be improved by adopting Quality of Service [1]. Due to fluctuation of routes and mobility of nodes, energy efficiency will not be improved in ad hoc network in the presence of packet dropping. The power of the transmitter can be adjusted according to support various applications. In this research, multicast routing Based energy efficient model is introduced to attain high network lifetime by adopting various strategies and routing methodologies.

2 Analytical Survey

Kuo et al. [2] explored the Energy Efficiency optimization using cross layer design. The energy unit was modeled using non convex mixed integer programming. This programming was formalized by considering scheduling, energy management and routing. The problem is optimized using non convex programming. The concept of branch and bound algorithm was used to identify the issues of energy during data transmission. Riasudheen et al. [3] proposed the energy management of cloud assisted ad hoc networks to extend the network lifetime. The communication between the head nodes and mobile nodes were frequently monitored and renewed Based on performance metrics of networks i.e., overhead, route failure and batter power of node etc. The maximum energy was spent on finding and connecting the mobile nodes. The fast local route recovery mechanism was adopted to reduce the energy consumption. The intermediate nodes were grouped together to form overlay network which consumes less energy if more link failure occurred.

Zhang et al. [4] developed an offline roadside scheduling algorithm to provide a better energy consumption. The concept of on/off scheduling was to determine the slots for packet forwarding towards the sink node through the channel. The size of contention window was adjusted according to the network overload. If the density is more, the size can be limited to reduce the packet loss during packet transmission. The optimization issues were solved by the non-linear programming to reduce the energy consumption. Meanwhile the sub optimal issues were solved by the non-linear programming model. Peng et al. [5] designed an energy efficient cooperative multi input multi output transmission for increasing network lifetime of ad hoc networks. A new cooperative strategy was followed Based on random distribution methods with various number of nodes. The synchronization and issues of internal packet transmission were solved using spatial modulation technique. The information of transmission was transmitted by cluster members with supporting nodes to achieve the flexibility. The energy consumption of the cooperative strategy was estimated and compared with existing schemes and shown the better performance.

Malekshan et al. [6] proposed the concept of joint transmission scheduling and power control mechanism to improve the network performance. Due to unbounded network region and high node density, the concept of asymptotic optimal scheduling and transmission power control was determined. The basic limits of spectrum and energy model were determined to analyze the optimal scheduling. The transmission power level was determined Based on optimal solution values. The continuous transmission at each network slot was scheduled to improve the energy utilization and spectrum efficiency. Tilwari et al. [7] presented multipath aware routing Based on node mobility, remaining energy and quality of links in the network. The multiple parameters were aggregated into a single value Based on Q learning concept in order to provide an optimal path decision. The status of nodes was evaluated in the presence of path estimation and topology sensing method to obtain stable routes in the convergence network region. During the selection of stable paths between source and sink node, least residual energy and more mobility nodes were avoided to cope with route failures and network lifetime enhancement.

Rao et al. [8] introduced the secure cryptography method integrated with energy efficient clustering method to balance security and energy in ad hoc networks. The proactive routing scheme was implemented with energy conservation scheme. The energy status and node mobility was focused in the routing hierarchy before data transmission process. The energy cost was estimated and attained Based on individual node energy estimation with the help of K-Means clustering along with Ad-hoc On Demand Distance Vector routing method. For security, the packets were protected with advanced encryption standard.

Ramya et al. [9] introduced the enhanced range routing with on demand routing to improve energy efficiency of network. Here only few nodes were participated for processing and receiving the data Based on signal strength to reduce energy consumption and overhead. An adaptive strategy was adopted to improve energy efficiency and transmission distance using enhanced range routing method. Here individual zones were particularly monitored to attain maximum network lifetime. Kanagasundaram et al. [10] proposed the multi objective ant lion optimizer to prolong the network lifetime and minimize the delay. The weight factor was calculated on shortest routes to improve the energy efficiency of individual node. The best and stable optimal path was selected to monitor the reputation metric, threat value and suspicious activity between the nodes. The degree of vulnerability was determined Based on energy conservation and misbehaving activity in the routes. The new performance metrics were introduced and tested for increasing the energy of link state routing. The multipoint relay path was selected Based on high integrity rate and maximum energy value.

Jubair et al. [11] presented a new link state routing called Bat Optimized Link State Routing (BOLSR) protocol to improve energy efficiency of network in the presence of high mobility nodes. The maximum energy was spent on route discovery and packet transmission period. The optimal paths were the solution to provide high residual energy to improve the network lifetime. Both link state routing and bat routing algorithm was used to identify the best routes Based on energy dynamic values. Fatima et al. [12] introduced the strategies for reducing energy consumption using specific energy modela and dynamic ad hoc on demand method. The power saving method was deployed to provide additional features of Wireless Local Area Network (WLAN). A multi hop relay model was taken into a consideration to improve coverage area with least energy consumption. Residual life battery monitoring model was adopted to focus on the energy value of WLAN and IEEE 802.16 standards and technologies.

Kaur et al. [13] have reviewed and presented different fault tolerant routing algorithms and protocols for ad hoc wireless networks. Various handling problems like node failures, link failures, and transmission power and energy dissipation were analyzed and solutions were given to those issues. The overall performance Based on throughput, reliability and network lifetime was recorded in the presence of fault tolerant routing schemes. Ravichandra et al. [14] presented Fault tolerant QoS Routing Protocol (FTQRP) to attain high tolerant route in the presence of mobile environment. Alternate routes are discovered if the route breaks occurs. Packets are sent through alternative routes to achieve more packet delivery ratio. Mobile nodes are randomly moving inside and outside the network. In previous work of this protocol, genetic algorithm was implemented to address routing with the help of network redundancies. In this QoS protocol, more fault tolerant rate has been improved than genetic algorithm.

Palaniappan et al. [15] introduced energy efficient QoS routing to estimate parameters of link reliability with the help of fuzzy logic technique. While adopting this approach, routing layer will be more robust. From the OSI architecture, link layer, routing and physical layer performs better. The Signal to Interference plus noise ratio can be calculated using physical layer. The neighbor status and back off time can be estimated for link layer. Data rate and data count information were calculated to decide the packet transmission status. Chaudhary et al. [16] have made an analysis on fault tolerant methodologies to route packets along the optimized paths. All the paths have threshold signal strength to achieve more energy efficiency. Route

discovery and route maintenance are continuously monitored to avoid packet loss in the presence of link mobility.

Tavakoli et al. [17] proposed efficient fault-tolerant routing algorithm for MANET. Network fault tolerance and natural redundancy was successfully improved using this algorithm. Initially, selection of backup routes and nodes were chosen by predicting reputation parameters. Fault tolerant routing will be initiated once the selection of backup of nodes was over. The primary route between pair of source and destination was estimated. Nallusamy et al. [18] introduced the new reliable protocol called Mobile Agent Based Energy Efficient Reliable routing protocol to improve the link cost metrics i.e., network load and link availability. All the mobile agents are randomly deployed and packets are transferred in a hop by hop manner once it reaches the destination. From this traversal, node agents can collect the combine link cost metrics and source agents may able to select the optimal path.

Rani et al. [19] have introduced the new concept of link optimization procedure to extract the bandwidth efficiency using window channel. It was considered that previous obstacles and solutions were found to improve the energy efficiency. The optimal network path was established from source to destination by considering link cost metrics and node trust parameters. Meena et al. [20] proposed the topology transparent routing to achieve the improvement in network performance. There are three different network scenarios adopted to attain more gain. Network was kept as static and dynamic. Energy estimation was done in the last scenario. Routing steps were modified according to the energy level of mobile nodes. The concept of shortest path mechanism was established to achieve high energy efficiency. Narayanan et al. [21] presented fault tolerant routing for selecting cluster head with maximum energy efficiency. The link failure was mitigated by deploying local repair method. This method was utilized for avoiding link breakages. However, this routing suffered from excessive routing overhead and more delay.

Nandhini et al. [22] developed an effective and secured message broadcasting model to achieve better results over authentication with least energy consumption. The secure broadcast model was used to minimize overhead Based on the evaluation of confidentiality and authentication through source node. The confidence correlation measure was calculated to find the authenticated route between source and neighbor nodes. Gaur et al. [23] introduced a multi-constraints integrated link Based multicast routing protocol while considering Quality of Service (QoS) metric to improve throughput, and improve bandwidth efficiency of MANET. The link stability factor was calculated to determine the number of stable links in the network. The authors used the concept of mesh Based routing to support mesh communication while reducing link failures. The proposed RLRA contains five sections. Section 1 deals with MANET overview and need for energy efficiency. Section 2 surveys the various methods and protocols relevant to proposed approach. Section 3 discusses the proposed approach that contains network model and routing methods. Section 4 deals with simulation results and last section concludes the proposed work.

The proposed work is contributed to improve reliability with following innovations

1. The path reliability metric is calculated Based on energy, bandwidth and delay values to ensure good network lifetime.
2. Establishment of optimum energy model is to increase network energy efficiency.
3. Link availability is determined to maximize the packet delivery ratio.
4. Cluster group with network density is identified to face fault failures through the calculation of fault tolerant ratio.

3 Reliable Load Balanced Approach

In this section, Reliable load Balanced approach is developed to improve energy efficiency of nodes in the network with optimal route selection in multicast route and energy efficient model. Before data transmission process, the network model is introduced to attain maximum energy.

3.1 Network Model

In this phase, the topology of MANET is derived as $T(n, r)$. Where n indicates nodes and r means routes. Both are connected by the devices i.e., edges. The reliability of link is expressed as l_r and residual energy of node is expressed as E_r .

3.2 Multicast Route Establishment Based on Path reliability

Multicast routes are established from source to sink whereas the secured data packets are forwarded through routes. The routes are able to withstand dynamic environment, but it is difficult to identify attackers in the coverage region. Mostly routes are used as disjoint routes. The remaining energy of the node and signal strength decides the cluster heads and members which forms cluster region. Mesh Based multicast routing is implemented to improve network connectivity by sending group of messages to many sink nodes. The link reliability is determined Based on minimum packet dropping and reliable transmission. This metric is determined from the link reliability (l_r), residual energy (E_r), delay (d) and bandwidth (BW). The link reliability is estimated as,

$$l_r = \frac{P_d - P_l}{P_T} - E_w \quad (1)$$

where P_d is the destination packets, P_l is the packets loss, P_T is the total packets and E_w is the energy wastage on packet loss and retransmission of packets. During bandwidth estimation, the channel capacity and periods of sleep node and active node during packet transmission are considered. In energy model, initial energy is E_i and transmission energy is E_t . The transmission energy is estimated Based on packet transmission N_t and reception N_r with respect to constant parameter (μ, v) and it is derived as,

$$E_t = N_t * \mu + N_r * v \quad (2)$$

The delay is measured from the propagation delay, processing delay and queuing delay. It is given as,

$$d = d_p + d_{pg} + d_q \quad (3)$$

The path reliability metric (P_k) is measured as,

$$P_k = P_1 * \left(\frac{BW_s}{BW_T} \right) + P_2 * \left(\frac{E_t}{E_i} \right) + P_3 * \left(\frac{d}{T_{max}} \right) + P_4 * \left(\frac{l_r}{l_n} \right) \quad (4)$$

where $P_1 + P_2 + P_3 + P_4 = 1$, T_{max} is the maximum time for synchronization, l_n is the number of links available in the network.

Fault tolerant routes are defined with less number of lost packets. Neighbor node checks the reliability of paths and hop count value and forward it to destination node. If the Sequence Number of the node is not matched, neighbor node will resend the RRREQ packets to source node. If it is matched, the message will be broadcasted to destination node. The destination node sends the reply packets containing path reliability count. CH chooses maximum reliability count and check the fault tolerability of the paths. The optimized fault tolerant route is discovered with having least energy nodes on active route inside the network region. Route error (RERR) message will be received if the energy of node falls below the

threshold value. Here the maximum transmission energy is 0.879 Joules as fixed in the simulation setup. CH creates and chooses alternative path to the destination. Mesh routes are created Based on high path reliability metric and number of fault tolerant routes with least cost metric.

3.3 Determination of Fault Tolerable Routes

Once the alternative paths are setup towards the destination node, neighbor node discovers the optimal paths Based on the link quality estimation. Link quality defines that number of packets can be carried out through the links which does not cause packet losses. It is calculated by estimating the Expected Transmission Period (ETP). This period ensures no packet losses during data transmission. This metric is used to find link capacity (lc) and packet size (ps). This ETP value will be stored in all mobile nodes including source and destination. It is given as,

$$ETP_k = ETC_k * \left(\frac{lc}{ps} \right) \quad (5)$$

where ETC is the expected transmission count for packets.

Fault Tolerable Routes (FTR) can be found as the sum of metrics of link, remaining energy, hop distance, and ETP. It is estimated as,

$$FTR = \left(\epsilon * re_k + \varphi * \frac{1}{d_{jk}} + \gamma * \frac{1}{ETP_k} + p_reliability \right) \quad (6)$$

where $\epsilon, \varphi, \gamma$ are the coefficients related to remaining energy, distance between two mobile nodes and expected transmission period. Source node chooses path with maximum FTR. Source node sends RRREQ message towards the next hop. Once it is confirmed, it is able to identify the presence of destination node. The flag will be set if the destination address matches with address in the header field of RRREQ. If not, the optimal route will be constructed towards the destination node.

3.4 Cluster Network Model

The cluster network model is illustrated to balance the load and energy. Cluster nodes are grouped together to form a cluster and select Cluster Head (CH). In each cluster, one anchor node will be set to monitor the behaviour of nodes and paths. The routes are computed Based on quality of links, remaining energy of node and delay metric. The availability of links and delay are estimated. The epoch is defined here to identify the movement of nodes from one location to another location with constant speed and same direction. It is not same for all mobile nodes. Constant epoch length defines different epoch size. The cluster multicast routes are established from CH to cluster members. The reason for choosing mesh routing is to provide global connectivity and optimal solution to link failures. The failure rate and delay is very low in mesh routing. Meanwhile it also supports cluster formation and discovery process. The recovery of routes can be quickly done with the help of multicast routes. CH is the source node and destination cluster members are the target nodes. These nodes are the end node who will complete the data transmission process. CH sends bulk of messages to cluster members by creating multicast routes. The routes are created and formalized for packet forwarding Based on link quality. Before that, link availability must be tested to obtain quality.

The link availability $L_A(\tau_{CH \text{ to } CM})$ is estimated between CH and destination cluster member if the constant epoch length persists. It is given as below,

$$L_A(\tau_{CH \text{ to } CM}) \triangleq \Delta A\{t_{CH \text{ to } t_{CM}} + \tau, \text{available}\} \quad (7)$$

If velocity is changed between two epochs, the link availability can be computed as,

$$L_A(\tau_{CH \text{ to } CM}) = L_A(\tau_{CHt}) + L_A(\tau_{CM}) \quad (8)$$

If the mobility of nodes are independent, the exponential distribution of link availability is given as,

$$L_A(\tau_{CH \text{ to } CM}) = [1 - E(\tau_{CH \text{ to } CM})]^2 = e^{-2\lambda\tau_{CH \text{ to } CM}} \quad (9)$$

The received signal strength indicator is used to identify the node location and node mobility inside or outside the region. The square distance between the nodes is degraded by the link quality if nodes are moved out of cluster. It is estimated Based on random variable α and given as,

$$L_q(\alpha) = \frac{\alpha + (\tau_{CH \text{ to } CM} - \alpha)}{\tau_{CH \text{ to } CM}} \quad (10)$$

Once the link quality is obtained, CH verifies the multiple link quality Based on threshold value. If links are fluctuated and low value, it will be isolated for packet forwarding.

3.5 Data Transmission Through Multicast Routing

In this phase, CH sends CHM_Req packets to all cluster members to initiate packet forwarding. Cluster members receive the request packets and replies *via* CHM_Rep packets to CH. The destination cluster members are determined to begin packet forwarding. Once confirmed, CH sends data packets to destination CM *via* optimal routes. If any packet loss occurs, destination CM sends failure token message to CH to reinitiate packet transmission. This token message contains packet failure information due to errors. It may occur due to path failure or path overload. The residual energy is maintained among all cluster members. If any packet loss occurs, destination CM sends failure token message to CH to reinitiate packet transmission. If any error in the packet found, it will be immediately corrected using forward error correction. Cluster members are the nodes which are actively participating to elect Cluster Head (CH). The illustration of data transmission in cluster multicast zone is shown in Fig. 1.

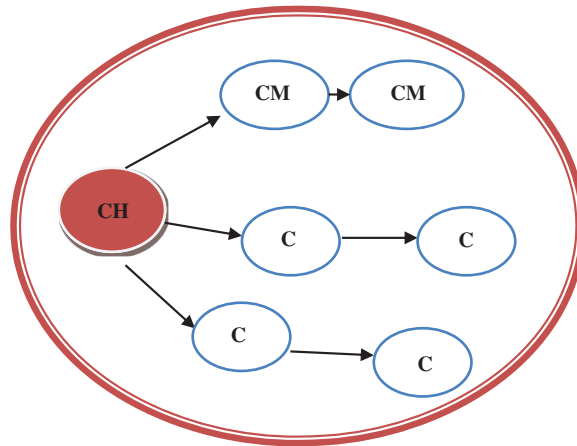


Figure 1: Data transmission in cluster multicast group

During data transmission, cluster messages are transmitted through optimal routes. It will be checked and confirmed by the CH.

3.6 Optimal Energy Model

In this phase, energy needs to be estimated during packet transmission and at the end of route maintenance phase. The energy consumed by the packets from node to node is evaluated. The energy spent (E_S) by CH and CM for packet forwarding is estimated as,

$$E_S = \sum_{r=1}^m \tau(nr, nr + 1) - \sum_{r=1}^m \tau_p(wr, wr + 1) \quad (11)$$

where r indicates residual energy, m means number of nodes and n indicates epoch size, w indicates energy wastage on packet dropping.

The residual energy is calculated as,

$$r_k = T_k - E_w \quad (12)$$

where T_k is the total energy allocated to nodes and E_w is the energy wasted on packet dropping. The transmitter E_t energy is given as,

$$E_t = \sum (E_T, E_{RD}) \times \tau \quad (13)$$

This energy is Based on energy spent for packet transmission E_T and route discovery process E_{RD} .

The receiving energy E_r is estimated as,

$$E_r = \sum (E_R, E_{PA}) \times \tau \quad (14)$$

This energy is Based on energy spent for packet reception E_R and packet arrival E_{PA} at sink node.

The total energy E_T is derived as

$$E_t = E_t + E_r + E_I \quad (15)$$

where E_I is the energy spent in idle mode. The total energy of node is also estimated Based on power spent for packet forwarding from CH to CM.

Total energy = Total energy for cluster group/packet delivery cost.

The algorithm 1 shows illustration of RLRA to provide high energy efficiency through optimal path.

Algorithm 1: RLRA algorithm

1. Start
 2. CH initiates route discovery process
 3. CM joins routing and finalize destination CM
 4. Obtain the link quality
 5. If threshold link quality is not met
 6. {
 7. Drop the route discovery process and reinitiate
 8. else
 9. Initiate packet forwarding
-

(Continued)

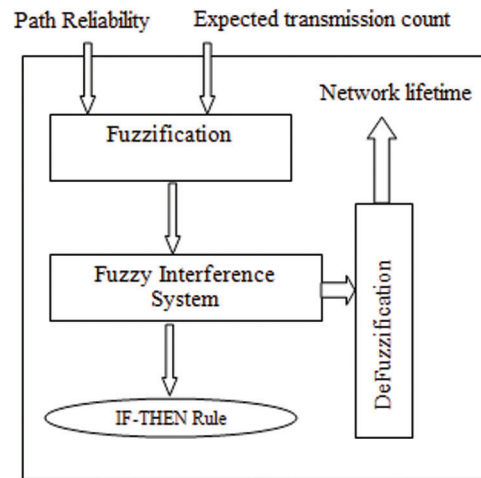
Algorithm 1 (continued).

10. }
11. Estimate energy on transmitting and receiving section.
12. Find total energy and network lifetime
13. End

From the above algorithm, the total energy and network lifetime of sensor networks are estimated through link quality determination and packet forwarding initialization. After route maintenance process, the total energy and network lifetime will be estimated.

Fuzzy decision model for Fault tolerant

Fuzzy decision mechanism is used using Mamdani Fuzzy model. The inputs to the fuzzification are path reliability and expected transmission count. It is converted as crisp values and given to fuzzy inference engine. The values are processed and given to defuzzification. The values are converted into single output i.e., network lifetime. If both crisp values are high, network lifetime will be high. Fig. 2. shows the illustration of fuzzy decision mechanism.

**Figure 2:** Fuzzy decision model**3.7 RLRA Frame Format**

The Tab. 1 shows the illustration format of RLRA. First two field occupies 4 bytes by the identity of cluster head and cluster member as well as link quality. The link quality field is used to provide optimal solution for link failure and Route ID occupies one byte. The energy status of node is shown to know the residual energy of node after packet transmission. Cyclic redundancy check is used to detect and correct the packet error that occupies 4 bytes.

Table 1: Frame format

CH and CM id	Link quality status	Route ID	Energy Status	CRC
2	2	1	4	4

4 Simulation Setup

The proposed approach is tested using network simulation tool. It is the open-source tool where it is user friendly. The used language for NS2 is the tool command language which is the resemble of C++. The simulation coverage area used for RLRA is $1000 \times 1000 \text{ sq} \cdot \text{m}$. The simulation settings are tabulated in Tab. 2. The following parameters are used to validate the performance The following QoS metrics are used to validate the performance of the proposed protocol with existing schemes.

Table 2: Simulator settings for RLRA

No. of mobile nodes	150 node
Routing protocol	AODV
Area size	$1000 \times 1000 \text{ sq} \cdot \text{m}$
Mobility model	Random walk
Traffic	Constant Bit Rate
MAC	IEEE 802.11
Frequency for transmission	2.4 GHz
Data packet rate	5 packets/sec

Propagation delay: It is the delay where the packets are propagated from node to node during transmission phase.

Network lifetime: It is the maximum energy after data transmission.

Packet delivery ratio: The ratio which is calculated from packets delivered to packets sent.

Overhead: It means that number of excessive packets present in link where packets may not able to reach sink node.

Energy efficiency: It is defined as the maximum energy obtained to the total available energy.

The proposed protocol RLRA is compared with previous schemes MOALO [10] and BOLSR [11], FTQRP [14].

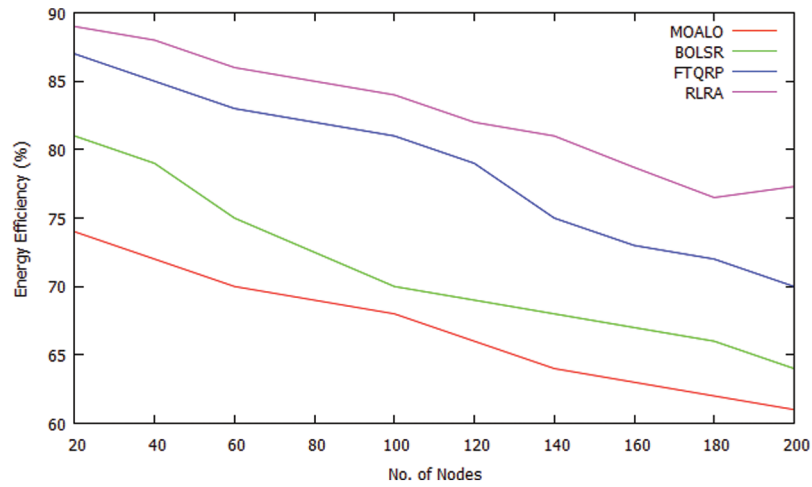
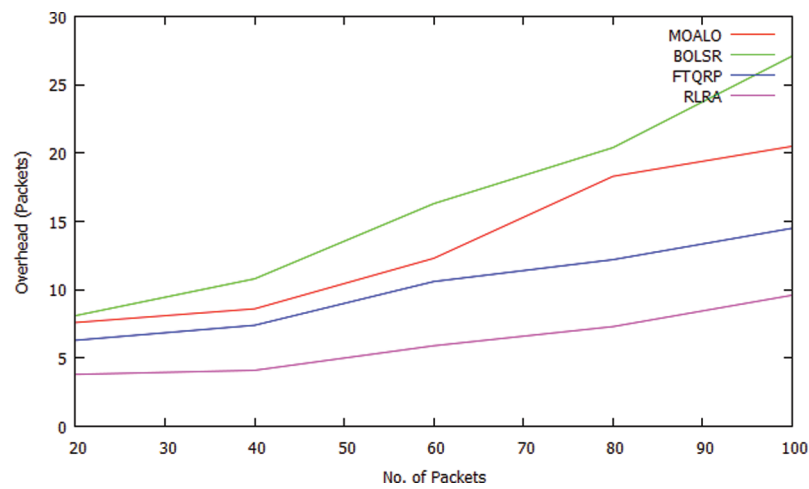
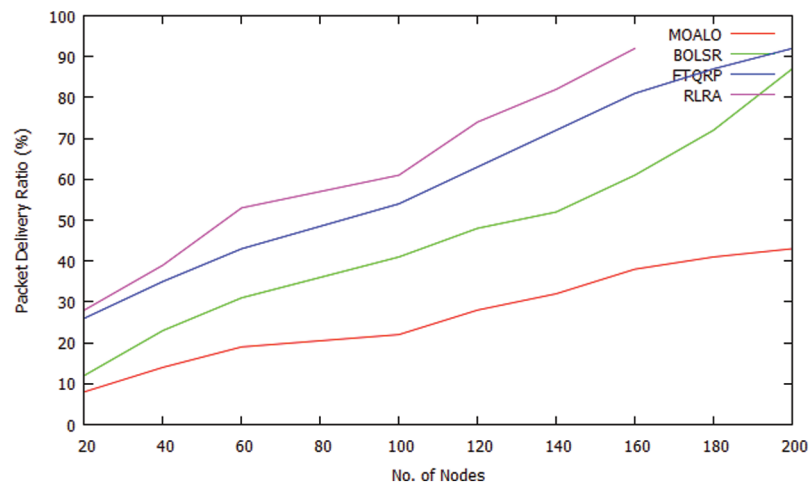
Fig. 3 illustrates the energy efficiency analysis of RLRA, FTQRP, BOLSR and MOALO. From the results, it is seen that RLRA achieves high energy efficiency than existing schemes due to presence of energy model by consuming less energy for transmission and reception.

Fig. 4 shows the overhead of proposed and existing schemes. The overhead of RLRA is less compared to existing schemes due to stable route discovery and link quality attainment.

Fig. 5 shows the performance of packet delivery ratio of RLRA and existing schemes. The RLRA achieves more packet delivery ratio from the results. It is because of optimal route selection and effective packet forwarding scheme.

Fig. 6 shows the results of propagation delay in x axis and simulation time in y axis. While varying the simulation time, the propagation delay of RLRA achieves low value compared to existing schemes.

Fig. 7 shows the results of network lifetime. From the results, RLRA attains more network lifetime due to least energy consumption of packets and optimal route selection. Tab. 3 shows the performance analysis between proposed system and existing system.

**Figure 3:** Energy efficiency vs. No. of nodes**Figure 4:** Overhead vs. No. of control packets**Figure 5:** Packet delivery ratio vs. No. of nodes

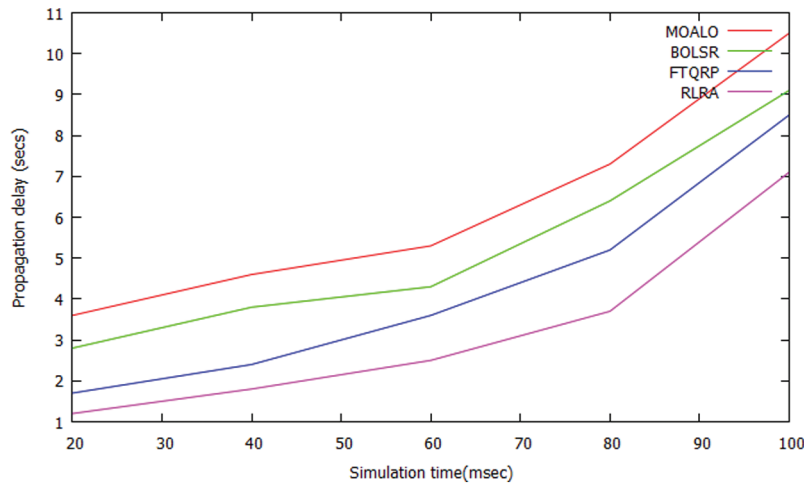


Figure 6: Propagation delay vs. Simulation time

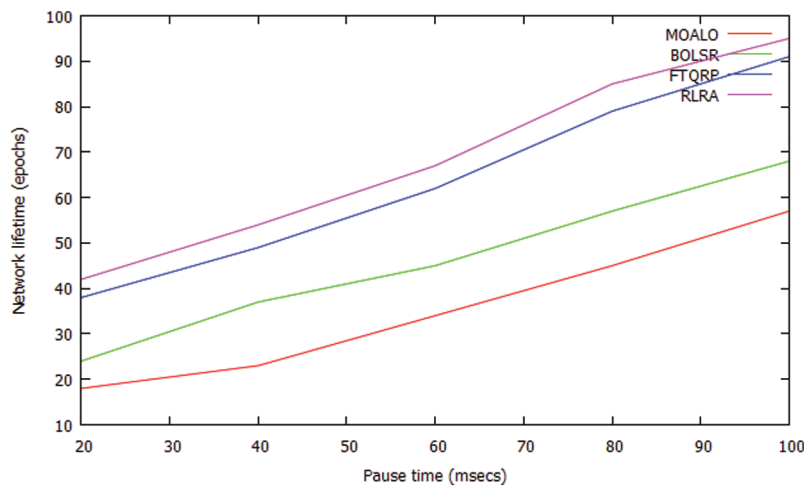


Figure 7: Network lifetime vs. Pause time

Table 3: Performance Analysis

Methods Parameters	MOALO	BOLSR	FTQRP	RLRA
Propagation delay (msecs)	3.6–10.5	2.8–9.1	1.7–8.5	1.2–7.1
Overhead (Pkts)	7.6–20.5	8.1–27.1	6.3–14.5	3.8–9.6
Packet delivery ratio (%)	8–38	12–61	26–81	28–92
Network lifetime (epochs)	18–57	24–68	38–91	42–95
Energy efficiency (%)	74–63	81–67	87–73	89–79

From the results, RLRA achieves more packet delivery ratio, more network lifetime and high energy efficiency, less delay and overhead than existing schemes.

5 Conclusion

In ad hoc networks, balancing both link failure and energy will be the major task. In ad hoc networks. In existing schemes, it is failed to balance both metrics. In our proposed model, RLRA is introduced to meet the challenges of ad hoc networks i.e., high energy efficiency and more network lifetime. Network model is introduced to decide the level of reliability and fault tolerant. Multicast routing is established from source to sink node Based on path reliability. The estimation of link quality is done Based on epoch size and length and the optimal multicast routes are discovered from cluster head to cluster member. Energy efficient model is integrated in the network to obtain total energy and save the residual energy. From the results, RLRA achieves more packet delivery ratio, more network lifetime and high energy efficiency, less delay and overhead than existing schemes.

Funding Statement: The authors extend their appreciation to the Deanship of Scientific Research at King Khalid University, Kingdom of Saudi Arabia for funding this workthrough General Research Project Under the grant number (RGP.1/262/42).

Conflicts of Interest: The authors declare that they have no conflicts of interest to report regarding the present study.

References

- [1] K. VinothKumar, T. Jayasankar, M. Prabhakaran and V. Srinivasan, "Fuzzy logic based efficient multipath routing for mobile adhoc networks," *Applied Mathematics & Information Sciences*, vol. 11, no. 2, pp. 449–455, 2017.
- [2] W. K. Kuo and S. H. Chu, "Energy efficiency optimization for mobile ad hoc networks," *IEEE Access*, vol. 4, pp. 928–940, 2016.
- [3] H. Riasudheen, K. Selvamani, S. Mukherjee and I. R. Divyasree, "An efficient energy-aware routing scheme for cloud-assisted MANETs in 5G," *Ad Hoc Networks*, vol. 97, pp. 102–121, 2019.
- [4] L. Zhang and Y. Wang, "An offline roadside unit on-off scheduling algorithm for energy efficiency of ad hoc networks," *IEEE Access*, vol. 6, no. 26, pp. 59742–59751, 2018.
- [5] Y. Peng, F. Al-Hazemi, H. Kim and C. Youn, "Design and optimization for energy-efficient cooperative mimo transmission in ad hoc networks," *IEEE Transactions on Vehicular Technology*, vol. 66, no. 1, pp. 710–719, 2016.
- [6] K. R. Malekshan and W. Z. Huang, "Joint scheduling and transmission power control in wireless ad hoc networks," *IEEE Transactions on Wireless Communications*, vol. 16, no. 9, pp. 5982–5993, 2017.
- [7] V. Tilwari, K. Dimyati, N. Hindia, A. Fattouh and I. Sadegh Amiri, "Mobility, residual energy, and link quality aware multipath routing in manets with q-learning algorithm," *MDPI, Applied Science*, vol. 9, no. 8, pp. 1–23, 2019.
- [8] K. P. K. Rao and T. Senthilmurugan, "Energy efficient clustering technique using k-means and aodv-aco routing with secured AES cryptography in MANET," *International Journal of Intelligent Engineering and Systems*, vol. 12, no. 3, pp. 292–302, 2019.
- [9] J. Ramya and M. Sumathi, "Efficient energy consumption in MANET by AODV," *ERR, International Journal for Research in Applied Science & Engineering Technology*, vol. 7, no. 12, pp. 853–860, 2019.
- [10] H. Kanagasundaram and K. Ayyaswamy, "Multi objective alo based energy efficient and secure routing OLSR protocol in MANET," *International Journal of Intelligent Engineering and Systems*, vol. 12, no. 1, pp. 74–83, 2019.
- [11] M. Ahmed Jubair, A. Salama, A. Mostafa, R. C. Muniyandi, H. Mahdin *et al.*, "Bat optimized link state routing protocol for energy-aware mobile ad-hoc networks," *Sensors*, vol. 11, no. 11, pp. 1–22, 2019.
- [12] L. N. Fatima, S. H. Mahin and F. Taranum, "Efficient strategies to reduce power consumption in MANETs," *Peer Journal of Computer Science*, vol. 5, no. 2, pp. 1–23, 2019.

- [13] K. Kaur and K. Kaur, "Recent trends toward fault tolerance techniques in MANET," *International Journal of Computer Applications*, vol. 120, no. 22, pp. 47–52, 2015.
- [14] M. L. Ravichandra and C. Reddy, "Fault tolerant QoS routing protocol for MANETs," in *Proc. IEEE Int. Conf. on Advanced Computing*, Bhimavaram, India, pp. 623–628, 2016.
- [15] S. Palaniappan and K. Chellan, "Energy-efficient stable routing using QoS monitoring agents in MANET," *EURASIP Journal on Wireless Communications and Networking*, vol. 13, pp. 1–11, 2015.
- [16] N. Chaudhary, E. Shiv Kumar Goel and N. Goel, "A deep analysis: Highly robust fault tolerant secure optimized energy ad-hoc networks methodologies for mobile nodes," *International Journal of Advanced Research in Computer Science and Software Engineering*, vol. 5, no. 7, pp. 540–543, 2015.
- [17] F. Tavakoli, M. Kamarei and G. Reza Asgari, "An efficient fault-tolerance routing algorithm for mobile ad-hoc networks," *Journal of Advances in Computer Research*, vol. 7, no. 2, pp. 23–40, 2016.
- [18] S. Nallusamy, S. Appavupillai and S. Ponnusamy, "Mobile agents based reliable and energy efficient routing protocol for MANET," *International Journal of Intelligent Engineering and Systems*, vol. 9, no. 3, pp. 110–116, 2016.
- [19] M. Rani and Er. Amit Chhabra, "Modified LA to optimize the performance of mobile ad hoc network," *International Journal of Engineering Science and Computing*, vol. 10, no. 35, pp. 1283–1286, 2015.
- [20] R. Meena, S. Raghuwanshi and Y. Kumar, "Threshold based energy efficient fault tolerance transparent scheme in MANET," *International Journal of Advanced Computer Technology*, vol. 5, no. 5, pp. 87–93, 2016.
- [21] A. E. Narayanan, R. Devi and A. Vincent Jayakumar, "An energy efficient cluster head selection for fault tolerant routing in MANET," *International Journal of Engineering and Technology*, vol. 5, no. 2, pp. 1281–1289, 2013.
- [22] J. Nandhini and D. Sharmila, "Secured message distribution based on multi-bit digital signature in mobile ad-hoc network," *International Journal of Advanced Engineering Technology*, vol. 8, no. 1, pp. 579–586, 2016.
- [23] M. S. Gaur, S. Todi, V. Rao, M. Tripathi and R. Kushwaha, "Multi-constraints link stable multicast routing protocol in MANETs," *Ad Hoc Networks*, vol. 63, no. 2, pp. 115–128, 2017.

Original Article

Brain Tumor Detection in MRI Images using Convolutional Neural Network Technique

R. Tamilaruvi¹, R. Vijayalakshmi², M. Ganthimathi³, R. Surendiran⁴, M. Thangamani⁵, S. Satheesh⁶

¹Department of Computer Science and Engineering, Annamalai University, Chidambaram, Tamil Nadu, India

²Department of Computer Science and Engineering, Velammal College of Engineering and Technology, Madurai, India

³Department of Computer Engineering, Government Polytechnic College, Dharmapuri, India

⁴School of Information Science, Annai College of Arts and Science, Kumbakonam, India

⁵Department of Information Technology, Kongu Engineering College, Tamilnadu, India

⁶Department of Computer Science and Engineering, Arjun College of Technology, Tamilnadu, India

²Corresponding Author : rvi@vcet.ac.in

Received: 30 October 2022

Revised: 03 December 2022

Accepted: 19 December 2022

Published: 31 December 2022

Abstract - A brain tumour is a type of cancer that is difficult to detect. As a result, it is more important for care to evaluate nodules swiftly and appropriately for both men and women. As a result, numerous approaches for detecting brain tumors in their early stages have been developed. A comparative comparison of multiple strategies based on machine learning and deep learning for brain tumor identification has been offered in this procedure. There have been far too many approaches for diagnosing brain tumours developed in recent years, the majority of which rely on MRI images. In addition, several classifier methods are used in conjunction with threshold segmentation algorithms to locate tumors using picture recognition. MRI gray scale images have been discovered to be more suitable for obtaining accurate results because of this method. As a result, most MRI scan images are used to detect tumors in the brain. Furthermore, the findings obtained from approaches based on machine learning and deep learning techniques were more accurate than those obtained from methods based on traditional deep learning techniques. The deep learning method was proposed using the Convolutional neural network to predict the outcome with high accuracy.

Keywords - Brain tumor, Convolutional neural network (CNN), Deep learning, MRI(magnetic resonance imaging), Threshold segmentation.

1. Introduction

In recent years, health informatics systems have been increasingly used to detect and monitor major diseases. Artificial learning-based information systems are used to monitor brain tumour disease. Brain tumors affect both men and women and are caused by uncontrolled cell proliferation in the brain. The brain is the physical body's command and control center. It is responsible for carrying out all activities across many connections and neurons. A brain tumour is one of the most dangerous disorders caused by the abnormal development of cells in the brain that affects the nervous system's activities. Brain tumours come in various shapes and sizes and can be either malignant or benign. Image processing is the process of examining and modifying a photograph to extract information from it. According to figures from the World Health Organization, cancer is the second largest cause of human death worldwide, accounting for an estimated 9.6 million deaths this year. Because of their aggressive nature, varied characteristics (types), and low relative survival rate, brain tumours are often regarded as

among the deadliest cancers. The goal of this study is to compile a list of reviews and technical literature on brain cancer diagnosis. It provides an outline of the current brain tumour treatment method. Image processing techniques were used to enhance the brain tumour in an MRI dataset.

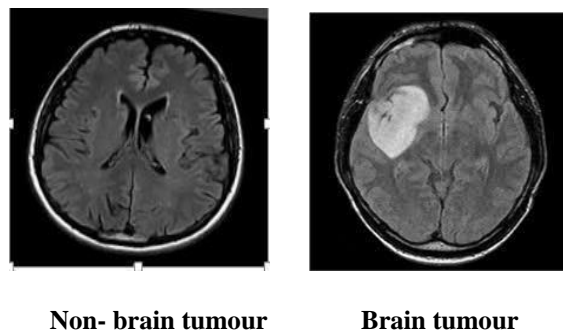


Fig. 1 Sample dataset MRI brain tumour images



2. Background

2.1. Brain Tumors and Magnetic Resonance Imaging

Brain tumours can be intra-axial (e.g., gliomas) or extra-axial (e.g., meningiomas or pituitary adenomas). Intra-axial brain tumours are particularly difficult to treat, especially at advanced stages, when they are usually discovered due to the symptoms caused by the mass effect on the surrounding brain. Treatment failure can be due to several factors, including the limited capacity of current imaging modalities to identify the boundaries of the lesion within the normal-appearing brain parenchyma. Hence, more advanced imaging techniques for assessing brain tumours and surrounding structures are critical to improving overall management. Extra-axial brain cancers also require special attention, as these tumours (such as pituitary adenoma and meningioma) can result in complications and long-term impairment.

MRI is the workhorse for brain tumour imaging in clinical practice providing structural, microstructural, functional, and metabolic information. Moreover, novel advanced imaging techniques are continuously developed to improve brain tumours' identification, characterization, and response assessment. Hence, much artificial intelligence (AI) applications in brain tumor imaging have been based on MRI.

2.2. Deep Learning

Deep Learning (DL) is a subfield of ML concerned with techniques inspired by neuroscience. However, Good fellow et al. noted that neuroscience is no longer the primary source of inspiration for deep learning. Recently, DL algorithms have established themselves as a critical component of medical image analysis tasks, such as object recognition, classification, and segmentation. CNNs represent the most often utilized DL algorithm for developing brain tumor classification and segmentation techniques. CNNs can learn the spatial relationships between voxels in an MRI scan. In

CNNs, multiple filters are hovered on an input image to learn different features that characterize the image.

A typical CNN model mainly consists of the following components: (i) input layer, (ii) convolution layer, (iii) activation function, (iv) pooling layer, (v) fully connected layer, and a (vi) output layer. The input layer feeds the input image into the network for processing by the successive layers. Convolution, pooling, and activation functions are used to extract high-level features from the image, whilst the fully connected layer is used for image classification, object segmentation, or object detection. The output layer generates the network's final prediction or results.

2.3. Vision Transformers

CNNs have demonstrated state-of-the-art performance in computer vision tasks, such as brain tumor segmentation and classification, over the last few years. However, CNNs cannot efficiently capture long-range information or dependencies due to their small kernel size. Long-range dependencies are those in which the desired output depends on image sequences presented at distant times. Due to the similarity of human organs, many visual representations in medical images are organized in sequence. Destruction of these sequences will significantly affect the performance of a CNN model. It is because the dependencies between medical image sequences (such as modality, slice, and patch) contain significant information. These long-range dependencies can be effectively handled by techniques that can process sequence relations. A self-attention mechanism in ViTs has the capacity to model long-range dependencies, which is very important for precise brain tumour segmentation. They achieve this by modelling pairwise interactions between token embedding, thus enabling ViT-based models to learn local and global feature representations. ViT has demonstrated promising performance on a variety of benchmark datasets.

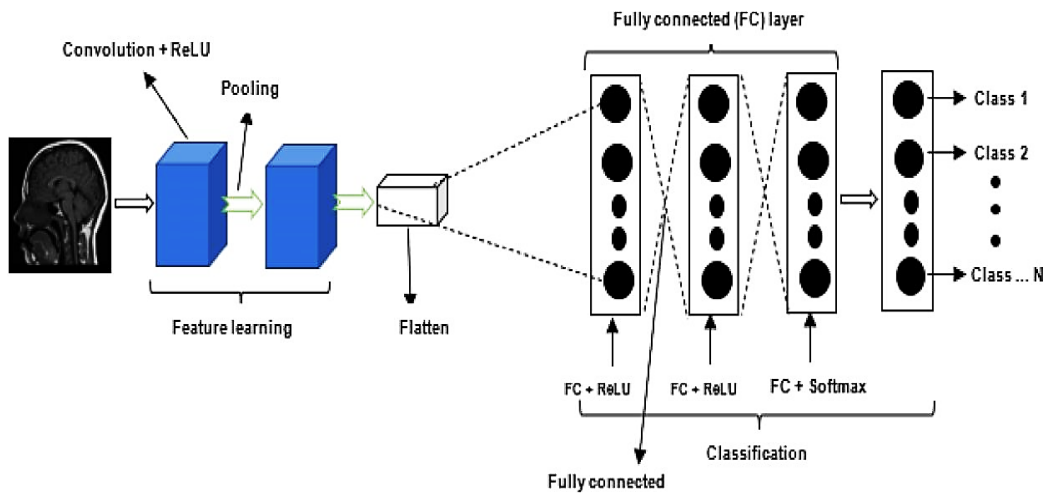


Fig. 2 The general architecture of a Convolutional Neural Network (CNN)

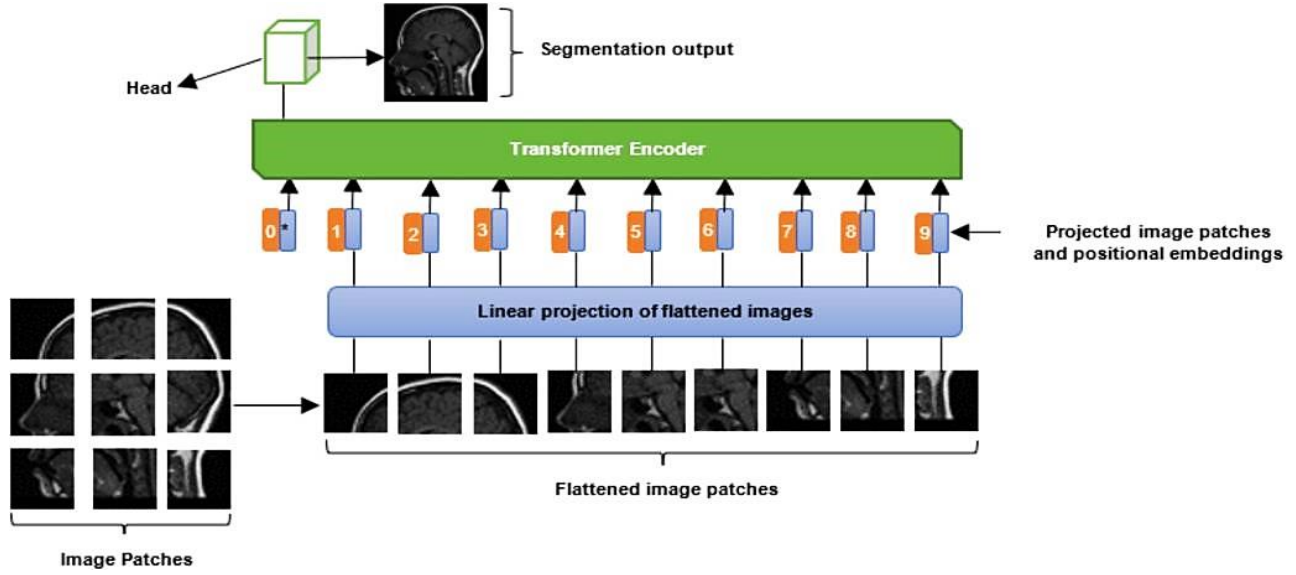


Fig. 3 Vision Transformers (ViT) model

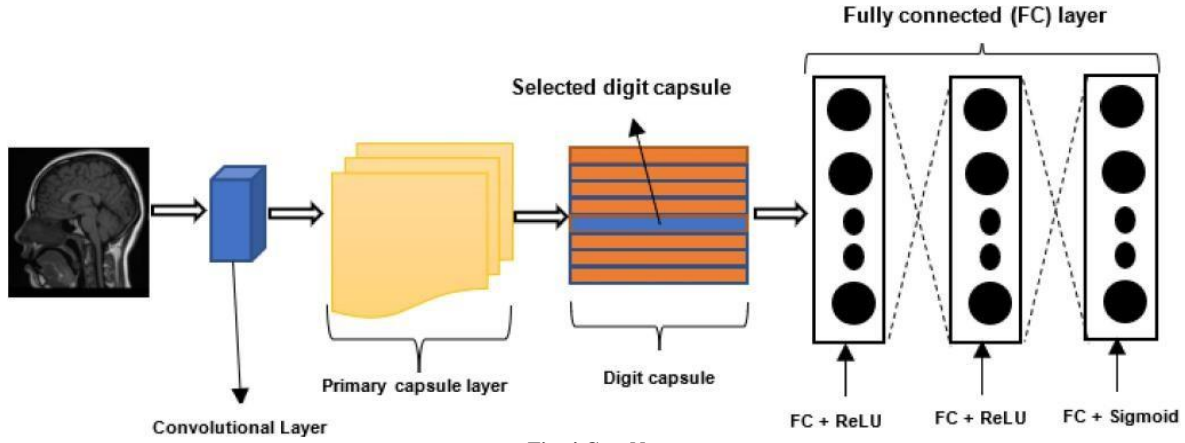


Fig. 4 CapsNet

2.4 Capsule Neural Networks

Despite the remarkable success of CNNs, they have some drawbacks. First, CNNs require vast datasets for training. Second, CNNs are typically not robust to affine rotations and transformations. Additionally, the routing mechanism employed by CNN's pooling layers is distinct from that employed by the human visual system. The CNN pooling layer routes all the information extracted from the image to all the neurons in the subsequent \times layer, neglecting essential details or little objects in the image. Hinton et al. designed the CapsNet to address the drawbacks of CNN. The general structure of a CapsNet is depicted in Figure - 4. A CapsNet is a three-layer network composed of the convolutional, primary capsule, and class capsule layers. The primary capsule layer is typically the first one, followed by an undetermined number of capsule layers. The class capsule layer follows the capsule layer. The convolutional layer extracts the feature and then transmits it to the primary capsule layer. The primary capsule performs a series of operations and transmits the resulting feature map to the digit

capsule. Typically, the digit capsule is composed of an $n \times m$ weight matrix, where n denotes the number of classes and m is the size of each digit capsule. The digit capsule is used to classify the input image before it is fed into the decoder. The decoder consists of three fully connected layers that are used to reconstruct or decode the selected digit capsule into an image.

Figure 3. Overview of a Vision Transformers (ViT) model. The image is partitioned into N small patches (e.g., 9 patches). Each image patch contains $n \times n$ pixels (e.g., 16×16 pixels). After partitioning, each image patch is flattened: each of the flattened image patches is fed into a linear projection layer to obtain a lower-dimensional linear embedding.

Moreover, positional embeddings are added to the sequence of image patches to ensure each image keeps its positional information. The input and position embedded sequences are fed into a standard transformer encoder for

training. The training can be conducted by an MLP or CNN head stacked on top of the transformer. The “*” symbol refers to an additional learnable (class) embedding that is appended to the sequence based on the position of the image patch. This class embedding is used to predict the class of an input image after self-attention updates it.

Figure 4. General scheme of a capsule neural network (CapsNet). A CapsNet is a three-layer network composed of the convolutional, primary capsule, and class capsule layers. The primary capsule layer is typically the first one, followed by an undetermined number of capsule layers. The class capsule layer follows the capsule layer. The convolutional layer extracts the feature and then transmits it to the primary capsule layer. The primary capsule performs a series of operations and transmits the resulting feature map to the digit capsule. CapsNet can recognize spatial and hierarchical relationships among objects in images. They are resistant to rotation and image transformations. Additionally, as shown in, CapsNet requires substantially less training data than CNN. Moreover, results reported in the literature show that CapsNet has the potential to improve the accuracy of CNN-based brain tumour diagnosis using a minimal number of network parameters.

It is worth noting that the pooling operation in CNNs makes them robust to small input transformations. However, for CNN to perform well, it must be trained on augmented data in terms of scale, rotation, and varying perspectives. Despite this, results reported in the literature indicate that, in some cases, CapsNet performs comparably to CNN models trained on augmented datasets. CapsNet does not need to be trained on large-scale or augmented data to produce excellent results. It makes it a suitable model for medical image datasets, which are typically small. For more information on CapsNet, please refer.

3. Literature Survey

Brain tumours can be located anywhere in the human brain and assume virtually any shape, size, or contrast (dissimilarity). It shows that ML-based solutions that can effectively and automatically classify and segment brain tumours are needed. The introduction of powerful computing devices and lower hardware prices have prompted the scientific community to develop numerous brain tumour segmentation and classification techniques. Some methods were designed with classical ML algorithms, while others were designed with CNN algorithms and CapsNet. This section reviews ML-based, CNN-based, CapsNet-based, and ViT-based brain tumour segmentation and classification techniques. These techniques are expected to assist medical practitioners in improving the accuracy and consistency of diagnosis.

3.1. Classical Machine Learning-Based Techniques

Numerous brain diagnostic systems have been developed using classical ML algorithms, including Support Vector Machines (SVMs), Random Forests (RFs), and k-Nearest Neighbor (kNN), to list a few. These algorithms are used alone or in combination with other ML algorithms or feature selection techniques. This section presents a survey of ML-based brain classification and segmentation techniques.

3.1.1. Brain Tumor Classification and Segmentation Using Hybrid Texture-Based Features

An image's texture is an important feature that can be used to identify different regions of interest. The texture of a region in an image is determined by the distribution of Gray levels across the image pixels. Jena et al. proposed a brain tumor classification and segmentation technique using texture features and multiple ML algorithms. The technique is divided into two stages: tumour classification and tumour segmentation. The MRI scans are pre-processed in the tumour classification stage, and texture features are extracted from the images using different texture extraction techniques. The following texture-based features were explored in the study: first-order statistical feature, Gray-level co-occurrence matrix (GLCM) feature, Gray-level run length matrix (GLRLM) feature, Histogram-oriented gradient (HOG) feature, Local binary patterns (LBP) feature, Cross-diagonal texture matrix (CDTM) feature, and simplified texture spectrum feature. All the features were extracted from 100 tumours and $100 \times$ non-tumour images. The extracted features were combined to form a feature vector matrix size 200 471. Subsequently, the feature vector matrix was used to train five ML algorithms: SVM, k-NN, binary decision trees, RF, and ensemble methods. The ensemble methods consist of seven algorithms: Adaboost, Gentleboost, Logitboost, LPboost, Robust-boost, RUSboost, and Totalboost. After training, the tumorous images were identified and used as input to a hybrid tumour segmentation technique designed in the study. The hybrid technique consists of k-NN and fuzzy C-means clustering algorithms. The hybrid technique was used to segment the tumour regions in the images. It was evaluated on two datasets based on the following performance metrics: average Dice similarity coefficient (DSC), average Jaccard similarity coefficient, and average accuracy. The dataset used to evaluate the model include BraTS2017, BraTS2019, and the Cancer Imaging Archive (TCIA). Experiments show that the ensemble methods produced the best result, achieving a classification accuracy of 96.98% and 97.01% for BraTS2017 + TCIA and BraTS2019 + TCIA, respectively. RF produced the second-best result, achieving an accuracy of 96.5% and 96.99% for BraTS2017 + TCIA and BraTS2019 + TCIA, respectively. The results also show that the segmentation technique produced a Dice similarity score and accuracy of 90.16% and 98.4%, respectively, for BraTS2017.

3.1.2. Brain Tumor Classification Using GoogleNet Features and ML

Sekhar et al. proposed a tumor classification model using a modified GoogleNet pre-trained CNN model and two ML algorithms: SVM and k-NN. In the study, the last three fully connected layers of the GoogleNet network were modified and fine-tuned on brain tumour images. After fine-tuning, the 1024 feature vector from the previous average pooling layer was extracted and used to train SVM and k-NN classifiers. The technique was evaluated on the CE-MRI dataset containing 3064 T₁w post-GBCA brain MR images from 233 patients. Experimental results show that GoogleNet produced precision and recall of 96.02% and 97.00% for glioma, respectively, using the softmax activation function. The model's performance was improved by over 2.5% when the SVM classifier was used. It achieved precision and specificity of 98.76% and 98.93% for glioma, respectively. The performance of GoogleNet was also improved by over 2.3% when the k-NN classifier was used. It produced

precision and specificity of 98.41% and 98.63% for glioma, respectively. It shows that features extracted from pre-trained CNN models can be used to build effective ML-based classifiers.

4. Methodology

This review includes papers published between 2019 and 2022. A few studies that were published before 2019 are also covered in this paper. Specifically, we focused on papers that developed brain tumor classification and segmentation approaches using ML, CNN, CapsNet, and ViT. The following databases for scientific literature were queried to find relevant articles: PubMed, Google Scholar, and ScienceDirect. We also queried the online database of the Multidisciplinary Digital Publishing Institute (MDPI) for journal articles. The following search terms were used for our queries: a brain tumor, segmentation, classification, and DL.

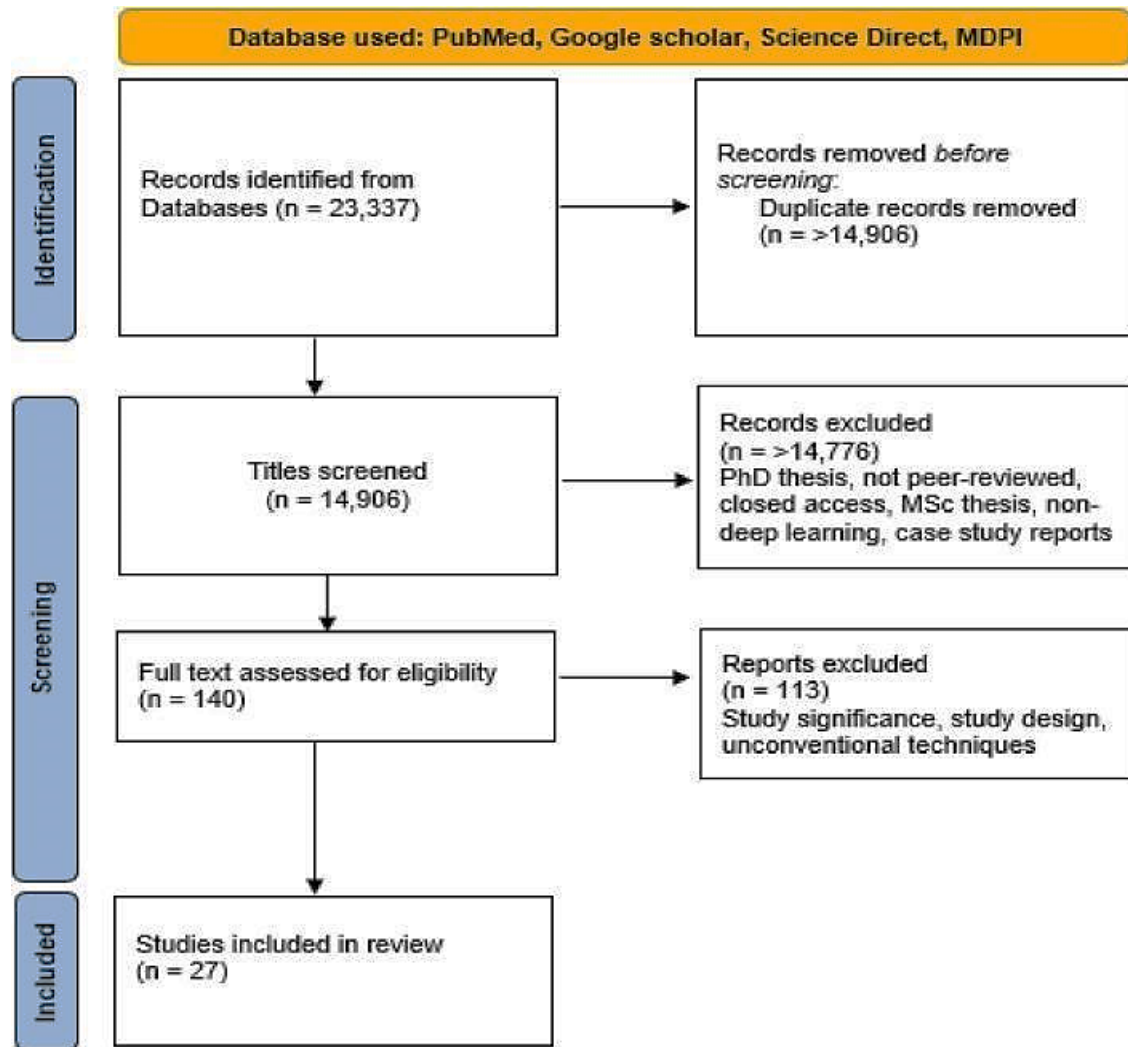


Fig. 5 Preferred Reporting Items for Systematic Reviews and Meta-Analyses (PRISMA) diagram of the proposed review on AI applications to brain tumour MRI

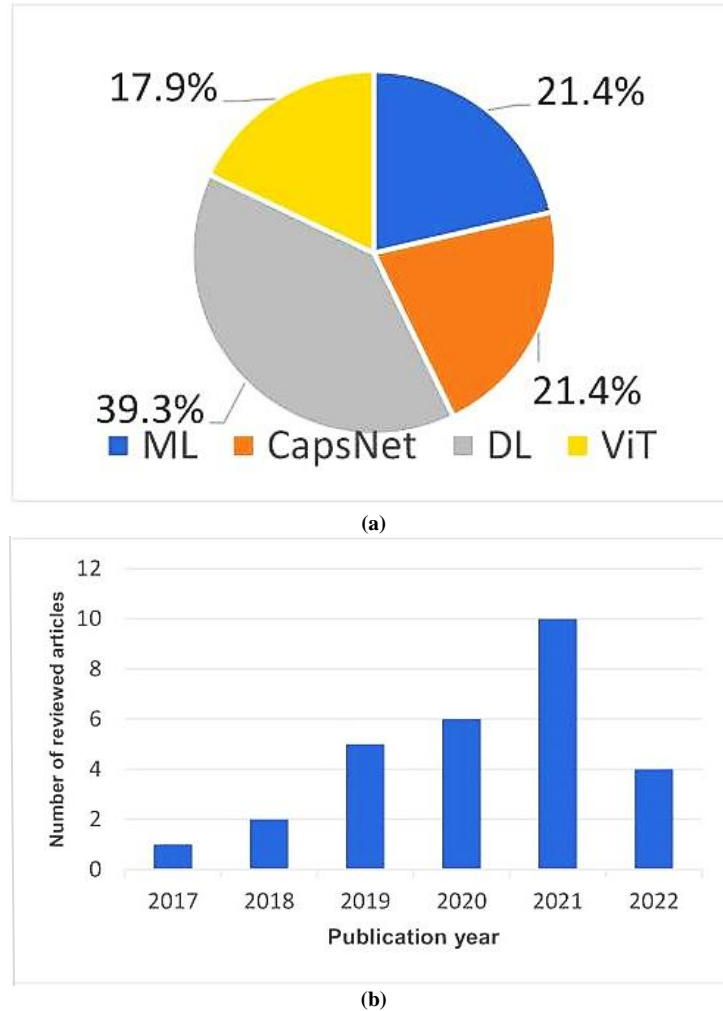


Fig. 6 Percentage of Articles reviewed for this study (a) Segmentation approaches wise (b) Year wise

In addition, the union of the outlined search terms was used with a set of terms relating to DL brain tumor segmentation and classification, including classic machine learning, convolutional neural networks, capsule networks, and transformers. The following inclusion criteria were used in this survey: conventional brain segmentation and classification techniques, deep learning, capsule networks, vision transformers, MRI images, and peer-reviewed. Ph.D. theses, M.Sc. theses, and case study papers were excluded from this study. Figure 5 shows the Preferred Reporting Items for Systematic Reviews and Meta-Analyses (PRISMA) diagram used for this survey. Figure 6 a and b illustrates the percentage of articles reviewed in this study and their publication year, respectively.

4.1. Datasets

The 3064 MRI T₁w post-GBCA images from 233 patients were used. The Medical Image Computing and Computer-Assisted Intervention (MICCAI) Society has funded numerous events and open challenges over the years to stimulate the development of DL tools and medical devices

for computer-aided diagnosis. Most studies used the datasets provided by the MICCAI Society to evaluate the efficiency of their techniques. Details of the other datasets are also shown in Table 1. As shown in the table, most of the benchmark datasets are small, making it challenging to build DL models from end to end.

4.2. Image Pre-Processing Techniques

Image pre-processing techniques can be used to improve the performance of DL-based techniques. Thaha et al. introduced a skull stripping and image enhancement technique for image pre-processing. Skull stripping removes signals from outside the brain, removing unwanted information and facilitating learning tasks. Image enhancement techniques are also utilized to further increase the image's quality, allowing for identifying essential features in the image. Sérgio et al. introduced an intensity normalization technique for image pre-processing. Results obtained in the study showed that intensity normalization combined with data augmentation produced good results.

One of the key challenges researchers face applying quantitative analyses to MRI scans is the presence of background interference, such as thermal noise and scanner-related artifacts. Thermal noise is typically triggered by random fluctuations within the MRI system, radiofrequency coils in the MRI scanner, and small movements of the patient during the scanning process. The presence of noise in an MR scan can reduce the quality of the image.

Training a CNN on noisy images can affect its ability to effectively extract tumour-related features, consequently affecting its accuracy and generalization performance. In view of this, some studies adopted denoising and contrast enhancement as pre-processing steps to improve the quality of MRI scans before training CNN models. Some studies also developed other techniques for reducing noise in MR images, including modified median noise filter, Wiener filter, and non-local means approach. More robust and effective denoising techniques are still required.

4.3. Performance Metrics

Several metrics were used to evaluate the performance of ML and DL techniques. Most studies used the Dice similarity coefficient to evaluate the performance of brain tumour segmentation techniques. The coefficients determine the amount of spatial overlap between the ground truth segmentation (X) and the network segmentation (Y). Some studies used average Hausdorff Distance for brain tumor segmentation. Many studies used classification accuracy, precision (or recall), sensitivity, and specificity to evaluate brain tumour classification

4.4. Classification

4.4.1. Convolutional Neural Network (CNN)

CNNs are a sort of deep learning system that uses a grid-like structure to process data. CNNs are a form of deep learning algorithm used to handle data related to space or time. CNNs are similar to other neural networks, but because they use a succession of convolutional layers, they add a layer of complexity. Convolutional layers are an essential part of Convolutional Neural Networks (CNNs). A typical CNN architecture is depicted in the diagram below,

Image identification and classification tasks frequently employ CNNs. CNNs can be used to recognize objects in an image or to classify an image as a cat or a dog, for example. CNNs can also be used to perform more complicated tasks, such as creating visual descriptions or recognizing image points of interest. CNNs can also be used to analyse time-series data like audio or text. CNNs are a strong deep learning tool that delivers cutting-edge outcomes in various applications.

The following are definitions for the various layers in the architecture depicted above:

Convolutional Layer

Convolutional layers are made up of a group of filters (also known as kernels) applied to an input image. A feature map represents the input image with the filters applied as the convolutional layer's output. Layers of convolutional neural networks can be stacked to produce more complicated models that can learn more intricate features from photos.

Pooling Layer

In deep learning, pooling layers are a sort of convolutional layer. The spatial size of the input is reduced by pooling layers, making it easier to process and needing less memory. Pooling also reduces the number of parameters and speeds up the training process. Pooling can be divided into two types: maximum pooling and average pooling. The maximum value from each feature map is used in max pooling, while the average value is used in average pooling. After convolutional layers, pooling layers are often employed to minimise the input size before it is fed into a fully connected layer.

Fully Connected Layer

In a convolutional neural network, fully-connected layers are one of the most fundamental layers (CNN) types. Each neuron in a fully-connected layer is entirely coupled to every other neuron in the previous layer, as the name implies; when the goal is to take the information learnt by the preceding layers and apply them to produce predictions, fully linked layers are often utilized near the conclusion of a CNN.

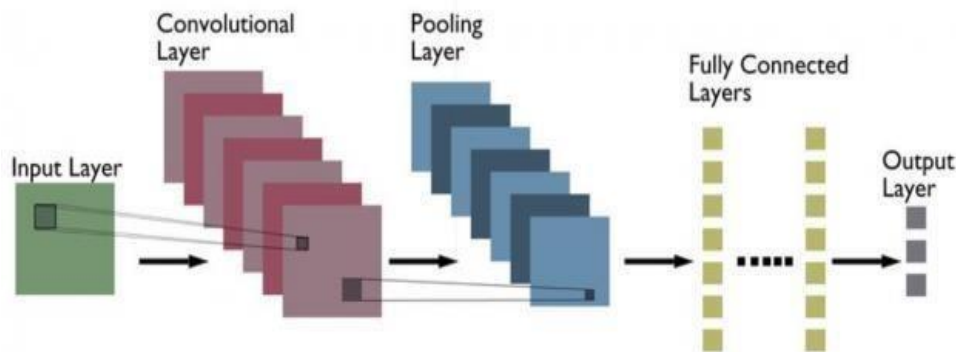


Fig. 7 CNN Architecture

Layer (type)	Output Shape	Param #
conv2d_1 (Conv2D)	(None, 65, 65, 32)	416
conv2d_2 (Conv2D)	(None, 65, 65, 32)	4128
batch_normalization_1 (Batch Normalization)	(None, 65, 65, 32)	128
max_pooling2d_1 (MaxPooling2D)	(None, 32, 32, 32)	0
dropout_1 (Dropout)	(None, 32, 32, 32)	0
conv2d_3 (Conv2D)	(None, 32, 32, 64)	8256
conv2d_4 (Conv2D)	(None, 32, 32, 64)	16448
batch_normalization_2 (Batch Normalization)	(None, 32, 32, 64)	256
max_pooling2d_2 (MaxPooling2D)	(None, 16, 16, 64)	0
dropout_2 (Dropout)	(None, 16, 16, 64)	0
flatten_1 (Flatten)	(None, 16384)	0
dense_1 (Dense)	(None, 512)	8389120
dropout_3 (Dropout)	(None, 512)	0
dense_2 (Dense)	(None, 2)	1026
Total params: 8,419,778		
Trainable params: 8,419,586		
Non-trainable params: 192		

Fig. 8 Layers that are used in our model (II) Prediction

It is a method of predicting Brain Tumours from a dataset. This project will effectively predict data from the dataset by improving the overall prediction outcomes.

4.5. Result Generation

The overall prediction will be used to create the Final Result. Some measures, such as accuracy, are used to evaluate the performance of this proposed approach.

CNN accuracy is : 86.44067645072937 % - 99.98620748519897 % Confidence This is its a Tumor

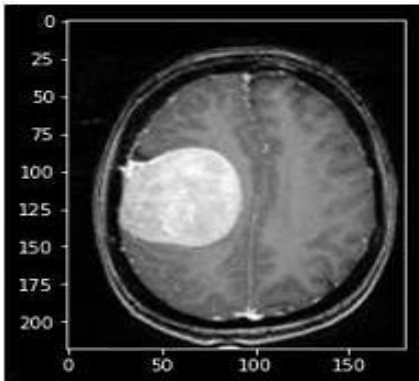


Fig. 9 The accuracy and result for the given input image

It will show the accuracy and result for the given input image (i.e.) whether that selected image has a brain tumor or not.

4.6. Experimental Results

The effectiveness of the proposed technique is assessed using accuracy.

4.6.1. Accuracy

One parameter for evaluating the classification model is accuracy. Accuracy is defined as the ratio of the total number of correct predictions to the total number of predictions.

$$\text{Accuracy} = \frac{TP+TN}{TP+TN+FN+FP}$$

Where,

TP(true positive) is the total number of images correctly classified.

TN(true negative) is the number of images correctly classified but not belonging to that class.

FP(false positive) is the number of images misclassified to some other classes.

FN(false negative) is the number of images belonging to one class but misclassified to another.

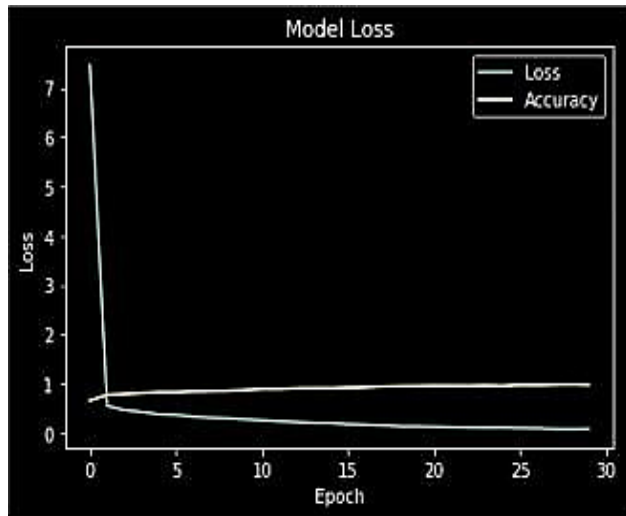


Fig. 10 Graph for accuracy and loss

The accuracy and loss graph denotes the below figure 10.

Here X-axis represents the number of training epochs, and Y-axis represents the model's loss.

5. Conclusion

A two-step approach for detecting brain tumour tissue was introduced in this process. The thresholding approach is combined with using a shape descriptor in this method. The thresholding algorithm groups picture pixels in the first phase, after which the image is binaries using a threshold value. Although tumour structures are formed in binary elements, they are frequently surrounded by healthy structures. The second step eliminates non-tumour tissues, only detecting those corresponding to the tumour. The CNN algorithm can be used to classify MRI images. It will improve the accuracy of brain tumor diagnosis.

References

- [1] L. M. De Angelis, "Brain Tumors," *The New England Journal of Medicine*, vol. 344, no. 2, pp. 114-123, 2001. *Crossref*, <https://doi.org/10.1056/nejm200101113440207>
- [2] Stewart BW, and C. P. Wild, "World Cancer Report 2014," Lyon, France: IARC Publications, 2014.
- [3] A.Ratna Raju, P.Suresh, and R.Rajeswara Rao, "Recent Advancements in the Automatic Detection and Segmentation of GBMs from Multimodal Brain MRI Images," *SSRG International Journal of Computer Science and Engineering*, vol. 2, no. 12, pp. 19-23, 2015. *Crossref*, <https://doi.org/10.14445/23488387/IJCSE-V2I12P105>
- [4] Brain, Other CNS and Intracranial Tumours Statistics, 2019. [Online]. Available: <https://www.cancerresearchuk.org/>
- [5] Anthony Behin et al., "Primary Brain Tumours in Adults," *Lancet*, vol. 361, no. 9354, pp. 323-331, 2003.
- [6] Fareed M.mohammed, Mustafa M.Essa, and Ahmed W. Maseer, "Comparison between MRI And CT-Scan in Diagnosis the Brain Tumor Images," *SSRG International Journal of Medical Science*, vol. 6, no. 5, pp. 1-4, 2019. *Crossref*, <https://doi.org/10.14445/23939117/IJMS-V6I5P101>
- [7] Antonios Drevelegas, "Imaging of Brain Tumors with Histological Correlations," Berlin, Germany: Springer, 2002.
- [8] T. Gayathri, and K. Sundeep Kumar, "AlexNet – Adaptive Whale Optimization – Multiclass Support Vector Machine model for Brain Tumour Classification," *International Journal of Engineering Trends and Technology*, vol. 70, no. 5, pp. 309-316, 2022. *Crossref*, <https://doi.org/10.14445/22315381/IJETT-V70I5P234>
- [9] Geert Litjens et al., "A Survey on Deep Learning in Medical Image Analysis," *Medical Image Analysis*, vol. 42, pp. 60-88, 2017. *Crossref*, <https://doi.org/10.1016/j.media.2017.07.005>
- [10] M. L. Goodenberger, and R. B. Jenkins, "Genetics of Adult Glioma," *Cancer Genetics*, vol. 205, no. 12, pp. 613-621, 2012. *Crossref*, <https://doi.org/10.1016/j.cancergen.2012.10.009>
- [11] D.Napoleon, and M.Praneesh, "Detection of Brain Tumor Using Kernel Induced Possiblistic C-Means Clustering," *International Journal of Computer Organization Trends and Technology*, vol. 3, no. 5, pp. 40-42, 2013.
- [12] David N Louis et al., "The 2016 World Health Organization Classification of Tumors of the Central Nervous System: A Summary," *Acta Neuropathol*, vol. 131, no. 6, pp. 803-820, Jun. 2016.
- [13] Dheeraj D, and Prasantha H S, "DR-UNET: A Hybrid Model For Classification of G lioma using Transfer Learning on MR Images," *International Journal of Engineering Trends and Technology*, vol. 69, no. 10, pp. 146-150, 2021. *Crossref*, <https://doi.org/10.14445/22315381/IJETT-V69I10P218>
- [14] Christopher M. Bishop, "Pattern Recognition and Machine Learning," Berlin, Germany: Springer-Verlag, 2006.
- [15] Sindhia et al., "Brain Tumor Detection Using MRI by Classification and Segmentation," *SSRG International Journal of Medical Science*, vol. 6, no. 3, pp. 12-14, 2019. *Crossref*, <https://doi.org/10.14445/23939117/IJMS-V6I3P103>
- [16] T. Rajesh, and R. Suja Mani Malar, "Rough Set Theory and Feed Forward Neural Network Based Brain Tumor Detection in Magnetic Resonance Images," *International Conference on Advanced Nanomaterials & Emerging Engineering Technologies*, pp. 240-244, 2013. *Crossref*, <https://doi.org/10.1109/ICANMEET.2013.6609287>
- [17] Narendra Mohan, "Tumor Detection From Brain MRI Using Modified Sea Lion Optimization Based Kernel Extreme Learning Algorithm," *International Journal of Engineering Trends and Technology*, vol. 68, no. 9, pp. 84-100, 2020. *Crossref*, <https://doi.org/10.14445/22315381/IJETT-V68I9P214>

- [18] K. Machhale et al., "MRI Brain Cancer Classification Using Hybrid Classifier (SVM- KNN)," *International Conference on Industrial Instrumentation and Control (ICIC)*, pp. 60–65, 2015.
- [19] Nidhi Mongoriya, and Vinod Patel, "Review The Breast Cancer Detection Technique Using Hybrid Machine Learning," *SSRG International Journal of Computer Science and Engineering*, vol. 8, no. 6, pp. 5-8, 2021. *Crossref*, <https://doi.org/10.14445/23488387/IJCSE-V8I6P102>
- [20] M. Shasidhar, Sudheer raja Venishetty, and B. Vijaya Kumar, "MRI Brain Image Segmentation Using Modified Fuzzy C-Means Clustering Algorithm," *Communication Systems and Network Technologies (CSNT), IEEE, Explore*, pp. 473–478, 2011. *Crossref*, <http://dx.doi.org/10.1109/CSNT.2011.102>
- [21] K. Aravinth Raaj, B. Joel Sherwin, and S. Sabeetha Saraswathi, "Automated Detection of Abnormalities in Chest X-Ray Images Using Convolutional Neural Networks," *International Journal of P2P Network Trends and Technology*, vol. 8, no. 2, pp. 18-24, 2018. *Crossref*, <https://doi.org/10.14445/22492615/IJPTT-V8I2P404>
- [22] Goswami, S, and Lalit Kumar P. Bhैया, "Brain Tumour Detection Using Unsupervised Learning Based Neural Network," *2013 International Conference on Communication Systems and Network Technologies, IEEE Explore*, pp. 573–577, 2013.
- [23] P.Kanmani, Dr.P.Marikkannu, and M.Brindha, "A Medical Image Classification using ID3 Classifier," *SSRG International Journal of Computer Science and Engineering*, vol. 3, no. 10, pp. 8-11, 2016. *Crossref*, <https://doi.org/10.14445/23488387/IJCSE-V3I10P105>
- [24] S. Khalid, Tehmina Khalil, and Shamila Nasreen, "A Survey of Feature Selection and Feature Extraction Techniques in Machine Learning," *Science and Information Conference*, pp. 372–378, 2014.
- [25] L. Deng, and D. Yu, "Deep Learning: Methods and Applications," *Foundations and Trends in Signal Processing*, vol. 7, no. 3–4, pp. 197–387, 2013.
- [26] Y. Lecun, Lenet-5, Convolutional Neural Networks, 2015. [Online]. Available: <http://yann.lecun.com/exdb/lenet>
- [27] M. Matsugu, K. Mori, Y. Mitari, and Y. Kaneda, "Subject Independent Facial Expression Recognition with Robust Face Detection Using a Convolutional Neural Network," *Neural Networks*, vol. 16, no. 5–6, pp. 555–559, 2003. *Crossref*, [https://doi.org/10.1016/S0893-6080\(03\)00115-1](https://doi.org/10.1016/S0893-6080(03)00115-1)
- [28] Y. Lecun, Y. Bengio, and G. Hinton, "Deep Learning," *Nature*, vol. 521, no. 7553, p. 436, 2015. *Crossref*, <https://doi.org/10.1038/nature14539>
- [29] Ibrahima Sory keita et al., "Classification of Benign and Malignant MRIs using SVM Classifier for Brain Tumor Detection," *International Journal of Engineering Trends and Technology*, vol. 70, no. 3, pp. 234-240, 2022. *Crossref*, <https://doi.org/10.14445/22315381/IJETT-V70I2P226>
- [30] Y. Lecun et al., "Gradient-Based Learning Applied to Document Recognition," *IEEE*, vol. 86, no. 11, pp. 2278–2324, 1998. *Crossref*, <https://doi.org/10.1109/5.726791>
- [31] A. Krizhevsky, I. Sutskever, and G. E. Hinton, "Imagenet Classification with Deep Convolutional Neural Networks," *Advances in Neural Information Processing Systems 25 (NIPS 2012)*, pp. 1097–1105, 2012.
- [32] Evangelia I Zacharakis et al., "Classification of Brain Tumor Type and Grade Using MRI Texture and Shape in a Machine Learning Scheme," *Magnetic Resonance in Medicine*, vol. 62, no. 6, pp. 1609–1618, 2009. *Crossref*, <https://doi.org/10.1002/mrm.22147>
- [33] T. Tamilselvi et al., "Deep Derma Scan: A Proactive Diagnosis System for Predicting Malignant Skin Tumor with Deep Learning Mechanisms," *International Journal of Engineering Trends and Technology*, vol. 70, no. 8, pp. 310-317, 2022. *Crossref*, <https://doi.org/10.14445/22315381/IJETT-V70I8P232>
- [34] El-Sayed AhmedEl-Dahshan et al., "Hybrid Intelligent Techniques for MRI Brain Images Classification," *Digital Signal Processing*, vol. 20, no. 2, pp. 433–441, 2010. *Crossref*, <https://doi.org/10.1016/j.dsp.2009.07.002>
- [35] Jun Cheng et al., "Enhanced Performance of Brain Tumor Classification via Tumor Region Augmentation and Partition," *PLOS ONE*, vol. 10, no. 10, 2015. *Crossref*, <https://doi.org/10.1371/journal.pone.0140381>
- [36] Rohan K. Gajre, Savita A. Lothe, and Santosh G. Vishwakarma, "Identification of Brain Tumor using Image Processing Technique: Overviews of Methods," *SSRG International Journal of Computer Science and Engineering*, vol. 3, no. 10, pp. 48-52, 2016. *Crossref*, <https://doi.org/10.14445/23488387/IJCSE-V3I10P114>
- [37] Mehmet Günhan Ertosun, and Daniel L Rubin, "Automated Grading of Gliomas Using Deep Learning in Digital Pathology Images: A Modular Approach with Ensemble of Convolutional Neural Networks," *AMIA Annual Symposium proceedings*, vol. 2015, pp. 1899–1908, 2015.
- [38] J. S. Paul et al., "Deep Learning for Brain Tumor Classification," *Biomedical Applications in Molecular, Structural, and Functional Imaging*, vol. 10137, 2017. *Crossref*, <https://doi.org/10.1117/12.2254195>
- [39] ZENG Runhua, and ZHANG Shuqun, "Improving Speech Emotion Recognition Method of Convolutional Neural Network," *International Journal of Recent Engineering Science*, vol. 5, no. 3, pp. 1-7, 2018. *Crossref*, <https://doi.org/10.14445/23497157/IJRES-V5I3P101>

- [40] Parnian Afshar, Konstantinos N. Plataniotis, and Arash Mohammadi, "Capsule Networks for Brain Tumor Classification Based on MRI Images and Course Tumor Boundaries," *ICASSP 2019 - 2019 IEEE International Conference on Acoustics, Speech and Signal Processing (ICASSP)*, 2019.
- [41] AminKabir Anaraki, Moosa Ayati, and Foad Kazemi, "Magnetic Resonance Imaging Based Brain Tumor Grades Classification and Grading Via Convolutional Neural Networks and Genetic Algorithms," *Biocybernetics Biomedical Engineering*, vol. 39, no. 1, pp. 63–74, 2019. *Crossref*, <https://doi.org/10.1016/j.bbe.2018.10.004>



APPLICATION OF PROBABILITY BASED SURPRISING MEASURE IN OUTLIER DETECTION

A.M.Rajeswari¹, B.Subbulakshmi², M.Nirmaladevi³ and M.Sivakumar⁴

¹ Associate Professor, Department of Computer Science and Engineering, Velammal College of Engineering and Technology, Madurai, India
amrtce@gmail.com

² Assistant Professor, Department of Computer Science and Engineering, Thiagarajar College of Engineering, Madurai, India.
bscse@tce.edu

³ Assistant Professor, Department of Computer Science and Engineering, Thiagarajar College of Engineering, Madurai, India.
nirmaladevi2004@gmail.com

⁴ Associate Professor, Department of Computer Science and Engineering, Thiagarajar College of Engineering, Madurai, India.
mskcse@tce.edu.

Article History: Received: 12.05.2023

Revised: 25.05.2023

Accepted: 05.06.2023

Abstract

Outlier detection was instigated as noise removal technique for enhancing the prediction accuracy of Machine Learning (ML) algorithms. In due course, outlier detection emerged as the phenomenon of mining rare/alarming patterns to assist in decision making process. Outliers can be point or collective types and can be detected by the supervised and unsupervised ML algorithms. Such algorithms have the probability of missing out certain point or collective outliers in high dimensional quantitative data. To overcome the aforementioned issue, this work proposes a Semi Supervised Outlier Detection (SSOD) algorithm with a probability based surprising measure 'Lift' for outlier detection. The performance proposed SSOD is benchmarked with the existing outlier detection ML algorithms. By studying performance of the algorithms, it is understood that the proposed SSOD with Lift measure outperforms the benchmarked ML algorithms.

1. Introduction

Outliers are the rare observations as in the case of weak performers in education data, ozone days in weather data, hike or dip in the shares sold in the stock market data, fatal cases in accident data, malignant cases in cancer data, etc. These rare occurring events always used to tip off the system or domain experts. Identifying such outliers will give an alarm and help in

taking the required precautionary measures. Based on the outlier score the rare observations will be weak outliers (noise) or strong outliers (help in decision making). "Usually, Noise possesses less outlier score than the actual Outliers [1]". Hence it makes a clear statement that identifying the outlier score of every observations is a must to segregate the rare cases from the normal observations and noise. Most of the existing works made

use of subjective measures [2], [3], [4], [5], [6] to detect the outliers in various domains, where the researcher considered the nature of the data along with their objective. The subjective measurements [7] require user interaction such as setting the threshold value for the measurement in order to prune outliers and, therefore, will be domain specific and dependent on the domain expert. But the proposed work contribute to fix a common objective measure (based only on the probability of occurrence of data) which can be suitable for pruning the outliers in a wide set of applications without user's interaction. Such a common measure to prune outliers is 'Lift' which is classified as 'Surprising measure' [7]. "Lift is used to measure the independency among the unexpected correlated item. The unexpected correlated items with high Lift value (one and above) represents the rare items (the nature of the outliers)" [8].

Outliers may be point (single occurrences here and there) or collective (occur in small group) outliers. The occurrence of ozone days in weather data, the pre-diabetic conditions of the patients in diabetes data and the hike, dip in the returns of the stock market are example of point outliers [9]. The occurrence of malignant cases in cancer data and weak performers in the examinations of education data falls under the collective outliers. The figure 1 gives the clear picture of these types of outliers.

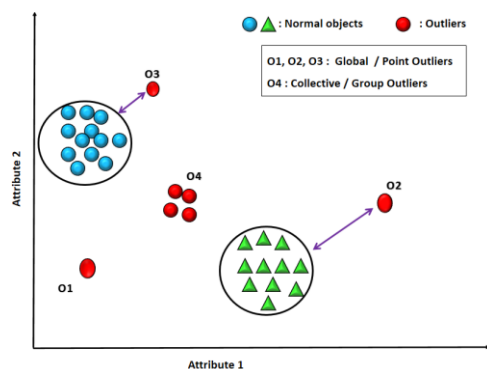


Figure 1. Types of Outliers.

classification (supervised) and clustering (unsupervised) are well suitable for detecting outliers based on single dimension, they will miss certain small groups of collective outliers like 'O4' in figure 1 and point outliers like 'O1', 'O2' and 'O3' of figure 1 in high dimensional data. A best suitable approach for detecting such outliers in high dimensional quantitative data is correlation based technique. A well-known correlation based approach is Association Rule Mining (ARM) [10], [11] an unsupervised learning algorithm.

The proposed method - SSOD (Semi Supervised Outlier Detection) makes use of the hybrid version of ARM (unsupervised) and classification (supervised) techniques and can be called as Associative Classification technique. The proposed SSOD algorithm make use of the class label only during the rule generation phase and not during the infrequent pattern generation phase. Since, the proposed associative classifier does not use the class label (target attribute) during the pattern generation phase we claim that this is a semi supervised based learning approach. By doing so, the algorithm will not miss the point outliers and also the small groups of collective outliers in multi-dimensional, multi-labeled and imbalanced database like stock market data. The performance of proposed method – SSOD along with the surprising measure 'Lift' in outlier detection is examined along with various conventional supervised and unsupervised outlier detection algorithms. The proposed method - SSOD found to outperform the benchmarked algorithms by detecting more precise outliers.

The rest of the manuscript is structured to have part 2 addresses the related work. Section 3 provides a detailed description of the preliminaries required to implement the proposed methodology. Section 4 deals with the algorithm and Section 5 details

the experiments performed with the proposed methodology - SSOD. Lastly, in Section 6, the proposed work has been summarized.

2. Related Work

When the databases have an adequate amount of normal and outlier samples then the supervised data mining algorithms will be used to detect outliers. In this supervised approach, the model is generated from the existing samples and based on this model the outliers can be identified. The samples if it is not perfect then outlier detection will be at risk. Similarly, to detect outliers, the unsupervised ML algorithms require number of clusters (groups) as user input and a proper measure with accurate threshold value from the domain experts to identify the outliers from the normal objects. For this reason, the proposed SSOD method adopts the semi-supervised associative classification technique and the surprising measure - Lift to extract outliers without any value defined by the user.

The mining of association rules (Apriori algorithm) is the first and most frequent pattern-based mining technique [10], [11]. Initially, this method was introduced to investigate the correlation between elements which frequently occur together. Subsequently, its application concentrates on the study of the correlation between infrequent elements as well. An algorithm called RARM [12] was proposed by Romero et al., to detect infrequent student behaviour and activities in an online learning environment by generating sets of rare items. The authors compared RARM performance with existing algorithms such as Apriori-Infrequent, Apriori-Reverse, and Apriori Rare. Unexpected temporal association rules are generated by an approach based on frequent models to alert equity market systems [3]. In this work, the normal behavior of objects in the stock exchange database is discovered with the help of Temporal Association Rules

(TAR). Then, the relationship between the characteristics of these rules over time is identified using quasi-functional dependency and, finally, a predefined measurement called "degree of dependency" is used to extract outliers. Also, the stock splits that occur during a particular period that alert the stakeholders for their investment were identified using TAR with 'residual leverage' as the pruning measure [2]. Unexpected episodes to detect the adverse drug reaction in the medical domain were identified using TAR [4], [5], [6]. Preetha et al., came up with a non-parametric FP-Growth algorithm to detect outliers [13]. All of the above work was performed with pre-defined fixed threshold values for all interesting measurements used to extract outliers.

Recent studies show that associative classification is spontaneous, effectual and has good classification accuracy [14], [15]. This method considers the rules with the highest confidence for classification. In imbalanced class distribution, the class rules which cover the minor groups are missed in classification technique due to the presence of least supportable classes. But Associative classification can generate Class Association Rules (CARs) which is supportable within the class rather than in the whole database [15], [16]. Thus it can generate a complete set of rules for classification.

3. Preliminaries

This section describes the basic requirements like the dataset considered for evaluation and the interesting measures that are used to detect the outliers by the proposed method.

3.1. Dataset used

In our previous work [9], we have shown that the detection of outliers by existing supervised and unsupervised machine learning algorithms falls short. Data sets such as Pima Indian Diabetes Dataset [17],

Education Dataset (our Student Department Data), Yahoo Finance Stock Market Dataset [18] are reviewed and

evaluated in our work [9]. The same data set is used for the assessment of the proposed methodology – SSOD.

Table 1. Specifications of the benchmark datasets

Database Name	Size	Dimensions	No of Classes	Classes	Imbalanced distribution of instances	Type of Outliers present
PIMA Indian Diabetes	768	9	2	Yes	500	Point and
				No	178	Point and Collective
Education	155	10	2	Pass	138	Point and
				Fail	16	Point
Stock Market	293	5	5	Volume1	212	Collective
				Volume2	14	Point
				Volume3	24	Point
				Volume4	19	No
				Volume5	24	Point

3.2. Interesting Measures used to extract outliers

The interesting measure used to prune the infrequent patterns from other patterns is ‘Support’. Support indicates the number of times the model has been found in the database. Support for the "A" model in the "D" database is computed as in equation 1.

$$\text{Support}(A) = \frac{P(A)}{|D|} \quad (1)$$

The measures that are used to extract the exceptional rules, ie., the infrequent CARs are ‘Rule Support’ and ‘Rule Confidence’. The exceptional CAR is of the form $A \rightarrow C$ [Support%, Confidence%]

which implies that, the likelihood of occurrence of ‘A’ set of patterns in class ‘C’ of the database ‘D’. The support and confidence values for the rule $A \rightarrow C$ are defined as in equations 2 and 3 respectively.

$$\text{Support}(A \rightarrow C) = \frac{P(A \wedge C)}{|D|} \quad (2)$$

$$\text{Confidence}(A \rightarrow C) = \frac{P(A \wedge C)}{P(A)} \quad (3)$$

Finally the interesting measure that is used to extract outliers from infrequent CAR is ‘Lift’. “Rare item sets with low counts (low probability) which per chance occur a few times (or only once) together can produce enormous lift values” [7]. This nature – ‘the enormous value’ of the Lift measure motivated us to generate the rare item sets by making use of it. The lift value for the infrequent CAR, $A \rightarrow C$ is defined as in equation 4.

$$\text{Lift}(A \rightarrow C) = \frac{P(A \wedge C)}{P(A) \wedge P(C)} \quad (4)$$

Outliers extracted by lift measurement from infrequently occurring CARs are assessed by the measurement called Coverage and Accuracy [19]. Let N_{COVERS} be the number of instances in the database ‘D’ covered by the LHS of exceptional CAR ie., the support(A) and N_{CORRECT} be the number of instances correctly classified by the exceptional CAR. The Coverage and Accuracy of the rule is computed as

per the equation 5 and equation 6 respectively.

$$\text{Coverage } (A \rightarrow C) = \frac{N_{\text{COVERS}}}{|D|} \quad (5)$$

$$\text{Accuracy } (A \rightarrow C) = \frac{N_{\text{COVERS}}}{N_{\text{CORRECT}}} \quad (6)$$

All the association technique based works discussed in the section 2 have used user defined thresholds for all the interesting measures to extract the rules. For assigning the pre-defined thresholds values for the measures, either prior knowledge about the data or domain experts' guidance is required. Also, threshold values are domain specific and vary for every application. Even the size of the data will cause change in the threshold values. Consequently, the proposed method generates threshold values for interesting measurements like Support and Lift

dynamically [20] depending on the data distribution. By doing so it is observed that the threshold values of the measures vary for different databases.

3.3. Understand outliers and their type in benchmark data sets.

The box plot is the best statistical visualization technique for interpreting outlier presence [21]. Consequently, an analysis of the plots was conducted on the datasets to be assessed. The outlier type present in these data sets is analyzed using the box plot. Figure 2 presents the analytical report for the box plot. In Figure 2, the presence of bubbles in the upper and lower whiskers of the cell indicates the presence of outliers. The emergence of bubbles in a group or points can be interpreted as collective and global outliers respectively.

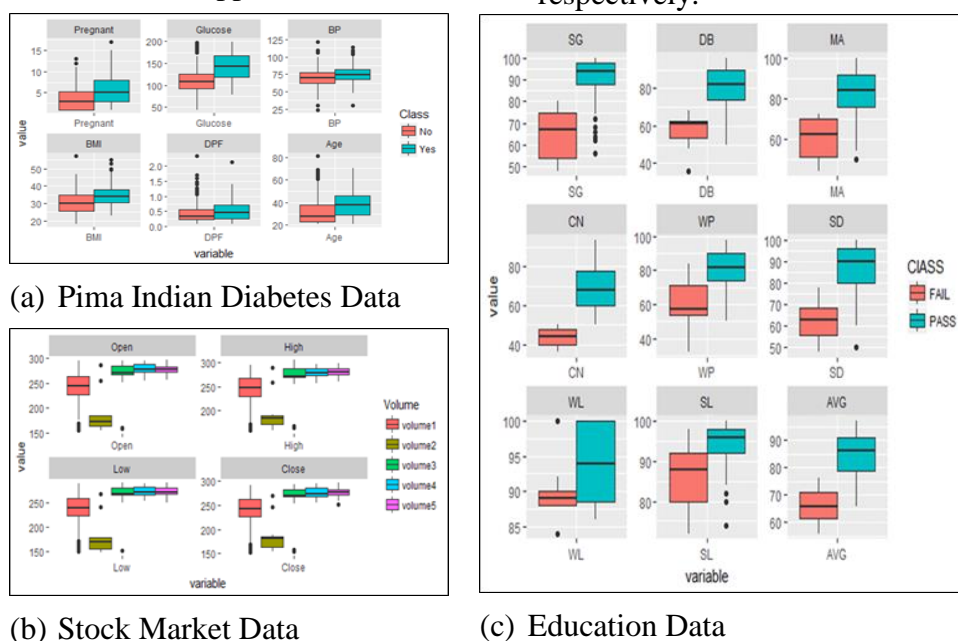


Figure 2. Analysis of outliers in the datasets examined for evaluation.

4. The Proposed Methodology

The proposed SSOD uses the ARM based associative classification approach for detecting outliers. The method dynamically computes the threshold value for the support measure to generate infrequent patterns. To prune outliers the surprising measures 'Lift' is used. The data set considered are all numeric in nature. Hence the numerical data are categorized before performing the mining process. This data constitutes the input of the SSOD algorithm. Candidate sets are generated, from which infrequent models are pruned by support measurement. The actual support of each candidate set is calculated as per the equation 1.

Then, the infrequent patterns are pruned using the dynamically computed support threshold as in the algorithm. Following the step in the algorithm, the higher level candidate sets are generated and the complete sets of infrequent patterns are pruned by the support threshold. After generating the complete infrequent pattern sets, the infrequent CARs are generated and the one with the high confidence are pruned as rare rules. Lastly, the surprising Lift measurement is used to prune outliers of the rare rules. The exceptional CARs with high confidence are alone considered to extract the outliers

Algorithm1: SSOD - Semi Supervised Outlier Detection

Input : Database - D, Initial Support - S

Output : A set of Temporal Outliers – Outlier

Notations Used : σ_{dynsup}^R - Max. Support, S_a - Actual Support, R - Rare Pattern sets,

C_k : Candidate pattern set of size k, L_k : Infrequent pattern set of size k

Data Preprocessing: */* Categorization of the numerical values */*

1. $D(A_1, A_2, \dots, A_n, \text{CLASS}) \rightarrow D^P(A_1.\text{LOW}, A_1.\text{MEDIUM}, A_1.\text{HIGH}, \dots, A_n.\text{HIGH}, \text{CLASS})$

Infrequent Pattern Generation: */* Infrequent pattern generation - APRIORI algorithm */*

2. $C_1 = \{ A_1.\text{LOW}, A_1.\text{MEDIUM}, A_1.\text{HIGH}, \dots, A_n.\text{HIGH} \};$

3. $L_1 = \text{Set of all } C_1 \text{ for which } S_a(C_1) < S; \quad // \text{ Where } S=0.2 \text{ the Initial Support}_{\min}$

4. $R = L_1;$

5. for ($k=2; L_{k-1} \neq \emptyset; k++$) do begin

6. $C_k =$ candidate sets generated from $L_{k-1};$

7. $L_k = \text{Set of all } C_k \text{ for which } S_a(C_k) < \sigma_{\text{dynsup}}^R$

8. $R = R \cup L_k;$

9. end for;

10. return R;

Outlier Pruning: */* Pruning low support with high confidence infrequent CARs with outlier pruning measure */*

11. Outlier = Outlier_Pruning (R);

Post Pruning: */* Redundant Outliers if any are eliminated */*

Algorithm2: Outlier_Pruning**Input** : D^P – Preprocessed data, R - Rare Pattern sets**Output** : A set outliers (exceptional CARs)**Notations Used** : R_{Conf} – Rule Confidence, R_{sup} - Rule support, R_{lift} - Rule Lift, L_k - Infrequent pattern set of size k , IRs – Infrequent Rules, ER_{pruned} – Outlier, $Supp_{threshold}$ – Max. Support, $Lift_{threshold}$ – Min. Lift**Infrequent Rule Generation:** */* Infrequent CARs from Infrequent Patterns set */*

1. $IRs = \emptyset$;
2. for all L_k in R do
3. Scan D^P
4. If the instance of D^P matches L_k
5. Then Generate CAR of the form $L_k \rightarrow CLASS$; // Rule of the form $A \rightarrow C$
/ where $L_k \in (A1.LOW, A1.MEDIUM, A1.HIGH, \dots, An.HIGH)$ */*
6. end if;
7. calculate R_{sup} , R_{Conf} and R_{Lift} for CAR;
8. $IRs = IRs \cup CAR$;
9. end for;
10. $Support_{threshold} = Mean(\sum R_{sup}(IRs))$; $Lift_{threshold} = Mean(\sum R_{Lift}(IRs))$;
- Outlier Pruning:** */* Pruning outliers ie, exceptional CARs from Infrequent CARs */*
11. $ER_{pruned} = \emptyset$;
12. for all rules in IRs do
13. $ER_{pruned} = ER_{pruned} \cup IR$ (with $R_{sup} \leq Supp_{threshold}$, $R_{Lift} \geq Lift_{threshold}$ and $R_{Conf} > 95\%$) ;
14. end for;
15. return ER_{pruned} ;

5. Results and Discussions

To evaluate the proposed method – SSOD, several experiments were carried out on the benchmarked datasets. The performance of SSOD along with the lift measures is evaluated based on various parameters like the time taken to detect outliers, heap space used to detect outliers, the number of outliers detected by the Lift

measure from the infrequent patterns. Also, the nature of the outliers extracted was observed. The observed results are tabulated in Table 2. The exceptional CARs with high Lift value (>1) are considered as outliers. The threshold value of Lift measurements is calculated dynamically as indicated in the SSOD algorithm.

Table 2. Performance of the proposed method - SSOD

Evaluation Parameters	Databases		
	PIMA Indian Diabetes	Education	Stock Market
1. User defined thresholds	Initial Support = 0.003	Initial Support = 0.003	Initial Support = 0.003
2. Thresholds	Max Supp. = 0.072	Max Supp. = 0.106	Max sup = 0.001
3. No. of Infrequent CARs	25	36	94
4. No. of Outliers	12	17	2
5. Heap space for outliers	44,507,136	5,908,122	5,571,344
6. Outliers'	0.716	0.568	0.306
7. Outliers'	98.91	98.52	99.92

The results presented in Table 2 show that the number of infrequent models generated and the heap space used differ for each data set. This is because, each dataset vary in size and dimensions. Though the user defined initial support value is kept uniformly, the threshold value of Support and Lift measures computed dynamically varies for each dataset. Also, the number of infrequent CARs generated varies for each dataset varies. Likewise, the number of outliers extracted, the heap space used to extract outliers, and the time required to detect outliers differ for each dataset. The highest coverage value for PIMA Indian diabetes dataset indicates the presence of a greater number of outliers, which may be understood from the box plot analysis in Figure 2. Consistently across the dataset,

the detection accuracy for outliers is almost 99%.

5.1. Analysis of the outliers generated

The natures of the outliers/Exceptional CARs generated for the datasets are examined and the inferences of the rules are interpreted. The sample outliers generated for Pima Indian Diabetes dataset, Education dataset and Stock market dataset and the implication of the exceptional CARs are listed in Table 3, 4 and 5 respectively. Based on the coverage value, the types of the outliers are identified. The high coverage value indicates the group / collective outliers and the low coverage values indicate the point outliers.

Table 3. Sample outliers detected from PIMA INDIAN diabetes dataset.

Exceptional CARs	Support	Confidence	Lift	Coverage	Implications	
					Risk Factors	Outlier Type
Age (Above 60) → No	0.003	1.000	1.019	0.214	Age factor	Point
DPF (Above 0.6) ^ BMI (26-30) → No	0.003	1.000	1.529	0.214	BMI level and hereditary factors	Point
DPF (Above 0.6) → No	0.131	0.924	1.396	14.11	Hereditary factors	Collective

Table 4. Sample outliers detected from EDUCATION dataset.

Exceptional CARs	Support	Confidence	Lift	Coverage	Implications	
					Risk Factors	Outlier Type
SG (80-89) → PASS	0.153	0.933	1.029	19.565	Higher marks in SG	Collective
SL (80-89) → PASS	0.196	1.000	1.106	14.304	Higher marks in SL	Collective
SD (50-59) ^ DB (60-69) → PASS	0.011	1.000	1.138	01.087	Border marks in SD	Point

Table 5. Sample outliers detected from STOCK MARKET dataset.

Exceptional CARs	Support	Confidence	Lift	Coverage	Implications	
					Risk Factors	Outlier Type
Close (210.33 -233.8) → Volume1	0.173	0.955	1.013	18.107	Close price is high	Collective
Low (177.08 -218.68) → Volume1	0.171	0.955	1.006	07.489	Low price is considerably low	Collective
Open (183.33 – 211.36) → Volume2	0.003	1.000	1.066	00.290	Open price is considerably low	Point
High (172.34 -183.36) → Volume2	0.008	1.000	1.025	00.246	High price is considerably low	Point

5.2. Performance of SSOD against conventional outlier detection methods

The performance of the proposed SSOD method is compared to existing classical outlier detection methods. The calibrated methods are Naive Bayes, Multi-class Classifier, K-Nearest Neighbor (KNN), Class outlier factor (COF), Distance based

algorithm, Density based algorithm, and Local outlier factor (LOF). The performance of the above mentioned algorithms are evaluated on the basis of assessment measures such as Precision, Recall and F-Score. The results are plotted, as shown in Figures 3, 4 and 5 respectively.

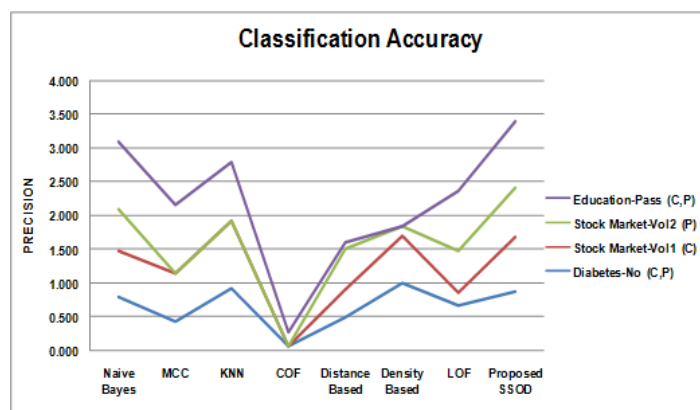


Figure 3. SSOD vs classical methods Accuracy of classification.

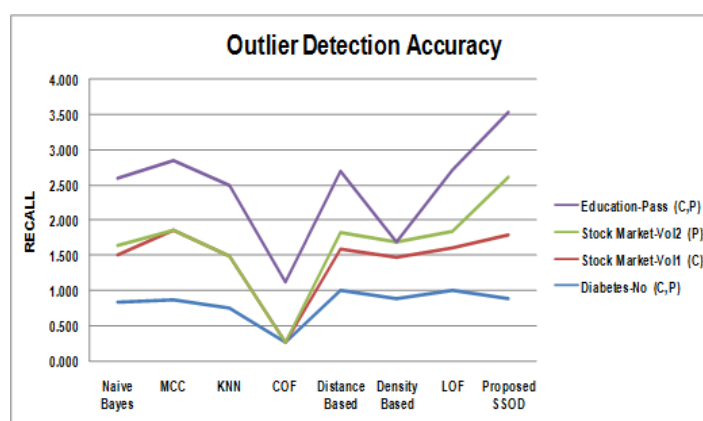


Figure 4. SSOD outlier detection accuracy compared to conventional methods.

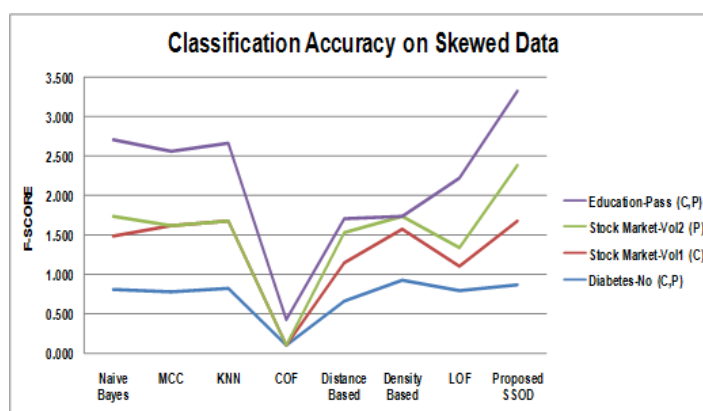


Figure 5. Efficiency of SSOD methods relative to conventional methods.

For simple understanding the alarming target classes with outliers are alone is considered to construct the graphs. For example, in the Education dataset, the 'Pass' target class with collective and point outliers is considered from which the risk

factors identified will be useful for improving the results. From the graphs, it is understood that COF algorithm perform very poor in predicting both the collective and point outliers. Though the algorithms like KNN, Naive Bayes and Distance

based performs better in few aspects, the proposed SSOD surpasses all the algorithms in all the aspects. Hence, we claim that the proposed SSOD algorithm along with the surprising measure 'Lift' is the better choice of identifying both the type of outliers.

6. Conclusion and Future Work

An overview of type of outliers and their presence in the databases has been discussed. The need for the surprising measure in outlier detection is explained. The limitations of supervised and unsupervised ML algorithms in outlier detection are discussed and how the proposed SSOD algorithm overcomes these limitations is also explained. The surprising measure Lift along with SSOD algorithm have been experimented with the databases like Pima Indian Diabetes dataset, Education dataset and Stock market dataset where point and collective outliers are present. Based on the results obtained, it is understood that the lift measure is capable of detecting both the point and the collective outliers fruitfully. Also, the performance of the SSOD with Lift as the outlier pruning measure has been examined against the existing conventional outlier detection algorithms like Naive Bayes, Multi-class Classifier, K-nearest neighbor, Class outlier factor (COF), Distance based algorithm, Density based algorithm, Local outlier factor (LOF) and found that the proposed method – SSOD, outperforms the benchmarked algorithms by precisely detecting more accurate outliers. Therefore, we conclude that the surprising Measure Lift is adapted to extract collective and point outliers from different multidimensional, multi-labeled and asymmetric data sets.

For future research the work can be examined by various outlier pruning measures to improve the accuracy level. Also, the algorithm can be tested on Big data.

References

- [1] C.C. Aggarwal. An introduction to outlier analysis. In *Outlier Analysis*, Springer, Cham, (2017). 1-34.
- [2] G. Bruno, and P.Garza. TOD: Temporal outlier detection by using quasi-functional temporal dependencies. *Data & Knowledge Engineering* (2010), 69(6), 619-639.
- [3] A.M. Rajeswari, C. Deisy, V. Abirami Nachammai, and G.V. Aishwarya. Temporal Outlier Detection on Quantitative Data using Unexpectedness Measure', 12th International Conference on Intelligent System Design and Applications, IEEE Proceedings, (2012), 420-424.
- [4] H. Jin, J. Chen, H. He, G. J. Williams, Chris Kelman, and M. O. Christine Keefe. Mining Unexpected Temporal Associations: Applications in Detecting Adverse Drug Reactions. *IEEE Transactions On Information Technology In Biomedicine*, (2018), 12(4), 488-500.
- [5] H. Jin, J. Chen, H. He, C. Kelman, D. McAullay, and C.M. O'Keefe. Signaling potential adverse drug reactions from administrative health databases. *IEEE Transactions on knowledge and data engineering*, (2010), 22(6) 839-853.
- [6] Y. Ji, H. Ying, P. Dews, A. Mansour, J. Tran, R.E. Miller, and R.M. Massanari. A potential causal association mining algorithm for screening adverse drug reactions in postmarketing surveillance, *IEEE Transactions on Information Technology in Biomedicine*, (2011), 15(3), 428-437.
- [7] M. Hahsler. A probabilistic comparison of commonly used interest measures for association rules. (2015) Available online at <http://michael.hahsler>.

- net/research/association_rules/measure
s. Html.
- [8] A.M. Rajeswari, and C. Deisy. "Prediction of risk factors for pre-diabetes using a frequent pattern-based outlier detection." *International Journal of Biomedical Engineering and Technology* (2020), 34(2), 152-171.
 - [9] A.M.Rajeswari et al., A comparative evaluation of supervised and unsupervised methods for detecting outliers. In *2018 Second International Conference on Inventive Communication and Computational Technologies (ICICCT)*, (2018), 1068-1073, IEEE.
 - [10] R. Agrawal, T. Imielinski, and A. Swami. Mining Association Rules between Sets of Items in Large Databases. In *Proceedings of ACM SIGMOD*, Washington DC, USA. (1993), 207– 216.
 - [11] R. Agrawal and R. Srikant. Fast Algorithms for Mining Association Rules in Large Databases. In *Proceedings of the 20th International Conference on Very Large Data Bases*. (1994), 478–499.
 - [12] C. Romero, J. R. Romero, J. M. Luna and S. Ventura. Mining rare association rules from e-learning data. in *Educational Data Mining*. (2010), 171-180.
 - [13] S. Preetha, and V. Radha. Enhanced outlier detection method using association rule mining technique. *International Journal of Computer Applications*. (2012), 42 (7), 1-6.
 - [14] H. Deng, G. Runger, E. Tuv, and W. Bannister. CBC: An associative classifier with a small number of rules. *Decision Support Systems*. (2014), 59, 163-170.
 - [15] L.T. Nguyen, B. Vo, T.P. Hong, and H.C. Thanh. CAR-Miner: An efficient algorithm for mining class-association rules. *Expert Systems with Applications*. (2013), 40 (6), 2305-2311.
 - [16] J. Alcala-Fdez, R. Alcala, and F. Herrera. A fuzzy association rule-based classification model for high-dimensional problems with genetic rule selection and lateral tuning. *IEEE Transactions on Fuzzy Systems*. (2011), 19 (5), 857-872.
 - [17] Pima Indian Diabetes database. (2022). Available online at <https://www.kaggle.com/datasets/uciml/pima-indians-diabetes-database>
 - [18] State Bank of India (SBI.NS). (2022) Available online at: <https://in.finance.yahoo.com/quote/SBIN.NS/history>
 - [19] J. Han, J. Pei, and M. Kamber. 2011, 'Data mining: concepts and techniques. Elsevier. (2011).
 - [20] C.K. Selvi, and A. Tamilarasi. Mining association rules with dynamic and collective support thresholds. *International Journal of Engineering and Technology*. (2009), 1 (3), 236-240.
 - [21] M. Krzywinski and N. Altman. Points of significance: visualizing samples with box plots. *Nature methods*. (2014), 11 (2), 119-120.

A GRAPH-BASED APPROACH FOR PERSONALIZED JOB RECOMMENDATION

B.Subbulakshmi¹, M.Nirmaladevi², A.M.Rajeswari³ and M.Sivakumar⁴

¹ Assistant Professor, Department of Computer Science and Engineering,
Thiagarajar College of Engineering, Madurai, India.
bscse@tce.edu

² Assistant Professor, Department of Computer Science and Engineering,
Thiagarajar College of Engineering, Madurai, India.
nirmaladevi2004@gmail.com

³ Associate Professor, Department of Computer Science and Engineering,
Velammal College of Engineering and Technology, Madurai, India
amrtce@gmail.com

⁴ Associate Professor, Department of Computer Science and Engineering,
Thiagarajar College of Engineering, Madurai, India.
mskcse@tce.edu

Abstract

In today's society, finding a job is more challenging than getting one. On-campus placements make it easier for students to access work at the best universities. But when students go into mainstream colleges, they face challenges. These students have to go through a plethora of web pages, which is a time-consuming process. Thus, a graph based recommendation engine on user competence and location is built. The proposed work facilitates the referral process so that students can obtain information about jobs that interest them with just a click. This approach aims to address gaps in previous literature, such as cold start issues, safety concerns, and scalability, in order to provide a more effective recommendation system. As a result, by providing a career that matches their interests, the recommendation system can significantly aid recent graduates and job seekers in realising their goals.

Keywords: Natural Language Processing, graph-based recommendation, similarity matrix.

1. Introduction

There is a huge group of skilled workers in India that is growing the fastest. With the internet, a plethora of opportunities is available. People spend the majority of their time looking for employment, while working employees who seek to change careers may not have enough opportunity to locate the perfect job. There is indeed a plethora of info on numerous websites. However, for beginners or job searchers, this activity is highly arduous because they must browse through dozens of websites to explore the ideal employment. Nowadays, recommendation systems are more popular. However, depending on the domain in which it is used, the type of recommendations supplied may differ.

Customized employment recommendations are more applicable as part of the employment referral system. A system which recommends jobs to users based on their past research has been designed to help job seekers find their ideal place of work. There are plenty of job search sites that present jobs that have been listed by recruiters. Numerous job search websites exist, such as Indeed, Internshala, LinkedIn and others. These sites may be used to search for jobs and apply with the help of the given links. These websites ask for personal information as well as educational background. These websites do include a filter option that can save time. However, the major issue is that recruiters can only post to a single website, which is not always available. Therefore, a fantastic opportunity for the users is lost. As well, searching all available websites takes a long time. Disclosure of personal information on several websites is risky too. Data leaks are very widespread nowadays. Based on the job recommendation system, several articles have been proposed.

2. Related Work

Author [1] proposed a referral system in which graduates are divided into groups depending on their academic performance and family economic circumstances. In addition, graduates' similarity scores and customized preferences are merged to recommend some suitable occupations. The disadvantage of this work

[1] is academic achievement and family background does not appear to be excellent features in grouping graduates. Miao Jiang et al., [2] proposed a referral system through which job applicants subscribe to mail alerts for new job postings that fit their professional interests. In this referral system, the set of features that reflect the click-through behavior of individual applicants was considered to group users. The drawback here is the gray sheep problem which means that there are always people whose taste does not correspond to anyone.

The various employment suggestion systems and their methods were analysed by Ravita Mishra and Sheetal Rath [3]. Additionally, they highlighted the drawbacks of each recommendation system, including scalability, security, and cold start issues.

Qingyu Guo et al., [4] proposed a system based on interactions within social networks, and a knowledge graph is constructed from there. The downside here is that the knowledge chart is user-based and the scalability issue will arise. A hybrid referral system that uses a web crawler to obfuscate data was proposed by Zhenqi Dong et al., [5]. Additionally, they built a group-based algorithm for content filtering and recommendations. The drawback in this situation is that web crawlers will scan and retrieve all the data from a website, whereas web scraping has a much more focused approach and objective. Ravita Mishra and Sheetal Rath [10] proposed a recommendation system that uses a Deep Semantic Structure Modelling (DSSM) system that uses the semantic representation of sparse data and represents the job description and skill entities in character trigram format, increasing the system's efficacy. Here the DSSM system is a combination of CNN, RNN and GNN. The drawback is that since it is a combination of three neural networks, it is more complicated which may lead to more memory and time.

3. Existing Methods

3.1 Job Search Websites

Jobs placed by recruiters are listed on job search websites. There are many websites for job searching, including LinkedIn, Internshala, and Indeed. By using the offered links, one can use these websites to look for employment and apply for it. We are required to enter details about our academic record and personal lives on these websites. Additionally, they feature a number of filter options that can be utilised to speed up search results. Despite its positive attributes, it is not always appropriate.

For example in LinkedIn, a new account was created and only user skills and location were added. When the jobs page opens, it is seen that there is no recommendation. From this point, one can search for the required jobs but no recommendation was provided. This is a major problem called the cold start problem. When the user gets some history, this system gives good recommendations.

In Indeed, a new user is created as usual, and only skills are added. Then the preferred location was selected. Based on these data, recommendations are suggested, but the recommendations provided were not up to the specific requirements as given by the user. In Internshala website, only preferred job titles can be selected in Fields of interest. This site doesn't have a great recommendation engine.

3.1.1 Drawbacks of Job Search Websites

- Hiring managers may not be able to publish on all job-searching platforms. Certain individuals may miss out on a wonderful offer, and researching all available websites is a time-consuming approach.
- It's risky to disclose all of your personal information on multiple websites. Data leaks are very wide spread nowadays.

3.2 Recommendation Engines

A job recommendation engine is a data filtering tool that employs machine learning algorithms to recommend the most relevant jobs to a particular user. Various algorithms with merits and downsides have been proposed in the literature.

3.2.1 Drawbacks of Recommendation Engines

- Cold Start problem: When a new item or user is added there won't be enough information for a recommendation.
- Security issue: User information is given which is not safe
- Scalability issue: The system is not scalable because it can't handle when the number of users or jobs goes over a limit.

4. Proposed Approach

To recommend jobs to the job seekers based on different parameters like job details which includes job description, required skills, job location and user data such as user skills, user-preferred location. In the proposed approach, memory-based content filtering recommendation algorithm is used. This algorithm requires the new characteristic or description of an item and user characteristics to recommend.

Collaborative filtering is not suitable for our approach as it recommends solutions based on other users' likes and dislikes. The job recommendation system is not dependent on other users' recommendations. The users have their own likes and dislikes. The gray sheep issue is a well-known issue that is occurring in this technique. The issue arises for a new unique user who does not fall into any set or group of like-minded users.

The proposed approach has the following objectives:

1. To scrape data from online to create an offline job dataset.
2. To construct a recommender model that can address the cold start issues and scalability issues.
3. To design an algorithm that is well suited for recommending jobs to job seekers based on skills, location and job description.

Figure 1 demonstrates the design of the proposed system. There are four layers to the system: an input layer, a database layer, a recommendation layer, and a user interface layer. The input layer gathers all pertinent data, including user information and job openings, from various websites using a web scraper. The data is saved in a secure and easy-to-recover container by the database layer, which is the second layer. At the recommendation layer, a recommendation engine is developed with all of this data to generate top recommendations. The UI layer is a user interface with three screens for listing recommendations, searching for relevant jobs, and seeing a job's detailed description.

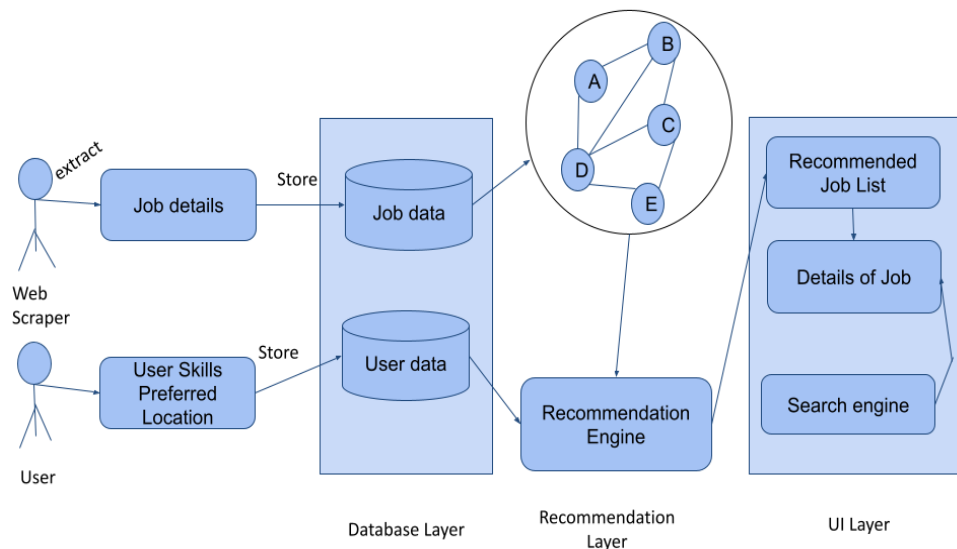


Figure 1. Design of Proposed System

Figure 2 shows the workflow of the recommendation algorithm and an explanation is provided below.

- Various job data are scraped from multiple websites, such as job descriptions, required skills, and job locations.
- The skills and preferred location of the user are acquired. Using these two inputs, the source is identified, which is a job in scraped data.
- Three different score matrices are created for the job description, skills, and location.
- Based on the different contribution scores, a single score matrix is constructed from the three different score matrices.
- On the single score matrix, a graph-based technique is used to get the best recommendations.

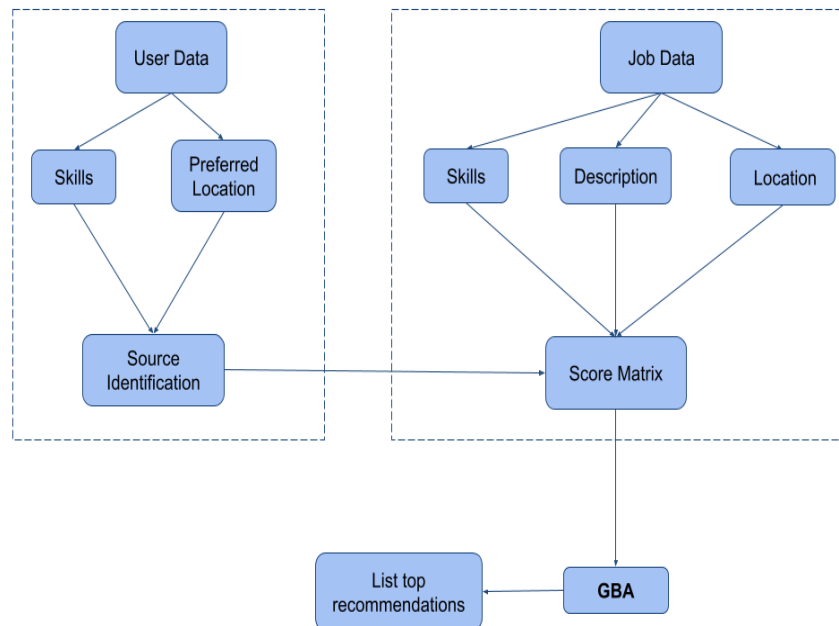


Figure 2. Workflow of Recommendation System

In the proposed approach, there is no breach of privacy because just the user's skills and preferred location are known. The user is not asked for any personal information. This approach provides a good level of security and privacy.

There is no scalability issue because only a job to job matrix is created that will contain only a finite number of job postings, and obsolete jobs are removed from the website itself and the job to job matrix is formed from real-time job postings.

There is also no difficulty with a cold start because if a new user joins, he or she will receive recommendations because the user-to-user matrix is not taken into account here. If a new job is posted, there is also no cold start issue because the new job will be scrapped and moved to the score matrix construction process. Hence it is taken into consideration in the recommendation list.

4.1 Extracting Job Details

Information about the project is obtained from the website "Internshala". Information is extracted from websites and online material using a process called web scraping. It is a cost-free way to obtain datasets and extract information. Additional analysis is done using this dataset.

Requests and BeautifulSoup are the two used packages. In order to swiftly extract DOM Elements, BeautifulSoup parses HTML into a machine-readable tree representation. It enables the extraction of certain table and paragraph elements with a specific HTML ID or Class. The HTML element would be obtained by requests from the URL and used as the input for BS to parse.

4.2 Preprocessing Extracted Job Details

Natural Language Processing or NLP is a field of Artificial Intelligence that gives machines the ability to read, understand and make sense of human languages. All basic preprocessing steps like removing stop words, lemmatization, converting all texts to lowercase, etc., were done. The package used is NLTK. NLTK, or Natural Language Toolkit, is a Python package you can use for NLP. Before analyzing the data, it must be preprocessed for better results.

4.3 Recommendation Engine - Graph-based Recommendation

4.3.1 Cosine Similarity:

The first step of this algorithm involves constructing three matrixes of similarity. Cosine similarity is a

measure of how similar two linguistic documents are. Text documents are converted into an n-dimensional vector form so they can be used to find similarity. The mathematical equation for the cosine similarity of two nonnull vectors is as per equation (1)

$$Similarity = A.B/||A|| ||B|| \tag{1}$$

The text is vectored using the vector TF-IDf (term inverse frequency of the document). 'TF' represents the number of times a term appears in a certain document. 'IDF' is a measure of the frequency or infrequency of a term appearing in the corpus of a document. The 'TF-IDf' is the value of a term within a document is the output of its 'TF' and 'IDF'. The higher the value, the more relevant are the words used in the document.

Skills to skills similarity matrix, job description to job description similarity matrix, and location to location similarity matrix are three similarity matrices. All of this information was gathered from the previously stated source. Skills are the skills that recruiters have mentioned on the website. Similarly, the website was used to obtain the job description and location. Figure 3 depicts an example of a skill-to-skill similarity matrix:

	c, python, java	reactjs, css, html, js
c , python, java	1	0.0000003
reactjs, css, html, js	0.0000003	1

Figure 3 Skill-to-Skill Similarity Matrix

A single matrix is created by combining these three matrices. The skills to skills similarity matrix accounts for 60% of the score. Similarly, the job description to job description matrix and the location to location matrix each contributed 30% and 10%, respectively.

4.3.2 User Input

The user's skill and the user's desired work location are taken as input.

4.3.3 Source identification

Based on the user's expertise, a source is identified. The source is nothing but a job from the scraped data. User skills and job skills are analyzed and the most relevant job is taken as the source.

4.3.4 Dijkstra Algorithm

There is a single similarity matrix that represents the similarity value. The distance matrix is formed by taking the difference. The mathematical equation for distance is given in equation (2).

$$distance = 1 - similarity \tag{2}$$

This distance graph has several nodes where every node is linked to several other nodes. If the minimum distance between each node from every other node is known, then it's easy to pick the top recommendations.

This need can be fulfilled by the Dijkstra algorithm. Negative edges are not needed, so remove them from the graph. Use this graph and source to implement the Dijkstra algorithm that provides the best recommendations.

5. Results and Discussions

5.1 Dataset:

Numerous job details were obtained from various sources, as well as user skills and preferred location. A dataset having test user's history is created. Userid and Job_Titles are two features in the user history. It is

obtained from the user through a Google form. The features in the job dataset include jobid, job_title, job description, and job location. Table 1 shows the job data fields extracted from multiple websites. Figure 4 represents sample data that belongs to various jobs. The first column is job id . Table 2 shows user data fields collected from users. Figure 5 represents a sample data entered by users through Google form.

Table 1. Job Data Fields

Field	Type
Job_id	int
Job Title	String
Job Description	String
Skills Required	String
Location	String

Table 2. User Data Fields

Field	Type
Timestamp	String
Enter your skills	String
Enter your location	String
Job_title_1	String
Job_title_2	String
Job_title_3	String
Job_title_4	String
Job_title_5	String

A	B	C	D	E
		<p>Key responsibilities:</p> <ol style="list-style-type: none">1. Prospect for potential new clients and turn this into increased business2. Work on cold calling as appropriate within your market or geographic area to ensure a robust pipeline of opportunities3. Meet potential clients by growing, maintaining, and leveraging the network4. Identify potential clients and the decision-makers within the client organization5. Research and build relationships with new clients6. Set up meetings between client decision-makers and the company's practice leaders/principles7. Plan approaches and pitches8. Work with the team to develop proposals that speak to the client's needs, concerns, and objectives9. Participate in pricing the solution/service10. Handle objections by clarifying, emphasizing agreements, and working through differences to a positive conclusion11. Use a variety of styles to persuade or negotiate appropriately12. Present an image that mirrors that of the client		
101	A-IT Sales Executive (B2B)	20	Client Relationship	Gurgaon,Bangalore

Figure 4 Sample Data of Jobs

Timestamp	Enter your skills	Enter your location	Job_title	Job_title	Job_title	Job_title	Job_title
2022/04/09 12:30:53 PM GMT+5:30	accounting excel office tally	bangalore	Accountant	Finance Executive	Associate Accountant	Finance Executive	Junior Accountant

Figure 5 Sample Data of User History

5.2 Sample Input and Output

User 1:

User 1 is expertise in both software testing and manual testing and his/her preferred location is Bangalore. The top recommendations are software development engineer in testing, software tester, QA tester, QA engineer and junior full stack developer. Hence the recommendations are mostly related to testing and QA and location for all those jobs also mostly Bangalore which are acceptable. Figure 6 represents users 1's input. Figure 7 represents recommendations for this user.

```
Enter your skills>manual testing software testing
Enter your location:bangalore
```

Figure 6 User 1's Inputs

predicted_title - List (20 elements)				predicted_location - List (20 elements)			
Inde.	Type	Size	Value	Inde.	Type	Size	Value
0	str	1	Software Development Engineer In Testing (SDET)	0	str	1	bangalore
1	str	1	Software Tester	1	str	1	bangalore
2	str	1	QA Tester	2	str	1	remote
3	str	1	QA Engineer	3	str	1	bangalore
4	str	1	Junior Full Stack Developer (Python + JavaScript)	4	str	1	bangalore

Figure 7 User 1's Recommendation List

User 2:

User 2 enters the respective skills and location as shown in Figure 8. Graphic designer, video editor, video editor, multimedia content analyst, and assistant video editor are the top recommendations provided. Since the skills are adobe related, the recommendations are also related to video editor and graphic designer. Figure 9 represents recommendations for this user.

```
Enter your skills:Adobe After Effects Adobe illustrator Adobe
photoshop Adobe Primere Pro Final Cut Pro Video Editing Video Making
Enter your location:Delhi
```

Figure 8 User 2's Inputs

predicted_title - List (20 elements)				predicted_location - List (20 elements)			
Index	Type	Size	Value	Index	Type	Size	Value
0	str	1	Graphic Designer	0	str	1	gurgaon
1	str	1	Video Editor	1	str	1	gurgaon
2	str	1	Video Editor	2	str	1	mohali
3	str	1	Analyst - Multimedia Content	3	str	1	kolkata
4	str	1	Associate Video Editor	4	str	1	delhi

Figure 9 User 2’s Recommendation List

User 3:
User 3 is expertise in Dart and Flutter. The top recommendations are flutter developer, flutter app developer, junior flutter developer, junior full stack developer and flutter developer. As skills are related to flutter, the recommendations produced are also related to Flutter development. Figure 10 represents user 3’s input. Figure 11 represents recommendations for this user.

Enter your skills:Dart Flutter
Enter your location:Bangalore

Figure 10 User 3’s Inputs

predicted_title - List (20 elements)				predicted_location - List (20 elements)			
Index	Type	Size	Value	Index	Type	Size	Value
0	str	1	Flutter Developer	0	str	1	noida
1	str	1	Flutter App Developer	1	str	1	remote
2	str	1	Junior Flutter Developer	2	str	1	remote
3	str	1	Junior Full Stack Developer	3	str	1	remote
4	str	1	Flutter Developer	4	str	1	bangalore

Figure 11 User 3’s Recommendation List

5.3 Performance Metrics

For the tests, user history from some users was used. The user history for a set of six users was collected and depicted in the Figure 12 and calculated based on recommendation results and user history, accuracy, recall and average accuracy. The algorithm had a pretty good recommendation.

A	B	C	D	E	F	G	H
Timestamp	Enter your skills	Enter your location	Job_title	Job_title	Job_title	Job_title	Job_title
2022/04/09 12:30:53 P	accounting excel office	bangalore	Accountant	Finance Executive	Associate Accountant	Finance Executive	Junior Accountant
2022/04/09 12:32:29 P	creative writing digital	delhi	Digital Marketing Spec	Digital Marketer	Digital Marketing Asso	Content Writer	Digital Marketing Executive
2022/04/09 12:55:58 P	adobe effect , adobe ci	mumbai	Jr. Executive Graphic I	Graphic Designer And	Graphic Designer	Associate Graphic Des	Junior Graphic Designer
2022/04/09 12:55:58 P	manual testing softwar	bangalore	Software Development	Software Tester	QA Tester	QA Engineer	Quality Assurance
2022/04/09 12:55:58 P	android flutter io kotlin	bangalore	Mobile App Developer	Flutter Developer	React Native Develop	Mobile App Developer	Flutter/Android Developer
2022/04/09 12:55:58 P	english proficiency spo	hyderabad	Associate Recruiter	HR Recruiter	Junior Recruitment Ex	HR Generalist	Junior Recruitment Executive

Figure 12 User History Data

When the "k" break occurs, the precision and recall are employed. Five was chosen for the k. Only the subset of rank 1 to k recommendations is used to derive precision and recall to cutoff k, P@k, and r@k. At cutoff k, precision and recall are employed. Five was the chosen k. P@k and r@k are the precision and recall calculated using only the subset of suggestions from rank 1 to k.

The Mean Average Precision (MAP) and Hit Rate (HR) metrics are utilised in this study to evaluate the effectiveness of the recommendation system. The mean of the average precision across all users is known as MAP. You receive awards from Average Precision for making sensible recommendations. HR is calculated by dividing the number of hits by the total number of occurrences.

Average Precision AP@N is defined as (3) if there is a need to propose N things and there are m relevant items in the entire space of items. Single data points, such as a single user, are covered by AP. Mean Average Precision MAP@N takes it a step farther by averaging all users' AP. The acronym MAP@N is calculated as in (4). The proposed recommendation approach gives the Mean Average Precision as 88.78%. Hit rate can be defined as in equation (5). The hit rate for the recommender system is 51%.

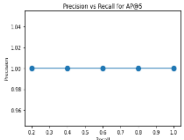
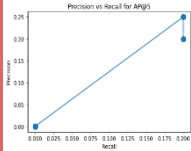
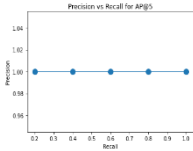
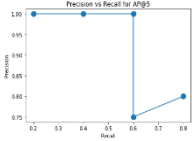
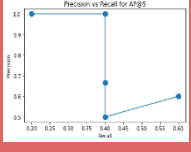
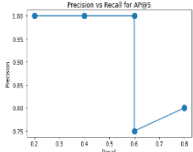
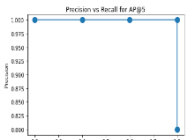
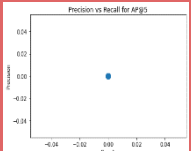
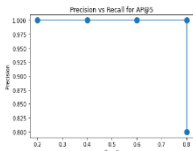
$$AP@N = (\frac{1}{m}) \sum_{k=1}^N (Precision@k \text{ if } k^{th} \text{ item is relevant}) \tag{3}$$

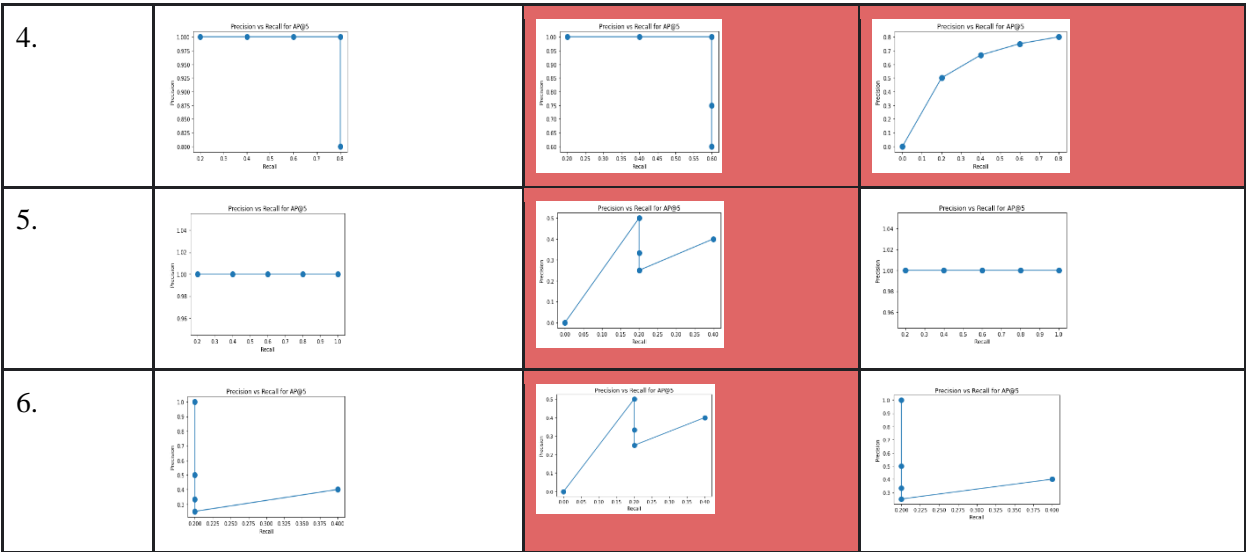
$$MAP@N = (\frac{1}{|U|}) \sum_{u=1}^{|U|} (AP@N)_u \tag{4}$$


$$Hit\ Rate(HR) = \frac{number\ of\ hits}{number\ of\ occurrences} \tag{5}$$

Graphical representations of Precision@k vs Recall@k for the randomly chosen user chosen for the presented approach and other typical approaches are shown in Table 3. In Table 3, each line represents the precision plot against a user recall produced by various approaches, as mentioned in the header.

Table 3. Graphical representation of precision vs recall at k = 5 for GBA, content based - skills and content based - description approaches

User IDs	The Proposed Approach	Content based - Skills	Content based - Description
1.			
2.			
3.			



Note:  This colour represents precision vs recall graph that shows variations from our approach

5.3.1 Analysis of graphs represented in Table 3

User 1: Both the proposed approach and the content-based approach (Description) produce a good graphical representation, with the precision of 1 at every k and recall steadily improving. The maximum recall attained is 1. In the content-based approach (skills) the maximum precision is 0.25 and again gradually decreases. The recall also follows the same. Here both our presented approach and content-based approach (Description) win since they give the best performance.

User 2: In the proposed approach and in content-based approach (Description) the precision starts at 1 but gradually decreases to 0.8 and recall gradually increases to 0.8. Precision starts at 1 and falls to 0.6 in a content-based approach (skills), whereas recall steadily climbs to 0.6. Here also both the presented approach and content-based approach (Description) win because of their better performance.

User 3: The precision of both the proposed approach and the content-based approach (Description) is 1 and recall progressively grows to 0.8. Content-based approach (skills) shows both precision and recall as 0. It is clearly seen that both the presented approach and content-based approach (Description) win.

User 4: In the proposed approach, precision is 1 in all cases, and recall gradually increases to 0.8. Content-based approach (skills) has a precision of 1 at all k and recall gradually increases to 0.6. In the content-based approach (Description), both recall and precision increases to 0.8. Here the presented approach wins.

User 5: Both the proposed approach and content-based approach (Description) have precision 1 at all k and the same follows for recall. The precision for this user in the Content-based approach (skills) fluctuates and when k = 5 it is 0.4 which is low. The recall gradually increases to 0.4 which is also considered low. It is clearly seen that both the presented approach and content-based approach (Description) win.

User 6: All three approaches have some similar fluctuations in their graph. In this case, all the approaches' performances are mostly similar.

Table 4 gives a clear picture that the proposed approach has a maximum number of wins. Various users get the best result in different approaches but the maximum wins are present in the proposed approach and it is to be noted that there is no loss in the proposed approach.

Table 4. Comparison among Graph Based Approach (proposed), content-based -skills and content-based - description approaches

User IDs	The Proposed Approach	Content based - Skills	Content based - Description
1.	win	loss	win
2.	win	loss	win
3.	win	loss	win
4.	win	loss	loss
5.	win	loss	win
6.	draw	draw	draw

Tables 3 and 4 indicate that, when taking into account the top 5 suggestions, the suggested technique provides good precision and recall scores. Draw means that all the approaches give consistent performance for user 6. Table 5 clearly shows that the offered approach outperforms prior approaches.

Table 5. Comparison of content based approaches and proposed approach

Evaluation Metric	The Proposed Approach	Content-Based Skills	Content- Based - Description
Mean Average Precision	88%	38%	81%
Hit Rate	51%	22%	48%

Table 6. Comparison of Existing Approaches

S.no	Existing approach	Drawback	How does this approach overcome these drawbacks?
1.	LinkedIn	Cold start problem	The approach presented in this paper does not have a cold start issue since the user skills and locations are the main attribute considered.
2.	Internshala	No matching recommendations	This Graph-based approach has a natural language-based recommendation engine that can recommend jobs based on user skills as mentioned earlier in the paper.
3.	Indeed	Extracts the job titles the user gives	Since this approach has recommendations based on skills that would do a better job than just matching the Title.

5.4 Why no to Collaborative filtering?

Collaborative filtering does not always lead to the desired outcomes. Here there is a possibility of a grey sheep problem. When collaborative filtering on the data that was collected from different users through google forms, the result was not satisfactory. Consider that there exists one user whose skills are flutter and dart; jobs that the user accessed is only mobile app developer. When a new user with the following skills android, flutter, kotlin, react native arrive, he only gets recommendations based on the already available user who has a history only on Mobile App developer. When the same user uses the proposed approach, he gets various recommendations related to a Mobile App Developer, a Flutter Developer, a React Native Developer, and a Java App Developer. Hence for job recommendation content-based is more suitable than a collaborative approach.

6. Conclusion

Nowadays, freshers and job seekers find it tough to select the most suitable profession on a variety of websites. This type of seeking wastes time and makes it harder to grow in one's job. Personalized recommendations are made to help people overcome such hurdles. To achieve this goal, job information is gathered from a variety of sources, and jobs are recommended based on work location, required skills, job description, user skills, and user's preferred location. As a result, personalized job recommendations are provided.

Comparisons on various approaches have been made. It was seen that there was a significant difference in the precision vs recall graph which was produced by various approaches. However, it was evident that this proposed approach gives more appropriate results than other approaches. By collaborating with businesses to publish job opportunities in an app and expanding the app to include course recommendations for the user's career path growth, this idea can be improved in the future. This algorithm can be used as a backend and the frontend can be developed so that users can see recommendations on the flow. This will be done so that this algorithm can be utilized and the application can be published for people to be used.

5. References

- [1] Qing Zhou, Fenglu Liao, Chao Chen, Liang Ge, "Job recommendation algorithm for graduates based on personalized preference", CCF Transactions on Pervasive Computing and Interaction, vol. 1, pp. 260–274, 2019.
- [2] Miao Jiang, Yi Fang, HuangmingXie, Jike Chong & MengMeng, "User click prediction for personalized job recommendation", World wide web, vol. 22, pp. 325–345, 2018.
- [3] Ravita Mishra, SheetalRathi, "Efficient and Scalable Job Recommender System Using Collaborative Filtering", Lecture Notes in Electrical Engineering book series, pp. 845–856, 2020.
- [4] Qingyu Guo; Fuzhen Zhuang; Chuan Qin; Hengshu Zhu; Xing Xie; HuiXiong; Qing He, "A Survey on Knowledge Graph-Based Recommender Systems", IEEE Transactions on Knowledge and Data Engineering, pp. 1-1, 2020.
- [5] Zhenqi Dong, ChunxiaLeng, Hong Zheng, "Employment Service System Based on Hybrid Recommendation Algorithm", Advances in Intelligent Systems and Computing book series, vol. 1, pp. 368–375, 2020.
- [6] D.Mhamdi, R.Moulouki, M.Y. El Ghoumari, M.Azzouazi, L.Moussaid, "Job Recommendation based on Job Profile Clustering and Job Seeker Behavior", The International Workshop on Artificial Intelligence and Smart City Applications (IWAISCA), vol. 175, pp. 695–699, 2020.
- [7] TanviTayade, RutujaAkarte, GayatreeSorte, RohitTayade, PritiKhodke, "Data Mining Approach to Job Recommendation Systems", EAI/Springer Innovations in Communication and Computing book series (EASICC), vol. 1, pp. 503–509, 2020.
- [8] Pradeep Kumar Roy, Sarabjeet SinghChowdhary, Rocky Bhatia, "A Machine Learning approach for automation of Resume Recommendation systems", International Conference on Computational Intelligence and Data Science (ICIDS), vol. 161, pp. 2318–2327, 2019.
- [9] HariniPriya B R, Kannimalar K, Saranya S B and Subbulakshmi B, "A Machine Learning Approach for Personalized Job Recommendation System", In: Rahul Srivastava and Aditya Kr. Singh Pundir (eds), New Frontiers in Communication and Intelligent Systems, SCRS, India, 2022, pp. 399-404. <https://doi.org/10.52458/978-81-95502-00-4-42>.

- [10] Mishra, R., & Rathi, S. (2022). Enhanced DSSM (deep semantic structure modelling) technique for Job recommendation. *Journal of King Saud University-Computer and Information Sciences*, 34(9), 7790-7802.



ANALYSIS OF PHOTONIC CRYSTAL BASED ALL-OPTICAL 4-PORT DIRECTIONAL COUPLER DESIGN USING FDTD METHOD

Anusooya V ^a, Ponmalar S ^{b*}, Manikandan M S K ^c, Sanjith S ^d, Gobalakrishnan S ^e

^a Department of Electronics and Communication Engineering, Amrita College of Engineering and Technology, Erachakulam, Kanyakumari, India - 629901, prof.v.anusooya@gmail.com

^b Department of Computer Science and Engineering, Velammal College of Engineering and Technology

Madurai, India – 625009, sponmalar1976@gmail.com

^c Department of Electronics and Communication Engineering, Thiagarajar College of Engineering,

Madurai, India – 625015, manimsk@tce.edu

^d Department of Digital Sciences, Karunya Institute of Technology and Sciences, Karunya Nagar, Coimbatore, Tamilnadu, India – 641114, drsanjith@gmail.com

^e Department of Nanotechnology, Noorul Islam Centre for Higher Education, Kumaracoil, Kanyakumari, India – 629180, gobalphd@gmail.com

Article History: Received: 12.05.2023

Revised: 25.05.2023

Accepted: 05.06.2023

Abstract

The ever-growing demand for larger integration density, higher bandwidth, and lower power consumption in conventional electronic technology has made photonics one of the key drivers in global data communications. The success and ongoing trend of nanophotonic anticipate a photonic roadmap leading to ultra-compact, broad bandwidth, high-speed optoelectronic devices. However, there is a severe deadlock imposed on the miniaturization of nanophotonic devices as long as conventional propagating light is used. This view dramatically changed due to the emerging field of nonlinear photonic crystals. To meet these purposes all optical 4-port Directional Coupler is a potentially important components for future optical integrated circuits. This project proposes the design of a Directional Coupler where the propagation of the electromagnetic wave is simulated at the wavelength of 1.55 μm in dielectric material Silicon of refractive index 3.4757 with the hexagonal lattice of the lattice constant of 0.750 μm in 2D photonic crystal using Finite Difference Time Domain (FDTD) method. The Photonic Bandgap (PBG) of the material can be observed using Plane Wave Expansion (PWE) method and a photonic bandgaps width of 0.148 GHz and 0.152 GHz at a normalized frequency of 0.379 GHz, 0.653 GHz respectively was obtained which leads to an opportunity for a number of applications that can be used in ultrafast optical circuits and future optical networks.

Keywords: Optical Computing, Photonic Crystal, Photonic Integrated Circuits, all-optical directional coupler, FDTD, PWE, Bandgap.

I. INTRODUCTION

Recently, digital computing suffers from limited bandwidth and lower speed when the number of users increases. By 2020, the demand for digital communication bandwidth is predicted to greatly exceed all existing technology. High-speed transmission, minimized energy losses, and parallel processing capability can be achieved, if you have used photons instead electrons as carriers. So finally optical computing coming into the picture. Optoelectronic devices require optical-electronic-optical conversion. To avoid speed limitations, all-optical processing solutions are the next step. But there exists a problem of enormous size in all optical conventional devices. So, the next step of nanophotonics arises. Microstructure photonic crystals serve as a platform on which to build devices in the order of wavelengths of light for future photonic integrated circuits. By creating point defects in the photonic crystal, a triangular lattice-based directional coupler was developed for all-optical switching [1]. A ring resonator based on a four-port wavelength demultiplexer was proposed by Saraniya [2]. By varying the index differences along each port various wavelengths can be obtained for tuning the device. Photonic crystal-based directional couplers are used as a platform to realize various optical devices such as wavelength selective devices, ring resonators, and wavelength demultiplexers [2-4]. All optical switches [5-8] and all-optical Logic Gates [9-11] can be implemented using directional couplers. It was suggested and shown that directional couplers could switch at short switching lengths while maintaining a wide bandwidth [12]. Ring resonator based two dimensional photonic crystals effectively designed and demonstrated all optical half adder circuits [13, 14] and optical combined half adder/subtractor [15].

Here, in this paper, we proposed a new hexagonal lattice based 4-port directional coupler by introducing line defect in the

photonic crystal. There is no mode overlapping and interference in the proposed design because of hexagonal lattices and defects. By removing the row of dielectric rods we can overcome the time delay and fabrication complexity. Finally, the simulation is performed at the wavelength of $1.55\ \mu\text{m}$ and a normalized frequency of 0.4839 GHz is obtained which is very suitable for a number of applications. The bandgap structure was determined through the utilisation of the plane wave expansion (PWE) technique.

II. DEVICE CONCEPT

The schematic diagram of a 4-port directional coupler is shown in Figure 1. It shows that a directional coupler is a passive device that acts as a building block of all-optical combinational circuits. The directional coupler can be configured by combining two linear waveguides in close proximity at the center portion of a certain length in terms of wavelength (λ). In this proposed work, we have considered 4 port directional couplers. Port 1 is considered as the input port, port 2 is the received port. Most of the output is received at this port. Port 3 is the reverse side port. No signal should be present due to reflection. In port 4, forward power can be measured.

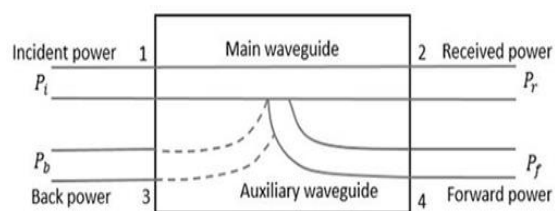


Figure 1. Schematic diagram of a 4-port directional coupler

Compared with the power at the received power port, the power at the forward power port is less. The directional coupler was constructed using dielectric rod type photonic crystal in a hexagonal lattice structure. It consists of two linear waveguides made by creating a line of

defects by removing two rows of atoms. When these waveguides are parallel because of the interaction of electromagnetic fields power can be coupled between the waveguides. Here, the phenomenon involved is the Kerr effect. In the directional coupler, any port can be the input.

A linear combination of symmetric and anti-symmetric modes was excited during the power incident at one waveguide. The excitation may be of constructing the modes in one waveguide and destructing the modes in other waveguides. A phase difference was introduced in the system due to the inequality in the propagation constants. The modal addition is present in the second waveguide and deletion is present in the first waveguide, when the total phase difference is π . Further signal propagation in the resulting length of the waveguide is happen when the phase difference is 2π , which leads to power transfer back to the first waveguide. Hence, the power coupling between the two waveguides will happen periodically.

III. DESIGN METHODOLOGY

In the proposed directional coupler structure, the lattice arrangement is hexagonal with a lattice constant of $0.750\ \mu\text{m}$. It consists of rods with silicon, a high refractive index of 3.4757, and radii of $0.2\ \mu\text{m}$ embedded in a background material with a low refractive index of 1 (air).

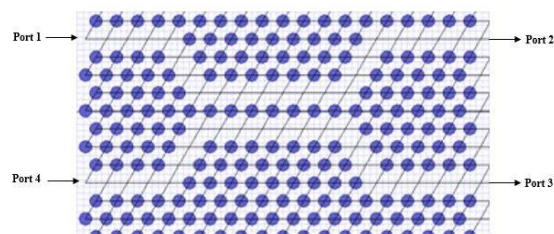


Figure 2. Design Layout of the proposed directional coupler

The directional coupler is made by removing a row of rods entirely as shown in Figure 2. So, there is no frequency overlap

between the waveguides. This is an improvement over previously reported similar structures.

The bandgap structure of the same can be observed by using the plane wave expansion method which is depicted in Figure 3. This structure has two photonic bandgap in TE mode within the normalized frequency range of 0.379 GHz, 0.653 GHz respectively.

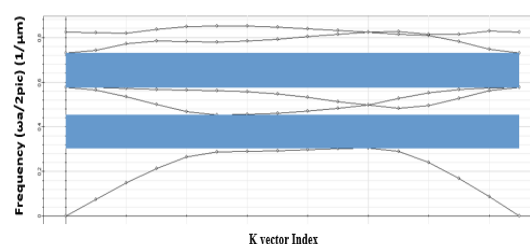


Figure 3. Bandgap structure

The frequency ranges are from 0.304484 to 0.45267 & 0.577229 to 0.729649 and the corresponding wavelength are from 3284 nm to 2209 nm & 1732 nm to 1371 nm. Between these two wavelength ranges, the low loss telecommunication wavelength 1550 nm lies in the second bandgap range could be considered for proposed directional coupler design. The point source is the radiation source. The wave radiated from the point source propagates through the directional coupler and the responses are observed at the observation points at port 1, port 2, port 3, and port 4.

IV. RESULTS AND DISCUSSION

The 2D Finite Difference Time Domain (FDTD) approach is utilized for the simulation in order to gain an understanding of how the suggested architecture functions. The input was given at both port 1 as depicted in Figure 4 and observations were made at all four ports of the directional coupler. The input amplitude of 0.12 (a.u) was given at input port 1 and the received signal amplitude at port 2 is 0.048 (a.u) and the forward signal

amplitude at port 3 is 0.052 (a.u), there will be a 0.02 (a.u) present at port 4. Similarly, The input amplitude of 0.12 (a.u) was given at input port 2 and observations were made at all the four ports as depicted in Figure 5. The time domain representation of all the four ports responses were depicted in Figure (6-9).

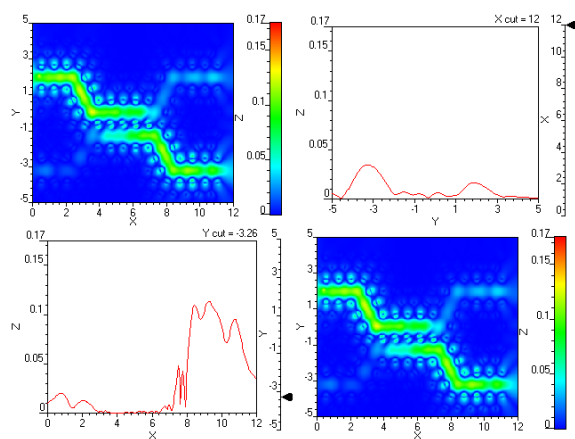


Figure 4. Directional coupler output for input at port 1

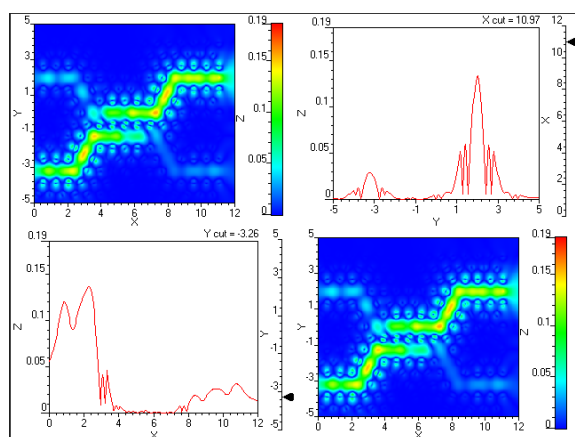


Figure 5. Output of directional coupler for input at port 2

In this proposed design of directional coupler, received power and forward power was partial present at port 3 & 4 and very less propagation was present at port 4. Figure 6 shows the incident power in the time domain at port 1 having the peak to peak amplitude of 0.12 (a.u) to -0.12 (a.u), and Figure 7 shows the received power in the time domain at port 2. The frequency

DFT of all the four ports powers were depicted in Figure 9.

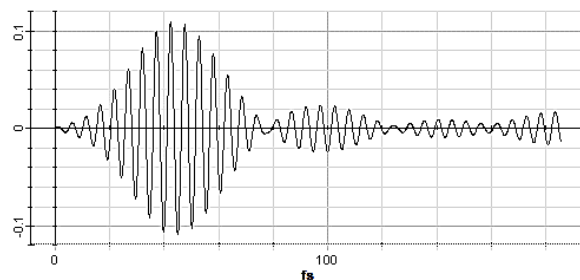


Figure 6. Incident power at port 1

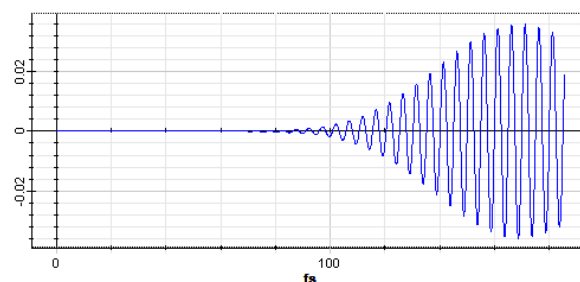


Figure 7. Received power at Port 2

Figure 8 shows the forward power in the time domain at port 3, and the reflected power which is very less as shown in figure 8. The response time of the proposed directional coupler is 100fs.

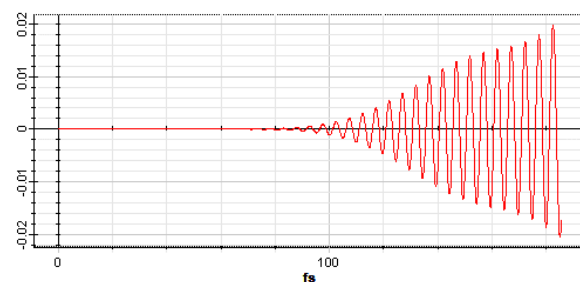


Figure 8. Forward power at port 3

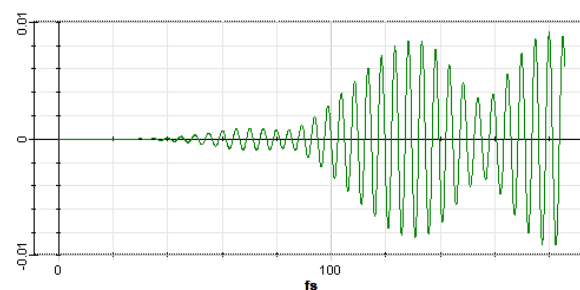


Figure 9. Backward power at port 4

The theoretical concepts of the 4 port bidirectional directional coupler were achieved effectively. The normalized frequency calculations were made both theoretically and practically depicted through Equations (1-5). The photonic bandgaps were calculated using the equations (6-7).

A. Calculation of normalized frequency

1) Theoretical calculation

Normalized frequency,

$$f_n = \frac{\omega a}{2\pi c} = \frac{a}{\lambda} \quad (1)$$

Where, a = lattice constant, c = velocity of light in meter/sec, ω = angular frequency in Hz.

$$f_n = \frac{0.750 \mu\text{m}}{1.55 \mu\text{m}}$$

$$f_n = 0.484 \text{ GHz} \quad (2)$$

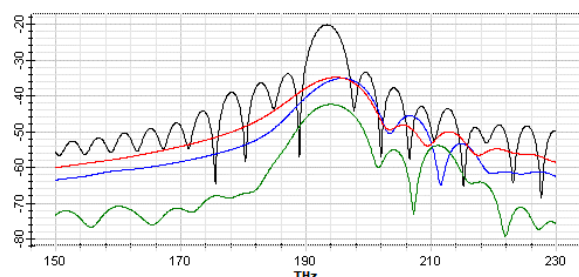


Figure 9. Frequency DFT in dB

2) Experimental calculation

The two Bandgaps are obtained using PWE method of simulation. The observed bandgaps are 0.304484 GHz to 0.45267 GHz and 304484 GHz 0.45267 GHz. The normalized frequency of the corresponding bandgaps are calculated based on the PWE methods are as follows.

So the normalized frequency f_{n1} & f_{n2} are,

$$f_{n1} = \frac{(0.304484 + 0.45267)}{2} \text{ GHz}$$

$$f_{n1} = 0.379 \text{ GHz} \quad (3)$$

$$f_{n2} = \frac{(0.577229 + 0.729649)}{2} \text{ GHz}$$

$$f_{n2} = 0.653 \text{ GHz} \quad (4)$$

The average normalized frequency is,

$$f_n = 0.516 \text{ GHz} \quad (5)$$

The Photonic Bandgap width PBG_1 is,

$$PBG_1 = (0.45267 - 0.304484) \text{ GHz}$$

$$PBG_1 = 0.148 \quad (6)$$

The Photonic Bandgap width PBG_2 is,

$$PBG_2 = (0.729649 - 0.577229) \text{ GHz}$$

$$PBG_2 = 0.152 \quad (7)$$

Among these two bandgaps the second gap lies between 0.577229 and 0.729649 was consider for the design of the proposed directional coupler.

V. CONCLUSION AND FUTURE SCOPE

To overcome the limitations of conventional digital computing, nanophotonic computing is performed through ultrafast optical components such as a directional coupler using nonlinear 2D Photonic Crystal (NPC). The optical directional coupler is designed by the dielectric rod type method with hexagonal lattices. The light wave propagation was observed using the FDTD method and the bandgap structures were analyzed using the Plane Wave Expansion (PWE) method. The performance of the photonic crystal based directional coupler was observed in terms of transmission and reflection. Due to the miniaturized design of the nanostructured bidirectional directional coupler, it will be used as a basic block of all-optical logic gates, all-optical combinational and all-optical sequential circuit designs.

Hence, the proposed optical component is very useful for ultrafast optical operations and future photonic integrated circuits. By using the proposed directional coupler optical switching can be performed and a number of applications can be developed

for optical networks which are kept for future work.

REFERENCES

- [1] Vakili, B., Bahadori-Haghighi, S. And Ghayour, R.. (2015) All-optical switching using a new photonic crystal directional coupler. *Advanced Electromagnetics*, 4(1), pp.63-67.
- [2] Talebzadeh, R., Soroosh, M., Mehdizadeh, F.A.R.H.A.D., (2016) Improved low channel spacing high quality factor four-channel demultiplexer based on photonic crystal ring resonators. *Optica Applicata*, 46(4).
- [3] Insu Park, Hyun-Shik Lee, Hyun-Jun Kim, Kyung-Mi Moon, Seung-Gol Lee, Beomhoan O, Se-Geun Park, And El-Hang Lee (2006) Photonic crystal power-splitter based on directional coupling, *Optical Society of America*, Vol. 12, No. 15.
- [4] Ghorbani, S., Mosalanezhad, R. And Ghadar, G.R., (2017) Design and Simulation of All Optical Photonic Crystal Wavelength Selective Devices Based on Directional Couplers for Optical Communication Systems. *Medbiotech Journal*, 1(04), pp.178-183.
- [5] Beggs. D.M, White.T.P, O'faolain.L And Krauss.T.F (2008) Design and Simulation of a Photonic Crystal Directional Coupler for the Use as an Optical Switch, *Eindhoven*, Vol. 11, No. 13.
- [6] Eshaghi. A, Mirsalehi.M.M, Attari.A.R And Malekabadi (2008) All Optical Switching Structure Using Non-Linear Photonic Crystal directional Coupler, *Progress in Electromagnetics Research Symposium*, Vol. 4652, pp. 77-85.
- [7] Han, Z., Moille, G., Checoury, X., Bourderionnet, J., Boucaud, P., De Rossi, A. And Combrié, S., (2015) High-performance and power-efficient 2×2 optical switch on silicon-on-insulator. *Optics Express*, 23(19), pp.24163-24170.
- [8] Nanda, R., Rath, R., Swarnakar, S., & Kumar, S. (2022) Design of All-Optical Directional Coupler Using Plasmonic MIM Waveguide for Switching Applications. *Plasmonics*, 17(5), 2153-2159.
- [9] Sharifi, H., Hamidi, S. M., & Navi, K. (2017). All-optical photonic crystal logic gates using nonlinear directional coupler. *Photonics and Nanostructures-Fundamentals and applications*, 27, pp-55-63.
- [10] De Oliveira, J. E., De Sousa, F. B., De Oliveira, J. M., De Oliveira, L. A., Da Silva, H. A. B., & Sabino, E. R. (2022) Analysis of the Behavior of an All-Optical NOT Logic Gate in a Photonic Crystal Directional Coupler. *Brazilian Journal of Development*, 8(4), pp-30365-30378.
- [11] Sharifi, H., & Maleknejad, M. (2021) Multi-functional all-optical photonic crystal logic gate using nonlinear directional coupler. *Optical and Quantum Electronics*, 53(12), pp-673.
- [12] Yamamoto, N., Ogawa, T. And Komori, K., (2006) Photonic crystal directional coupler switch with small switching length and wide bandwidth. *Optics Express*, 14(3), pp.1223-1229.
- [13] Shamsi, A., (2021) A high speed all optical half adder using photonic crystal based nonlinear ring resonators. *Journal of Optical Communications*.
- [14] Parandin, F., Sheykhan, A., (2022) Design of an all-optical half adder based on photonic crystal ring resonator. *Optical and Quantum Electronics*, 54(7), p.443.
- [15] Pakrai, F., Soroosh, M. And Ganji, J., (2022) A novel proposal for an all optical combined half adder/subtractor. *Optical and Quantum Electronics*, 54(8), p.51

RESEARCH ARTICLE

Photonics Technology

Simulation and numerical analysis of SOA- based all optical NAND gate for high data rate communication

V Anusooya¹, S Ponmalar², MSK Manikandan³ and S Gobalakrishnan⁴

¹ Department of Electronics and Communication Engineering, Amrita College of Engineering and Technology, Tamil Nadu 629901, India.

² Department of Computer Science and Engineering, Velammal College of Engineering and Technology, Tamil Nadu 625009, India.

³ Department of Electronics and Communication Engineering, Thiagarajar College of Engineering, Tamil Nadu 625015, India.

⁴ Department of Nanotechnology, Noorul Islam Centre for Higher Education, Tamil Nadu 629180, India.

Submitted: 18 February 2022; Revised: 15 August 2022; Accepted: 28 October 2022


Abstract: As a result of the development of advanced semiconductor-based optical switching devices and their commercialization, concepts and technologies in all-optical signal processing have evolved significantly in the past few years. Universal gates are required for the realization of logical processes in photonic computing. In this study, a straightforward and small-footprint all-optical NAND gate was created utilizing semiconductor optical amplifier and simulated at high data rates between 10 to 40 Gbps. Numerical analysis of the performance of the suggested NAND gate for various input combinations and semiconductor optical amplifier (SOA) is shown. A numerical study is carried out by varying the wavelength, injection current, confinement factor, and optical elements such as sources, amplifiers, and filters. Unique results were obtained at a 10 Gbps to 40 Gbps data rate for NRZ-L user-defined bit sequences. This type of all-optical NAND gate will be the perfect alternative in the field of all-optical computing to realize a high-speed optical communication network. An extinction ratio of 15.323 dB is achieved at a high data rate of 40 Gbps. The output spectrum of the designed NAND logic is also obtained for a wide input spectrum and the system responds selectively to the input wavelength at 1548.3 nm, which is the probe signal wavelength.

Keywords: Cross-gain modulation, erbium doped fibre amplifier, extinction ratio, gain saturation, optical logic gate, semiconductor optical amplifier.

INTRODUCTION

Considerable research has gone into making all-optical integrated circuits, which are widely useful for doing ultrafast computing to handle ultrahigh bandwidth in the field of communication engineering technology. This technology is very helpful in developing miniaturized and noise-free integrated circuits, which are very difficult to realize using conventional electronic components. Among all the digital logic gates, these are the primary elements for performing any kind of function in electronic circuits. Therefore, similar kinds of gates will be replaced by optical logic gates so that all functions can be done with light.

All-optical logic gates are unique due to their small physical size, negligible electronic interference, excellent immunity against short circuits, and high bandwidth transmission with negligible loss. Implementing a nonlinear medium is essential to complete the design of an all-optical system which plays a major role in modulating the input light signals into the desired output. At a data rate of 80 Gbps, the configuration of the NAND logic gates employing a semiconductor optical amplifier (SOA) and PC-SOA with Mach-Zehnder interferometer (MZI) structure has been designed to achieve an extinction ratio of 7.1 dB and 16.2 dB, respectively (Heydarian *et al.*, 2022). In addition, a three-input all-optical NAND gate that makes use of polarisation rotation in an SOA was demonstrated. The goal of this demonstration was to achieve a high extinction ratio with an unsaturated gain of 30 dB, despite the fact that the output signals had non-uniform amplitudes (Mukherjee & Raja, 2020).

* Corresponding author (v.anusooya@gmail.com;  <https://orcid.org/0000-0003-2608-5738>)



This article is published under the Creative Commons CC-BY-ND License (<http://creativecommons.org/licenses/by-nd/4.0/>). This license permits use, distribution and reproduction, commercial and non-commercial, provided that the original work is properly cited and is not changed in anyway.

The design of all-optical logic gates comprises an encoding system, a frequency generator, and a frequency converter. For the representation of binary states, hybrid encoding techniques are preferred. A four-wave mixing semiconductor amplifier was adopted to develop a frequency generator, and a cross-polarization rotation effect was adopted to develop a frequency converter. With these designed components, a universal all-optical NAND logic system has been studied (Mukherjee *et al.*, 2019). The use of filters along with SOA can help improve the efficiency of the NAND gate.

Continuous improvement is made by the research community from the existing SOA-based NAND gate designs into the SOA-MZI configuration, which enables high switching efficiency, ER ratio, and high bit rate operation (Mehra *et al.*, 2012). To achieve miniaturization, an integrated SOA-based MZI was used at a data rate of 10 Gbps, which opens a new horizon to realize all-optical routing (Ye *et al.*, 2006). The enhancement of the existing design has been attained by introducing a distributed Bragg reflector laser integrated SOA. By increasing the signal rate between 1.25 Gbps and 10 Gbps, the extinction ratio was reduced from 28 dB to 6 dB (Yu *et al.*, 2014).

Kim *et al.* (2006a) found that the NAND, NOR, and their combinations have the best chance of being able to do all kinds of logical operations in the future high-capacity optical communication networks. Excellent recovery time and high-speed operations have been achieved at 5 ps and 10 Gb/s, respectively, using nonlinear vertical-cavity semiconductor gates (Porzi *et al.*, 2008). All-optical AND and NAND gates were designed using silicon-based micro ring resonators, which showed the free carrier dispersion effect (Ibrahim *et al.*, 2003). To achieve 15 dB at 10 Gbps, one research team developed a structure with parallel SOA and MZI logic gates. These gates include XOR, OR, NOR, and NAND (Kim *et al.*, 2006b).

To obtain an ER of 11 dB and a low penalty of 2.3 dB with a gate operating data rate of 42.6 Gbps, differently switched SOAs are used in a MZI configuration (Dailey *et al.*, 2009). The design and modelling of an all-optical NAND gate employing an SOA with a high ER of 15.323 and a data rate of 40 Gbps are reported in this research. The necessary mathematical support from the current literature is used to effectively address the theoretical background of the EDFA and SOA. User defined random input sequences were used in the NAND gate simulations, and the accompanying numerical analyses are documented. The performance of the designed NAND operation was compared with those reported previously.

MATERIALS AND METHODS

Design arrangement

Figure 1 shows the block diagram of the proposed SOA-based all-optical NAND gate. It consists of an EDFA along with a TWSOA, which is the important optical component for the design of the NAND gate. As input sequences, A and B are combined by the optical multiplier and amplified by the EDFA, whereas the reference or probe signal from a continuous wave laser is combined with the amplified input data by an X-coupler. Continuous laser light from port 3 can be used as a reference signal to achieve an all-optical NAND gate function.

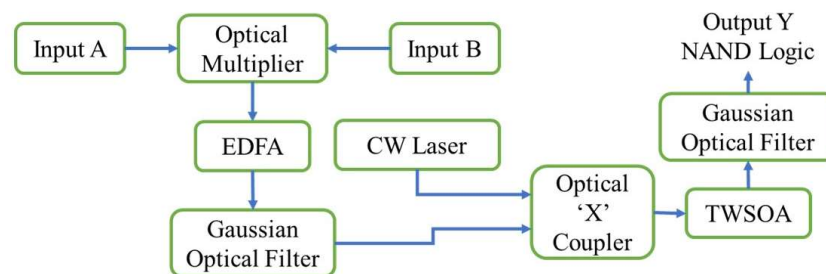


Figure 1: Block diagram representation of proposed NAND gate

Working principles of NAND logic

In the principles of operation, the two binary inputs A and B are converted into an analog waveform using an optical pulse generator, and will be given to the multiplier, which generates the multiplication of binary data. It looks like an AND logic operation. The Erbium-Doped Fibre Amplifier is used to boost the output of the multiplier. It has the lowest loss in all of the optical fibre telecommunication wavelength bands, so it can also be used to make up for signal loss as it travels.

The amplified data is further processed through a tuned Gaussian optical filter to get a specific centre wavelength. A continuous wave laser is employed to generate a probe or reference signal. An optical X coupler receives a combined input and probe signal simultaneously and its outputs are fed to a TWSOA where cross gain modulation (XGM) of carrier induced changes takes place in accordance with the changes in the input A and B (intensity modulation). During cross gain modulation, the gain is changed in SOA by the effect of gain saturation.

The modulated output wavelength of continuous wave (CW) laser is caused by gain variations of the intensity modulated input signals. The output of SOA module carries data that precisely matches the intensity-modulated input signals. The output signal is influenced by the directional characteristics of two signals, such as the reference signal and combined input signals, which can both enter the SOA in a co-directional or counter-directional manner. The optical bandpass filter receives the output of the amplifier.

The Gaussian optical filter centred at wavelength 1548.3 nm and bandwidth 40 GHz selects the desired NAND operation. To get the optimum performance, the SOA parameters were adjusted. When inputs A and B are high, XGM can be generated at SOA, producing a low output (logic 0). If any one of the inputs is low, then the multiplier output is also low and then the output of SOA corresponds to CW laser only, which is the logic high output (logic 1). By filtering and amplifying the power of the CW laser, the NAND output can be seen.

The 'X' coupler is used to couple the output of the multiplier and the output of the CW laser; the coupling coefficient selected was 0.5 dB. The semiconductor optical amplifier receives the coupler output as its input. When either input A or B, or both, is low, a high-power output is produced. Because the multiplier output is low, cross gain modulation cannot take place. On the other hand, the CW laser reference signal makes the logic output high.

The XGM modulated signal can be generated with the combined use of the multiplier output and the signal from the continuous wave laser, whereas the output of the multiplier is high when all the two inputs are logic high. The Gaussian optical filter is used to select a preferred centre frequency from the SOA output and to remove unwanted noise. Then the output will be considered as logic "0". At least one of the inputs goes to zero (low), the output logic becomes logic "1", which indicates that the constructed logic gate reflects the NAND operations.

Theoretical background of EDFA and SOA

Erbium-doped fibre amplifiers (EDFA) are used to boost signals with a loss of less than 0.2 dB/km in the 1550 nm wavelength range. The amplification is purely optical and independent of the data rate (Durhuus *et al.*, 1996). The proposed NAND gate has EDFA parameters of 2.2 μm for the core radius and doping radius. The EDFA's numerical aperture is 0.24, and the losses at 1500 nm are 0.1 dB/m. The wavelength and power for forward transmission are 1553 nm and 100 mW, respectively. Similar to this, the EDFA's backward pump wavelength and power are 980 nm and 0 mW, respectively. This demonstrates that there will be no back reflection while the gate is operating.

Simulated emission is the guiding principle behind the operation of the amplifier in erbium-doped fibre (Nakazawa *et al.*, 1989). When the data is introduced into the fibre at a wavelength ranging from 1520 nm to 1560 nm, the desired result of stimulated emission can be attained. During the stimulated emission process, the signal is amplified by the photon that is just made (Agrawal, 1997).

The rate equation stated the working principles of EDFA. The population of the upper, middle, and ground state is represented by P_u , P_m and P_g , respectively. When T_p is the pumping rate, T_{ab} is the absorption of photons from the signal and τ_{12} is the lifetime of spontaneous emission, the following equations can be written as

$$\frac{dP_g}{dt} = \frac{P_m}{\tau_{mg}} + T_{ab}(P_m - P_g) - T_p(P_g - P_u), \quad \dots(1)$$

$$\frac{dP_m}{dt} = \frac{P_u}{\tau_{um}} - T_{ab}(P_m - P_g), \quad \dots(2)$$

$$\frac{dP_u}{dt} = -\frac{P_u}{\tau_{um}} + T_p(P_g - P_u). \quad \dots(3)$$

In a SOA, population inversion refers to the condition, in which the population of electrons in the conduction band exceeds the population of holes in the valence band, $P_m > P_g$. Under steady state conditions, the time derivatives are not present. Since the photon lifetime at state u is much smaller than the lifetime of a photon at state m , the population of the excited state is defined by the Boltzmann distribution, β .

$$\text{The population of upper level is } P_u = P_m e^{-\frac{E_u - E_m}{kT}} = \beta P_m, \quad \dots(4)$$

$$\text{where } \beta = e^{-\frac{E_u - E_m}{kT}},$$

$$\text{From (1), } \frac{P_m}{\tau_{mg}} + T_{ab}(P_m - P_g) - T_p(P_g - P_u) = 0.$$

This gives the inversion level as

$$n = \frac{P_m}{P_m - P_g} = \frac{(T_p + T_{ab})\tau}{T_p\tau(1 - \beta) - 1}. \quad \dots(5)$$

Equations (1) to (4) related with population inversion, while (5) shows the degree of inversion needed for a signal to successfully flow through the EDFA (Desurvire, 1994). The inversion level n is thus related to both the probe and input signal powers, probe signal wavelength through β (Sabella & Lugli, 1999).

The nonlinear optical effect and the carrier density of SOA can be theoretically analysed by rate equations (Ishikawa, 2008). The device considered for this work is the Travelling Wave Semiconductor Optical Amplifier (TWSOA), which is used to amplify modulated light signals in which the input signal power and the internal noise have an impact on the gain of SOA. Gain saturation will occur if the input power is high, which will decrease the lasing operation in SOA (Liou *et al.*, 1997), which will result in low output.

The carrier recombination lifetime decides the gain dynamics of the SOA and the condition underneath specified appears the carrier density which is created spatially along the whole length of the active region of the device. The carrier recombination lifetime decides the gain dynamics of the SOA and the condition underneath specifies the carrier density, which is created spatially along the whole length of the active region of the device. It combines the forward and turn-around traveling signal as well as the ASE mentioned in (6) (Manimaran & Madhan, 2020). The dynamic equation for the change in carrier density inside the device's active zone is provided by

$$\frac{dn(z)}{dt} = \frac{1}{edLW} - R(n(z)) - \frac{\Gamma}{dw} \left\{ \sum_{k=1}^{N_s} [g_m(v_k, n(z))(N_{sk}^+(z) + N_{sk}^-(z))] \right\} - \frac{2\Gamma}{dw} \left\{ \sum_{k=1}^{N_m-1} [g_m(v_k, n(z))K_j(N_j^+(z) + N_j^-(z))] \right\}, \quad \dots(6)$$

where Γ is the confinement factor, g_m is the material gain, while L , W are the length and the width of the active region of the SOA, respectively. The recombination rate is $R(n(z))$, an emitted photon in the positive and negative Z-direction are $N_{sk}^+(z)$ and $N_{sk}^-(z)$. For the transverse electric (TE) mode, the spontaneous emission

photon rate is $N_j^+(z)$, and for the transverse magnetic (TM) mode, it will be $N_j^-(z)$. The carrier density can be altered within the active region by varying a few parameters or processes which are shown in (6). The infused current, unconstrained radiative and nonradiative recombination, forecast recombination process of carriers, invigorated recombination by the signal, and ASE photons. In the case of a traveling wave amplifier, the mirror losses will not affect the photon lifetime (Eisenstein, 1989; Obermann *et al.*, 1997). In the proposed system, the parameters chosen for the SOA are confinement factor $\Gamma = 0.35$, length $L = 0.5$ mm, width $W = 3$ μm , height $H = 80$ nm, Line width enhancement factor = 5, differential gain $A_d = 27.8 \times 10^{-021} \text{m}^2$.

RESULTS AND DISCUSSION

The study of this numerical simulation explored the dynamics transfer characteristics of the NAND gate for user-defined or random sequence input of A and input B with a data rate of 40 Gbps. The wavelength of 1553.05 nm and 1557.75 nm was selected for A and B with a power of -1.21 dBm and -0.223 dBm, respectively. The centre wavelength of the Gaussian optical filter is 1555.40 nm, which is the average wavelength of both inputs A and B, whereas the wavelength, injection current, and power of the probe or reference signal are 1548.3 nm, 0.95A, and -2.6 dBm, respectively.

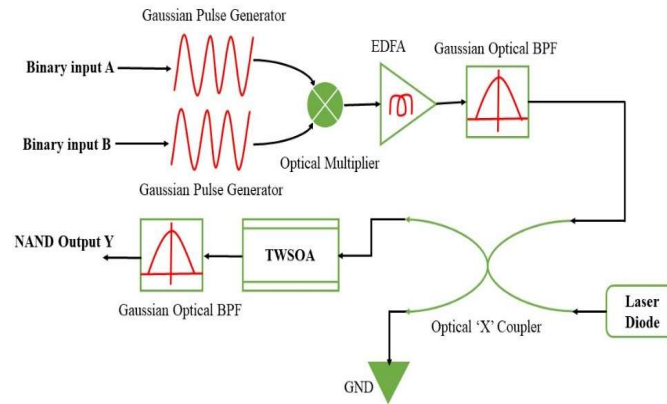


Figure 2: The schematic diagram of the proposed NAND gate design

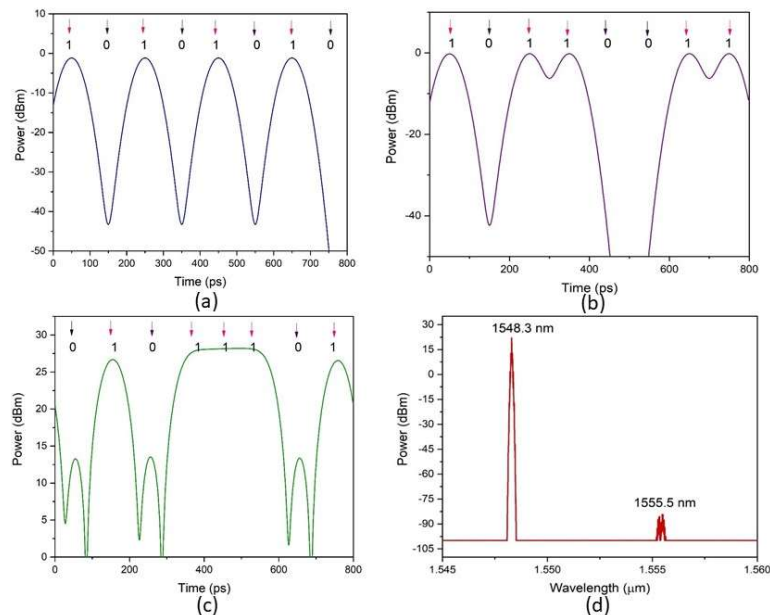


Figure 3: (a). Input sequence A; (b) Input sequence B; (c) Output of NAND logic; (d) Output Power spectrum of designed NAND logic.

The SOA parameters are set as 0.5 mm length, 3 μm width, 80 nm height, and the optical confinement factor is 0.35. The centre wavelength of the Gaussian optical filter placed before SOA is 1555.4 nm and after SOA is 1548.3 nm. Figure 2 shows the schematic of the proposed NAND gate. Figures (3a) and (3b) represent the user-defined input sequence of A: 10101010 and B: 10110011, and Figure (3c) shows the output of NAND logic Y: 01011101. From the NAND gate logic output, we observe that, the output power for logic 1 is 28.575 dBm and the output power for logic 0 is 13.252 dBm. The figure (3d) shows the output spectrum of the NAND logic and it was measured for different wavelengths ranging from 1545 to 1560 nm. The system gives a highly selective response at a 1548.3 nm input wavelength with about 28.5 dBm of output power. All other wavelengths are forbidden from transmission. Around 1555.5 nm, a small output signal (-82 dBm) arises, but it is negligible when compared to 28.5 dBm. Table 1 shows the proposed NAND gate logic output for user-defined input sequences with corresponding logical outputs with power in dBm.

Table 1: Truth table for NAND gate logic (user defined input)

User defined sequence		NAND gate logic	Output power
Input 1 logic	Input 2 logic	$y = \overline{A * B}$	(dBm)
1	1	0	13.252
0	0	1	28.575
1	1	0	13.252
0	1	1	28.575
1	0	1	28.575
0	0	1	28.575
1	1	0	13.252
0	1	1	28.575

Numerical analysis

The analysis of the proposed design can be performed by varying the parameters as well as the optical components. Different wavelengths of output for NAND logic can be observed. At a wavelength of 1548.3 nm, the performance of the pump laser is compared with the CW laser output shown in Figure 4. Even though the optical output power of the pump laser is more stable than the CW laser output, we have chosen a continuous wave laser, which is mainly used in optical low-loss applications.

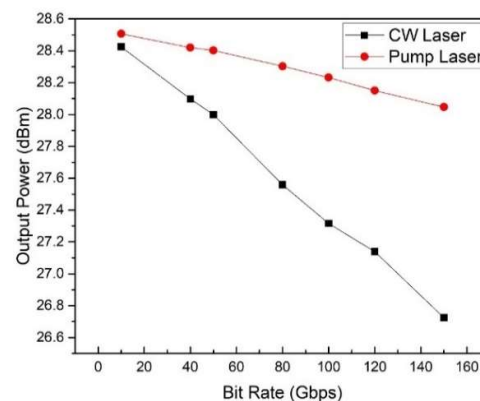


Figure 4: Output optical power at various data rates for CW and pump lasers

The impact of various types of amplifiers on the output power of NAND logic can be seen in Figure 5, in which we observe that the output is greater in optical fibre amplifiers and TWSOA. Likewise, filters were also tested to identify the better performance of the proposed logic gate. In the input stage of the proposed system, the impact of filters is high, but in the case of filters at the output stage, no impact is there, as mentioned in Table 2.

Table 2: Types of filters (vs) output power at $\lambda = 1548.3$ nm and bandwidth= 10 GHz

Sl. no	Types of filters	Output power (dBm)
1	Trapezoidal optical filter	27.416
2	Gaussian optical filter	28.575
3	Butterworth optical filter	28.202
4	Bessel optical filter	28.202
5	Fabry Perot optical filter	24.217
6	Optical digital filter	26.622
7	Periodic optical filter	28.231

The selected components from the analysis can be used for the design of a universal optical NAND gate. Figure 4 shows the relationship between the optical laser source and the operating data rate. Here the same structure can be further tested for various data rates of 10 Gbps to 200 Gbps.

Finally, the required performance can be attained at a bit rate from 10 Gbps to 40 Gbps. Afterward, its output power value can be reduced considerably, and finally, no proper transmission has occurred at a speed of 180 Gbps to 200 Gbps. The rate of change of output power for pump laser and CW laser was calculated from the plot based on the simulated output values of 0.00382 dBm/Gbps and 0.0126 dBm/Gbps, respectively. In order to improve the quality of the output signal, it is recommended to use the appropriate filter in front of the SOA.

In this study, various filters have been analysed and their outputs are observed and listed in Table 2. From the tabulated values, it is obvious that the Gaussian filter and Periodic Optical filter showed better output power compared to other filters, and their output power values are 28.575 dBm and 28.231 dBm, respectively. Since the Gaussian optical filter shows the best output power and also has an optimum shape to get high resolution in the output, it has been selected for the development of the NAND gate logic system.

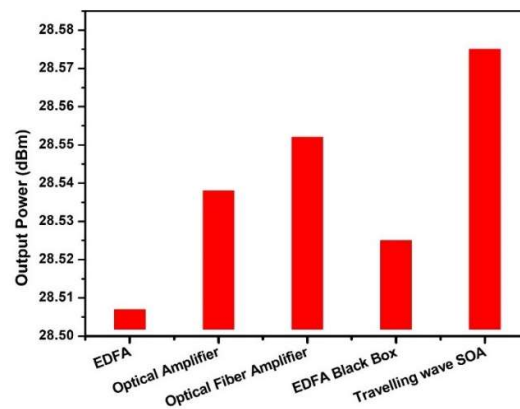
**Figure 5:** Output optical power for different amplifiers

Figure 6, shows the tuning of the wavelength of the carrier signal in order to get the maximum output power, which will favour efficient information transmission. After doing a large-scale variation from 1400 nm to 1600 nm, it has been identified that the system responds better around 1548 nm. Then, the signal wavelength varied from 1548.0 to 1548.9 nm with an increment of 0.1 nm. The output power is maximal when the wavelength is set as 1548.3 nm. The output power drastically decreases on the higher and lower side of the spot of 1548.3 nm, which can be interpreted as the window being optimum for the proposed system. The third optical window, which has a wavelength between 1400 and 1600 nm, was identified in the literature as an appropriate one for achieving low-loss transmission.

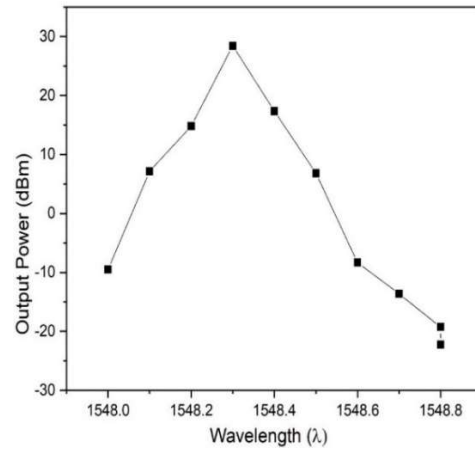


Figure 6: Wavelength (vs) output optical power using CW laser.

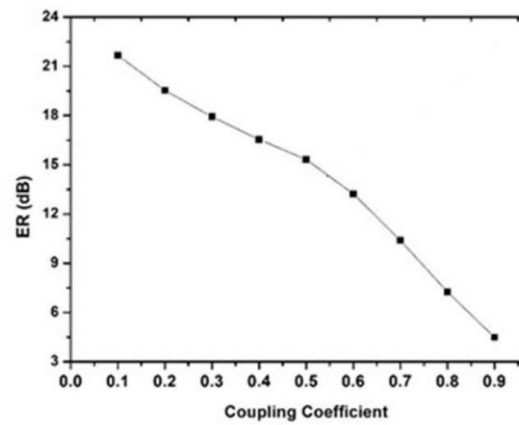


Figure 7: The response of ER to variation in coupling coefficient.

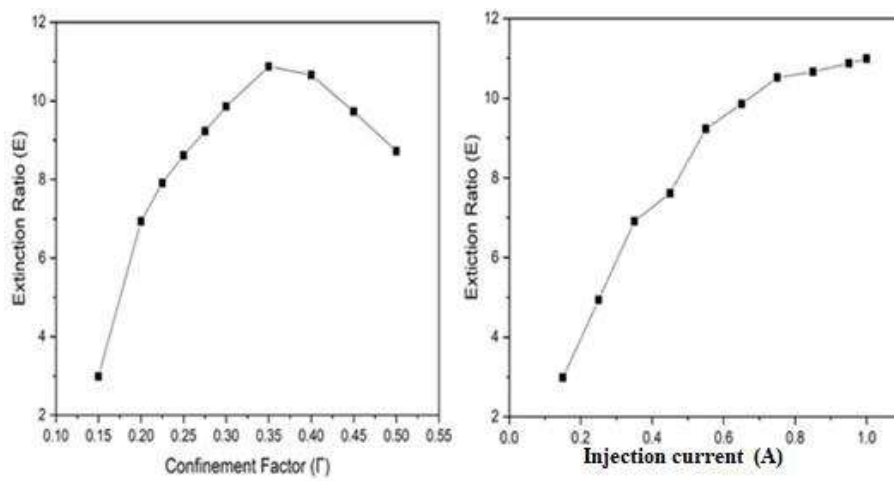


Figure 8: Relationship between confinement factor, injection current and extinction ratio at 10 Gbps data rate.

In telecommunications and optical systems, the extinction ratio (ER) is a measure of the contrast or ratio of power between the "on" and "off" states of an optical signal which considered as an important factor in evaluating the performance of the system at a particular data rate.

The performance of the NAND gate is verified using the Extinction Ratio (ER) as shown in Figure 7, by adjusting the coupling coefficient of the X-coupler. According to this, ER ratio increases if the coupling coefficient is smaller than 0.5. The ER is decreased-when the coupling coefficient lies between 0.5 and 0.9. The NAND logic operation will not function correctly, after the coupling coefficient approaches one. The coupling coefficient selected for the current work is 0.5 in order to achieve an appropriate NAND gate logical operation at a high data rate of 40 Gbps. Moreover, both the confinement factor and injection current varied independently and the extinction ratio based on the output results is shown in Figure. 8. The confinement factor and the injection current of 0.35 and 0.95 A, respectively, produced an excellent extinction ratio of 15.323 dB. The same high extinction ratio can be maintained for the high-speed data rate of 10 Gbps to 40 Gbps. Similarly, the important parameters such as the Extinction Ratio (ER) and Bit Error Rate (BER) were calculated and listed in Table 3.

Table 3: Calculated parameters of the designed NAND logic system

Sl. No	Parameters	Metrics
1	Extinction ratio	15.323 dB
2	Bit error rate (BER)	4.27×10^{-26}

Table 4: Comparison of NAND gate designs

Sl. no.	Author name and year	Title	Optical components used	Data rate (Gbps)	Extinction ratio (dB)
1	Heydarian <i>et al.</i> , 2022	Design and analysis of an all-optical NAND logic gate using a photonic crystal semiconductor optical amplifier based on the Mach–Zehnder interferometer structure	SOA	80	7.1
2	Mukherjee <i>et al.</i> , 2019	All-optical logic gate NAND using semiconductor optical amplifiers with simulation	PC-SOA	80	16.2
3	Oliveira <i>et al.</i> , 2019	New design of all-optical logic universal NAND gate formed by NOT (A AND B) gates using Michelson Interferometer based on semiconductor optical amplifier	Two SOA	10	13.0
4	Yu <i>et al.</i> , 2014	All-optical decision gate with extinction ratio improved scheme using a SOA-DBR laser	SOA- MI	10	-
5	Mehra <i>et al.</i> , 2012	All optical universal logic Gates Design and Simulation using SOA	SOA- DBR Laser	10	24
6	Mehra <i>et al.</i> , 2012	SOA based all-optical NAND gates and their comparison	Two SOA	40	8.75
7	Nakarmi <i>et al.</i> , 2012	Demonstration of all-optical NAND gate using single-mode Fabry–Pérot laser diode	SOA- filter	80	9.73
			SOA- MZI	80	11.09
			Fabry Perot laser diode	10	14.6

We deduce from the comparison table that the majority of research on the design of all-optical NAND gates for optoelectronic integrated circuits has a data rate of 10 Gbps. If the data rate rises, the extinction ratio may decline. With a single SOA and filter combination, the NAND gate in the proposed work is created with a high data rate of 40 Gbps and an enhanced extinction ratio of 15.323 dB.

CONCLUSION

A unique all-optical NAND gate using a single TWSOA has been developed and implemented in this study, and by numerical simulation, a high ER of 15.323 dB at a data rate of 10 Gbps to 40 Gbps is achieved. Additionally, the functionality of all-optical NAND gate is examined in various scenarios. By adjusting the input data, SOA, CW laser, or optical filter parameters, the maximum extinction ratio for the NAND gate was achieved. Calculated values for the ER and BER were 15.323 dB and 4.27×10^{-26} respectively.

Conflict of interest

The authors declare that there is no conflict of interest.

Acknowledgement

The authors acknowledge the Department of Electronics and Communication Engineering, Government College of Engineering Tirunelveli for providing software facility for the successful completion of the proposed work.

REFERENCES

- Agrawal G.P. (1997). *Fiber-optic Communication Systems*, 2nd edition. John Wiley & Sons, Inc., USA.
- Desurvire E. (1994). *Erbium Doped Fiber Amplifiers*. John Wiley & Sons, Inc., USA.
- Dailey J.M., Ibrahim S.K., Manning R.J., Webb R.P., Lardenois S., Maxwell G.D. & Poustie A.J. (2009). 42.6 Gbit/s fully integrated all-optical XOR gate. *Electronics Letters* **45**(20): 1047–1049.
- Durhuus T., Mikkelsen B., Joergensen C., Lykke Danielsen S. & Stubkjaer K.E. (1996). All-optical wavelength conversion by semiconductor optical amplifiers. *Journal of Lightwave Technology* **14**(6): 942–954.
DOI: <https://doi.org/10.1109/50.511594>
- Eisenstein G. (1989). Semiconductor optical amplifiers. *IEEE Circuits and Devices Magazine* **5**(4): 25–30.
DOI: <https://doi.org/10.1109/101.29899>
- Heydarian K., Nosratpour A. & Razaghi M. (2022). Design and analysis of an all-optical NAND logic gate using a photonic crystal semiconductor optical amplifier based on the Mach-Zehnder interferometer structure. *Photonics and Nanostructures-Fundamentals and Applications* **49**: 100992.
DOI: <https://doi.org/10.1016/j.photonics.2022.100992>
- Ibrahim T.A., Grover R., Kuo L.C., Kanakaraju S., Calhoun L.C. & Ho P.T. (2003). All-optical AND/NAND logic gates using semiconductor microresonators. *IEEE Photonics Technology Letters* **15**(10): 1422–1424.
DOI: <https://doi.org/10.1109/LPT.2003.818049>
- Ishikawa H. (2008). Ultrafast all-optical signal processing devices. In: *Ultrafast All-Optical Signal Processing Devices*. John Wiley & Sons, Inc., USA.
DOI: <https://doi.org/10.1002/9780470758694>
- Kim J.-Y., Kang J.-M., Kim T.-Y. & Han S.-K. (2006a). All-optical multiple logic gates with XOR, NOR, OR, and NAND functions using parallel SOA-MZI structures: theory and experiment. *Journal of Lightwave Technology* **24**(9): 3392–3399.
DOI: <https://doi.org/10.1109/JLT.2006.880593>
- Kim J.-Y., Kang J.-M., Kim T.-Y. & Han S.-K. (2006b). 10 Gbit/s all-optical composite logic gates with XOR, NOR, OR and NAND functions using SOA-MZI structures. *Electronics Letters* **42**(5): 303–304.
DOI: <https://doi.org/10.1049/el:20063501>
- Liou K.Y., Koren U., Burrows E.C., Zyskind J.L. & Dreyer K. (1997). A WDM access system architecture based on spectral slicing of an amplified LED and delay-line multiplexing and encoding of eight wavelength channels for 64 subscribers. *IEEE Photonics Technology Letters* **9**(4): 517–519.
DOI: <https://doi.org/10.1109/68.559407>
- Manimaran P. & Madhan M.G. (2020). Bandwidth characteristics of TWSOA based inline detector configurations for near infrared communications. *Optical and Quantum Electronics* **52**(1): 32.
DOI: <https://doi.org/10.1007/s11082-019-2143-y>
- Mehra R. & Tripathi J.K. (2012). All optical universal logic gates design and simulation using SOA. *IJCEM International Journal of Computational Engineering and Management* **15**: 41–45.
- Mehra R., Jaiswal S. & Dixit H. K. (2012). SOA based all-optical NAND gates and their comparison. 2012 *Third International Conference on Computer and Communication Technology*, 23-25 November, Allahabad, India, pp. 175–177.
DOI: <https://doi.org/10.1109/ICCCT.2012.42>

- Mukherjee K. & Raja A. (2020). Three Input NAND gate using semiconductor optical amplifier. *2020 IEEE VLSI Device Circuit and System (VLSI DCS 2020)*, Kolkata, India, 18–19 July, pp. 142–145.
- Mukherjee K., Raja A. & Maji K. (2019). All-optical logic gate NAND using semiconductor optical amplifiers with simulation. *Journal of Optics* **48**(3): 357–364.
DOI: <https://doi.org/10.1007/s12596-019-00555-9>
- Nakarmi B., Rakib-Uddin M., Hoai T. Q. & Won Y. H. (2010). Demonstration of all-optical NAND gate using single-mode Fabry–Pérot laser diode. *IEEE Photonics Technology Letters* **23**(4): 236–238.
DOI: <https://doi.org/10.1109/LPT.2010.2098863>
- Nakazawa M., Kimura Y. & Suzuki K. (1989). Efficient Er³⁺-doped optical fiber amplifier pumped by a 1.48 μm InGaAsP laser diode. *Applied Physics Letters* **54**(4): 295–297.
- Oliveira J.M., Silva H.A.B.D., Oliveira L.A.D., Sousa F.B.D., Oliveira J.E.D., Sousa F.M.D. & Costa M.B.C. (2019). New design of all-optical logic universal NAND gate formed by NOT (A AND B) gates using Michelson interferometer based on semiconductor optical amplifier. *Journal of Computational and Theoretical Nanoscience* **16**(7): 2712–2719.
DOI: <https://doi.org/10.1166/jctn.2019.8236>
- Obermann K., Koltchanov I., Petermann K., Diez S., Ludwig R. & Weber H. G. (1997). Noise analysis of frequency converters utilizing semiconductor-laser amplifiers. *IEEE Journal of Quantum Electronics* **33**(1): 81–88.
DOI: <https://doi.org/10.1109/3.554895>
- Porzi C., Guina M., Bogoni A. & Potì L. (2008). All-optical NAND/NOR logic gates based on semiconductor saturable absorber etalons. *IEEE Journal of Selected Topics in Quantum Electronics* **14**(3): 927–937.
DOI: <https://doi.org/10.1109/JSTQE.2008.919754>
- Sabella R. & Lugli P. (1999). High speed optical communications. In: *High Speed Optical Communications*, pp. 207–232. Springer, USA.
DOI: <https://doi.org/10.1007/978-1-4615-5275-8>
- Ye X., Ye P. & Zhang M. (2006). All-optical NAND gate using integrated SOA-based Mach-Zehnder interferometer. *Optical Fiber Technology* **12**(4): 312–316.
DOI: <https://doi.org/10.1016/j.yofte.2005.12.001>
- Yu L.-Q., Lu D. & Zhao L.-J. (2014). All-optical decision gate with extinction ratio improved scheme using an SOA-DBR laser. *IEEE Photonics Technology Letters* **26**(21): 2126–2129.
DOI: <https://doi.org/10.1109/LPT.2014.2349274>



PREDICTING ENERGY USAGE FOR SMART HOME USING SMART SWITCH

Mrs.C.B.Selva Lakshmi ¹, Assistant Professor, Velammal College of Engineering and Technology, Madurai,
cbselak08@gmail.com

Dr.A.Radhika ², Associate Professor, Velammal College of Engineering and Technology, Madurai,
ark@vcet.ac.in

ABSTRACT

The Smart switch is a switch that measures the future trends of electricity consumption, it is a product that is much needed in today's world where electricity plays an important role that is being consumed by industries and domestics on regular basis. The demand and supply of the relationship of electricity are always at troubles in critical times. It raises power cuts. The main reason for this problem is that prediction of the electricity consumption trend is not well predicted. Presently, we use the human expertise of senior members of the electricity board to predict the trends. However, it may not be well in a situation where the demands are changing dynamically. Hence, we need to analyse the prediction trends through computing models. Machine learning is a computing model that uses existing data to predict the future trends of existing data. This project presents a smart switch to predict the load trends of electricity in domestic using machine learning. This agent comes with hardware and software components. The hardware component is a programmed switch that supplies the current to the appliances. This switch is programmed in such way that it measures the current flow consumption and duration using Arduino and Current Sensors. The measured information will be sent to the database. The database will keep collecting information 24x7(until the switch is ON). The software component brings a backend processing unit that is connected to the databases. The collected Dataset is then processed through a machine learning analyzer to predict the trends of load consumption.

KEYWORDS: Machine Learning, Regression, Electricity prediction, ACS712Current Sensor.

1.INTRODUCTION

The Smart switch is a normal switch which is connected to current sensors. The current sensors collect the power consumption of the equipment which is connected to the switch.

This project brings an awareness to the people using the smart switch about their own consumption of electricity. This will help themselves saving money and the society in saving the resources. The supply and demand issues will also come to an end when people are more aware about their daily consumption of power. The supply and demand issues arise when the demand is more than the supply. The supply and demand issues in the recent times troubles us a lot, this happens when the people are not aware about their electricity usage patterns, added to, the people are paying more charges for their electricity than for what they use, this becomes a loss for them too. So, our plan is to devise a smart electrical switch that automatically reads the power consumption information, load it in a database, analyze and forecast the future trends of power consumption which will help the domestic people in their daily usage.

II. LITERATURE SURVEY

Smart grid and smart metering technologies allow residential consumers to monitor and control electricity consumption easily. [1] The real-time energy monitoring system is an application of the smart grid technology used to provide users with updates on their home electricity consumption information. This paper aims to forecast a month ahead of daily electricity consumption time-series data for one of the real-time energy monitoring system named beLyfe. Four separate multistep Long Short Term Memory LSTM neural network sequence prediction models such as vanilla LSTM, Bidirectional LSTM, Stacked LSTM, and Convolutional LSTM ConvLSTM has been evaluated to determine the optimal model to achieve this objective. A comparison experiment is performed to evaluate each multistep LSTM model performance in terms of accuracy and robustness. Experiment results show that the ConvLSTM model achieves overall high predictive accuracy and is less computationally expensive during model training than remaining models.

[2] With increasing of distributed energy resources deployment behind-the-meter and of the power system levels, more attention is being placed on electric load and generation forecasting or prediction for individual residences. While prediction with machine learning based approaches of aggregated power load, at the substation or community levels, has been relatively successful, the problem of prediction of power of individual houses remains a largely open problem. [3] This problem is harder due to the increased variability and

uncertainty in user consumption behavior, which make individual residence power traces be more erratic and less predictable

[4] Prediction of electric power consumption has recently become one of the important domains, not only for the electrical utilities, but also for the consumers of the electricity. In the recent time, the demand of accurate electric power consumption prediction has been increased and is considered as an integral part for electric utility in planning and scheduling of electricity distribution from the power system. Accurate prediction enabled to better manage of electric usage[5]. A review of the recent electric consumption prediction techniques will be presented in this paper in the context of different power consumption prediction applications. [6] This study focusses a comprehensive survey of the existing methods employed for power consumption prediction process and a comparative study has been performed on different models based on the three methods. [7] The predicted results of the models are evaluated by using the performance metrics such as Mean Square Error (MSE), Root Mean Square Error (RMSE), Mean Absolute Error (MAE), and Mean Absolute Percentage Error (MAPE) metric

III. PREDICTION AND METHODOLOGIES

The real time data is generated using python programs in a .csv format, the real time data are collected using ACS712 sensors, which is a current sensor that is used to monitor the power consumptions of the connected equipment. ACS712 is an AC or DC current sensor, it is connected to a switch, when the switch is powered on the current sensor starts to read the raw data of the connected equipment, the Arduino IDE is used to convert the raw data into power and energy. The reading are recorded in an excel sheet in the .csv format.

Recurrent Neural Network (RNN) is a part of Artificial Neural Network which will be primarily work for time series data or sequential data. Standard Neural Networks algorithms only work for the data points that is independent of each other. If we have the series of data that rely on the past data, then we have to make changes in the neural network. Recurrent Neural Network (RNN) has the idea of “memory” which helps to store the old states to predict next output order.

Long Short-Term Memory (LSTM) is an Recurrent Neural Network (RNN) Algorithm

which was used in domain of Deep Learning. Long Short-Term Memory Model was not like the standard feed forward neural networks, It has feedback connections. LSTM can process both single data points (e.g. Images) and entire sequences of data (e.g. speech or videos). LSTM units contains input gate, output gate, forget gate and a cell. These gates is to regulate the information flow in and out of cell. LSTM Networks were used to classify, process and to make predictions using the time series data.

The Real time data collected from the current sensor with Arduino is in the format, date with time and the power usage that was calculated from the raw current sensor output. The dataset is then evaluated for duplicate entries and it will be removed. The time series data is then trained and tested. The forecasting is done for 'n' steps ahead using the full data that is dataset has. If the dataset contains huge data then the predicted data will have more accuracy when compared to the less data in data set. The training set is observed for loss and accuracy by providing optimal epoch number. If the epochs were higher, then the data training data will take more time and the accuracy will also be affected. The output of the model is the forecasted power usage which is actually seven days from the date of last value in the data set and the train data which was compared with actual data set that shows the accuracy of the predicted data. The outputs will be in the form of graph. By using those predicted values the Bill for power consumption is generated.

IV. WORKING & IMPLEMENTATION

The load (bulb) is connected to the socket having the smart switch which is connected to the current sensor. The current sensor readings are recorded which Arduino and using the desktop/laptop and the Machine Learning algorithms are used to predict the future trends. Then the predicted electricity consumption is calculated and the respective bills are generated and sent to the end user via e-mail. Figure 1 shows the System Architecture

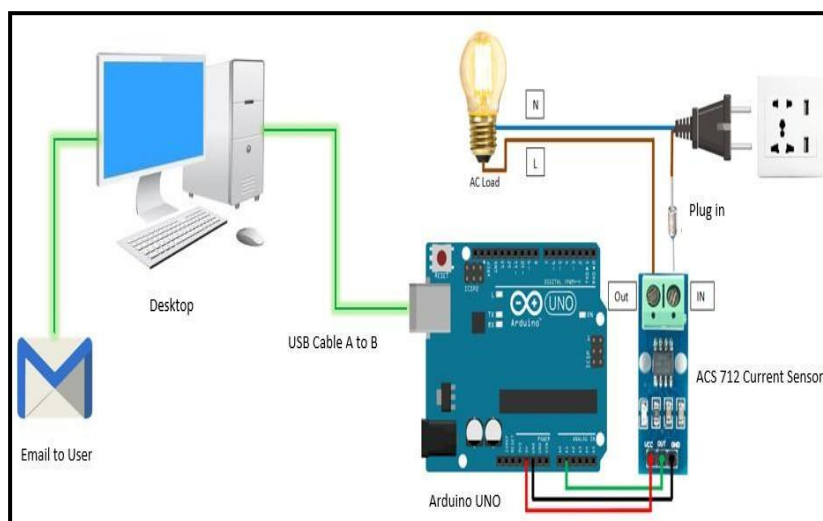


Figure 1 System Architecture

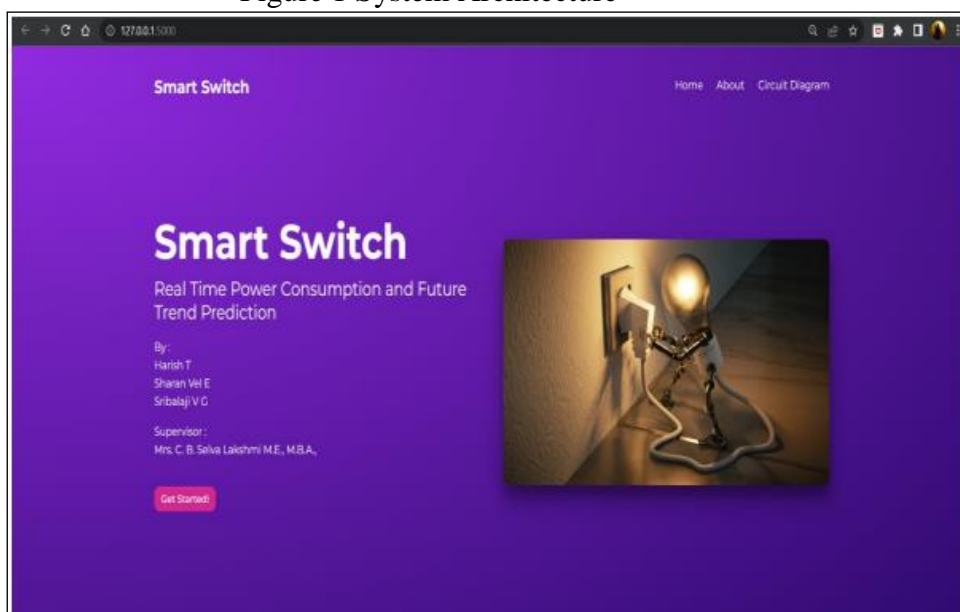


Figure 2 Home Page

Figure 2 shows the home page is the first page that appear while project gets executed. It starts from here, this page consists of the title, team member names along with the get started button

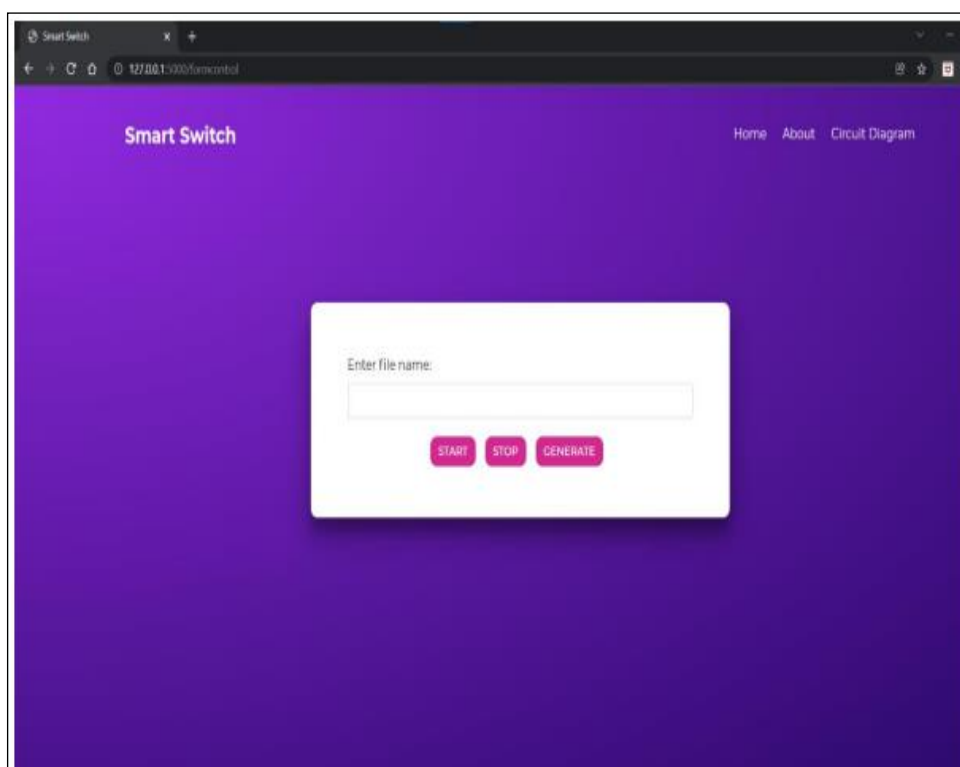


Figure 3 Get Started Page

Figure 3 shows the Get Started page where the operations of the project take place. The following steps are to be followed:

1. The file name of the excel should be given in the textbox given
2. After entering the file name the start button should be clicked (Note: Ensure that the sensors and Arduino are well connected and plugged in)
3. Once the start button is clicked the readings of the equipment are measured and recorded in the created excel sheet.
4. After enough readings are taken the Stop button is clicked to stop the recording of the consumption
5. Click the generate button to start the analysis of the dataset collected, once the analysis is done by the algorithm, the prediction is displayed in the form of graph

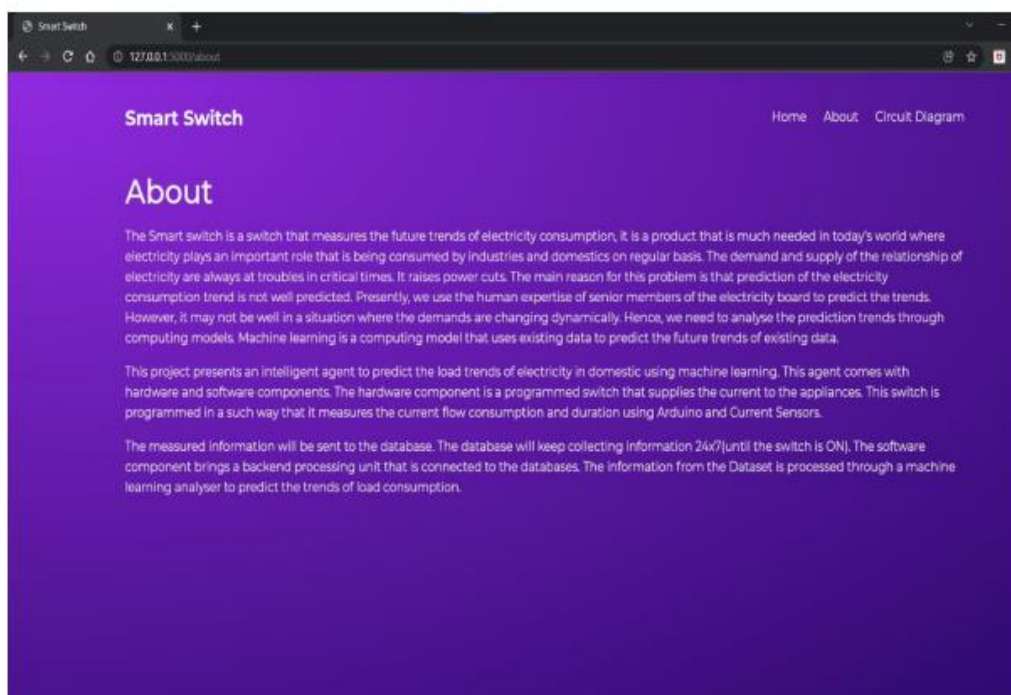


Figure 4 About Page

this page consists of the circuit diagram of the project, this can be used to ensure the connections before clicking the start button in the get started page. Figure 4 shows the About Page



Figure 5 Prototype

Figure 5 shows the prototype which consists of the following:

- Arduino
- Switch
- Plug
- Current sensor
- USB-B TO USB-A cable
- Bulb (Load)

V. PREDICTION AND BILL GENERATION

Once the generate button is pressed in the Get Started page the prediction starts and the bill is generated. Below are the images of the predicted values and the bill generated.

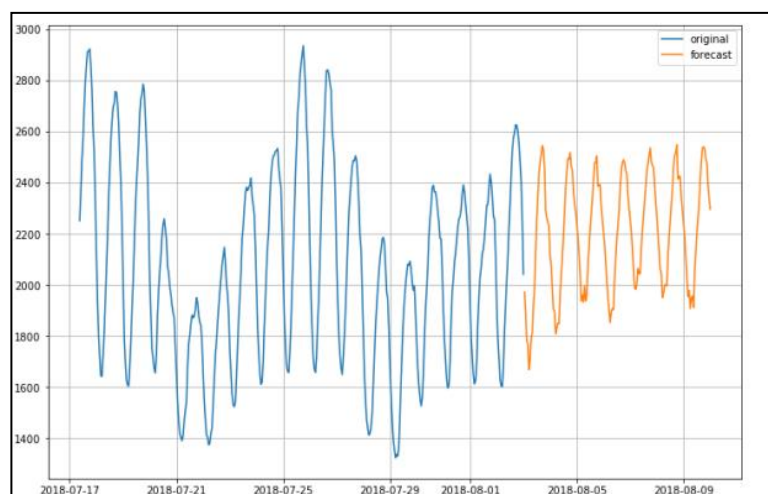


Figure 6 Predicted Graph

The orange line shows the predicted values of the equipment's and below is the sample of the predicted bill has been calculated. Figure 6 shows the Predicted calculations made is generated as a bill and sent it via e-mail to the users.

VI. CONCLUSION

aims to bring awareness about the electricity consumption to people and people can use it in their homes to predict their electricity consumption trends and reduce their electricity usage to save electricity costs. This also helps the electricity board to control the supply and demand issues, since the people will limit their usage to certain level. The user will get a predicted bill

so that he/she can have a idea about their own consumption of power. This can help to reduce the charges of electricity.

REFERENCES

- [1] .S. Duerr, C. Ababei, and D. M. Ionel, "Smartbuilds: An energy and power simulation framework for buildings and districts," IEEE Transactions on Industry Applications, vol. 53, no. 1, pp. 402–410, 2017.
- [2].R. E. Alden, P. Han, and D. M. Ionel, "Smart plug and circuit breaker technologies for residential buildings in the us," in 2019 8th International Conference on Renewable Energy Research and Applications (ICRERA), 2019, pp. 1018–1021.
- [3].K. Amarasinghe, D.L. Marino, and M. Manic, "Deep neural networks for energy load forecasting," IEEE Int. Symposium on Industrial Electronics (ISIE), 2017.
- [4].P. Chen, W. Li, Y. Chen, K. Guo, and Y. Niu, "A parallel evolutionary extreme learning machine scheme for electrical load prediction," IEEE Computing Conference, 2017.
- [5] Electricity consumption prediction based on LSTM neural network. Xu Yaoqiang, Fang Leheng, Zhao Donghua, et al. Electr Power Big Data 2017;(8):25–9, 14
- [6] Xu Aidong, Guo Yanwen, Wu Tao, et al. Household electricity consumption prediction based on Bi-LSTM. Ind Control Comput 2020;33(04):11–3
- [7] Study on Power Energy Consumption Model for Large-scale Public Building. Ma, Y.; Yu, J.Q.; Yang, C.Y.; Wang, L. In Proceedings of the 2010 2nd International Workshop on. IEEE Intelligent Systems and Applications, Wuhan, China, 22–23 May 2010; pp. 1–4.
- [8] Predicting residential energy consumption using CNN-LSTM neural networks, TaeYoungKim, Sung-BaeCho, ScienceDirect(Elsevier Ltd), 2019/182/4

[9] A Survey on Electric Power Consumption Prediction Techniques, Antara Mahanta Barua, International Journal of Engineering Research and Technology (IJERT) Pradyut Kumar Goswami, 2020/13/10

[10] Electric Energy Consumption Prediction by Deep Learning with State Explainable Autoencoder, Jin-Young Kim and Sung-Bae Cho, MDPI (Energies), 2019/12/4



RESPONSIVE WEB DESIGN WITH CHATBOT FOR AGRICULTURAL WEBSITE

P.Alli¹, Department of Computer Science and Engineering, Velammal College of Engineering and Technology, Madurai

Dr. J. Dinesh Peter², Department of Computer Science and Engineering, Karunya Institute of Technology and Sciences, Coimbatore

C.B.Selva Lakshmi³, Department of Computer Science and Engineering, Velammal College of Engineering and Technology, Madurai

Harini K K⁴, UG Student, Department of Computer Science and Engineering, Velammal College of Engineering and Technology, Madurai
Corresponding author - cbselak08@gmail.com

ABSTRACT

E-Commerce Agricultural websites provide an interaction between farmers and customers. However, many of these websites are not designed to be accessible on mobile devices, which can limit their effectiveness in reaching a broad audience. In this paper, we present a responsive web design for e-commerce agricultural websites, which allows interaction across a range of devices and screen sizes. It allows customers to shop for products from the comfort of their own homes, without having to physically visit a store. This can be particularly useful for customers who live in remote or rural areas. Chatbots are used to provide customers with quick and convenient customer support, personalized recommendations, help in resolving customer issues, and learning about products and services. Chatbot is developed to help farmers to get to know about the crop that suits their environment and provide various agriculture-related details. It also helps the farmers get to know about current weather details. With the growing technology and internet services the information related to the government agricultural schemes are now available on internet which are provided by the chatbot. And crops are also recommended according to the weather by chatbot. So, the motivation of this paper is to provide the farmers of our country with easy to use website for their benefit so that they can get all the information related to agriculture.

Keywords E-Commerce, Chatbot, Crop Recommendation, Responsive Website

INTRODUCTION

Agriculture is the strength of Indian economy and 70% of India's total population is primarily dependent on agriculture for their employment. With the global population expected to reach 9.7

billion by 2050, agriculture has become an increasingly important area of research and development as the demand for food and other agricultural products continues to grow. The design and development of agricultural websites can also incorporate features such as e-commerce functionality, which allows farmers and other users to purchase agricultural products and services online. This can improve access to markets for farmers and provide greater convenience for buyers. Agricultural websites can also play a critical role in promoting sustainable agriculture practices and raising awareness about environmental issues in the agriculture industry. The main objective of this project is to ensure a direct line of communication between the User and the farmer. A farmer can also sell his product directly to the customer and he will get the profit.

Chatbots can provide customers with quick and convenient support, as they are available 24/7 and can respond to queries instantly. Chat bot acts as a virtual assistant for farming business. Farmers can use this chat bot for conversational purposes. This can save customers time and effort, and help resolve issues more efficiently. Chatbots can also assist farmers in resolving issues related to crop recommendation, government provided schemes and assist farmers to nearby Direct Purchase Centre. And also, the chatbot help the farmers to schedule appointment with the experts to clarify their issues.

II.LITERATURE SURVEY:

[1] Prof. Kumbharde M. V., GhodkeTushar D., DevdeNitin N., AgwanSagar C. and KudalYogesh N developed a website and as well as a mob app which will help the end users (farmers) to access the information related to agricultural in an efficient and easy way. This web and mob app provides information about prediction about the crops production, agricultural bank loan and different government schemes.

[2] Prof. A. A. Bamanikar., Harshal Awate., Jay Katre., Hritik Rasal., Akshaya Mahadik developed a system for direct selling of farmer's products to the customer without any middleman. This application also has a "CHAT BOT" through which users can communicate with it. Also, there is a weather map for the farmer to use in order to check which crop will grow at a certain time in this project. Data mining techniques like PAM, CLARA, DBSCAN and Multiple Linear Regression are necessary for accomplishing practical and effective solutions for this problem.

[3] Prof. Manisha Pise., Dhananjay Girsawale., Siddhant Chilke., Praful Ramedwar., Shivam Longadge developed a website where buyer and seller can sell their products at best rate and eliminate the middlemen or third party. Every farmer is given an individual login id, with which

their information is recorded in a database and linked to a related bank for secure transactions. In this system Farmers can first submit their produce with an estimated ultimate price.

[4] Prof.Naina Palandurkar., Pritam Ramteke., Sandeep Pathak., Pooja Raut., Pradnya Sarade proposed a Website for Farmers to Sell Vendors Directly is intended to provide an online platform that will help farmers from Indian cities sell their products directly to customers without the help of intermediaries or agents. This website will serve as a unique and safe way to do agricultural marketing. This new site allows good farmer, sellers and sellers to communicate. It allows farmers to log in and sell a product published by other farmers.

[5] Rahul Singh Chowhan, Purva Dayya, Dr. U.N. Shukla proposed a E-Agriculture to enhance agricultural in addition to rural improvement by using various facts and verbal exchange techniques. The inspiration to use full-fledged potential of ICTs for agriculture capability building, and marketing has existed for a long time. It's far just most currently the dissemination of records started out harnessing ICTs extra efficaciously for better provider delivery to the farmers.

[6] Sindhu M R, Aditya Pabshettiwar, Ketan.K.Ghumatkar, Pravin.H.Budhehalkar, Paresh.V.Jaju paper says that Farming is the Prime Occupation in India in spite of this, today the people involved in farming belongs to the lower class and is in deep poverty. The Advanced techniques and the Automated machines which are leading the world to new heights, is been lagging when it is concerned to Farming, either the lack of awareness of the advanced facilities or the unavailability leads to the poverty in Farming. Even after all the hard work and the production done by the farmers, in today's market the farmers are cheated by the Agents, leading to the poverty.

[7] Sumitha Thankachan, Dr. S. Kirubakaran paper states that Technological importance has been a great support for making decisions in various fields especially in agriculture. The development of agriculture has been on under development for the past few years due to lack of Agriculture knowledge and environmental changes. The main aim of this paper is to reach farmers for their awareness, usage and perception in e-Agriculture. The study used statistical survey design technique to collect data from farmers for their awareness in e-Commerce.

[8] Dr. Deshmukh Nilesh Kailasrao "ICT for Indian Agricultural Informatics Developments", It aims to focus on key factors discovered for effective utilization of Information Communication

Technology for agricultural boost up, at least on the surface, with supportive of evidence here in. Some issues discussed concern with how information technologies contribute to the wide sphere of agricultural and rural developments, as they are two sides of a coin. Provide IT- ICT based services in Asian region.

III.METHODOLOGY

We used languages such as HTML, CSS, JAVASCRIPT And PHP According to previous drawbacks in the sites and app. We discovered a Website with an easy user interface. In our website where buyer and seller can sell their products at best rate. Eliminating the middleman i.e third party person or a brokers. All the Buyers and Sellers details are stored in database by using MySQL Database. Figure 1 depicts the overall architecture of the proposed system.

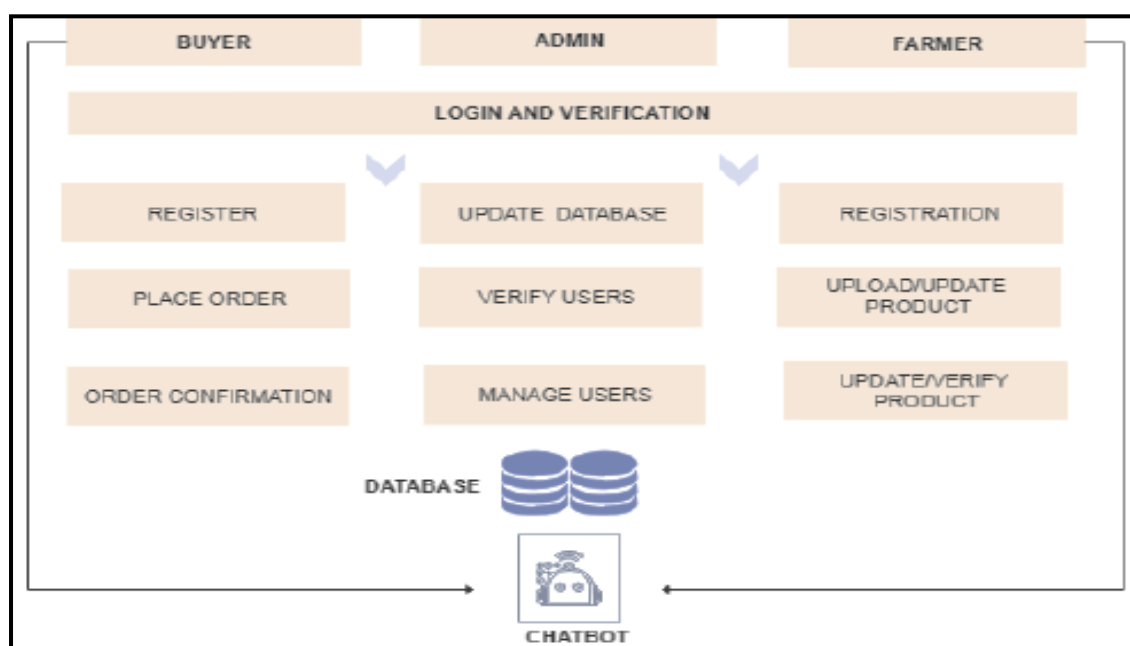


Figure 1 Overall Architecture -Proposed System

IV.EXISTING SYSTEM:

Most of the existing systems have the feature of selling the farmer's crops to the end customers. They don't provide any other necessary information like current weather and direct purchase centre details. The farmers are unaware of the schemes that are offered by the government. Since they can help farmers in various ways, an agricultural website needs to provide those details. In addition, many of these websites are demanding some kind of subscription fee from the farmers which makes them unreliable. In most of the existing systems, the farmer must

log in with the necessary information and provide the details about the crops that they want to sell. Here, the farmers can have difficulty in using that interface. Hence, the applications that has been developed earlier were not efficient and effective for use.

A. Modules of Website Implementation:

- **ADMIN MODULE:**

Admin is a first step in a process, and the farmer or consumer must be logged in before moving on to the next step. The information about the admin is saved in MySQL Database if the user already has an account they do not need to establish a new one, simply input their username and password. The admin can remove the unauthorized products. Figure 4 shows the Admin module

- **FARMER MODULE:**

In this module the farmers can sell their product online just by adding their products category wise .Figure 2 shows the Login module and Figure 3 shows farmers module.

- **CUSTOMER MODULE:**

The customer registers himself with proper details. After logging in he is redirected to the homepage where he/she is able to see all the products which are uploaded by the farmers as well as he can buy those product with preferred quantity. Figure 14 shows the Customer module.

- **CART MODULE:**

In the cart module the system adds the selected products to cart and total amount is displayed. Figure 7 shows the Cart Module.

- **CHECKOUT MODULE:**

In the checkout module the details of the customers to be given. Then place the order. Figure 8 shows the checkout module

- **ORDER MODULE:**

In the order module the details of the orders are displayed with the delivery date. Figure 9 shows the order module

B. Modules of CHATBOT Implementation:

- **Data Collection:**

Gather the scheme and subsidy information from the corresponding government websites to be stored on the data sheets. Also, collect and store the location details of the direct purchase centers and soil testing labs.

- **Data Preparation:**

The data that has been identified in the previous stage is unstructured. We need to organize and validate the collected data into a structured and desired format so that it can be stored on to the data sheets.

- **Design the workflow:**

For each entity i.e, customer and farmer decide on their needs that we are going to satisfy. Based on the identified requirement, design the flow of the chatbot conversation.

Farmers: The basic requirements for the farmers include getting to know about current weather details, direct purchase center and soil testing lab location details, schedule, reschedule or cancel an appointment with the experts and most importantly to register to sell their crops to consumers by providing the necessary details such as quantity, price, their name and location.

So, in the initial interface, farmers will be shown the options given below,

- a. Expert Sessions
- b. Register crops
- c. Weather Forecast
- d. Soil Testing Labs
- e. Direct Purchase Centers

Customers: The only requirement for the customers is to buy the commodity from the list of available ones. If the desired crop is not available, then we'll get the email to send a notification if it is available in future. For customer, the initial interface will have,

- a. Buy Crop
- b. Available Product list

V.IMPLEMENTATION AND DEPLOYMENT

Code the identified workflow and make the necessary integrations with external apps using API. Integrations with the external and internal services are done using webhook. Finally, deploy the web app using any deployment platform.

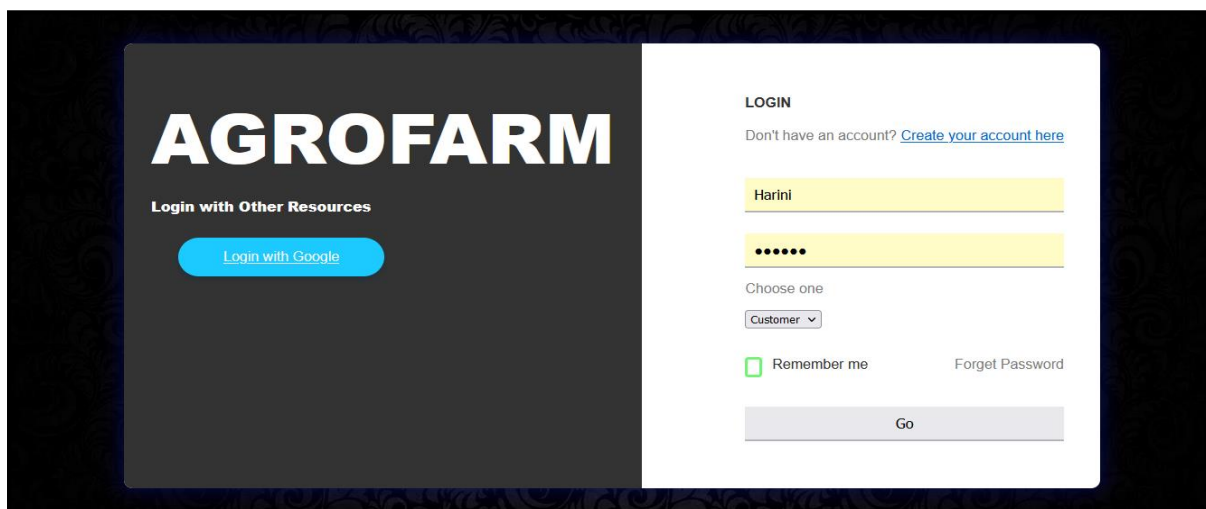
LOGIN:

Figure 2 Login Module

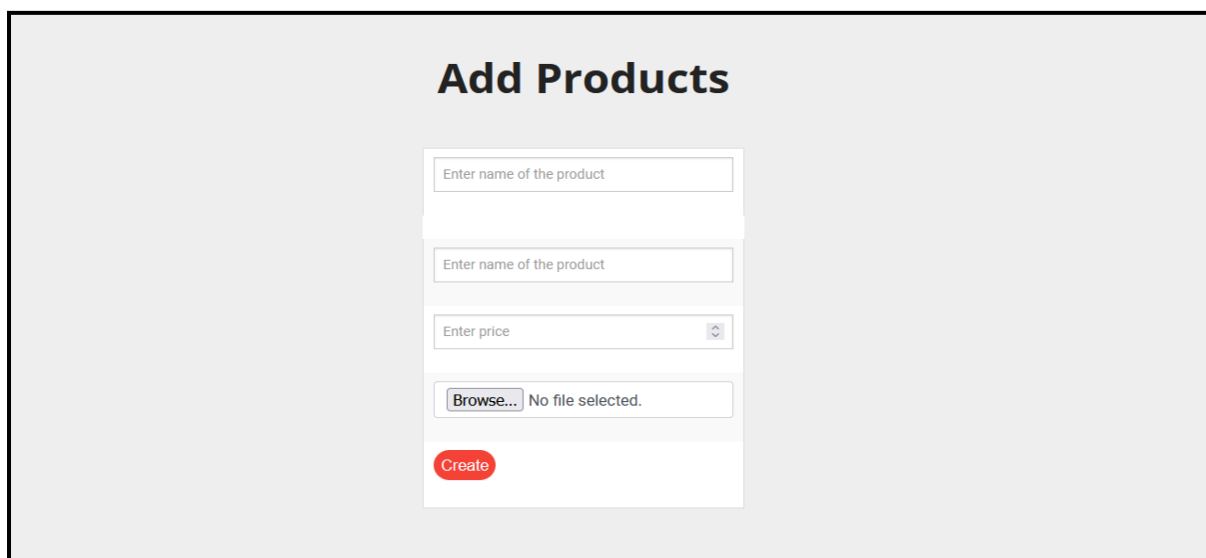
FARMER'S MODULE:

Figure 3 Farmer's Module

ADMIN MODULE:

Manage Settings					
S.No	Farmer Id	Name	Price	Status	
1	105	Orange	150.00	1	Delete Farmer
2	106	Strawberry	100.00	1	Delete Farmer
3	108	Blueberry	55.00	1	Delete Farmer
4	107	Mango	40.00	1	Delete Farmer
5	0	Green Apple	40.00	1	Delete Farmer
6	0	Grapes	40.00	1	Delete Farmer
7	0	Pine Apple	160.00	1	Delete Farmer

Figure 4 Admin Module

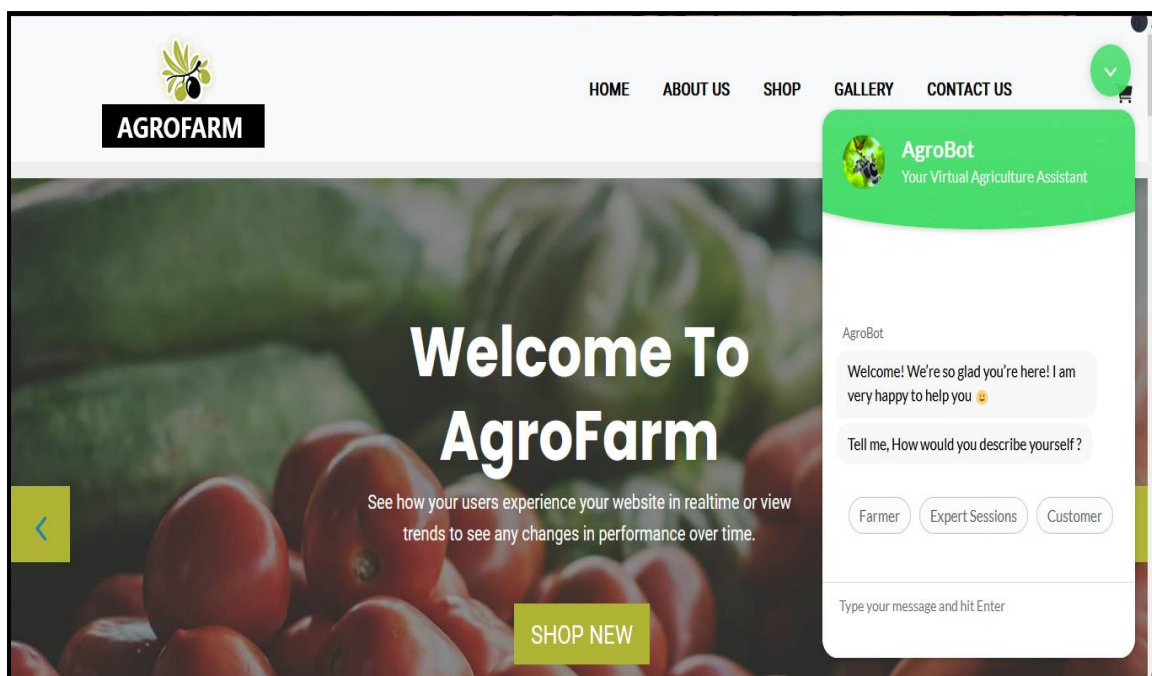
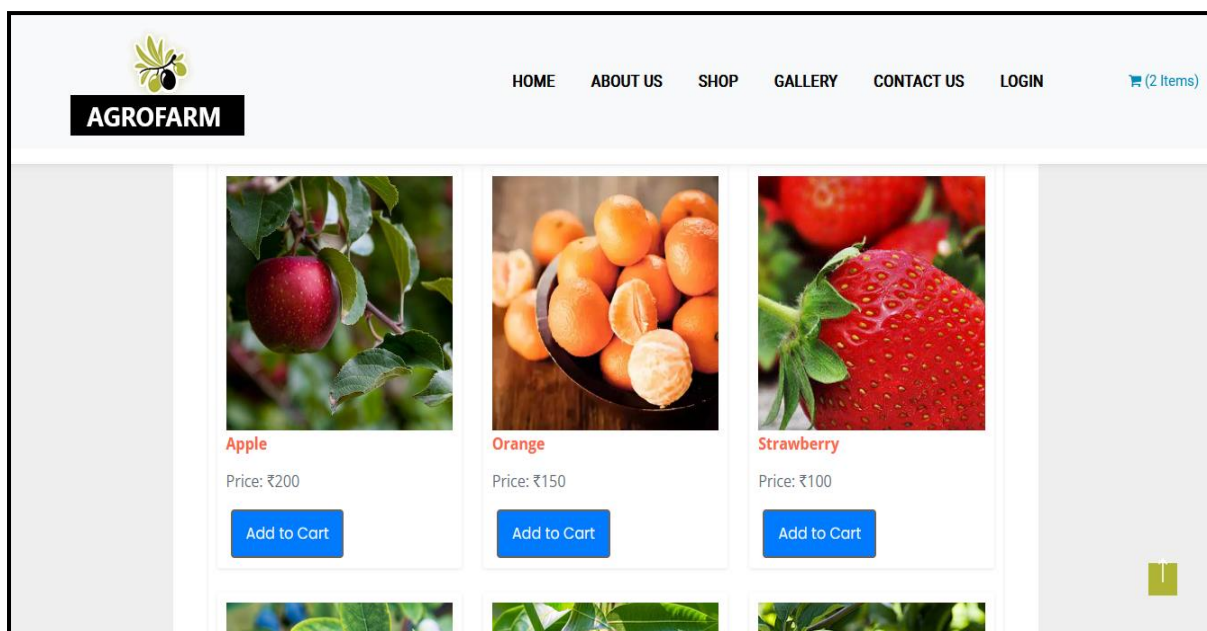
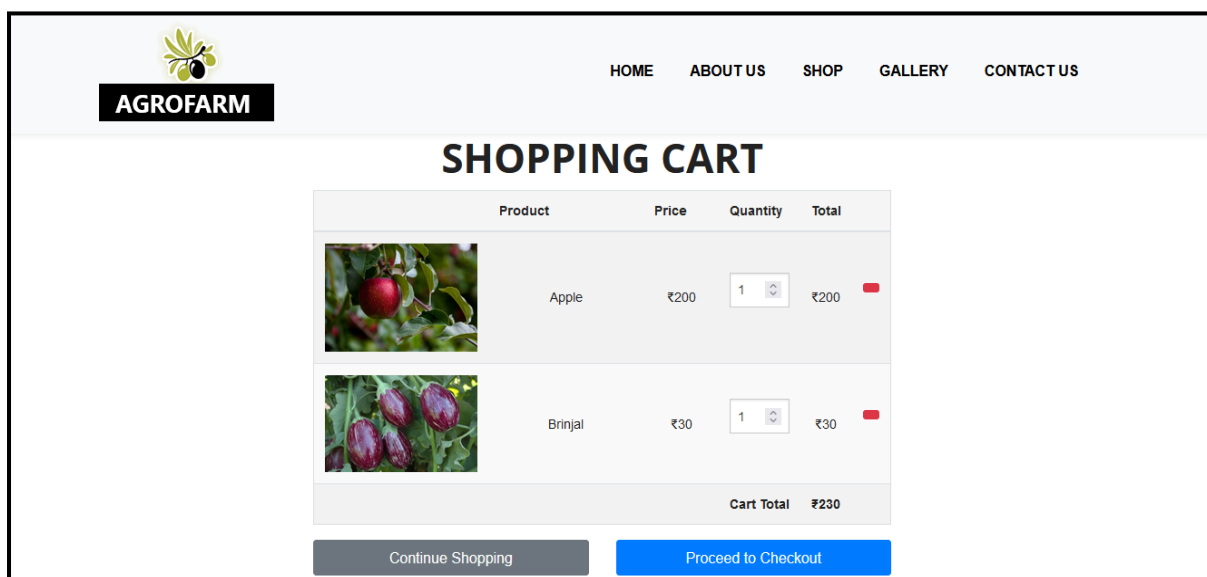
HOME PAGE:

Figure 5 Home Page

SHOP MODULE:**Figure 6 Shop Module****CART MODULE:****Figure 7 Cart Module**

CHECKOUT MODULE:
Figure 8 Checkout Module**ORDER MODULE:**

Product	Price	QTY	Sub Total
Apple	₹200	1	₹200

Figure 9 Order Module

CONTACT US PAGE:

Figure 10 Contact us Page

CHATBOT:

Figure 11 ChatBot

FARMERS:

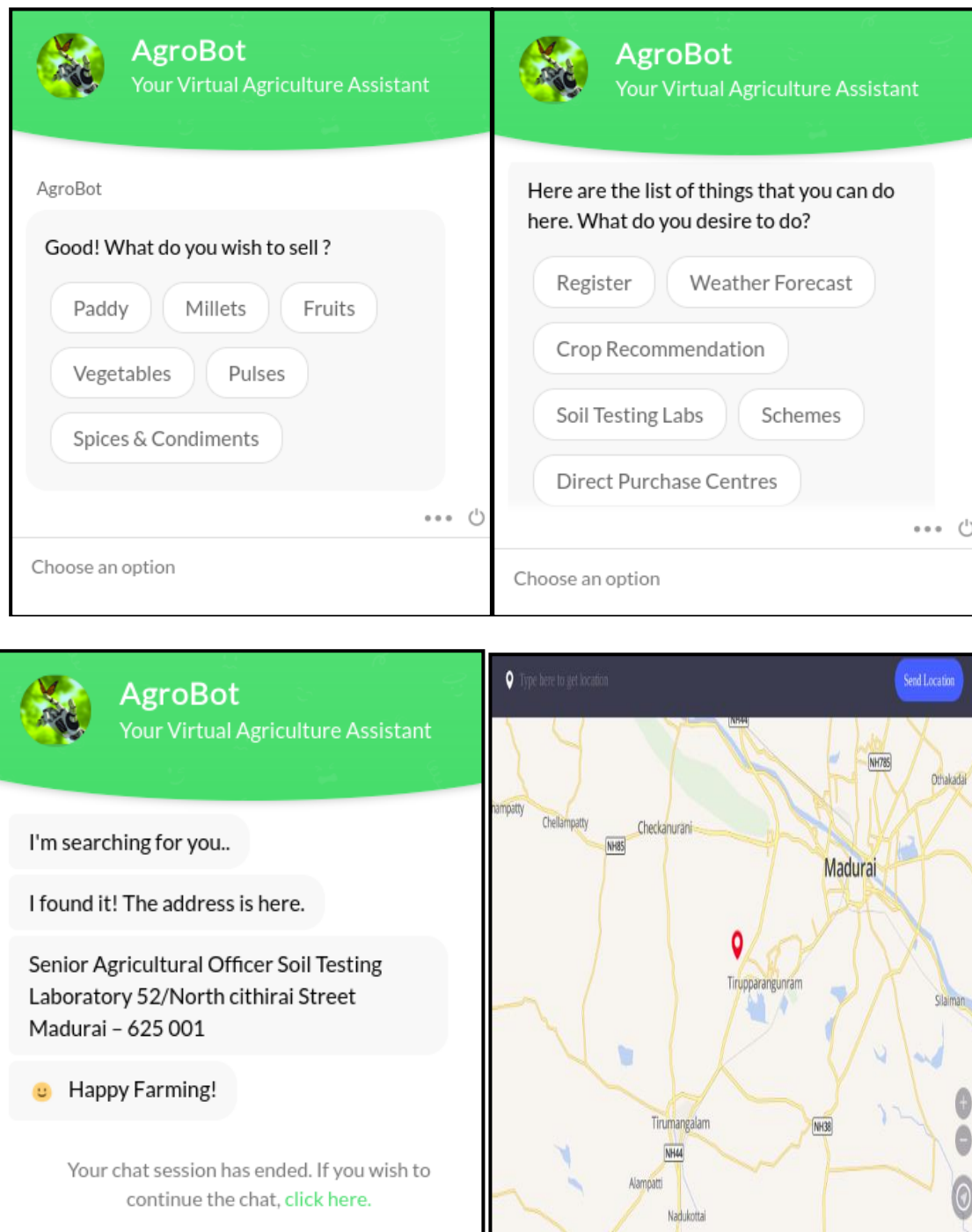
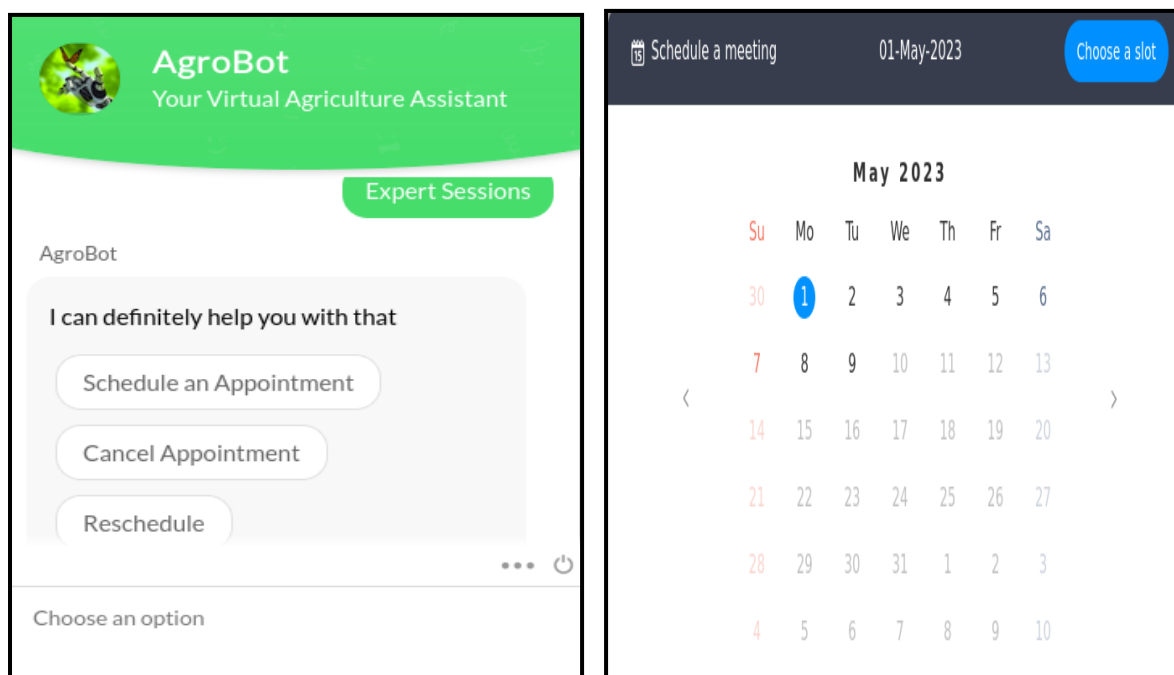
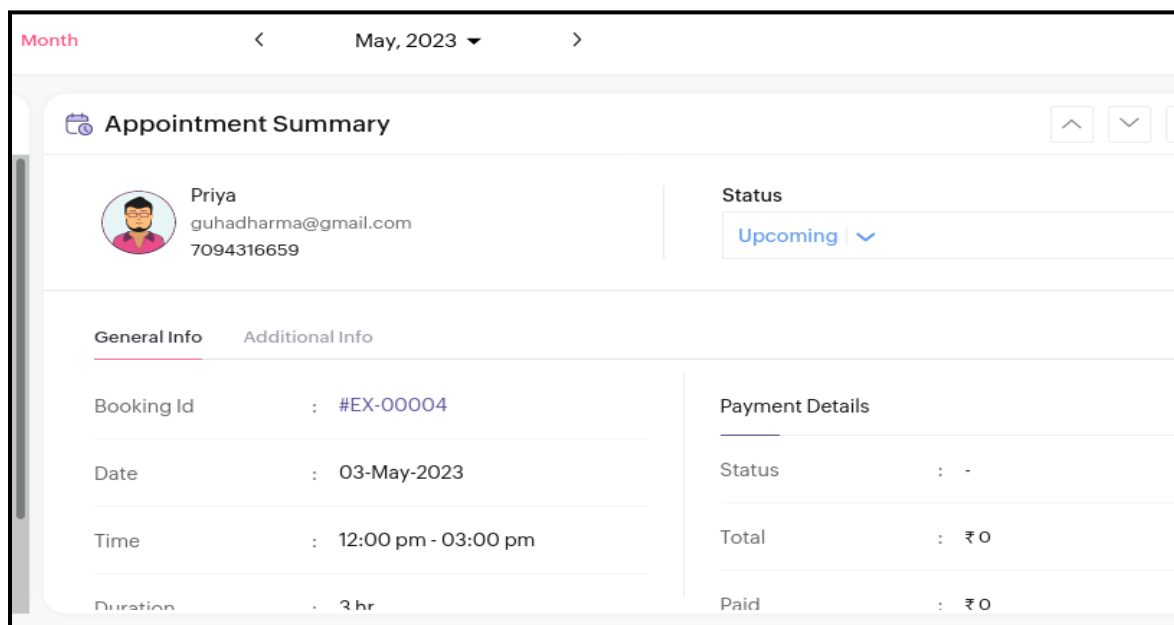


Figure 12 Farmers Page

EXPERT SESSIONS:


The top section shows the AgroBot interface with a green header. It includes a profile picture of a robot, the name 'AgroBot', and the tagline 'Your Virtual Agriculture Assistant'. A green button labeled 'Expert Sessions' is visible. Below this, a chat bubble from 'AgroBot' says 'I can definitely help you with that' and contains three buttons: 'Schedule an Appointment', 'Cancel Appointment', and 'Reschedule'. At the bottom of the chat area, it says 'Choose an option'.

The right section shows a calendar for May 2023. The header includes a calendar icon, the text 'Schedule a meeting', the date '01-May-2023', and a blue button 'Choose a slot'. The calendar grid shows the days of the week (Su, Mo, Tu, We, Th, Fr, Sa) and the dates. The date '01' is highlighted in blue.



The bottom section shows the 'Appointment Summary' page. It features a header with 'Month', navigation arrows, and 'May, 2023'. The main content area includes a profile picture of a person, the name 'Priya', email 'guhadharma@gmail.com', and phone number '7094316659'. To the right, the 'Status' is 'Upcoming'. Below this, there are two tabs: 'General Info' and 'Additional Info'. The 'General Info' tab is active and shows 'Booking Id : #EX-00004', 'Date : 03-May-2023', 'Time : 12:00 pm - 03:00 pm', and 'Duration : 3 hr'. To the right of these details is a 'Payment Details' section showing 'Status : -', 'Total : ₹ 0', and 'Paid : ₹ 0'.

Figure 13 Expert Sessions

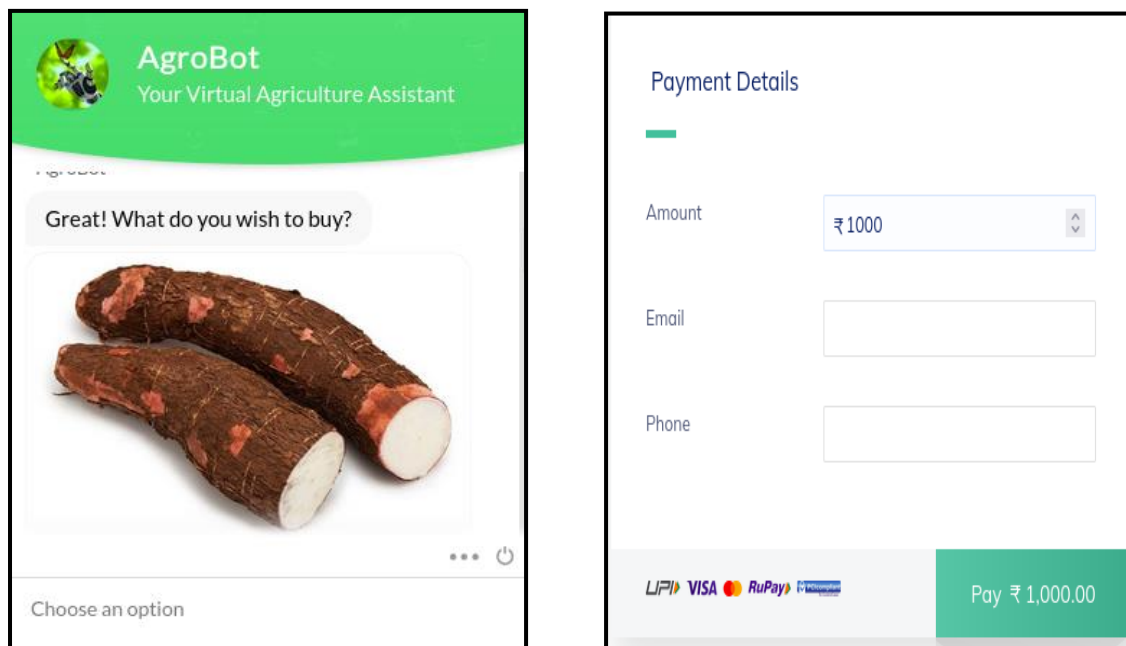
CUSTOMERS:

Figure 14 Customers

VI CONCLUSION

An interactive Chatbot connected to an Agricultural website which helps in providing efficient communication between farmers and agricultural experts. Most of the farmers do not have proper knowledge of sites and applications. they often don't have an idea of online product posting ,web applications etc ,but our proposed system is much easier to access by them without the involvement of third party and middlemen .Through this portal farmers can get much profit by selling their products online.If farmer has any doubts they can clarify it by receiving personalized advice from agricultural experts on issues such as soil quality, pests and disease control through chatbot. It also enhances customer service by helping farmers build stronger relationships with their clients and increase customer satisfaction. The location of nearest soil testing labs can also be viewed by farmers and crop recommendation for the particular type of soil will also be suggested. The information about various schemes provided by government can also be viewed. The details about Direct Purchase Centres and Open Weather Forecast with real time weather updates which helps in making decisions about planting, harvesting and other activities are also available. Overall chatbot have the potential to transform the agriculture industry by providing farmers with quick and efficient access to agricultural advice and information. Hence, in order to avoid the drawbacks of the

currently available systems we are developing an Chatbot connected to an agricultural website that will be more efficient to use.

REFERENCES:

1. Dhananjay Girsawale,Siddhant Chilke,Praful Ramedwar,Shivam Longadge Prof. Manisha Pise “Farmkart: E-Commerce Website for farming related products” International Journal of creative research thoughts - June 2022.
2. Pritam Ramteke,Sandeep Pathak,Pooja Raut, Pradnya Sarade, Prof.Naina Palandurkar “Development of Web Based System for Farmer to Consumer Product Selling Through Direct Marketing” International Journal of creative research thoughts -March 2020.
3. R Sneha Iyer, R Shruthi, K Shruthi, R Madhumathi “Spry Farm: A Portal for Connecting Farmers and End Users”. 2021 7th IEEE International Conference on Advanced Computing and Communication Systems (ICACCS),03 June 2021.
4. Karpagavarsini.R, Karthiksaran.T, Promodh.K.K , Thabuvelan.S , Senthilkumar.C “E-Farming based application of Agricultural Products from farm to Customer” International Journal of creative research thoughts - 4 April 2022.
5. Soumalya Ghosh, A. B. Garg, Sayan Sarcar, P.S.V.S Sridhar, Ojasvi Maleyvar, and Raveesh kapoor Krishi-Bharati: “An Interface for Indian Farmer”, Proceedings of the 2014 IEEE Students' Technology Symposium, 28 Feb.-2 March 2014, Kharagpur, India.



Vol. XVI & Issue No. 3 March - 2023

INDUSTRIAL ENGINEERING JOURNAL

A Systematic Review and Meta-Analysis of Digital Eye Strain

Mrs.C.B.Selva Lakshmi¹, Assistant Professor, Velammal College of Engineering and Technology, Madurai,
cbsl@vcet.ac.in

Dr.A.Radhika², Associate Professor, Velammal College of Engineering and Technology, Madurai,
ark@vcet.ac.in

R .Anu³, PG Student, Velammal College of Engineering and Technology, Madurai
anushasha1327@gmail.com

S.Reshma⁴,UG Student,Velammal College of Engineering and Technology, Madurai

ABSTRACT:

Computers have become a vital part of our workplaces. Millions of computer users spend at least more than two hours in front of a computer screen daily. This excessive use of computers leads to a disorder known as “Computer Vision Syndrome”. Most of the computer users suffer from CVS. CVS causes irritation, redness of the user's eye. A real time method to detect the redness of eye and to prevent Computer Vision Syndrome (CVS). In these days nearly 8 to 9 people in 10 forgot to blink their eyes while watching laptops, smartphones, tablets, etc. Improper blinking cause's dryness in eyes and also long term viewing of screens without any proper eye exercises and precautions causes eye strain. Computer Vision Syndrome or Digital Eye Syndrome is caused due to the usage of screens. Symptoms of CVS are eye strain, itching of eyes, pain around eyes, redness of eyes, and tiredness of eyes. The main idea of this method is to detect blink count of a person using SVM(Support Vector Machine) is a supervised machine learning model or classifier which is a trained model used to predict whether the person is blinking or not. Blink count or blink ratio data is used to ensure whether the person is blinking at a proper rate or not. CNN (Convolution Neural Network) is used to find the redness in eyes. The CNN model is pretrained with datasets in which a person image is given to the model and the eye of that person is separated and the redness is detected in the white area of the eye (selera) by separating into pixels. With the help of these data's, we can predict or tell whether a person has CVS or to prevent from CVS.

KEYWORDS:

Eye detection, Face detection, Landmark Plotting, Blink detection, detection accuracy, support vector machine

1. INTRODUCTION

Computer vision syndrome (CVS) is a condition resulting from focusing the eyes on a computer or other display device for protracted, uninterrupted periods of time and the eye's muscles being unable to recover from the constant tension required to maintain focus on a close object. Some symptoms of CVS include headaches, blurred vision, neck pain, fatigue, eye strain, dry eyes, irritated eyes, double vision, vertigo/dizziness, polyopia, and difficulty refocusing the eyes. These symptoms can be further aggravated by improper lighting conditions (i.e. glare, strong blue-spectrum backlights,[citation needed] or bright overhead lighting) or air moving past the eyes (e.g. overhead vents, direct air from a fan). Digital eye strain has been shown to have a significant impact on both visual comfort and occupational productivity, since around 40% of adults and up to 80% of teenagers may experience significant visual symptoms (principally eye strain, tired and dry eyes), both during and immediately after viewing electronic displays.

The concept of eye blink detection is to detect the eye of the person and plot the landmarks using dlib which is the python library for facial detection. OpenCV is used to capture the video of the person sitting in front of the system and the video frames of given to the landmarks predictor of the dlib. The facial landmarks are plotted on the detected face. With help of the landmarks of the eye, the eye is detected and change in the aspect ratio is used to say whether the person is blinking or not. But the eye aspect ratio will change based on the environmental conditions. Sometimes the blink counts cannot be perfect or blink detection is not perfect. The counts will keep on increasing even if the person is opening his eye.

To overcome this problem, this paper tells how to increase the accuracy of blink detection and detect the eye redness using deep learning.

2. BLINK DETECTION

A SVM is a classifier based on the use of hyper planes to discriminate two or more classes. It is a learning tool originated in modern statistical learning theory and it was invented by Vladimir Vapnik . An optimal hyper plane in SVM maxims the margin between classes and generalize the learning process for classification. For linear classification, when the classes are classified using linear decisions, there exists a linear function for the SVM's hyperplane of the form: SVM (Support Vector Machine) is a supervised deep learning model is used to increase the accuracy of the eye blink detection.SVM is a model which is trained with Eye Aspect Ratio(EAR) features. The EAR of the eye varies with position of the eye. If the eye is fully opened then the EAR will be a constant value until the eye is closed.If the eye is closed then the EAR of the eye will completely become zero.This EAR is determined by the manipulation of the landmarks of the

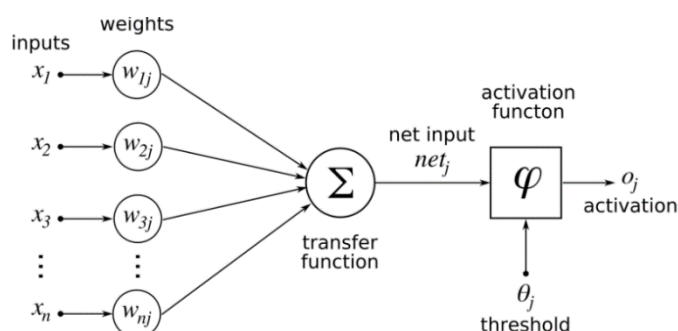


Figure 1 Structure of the artificial neuron

eye.This EAR is give as a input to the SVM which is pretrained with various EAR features. Then the trained features of SVM is used to predict whether a person is blinking or not.SVM has more accuracy than using OpenCV with dlib. SVM can produce the results upto 95% accuracy. With the help of the EAR data we can say a person whether he is blinking or not.This model also detects various blink patterns.

3. EYE REDNESS DETECTION

Eye redness detection is a process to detect redness in eyes by using Convolution Neural Network(CNN).Some of the tasks CNNs are typically used for include Image Classification, Image Segmentation, Computer Vision, with applications even in other areas like NLP, Time-Series and Recommender Systems. Convolutional neural networks are composed of multiple

layers of artificial neurons. Artificial neurons, a rough imitation of their biological counterparts, are mathematical functions that calculate the weighted sum of multiple inputs and outputs an activation value. The CNN module is trained with the several images containing eye with redness. The pretrained model is used to predict the eye redness. With this detection we can say that whether a person is having a eye strain or not. If a person is having eye strain then we can intimate him.

4. PREVENTION OF COMPUTER VISION SYNDROME

Making a short break, stretching the muscles, change of scenery and a quick walk around the office have been shown to improve productivity and reduce ocular symptoms of stress. Working nonstop for more than 4 hours has been associated with eye strain. Frequent short break can restore and relax the accommodative system of the eyes and preventing ocular strain and visual fatigue. Workers who have recurrent symptoms of computer vision syndrome are encouraged to get proper optometrist review and assessment

Dry eyes secondary to decreased blink rate can be easily managed by applying lubricating eye drops or artificial tears. Patients are advised to consult their doctor first if they have any ocular symptoms before applying this eye lubricating solution although they are available over the counter in pharmacy. Workers who are using contact lens must be more careful with any ocular symptom which started acutely such as pain and redness. Complications following prolonged contact lens usage such as cornea ulcer must be excluded by proper ophthalmological assessment and examination before one can say that the symptoms are due to computer vision syndrome.

Use of proper corrective glasses for refractive errors such as myopia, astigmatism and presbyopia is important to prevent further deteriorating of the ocular symptoms which can lead to poor work performance and the poor quality of life. Workers who have history of medical illnesses such as diabetes mellitus and connective tissue disease affecting the eyes must get referral to see ophthalmologist without delay.

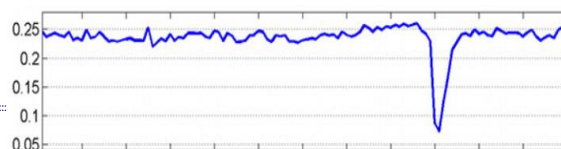


Figure 2: Eye Aspect ratio

CONCLUSION:



Figure 4: *Facial landmarks*

Computer vision syndrome is a new problem that has emerged in this century following increase

Eye aspect ratio will be larger and relatively constant over time when eye is open

Eye aspect ratio will be almost equal to zero when a blink occurs

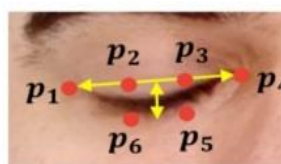
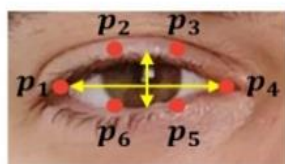


Figure 3: *Eye aspect ratio during eye open and eye close*

usage of computer both at home and at work. There is a correlation between ocular symptoms such as pain, redness, dryness, blurring of vision, double vision and other head and neck sprains and computer usage. Prevention remains the main strategy in managing of computer vision syndrome. Modification in the ergonomics of the working environment, patient education and proper eye care are important strategies in preventing computer vision syndrome. We have implemented an eye detection and face detection from the web cam video for Computer Vision Syndrome. Our algorithm successfully detect the eye and face from the web cam video. We are planned to extend these ideas in mobiles also as most of them spent lot of times on mobile phones. As most of IT person suffering from computer vision syndrome this idea will help to protect their eyes (or) help them to prevent Computer Vision Syndrome.

REFERENCES

- [1] Young-Joo Han, Wooseong Kim, and Joon-Sang Park, "Efficient Eye-Blinking Detection on Smartphones: A Hybrid Approach Based on Deep Learning", Volume 2018 Article ID 6929762
- [2] Warapon Chinsatit and Takeshi Saitoh, "CNN-Based Pupil Center Detection for Wearable Gaze Estimation System", Volume 2017 Article ID 8718956
- [3] Dhaval Pimplaskar, Dr. M.S. Nagmode, Atul Borkar, "Real Time Eye Blinking Detection and Tracking Using OpenCV", 2248-9622, Vol. 3, Issue 5, Sep-Oct 2013, pp. 1780-1787
- [4] Marc Lalonde, David Byrns, Langis Gagnon, Normand Teasdale, Denis Laurendeau, "Real-time eye blink detection with GPU-based SIFT tracking", IEEE DOI: 10.1109/CRV.2007.54
- [5] Jong Bin Ryu; Hyun S. Yang; Yong-Ho Seo, "Real Time Eye Blinking Detection Using Local Ternary Pattern and SVM", IEEE DOI: 10.1109/BWCCA.2013.105
- [6] Guilei Hu, Yang Xiao, Zhiguo Cao, Lubin Meng, Zhiwen Fang, Joey Tianyi Zhou, Junsong Yuan, "Towards Real-Time Eyeblink Detection in the Wild: Dataset, Theory and Practices", IEEE Transactions on Information Forensics and Security Volume: 15
- [7] T. R. Akinbinu and Y. J. Mashalla, "Impact of computer technology on health: Computer Vision Syndrome", Medical Practice and Review, vol. 5, pp. 20-30, 2014.
- [8] M Divjak and H. Bischof, "Eye blink based fatigue detection for prevention of Computer Vision Syndrome", MVA 2009 IAPR conference on machine vision applications, 2009.

Revathy, J. Shanthalakshmi - Aut... x J. Shanthalakshmi Revathy - Go... x Scopus preview - Scopus - Shu Ji... x Shu Ju Cai Ji Yu Chu Li/Journal o... x 2 Improving Heart Disease Diagn... x

ieeexplore.ieee.org/document/10089378

IEEE.org | IEEE Xplore | IEEE SA | IEEE Spectrum | More Sites

Subscribe Cart Create Account Personal Sign In

IEEE Xplore® Browse My Settings Help Institutional Sign In

All

ADVANCED SEARCH

Books > Machine Learning for Healthca... > 2 Improving Heart Disease Diagnosis usi...

2 Improving Heart Disease Diagnosis using Modified Dynamic Adaptive PSO (MDAPSO)

Publisher: River Publishers

Cite This PDF

Book Chapter is part of: Machine Learning for Healthcare Systems: Foundations and Applications

Editor(s): C. Karthik ; M. Rajalakshmi ; Sachi Nandan Mohanty ; Subrata Chowdhury

Abstract

Chapter Abstract:

The introduction of digital technology in the healthcare industry is marked by ongoing difficulties with implementation and use. Slow progress has been made in unifying different healthcare systems, and much of the world still lacks a fully integrated healthcare system. The intrinsic complexity and development of human

More Like This

Improving the heart disease diagnosis by evolutionary algorithm of PSO and Feed Forward Neural Network
Published: 2016

Using PSO Algorithm for Producing Best Rules in Diagnosis of Heart Disease
Published: 2017

Show More

Feedback

Revathy, J. Shanthalakshmi

Edit profile

3 Documents Cited by 0 Preprints 5 Co-Authors Topics 0 Awarded Grants

Note:

Scopus Preview users can only view an author's last 10 documents, while most other features are disabled. Do you have access through your institution? Check your institution's access to view all document features.

3 documents

Export all Save all to list

Sort by Date (newest)

View list in search results format

View references

Set document alert

Book Chapter

Improving heart disease diagnosis using modified dynamic adaptive PSO (MDAPSO)

0 Citations

Revathy, J.S., Anchitaalagammai, J.V., Hariharasitaraman, S.

Machine Learning for Healthcare Systems: Foundations and Applications, 2023, pp. 19-33

Show abstract Related documents

Conference Paper • Open access

Factors influencing the use of Deep Learning for Medicinal Plants Recognition

0 Citations

Anchitaalagammai, J.V., Revathy, S.L.J.S., Kavitha, S., Murali, S.

Journal of Physics: Conference Series, 2021, 2089(1), 012055

Show abstract Related documents



A CRITICAL SURVEY ON EFFICIENCY AND SECURITY OF INTERNET OF THINGS BASED INTELLIGENT TRANSPORT SYSTEM

939

K.Santha Sheela

Assistant Professor, CSE Department, Velammal college of engineering and technology Madurai-625009

santhasheela2022@gmail.com

Dr.A.Radhika

Associate professor,EEE, Velammal college of engineering and technology Madurai-625009

aradhika80@gmail.com

Corresponding author: **santhasheela2022@gmail.com**

ABSTRACT

With urbanization and increase in population and vehicle usage, transportation sector and people experience major challenges like traffic congestion, high accident rates, transportation delay, and air pollution. Nowadays, it has become a challenge to manage crowd and vehicular traffic in a way that is both efficient and safe in transportation. Traditional transport management system is ineffective in terms of time, cost, energy consumption, security, and quality of service (QoS). The Internet of Things (IoT) integration into transportation systems has helped alleviate such issues, while also facilitating the collection of useful commuting data that has led to the development of intelligent transport systems (ITS). Though ITS helps in reducing traffic congestion, accident rates, transportation delay, and air pollution, it is associated with certain challenges like cyber-security and energy efficiency issues. Hence, we presented a survey on recent techniques involved in enhancing energy efficiency and security of vehicular communication in IoT-based-ITS. Initially, architecture of ITS involving different layers, including data collection, sharing, and storage layers, is discussed. Then various applications and challenges in IoT-based-ITS are explained. Following this, recent approaches involved in mitigating the challenges encountered by IoT-based-ITS, are presented in this survey. Future trends to be incorporated in ITSs for alleviating efficient traffic control, monitoring, and management are also discussed.

Keywords: *Internet of Things (IoT), Intelligent Transport System (ITS), Traffic, Communication, Security, Efficiency.*

DOI Number: 10.48047/NQ.2022.20.20.NQ109094

NeuroQuantology2022;20(20): 939--949

I. INTRODUCTION

Transportation infrastructure has a significant role in a country's ability to compete globally, its economic health, and its level of productivity. Currently, transportation networks are crucial to almost every aspect of modern life. Forty percent of people, on average, are out and about for an hour or more every day, according to a recent survey. People's reliance on transportation networks has increased dramatically in recent years, posing new possibilities and problems for these networks.

Cities grow in size as their populations do, and with that come a corresponding growth in the total number of automobiles on the road. The contemporary city's daily routine and environment are both negatively impacted by the widespread traffic congestion that has emerged as a global issue in recent years. Transport-related difficulties include, but are not limited to, delays in departure times, excessive fuel use, and increased pollution levels. Developing and developed countries alike have challenges from the environmental



noise, air pollution, energy waste, and other elements afflicting modern transportation in big cities. These issues have arisen as a result of the rapid pace of urbanization, motorization, modernization, the growth of the urban population, the proliferation of faster vehicles, the saturation of the urban transport system, and other factors. Consequently, there has been a rise in the frequency of accidents. The end effect is a high number of people dying in traffic accidents. According to WHO, road accidents account for more than 100 million deaths and up to \$500 billion in annual economic losses throughout the world every year. As a consequence of inadequate or delayed medical attention, more over half of all accident victims die (Goyal et al. 2022). Since this is the case, traffic management officials have a formidable obstacle in keeping tabs on the flow of traffic.

There is, without a doubt, a need to both lessen the number of traffic accidents and identify them after they have already happened, so that their aftermath may be lessened. Traffic jams might occur due to numerous reasons like natural hazards, tree falls, flooding, avalanches, and other forms of natural road hazards pose a threat to public safety. For intelligent transport networks to be realized, conventional traffic management needs a large number of calculations and a wide range of information. Transport management system has several limitations and is constrained by existing technologies. As the world becomes increasingly interconnected and information technology advances at a rapid pace, conventional modes of transportation can no longer keep up with the demands of economic and social progress. As a result, intelligent transportation has emerged as the industry standard, ushering in a new era of innovation in the realm of urban transportation. Integration

of vehicles into intelligent transportation networks paves the way for more smart traffic management; detection, prediction, and avoidance of collisions; detection of malicious or anomalous activity inside a specific vehicular network; and authentication and other forms of security.

ITSs refer to the use of modern forms of communication and computing to solve issues plaguing more traditional modes of transportation. To make the transportation system more secure, reliable, efficient, accessible, and environmentally friendly, these companies use cutting-edge technology in these areas. Wired systems, which are a part of traditional ITS, are not very adaptable. Millions of IoT-enabled devices are needed to realize the vision of smart and intelligent transportation. By quickly detecting environmental restrictions, sending the detected data, and presenting a detailed report utilizing visualization tools, the IoT application in ITS promises to expand the range of services available to users. By 2020, according to a Gartner forecast, the Internet of Things will include 30 billion linked smart cars capable of sensing, communicating, operating, and maybe acting upon one another. To increase efficiency, lessen congestion, make roads safer for drivers, save resources, and safeguard the environment, countries often use the ITS approach (Zhang et al. 2020). The advantages of ITSs are illustrated in figure 1. By using the Internet of Things, transportation systems can increase carrying capacity, enrich the passenger experience, and make cargo delivery more reliable, efficient, and secure. By combining smart traffic management with citywide sensor networks, the police, emergency services, and other government agencies can better monitor the city as a whole and react more quickly to calls for assistance.



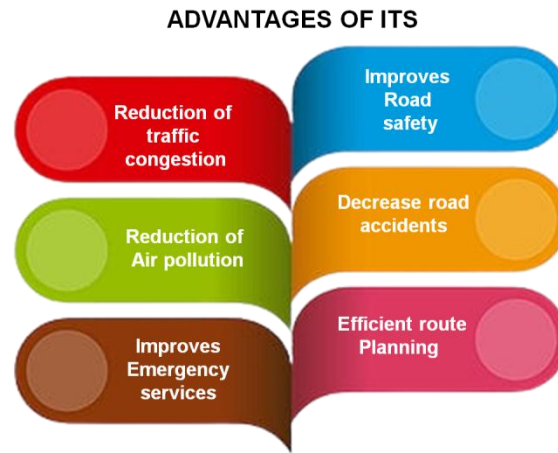


Figure 1: Major Benefits of Intelligent Transport System

ITS offers smarter opportunities but has certain challenges in implementing ITS. Due to the heterogeneous nature of the connected vehicle environment in ITS, algorithms must be developed to give in-vehicle communication devices the intelligence they need to make decisions based on factors such as the QoS parameters of the requested application and the current traffic/environmental conditions. Similarly, information security mechanisms must be developed to guarantee the safe transfer of sensitive traffic/accident data. Emergency applications require a network connection with low delays. The real-time nature of applications, the rapid mobility of vehicles, the broad range of relative speeds between nodes, and the large number of system and application related requirements all provide technical obstacles in ITS implementation. A comprehensive survey on applications, challenges, recent approaches that are utilized in enhancing energy-efficiency and security of ITSs is less available. This motivated us to conduct this survey. This survey presents the overview of benefits and challenges in ITSs, and emerging techniques in improving energy efficiency, security, time efficiency, and QoS of vehicular communication in ITS.

II. ARCHITECTURE OF INTELLIGENT TRANSPORT SYSTEM

IoT-based ITSs have been created that can consolidate many different types of infrastructure into a single operating unit, such as those responsible for sensing, communication, information distribution, and traffic management. Data collection, data analysis, data/information transfer, and data storage are the fundamental building blocks of any ITSs. Figure 2 depicts the different layers in ITS.

Data Acquisition layer: The data-collection elements of the transportation system gather all visible data for the aim of assessing the present traffic condition (including, but not limited to, traffic volume at a specific location on the road network, average travel time for a certain road segment, ridership on a specific transit line, etc.). As sensing and imaging technology improves, alternatives like video cameras and radio-frequency identification (RFID) scanners are being considered more seriously for use in traffic data collection (Torre-Bastida et al. 2018). Mobile, position, improbable occurrences, natural dangers, etc. are just some of the data that may be gleaned from a vehicle's on-board device or sensor (OBD) with the use of OBUs (on-board units). Each car will include a GPS receiver, accelerometer, speedometer, and gyroscope, all of which will capture relevant data.



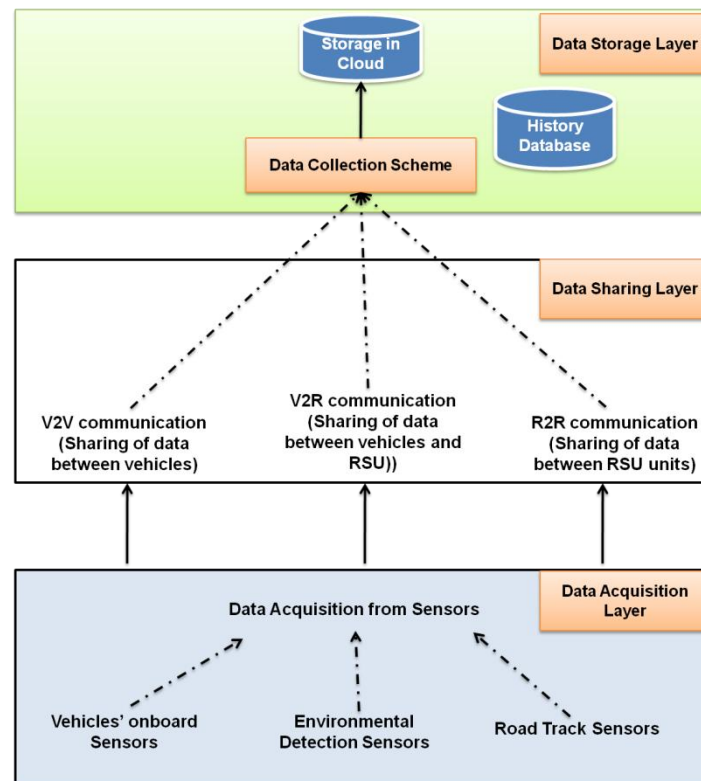


Figure 2: Layers in IoT enables ITS

Data sharing layer: After being received by OBU, the data will be processed, evaluated, and severity predictions made before being relayed to nearby cars and RSUs. With this system, automobiles communicate sensor data with one another and RSUs (Road side units). The vehicles and RSUs in IoT enables ITS use the communication channels to transfer information regarding traffic conditions, road status, or uncertain incidents. Fitah et al. 2018 employed Dedicated Short Range Communication (DSRC) protocol for low latency networking in ITS. Vehicle-to-vehicle communication (V2V), Vehicle-to-RSU (R2R), RSU-to-RSU (R2R), RSU-to-cloud (R2C) can occur in vehicular environment of ITS.

Data storage layer: The traffic/accident data generated and exchanged between vehicles and RSUs will be stored in the cloud (Finogeev et al. 2019). In the event of an emergency, the cloud-stored data will notify the relevant authorities (such as Google Maps or the Environmental Protection Agency) and immediately begin

providing services (including evacuation routes and response teams) in response. New vehicles entering the road where the incident took place are given a warning and encouraged to choose another route.

III. Applications of Intelligent Transport System

This section shows some of the applications of ITS like traffic monitoring and management, congestion avoidance, and accident detection and enhancing emergency services in smart cities.

a) Traffic Monitoring and Management

The registration of vehicle data to the RSU is the initial stage in the traffic management concept in ITS. The location where the vehicle is expected to arrive is also specified. One area's traffic data is collected by a roadside sensor that is linked to another in a different area. One possible vehicle route and its associated traffic data are studied. If the first suggested path is doable, it is offered. If not, the next option is explored, and so on. Because of this, the car is sent along the most efficient path possible,



helping to ease congestion in populated regions (Fantin Irudaya Raj and Appadurai 2022). Figure 3 shows an example of congestion avoidance in ITS. Eswaraprasad et al. 2017 suggested new IoT dependent Traffic Management that uses a “hybrid artificial neural network with a hidden Markov model (HANN-HMM)” to make short-term decisions on management of traffic for more precise and time-efficient traffic clearing in intelligent transportation systems. Kuppusamy et al. 2019 propose a smart traffic control framework based on a combination of a locally hosted traffic smart server, an optimised regression algorithm, and a server in the cloud to speed up the processing of traffic signals and thus decrease congestion, emissions, and the amount of time vehicles spend waiting at intersections. In order for ITS applications to be successful, an efficient traffic flow prediction system must be implemented to cope with potential road situations in advance.

Boukerche, A. aims to improve the accuracy of traffic flow forecasts by using machine learning. In 2020, researchers Wang, J., and Wang, J. examined several machine learning techniques. By combining unsupervised online incremental machine learning, deep learning (DL), and deep reinforcement learning, Nallaperuma et al. 2019 offered a comprehensive smart traffic management platform (STMP). The STMP unifies the various big data sources, classifies traffic incidents into those that occur frequently and those that don't, and uses that information to improve such things as traffic flow forecasting, commuter sentiment analysis, and the efficiency with which traffic control decisions are made. A new DL framework named “Spatial-Temporal Graph Attention Networks” was introduced by Zhang et al. 2019 to capture dynamic spatial interdependence of traffic networks for traffic data analysis.

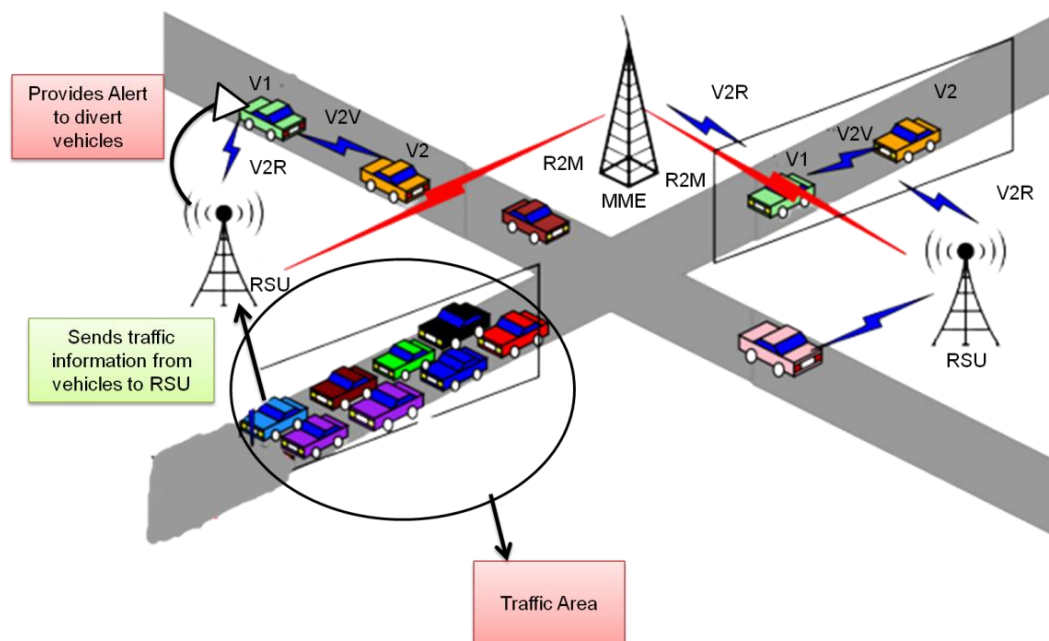


Figure 3: Traffic monitoring and congestion avoidance in IoT enabled ITS

b) Enhancement of emergency services

The victim's chance of survival is directly related to how quickly an ambulance can get them from the scene of the accident to the hospital. Most

people injured in car accidents do not suffer life-threatening injuries, and may be saved if emergency workers get to them quickly enough. An automatic accident detection and

alert system must exist in ITSs to overcome this situation. For this reason, pinpointing the scene of an accident and communicating this data to responding authorities as quickly as possible is crucial if we are to increase the likelihood that the victim will be saved. The hospital's emergency room receives word of the incident and sends an ambulance to the accident site (Dar et al. 2019). Figure 4 shows the transfer of accident message to hospitals in IoT based ITS. The DeepCrash system, proposed by Chang et al. 2019, is a cloud dependent DL server and cloud dependent management platform for the Internet of Vehicles (IoV), which consists of an

in-vehicle infotainment telematics platform with a front camera and a vehicle self-collision detection sensor. Hadiwardoyo et al. (2018) presented Messiah, an Android app that may alert normal vehicles regarding the presence of emergency vehicles like fire brigades, ambulances, and police cars so that drivers can make informed decisions on where to go. Using blockchain technology, Vangala et al. 2020 created a certificate-based authentication mechanism, BCAS-VADN, for ITS's vehicle accident detection and notification. Bhatti et al. 2019 introduced a new IoT-based solution for smart cities to report and record accidents.

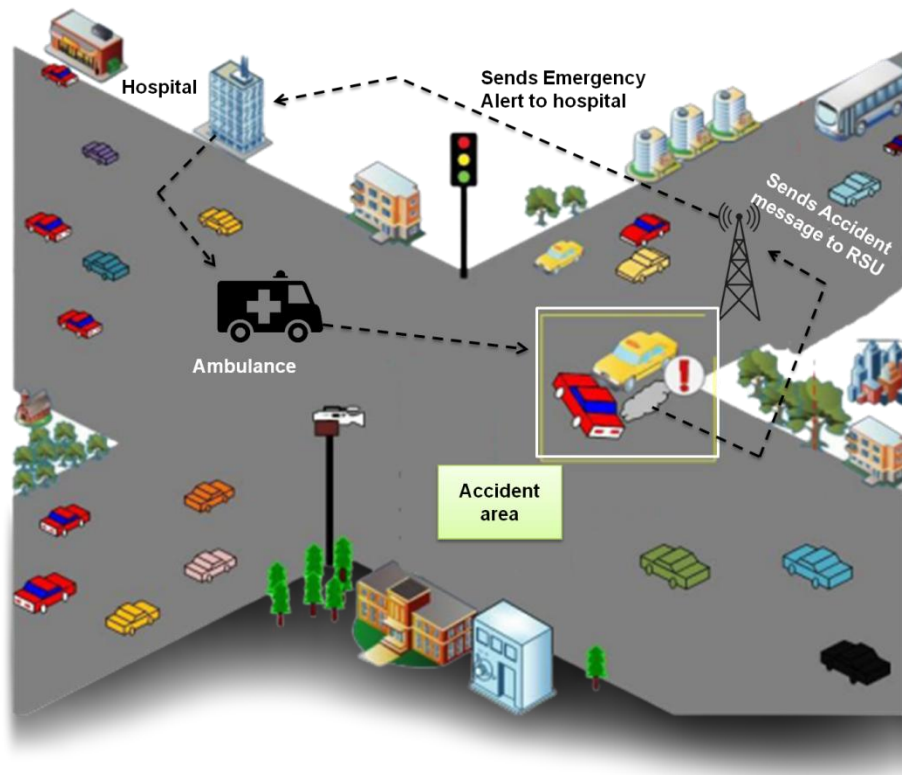


Figure 4: Accident detection and emergency alert scheme in ITS

IV. CHALLENGES IN ITS

The following sections explore some of the difficulties inherent in implementing effective ITS in smart cities. Due to factors like increased vehicle mobility and frequent link disconnection, the routing procedure in such networks is difficult. There are numerous constraints that must be overcome in order to

design an effective routing protocol that fulfills latency constraints with minimal overhead (Fatemidokht et al. 2021). New obstacles for ITS are effective traffic segregation, interference management, and allocation of available resources. Improved dependability requires effective suppression of interference from co-

channel use or neighboring channels (Sedar et al. 2020).

The authentication of highly mobile cars is another issue for security and privacy in vehicular clouds, as is the complexity of trust relationships between various vehicular nodes. Improving ITS's information distribution reliability and efficiency requires defining selected network coding techniques, which is a difficulty in and of itself. Data-centric trust and verification, anonymity, privacy, and responsibility of traffic data sent in ITSs provide unique challenges that must be identified and

managed via thorough risk analysis and management (Camacho et al. 2019). Furthermore, a crucial responsibility in ITSs is the identification of malevolent vehicles. Malicious attackers/malicious vehicular nodes in ITS might transfer new/modified traffic data or emergency alert data (false data) to other vehicular nodes which makes vehicular nodes to carry out wrong travel decisions. In addition, they can prevent emergency data alerts to reach other vehicular nodes which result in traffic congestion and road clashes. Figure 5 shows the malicious attack occurring in ITS.

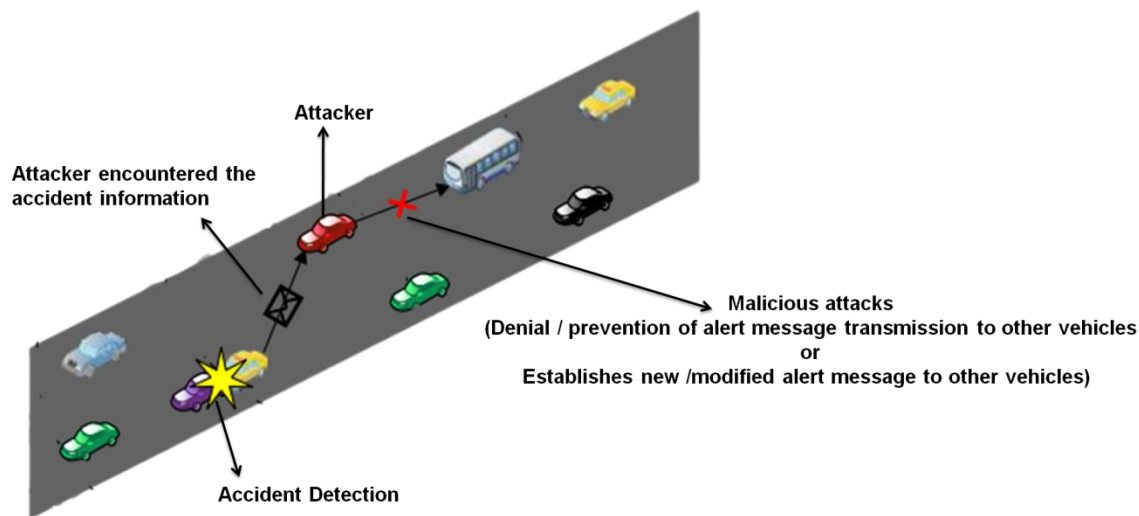


Figure 5: Occurrence of malicious attacks in ITS

When it comes to V2X communication, high precision for relative and absolute positioning, trajectory alignment, etc., is challenging to attain due to the increased mobility of the devices involved and the dynamic nature of network topologies. Harsh propagation conditions caused by the V2X dynamics, such as high delay spread and Doppler effect, owing to moving receivers, transmitters, and scatter devices, prevent the seamless and instantaneous monitoring of traffic. Maintaining confidentiality and integrity of communication across the entire network of ITS devices is a challenging task (Hahn et al. 2019; Ali et al. 2018). There may be many research programs

dedicated to linked vehicles at the moment, but the biggest obstacle is raising enough public awareness to encourage governments and automakers to fund the installation of the essential technology and infrastructures in cars, streets, and highways.

V. TECHNIQUES TO ENHANCE ENERGY EFFICIENCY OF ITS

Communication between cars and infrastructure is a key feature of ITS, but it is limited by the high power requirements of embedded wireless sensor nodes in the road network (Bhardwaj et al. 2019). For this reason, studying methods to lessen ITS's energy footprint has become a priority. Cooperative

communications in ITS networks, as suggested by Peng et al. 2019, is one approach to lowering the network's overall power usage. Because of the limited resources of edge nodes, a greater number of data packets will be lost due to the nodes' heavy energy consumption and short battery life. In 2020, Sodhro et al. will release a study proposing an unique 5G-driven reliable algorithm and a 5G-dependent self-adaptive green (that is energy-efficient) algorithm to enhance the energy efficiency of vehicle communication in ITS. Sodhro et al. 2019 employed a "QoS-aware, green, sustainable, reliable and available (QGSRA)" algorithm to support energy efficiency (greenness), sustainability, reliability (less traffic data loss), and availability (higher coverage) in multimedia transmission in V2V across emerging edge computing networks powered by the IoT in ITS. Kuppusamy et al. 2020 optimized the energy of metro systems by incorporating improved genetic algorithm with LSTM. The current state of IoT-ITS surveillance relies on fixed infrastructure-based sensing applications, which result in many network overheads and failures due to their exorbitant energy consumption. Drones were proposed as a gateway for "Low-Power Wide Area Networks" by Sharma et al. 2018, who also proposed a communication strategy depending on stress, energy consumption, and resilient factor of the area all of which contribute to precise localization, enhanced coverage, and energy-efficient surveillance with reduced overheads, redundancies, and isolations. To improve the QoS offered by ITS, Cao et al. 2022 investigated the problem of intelligent resource allocation inside B5G-enabled VANETs. To solve the problems of resource allocation in ITS's vehicular communication and connection, Manogaran et al. 2022 introduced the "Permissible Service Selection and Allocation" technique. To minimize computational resource available at the nodes in ITSs and maximize V2X

service placement in a hybrid edge environment, Moubayed et al. 2020 used the Greedy V2X Service Placement Algorithm.

VI. TECHNIQUES FOR SECURING COMMUNICATIONS IN IoT based ITS

This section deals with emerging approaches to mitigate malicious activities in IoT based ITS for establishing secured transmission of traffic/accident data. To protect against adversarial assaults in ITS, Yamany et al. 2021 offered a unique "Optimized Quantum-based Federated Learning (OQFL)" framework for performing automated hyperparameter adjustments for federated learning. For the purpose of uncovering malicious network activities in traffic data transmission, Ashraf et al. 2020 described a DL-dependent Intrusion Detection System (IDS) for ITSs that makes use of Long Short Term Memory (LSTM). It was recommended by Javed et al. 2020 that an "Outlier Detection, Prioritization, and Verification (ODPV)" protocol be used to more effectively separate out erroneous data and enhances the quality of traffic management choices. Specifically, ODPV use the isolation forest method to identify anomalies, fuzzy logic to rank them in importance, and C-V2X communications to confirm their authenticity. To address the issue of traffic data vulnerability, Abbas et al. 2021 suggested a decentralised data management system for secured smart transportation that makes use of IoT and blockchain in a sustainable smart city setting. Tyagi and Dembla 2019 suggested a method for improved network connection and security against assaults on routing protocols in ITS. This technique allows for the identification of an attacker node or a chain of attacker nodes, and the IP addresses of the identified attacker nodes are excluded from the ITS network. To safeguard the identity and position of vehicles in ITS, Bao et al. 2019 presented a decentralised blockchain dependent system for pseudonym management. Haydari et al. 2018 suggested a



new approach depending on non-parametric statistical anomaly detection to identify and defend against distributed denial of service attacks in ITS. A LSTM dependent SQL injection attack detection system that can automatically learn the most useful data format of attacks was developed by Li et al. in 2020. Ju et al. 2020 provide a modified generalised likelihood ratio technique to identify and quantify sensor deception attacks in ITS. Blockchain and DL modules are used to offer two levels of security and privacy in ITS by Kumar et al. 2021. A blockchain module is first created to securely transport ITS data between automobiles and RSUs, and an enhanced Proof of Work (ePoW) method depending on smart contracts is then created to ensure data integrity and prevent data poisoning attacks. Second, to protect against inference attacks, a DL module is created that uses the LSTM-AutoEncoder approach to encode ITS data into a new format. Finally, "Attention-based Recurrent Neural Network" uses the encoded data to identify intrusive occurrences in ITS infrastructure.

VII. CONCLUSION

The globe over, especially in densely populated urban and suburban regions, transportation infrastructure is under growing strain, and improvements are urgently needed. ITSs are designed to increase safety, productivity, and command of transportation networks by sharing contextual data inside such networks and their surrounding communities. New mobility technologies like IoT must be used, integrated, and implemented to improve ITS. In this paper, we've outlined a few of the most promising new techniques that may improve energy-efficiency, sustainability, reliability, and security of ITS. The survey provides deep insights into applications and challenges in implementing ITS. We suggest that the future of sustainable transportation solutions and increased road safety lies in the seamless

integration of the IoT and decentralized technologies with ITS. The limitations of the presented survey are that applications of big data technology in improving decision making process for vehicular nodes in ITSs are not discussed. In the future, applications of big data technology in improving decision making process for vehicular nodes in ITS must be studied.

Reference

1. Eswaraprasad, Ramkumar, and Linesh Raja. "Improved intelligent transport system for reliable traffic control management by adapting internet of things." In 2017 International Conference on Infocom Technologies and Unmanned Systems (Trends and Future Directions)(ICTUS), pp. 597-601. IEEE, 2017.
2. Goyal, S.B., Bedi, P. and Kumar, J., 2022. Realtime accident detection and alarm generation system over IoT. In *Multimedia Technologies in the Internet of Things Environment*, Volume 2 (pp. 105-126). Springer, Singapore.
3. Zhang, H. and Lu, X., 2020. Vehicle communication network in intelligent transportation system based on Internet of Things. *Computer Communications*, 160, pp.799-806.
4. Kuppusamy, P., Kalpana, R. and Venkateswara Rao, P.V., 2019. Optimized traffic control and data processing using IoT. *Cluster Computing*, 22(1), pp.2169-2178.
5. Yamany, W., Moustafa, N. and Turnbull, B., 2021. OQFL: An Optimized Quantum-Based Federated Learning Framework for Defending Against Adversarial Attacks in Intelligent Transportation Systems. *IEEE Transactions on Intelligent Transportation Systems*.



6. Peng, Y., Li, J., Park, S., Zhu, K., Hassan, M.M. and Alsanad, A., 2019. Energy-efficient cooperative transmission for intelligent transportation systems. *Future Generation Computer Systems*, 94, pp.634-640.
7. Sodhro, A.H., Pirbhulal, S., Sodhro, G.H., Muzammal, M., Zongwei, L., Gurtov, A., de Macêdo, A.R.L., Wang, L., Garcia, N.M. and de Albuquerque, V.H.C., 2020. Towards 5G-enabled self adaptive green and reliable communication in intelligent transportation system. *IEEE Transactions on Intelligent Transportation Systems*, 22(8), pp.5223-5231.
8. Fatemidokht, H., Rafsanjani, M.K., Gupta, B.B. and Hsu, C.H., 2021. Efficient and secure routing protocol based on artificial intelligence algorithms with UAV-assisted for vehicular ad hoc networks in intelligent transportation systems. *IEEE Transactions on Intelligent Transportation Systems*, 22(7), pp.4757-4769.
9. Sodhro, A.H., Obaidat, M.S., Abbasi, Q.H., Pace, P., Pirbhulal, S., Fortino, G., Imran, M.A. and Qaraqe, M., 2019. Quality of service optimization in an IoT-driven intelligent transportation system. *IEEE Wireless Communications*, 26(6), pp.10-17.
10. Camacho, F., Cárdenas, C. and Muñoz, D., 2018. Emerging technologies and research challenges for intelligent transportation systems: 5G, HetNets, and SDN. *International Journal on Interactive Design and Manufacturing (IJIDeM)*, 12(1), pp.327-335.
11. Torre-Bastida, A.I., Del Ser, J., Laña, I., Ilardia, M., Bilbao, M.N. and Campos-Cordobés, S., 2018. Big Data for transportation and mobility: recent advances, trends and challenges. *IET Intelligent Transport Systems*, 12(8), pp.742-755.
12. Fitah, A., Badri, A., Moughit, M. and Sahel, A., 2018. Performance of DSRC and WIFI for Intelligent Transport Systems in VANET. *Procedia Computer Science*, 127, pp.360-368.
13. Fantin Irudaya Raj, E. and Appadurai, M., 2022. Internet of Things-Based Smart Transportation System for Smart Cities. In *Intelligent Systems for Social Good* (pp. 39-50). Springer, Singapore.
14. Finogeev, A., Finogeev, A., Fionova, L., Lyapin, A. and Lychagin, K.A., 2019. Intelligent monitoring system for smart road environment. *Journal of Industrial Information Integration*, 15, pp.15-20.
15. Ashraf, J., Bakhshi, A.D., Moustafa, N., Khurshid, H., Javed, A. and Beheshti, A., 2020. Novel deep learning-enabled LSTM autoencoder architecture for discovering anomalous events from intelligent transportation systems. *IEEE Transactions on Intelligent Transportation Systems*, 22(7), pp.4507-4518.
16. Nallaperuma, D., Nawaratne, R., Bandaragoda, T., Adikari, A., Nguyen, S., Kempitiya, T., De Silva, D., Alahakoon, D. and Pothuhera, D., 2019. Online incremental machine learning platform for big data-driven smart traffic management. *IEEE Transactions on Intelligent Transportation Systems*, 20(12), pp.4679-4690.
17. Zhang, C., James, J.Q. and Liu, Y., 2019. Spatial-temporal graph attention networks: A deep learning approach for traffic forecasting. *IEEE Access*, 7, pp.166246-166256.
18. Boukerche, A. and Wang, J., 2020. Machine Learning-based traffic prediction models for Intelligent



- Transportation Systems. Computer Networks, 181, p.107530.
19. Dar, B.K., Shah, M.A., Islam, S.U., Maple, C., Mussadiq, S. and Khan, S., 2019. Delay-aware accident detection and response system using fog computing. *Ieee Access*, 7, pp.70975-70985.
 20. Chang, W.J., Chen, L.B. and Su, K.Y., 2019. DeepCrash: a deep learning-based Internet of vehicles system for head-on and single-vehicle accident detection with emergency notification. *IEEE Access*, 7, pp.148163-148175.
 21. Javed, M.A., Khan, M.Z., Zafar, U., Siddiqui, M.F., Badar, R., Lee, B.M. and Ahmad, F., 2020. ODPV: An efficient protocol to mitigate data integrity attacks in intelligent transport systems. *IEEE Access*, 8, pp.114733-114740.
 22. Hadiwardoyo, S.A., Patra, S., Calafate, C.T., Cano, J.C. and Manzoni, P., 2018. An intelligent transportation system application for smartphones based on vehicle position advertising and route sharing in vehicular ad-hoc networks. *Journal of Computer Science and Technology*, 33(2), pp.249-262.
 23. Vangala, A., Bera, B., Saha, S., Das, A.K., Kumar, N. and Park, Y., 2020. Blockchain-enabled certificate-based authentication for vehicle accident detection and notification in intelligent transportation systems. *IEEE Sensors Journal*, 21(14), pp.15824-15838.
 24. Bhatti, F., Shah, M.A., Maple, C. and Islam, S.U., 2019. A novel internet of things-enabled accident detection and reporting system for smart city environments. *Sensors*, 19(9), p.2071.
 25. Hahn, D., Munir, A. and Behzadan, V., 2019. Security and privacy issues in intelligent transportation systems: Classification and challenges. *IEEE Intelligent Transportation Systems Magazine*, 13(1), pp.181-196.
 26. Ali, Q.E., Ahmad, N., Malik, A.H., Ali, G. and Rehman, W.U., 2018. Issues, challenges, and research opportunities in intelligent transport system for security and privacy. *Applied Sciences*, 8(10), p.1964.
 27. Sedar, R., Kalalas, C., Vázquez-Gallego, F. and Alonso-Zarate, J., 2021. Intelligent transport system as an example of a wireless IoT system. In *Wireless Networks and Industrial IoT* (pp. 243-262). Springer, Cham.
 28. Bhardwaj, K.K., Khanna, A., Sharma, D.K. and Chhabra, A., 2019. Designing energy-efficient IoT-based intelligent transport system: need, architecture, characteristics, challenges, and applications. *Energy Conservation for IoT Devices*, pp.209-233.
 29. Kuppusamy, P., Venkatraman, S., Rishikeshan, C.A. and Reddy, Y.P., 2020. Deep learning based energy efficient optimal timetable rescheduling model for intelligent metro transportation systems. *Physical Communication*, 42, p.101131.
 30. Sharma, V., You, I., Pau, G., Collotta, M., Lim, J.D. and Kim, J.N., 2018. LoRaWAN-based energy-efficient surveillance by drones for intelligent transportation systems. *Energies*, 11(3), p.573.
 31. Cao, H., Garg, S., Kaddoum, G., Hassan, M.M. and AlQahtani, S.A., 2022. Intelligent Virtual Resource Allocation of QoS-Guaranteed Slices in 5G-Enabled VANETs for Intelligent Transportation Systems. *IEEE Transactions on Intelligent Transportation Systems*.
 32. Manogaran, G., Gao, J. and Nguyen, T.N., 2022. Optimizing Resource and Service Allocations for IoT-Assisted



- Intelligent Transportation Systems. IEEE Transactions on Intelligent Transportation Systems.
33. Moubayed, A., Shami, A., Heidari, P., Larabi, A. and Brunner, R., 2020. Edge-enabled V2X service placement for intelligent transportation systems. IEEE Transactions on Mobile Computing, 20(4), pp.1380-1392.
 34. Abbas, K., Tawalbeh, L.A.A., Rafiq, A., Muthanna, A., Elgendy, I.A., El-Latif, A. and Ahmed, A., 2021. Convergence of blockchain and IoT for secure transportation systems in smart cities. Security and Communication Networks, 2021.
 35. Tyagi, P. and Dembla, D., 2019. A secured routing algorithm against black hole attack for better intelligent transportation system in vehicular ad hoc network. International Journal of Information Technology, 11(4), pp.743-749.
 36. Bao, S., Cao, Y., Lei, A., Asuquo, P., Cruickshank, H., Sun, Z. and Huth, M., 2019. Pseudonym management through blockchain: Cost-efficient privacy preservation on intelligent transportation systems. IEEE Access, 7, pp.80390-80403.
 37. Haydari, A. and Yilmaz, Y., 2018, November. Real-time detection and mitigation of DDoS attacks in intelligent transportation systems. In 2018 21st International Conference on Intelligent Transportation Systems (ITSC) (pp. 157-163). IEEE.
 38. Ju, Z., Zhang, H. and Tan, Y., 2020. Distributed deception attack detection in platoon-based connected vehicle systems. IEEE transactions on vehicular technology, 69(5), pp.4609-4620.
 39. Li, Q., Wang, F., Wang, J. and Li, W., 2019. LSTM-based SQL injection detection method for intelligent transportation system. IEEE Transactions on Vehicular Technology, 68(5), pp.4182-4191.
 40. Kumar, R., Kumar, P., Tripathi, R., Gupta, G.P., Kumar, N. and Hassan, M.M., 2021. A privacy-preserving-based secure framework using blockchain-enabled deep-learning in cooperative intelligent transport system. IEEE Transactions on Intelligent Transportation Systems.





Facial Expression Detection Using CNN with MediaPipe

Mrs.V.Lavanya¹, Mr.K.Azarudeen², Dr.G.Vinoth Chakkaravarthy³,
Mrs.CB.Selvalakshmi⁴

¹Assistant Professor, Department of CSE, Velammal College of Engineering and Technology, Madurai.

²Assistant Professor, Department of CSE, Velammal College of Engineering and Technology, Madurai.

³Associate Professor, Department of CSE, Velammal College of Engineering and Technology, Madurai.

⁴Assistant Professor, Department of CSE, Velammal College of Engineering and Technology, Madurai.

ABSTRACT

Facial recognition has recently become very important in the fields of artificial intelligence, robotics, security, trade, etc. It can be used in stress analysis in industries by capturing the faces of the employees and by analysing their emotions in order to put forward the suitable therapies for cure in required. Face recognition can also be used in shopping malls to analyse the facial expressions of the users while purchasing various products, thus capturing their interests for purchasing the same. This can then be used together with the other data for the process of data analysis and further promotions for the users in terms of their liking products. In order to analyze facial expressions, a variety of techniques are employed, including support vector machines, the k-nearest neighbor algorithm, and multilayer perceptron. Although there are numerous ways to recognize expressions using machine learning and artificial intelligence techniques, this project makes an attempt to use Convolutional neural networks and MediaPipe to identify various expressions from the faces and classify them appropriately. In order to learn face representation from a smaller data set, this project suggests modifying a Convolutional neural network. Convolutional neural networks are well known to have a higher accuracy when compared to traditional machine learning methods. Our system continuously captures the images of the user using Webcam and analyses the facial expressions accordingly using a convolutional neural network and to identify the mood of the user which can be used for further analyses.

Keyword: CNN, FER, MediaPipe.

1. INTRODUCTION

Facial expression detection, in today's world, is one of the most important features of human emotion recognition. Facial Expression can be defined as the facial changes observed in a person in response to the person's internal emotional state, intentions, or social communication. Automated facial expression recognition has a large variety of applications nowadays, such as neuromarketing, data-driven animation, sociable robotics, interactive games and many other human-computer interaction systems. Basically, expression recognition is a task performed by human beings on everyday basis, effortlessly. However, it is not yet easily performed by computers. In specific situations, such as frontal face, controlled settings, and high-resolution photos, several contemporary systems have also demonstrated accuracy levels more than 95%. However, these only seem to be deceptive high-accuracy. Furthermore, most of the issues that face expression recognition systems face in actual situations are not adequately represented by these systems. The use of deep learning in expression detection is mainly for obtaining higher accuracy even for dynamic sequence of input received from webcam live. However, deep learning methods require huge dataset for obtaining such accuracies.

Facial expression data is not as large as required by deep networks. Hence, the proposed system attempts to use a modified CNN and media pipe that can work on even small datasets and ensure that the required accuracy is obtained. The modified CNN, which helps obtain high accuracy even with limited dataset uses data augmentation to recreate large datasets from the available data by processes.

2. LITERATURE SURVEY

Different facial muscles contract to produce facial expressions, which temporarily deform our eyes, noses, lips, cheeks, and other facial features. From person to person, it differs. This survey provides a thorough explanation of the various techniques used for facial expression analysis.

2.1 Judgement based approach

The messages that the facial expressions convey are the main focus of approaches that rely on judgement. Based on the consensus of the experts or coders, or "ground truth," the facial expressions are categorised into a set of emotions. The majority of facial expression analyses fall into one of the six basic emotion classes listed by Ekman and Friesen in Constants across culture in the face and emotions in 1971.

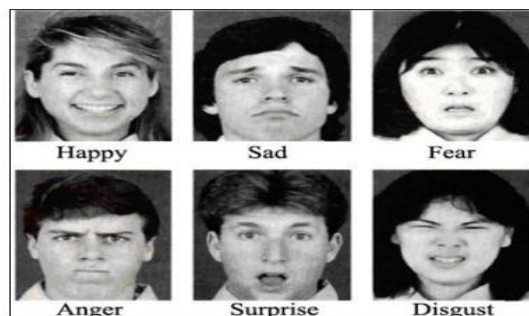


Figure 1 Six Basic Emotions

Sign based approaches

Facial expressions are abstracted and described by their location and intensity in sign-based approaches. Therefore, all potential perceptions that might be present on a face make up a comprehensive description framework. Ekman and Friesen's 'A technique for the measurement of facial movement' from 1978 contained the FACS (Facial Action Coding system) proposal. For the description of facial expressions in terms of location and intensity, FACS uses 44 action units. In 1983, Izard, Dougherty, and Hembree proposed a system for identifying affect

Upper Face Action Units					
AU 1	AU 2	AU 4	AU 5	AU 6	AU 7
Inner Brow Raiser	Outer Brow Raiser	Brow Lowerer	Upper Lid Raiser	Cheek Raiser	Lid Tightener
*AU 41	*AU 42	*AU 43	AU 44	AU 45	AU 46
Lid Droop	Slit	Eyes Closed	Squint	Blink	Wink
Lower Face Action Units					
AU 9	AU 10	AU 11	AU 12	AU 13	AU 14
Nose Wrinkler	Upper Lip Raiser	Nasolabial Deepener	Lip Corner Puller	Cheek Puffer	Dimpler
AU 15	AU 16	AU 17	AU 18	AU 20	AU 22
Lip Corner Depressor	Lower Lip Depressor	Chin Raiser	Lip Puckerer	Lip Stretcher	Lip Funneler
AU 23	AU 24	*AU 25	*AU 26	*AU 27	AU 28
Lip Tightener	Lip Pressor	Lips Part	Jaw Drop	Mouth Stretch	Lip Suck

expressions by

Figure 2

holistic judgements that included coding schemes like EMFACS, MAX, and AFFEX.

2.2 Reliability of ground truth coding

The labeling of employed databases to recognize or interpret facial expressions has improved recognition accuracy with respect to timing and intensity estimations. Ekman specifies certain points to be addressed while measuring facial expressions in 'Handbook of methods in non-verbal behavioural research' in 1982.

2.3 Automatic face expression analysis

As faces differ from person to person, automatically analysing facial expressions is a difficult task. Automatic facial expression analysis involves facial acquisition, facial feature extraction and analysis.

2.4 Face acquisition

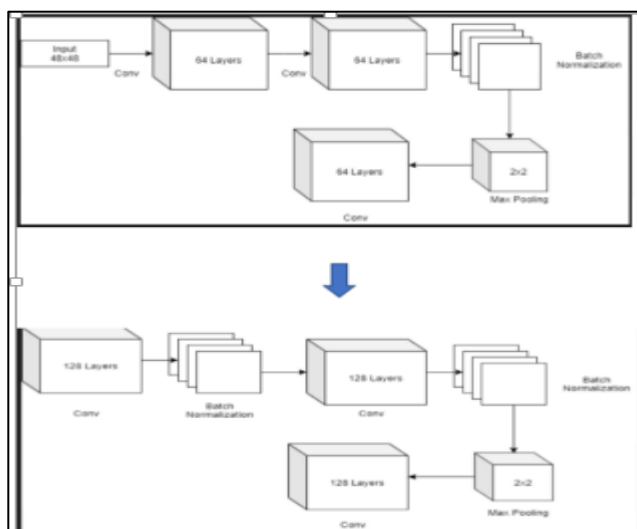
Face recognition is automatic in complicated settings with crowded backgrounds. Using the active appearance models described by Lanitis, Taylor, and Cootes in their 1997 paper "Automatic interpretation and coding of face images using flexible models," this may be accomplished. Hong tracked faces in real time by utilising the steffens person spotter technology. Depending on the viewing angle and distance for a certain face, several facial

expressions will show. In order to normalise test faces in accordance with the general face models stated in "Transactions on pattern Analysis and machine intelligence," distinguishing facial characteristics like the eyes, ears, and nose serve as reference points. Another important factor in face recognition is illumination. According to 'Proceedings of Circuits, Systems, Communications, and Computers' from 1999, Gabor wavelets can be used to lessen changes in light.

3. NEURAL NETWORK DESIGN

The main component in an emotion detection system built using deep learning is the neural network. The neural network deployed in this system will be Convolution Neural Network (CNN). TensorFlow and Keras. The model is designed using TensorFlow and Keras package. Usually, a neural network that is developed is trained by means of forward propagation and backward propagation. Computational graphs are constructed to compute gradients effectively. These gradients are used in the back propagation process while training our model, thus implementing gradient descent. The data structure for the computational graph is implemented by it, as the functions of each of the weights are defined. Hence, while training, TensorFlow makes it easier for the model to compile and run faster and effectively. Fast numerical computing is made possible by the open source library TensorFlow. The Apache 2.0 open source licence was used for its creation and maintenance by Google. Although the C++ API is accessible, the API is formally for the Python programming language. TensorFlow was created for use in both production systems and research and development systems, including but not limited to RankBrain in Google search and the entertaining DeepDream project. This makes it different from other numerical libraries intended for use in Deep Learning like Theano. Mobile devices, large scale distributed systems with hundreds of machines, single CPU systems, GPU systems, and GPU-enabled systems can all run it. Hence, the models can be easily created using Keras, but it uses TensorFlow as its backend. Therefore, there is no issues related to performance when Keras is compared with TensorFlow. Keras has various types of models, layers, activations, optimizers, initializers, and many more to build a neural network easily.

3.1 Architecture design of CNN



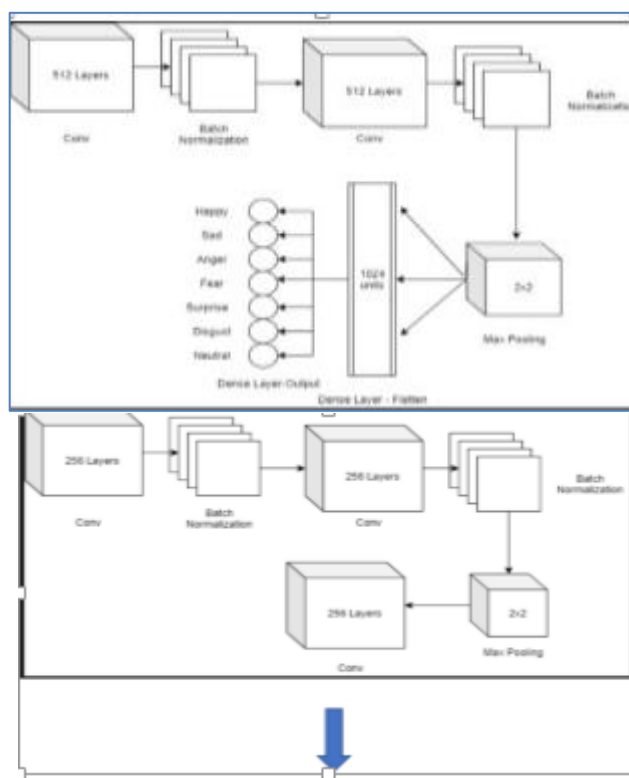


Figure 3 CNN architecture design

The structure of the architecture is as follows:

- The image input is fed having a dimension of 48*48
- The input is then applied to two convolution layers with 64 filters of the kernel size 3*3.
- Followed by batch normalization of the output from the convolution layer maximum pooling of size 2*2 is then performed with stride 2*2.
- The output from max pooling is fed to another convolution layer of 64 filters with 3*3 kernel size.
- All the above layers are illustrated in the block diagram 1.3(a)
- A convolution layer with 128 filters and a kernel size of 3*3 receives the output from the convolution layer of 64 filters.
- An additional convolution layer with 128 filters and a batch normalisation layer are added after this.
- The output from this process is fed to a convolution layer with 128 filters. Next, a max pooling operation of size 2*2 is carried out.
- All the above layers are illustrated in the block diagram 1.3 (b)
- The same pattern of layers as in the block diagram 1.3(b) is followed in the next set of layers also but with each convolution layer having 256 filters and later with 512 filters.
- The output of the final pooling layer is flattened to create a set of dense layers with 1024 units.

- The final dense layer with seven classification outputs is then applied.

3.2 Dataset

A machine learning platform called Kaggle provided the dataset that was used to train and test the CNN. Anger, disgust, fear, happiness, sadness, surprise, and neutral are the seven emotions that are labelled on each of the 48x48-pixel grayscale images of faces in the FER2013 dataset. The Facial Expression Recognition Challenge on Kaggle was the original competition for which Pierre-Luc Carrier and Aaron Courville produced the dataset. A total of 35,887 images make up the dataset. The FER2013 dataset includes images that are presented in CSV (Comma-Separated Values) format, where each row corresponds to an image with pixel values and an emotion label. There is a training set, a public test set, and a private test set for the FER2013 dataset. 28,709 images make up the training set, while 3,589 images each make up the public and private test sets.

```
Preprocessing Done
Number of Features: 48
Number of Labels: 7
Number of examples in dataset:
```

Figure 4 Dataset Details

3.3 Training and Testing on dataset

Any CNN network needs to be trained and tested before deployment on dataset. For training and testing the dataset mentioned in section 3.2 was used. The testing accuracy of 66.369 % is obtained.

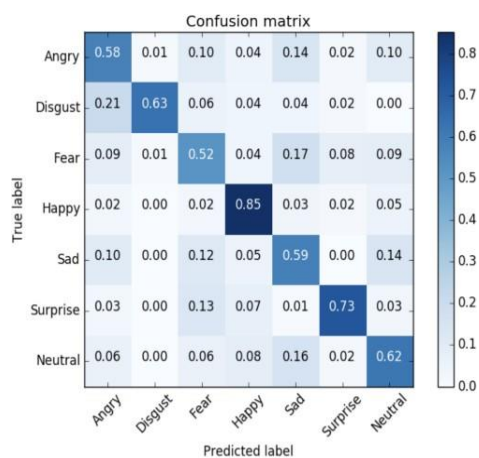


Figure 3.4 Confusion Matrix

Figure 5 Confusion matrix

SYSTEM IMPLEMENTATION

This chapter is about the prototype implementation. It discusses about the various

modules implemented and overall conceptual architecture of the system.

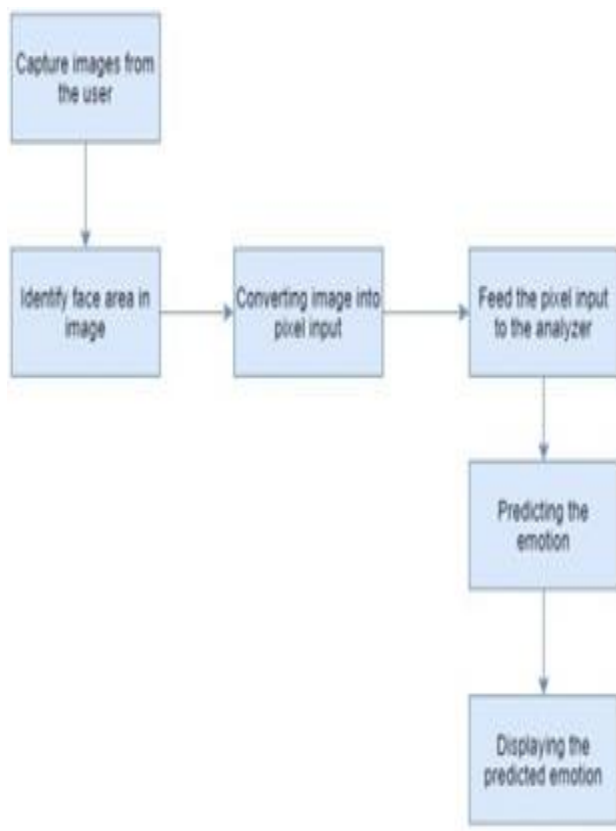


Figure 6 Conceptual Architecture

3.4 Conceptual architecture

The conceptual architecture visually describes the various aspects of the system at a higher level. This Conceptual Architecture's main goal is to make the system understandable. The system takes the image from web camera as input data. The captured image input is given to the pre-processor in which the face area is recognized from the image input. The pre-processed image is converted into pixels and fed into the model for prediction. The model trained using CNN is used for prediction. The model generates the suitable emotion prediction using the trained data. The prediction is then displayed to the user as output. The overall workflow between the various components is described in the following block diagram of the proposed system.

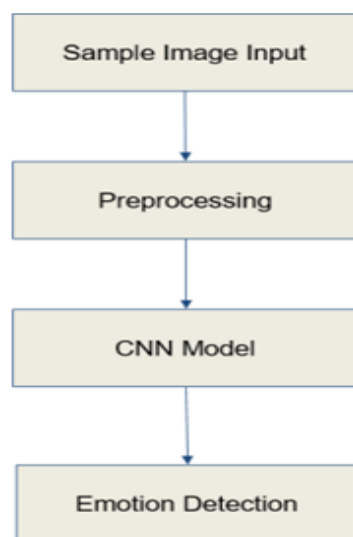


Figure 7 Flow of Components

3.5 Input module

Input module captures facial inputs of the user from the web camera and feeds the input for further processing and for final prediction of the mood of user. This is done using **emotion.py** module in python.

3.6 Pre Processing module

Pre Processing module is used to process the input image so that it can be fed into the trained model for prediction. The image input generated from the camera is pre-processed in this module. The image is processed, and the facial component is identified. This is done with google MediaPipe face detection module. All this is done using **cv2 module** in python.

3.7 Analyzer module

The faces detected using the cascade classifier are resized to 48*48 size and normalized. After completing all this, the resultant array will be provided as the input to the CNN. All this is also done using **cv2 module** and **NumPy** in python.

3.8 Emotion detector

The Emotion Detector module is designed based on **Convolutional Neural Networks** model which is popularly used for image classification.

4. OUTPUT AND EVALUATION

Output during training

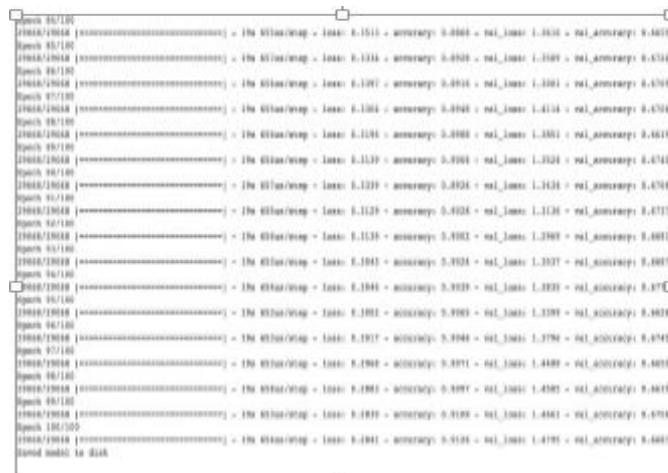


Figure 8 Training Output

Output from the emotion detector

- Output Evaluation on images taken from internet. These images are taken in well lighted conditions in professional camera. This was processed in the implemented system.

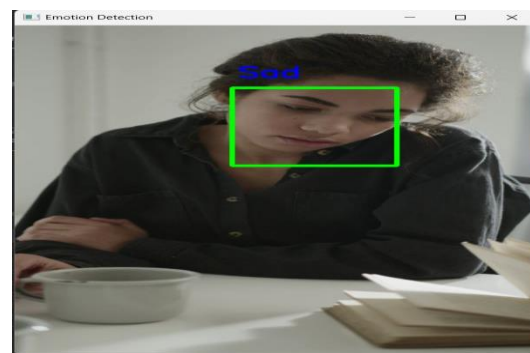


Figure 9 Images from Laptop

APPLICATION AND FUTURE SCOPE:

Application:

The product's scope is multi-fold. It can be used as a part of numerous applications. Some of the scopes of this system are discussed below. The system has the ability to recognize and monitor a user's mental state. To view customer feedback and improve the business, the system is also used in mini-marts and shopping centers. Using the emotional intelligence of a person that this system can identify, clever marketing is possible. The system can be installed in crowded areas like airports, train stations, or bus stops to detect people's faces and facial expressions. The system may sound an internal alarm if it notices any suspicious emotions, such as anger or fear. The system can also be employed for educational purposes, such as receiving feedback based on how a student is acting in class. It can also be used as plugins to monitor mentally disordered patient's behavior at difficult level. System is fully automatic and has the capability to work with video feeds as well as images. It can recognize spontaneous expressions. This makes the system capable of being used even in Digital Cameras where in it is tuned such that the image is captured only when the person smiles or similar emotions. It can feature as added plugin in home automation. For instance, rooms in the house can set the lights, television to a person's current mood by figuring out his/her expression when he/she enters.

Future scope:

The developed system is restricted only to predict the emotion of the facial expression captured at an instance of time by the system. The system can be extended to predict the emotion of the user captured over a sequence of period i.e a video input as a sequence of images to train the model. It can be expanded to forecast emotions based on the user's vocal input, or forecast emotions based on user sound patterns. This system can be delivered as a plug-in feature so that it can be incorporated with many applications that use this feature(emotion detection) in it.

CONCLUSION:

Thus, the purpose of this project has been achieved by efficiently predicting the emotion of the corresponding facial expression captured by the system. This has been achieved by using a trained Convolutional Neural Network architecture. The model has been successfully trained with sufficient input output samples and has produced a decent prediction accuracy as well. The performance has been improved by using increased kernel filters and sufficient dropout percentage so as to ensure the required features are captured and learnt by the model as well as the model does not overfit for the training samples.

REFERENCES

- [1] Jie Wang, Zihao Li, "Research on Face Recognition Based on CNN", 2018 IOP Conf. Ser.: Earth Environ. Sci. 170 032110.
- [2] <https://towardsdatascience.com/an-intro-to-deep-learning-for-facerecognition>.

- [3] Andre Teixeira Lopesa, Edilson deAguiarb, Alberto F. De Souzaa, Thiago Oliveira-Santosa, “Facial Expression Recognition with Convolutional Neural Networks: Coping with Few Data and the Training Sample Order”.
- [4] Chalciya Elizabeth Rani P1, Dr. H.P. Mohan Kumar2 "Facial Emotion Detection Using Keras ".
- [5] Prathwini, Roshan Fernandes, Anisha P Rodrigues "Emotion Detection in Multimedia Data Using Convolution Neural Network".
- [6] Amr Mostafa, Mahmoud I. Khalil, Hazem Abbas " Emotion Recognition by Facial Features using Recurrent Neural Networks ".
- [7] " Human Emotion Detection Using Open CV " Mallika Srivastav, Prakhar Mathur, T. Poongodi, Shrddha Sagar, Suman Avdhesh Yadav.
- [8] Sarwesh Giri, Gurchetan Singh, Babul Kumar, Mehakpreet Singh, Deepanker Vashisht, Sonu Sharma, Prince Jain " Emotion Detection with Facial Feature Recognition Using CNN & OpenCV “
- [9] Ninad Mehendale,”Facial emotion recognition using convolutional neural networks”.
- [10]Akriti Jaiswal, A. Krishnama Raju, Suman Deb " Facial Emotion Detection Using Deep Learning ".



An Approach for Intersection Prevention in Transmission Channel Using Correlation Matrix and Tree Construction Model in V2X Framework

T. Graceshalini¹ · S. Jenicka²

Accepted: 7 January 2022

© The Author(s), under exclusive licence to Springer Science+Business Media, LLC, part of Springer Nature 2022

Abstract

Typically, the delivery of information in vehicular ad hoc networks (VANETs) is regarded as a demanding one because of high mobility and invariable topological difference. One major concern in VANET framework is the occurrence of simulated intersection at which the packet reception probability become complicated for predicting and the model turn out to be complex highly. So as to overcome this dispute, a new framework is introduced which in turn prevents the intersection among the transmission path. Initially, the system model is initialized and the availability of channel is estimated. Based on the strength and size of data to be transmitted, the availability of channel is computed. After that, the best forwarding zone computation is made for minimizing the redundant data packets flow. To check the priority of packet and occurrence of packet collision, tree construction based data strength transmission is employed at last, the prevention of intersection or collision between the transmission channel is checked by means of correlation matrix based intersection prevention approach by monitoring the neighbor node. Then, the data packets were forwarded in an efficient manner without any intersection between the frames. The performance analysis is estimated in terms of network lifetime, packet delivery ratio, packet collision; inter node collision, throughput, and end-to-end delay.

Keywords Vehicular ad hoc networks · Intersection · Forwarding zone computation · Correlation matrix-based intersection prevention · Tree construction · Availability of channel

1 Introduction

In VANET the demand of immense traffic rate leads to the continuous growth of bandwidth demand. The service of VANET becomes highly advanced for the enhancement of traffic efficiency and road safety improvement on targeting a highly comfortable driving and the

✉ T. Graceshalini
graceshaliniphd@gmail.com

¹ Velammal College of Engineering and Technology, Madurai, Tamil Nadu, India

² Vellore Institute of Technology, 632 014 Vellore, India

experience of traveling. For addressing such a requirement of capacity, it is essential to ensure the exploitation of optimal radio resources that were available [1]. The direction and speed of the necessitate vehicles need to alter their distance and position recurrently. As a result, the vehicles have to keep on altering their point of communication at the time of vehicle information transmission mechanism [2]. All through handover or handoff, vehicles block their receiving services from their communication points that were connected previously and connect with another for the receiving services [3, 4]. VANETs consist of some special features that involve road pattern restrictions, large-scale network sizes, self-organization, high mobility, no constraints of energy, etc. [5]. The vehicular network is considered a challenging technology that provides smart vehicles for exchanging wireless information between them to attain the excess safer and convenient system of transportation. This information might comprise data regarding the conditions of traffic, adaptive assistance of trips, alarms, and warnings, and availability of parking gas stations with information applications.

VANET is regarded as the extended mobile ad-hoc networks application that finds out new routes to the points of communication during handoff time. The communicating vehicle prompts re-routing for the discovery of new communication points positioned further away or nearby [6, 7]. The procedure of Handoff provided for VANET should ensure flawless performance on behalf of supporting these applications. Because of the vehicle's direction and unpredictable velocity, in VANETs handoff is a challenging task [8, 9]. The application of VANET requires the moving vehicle's position to assist specific user services. In VANET, the localization of a conventional global positioning system (GPS) does not assure the position-based application due to availability concerns, signal errors, localization proximity, communication management, and handoff. These are the incorporated blocks and disputes for the management of mobility (MM) in VANETs [10, 11].

In the scenario of urban VANET, usually vehicles are not dispersed consistently in the region of the City road. For these, the network might be fragmented and the proficient communication among V2X gets affected [12, 13]. In addition, the existence of the impediment like other constructions or buildings could be the interruption basis to a radio signal, which in turn leads to communication failure, as they are in the communication zone of each other. Most of the routing protocols proposed intended for Urban VANETs do not allow the probable hindrance with a negative routing impact, which in turn designates that the data flow direction system towards the destination because of the existence of the obstacle was a significant research concern. One more significant aspect is a forwarding zone selection in that way. After that, the possible selection of forwarding nodes on the forwarding zone is one more challenge for efficient data transmission. Also, the occurrence of intersections due to topology changes is considered a major dispute in VANET. This makes VANET framework a more challenging one for delivering information. To overcome this drawback, an effective protocol is presented in this work.

The remaining part of the paper is organized as follows: Sect. 2 offers various existing mechanisms presented so far. Section 3 provides the proposed algorithm and performance estimation were provided in Sect. 4. Section 5 offers the concluding statement.

2 Related Work

This section is a description of the various existing mechanisms employed so far.

A system is presented [8] for Adaptive intersection selection using the Ant Colony Optimization approach, a problem of finding a challenging route concern for the multiple QoS constraint. In addition, the outcomes in the urban framework reveal that the AISM outperforms the traditional protocols by extensive simulation environment in terms of Packet delivery ratio, hop count, and average delay [14]. An adaptive multi-channel medium access control (MAC) high-throughput protocol, specifically, AHT-MAC [15] was proposed that could manage the transmission of data over SCHs. Through this AHT-MAC, the range of data broadcasting was attuned by the range of beacon transmission over CCH so that a transmitting node might establish suitable candidate's communication and arrange resources available for both communication nodes before transmission.

A scheme of link quality-dependent dissemination of security messages on behalf of urban VANETs was presented [16]. The wide-ranging connectivity of the physical channel computation technique was suggested for estimating the probability of connectivity among vehicles precisely. A score-dependent mechanism of priority allocation was suggested for candidate forwarders (CFs) to manage the controversy between CFs.

The authors [17] utilized the controller SDN for mitigating the congestion of Vehicle-to-Vehicle communications even as routing information on the segments of road. This was attained by competent VANET bandwidth utilization on the road segments. In contradiction of current assistance, the suggested SDN controller offers a new mechanism of routing which considers the other traditional routing paths that were relaying information in VANET already. A new routing request was found out so that no road segment gets congested through the multiple crossing routing paths.

Intermittent hello packets were suggested [14] for the establishment of the neighboring list that furthermore employs information regarding the neighbors [15], with the dynamic neighbor distance and neighbors direction, for the selection of forwarding node [16]. A hybrid of neighbor and distance list forwarding broadcast protocol was considered. This article in turn mainly focuses on decreasing the delay of broadcast and enhancing the range of dissemination in VANET thereby avoiding the impacts of changing the topology of the network [17]. The road vehicles density was a significant aspect for the application of time-critical security [18].

The authors [19] suggested an approach of Multi-metric Power Control (MPC), that employs channel states and application requirements for determining a broadcast power intended for safety communication. The MPC offers a best-effort scheme for satisfying the range of coverage necessity of a message as signified through the application. Additionally, the perception differentiated among types of messages for providing coverage discrimination.

The authors [20] considered a design of physical (PHY)/MAC cross-layer depending on transmit power adaptation (TPA) and transmit antenna selection (TAS). A spatial multiplexing zero-forcing Bell-labs layered space-time (ZF-VBLAST) was considered over time-varying multiple-input and multiple-output (MIMO) flat fading channel that was to be implemented in the vehicle-to-vehicle (V2V) communication.

A Trunk Road dependent Protocol of Geographic Routing in Urban VANETs (TRGR) [21] was presented. This protocol in turn aims at resolving the data acquisition problem in the traditional system of trunk coordinated control mechanism. On considering the real physical distinctiveness of trunk lines, it formulates the entire utilization of trunk lines traffic flow and the neighboring road network, offers a transmission of real-time data routing design, and provides a vehicle network routing protocol in this particular form.

The authors [22] suggested a WAVE acquiescent improvement to the existing protocol IEEE 802.11p that targets the delivery of prioritized safety information whereas

provisioning the dissemination of the non-safety messages at the same time. The suggested technique relies on the generation of dynamic beacons for mitigating the congestion of channels and incompetent utilization of bandwidth through reducing the beacon's transmission frequency [23]. An effective strategy of charging information transmission (ECTS) [19] on behalf of Spatio-temporal coordinated services of vehicle-to-vehicle (V2V) charging was considered. In particular, depending on the mobile edge computing (MEC) concepts and hybrid vehicular ad hoc networks, a scalable and effective framework of communication was designed initially to shrink the costs of communication.

The authors [24] highlighted the major intention of introducing an optimal route path process for minimizing the link failure chances and energy consumption reduction of nodes in the network. In this article, an algorithm of the modified route optimal path at which the nodes were in cluster form was projected in the direction of achieving this objective. In this, the scheme of mobility prediction was employed for the stability of the network, and the two-tier method was employed in the minimization of energy consumed in the course of a Location Aided Routing (LAR) protocol.

The behavior of the network [25] was analyzed in a sensible area of simulated intersection wherever the packet reception probability becomes complicated for predicting and the model turns out to be complex highly. In that situation, a critical analysis was presented on the current US and EU decentralized congestion control protocols performance whereas their performance was estimated regarding the accuracies of tracking needed by the application of Intelligent Transportation System (ITS).

A collision avoidance scheme was presented in [26] for VANETs. A modified K-medoids algorithm was presented for clustering bi-directional traffic. The collision probability was estimated to expected nodes states. The presented strategy is better in offering minimized collision rate, overhead, and transmission latency. However, the delay and throughput were not improved.

The authors in [27] presented an adaptive MAC protocol in VANET. The potential impact on throughput and delay rate was considered in this approach. The performance analysis offers a reduced delay rate with improved throughput. However, the collision and intersection of packets were not considered in this approach.

Though there were several techniques employed so far there were some limitations like low throughput, reduced PDR, high packet collision ratio, high delay, and so on to overwhelm these limitations, the presented technique focuses on presenting a novel approach.

3 Proposed Work

This section depicts the proposed adaptive intersection-based channel selection strategy in detail. The flow of the proposed technique is shown below (Fig. 1).

3.1 Node Deployment

Let us envisage a VANET environment that consists of vehicles, which is a typical scenario in urban areas. The initialization of the system model is made at first by considering the number of transmitters, number of receivers, number of packets, packet size, number of frames, frame size, data strength, and number of iterations based on the vehicle node. The number of iterations can be varied as per the number of vehicles considered. The packet collision for each vehicle is being initialized. It was assumed that there was N number of

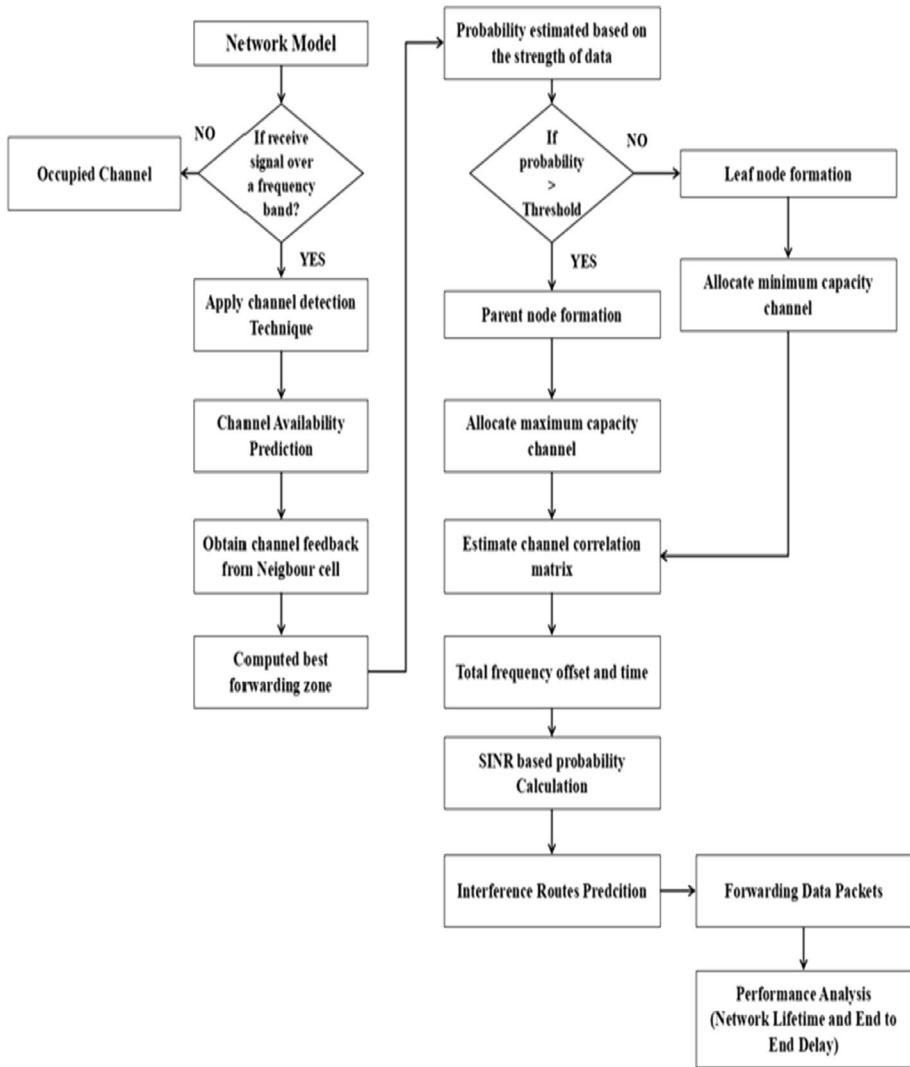


Fig. 1 Flow of proposed strategy

nodes that were moving at some distance as per the reference region model of group mobility. The entire nodes in the model have an equivalent range of transmission. Each node is capable of transferring information to the neighboring nodes.

3.2 Channel Availability and Best Forwarding Zone Prediction

After the initialization of parameters, the request for all available channels is made in case the user is ready to transmit data. Based on the strength and size of data to be transmitted, the availability of the channel is computed. The channel availability is offered based on the priority of data packets or messages that were to be transmitted. Users are transmitting

either or in handoff mode on various timestamps. Depending on the arrival of the user, the subcarrier should assign an appropriate channel or frame for users. Then, the computation of the best forwarding zone is made. To minimize the redundant data packets flow, the forwarding zone is being set so that the entire nodes present in the zone were in the wireless range of one another. For achieving these criteria, the forwarding zone with sector shape having the best angle of 60° towards the destination is being set. This fixed forwarding angle in turn limits the maximum distance in the forwarding zone. This in turn will allow the nodes present in the forwarding zone to heed each other's transmission of the packet, in that way allowing only one node to communicate the data packet in the forwarding zone.

3.3 Tree Construction Based on Strength of Transmission Data

In this, the packets are prioritized by constructing the key that is based on the number of users, route nodes, shift center point of a packet, packet size, the bandwidth of packet, and the number of packets received. This is done based on each transmitter and receiver tree, and their channel availability. This key construction is made through the novel approach termed tree construction based on strength of transmission of data to check the priority of packet and occurrence of packet collision. This tree construction mainly depends on the strength of the user and packet size. For each node and available channel, the λ (threshold) is increased in each iteration. The algorithm for this tree construction-based transmission of data is shown below:

Algorithm 1: Tree-based data strength Priori

Input: Frame packet from each vehicle V_{P_f} (data,
packet priority DP)

Output: formed data Priority tree

$PT_{high}, PT_{medium}, PT_{low}, PT_{normal}$

Step 1: read the input V_{P_f} from the vehicle node with
header information.

Step 2: Check the header and separate data packet
based on weight value from the vehicle.

Step 3: Construct the priority table in tree formation,

if DP need

if $V_{P_f} == PT_{high}$ then

Add the packet to the root node of the tree

Send the packet to the scheduler

elseif $V_{P_f} == PT_{medium}$

Add the packet to the parent node of the tree

Send the packet to the scheduler

elseif $V_{P_f} == PT_{low}$

Add the packet to the leaf node of the tree

Send the packet to the scheduler

else

Add the packet to either parent or leaf node
of the tree

Send the packet to the scheduler

end

else

if $pckt_{deadline} < Tr_{time}$

Add the packet to the root node of the tree

else

Add the packet to the normal node list and
append it with the parent leaf node.

end

end

In the tree construction-based data strength priority, the input is the frame packet from each vehicle. Initially, the information from the vehicle is read from the header information. By checking the header, the data packet is separated based on the vehicle's weight value. In the form of a tree, the priority tree is constructed. The packet with high priority is added to the root node of the tree by sending a packet to the scheduler. Similarly, the packet of medium priority is added to the leaf node of the tree by sending a packet to the scheduler. Likewise, those packets with low priority are added to either parent or leaf node of the tree by sending the packet to the scheduler. If the deadline of the packet is less than transmission time, the packet is added to the root node of the tree, or else the packet is added to the normal node list and is appended with the parent leaf node.

3.4 Prevention of Intersection Routes

During this data transmission process, there will be some occurrence of intersection. To evade this type of intersection between the channel and data transmission, the concept of intersection routes prevention by monitoring neighbor nodes was introduced. In this, the initialization of vehicle correlated matrix and vehicle user gain is made. Then for each correlated matrix of the vehicle, their minimum Eigenvector of data strength is estimated. To achieve SINR threshold, vehicle 1 with the N1 channel must satisfy the probability condition. The noise power spectral density is computed which in turn describes the intersection that occurred among the vehicles. The Eigenvector estimation step is carried till the fixed base station is attained for the transmission of data. These steps were carried similarly for vehicle 2.

In the prevention of intersection routes, correlation matrix formation is introduced in which the probability, data strength, available gain of the path, availability of base station is considered. The request from the neighbor or another frame causes intersection which leads to the formation of another route. To prevent this, the intersection prevention approach is employed. The power spectral probability is estimated AND by increasing the number of nodes, the collision that occurred is checked and prevented.

Algorithm 2: Prevention of the intersection of Nodes:

1. Initialize vehicle correlated matrix $C_1 C_2$ and vehicle user gains, h_1 and h_2 .
2. For each correlated matrix of vehicle 1 C_n^1 , where $n=1,2,...,N_1$, it's a minimum eigenvector of data strength.
3. For vehicle 1 uses a channel N_1 , to achieve its SINR threshold, the following probability it should be satisfied,

$$\frac{P_{V_1}^n}{N_0 + \sum_{i=1}^K P_{V_i}^n G_{V_i}^n} \geq \gamma$$

Here, N_0 is the noise power spectral density, $\sum_{i=1}^K P_{V_i}^n G_{V_i}^n$ describes the total interference of the vehicles that utilize the channel N_1 . γ is the SINR threshold. K indicates all vehicles which are available in the network.

4. Repeat step 2 until a fixed base station is obtained for data transmission.
5. For each correlated matrix of vehicle 2 C_n^2 , where $n=1,2,...,N_2$, it's a minimum Eigenvector of data strength.

6. For vehicle 2 who uses a channel N_2 , to achieve its SINR threshold, the following probability should be satisfied,

$$\frac{P_{V_2}^n}{N_0 + \sum_{i=1}^K P_{V_i}^n G_{V_i}^n} \geq \gamma$$

Here, N_0 is the noise power spectral density, $\sum_{i=1}^K P_{V_i}^n G_{V_i}^n$ describes the total interference of the vehicles that utilize the channel N_2 . γ is the SINR threshold. K indicates all vehicles which are available in the network.

7. Repeat step 4 until a fixed base station is obtained for data transmission.
-

Thus, the intersection of nodes will be prevented by monitoring the neighbor nodes. At last, the data packets were forwarded efficiently. At last, the performance analysis is estimated in terms of collision rate and end-to-end delay.

4 Performance Analysis

The performance analysis of the proposed system is estimated and the outcomes are provided in this section. The comparative analysis is made with existing techniques [28, 29]. The data rate is 6 Mbps. The computation of performance was made in terms of collision rate, PDR, and delay.

The performance analysis of the packet collision ratio is signified in Fig. 2. The packet collision ratio for vehicle density 100, 200, and 400 is estimated concerning location.

PDR is referred to as the amount of traffic amount that gets at the destination effectively similar to the fraction of generated traffic by the source node. Figure 3 depicts that the packet delivery ratios of estimated V1, V2, V3, and V4 concerning the vehicle density.

Average E2E delay signifies the time difference between the packet reception through the target and the instant the source created it; this covers all delays possible

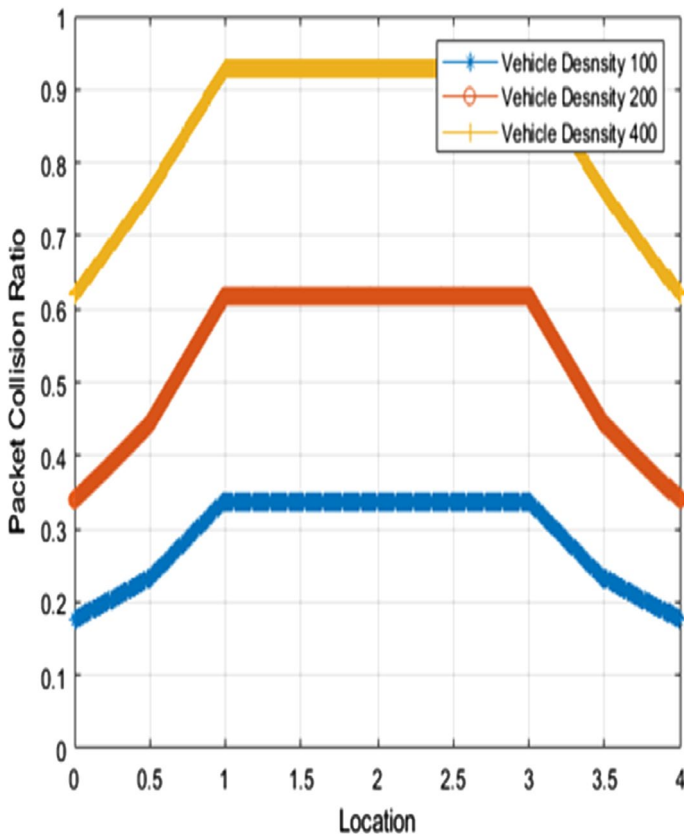


Fig. 2 Performance analysis of packet collision ratio

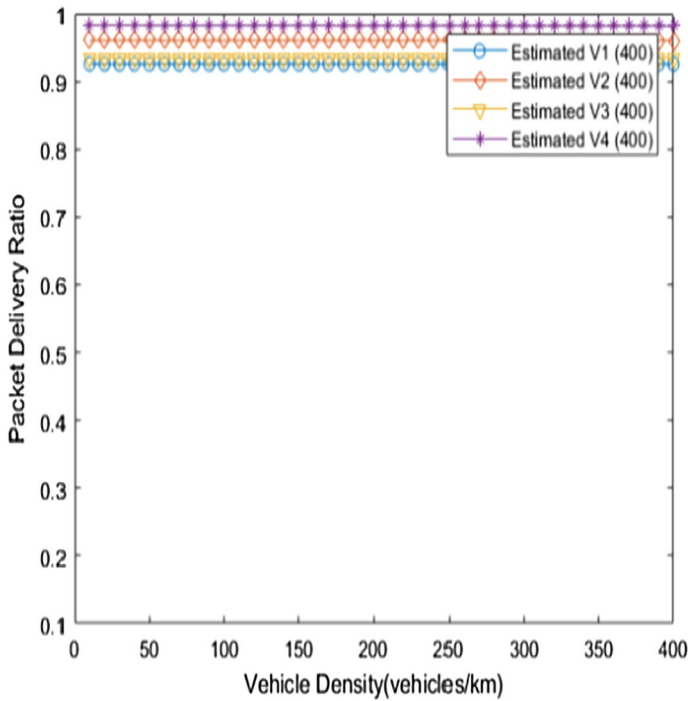


Fig. 3 Performance analysis of packet delivery ratio

encountered through a packet. Figure 4 depicts that the Average E2E delay of estimated V1, V2, V3, and V4 concerning the vehicle density.

Figure 5 is the representation of performance analysis of standard deviation versus vehicle density. The performance analysis is carried out in terms of estimated vehicles V1, V2, V3, and V4. The standard deviation increases concerning estimated vehicles increment.

The outage probability in terms of vehicle density is depicted in Fig. 6. The comparative analysis is carried out between the proposed technique and NOMAD₃ which shows that the proposed mechanism is having a better outage probability which increases gradually.

The average achievable rate in terms of vehicle density is represented in Fig. 7. The comparative analysis is carried out between the proposed technique and NOMAD₃ which shows that the proposed mechanism is having a better achievable rate in an average and turn decreases slowly.

Figure 8 is the representations of comparative analysis of inter-node collision versus initial relative distance (m). The analysis is carried out between the existing techniques like NoCCA, C-RACCA, CCM, P-DACCA, and the proposed methodology. The inter-node collision is low for the proposed system on comparing other methodologies.

Figure 9 is the depictions of comparative analysis of inter-node collision versus node speed (m/s). The comparison was carried out between the existing techniques like NoCCA, C-RACCA, CCM, P-DACCA, and the proposed methodology. The internode collision is low for the proposed system on comparing other methodologies. As the speed of the node increases, the inter-node collision increases gradually.

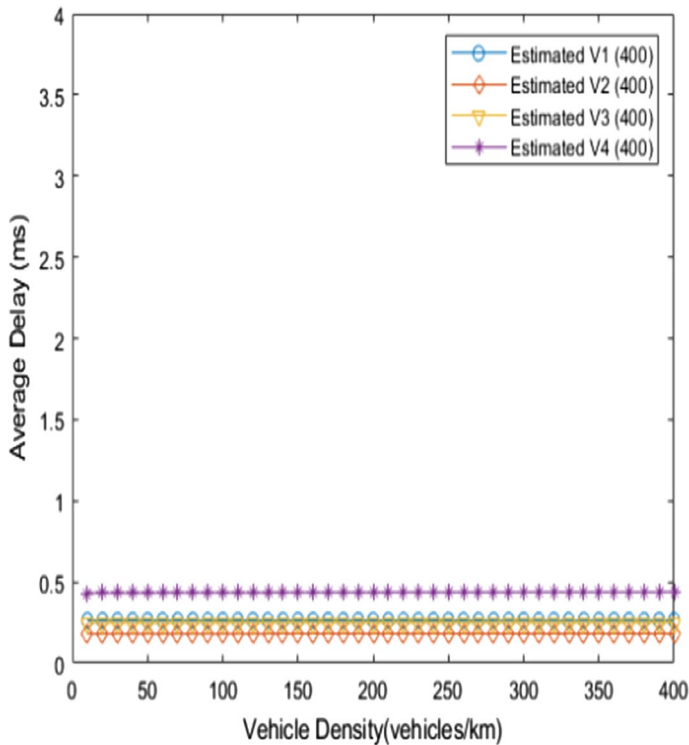


Fig. 4 Performance analysis of average delay (ms)

The average transmission delay in terms of data packet length is represented in Fig. 10. The comparative analysis is carried out between the proposed technique and existing techniques like VCI, CA MAC, APDM, and MP-MAC which shows that the proposed mechanism is having lower transmission delay in an average which increases with the length of the data packet.

The comparative analysis of throughput in terms of the number of vehicles is represented in Fig. 11. The comparative analysis is carried out between the proposed technique and existing techniques like VCI, CA MAC, APDM, and MP-MAC which shows that the proposed mechanism is having better throughput performance which decreases with an increase in the number of vehicles.

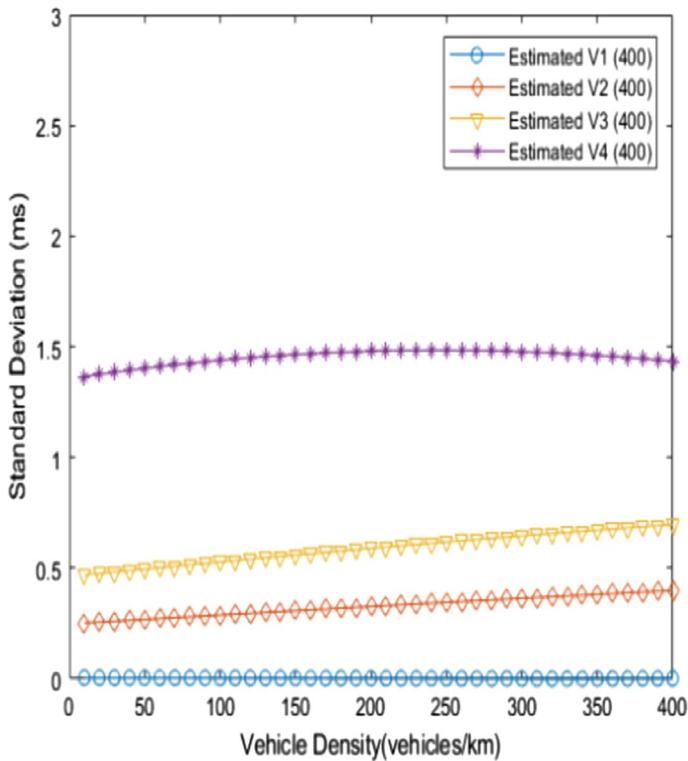


Fig. 5 Performance analysis of standard deviation versus vehicle density

5 Conclusion

An efficient technique was introduced for the mitigation of intersection occurrence in the channel availability, which is an attempt towards offering a safe transmission environment. This V2V approach addresses internodes collision avoidance. The computation of the best forwarding zone was made for minimizing the redundant data packets flow. To check the packet priority and packet collision, tree construction-based data strength transmission was introduced. Then, the prevention of intersection or collision between the transmissions channels was checked by correlation matrix-based intersection prevention technique on monitoring the neighbor node. After that, the data packets were efficiently forwarded without any intersection

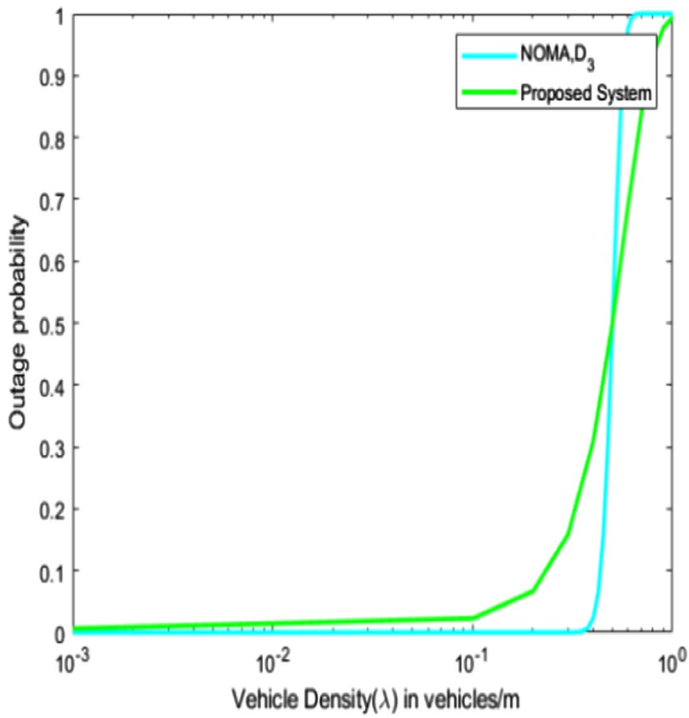


Fig. 6 Performance analysis of outage probability versus vehicle density

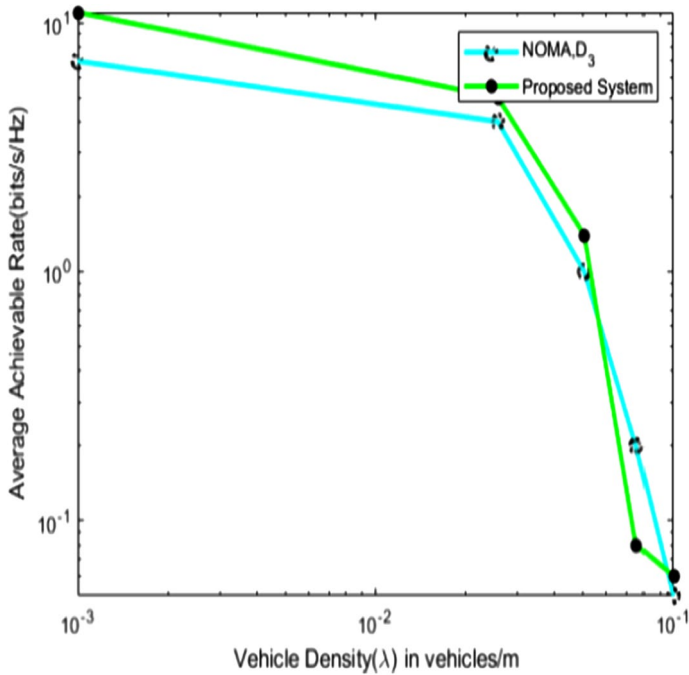


Fig. 7 Performance analysis of average achievable rate

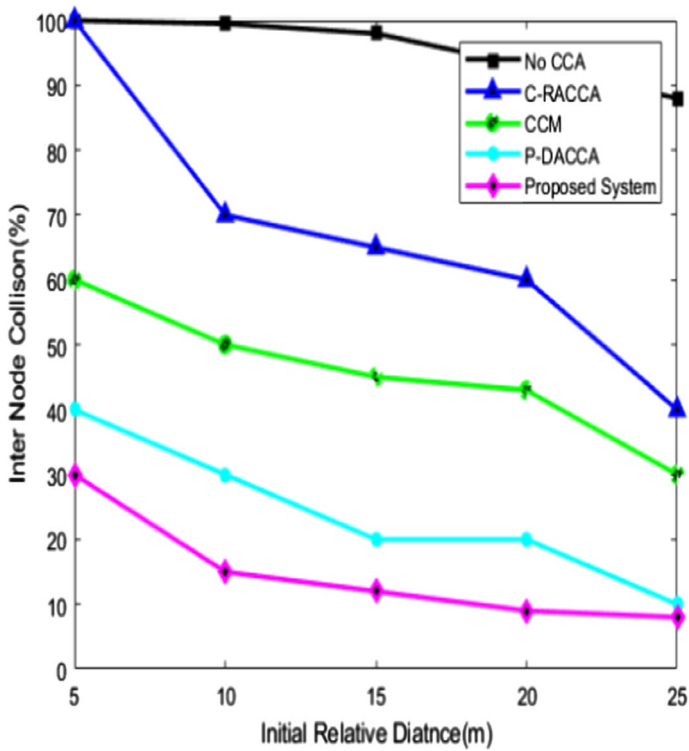


Fig. 8 Comparative analysis of internode collision versus initial relative distance

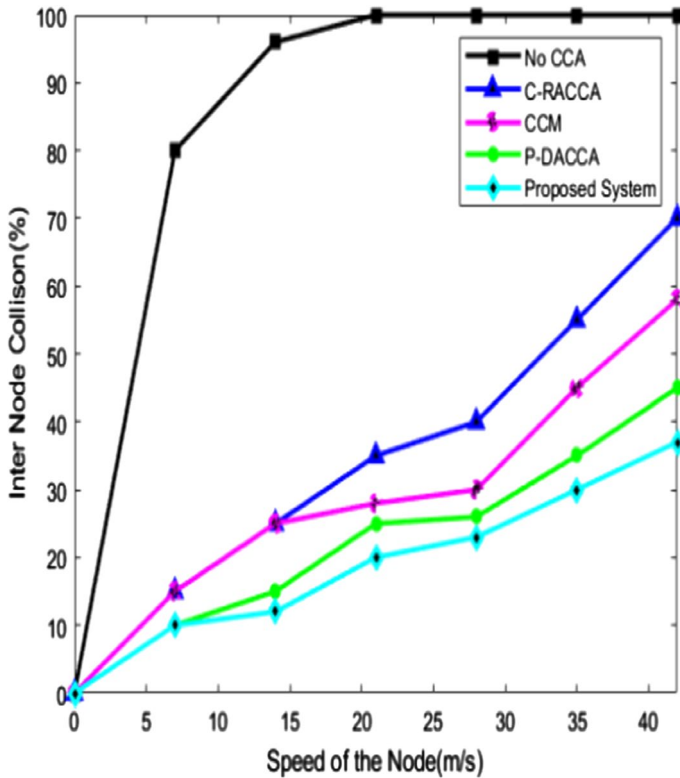


Fig. 9 Comparative analysis of Internode collision versus speed of the node

between the frames. The performance analysis was made and comparisons were carried with existing techniques in terms of packet delivery ratio, packet collision, internode collision, end-to-end delay, and throughput. Analysis shows that the presented technique offers reduced

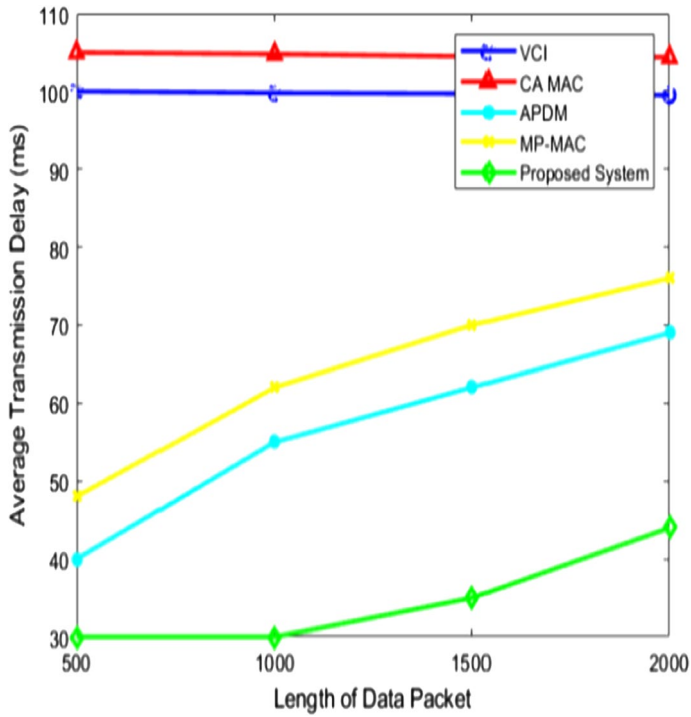


Fig. 10 Comparative analysis of average transmission delay (ms)

delay, minimized collision rate, increased throughput, increased outage probability. Thus, the proposed system was better than the existing techniques.

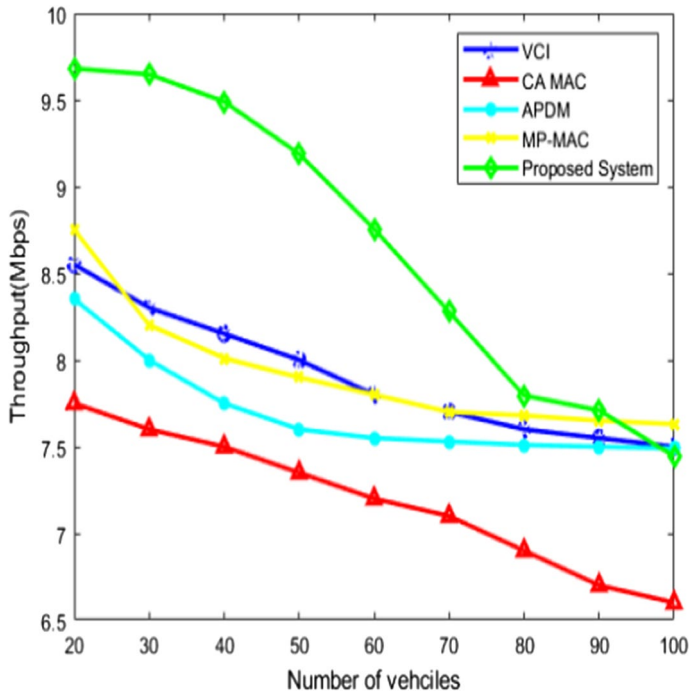


Fig. 11 Throughput analysis

Funding The authors did not receive support from any organization for the submitted work.

Declarations

Conflict of interest The authors have no conflicts of interest to declare that are relevant to the content of this article.

References

- Chandren Muniyandi, R., Hasan, M. K., Hammoodi, M. R., & Maroosi, A. J. (2021). An improved harmony search algorithm for proactive routing protocol in VANET. *Journal of Advanced Transportation*, 2021, 1.
- Kazi, A. K., & Khan, S. M. (2021). DyTE: An effective routing protocol for VANET in Urban scenarios. *Engineering, Technology & Applied Science Research*, 11(2), 6979–6985.
- Dutta, R., & Thalare, R. (2017). A review of various routing protocols in VANET. *International Journal of Advanced Engineering Research and Science*, 4(4), 221.
- Smiri, S., Abbou, A. B., Boushaba, A., Zahi, A., & Abbou, R. B. (2021). WA-GPSR: Weight-Aware GPSR-Based Routing Protocol for VANET. *International Journal of Interactive Mobile Technologies*, 15(17), 69.
- Baker, T., García-Campos, J.M., Reina, D.G., Toral, S., Tawfik, H., Al-Jumeily, D., Hussain, A. (2018). Greeadv: an energy-efficient routing protocol for vehicular ad hoc networks. In *International conference on intelligent computing*, 2018, pp. 670–681: Springer.
- Ghorai, C., & Banerjee, I. (2018). A robust forwarding node selection mechanism for efficient communication in urban VANETs. *Vehicular Communications*, 14, 109–121.

7. Garnepudi, P., & Venkatesulu, D. (2021). Vehicle direction-based B-MFR routing protocol for VANET. *Evolution in computational intelligence* (pp. 659–668). Springer.
8. Srivastava, A., Prakash, A., & Tripathi, R. (2020). An adaptive intersection selection mechanism using ant Colony optimization for efficient data dissemination in urban VANET. *Peer-to-Peer Networking and Applications*, 13, 1375.
9. Taleb, A. A. (2018). VANET routing protocols and architectures: An overview. *JCS*, 14(3), 423–434.
10. More, S., & Naik, U. (2018). Novel technique in multihop environment for efficient emergency message dissemination and lossless video transmission in VANETS. *Journal of Communications and Information Networks*, 3(4), 101–111.
11. Purkait, R., & Tripathi, S. (2020). Fuzzy logic based multi-criteria intelligent forward routing in VANET. *Wireless Personal Communications*, 111, 1871.
12. Liu, L., Chen, C., Wang, B., Zhou, Y., & Pei, Q. (2019). An efficient and reliable QoF routing for urban VANETs with backbone nodes. *IEEE Access*, 7, 38273–38286.
13. Liu, W., He, X., Huang, Z., & Ji, Y. (2019). Transmission capacity characterization in VANETs with enhanced distributed channel access. *Electronics*, 8(3), 340.
14. Belmekki, B. E. Y., Hamza, A., & Escrig, B. (2020). Performance analysis of cooperative NOMA at intersections for vehicular communications in the presence of interference. *Ad Hoc Networks*, 98, 102036.
15. Cao, Y., Zhang, H., Fang, Y., & Yuan, D. (2020). An adaptive high-throughput multi-channel MAC protocol for VANETs. *IEEE Internet of Things Journal*. <https://doi.org/10.1109/JIOT.2020.2990568>
16. Zhang, X., Miao, Q., & Li, Y. (2018). An adaptive link quality-based safety message dissemination scheme for urban VANETs. *IEEE Communications Letters*, 22(10), 2104–2107.
17. Rayeni, M.S., & Hafid, A. (2018) Routing in heterogeneous vehicular networks using an adapted software-defined networking approach. In *2018 Fifth international conference on software defined systems (SDS)*, 2018, pp. 25–31: IEEE.
18. Huang, Q., & Liu, F. (2017). An efficient adaptive broadcast protocol for different scenarios in VANETs. *Recent Patents on Computer Science*, 10(2), 131–139.
19. Shah, S. A. A., Ahmed, E., Xia, F., Karim, A., Qureshi, M. A., Ali, I., & Noor, R. M. D. (2018). Coverage differentiation based adaptive tx-power for congestion and awareness control in Vanets. *Mobile Networks and Applications*, 23(5), 1194–1205.
20. Triwinarko, A., Dayoub, I., Zwingelstein-Colin, M., Gharbi, M., & Bouraoui, B. (2020). A PHY/MAC cross-layer design with transmit antenna selection and power adaptation for receiver blocking problem in dense VANETs. *Vehicular Communications*, 24, 100233.
21. Wu, D., Li, H., Li, X., & Zhang, J. (2019). A geographic routing protocol based on trunk line in VANETs. In *Cyberspace data and intelligence, and cyber-living, syndrome, and health*. Springer, pp. 21–37.
22. Gupta, N., Prakash, A., & Tripathi, R. (2017). Adaptive beaconing in mobility aware clustering-based MAC protocol for safety message dissemination in VANET. *Wireless Communications and Mobile Computing*, 2017, 1.
23. Li, G., Gong, C., Zhao, L., Wu, J., & Boukhatem, L. (2020). An efficient reinforcement learning based charging data delivery scheme in VANET-enhanced smart grid. In *2020 IEEE International conference on big data and smart computing (BigComp)*, pp. 263–270: IEEE.
24. Agballa, U., Obiniyi, A., & Ayeni, B. (2019). Design of an improved energy efficient routing protocol in VANET using a modified route-optimal path algorithm. *Reason*, 12(18).
25. Iza-Paredes, C., Mezher, A. M., Aguilar Igartua, M., & Forné, J. (2018). Game-theoretical design of an adaptive distributed dissemination protocol for VANETs. *Sensors*, 18(1), 294.
26. Haider, S., Abbas, G., Abbas, Z. H., Boudjit, S., & Halim, Z. (2020). P-DACCA: A probabilistic direction-aware cooperative collision avoidance scheme for VANETs. *Future Generation Computer Systems*, 103, 1–17.
27. Nguyen, V., Khanh, T. T., Pham, X. Q., Lee, G. W., & Huh, E. N. (2020). Performance analysis of adaptive MAC protocol in VANETs considering the potential impact on throughput and transmission delays. *International Journal of Communication Systems*, 33(1), e4172.
28. Haider, S., Abbas, G., Abbas, Z. H., Boudjit, S., & Halim, Z. (2020). P-DACCA: A probabilistic direction-aware cooperative collision avoidance scheme for VANETs. *Future Generation Computer Systems*, 103, 1–17.
29. Nguyen, V., Khanh, T. T., Pham, X. Q., Lee, G. W., & Huh, E. N. (2020). Performance analysis of adaptive MAC protocol in VANETs considering the potential impact on throughput and transmission delays. *International Journal of Communication Systems*, 33(1), e4172.

Publisher's Note Springer Nature remains neutral with regard to jurisdictional claims in published maps and institutional affiliations.



Dr. T. Graceshalini completed her under graduation in Computer Science and Engineering at Magna College of Engineering, Tiruvallur, Tamil Nadu. Later she finished her post-graduation in the same discipline from Velammal College of Engineering and Technology, Madurai. Also she completed M.B.A (System Software) from Madurai Kamaraj University, Madurai. She was awarded Ph.D. in the same discipline in 2022. Her primary research interest in Vanets and Wireless Sensor Networks.



Dr. S. Jenicka completed her under graduation in Computer Science and Engineering at Thyagarajar College of Engineering, Madurai, Tamil Nadu in 1994. Later she finished her post-graduation in the same discipline in 2009 from Manonmaniam Sundaranar University, Tirunelveli. She was awarded Ph.D. in the same discipline in 2014. Her interests include Satellite image processing and texture segmentation. She has several notable online publications with citation indices.

A RYU-SDN Controller-Based VM Migration Scheme Using SD-EAW Ranking Methods for Identifying Active Jobs in the 5G Cloud Framework

Grace Shalini T., Velammal College of Engineering and Technology, India
Rathnamala S., Sethu Institute of Technology, India

ABSTRACT

The presented scheme focuses on active jobs live migration among VMs in 5G cloud framework depending on the software defined networks (SDN) to improve QoS in cloud framework. In this approach, RYU SDN controller is employed, which provides software components that allows software developers to extend network management and control applications for utilizing the features of SDN controller. It currently supports variety of southbound protocols such as OpenFlow, OF-Config, NETCONF, etc., whereas the proposed system uses Mininet prototype network. The destination server selection in the data centre is based on the server distinction based equivalent active weights (SD-EAW) ranking methods. The weight computation necessitate was to recognize non-active and active jobs. A presented SD-EAW scheme utilizes Pareto distribution for the recognition of active and inactive jobs in both continuous and discrete intervals of time. The presented SD-EAW algorithm functions well over all traditional approaches and in turn offers an optimum solution through minimizing the cloud environment's make span.

KEYWORDS

5G Cloud Environment, Mininet Prototype Network, SDN-Enabled Cloud Data Centres, Server Distinction Based on the Equivalent Active Weights (SD-EAW) Ranking, Virtual Machine (VM) Migration

1. INTRODUCTION

In today's world, the network solution is being developed for advanced networks at the steady pace. The mobile device proliferation, strategies of server virtualization, and the cloud framework were the finest opinions in a conventional network structure (Varghese, 2018), because of the advanced technologies advancement (Stergiou, 2018). Nowadays, the system links a databases variety of servers over several domains of network. Consequently, multiple server and client scenarios are needed. Accordingly, the traffic in the trends could vary. The enterprise company supplies private and public providers of cloud which should be supple in retrieving storage, software, and further IT

DOI: 10.4018/IJCAC.319031

This article published as an Open Access article distributed under the terms of the Creative Commons Attribution License (<http://creativecommons.org/licenses/by/4.0/>) which permits unrestricted use, distribution, and production in any medium, provided the author of the original work and original publication source are properly credited.

tools on-demand (Senyo, 2018). This in turn could be resolved by offering infrastructures of network over software defined networks (SDN). This could become prevalent nowadays for the reason of SDN benefits, like reliability, innovation, scalability, and testing (Amoore, 2018). The information plane comprises the network components managed like OpenFlow or Off-switches of a control plane. This in turn permits the shared knowledge in the networks application layer which offers features of network like load balancing, routing, and detection of intrusion (Langmead, 2018).

Presently, cloud computing is developing over several benefactors and the outdated set-ups of cloud that are being replaced through the technology revolution. By the way, this approach focusses on issues of load balancing, one of the major issues in cloud computing. A deprived algorithm of load balancing might outcome in utmost make span. The make span time was distinct as general time of the cloud environment completion. The solutions with respect to the issues of load balancing were given by means of traditional systems. However, only a fewer traditional system. The network objective of 5G cloud was capable of attaining optimal cellular networks performance (Ge, 2014). Several prevailing approaches focused on the virtual machines migration that comes at load balancing problems of the cloud environment. However, it was too essential for considering the migration of jobs over virtual machines in cloud environment.

There were two kinds of jobs in the environment of cloud. One is the active one and the other is the inactive one. The job was supposed to be an active one once their lifetime could not be projected at the environment. The time of those active jobs' completion might fall at some exponential time and thus this becomes a NP-hard issue. The presented research work offers an optimal active jobs migration over the VM in cloud for solving load balancing problems. For performing these active jobs live migration over virtual machines, SD-EAW ranking algorithm was presented. The algorithm in turn hypothesizes an instruction queue for storing environment's active jobs and employs Pareto distribution for the intention of jobs lifetime on behalf of recognizing the dynamic jobs weight. The algorithm process and job weights calculation are offered by the proposed scheme. The presented SD-EAW process was compared with traditional outcomes in the optimum outcome on minimizing make span of cloud framework.

The remaining portion of the proposed system is structured as shown: section 2 is the detailed description of related works employed so far. Section 3 is the detailed explanation of the proposed mechanism. The performance analysis of the proposed system is depicted in section 4. Finally, the conclusion part is deliberated in section 5.

2. RELATED WORKS

(Abdelmoniem, 2016) presented the VM and SDN-capable switches along with SDN-driven in cast frame depending on SDN controller and hyper speed/switch package. This in turn estimates the smaller testbed performance, larger and NS2 environment over the usual implementation of presented approach. The Load balancing was regarded as the crucial portion of cloud framework all through the period. There were 'n' literatures number that were available for the issues related to load balancing. The cloud environment concentrates on some more main intentions like the utilization of proper resource, algorithm of optimal scheduling for minimizing the environments make span, efficient utilization of resource clustering policy and the optimum policy of job migration so as to ensure the effective load balancing framework. In one such traditional system, it was said that job migration policy was concentrated on producing the effective cloud environment. From this regard, several literatures were analyzed for the better knowledge of job migration policies and their parameters. Various migration categories include virtual machine migration, resource migration and several other kinds of migrations that were occurred by several other domains.

The issues employed over overloaded and underloaded situation were addressed (Mishra, 2020) over the load balancing algorithms classification. The algorithm of load balancing was categorized as dynamic and static strategy. The dynamic approach was classified further as online mode and

offline mode. This review classifies the replication outcomes of several algorithms of load balancing depending on parameters like energy consumption, resource utilization and make span. In (Tchernykh, 2015), the issues were discussed in job migration time of completion whereas provisioning the cloud environment resources. A review was carried out on the vital uncertainty causes that lies in the provisioning of resources in the environment of cloud. The algorithm of weighted round robin process (Devi, 2016) was presented for mitigating the un-active tasks for sharing the cloud resource on cloud framework in an effective manner. For doing so, the capabilities like task length depending on the concentrated and categorized the factors of load balancing issues like overloaded, underloaded, and the balanced one. In this approach a new scheme (Deshpande, 2017) was analyzed over a designed prototype for handling traffic. A prototype of this kind was employed intended for VMs only with the virtual machines that have source machines pre-copy and the post-copy at the destination machine. The system's load balancing was carried out by two methodologies (Forsman, 2015) termed pull and push method. Those two methods in turn offer live migration over the systems.

The explicit study on virtual machine migration and the dynamic voltage frequency scaling datacenters of cloud were presented (Shirvani, 2020) so as to enhance the cloud environment performance. The minimized range of power consumption was being utilized for differing virtual machines depending on the incoming jobs. Several issues, challenges, moderations of performance, parameter intended for VM migration were being mentioned. The active live migration depending on the migration of memory was employed for offering the optimal time of migration (Noshay, 2018), transmission of data time and the virtualized cloud environment downtime. A policy of novel resource clustering (Mohan, 2019) termed differentiation of resource depending on the potential of node equivalence algorithm (RDENP) for solving the issues of load balancing in the simulated environment of wireless personal cloud.

An Effectual evaluation model of performance depending on the Poisson process and continuous Markov chain was offered for offering optimal solutions intended for the clusters of resource at the environment of cloud (Kowsigan, 2019). So as to offer enhanced cloud environment reliability the hierarchy-based resource clustering process was employed for minimizing the complexity of time in the selection of resource (Zhao, 2018). So as to enhance the cloud environment scheduling, the issues of resource provisioning were addressed by means of graph model (Kliazovich, 2016). QoS based scheduling and cost algorithm (Wang, 2017) was presented for handling the disputes in the environment of wireless cloud (Madni, 2016). So as to process the data streaming in cloud effectively, Markov chain prediction method was suggested (Zhang, 2015). Markov chain's Hurst exponent was projected for attaining the effective utilization of resource in cloud framework on considering the virtual machines behavior (Lu, 2015).

3. PROPOSED WORK

This section offers the detailed explanation of proposed system. RYU SDN controller is employed in this work that offers software components and allows the software developers for extending the control applications and network management for the utilization of SDN controller features. This in turn supports the diverse range of south band protocols currently like OpenFlow, OF-Config, NETCONF and so on, whereas the presented system employs Mininet network prototype. The selection of destination server in the data center depends on server distinction based Equivalent active weights (SD-EQA) ranking algorithm. The presented SD-EAW algorithm in turn focusses on the weight calculation for each and every job in the cloud framework. A weight calculation necessity was to recognize active and non-active jobs. The proposed SD-EAW scheme employs Pareto distribution for the recognition of continuous and discrete time intervals. The presented algorithm of migration functions well than other traditional techniques and in turn offers the optimal solution on diminishing the make span of the cloud framework.

2.1 Formulation of Parameter

By means of job's speaking lifetime, mentions to the job extent generally. The job's lifetime is intended as overall job utilization presently in addition to in imminent iterations. The future lifetime calculation of job is a challenging procedure, as a lifetime falls under the exponential distribution. At those situations, the active jobs movement turns out to be a non-deterministic polynomial concern. The SDN dependent method for cloud is effectual on keeping QoS. The jobs lifetime calculation outcomes in an increasing order for example, in the future jobs of the environment having the similar lifetime entirely. This might limit jobs to migrate or wander from one processor to the other one in the server. Thus, the agent migrating in turn comes under the impasse condition for selection of job that were to be migrated. Because of this, the entire traditional techniques concentrated only on the non-active job migration. For the reason of exponential distribution, lifetime might gradually enhance for the part of active job that are unexecuted. By the way, the exponential distribution turns out to be a pareto distribution in the presented approach. The pareto distribution in turn creates an exponential distribution as restrained distribution, because of this active job's lifetime are calculated easily. The job's lifetime comes in two types; one is job lifetime which in turn surpasses the limit and the job's lifetime is another one that comes under the limit. In this mentioned limit, roughly for instance 'Y'. at this time, exponential distribution initially is then expressed as shown below:

$$\bar{G}(Y) = e^{-\lambda Y} \quad (1)$$

$$\bar{G}(Y) = P\{\text{Lifetime of the job} > Y\} \quad (2)$$

This term is specified in the measured distribution as shown above. From the above-mentioned equation, it is mentioned obviously that the lifetime of job was more than limit. From this, it is summarized that there was a solution intended for computation of active job's lifetime, lifetime of job should be either above/below the limit as in the equation (1) exponential distribution it was not so easy to compute the lifetime of job. \bar{G} signifies the function distribution, P signifies the function of probability, λ signifies to rate of the jobs arrival and e denotes to exponential value. The equation above might be revised consistent with both cases: below and greater than limit as:

$$P\{\text{Lifetime of the job} > Y \mid \text{Lifetime of the job} > ET\} = \frac{ET}{Y} \quad (3)$$

Here, ET signifies the time estimated. The expected time falls under job's lifetime state at some limit. Beyond the limit, the job's lifetime condition might be considered as the extension generally, however the solution will be recognized in the time of polynomial over the value of the measured Pareto distribution. This pareto distribution in turn offers the flexibility on attaining the solution that ranges from 0 to 2. From this approach, the flexibility varied from 0.7 to 1.1. in this, the lifetime of job might be broken to several portions for attaining the solution over pareto distribution flexibility. The distribution will be equated again consistent with a flexibility by way of specified equation as shown. In this, the flexibility is being revealed as β :

$$\bar{G}(Y) = \frac{ET}{Y\beta} \quad (4)$$

The Pareto distribution characteristics is essential highly and is employed through several business products for identifying the actual loss and profit in the entire turns of the specified artefact. The pareto distribution was employed once there is the exponential distribution rate chance in the real-world issues.

The pareto distribution is then associated by their flexibility as follows:

$$\bar{G}_y(y) = P\{Y > y\} = y^{-\beta}, \text{ for } y \geq ET \quad (5)$$

where:

$0 < \beta < 2$ is called Pareto(β) flexible distribution

The other significant entity intended for employing Pareto distribution was that their rate of failure was least and also the rate of failure is then reduced on behalf of the imminent iterations. It is revealed by the computation provided below as follows:

$$\bar{G}(y) = P\{Y > y\} = y^{-\beta}, y \geq ET \quad (6)$$

where:

$$G(y) = P\{Y < y\} = ET - x^{-\beta}, y \geq ET$$

$$g(y) = \frac{dG(y)}{dy} = \beta y^{-\beta-ET}, y \geq ET$$

$$r(y) = \frac{g(y)}{G(y)} = \frac{\beta y^{-\beta-ET}}{y^{-\beta}} = \frac{\beta}{y}, y \geq ET$$

As of the above calculations this has been noted clearly that:

$$\int_1^{\omega} g(y) dy = \int_1^{\omega} \beta y^{-\beta-ET} dy = ET \quad (7)$$

By the way, the claims of $g(y)$ Pareto distribution is an assessable PD (probability distribution) on relating exponential distribution. The failure rate of the pareto distribution in turn declines gradually for example $r(y) = \frac{\beta}{y}$ declines with y. Even Pareto distribution's variance and mean can too be considered in cases similar to $\beta \leq ET$. At this time the function of density is united once $0 < \beta \leq ET$ and equated as shown:

$$Job[remaining Lifetime | size = \beta] ET = \infty \quad (8)$$

Over Pareto distribution, it is probable for computing the lifetime of several jobs in case of $\beta = ET$. For instance, this is probable to recognize the lifetime of Job1 probability to of lifetime of Job2 probability in case of $Job2 > Job1$, wherever $\beta = ET$. The result is an intellectual one, at which the job migration is shown in the server:

$$P\{Lifetime > Job2 | Life = Job1\} ET = \frac{ET / Job2}{ET / Job1} = \frac{Job1}{Job2} \quad (9)$$

By this expression, in case of distribution of Pareto ($\beta = ET$), distribution might be interpreted as follows:

- A probability of particular job having ET lifetime and in turn exploits $\geq ET$ around T, the make span is $\frac{ET}{T}$.
- In 50% of the jobs, for Jobs that has ET lifetime, might have lifetime $\geq ET$.
- The particular job probability having T lifetime and in turn exploits $\geq T$ about Tn, lifetime is $\frac{ET}{Tn}$.

The Pareto distribution's measured distribution offers both lifetimes' data measured below the limit and over limit. Through this, the Pareto distribution property, values will be computed altogether and the results were achieved. For formulating jobs lifetime in a structure, Bounded Pareto distribution might be employed. The Bounded pareto distribution (f, q, β) is specified as:

$$g(y) = \beta y^{-\beta-ET} \cdot \frac{f^\beta}{1 - \left(\frac{f}{q}\right)^\beta} \quad (10)$$

Here, $f \leq y \leq q$ and $0 < \beta < 2$.

The expression:

$$\frac{f^\beta}{1 - \left(\frac{f}{q}\right)^\beta}$$

that integrates the function of density among f and q might move in ET range since this has been normalized already.

For handling the jobs that exceeds the lifetime limit, weighted End property might be employed. As per the job's assets, jobs having lifetime under limit might be united over the jobs combinations that has lifetime limit higher. On doing this, the jobs serving has the demand that has lifetime beyond the limit that might come down. The weighted end property is being employed through the Bounded and the Normal Pareto distributions. Because of their asset, the presented approach employs the Pareto distribution intended for the entire kinds of lifetime computation of the job. The job's lifetime calculation shows a dynamic part in recognizing the rate of arrival, waiting time, time of response and the time of job service at the stated framework. A novel attempt was carried out for migrating

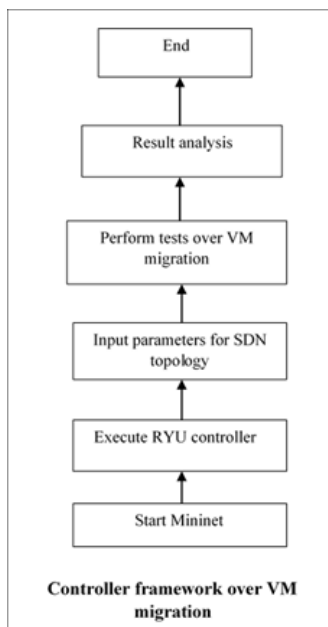
the active jobs in spite of older job in the environment. In the point of economic view, the Pareto distribution is being employed in several circumstances for identifying particular solutions to specific issue in an entire dimension like specified through problem parameters. This is one such purpose for selecting Pareto distribution in present approach for identifying thorough lifetime of job since this is mentioned as an exponential distribution factor previously.

2.2 RYU-SDN Controller Using Mininet Prototype Network

Ryu is one such popular controllers among industry having NTT lab support having an active community documentation in depth. Ryu is written entirely in Python and it employs green threads for implementing the multithreading. This in turn offers provides software components that allows software developers to extend network management and control applications for utilizing the features of SDN controller. It currently supports variety of southbound protocols such as OpenFlow, OF-Config, NETCONF, etc, whereas the proposed system uses Mininet prototype network. This supports a huge range of third party libraries which includes Open vSwitch Python buildings and aids in parse VLAN, MPLS, and so on of various protocol packets. Also, it supports sFlow and Netflow protocols that were specific to the management of network traffic. Ryu in turn supports till the version of OpenFlow 1.4. this employs encoder and decoder library for the OpenFlow packets and in turn comprises OpenFlow controller in its heart. This comprises of major executables termed Ryu manager where they listen to the specified IP address and on the 6633 ports, a typical OpenFlow port. In the Ryu structure, the major components include event management, messaging service and so on.

Mininet employs process-based virtualization for running the switches and the hosts in the operating system. This in turn requires each process having their individual routing and the ARP table, and the network interfaces. The Hosts are emulated as the bash process at which each code runs like a normal Linux shell. The virtual Ethernet (Veth) is employed for connecting all network devices. The application of Mininet can be installed either on the traditional Linux system or this could be downloaded in the prepackaged VM that runs on VirtualBox.

Figure 1. Controller framework over VM migration



The Open Flow Protocol Specification of the SDN controllers allows the controllers for informing switches at which place the data packets are to be delivered. Open Flow is regarded as the one which permits the researchers for performing the protocols that are experimental on the networks that was used daily in addition it specifies the messages formats that migrate from one controller to the others. Open Flow is applied to the commercial device network like routers, switches, and wireless access points as a capability that offers structured connection for allowing researchers to conduct tests deprived of manufacturers that discloses its devices' network internal operations. OpenFlow is regarded as the one that is now adopted by major suppliers, besides the switches underlying were available in the marketplace nowadays.

Open Flow Controller is an object contact system utilizing the Open Flow Protocol requirements with the underlying switches. The controller OpenFlow in most instances is a software that are high-level and manages several switches in OpenFlow logically. An OpenFlow is an internet connection among the Open Flow button in addition to Open Flow controller that is used to handle the switch by the controller.

In this approach, Mininet is used to build the RYU controller SDN network. Mininet network emulator is employed which is employed for running the experiment. This Mininet in turn creates the

Figure 2. Event handling representation of RYU controller

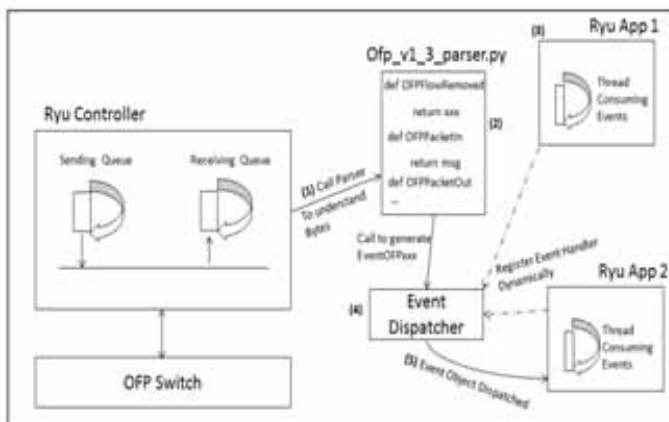
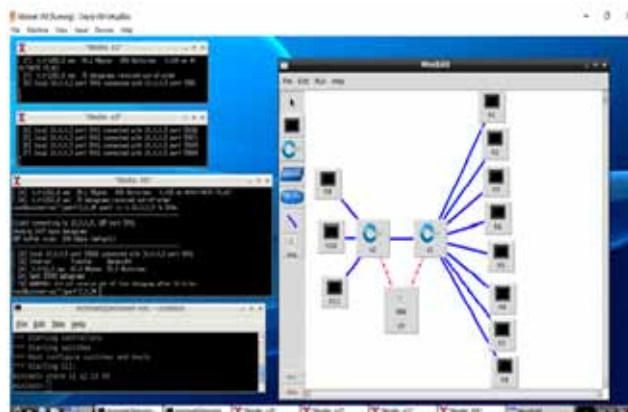


Figure 3. Representation of Mininet VM



virtual realistic network that runs in real kernel, application and switch code on the single machine at minimum time period with an interface of command line.

2.3 Ranking Methods Using Server Distinction Based Equivalent Active Weight (SD-EAW)

The presented SD-EAW algorithm in turn concentrates on the calculation of weight for each and every job of the cloud framework. The weight computation need is to recognize the non-active and active jobs in both continuous and discrete intervals of time. The approach of SDN for the cloud framework is an efficient one on offering higher range of QoS. Once after the active job's identification, these jobs were migrated depending on the algorithms procedure for offering efficient load balancing cloud framework. At first, the jobs weight is checked for identifying if the weight of job is equal. This is carried out for performing the job scheduling among VMs. The VMs might process varied weights of the job.

Once after this computation, the jobs that were higher than the time estimated were forwarded in the instruction Queue, the Queue that is presented for SD-EAW process. The jobs that are having higher time of estimation are regarded as the active jobs by means of Pareto distribution computation. On following this, the cloud framework make span was reduced and the efficient cloud environment is then developed. The minimum VM in the sense loaded, this means not only the VM consist of lesser jobs number, the VMs having minimum time for completion of assigned tasks were supposed to be the virtual machines that are loaded least.

Algorithm 1: Proposed Sd-Eaw Scheme

Input: Active Jobs (J_1 to J_n), Weights (Wg) of active jobs
Components used: Cloud's Virtual Machine (VM)

Output: Migration Performed $\left(\sum_{n=1}^8 J_n * VM_n \right)$

Begin Migration

Compute $n * n$ ($VM_{n1}, n2$); Estimating $VM_{n1} \neq VM_{n2}$

i.e VM_{n1} is distinct with VM_{n2}

/* VM_{n1} is distinct with VM_{n2} indicates that both the VMs have different workload. Here

for easy evaluation we took only two VMs for this algorithm structure. This algorithm

will work for 'n' number of VMs*/

Declare (($VM_{n1}, n2$), Wgs) = (J_1 to J_n)

/*indicates the weights of the active jobs are given to the VMs in the cloud environment*/

if (J_1 to J_n) = =Y

/*Y indicates the distinct property of the job weights. This property achieved by the weight calculation of jobs through Pareto distribution*/

Then

Differentiate (J_1 to J_n)

/*Jobs are differentiated. Each job has different weight Checked among the 'n' jobs*/

else (J_1 to J_n) = =Z

/*Z indicates equivalent property of the job weights*/

End if

While (J_1 to J_n) = = Y

$$\{ \text{Schedule} = (J_1, \dots, J_n) * \sum_{n=1}^{\infty} VM_n \}$$

Check $(J_1 \text{ to } J_n) = \sum_{n=1}^{\infty} VM_n \notin ET$

the algorithm checks whether the jobs scheduled to the VMs are below the estimated time (ET)/

if $(\sum_{n=1}^{\infty} VM_n \geq ET)$

Then

Migrate the jobs to some other VMs

if a job processing in a VM is superior to the time estimated at which stall the specific VM, for avoiding this job migration to another least loaded VM/

End if

Migration Process

$$\frac{J_1}{J_1 \text{ to } J_n} > ET \rightarrow I_q$$

/*The job which is higher on comparing time estimated (ET) to forward Instruction Queue*/ From this line the job will be served to the least loaded VM*/

Migrate

$$\frac{I_q(J_1)}{J_1 \text{ to } J_n} \rightarrow \sum_{n=1}^{\infty} J_n * VM_n$$

/*From this queue the job will be served to the least loaded VM*/

On promoting the active jobs to the queue instruction, this is done on the initial stage by themselves because of their environment's service time that has been reduced. As the active jobs might take excess time for processing, the residual jobs should have to wait in the pool of scheduling for processing till the active jobs complete their execution process. The presented SD-EAW algorithm functions well over all traditional approaches and in turn offers an optimum solution through minimizing the cloud environment's make span.

4. PERFORMANCE ANALYSIS

The performance analysis of the proposed system is depicted in this section. The comparative analysis of the proposed and existing system (Mekala, 2019) in terms of VMM, SLA violation time, SLA violation of SLATAH (SLAV of each active host), energy consumption is estimated at the utilization rate of resource $\delta=0.31$ 0.25, for evaluating the impacts and the outcomes attained are shown in this section.

4.1 Performance Metrics

The performance metrics are described which is employed for estimating the response time and the accuracy of proposed algorithm:

Table 1. Comparative analysis of proposed and existing system

Algorithm	Energy (kWh)	VMM	SLAV (10 ⁻⁵)	SLATAH (%)
Initial	285.05	570	0.9210	0.03549
RFAware	260.34	515	0.8321	0.03975
Sercon	245.79	426	0.7456	0.03112
ERVS (δ=0.31)	210.14	369	0.4123	0.02559
ERVS (δ=0.25)	211.50	375	0.4910	0.02971
SD-EAW(δ=0.31) (proposed)	209.38	341	0.4011	0.02122
SD-EAW(δ=0.25) (proposed)	210.04	356	0.4872	0.02463

1. The energy consumption refers to the utilization of total amount of energy of the cloud data centers and is defined by the following equation:

$$EC = \sum_{m=1}^{b_m} \int_t^0 (\alpha_u \cdot Max(\alpha_i) + (1 - \alpha_u) \cdot Max(\alpha_i) \cdot d_i^{mips}(t)) dt \quad (11)$$

Here, m signifies the number of VM, $\alpha_u = 0.7$ and it refers to the energy consumption that are unused by the server, $Max(\alpha_i) = 250W$ and is defined as the utilization of energy by host at their running condition and $d_i^{mips}(t)$ represents the CPU utilization at time t.

2. SLAV (service level agreements violation) is referred to the combination of both PDF and SLATAH metrics.
3. SLATAH (SLA violation time of each active host) is defined as the time proportion at which the active hosts consist of 100% utilization of CPU and is represented by the following equation:

$$SLATAH = \frac{1}{M} \sum_{i=1}^M \frac{T_{SLA_i}}{T_{ACT_i}} \quad (12)$$

Here, M is represented as the number of PM (physical machine), and T_{SLA_i} signifies the time of SLA violation at ith PM and T_{ACT_i} is signifies as the ith PM active time.

4. The migration process's performance degradation (PDM) is represented by the following equation:

$$PDM = \frac{1}{p} \sum_{j=1}^p \frac{PD_j}{CD_j} \quad (13)$$

Here, p signifies the VMs total number, PD_j is a performance deprivation that is determined that could be restrained intended for further 10% CPU utilization of the j th VM that are instigated by migrations and CD_j refers to a total CPU capacity that is required by j th VM.

Hence:

$$SLAV = SLATAH \times PDM$$

4.2 Comparative Analysis of Proposed and Existing Technique

The energy consumption analysis is estimated for the proposed algorithm and is compared with existing techniques and is shown in Table 1.

Figure 4 is the representation of number of migrations for varied range of VMs. The analysis is estimated and is compared with existing techniques like Initial, RFAware, Sercon, ERVS, and proposed strategy. The analysis shows that the proposed system is better on comparing existing techniques.

Figure 5 is the illustration of energy consumption analysis for varied range of VMs. The analysis is estimated and is compared with existing techniques like Initial, RFAware, Sercon, ERVS, and proposed strategy. The analysis shows that the proposed system is better on comparing existing techniques.

Figure 6 shows the energy consumption before and after migration process of VMs. From the analysis it was evident that the energy consumption after migration is lower than before migration process.

Figure 7 shows the resource utilization before and after migration process of VMs. From the analysis it was evident that the resource utilization after migration is higher than before migration process.

The comparative analysis of proposed and existing techniques are carried out for the SLAV to prove the effectiveness of proposed system and is shown in figure 8.

The comparative analysis of proposed and existing techniques is carried out for the task completion time in terms of cloudlet ID to prove the effectiveness of proposed system and is shown in figure 9.

Figure 10 is the depiction of makespan representation of proposed SD-EAW approach illustration simulated for number of VMs.

Figure 4. Number of migration analysis

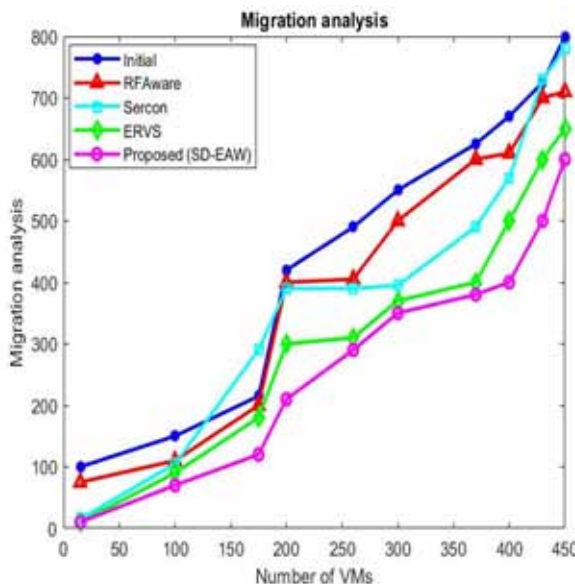


Figure 5. Energy consumption analysis

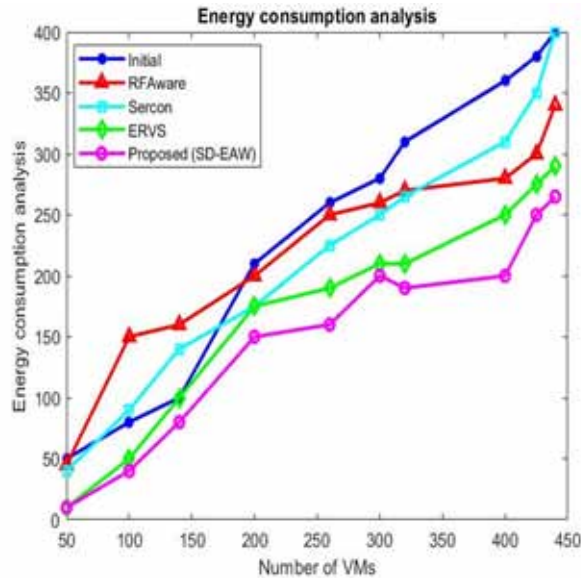


Figure 6. Analysis of energy consumption before and after migration

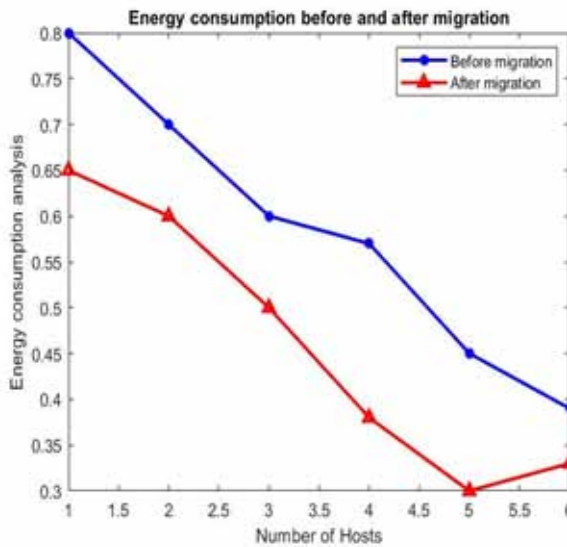


Figure 11 illustrates the resource utilization rate of the host of proposed system at which most of the node consist of good balance and resource utilization extremely. Thus, from the evaluation, it was evident that the migration count is reduced adequately and in turn preserves the consumption of energy. Thus, the proposed system is said to be effective than other traditional techniques.

Figure 7. Analysis of resource utilization before and after migration

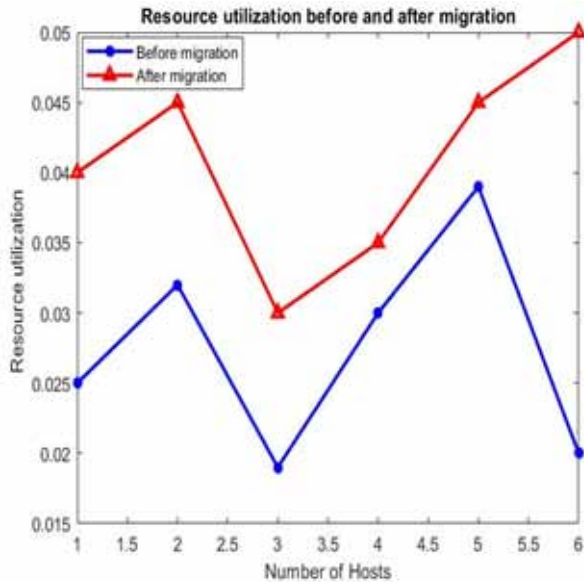
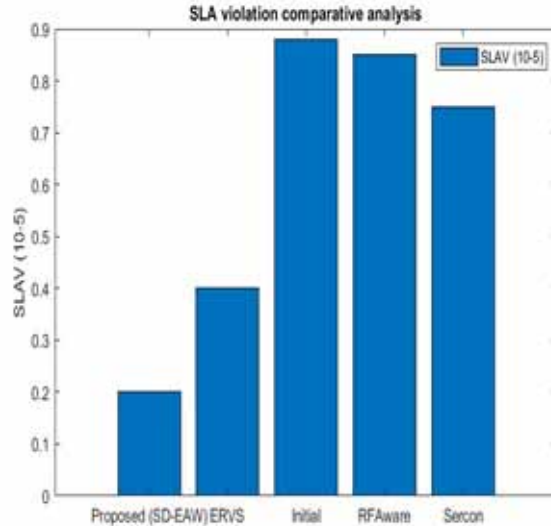


Figure 8. Comparative analysis of SLAV



5. CONCLUSION

In this approach, an efficient cloud environment is built based on SDN for producing the optimal solution and thus to maintain QoS for cloud framework. An efficient load balancing mechanism termed SD-EAW ranking algorithm was presented for the live migration of active jobs over several virtual machines was implemented in a real cloud testbed. In the proposed approach experiment, several heterogeneous resources were considered for processing the jobs. The presented technique employs

Figure 9. Comparative analysis of task completion time

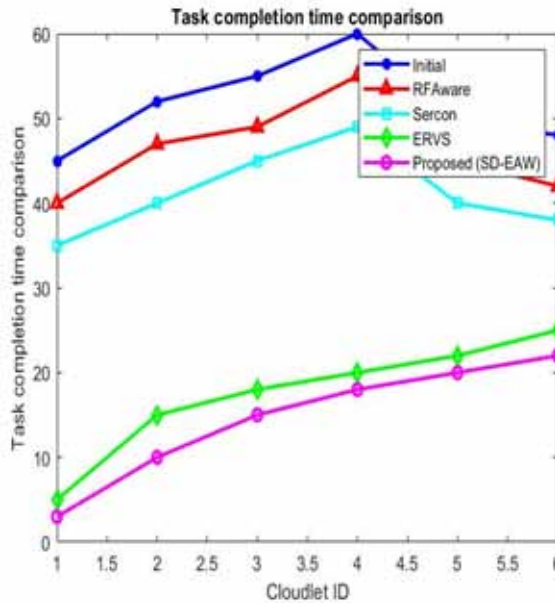


Figure 10. Make span representation of proposed SD-EAW approach

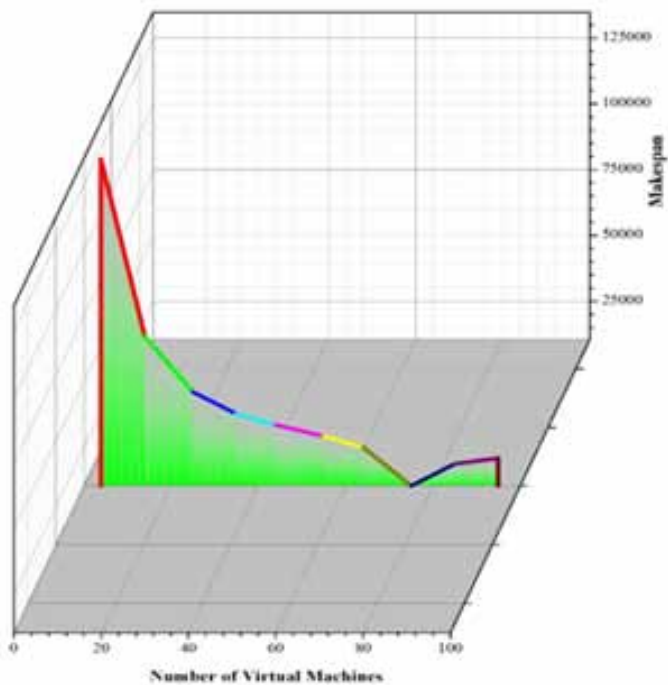
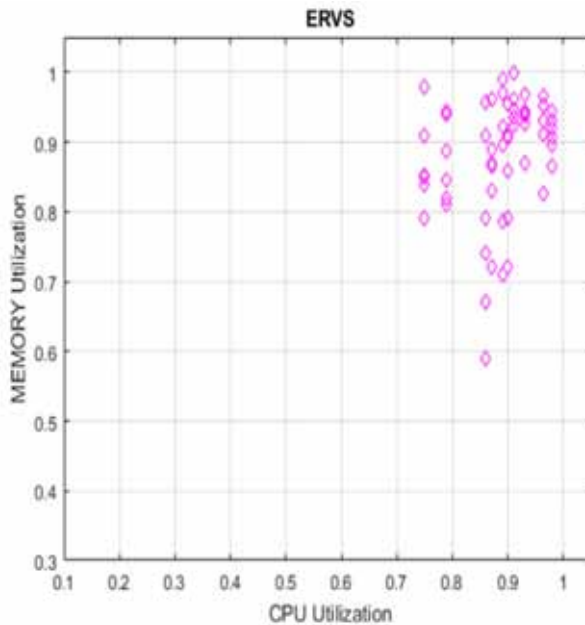


Figure 11. Resource utilization rate using proposed approach



Ryu-SDN controller with Mininet that provides software components that allows software developers to extend network management and control applications for utilizing the features of SDN controller. Also, the presented approach exploits Pareto distribution for computing the exact lifetime of active jobs. The presented technique performs well for producing optimal make span and migration time for 5G cloud framework. The performance is estimated in terms of consumption of energy, utilization of resource, migration analysis, and task completion time analysis. The rate of resource utilization of proposed system host at which most of the node consist of good balance and resource utilization extremely. Thus, from the evaluation, it was evident that the migration count is reduced adequately and in turn preserves the consumption of energy. Thus, the proposed system is said to be effective than other traditional techniques.

CONFLICT OF INTEREST

The authors of this publication declare there is no conflict of interest.

FUNDING INFORMATION

No Funding Information. This research received no specific grant from any funding agency in the public, commercial, or not-for-profit sectors.

REFERENCES

- Abdelmoniem, A. M., & Bensaou, B. J. C. D. (2016). *SDN-based incast congestion control framework for data centers: Implementation and evaluation*.
- Amoore, L. (2018). Cloud geographies: Computing, data, sovereignty. *Progress in Human Geography*, 42(1), 4–24. doi:10.1177/0309132516662147
- Deshpande, U., & Keahey, K. (2017). Traffic-sensitive live migration of virtual machines. *Future Generation Computer Systems*, 72, 118–128. doi:10.1016/j.future.2016.05.003
- Devi, D. C., & Uthariaraj, V. R. (2016). Load balancing in cloud computing environment using improved weighted round robin algorithm for nonpreemptive dependent tasks. *TheScientificWorldJournal*, 1–14. doi:10.1155/2016/3896065 PMID:26955656
- Forsman, M., Glad, A., Lundberg, L., & Ilie, D. (2015). Algorithms for automated live migration of virtual machines. *Journal of Systems and Software*, 101, 110–126. doi:10.1016/j.jss.2014.11.044
- Ge, X., Cheng, H., Guizani, M., & Han, T. (2014). 5G wireless backhaul networks: Challenges and research advances. *IEEE Network*, 28(6), 6–11. doi:10.1109/MNET.2014.6963798
- Kliazovich, D., Pecero, J. E., Tchernykh, A., Bouvry, P., Khan, S. U., & Zomaya, A. Y. (2016). CA-DAG: Modeling communication-aware applications for scheduling in cloud computing. *Journal of Grid Computing*, 14(1), 23–39. doi:10.1007/s10723-015-9337-8
- Kowsigan, M., & Balasubramanie, P. (2019). An efficient performance evaluation model for the resource clusters in cloud environment using continuous time Markov chain and Poisson process. *Cluster Computing*, 22(S5), 12411–12419. doi:10.1007/s10586-017-1640-7
- Langmead, B., & Nellore, A. (2018). Cloud computing for genomic data analysis and collaboration. *Nature Reviews. Genetics*, 19(4), 208–219. doi:10.1038/nrg.2017.113 PMID:29379135
- Lu, C.-T., Chang, C.-W., & Li, J.-S. (2015). Vm scaling based on hurst exponent and markov transition with empirical cloud data. *Journal of Systems and Software*, 99, 199–207. doi:10.1016/j.jss.2014.10.011
- Madni, S. H. H., Abd Latiff, M. S., & Coulibaly, Y. (2016). Resource scheduling for infrastructure as a service (IaaS) in cloud computing: Challenges and opportunities. *Journal of Network and Computer Applications*, 68, 173–200. doi:10.1016/j.jnca.2016.04.016
- Mekala, M. S., & Viswanathan, P. (2019). Energy-efficient virtual machine selection based on resource ranking and utilization factor approach in cloud computing for IoT. *Computers & Electrical Engineering*, 73, 227–244. doi:10.1016/j.compeleceng.2018.11.021
- Mishra, S. K., Sahoo, B., & Parida, P. P. (2020). Load balancing in cloud computing: A big picture. *Journal of King Saud University-Computer and Information Sciences*, 32(2), 149–158. doi:10.1016/j.jksuci.2018.01.003
- Mohan, K., & Palanisamy, B. (2019). A novel resource clustering model to develop an efficient wireless personal cloud environment. *Turkish Journal of Electrical Engineering and Computer Sciences*, 27(3), 2156–2169. doi:10.3906/elk-1807-187
- Noshy, M., Ibrahim, A., & Ali, H. A. (2018). Optimization of live virtual machine migration in cloud computing: A survey and future directions. *Journal of Network and Computer Applications*, 110, 1–10. doi:10.1016/j.jnca.2018.03.002
- Senyo, P. K., Addae, E., & Boateng, R. (2018). Cloud computing research: A review of research themes, frameworks, methods and future research directions. *International Journal of Information Management*, 38(1), 128–139. doi:10.1016/j.ijinfomgt.2017.07.007
- Shirvani, M. H., Rahmani, A. M., & Sahafi, A. (2020). A survey study on virtual machine migration and server consolidation techniques in DVFS-enabled cloud datacenter: Taxonomy and challenges. *Journal of King Saud University-Computer and Information Sciences*, 32(3), 267–286. doi:10.1016/j.jksuci.2018.07.001
- Stergiou, C., Psannis, K. E., Kim, B. G., & Gupta, B. (2018). Secure integration of IoT and cloud computing. *Future Generation Computer Systems*, 78, 964–975. doi:10.1016/j.future.2016.11.031

Tchernykh, A., Schwiegelsohn, U., Alexandrov, V., & Talbi, E. (2015). Towards understanding uncertainty in cloud computing resource provisioning. *Procedia Computer Science*, 51, 1772–1781. doi:10.1016/j.procs.2015.05.387

Varghese, B., & Buyya, R. (2018). Next generation cloud computing: New trends and research directions. *Future Generation Computer Systems*, 79, 849–861. doi:10.1016/j.future.2017.09.020

Wang, Z., Wu, J., Wu, Y., Deng, S., & Huang, H. (2017). QoS aware dynamic pricing and scheduling in wireless cloud computing in *2017 IEEE 56th Annual Conference on Decision and Control (CDC)* (pp. 3702–3707). IEEE.

Zhang, Q., Chen, Z., & Yang, L. T. (2015). A nodes scheduling model based on Markov chain prediction for big streaming data analysis. *International Journal of Communication Systems*, 28(9), 1610–1619. doi:10.1002/dac.2779

Zhao, Y., Liu, J., Fang, Q., Xu, L., Du, C., & Xiaoqun, Y. (2018). A strategy for improving NetClust server placement for multicloud environments. *Turkish Journal of Electrical Engineering and Computer Sciences*, 26, 115–124. doi:10.3906/elk-1704-206

Grace Shalini T. completed her PhD from Anna University Chennai, Tamil Nadu and under graduation in Computer Science and Engineering at Magna College of Engineering, Tiruvallur, Tamil Nadu. Later she finished her post-graduation in the same discipline from Velammal College of Engineering and Technology, Madurai. Also she completed M.B.A (System Software) from Madurai Kamaraj University, Madurai. Her primary research interest in Vanets and Wireless Sensor Networks.

Rathnamala S. is working as an associate professor and has 15 years of teaching experience.

[Home](#) > [Multimedia Tools and Applications](#) > [Article](#)[Published: 11 March 2023](#)

A bio-inspired fall webworm optimization algorithm for feature selection and support vector machine optimization for retinal abnormalities detection

[B. Sakthi Karthi Durai](#)  & [J. Benadict Raja](#)[Multimedia Tools and Applications](#) (2023)21 Accesses | 1 Altmetric | [Metrics](#)

Abstract

The early detection of retinal abnormalities such as diabetic retinopathy (DR) can be performed using the computerized analysis of retinal fundus images. The most significant complications associated with the DR detection are noise artifacts occurred as a result of unsuitable illumination, the overlapping of blood vascular structure and lesions as they have same intensities, and missing of data happened due to the analysis of large amount of data. Hence the improved technique capable of overcoming all these limitations must be presented in early detection of DR and other retinal abnormalities. Some of previous blood vessel segmentation methods provide better accuracy with normal retinal images and requires less computation time. In this work, an automated process using an optimized SVM

classifier and a new feature extraction is presented. The proposed feature extraction process is sum of minimum (SOM) local difference pattern (LDP) (SOMLDP) which is developed from the computation of difference between pixels. This feature extraction produces precise feature information with reduced size. In addition, feature selection process is employed to select more important features, using a new optimization algorithm developed from the behavior of fall webworm (FWW) species. FWW optimization algorithm is also applied for the optimal tuning of support vector machine (SVM) classifier. The main objective of the paper is to present an automated detection of DR with more accuracy, less memory and reduced computation time. The performance of proposed technique is validated with publicly available standard dataset Messidor-2 by evaluating the metrics such as sensitivity, specificity and accuracy. The simulation results depict that sensitivity, specificity and accuracy of 0.8235, 0.9892 and 0.9879 is attained respectively. The FWW optimization algorithm is also validated by analyzing the computation time performance and comparing the performance of FWW algorithm with other optimization algorithms.

This is a preview of subscription content, [access via your institution](#).

Access options



Sharing Personal Health Data by Blockchain with Cloud Storage Technologies

Balamuralikrishnan G¹ Assistant Professor, Dept of CSE, VCET

Balakrishnan G² Associate Professor, Dept of CSE, FMCET

V.Rajeshkannan³ Assistant Professor, Dept of CSE, KCET

DR R.Ramya⁴, Associate Professor, Dept of CSE, KCET

A.Alagar⁵, Assistant professor, Dept of CSE, SIT

Abstract—The development of wearable technology and mobile computing leads to the generation of huge amounts of personal data. Every second, many data related to health is being created and amassed continuously. As these personal datasets include important information about the users, they have to be treated as an asset for these users. Also they have to be controlled and managed by the person who generated those data. Many service providers have been established to manage these datasets and to keep them safe. These service providers project the problems for data security and prevent data exchange. These individual health records are very important sources. In this paper, we exhibit a theoretical approach for sharing continuously dynamic personal health data leveraging block chain technology and cloud storage to share health-related data in an open and secure way. In addition, to have control over data quality, we also develop a data quality inspection module based on machine learning approaches. The proposed system's main objective is to give users the ability to possess, manage and share their personal health data in a secured way that go along with the General Data Protection Regulation (GDPR) additionally, it gives users of commercial data and researchers an effective approach to get high-quality personal health data for both of those things.

INTRODUCTION

People and technology have become inseparable as they were using various kinds of smart devices like smart phones, smart watches, smart bands. These devices use various health-related applications such as remote diagnosis. We have to be grateful to the rapid development of mobile computing, wearable technology and wireless sensing. This helps us to monitor diseases and to look after elderly person as it predicts the disease earlier and make people health conscious. These devices provide a significant amount of data on a person's health, and this data is useful for both academic and commercial healthcare research. proper sharing of personal health data by the patients, researcher's, business's and also by the entire public health care system is always important. Health data should be owned and managed by the respective users themselves as a personal asset but in practise they are frequently managed by various service providers, device manufacturers, or dispersed across several healthcare systems. As these centralised data warehouses and authority providers are desirable targets for cyberattacks, it generally creates obstacles for data sharing and

compromises data security and privacy. Due to cryptocurrencies, the blockchain technology has significantly increased in popularity in recent years, particularly in the financial sector. For instance, since its initial introduction in 2008. Bitcoin has drawn interest from the research community across a range of academic disciplines and has become widely accepted because of its distinctive features, such as lack of control which is centralized, an assumed high of innominateness and distributed consensus over decentralised networks. Multiple parties' cooperation is prerequisite for the decryption of the data. With that cooperation blockchain solutions could reduce the risks of data breaches. This is also possible by using threshold encryption of data combined with public key framework. The blockchain-based data sharing system might significantly streamline the process of acquiring data for research and commercial initiatives and give users the chance to acquire ownership and privileges over their own data and profit from them. Additionally, it provide greater data control to help the user to keep an eye on all the actions using those data. The purpose of this paper is to put forward the significance of sharing personal health data based on blockchain and cloud

storage technologies . this paper also highlights how these technologies provide safe and secured sharing system. it also brings out how these systems backup researchers and consumers of commercial data in obtaining the data they demand efficaciously in a clear manner and in union with data regulations like GDPR.

II. RELATED WORK

The way of using personal data created by mobile and wearable technology has always to develop the standard of health care system. generated immense interest among researchers. One of the barriers for these investigations is data collection as it is naturally costly and time consuming . the worries about the security of their data make most people to keep their medical and other data related to their health confidential and are not ready to share them, A decentralised network of peers and a public ledger can be used to provide reliable and auditable computing, as shown by the financial industry's adoption of blockchain technology. Recently, there have been a lot of research about using blockchain technology in industries other than finance. The research in from 2015 utilised blockchain to safeguard data privacy for individuals. A protocol developed by the authors changes a blockchain into an automatic access-control manager that ensures the users the complete control of the data and it eradicate the dependency of the users on third party for data sharing . the utilization of blockchain technology in manging healthcare data has been focused in many research papers since 2016.the research described in proposed an application structure based on blockchain called Healthcare Data Gateway (HGD). This provide a system which guarantees the patients to share their data securely and provide a complete control over the data sharing without involving privacy.it provided an efficient means of improving health care systems intelligence in the process of protecting the privacy of patient data. Electronic Health Records(EHRs) manages the data using blockchain technology. The study in [3].created a decentralized management system to maintain the health record called MedRec. This system enables easy access to the medical records of the patients across multiple doctors and various sites for treatment and also it provide a clear log of their medical history. The studies described above mostly focused on utilising blockchain to manage static health data like Electronic Medical Records

(EHRs) (EMRs). The EMR comprises information that is mostly constant over the course of a patient's life, such gender, blood type, fingerprint, etc., or that changes gradually, like age, weight, height, disease history, etc.

The ability to store and share data inside the blockchain is made possible by the fact that this form of data often requires less storage space.This kind of static data only makes up a small portion of the total health data in the majority of real-world healthcare applications. Mobile and wearable devices, which are extensively used, generate significant volumes of dynamic data with frequent and big data sizes. For instance, the accelerometer within a smart watch produces data at a high frequency, producing millions of records every day with a maximum data size of several terabytes. It is challenging to store and share directly inside the blockchain because to the high changing frequency and size. A roadmap for a blockchain-enabled, decentralised personal health data ecosystem was put forth in a recent paper published in [1]. In order to help regulators overcome their issues and give people back control over their personal data, including medical records, the authors proposed the idea of a safe and transparent distributed personal data marketplace using blockchain and deep learning technologies. To offer an offchain storage option for huge biomedical data files, they integrated cloud storage into the ecosystem. In contrast to the majority of prior blockchain applications, a unique position called a data validator was added alongside the conventional roles of data contributor/generator and data consumer. The purpose of data validators is to verify or certify the accuracy of the data provided or generated by the users. Only data that has been verified or confirmed by data validators is made available to the public. The issue of gaining control over the data quality is resolved by this approach. Although most static and gradually changing health data may be controlled using this way, handling high frequency, large-volume data, like that from accelerometers, remains difficult. Manually validating these types of data may be time-consuming and require a lot of effort. Advanced techniques, such as machine learning and data mining, are required to manage such a massive volume of data. For many years, there has been a lot of interest in the research on evaluating massive data generated by wearable technology [4], [5], [6], [7], and [8]. For instance, the study of [9] assessed the degree of tremor in individuals with Essential

Tremor using the acceleration data obtained from a smart watch.

For Human Activity Recognition (HAR) tests, the researchers used a deep learning algorithm in [10] and found satisfactory results can be used to assess the calibre of data generated by wearable and mobile devices, similar to deep learning. In this paper, I presented a novel method for sharing personal health data that is enabled by blockchain, cloud computing, and machine learning technologies. This method was encouraged by the before mentioned studies.

III RESEARCH SCOPE

According to [1], health data can generally be split into dynamic and static data. The term "static data" refers to personal information that has remained largely constant over the course of a person's life, such as a person's DNA or fingerprint. The dynamic data shows the user's activities throughout time, such as electroencephalogram (EEG) heart rate data, or the status of the organism at the time of sampling, such as blood test data.

The dynamic data can be further broken down into variables that change quickly, like acceleration variables, and variables that change gradually, like height and weight variables, etc.

The health data can be separated into continuous data and instant data depending on the data gathering method. The continuous data is gathered over a period of time and shows the user's status or activities throughout that time. Continuous data are typically dynamic time series data that change quickly. The instantaneous data, in contrast, are acquired through a single measurement. The instant data may be dynamic data that changes over time or immutable static data. The classification methods are not based on the health indicators that the data represent, but rather on the type of data and the data gathering techniques. The same health indicator's data may fall under several categories. The number of heartbeats per minute, for instance, can be used to convey the status of the heartbeat and is an example of instantaneous dynamic data. However, when the heartbeat is monitored with EEG over a period of time, the data that is gathered is still of the same heartbeat but is continuous-dynamic

This study mainly focus on the continuous -dynamic data as it makes up the majority of the data created by wearable and mobile devices. The

below mentioned figure picturizes this sort of data. There aren't many research on this subject because they typically occur frequently, are big in size and it is hard to be shared or saved using the similar techniques used to store other types of health data

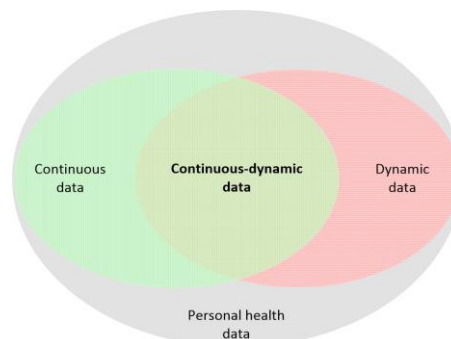


Fig. 1. Personal data categories and the study scope of this paper

A. General Data Protection Regulation:

The new General Data Protection Regulation (GDPR) [2] of the European Union went into force in May 2018. The present data protection directive, which was enabled in 1995 will be replaced by this GDPR. This is one of the most significant updates to data privacy regulation in recent memory. The regulation's main objective is to harmonise data privacy regulations across Europe, with a focus on empowering and safeguarding the privacy of EU individuals. The problem of user permission is one of the most important ones. The rule stipulates that the service provide should give a clear explanation of the purposes for the usage of the user's consent and similarly the user must have the same ease in giving and withdrawing consent. If the user withdraw his consent, the service provider is supposed to destroy the data related to that particular user. In addition, the user has the right to access, which requires that, upon request, the service provider or business disclose whether or not it is processing the user's personal data as well as its intended use. All information must be made available to the user by the service provider in a machine-readable format. The user has the right to get the information from the controller in a machine readable format and can transfer it to another controller .this right to data portability is alike to the right of access. Companies which break the above mentioned rule will be subject to fines up to 20 million euros or 4% of their revenue.

CONCEPTUAL DESIGN

The proposed health data storage and sharing system's design has been depicted in the figure 2. In this system there are three defined roles

- Users: to create, upload, and sell personal health data in exchange for money or services.
- Key keepers: to store the secret keys for encrypting and decrypting data after a user uploads it, then release the keys to users once a transaction is authorised. Every transaction that is accepted will result in financial rewards for them.
- Customers: to purchase user data and offer users and key keepers financial or service incentives.

A related App was created for each role to assist users in achieving their goals.

Users: User app is a mobile computing service such as a smartphone or tablet. It can transfer with different health-related data, wearable devices or sensors such as Bluetooth. The corresponding sensors' APIs provide support for data collecting. The quality score of the raw data can be get by passing them through a quality validation module. A brief discussion about this module will be done later. After validation, the raw data will be combined with different identification marker.

To simply describe the data, use the title, Data Type is used to specify the kind of the data, Size is used to specify its size, Quality is used to specify its calibre, etc. If necessary, certain static personal information, such as gender, age, and weight, could also be incorporated. The next step is that the combined data will be compressed and encrypted. Then, the encrypted data will be put on a cloud. Data encryption keys will be divided up into shares and given to key keepers. Following that, a transaction will be created and disseminated to all blockchain nodes. The transaction includes the user's public key, a hash reference that connects to encrypted data, basic details, the dataset's price, etc

Key keeper App: This app generally runs on a local device that is connect to the internet service or on a cloud server. This app will keep the key shares securely which is received from the system. After validation of the dat shares, it will get a notice to release the related key share to the customer who made that transaction.

Customer App: this app is also similar to the keykeeper app as it connects to the internal or on a cloud server. This provide all the available datasets to the customer and permit them to close the type of datasets they prefer. After choosing the dataset, the customer will be guided by the app to make a transaction for buying that dataset. then this transaction is validated the customer app will get a link to the encrypted data and the decryption keys from the key keepers. Finally ,it enables the customer to download the date and decrypt them with the private keys.

The following sections describe the core modules and its function of the proposed system.

1.validation of data quality:

This study mainly focus on continuous - dynamic data. Typically, these data are produced by common sensors. The devices' APIs make it possible to access the sensor data.

To ensure that the data is valid in accordance with specific validation patterns or checks, advanced machine learning techniques can also be used to evaluate the pattern of the acquired data. We can use it to verify the data's accuracy from a hardware and software perspective.

Hardware aspect: once, a new device is linked to the user app, the user app will gather hardware details about that device and any embedded sensors. A device or sensor is recognised as certified hardware and the data it generates is dependable if it comes from a validated manufacturer. Otherwise, the App won't allow it to connect. A well-maintained database of approved manufacturers and gadgets should be created in advance for this purpose.

3.Software aspect: With the aid of cutting-edge machine learning methods, it is feasible to accurately categorise the patterns in a time series collection. Numerous studies have been conducted on this subject. For example, it can identify a user's daily activities using information gathered from an accelerometer built into wearable technology [9], [10], [11]. We can build reliable classifiers for various health data using comparable machine learning techniques. The nonsensical data and sounds will be removed, leaving only the data with predetermined features saved. Here, a relative criteria for data quality is used. Consider the aforementioned acceleration data as an example and visualise how a smart watch would collect the user's acceleration data over the course of a 24-hour

period. Sleep will be distinct from other daily activities in the quality validation methods. The data corresponding to the sleep time may be categorized as high quality data or noise based on the user's decision to share data related to sleep or daily activities ,

2) Data sharing transaction validation: The blockchain module is one of the system's main building blocks. It's employed to protect the data-sharing procedure. Ethereum1, Hyperledger Fabric2, and other decentralised blockchain application platforms are currently accessible. These platforms make it simple for developers to make blockchain applications. In this study, we decide to use Ethereum as the system's development framework. Developers can create and issue their own cryptocurrency or tradeable digital token on the Ethereum platform, which can be used as money, a proxy for assets, or a digital share. The contract will be instantly compatible with any wallet, other contract, or exchange that also uses this standard because these tokens use a standard coin API.

Another crucial factor in selling or exchanging personal data with data consumers or commercial entities is that the data must be adequately anonymized to comply with GDPR laws [2]. For instance, personal demographic information like name, address, and person identifiers will be correctly erased or hashed so that the final dataset supplied to the consumer complies with data standards like GDPR [2].

Cloud storage : the main objective of including

cloud storage in the data sharing system is that it provides a huge dataset as an off-chain storing option. In a long-term process, continuous dynamic data are often acquired at high frequency. The following accelerating data can be considered as an illustration. The data gathered in a single day may be several terabytes.

4. Data encryption: To maintain security and privacy, the user App will encrypt the data before uploading it to the cloud using symmetric-key techniques like Rijndael AES in conjunction with a threshold encryption scheme [1], and other methods. Then, using Shamir's secret sharing approach , the symmetric key for decrypting the data will be divided into several shares, and the key shares will be given out to various key keepers. The total number of key keepers and the blockchain security model define the required minimum number of key keepers to decode the data [1]. In order to access the encrypted data, The link and authentication to the data must be obtained. Then, in order to decrypt the data, he or she must obtain sufficient key shares of the encryption key. Theoretically, individuals can only access these details through a transaction that has been validated and confirmed by blockchain nodes.

5. Crypto token: It is necessary to offer users incentives when they submit their personal data in order to motivate them to do so. Health-related services, such as disease monitoring and diagnosis, might be advantageous, but this approach might not be appropriate in every circumstance. In some circumstances, it is preferable to offer some sort of

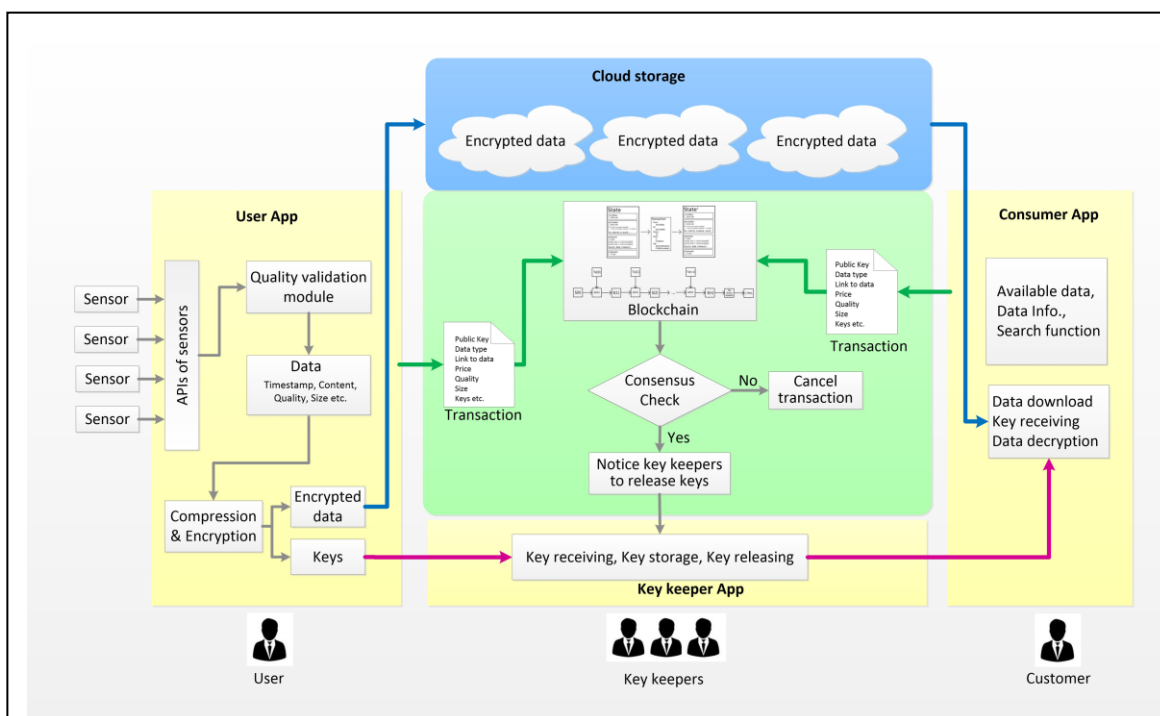


Fig. 2. The general architecture and workflow of the proposed system

financial benefit.

For a variety of reasons, such as the requirement to carry out an enormous number of microtransactions across numerous zones and among an equally enormous number of different types of participants, exchanging personal information for currency may be problematic. In line with [1], we recommend our own cryptocurrency token called Personal Health Data coin (PHD coin), which can be created or mined by storing data on a system with a blockchain to help with transactions. When the network has enough nodes and users, it is anticipated to facilitate exchange with other digital currencies or real currencies in the future.

6. Overall workflow: As seen in figure 2, there are three pipelines involved in interactions between users, key keepers, and customers: blockchain transactions, encrypted data transfers, and key sharing for decryption. The general process looks like this:

- Step 1: Using the user app, the user gathers, compresses, and encrypts data. The information will then be uploaded to a cloud storage system, and the key shares will be sent to the key holders.
- In step 2, a transaction will be created to inform the other users that the data has been uploaded and is ready for sharing. This transaction will be added to the blockchain via a consensus process after the user confirms it, and consumers and data verifiers will be able to see it.
- Step 3: The data validator will run data-mining and machine-learning algorithms on the data as part of the validation of the data to ensure that the data is valid in accordance with rules and specifications. The data validator will then certify that the data is valid in accordance with the provided guidelines.
- In step 4, a client selects the data they wish to purchase, confirms that it has been approved by the necessary data validators, and then establishes a transaction to do so.

The customer will sign the transaction, and it will then be added to the blockchain.

- In Step 5, the data purchase transaction will be verified using the consensus algorithm. The transaction will be allowed if the consumer has adequate balance (PHD coins) to pay for the data. A specific quantity of PHD coins will be given to the smart contract in accordance with the price of the data, and the workflow advances to step 6.

Otherwise, the transaction will be declined, and step 3 of the procedure will be resumed.

The key keeper of the associated dataset will be notified in Step 6 that a transaction to buy the data has been authorised. Then, using an authenticated communication channel, key keepers give the client access to their key shares of the relevant dataset.

Step 7: A predetermined rule will be used to the distribution of the PHD currencies saved in the smart contract among the accounts of the user and the key keepers.

- In step 8, the customer is given access to the encrypted data through a link and sufficient key shares to decrypt it. The data can then be downloaded and decrypted by the user from the cloud storage. The workflow comes to an end since the data are usable.

DATA SECURITY ANALYSIS

The data security of the proposed system depends on the following setups

The data kept in the cloud provide limited access to the user. One has to know the address and get authentication in order to access the encrypted data. the data is encrypted before being uploaded to the cloud storage, in order to check the storage system from data leakage single symmetric key is used by multiple key keepers for the decryption of data. As a result, the compromise of the data.

The data transaction process is further secured by the use of the hash function and public-key signature techniques in blockchain contracts. without the permission of the user no personal information will be involved as it provide the facility to use pseudonyms.

The blockchain-based public key infrastructure(PKI) enables key keepers to generate verified communication channels with another participants. It secures the symmetric decryption key for the transmission and storage of data

The procedure of sharing data was the main subject of this investigation. The main focus of this work is not the data security concerns that arise after the data has been purchased and delivered to the customer, such as data leakage caused intentionally or unintentionally by the customer. Existing security mechanisms for data in use and at rest [11] could be used to provide this protection, but it is outside the focus of the current paper

CONCLUSION

In this research paper, I presented a blockchain-based, cloud-based, and machine learning-based method for sharing personal health data. It enables consumers to easily and securely own, control, and share their personal health data while also gaining advantages. Within the framework of health-related data from wearables and mobile devices, we initially divided personal health data into various groups based on data characters (dynamic and static data) and the data gathering methods (continuous and instant data). We suggested employing various approaches to transfer the continuous dynamic data of huge size using hash references to the storage place.

Second, by combining blockchain and cloud storage, our suggested approach got over the continuous-dynamic health data's size restriction. Additionally, I suggested that huge amount of health-related data may be saved on cloud and shared as metadata or transactional data. A data quality validation module was also included in this system as it control the data quality from the aspects of both hardware and software supported by machine learning techniques.

REFERENCES

- [1] P. Mamoshina, L. Ojomoko, Y. Yanovich, A. Ostrovski, A. Botezatu, P. Prikhodko, E. Izumchenko, A. Aliper, K. Romantsov, A. Zhebrak et al., "Converging blockchain and next-generation artificial intelligence technologies to decentralize and accelerate biomedical research and healthcare," *Oncotarget*, vol. 9, no. 5, p. 5665, 2018. 1, 2, 5, 6
- [2] The European Parliament, "Regulation (eu) 2016/679 of the european parliament and of the council of 27 april 2016 on the protection of natural persons with regard to the processing of personal data and on the free movement of such data, and repealing directive 95/46 (general data protection regulation) [GDPR]," *Official Journal of the European Union*, vol. 59, no. L119, pp. 1–88, 05 2016. 1, 3, 4
- [3] A. Ekblaw, A. Azaria, J. D. Halamka, and A. Lippman, "A case study for blockchain in healthcare: "medrec" prototype for electronic health records and medical research data," in *Proceedings of IEEE open & big data conference*, vol. 13, 2016, p. 13. 2
- [4] S. Chernbumroong, S. Cang, A. Atkins, and H. Yu, "Elderly activities recognition and classification for applications in assisted living," *Expert Systems with Applications*, vol. 40, no. 5, pp. 1662–1674, 2013. 2
- [5] C. A. Ronao and S.-B. Cho, "Human activity recognition with smartphone sensors using deep learning neural networks," *Expert Systems with Applications*, vol. 59, pp. 235–244, 2016. 2
- [6] C. Pulliam, S. Eichenseer, C. Goetz, O. Waln, C. Hunter, J. Jankovic, D. Vaillancourt, J. Giuffrida, and D. Heldman, "Continuous in-home monitoring of essential tremor," *Parkinsonism & related disorders*, vol. 20, no. 1, pp. 37–40, 2014. 2
- [7] M. A. Alsheikh, A. Selim, D. Niyato, L. Doyle, S. Lin, and H.-P. Tan, "Deep activity recognition models with triaxial accelerometers," in *AAAI Workshop: Artificial Intelligence Applied to Assistive Technologies and Smart Environments*, 2016. 2
- [8] M. Ermes, J. Parkkila, J. Mänty, J. Arvi, and I. Korhonen, "Detection of daily activities and sports with wearable sensors in controlled and uncontrolled conditions," *IEEE transactions on information technology in biomedicine*, vol. 12, no. 1, pp. 20–26, 2008. 2
- [9] X. Zheng and J. Ordieres-Mere, "Detection and analysis of tremor using a system based on smart device and nosql database," in *Industrial Engineering and Systems Management (IESM), 2015 International Conference on. IEEE*, 2015, pp. 242–248. 2, 4
- [10] Y. Chen and Y. Xue, "A deep learning approach to human activity recognition based on single accelerometer," in *Systems, man, and cybernetics (smc), 2015 IEEE international conference on. IEEE*, 2015, pp. 1488–1492. 2, 4
- [11] M. Zeng, L. T. Nguyen, B. Yu, O. J. Mengshoel, J. Zhu, P. Wu, and J. Zhang, "Convolutional neural networks for human activity recognition using mobile sensors," in *Mobile Computing, Applications and Services (MobiCASE), 2014 6th International Conference on. IEEE*, 2014, pp. 197–205. 4
- [12] J. Daemen and V. Rijmen, *The design of Rijndael: AES-the advanced encryption standard*. Springer Science & Business Media, 2013. 5

Traffic Sign Recognition using Deep Learning

C. B.Selva Lakshmi ¹, Assistant Professor

Department of CSE, Velammal College of Engineering and Technology, Madurai

cbselak08@gmail.com

Nishanthi V², Mathumitha M.³, Keerthika R.⁴, Isha Parasu B⁵

^{2,3,4,5}UG Student, Department of CSE, Velammal College of Engineering and Technology, Madurai, Tamil Nadu

Abstract

Traffic sign recognition (TSR) has been an essential part of driver-assistance systems, which can assist drivers in avoiding a vast number of potential hazards and improve the experience of driving. However, the TSR is a realistic task that is full of constraints, such as visual environment, physical damages, partial occasions, etc. To deal with such constraints, convolutional neural networks (CNN) are widely used to extract the features of traffic signs and classify them into corresponding classes. The system consists of three stages: traffic sign detection, refinement, and classification. The detection and refinement are performed using CNN, while the classification is achieved with a proposed Convolutional Neural Network (CNN) architecture. We introduced the extended version of the German Traffic Sign Detection Benchmark (GTSDB) or GTSRB, labeled in a pixel manner (masks), with 11 classes grouped into 8 categories.

Keywords - Deep learning, Traffic sign recognition - CNN, dataset, traffic signs, traffic sign classification.

1. INTRODUCTION

Nowadays, intelligent autonomous vehicles, together with advanced driver assistance systems (ADAS), deal with the problem of traffic sign recognition. Traffic sign recognition using deep learning is a computer vision project that involves training a model to recognize different traffic signs in real time. In this project, we will use deep learning techniques to train a neural network that can identify traffic signs from images. To start, we need to download the dataset containing images of traffic signs. One of the most popular datasets for traffic sign recognition is the German Traffic Sign Recognition Benchmark (GTSRB) dataset. It contains more than 50,000 images of traffic signs from different angles and lighting conditions. Once we have the dataset, we can start building our neural network. We will be using Python programming language and the TensorFlow library to create our model. The TensorFlow library provides a high-level interface for building deep learning models, making it easier to implement complex neural networks [1]

our model, we will use a convolutional neural network (CNN). CNNs are widely used in computer vision tasks because they can extract features from images and learn to recognize patterns. Our CNN will have several layers, including convolutional layers, pooling layers, and fully connected layers. The first layer of our CNN is the input layer, where we feed the images from the dataset. The next few layers are convolutional layers that apply filters to the input images, extracting important features. The pooling layers are then used to reduce the size of the feature maps and make the model more efficient. Finally, the fully connected layers are used to classify the images based on the extracted features. Once we have built our model, we can start training it on the dataset. We will use the backpropagation algorithm to update the weights of the neural network and minimize the loss function. The loss function measures the difference between the predicted output of the model and the true label. After training, we can test our model on a separate test dataset and evaluate its performance [3]. We can use metrics such as accuracy, precision, recall, and F1 score to evaluate the model's performance. Once we are satisfied with the performance of our model, we can use it to classify new traffic sign images in real time. We can use the OpenCV library to capture images from a camera or a video feed and use our model to recognize the traffic signs. In summary, traffic sign recognition using deep learning is a challenging but rewarding project that involves building a convolutional neural network to recognize different traffic signs from images. With the help of Python and TensorFlow, we can create a model that can identify traffic signs in real time, making roads safer for everyone.

II.PROBLEM DEFINITION

Classifying traffic signs is a very important task for autonomous driving systems, as the safety of everyone as well as the passenger depends on it [4-8]. Depending on the country, traffic signs possess a variety in their visual appearance, making it harder for classification systems to succeed. Nowadays, intelligent autonomous vehicles, together with advanced driver assistance systems (ADAS), deal with the problem of traffic sign recognition. It is a challenging real-world computer vision problem due to the different and complex scenarios they are placed into. The proposed system will help understand the problem and provide a systematic way of approaching it.

III. OBJECTIVES

Overall, the ultimate objective of this report is to complete the customized traffic-sign recognition and figure out which state-of-art networks better fit into this project. Firstly, to recognize traffic sign, the first process is where dataset is generated as the quality of the actual data will have an impact on the result of network and models. Next is the tuning process of detectors and classifiers will be introduced, and we will adjust the neural networks from the following : (1) Experiments performed on different algorithms, (2) Validation and evaluation based on the chosen models, (3) Parameter tuning process. Finally, the report will summarize the pros and cons across the applied algorithm systems and find the best system for traffic-sign recognition.

IV.LITERATURE SURVEY

Traffic sign recognition (TSR) has benefited a large number of realistic applications, such as driver assistance systems, autonomous vehicles, and intelligent mobile robots since they have delivered the current state of traffic signs into various systems.

A. Real-Time Traffic Sign Recognition Based on Efficient CNNs in the Wild [9]

Year: Mar. 2018.Author: J. Li and Z. Wang,

Methodology

A complete pipeline of traffic sign recognition is proposed, which is superior to the majority of previous work, considering generality, reliability and run time.

B. A computer vision assisted geoinformation inventory for traffic infrastructure [2]

Year: 2010.Author: S. Segvić, K. Brkić, Z. Kalafatić, V. Stanisavljević, M. Ševrović,

D. Budimir and I. Dadić

Methodology

The developed techniques were tested on triangular warning signs from the superclass A. The superclass A is chosen as a model subset due to its prevalence in our videos. All algorithms have been trained on the training set T2009 containing about 2000 triangular signs collected in 2009 using an interlaced camera.

C. Simultaneous Traffic Sign Detection and Boundary Estimation Using Convolutional Neural Network[10]

Year: 2018.Author: Hee Seok Lee and Kang Kim

Methodology

The efficient traffic sign detection method is proposed where locations of traffic signs are estimated together with their precise boundaries. To this end, the object bounding box detection problem is generalized and formulated an object pose estimation problem, and the problem is effectively modeled using CNN based on the recent advances in object detection networks.

D. Towards real-time traffic sign detection and classification

Year: .2016. Author: Yi Yang, Hengliang Luo, Huarong Xu, and Fuchao Wu

Methodology

Aim of this project is to address the problem of real-time traffic sign recognition. To this end, two fast algorithms for traffic sign detection and classification is proposed, respectively.

E. Thai Traffic Sign Detection and Recognition Using Convolutional Neural Networks

Year: .2018.

Author: Mohamed Shahud, Jigyasa Bajracharya

Methodology:

After careful consideration and analysis of cost and benefit, use Yolov3 dark net developed by Joseph Redmon . There are 2 main reasons. First, Yolov3 is really fast, which makes it ideal for use in a real time application such as detecting traffic signs.

V.PROPOSED SYSTEM

We introduced the extended version of the German Traffic Sign Detection Benchmark, labeled in a pixel manner with 42 classes grouped into 8 categories. which is used to design the task of semantic segmentation of traffic signs. It is an extension of the original GTSDDB dataset, which contains only bounding box annotations for traffic signs. The extended version of GTSDDB with pixel-level annotations is a valuable resource for researchers and practitioners working on the development of computer vision algorithms for traffic sign detection and recognition, as well as for the evaluation and comparison of existing methods. Figure 1 shows the system architecture of the proposed model.

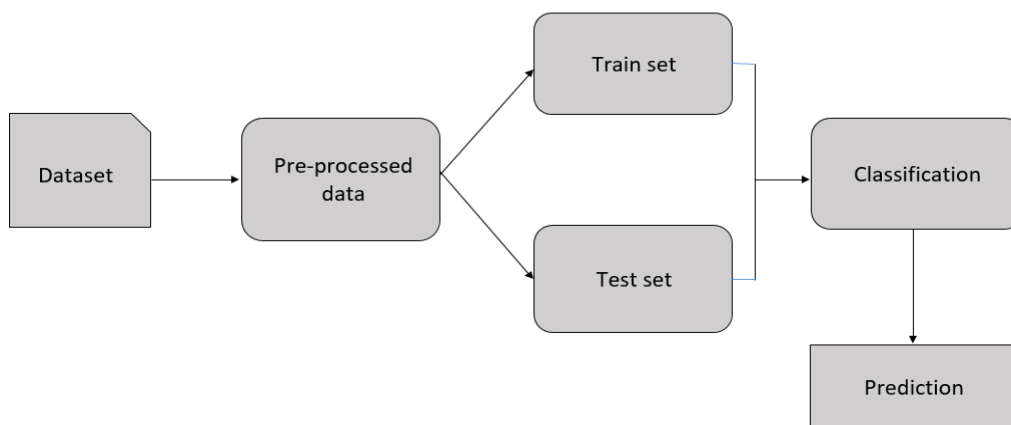


Figure 1. System Architecture

A).DATASETS

The images of our proposed European dataset are composed of publicly available datasets and of sequences recorded in Belfort, France, and surroundings during Spring and Summer from 2014, 2015, and 2018. The sequences are composed of urban and rural environments and cover daytime and sunset conditions. The public datasets(refer figure 2) are composed of different scenarios (urban, rural, highway) mostly captured during the daytime.



Figure 2. Sample Dataset

The flow diagram of the proposed work is shown below in figure 3 through which the entire flow of the

proposed model is implemented on the signal dataset.

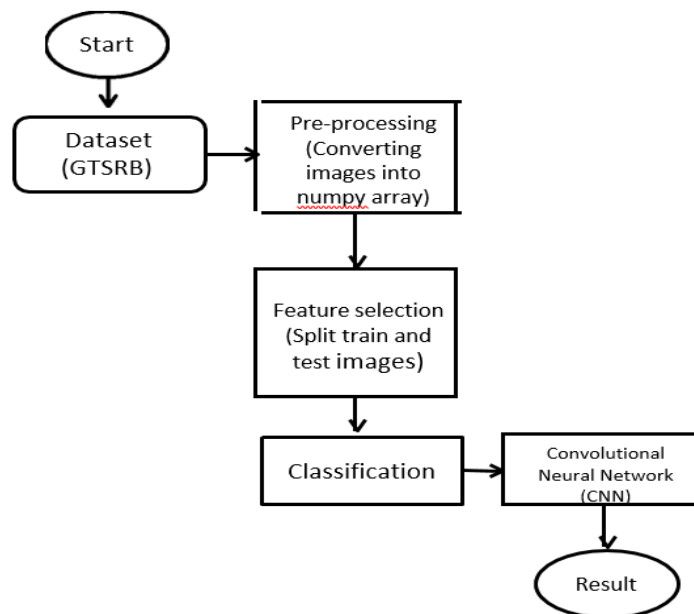


Figure 3. Flow Diagram

B. DATA SELECTION AND LOADING

The data selection is the process used for selecting the German Traffic Sign Recognition Dataset. In this paper, German Traffic Sign images from the GTSRB dataset (refer figure 4) are used to find traffic signs.



Figure 4 GTSRB dataset

C. DATA PREPROCESSING

Image Data pre-processing is the process of getting rescaled data from the dataset.

- Resize image from the dataset
- Getting data

Resize image dataset: Rescale the German Traffic Sign image (from the GTSRB dataset) size into 200.
Getting data: The categorical data are defined as variables with a finite set of rescaled values. Most deep learning algorithms require array input and output variables.

D. FEATURE SELECTION

Data splitting is the act of partitioning data from the dataset (GTSRB) into two portions. One Portion of the data is used to develop a predictive model. Another is to evaluate the model's performance. Separating data into training and testing sets is an important part of evaluating data mining models. When you separate a data set into a training set and testing set, most of the data is used for training, and a smaller portion of the data is used for testing.

E. CLASSIFICATION

CNN In deep learning, a convolutional neural network (CNN, or ConvNet) is a class of deep neural networks, most commonly applied to analyzing visual imagery. CNNs are regularized versions of multilayer perceptrons. Multilayer perceptrons usually mean fully connected networks, that is, each neuron in one layer is connected to all neurons in the next layer. The "full connectedness" of these networks makes them prone to overfitting data. Typical ways of regularization include adding some form of magnitude measurement of weights to the loss function. CNNs take a different approach towards regularization: they take advantage of the hierarchical pattern in data and assemble more complex patterns using smaller and simpler patterns. Therefore, on the scale of connectedness and complexity, CNNs are on the lower extremity.

F. PREDICTION

It is a process of predicting the GTSRB from the dataset. This project will predict the data by enhancing the performance of the overall prediction results (refer figure 5 (a) & (b)). The Final Result will get generated based on the overall classification and prediction.

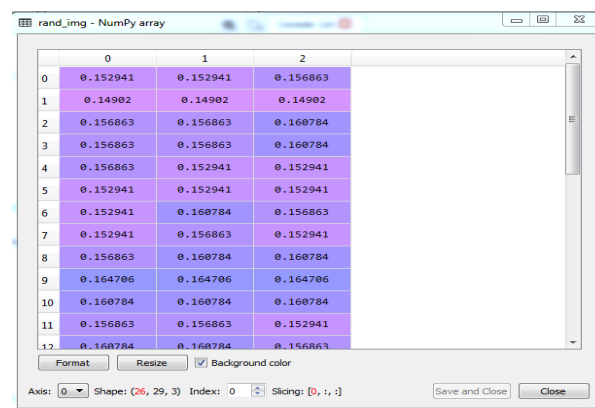


Figure 5 (a). Predicted Results

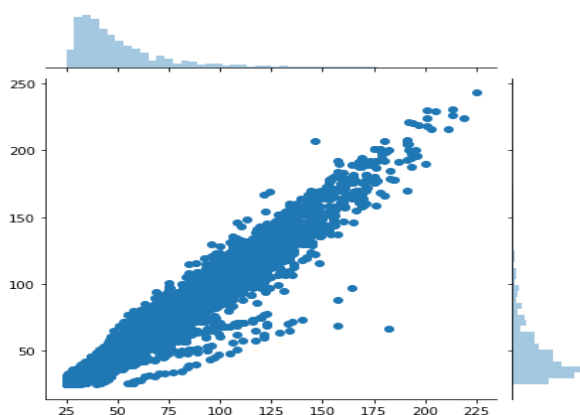


Figure 5 (b). Predicted Results for different values

VI.CONCLUSION

In this work, Traffic light detection in a European urban environment. The traffic sign digital images are used as the input of the data. The sign images are fed into the pre-processing method. In the pre-processing method, all the input digital images are resized. Then it is processed into the feature selection method. In the feature selection method, the digital image data set is split into training and testing datasets. The classification deep learning algorithm is used to predict the traffic sign images. Convolutional Neural Network is used to increase the overall performance of the detection of traffic sign detection also to improve the accuracy of the system.

In the future, the traffic sign detection method will be applied to vehicles. And also it will detect the traffic light signs and signal in distance measurement. It will also help to detect the signs and control the vehicle using a sensor device. Our process is detection the signs in the form of images and their pixels. It will help to avoid accidents and make them aware of traffic rules.

REFERENCES

1. C. Grigorescu and N. Petkov, "Distance sets for shape filters and shape recognition," *IEEE Trans. Image Process.*, vol. 12, no. 10, pp. 1274–1286, Oct. 2003
2. S. Šegvic et al., "A computer vision assisted geoinformation inventory for traffic infrastructure," in *Proc. 13th Int. IEEE Conference Intell. Transport System (ITSC)*, Sep. 2010,
3. F. Larsson and M. Fels berg, "Using Fourier descriptors and spatial models for traffic sign recognition," at *Proc. Scand. Conf. Image Anal. Berlin, Germany: Springer*, 2011,
4. R. Timofte and L. Van Gool, "Sparse representation-based projections," in *Proc. 22nd Brit. Mach. Vis. Conf. (BMVC)*, 2011.
5. Mogelmose, M. M. Trivedi, and T. B. Moeslund, "Vision-based traffic sign detection and analysis for intelligent driver assistance systems: Perspectives and survey," *IEEE Trans. Intell. Transp. Syst.*, vol. 13, no. 4, Dec. 2012.
6. S. Hou ben, J. Stallkamp, J. Salmen, M. Schlipsing, and C. Igel, "Detection of traffic signs in real-world images: The German traffic sign detection benchmark," in *Proc. Int. Joint Conf. Neural Netw. (IJCNN)*, Aug. 2013, pp. 1–8.
7. G. Serna and Y. Rui chek, "Classification of traffic signs: The European dataset," *IEEE Access* in 2018.
8. H. Luo, Y. Yang, B. Tong, F. Wu, and B. Fan, "Traffic sign recognition using a multi-task convolutional neural network," *IEEE Trans. Intell. Transp. Syst.*, vol. 19, no. 4, , Apr. 2018.
9. J. Li and Z. Wang, "Real-time traffic sign recognition based on efficient CNNs in the wild," *IEEE Trans. Intell. Transp. Syst.*, vol. 20, no. 3, Mar. 2018.

10. H. S. Lee and K. Kim, "Simultaneous traffic sign detection & boundary estimation using convolutional neural network," IEEE Trans. Intell. Transp. Syst., vol. 19, no. 5, May 2018.

DETECTING DISASTER, SAVING LIVES WITH RFID AND AWS CLOUD

¹Mr.G.BalaMurali Krishnan B.E.,M.E, Assistant Professor, Department of Computer Science and Engineering, Velammal College of Engineering and Technology,

²Deepthiha R, Undergraduate Student, Department of Computer Science and Engineering, Velammal College of Engineering and Technology,

³Dharshana T, Undergraduate Student, Department of Computer Science and Engineering, Velammal College of Engineering and Technology,

⁴Kamalika P, Undergraduate Student, Department of Computer Science and Engineering, Velammal College of Engineering and Technology,

⁵Sharmila S, Undergraduate Student, Department of Computer Science and Engineering, Velammal College of Engineering and Technology,

Abstract

This project is focused on designing and implementing an IOT-based disaster monitoring system that can monitor water level, air conditions, and high-frequency vibrations in real-time. The system will use sensors to collect data, which will be stored in the AWS cloud. The system will also record any slight changes in the monitored parameters, allowing for early warning and timely response to disasters. The system will additionally utilize RFID technology to detect people who are trapped in disaster-prone areas. The data from the RFID will be uploaded to the cloud, providing real-time tracking of the affected individuals. The system's main goal is to enable effective disaster management, reduce damage caused by disasters, and save lives. The project is expected to contribute to advancing the field of disaster management and bring significant benefits to society.

Keywords-IoT (Internet of Things),Sensors, Real-time monitoring,Naturaldisasters, Emergency,IOT- Cloud, Wireless networks, Remote sensing, Environmental monitoring, Sensor fusion

1.Introduction

Earth quake, Flood,Cyclone is a natural disaster where an area of land that get instantly damaged lives. An earthquake is a sudden and rapid shaking of the earth's surface, caused by the shifting and movement of tectonic plates beneath the surface. Earthquakes can range from minor tremors to major, destructive events that can cause significant damage to buildings, infrastructure, and communities. The strength of an earthquake is measured on the Richter scale, which assigns a numerical value based on the magnitude of the shaking. Earthquakes can trigger other natural disasters such as landslides, tsunamis, and volcanic eruptions. Flood may occur in many areas in different ways due to overflow of streams, rivers, lakes or oceans or as a result of excessive rain A warning system is necessary to take precautionary measures and be more prepared to overcome its effects. A cyclone is a weather phenomenon characterized by strong, rotating winds around a center of low pressure. Cyclones can form over warm ocean waters and are fueled by the release of heat energy from the ocean. Cyclones are classified based on their wind speeds, with tropical cyclones being the most common type. Tropical cyclones, also known as hurricanes or typhoons, form over tropical and subtropical waters and can cause significant damage when they make landfall. Cyclones are accompanied by heavy rainfall, thunderstorms, and storm surges, which can cause flooding and landslides. This project aims at alerting the authorities about an imminent areas by monitoring the water level at flood prone areas ,change in air conditions ,high frequency vibrations which have high impact on that area. Every information is recorded and store in the AWS Cloud with is a RFID(Radio Frequency Identification) to send the alert message to the emergency contact provided data to the RFID.

2.Literature Survey

Large-Scale Automatic Vessel Monitoring Based on DualPolarization Sentinel-1 and AIS Data proposed by R.Pelich *et al.* This research proposes a method for ship detection and characterization from SAR data using dual-polar metric descriptors. The method uses automatic algorithms based on the dual-polarization coherence of Sentinel-1. The proposed methodology is tested on Sentinel-1 data acquired over two different areas, the English Channel and Pacific coastline of Mexico. The results show a high detection rate for vessels larger than 60m, and the complementarity of SAR in detecting dark vessels.

Earth observation applications for coastal sustainability: potential and challenges for implementation proposed by E. Politi, S. K. Paterson, R. Scarrott, E. Tuohy, C.

O'Mahony, and W. C. A. Cámara-García. This article discusses the role of Earth observation (EO) in sustainable coastal management. While EO can provide much-needed spatiotemporal information for historical analysis and mapping, its uptake is limited by technical and methodological challenges, as well as governance issues. The article presents examples of how EO can contribute to decision-making in the coastal water zone, and discusses opportunities and challenges for a more solution-led approach to sustainable coastal management, framed by international agreements such as the United Nations Agenda 2030 and the Convention on Biological Diversity.

Shoreline Rotation Analysis of Embayed Beaches by Means of In Situ and Remote Surveys proposed by D. Di Luccio *et al.* This study aims to understand the possible rotation of embayed beaches in Italy over a 64-year period. Differential Global Positioning System (DGPS), GPS RTK, low-altitude aerial imagery, and satellite polar metric Synthetic Aperture Radar (SAR) measurements were used to collect data. Results suggest a correlation between coastline rotation and wave directional shift. The study also investigates the limitations of remote survey methods for identifying shoreline rotation.

A Hierarchical Split-Based Approach for Parametric Thresholding of SAR Images: Flood Inundation as a Test Case proposed by M. Chini, R. Hostache, L. Giustarini, P. Matgen, This study proposes a hierarchical split-based approach to parameterize distribution functions for SAR imagery thresholding algorithms. The method is integrated into a flood-mapping algorithm and tested using SAR images of a flood event along the Severn River in the UK. The results show promising classification accuracies and similarity to a benchmark method based on manual tile selection.

3. System Analysis

3.1 Existing System

The existing is real time flood monitoring system with Wireless Sensor Networks. We observed that this system cannot provide or measures the different environment conditions using Wireless Sensor Networks, and also noticed that the existing WSN of flash flood alerting cannot provide forecasting of future disasters. So in this case of floods it takes more time to send message to the people living in the nearest area so that the people could not save their lives. Usually the flood cannot be predicted but the early detection can be made it means the early alerting system with the help of continuous monitoring can be useful to reduce the loss caused by the floods& Earth quakes.

3.2 Proposed System

Smart Flood & Earthquake, Cyclones Monitoring System is developed to alert the public closest to the area when there is upcoming flood & Earthquake, Cyclone. The collected data from the sensor are gathered and will be forwarded to microcontroller and data will be stored in the AWS Cloud. Then, data will be analyzed and compared. This project will update the data collected and also the admin will able to details of the people who got stucked into disaster. The Server automatically sends an alert message to the emergency contacts.

4.Future Scope

Thus, an efficient and also a cheap solution to a real time Disaster monitoring and early warning system could be provided with plenty of potential for further improvements and optimization on the system side. It can further improved by sending messages to the public places. These experiments were performed at the same camera distance and ambient weather condition. The effect of distance can be added in the next modification As a future modification one could integrate the

camera into an Unmanned Aerial Vehicle platform so that it can be used to analyze real time flood level by moving overwater and into remote areas, which is a more complex extension.

5. Methodology

The methodology of this project is focused on designing and implementing an IOT-based disaster monitoring system. The system will use sensors to collect real-time data on water levels, air conditions, and high-frequency vibrations. This data will be stored in the AWS cloud and analyzed for any slight changes, allowing for early warning and timely response to disasters. RFID technology will also be utilized to detect people who are trapped in disasterprone areas, and their data will be uploaded to the cloud for real-time tracking. The main goal of the system is to enable effective disaster management, reduce damage caused by disasters, and save lives. By utilizing this approach, we hope to contribute to advancing the field of disaster management and bringsignificant benefits to society.

6. System Design

The block diagram of the proposed System is consists of Accelerometer Sensor, Vibration Sensor, MQ 135 Sensor are the sensors to monitor the Flood, Earth Quake and Cyclones. The Arduino with Node mcu is to record the data send to the cloud. The ESP 8266 is Wi-fi Module to communicate with Cloud Server. Then RFID is used to detect the people who stuck during the disaster through sending them alert message to the emergency contact number.

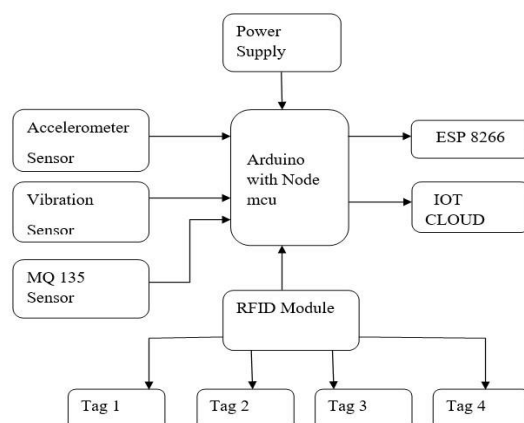


Figure 3 – Block Diagram

6.1 Accelerometer sensor

An accelerometer sensor is a tool that measures the acceleration of any body or object in its instantaneous rest frame. It is not a coordinate acceleration. Accelerometer sensors are used in many ways, such as in many electronic devices, smart phones, and wearable devices, etc.

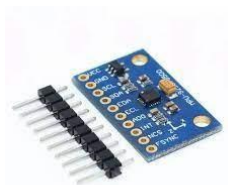


Figure 2 – Accelerometer sensor

6.2 Vibration Sensor

A vibration sensor, or vibration detector, measures vibration levels in machinery for screening and analysis. Maintenance teams use industrial vibration sensors for condition monitoring, giving them insight into the magnitude and frequency of vibration signals.



Figure 3 – Vibration sensor

6.3MQ 135 Sensor

An MQ135 air quality sensor is one type of MQ gas sensor used to detect, measure, and monitor a wide range of gases present in air like ammonia, alcohol, benzene, smoke, carbon dioxide, etc. It operates at a 5V supply with 150mA consumption.



Figure 4 - MQ 135 Sensors

6.4RFID Module

EM18 is a RFID reader which is used to read RFID tags of frequency 125 kHz. After reading tags, it transmits unique ID serially to the PC or microcontroller using UART communication or Wieg and format on respective pins. EM18 RFID reader reads the data from RFID tags which contains stored ID which is of 12 bytes. RFID is an acronym for “radio-frequency identification” and refers to a technology whereby digital data encoded in RFID tags or smart labels (defined below) are captured by a reader via radio waves. RFID is similar to barcoding in that data from a tag or label are captured by a device that stores the data in a database. RFID, however, has several advantages over systems that use barcode asset tracking software. The most notable is that RFID tag data can be read outside the line-of-sight, whereas barcodes must be aligned with an optical scanner. If you are considering implementing an RFID solution, RFID belongs to a group of technologies referred to as Automatic Identification and Data Capture (AIDC). AIDC methods automatically identify objects, collect data about them, and enter those data directly into computer systems with little or no human intervention. RFID methods utilize radio waves to accomplish this. At a simple level, RFID systems consist of three components: an RFID tag or smart label, an RFID reader, and an antenna. RFID tags contain an integrated circuit and an antenna, which are used to transmit data to the RFID reader (also called an interrogator). The reader then converts the radio waves to a more usable form of data. Information collected from the tags is then transferred through a communications interface to a host computer system, where the data can be stored in a database and analyzed at a later time.

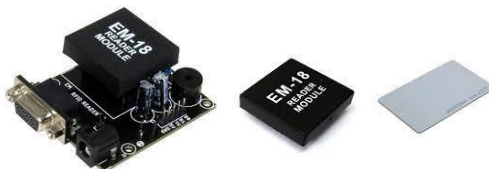


Figure 5 –RFID Module

6.5 IOT Cloud

The Node MCU (ESP8266) is a microcontroller with an inbuilt Wi-Fi module. The total pins on this device are 30 out of which 17 are GPIO (General Purpose Input/output) pins which are connected to various sensors to receive data from the sensors and send output data to the connected devices. The Node MCU has 128KB of RAM and 4MB flash memory storage

to store programs and data. The code is dumped into the Node MCU through USB and is stored in it. Whenever the Node MCU receives input data from the sensors, it crosschecks the data received and stores the received data.

6.6 Power Supply

Power supply is an electrical device which supplies electric power to an electrical load. The first function of a power supply is to convert electric current from a source to the correct voltage, current and frequency to power up the load. As a result, power supplies are also referred to as electric power converters. Some power supplies are separate standalone pieces of equipment while others are built into the load appliances that they power.

6.7 IOT (WI-FI module ESP8266)

The NodeMCU (ESP8266) is a microcontroller with an inbuilt Wi-Fi module. The total pins on this device are 30 out of which 17 are GPIO (General Purpose Input/output) pins which are connected to various sensors to receive data from the sensors and send output data to the connected devices. The NodeMCU has 128KB of RAM and 4MB flash memory storage to store programs and data. The code is dumped into the NodeMCU through USB and is stored in it. Whenever the NodeMCU receives input data from the sensors, it crosschecks the data received and stores the received data. Depending on the data received it sends a pulse to the Relay Module which in-turn acts as a switch to on or off the pump. The operating frequency of the NodeMCU ranges from 80 to 160 MHZ and the operating voltage of this device range from 3 to 3.6V. The Wi-Fi module presents in the NodeMCU range from 46 (indoors) to 92 (Outdoors) Meters.

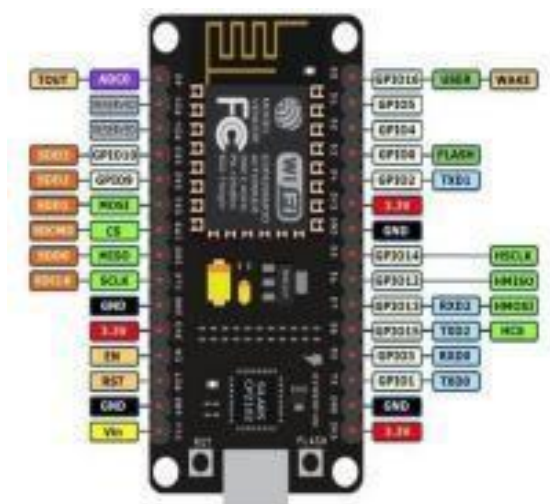


Figure 6- WI-FI module ESP8266

7. Working

7.1 Software Employed :

Arduino IDE The arduino software (IDE) is open source software, which is used to program the Arduino boards, and is an integrated development environment, developed by arduino.cc. Allow to write and upload code to arduino boards. And it consists of many libraries. Arduino software (IDE) is compatible with different operating systems (Windows, Linux, Mac OS X), and supports the programming languages (C/C++). The Arduino software is easy to use for beginners, or advanced users. It uses to get started with electronics programming and robotics, and build interactive prototypes. So Arduino software is a tool to developed new things. And create new electronic projects, by Anyone (children, hobbyists, engineers, programmers, etc).

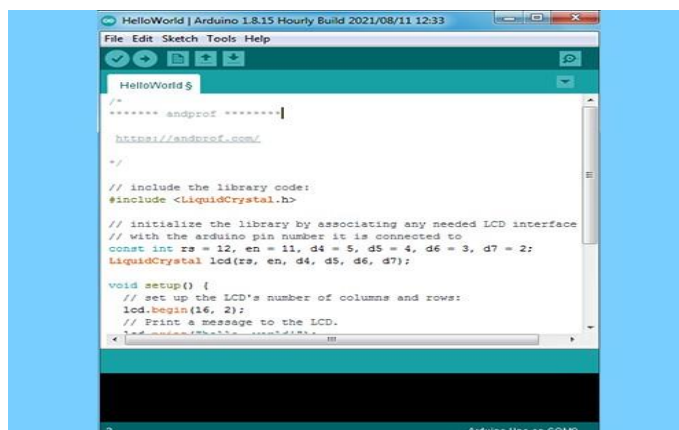


Figure 7- Arduino software interface

Menus section: Menus are the main menus of the program, and they are 5 menus (File, Edit, Sketch, Tools, Help), and they are being used to add or modify the code that you are writing.

Toolbar section: The toolbar is the most important section in the Arduino software, because it contains the tools that you will use continuously while programming the Arduino board. These tools are:

Verify: this button use to review the code, or make sure that is free from mistakes.

Upload: this button is use to upload the code on the arduino board.

New: this button use to create new project, or sketch (sketch is the file of the code).

Open: is use when you want to open the sketch from sketchbook.

Save: save the current sketch in the sketchbook. **Serial monitor:** showing the data which have been sent from arduino. **Code editor section:**

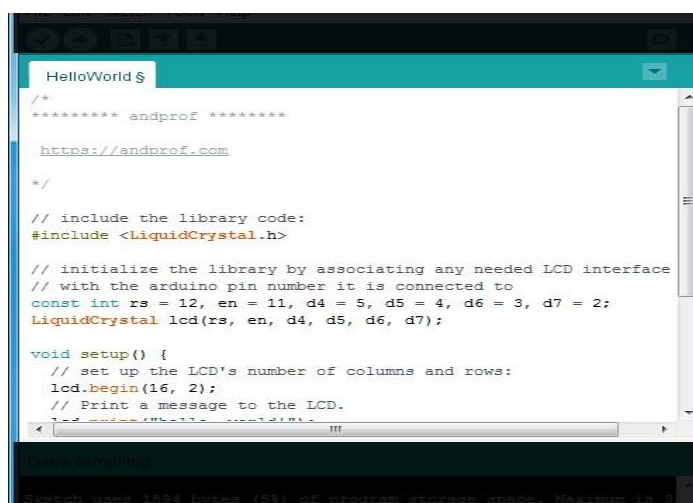


Figure 10-code editor section Code editor is liberator of codes, is the white space in the program, in which codes are been writing, and modifying on it.

Status bar section: Status bar is a space can be found down the code editor, through it showing the status of operation's completion (compiling, uploading, etc)

Program notifications section: Program notifications this program showing you the mistakes of codes, and some problems that can be face you during the programming process. And clarifies to you the type of the mistake or the problem which happened and it reason. And it presents some instruction through it, which you have to apply to process the mistake or the problem.

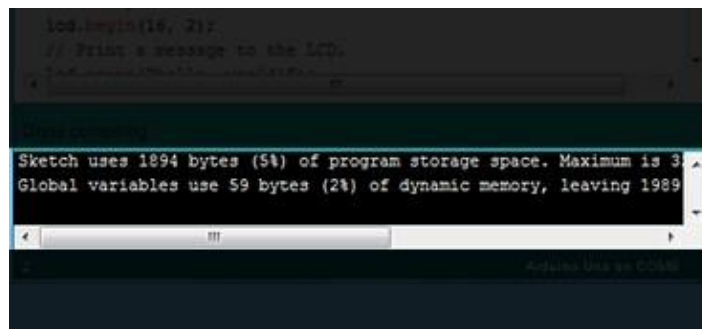


Figure 12-Program notifications section

Serial port & Board selections: Serial ports selections is a space in which the program showing you the type of the port which is used to connect the arduino by computer.

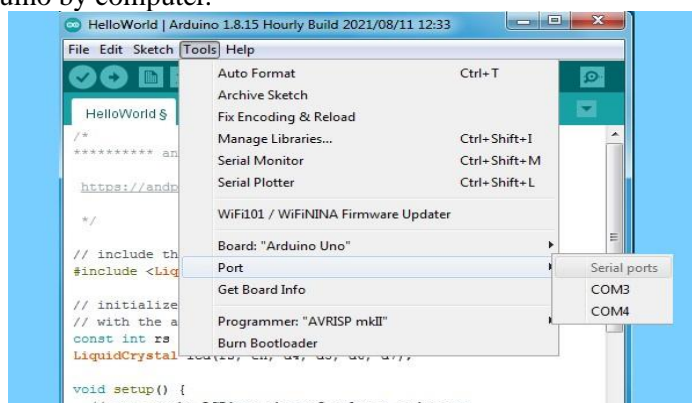


Figure 13- Serial port selection

Board selections is a space in which the program showing you the type of the arduino board.

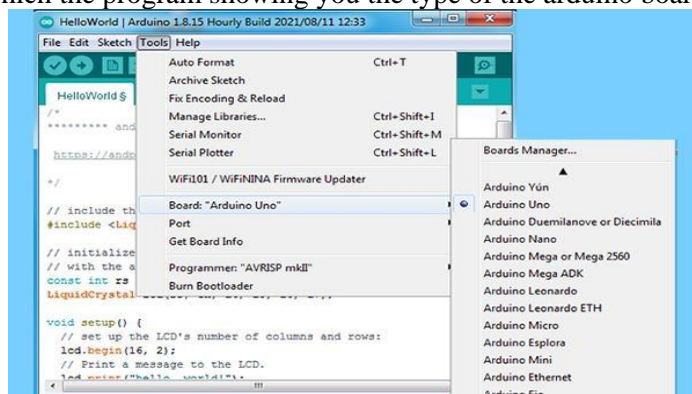


Figure 14-Board selection

7.2 Hardware Employed

NodeMCU ESP8266: The ESP8266 is, the name of a microcontroller designed by Expressive Systems. It is a self-contained Wi-Fi networking solution offering as a bridge from the existing microcontroller to Wi-Fi and is also capable of running self-contained applications. For less than \$3, it can monitor and control things from anywhere in the world – perfect for just about any IOT project.

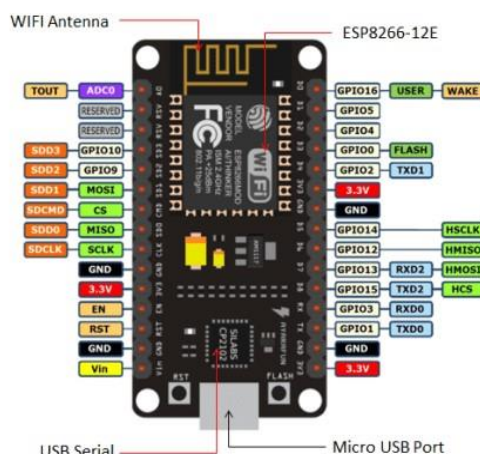


Figure 14 - Pin out

The **NodeMCU_ESP8266** has 30 pins in total out of which there are 17 GPIO pins. GPIO stands for General Purpose Input Output. There are the 9 digital pins ranging from D0-D8 and there is only one analog pin A0, which is a 10 bit ADC. The D0 pin can only be used to read or write data and can't perform other options. The ESP8266 chip is enabled when the EN pin is pulled HIGH. When pulled LOW the chip works at minimum power. The board has a 2.4 GHz antenna for a long-range of network and the CP2102 is the USB to TTL converter. The development board equips the ESP-12E module containing ESP8266 chip having **Ten silica Xtensa® 32-bit LX106 RISC** microprocessor which operates at 80 to 160 MHz adjustable clock frequency and supports RTOS. There's also **128 KB RAM and 4MB of Flash memory** (for program and data storage) just enough to cope with the large strings that make up web pages, JSON/XML data, and everything we throw at IOT devices nowadays. The ESP8266 Integrates **802.11b/g/n HT40 WiFi transceiver**, so it can not only connect to a Wi-Fi network and interact with the Internet, but it can also set up a network of its own, allowing other devices to connect directly to it. This makes the ESP8266 NodeMCU even more versatile.

Power Requirement: As the operating voltage range of ESP8266 is **3V to 3.6V**, the board comes with an LDO (low dropout) voltage regulator to keep the voltage steady at 3.3V. It can reliably supply up to 600mA. It has three 3v3 pins along with 4 GND pins. The power supply is via the onboard **Microbe USB connector**. Alternatively, if you have a regulated 5V voltage source, the **VIN pin** is used to directly supply the ESP8266. Moreover, it requires 80mA Operating Current and 20 μ A during Sleep Mode.

Various Peripherals and I/O: The ESP8266 supports *UART*, *I2C*, *SPI* communication protocols. It also has 4 PWM channels which can be used to drive motors, the brightness of the LED, etc. Moreover, there are 2 channels of the UART protocol. The **ADC (A0)** can be used to control any analog device. The **CMD** is the Chip select pin used in the SPI protocol.

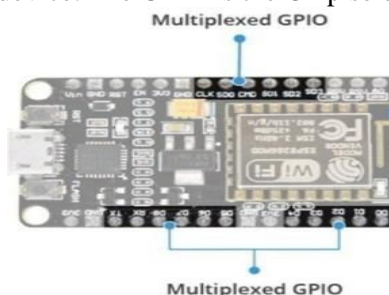


Figure 15- Peripherals & I/O

On-Board buttons and LED: ESP8266 has 2 onboard buttons along with an on-board LED which connects with the D0 PIN. The two buttons are FLASH and RST. **FLASH pin**– It is to download new programs to the board
RST pin – It is to reset the ESP8266 chip



Figure 16The LED On-board of ESP8266

Development Platforms: The prominent platforms include the Arduino IDE and the Explorer IDE. Other development platforms that can be equipped to program the ESP8266 are the Espruino – JavaScript SDK and firmware closely emulating Node.js, or Mongoose OS – An operating system for IOT devices.

8.Result

The existing disaster detection system is capable of identifying natural disasters, but lacks the capability to store data efficiently. The proposed system, however, not only detects disasters but also stores data in the cloud, allowing for quick access and analysis. By utilizing cloud storage, the proposed system ensures that critical information is not lost and can be easily retrieved by disaster response teams. This improves response times and helps save lives. Overall, the proposed system is a more efficient and effective way to manage disaster data.

9.Conclusion

In conclusion, the proposed system offers real-time monitoring which is crucial for disaster management. By using RFID technology, the system can also detect the number of people stuck in the affected areas, allowing for better response and rescue operations. This is particularly important during periods when there are drastic changes in environment conditions. Overall, the system's ability to monitor and detect changes in environment conditions and people's locations using RFID makes it a valuable tool in disaster management and can help save lives.

10.References

- [1] A. H. Hartog, an Introduction to Distributed Optical Fiber Sensors. Boca Raton, FL, USA: CRC, 2017 [2] Z. He and Q. Liu, "Optical fiber distributed acoustic sensors: A review," J. Lightw. Technol., vol. 39, no. 12, pp. 3671–3686, 2021
- [3] P. Stajanca, S. Chruscicki, T. Homann, S. Seifert, D. Schmidt, and A. Habib, "Detection of leak-induced pipeline vibrations using fiber—optic distributed acoustic sensing," Sensors, vol. 18, no. 9, 2018, Art. No. 2841 [4] P. G. Hubbard et al., "Dynamic structural health monitoring of a model wind turbine tower using distributed acoustic sensing (DAS)," J Civil Struct. Health Monit. vol. 11, pp. 833–849, 2021
- [5] Enhanced Flood Detection System using IoT A. Pravin;T.Prem Jacob;R. Rajakumar,2021
- [6] Extreme Weather Event (Cyclone) Detection in India Using Advanced Deep Learning Techniques. Atharv Dabhade; Samshitha Roy;Marwa S. Moustafa;Sayed A.Mohamed;Reda El Gendy;Shovan Barma,2021
- [7] IoT-Based Disaster Detection Model Using Social Networks and Machine Learning. Khalid Alfalqi;MartineBellaiche,2021
- [8] Implementation of Flood Warning System using IoT.E Devaraj Sheshu;N Manjunath;S Karthik;U Akash[9] Systematic Mapping Study on RFID Technology. Achraf Haibi;Kenza Oufaska; Khalid El Yassini;Mohammed Boulmalf;Mohsine Bouya,2022



AN IOT- BASED AUTO CONTROLLED SYSTEM FOR ELECTRICAL APPLIANCES BASED ON HUMAN MOVEMENT IN SMART ROOMS

Dr. G. Vinoth Chakkaravarthy, Paarkavi Priya S, Harshini T, Kharshitha Bhuvani E, Divya Sri N

gvc@vcet.ac.in, paarkavi19092001@gmail.com, harshinit1608@gmail.com,
kharshithabhuvani@gmail.com, divyasri7702@gmail.com

Velammal College of Engineering and Technology, Madurai

Article History: Received: 12.05.2023

Revised: 25.05.2023

Accepted: 05.06.2023

Abstract

The ever-growing demand for larger integration density, higher bandwidth, and lower power
Over the past few years, due to the increase in consumption of daily usage resources, there has been rapid growth in demand for energy. Energy is derived from fossil fuels and as time passes fossil fuels deplete. So, we are in immediate need of an energy conservation system. For the implementation of this system, the Internet of Things (IoT) provides the solution to perform the tasks. This paper presents a cost-efficient, and energy-efficient Internet of Things (IoT) based system where different devices can be connected over the Internet resulting in conserving energy. Also, this paper proposes an additional feature of saving time by turning manual work into automatic, that is to automate the user attendance system. The proposed prototype of "IoT Based Electricity Conservation and Biometric Attendance System" focuses on integrating the above two functionalities and can be accomplished using a PIR sensor and fingerprint sensor. If the PIR detects any motion, it sends a signal to NodeMCU which in turn triggers the relay to turn on the lights and turn off if no motion is detected. The fingerprint sensor scans the biometric of the person and marks attendance for that day.

Keywords-PIR sensor, NodeMCU, Energy conservation, Fingerprint sensor, Automation, Internet of Things, Cost-effective, Time conserving, Energy efficient.

I. INTRODUCTION

Using IoT (Internet of Things), devices with different functionalities can be connected over the Internet. In this project, two different features need to be integrated so the concept of IoT is used. The modules of this project are Energy Conservation System and Biometric Attendance System. Energy conservation involves turning on/off the lights if there are people in the near surroundings. In [1], to detect the presence of people PIR sensor is used. A PIR sensor is a type of IR sensor that monitors variations in the temperature

radiated by nearby objects to detect motion. When motion is detected the PIR sensor outputs a high signal on its output pin which acts as an input to NodeMCU. NodeMCU is a microcontroller that is featured with Wi-Fi capabilities, analog pins, digital pins, and serial communication protocols. The logic signal from the PIR sensor can be read by NodeMCU which in turn sends a signal to the relay [1]. Then the relay supplies the volt to the connected devices which can be a bulb, a tube light, a fan, or any other electrical device. Thus, the control of the light intensity is accomplished through NodeMCU [2].

The second part of this project is to maintain an automated biometric attendance system through a fingerprint scanner. In [3], the fingerprint scanner used here is an optical fingerprint scanner which is quick and produces accurate results. This provides a good 2D image and a high resolution of the exact picture. This scanner uses an LED (Light Emitting Diode) light to illuminate the finger. The fingerprint image is scanned and developed by the sensor by identifying the light and dark regions produced by the fingerprint ridges and deduced by [3]. When a person touches their finger on the glass plate, which has a rough surface, the scanning process begins. Initially, when a new user comes in, they have to register their fingerprint through the website and their biometrics will be saved along with the user's information. Once registration is done, the device can recognize the fingerprint through already saved templates and mark the attendance of the users accordingly. Further, the user logs can be exported to excel and can be considered for further use [4].

Following are the sections that make up the remainder of the paper. The next section of the paper, section II narrates related works and problem statements. Section III presents process flow, a conceptual model that includes a flow chart, connection, and implementation. The results & discussion and conclusion are given in section IV which closes the paper by suggesting future research directions.

II. RELATED WORKS

Some of the previous works related to this paper are listed in this section. It has been recognized that IoT technologies play a crucial role in energy conservation in a variety of domains, including industry, transportation, health, and smart cities.

R. Yasodharan et.al stated that their IoT project will help the staff present in the classroom to allow them to control the classroom using an Android application.

The overall system design is mainly based on Arduino Mega 2560. The Android application is developed using Blynk software or Blynk android application. We can supervise the state of sensors connected to the Arduino board and we can control the modules by simply enabling some options in the Android application on our smartphone [5].

In their paper, Isanka Diddeniya, Niroshan Gunawardana, Kaveendra Maduwantha, Kaveenga Koswattage, Mahadurage Viduni Randima, and Vasanthapriyan proposed a cost-effective energy-efficient Internet of Things (IoT) based device controlling system that can be used with minimum user interaction, in the case of operating any electrical device. The proposed prototype of "IoT Based Energy Efficient Smart Classroom" is implemented to reduce the wastage of electricity in a lecture hall at the Sabaragamuwa University of Sri Lanka. The system controls the operations of electrical devices (such as ON/OFF) by identifying the presence of humans in a specific area [6].

In the year 2021, Mohd Wafi Nasrudin, Nur Asyikin Nordin, Iszaidy Ismail, Mohd Ilman Jais, Amir Nazren Abdul Rahim, and Wan Azani Mustafa proposed that electricity-saving can be achieved through the efficient use of energy such as turning off lights and electrical appliances when not in use. Therefore, this work proposed the smart classroom for electricity-saving with an integrated IoT System to prevent wasting electricity in the classroom. The main objective of this work is to control the lighting systems and fans by using the IoT application and sensor system. Blynk application software is used to display the status of the classroom[7].

Tripti Jain et-al present light on simple, easier, and portable methods for student attendance in which IoT is used. The student's attendance is recorded using a fingerprint-based biometric scanner and then data is secured safely over cloud

storage. The system averts the proxy attendance, time will also be saved, thereby the reliability of students' attendance information is also maximized. The student's data are loaded securely over the cloud and can be easily fetched according to the need [8].

III. PROBLEM STATEMENT

There has been an increase in the use of energy in India since 2000, with coal, oil, and solid biomass accounting for 80% of

the demand. Economic development, a growing population, and technological advancements are all contributing factors to increased energy consumption. Due to the fact that most of these resources are mostly non-renewable resources, they get depleted over time. It would be difficult for living things to live if all resources ran out. So, we should start conserving the remaining resources for future needs. Also, we need to start working on time management. Effective time management helps us to achieve our goals faster and increase productivity.

IV. CONCEPTUAL MODEL

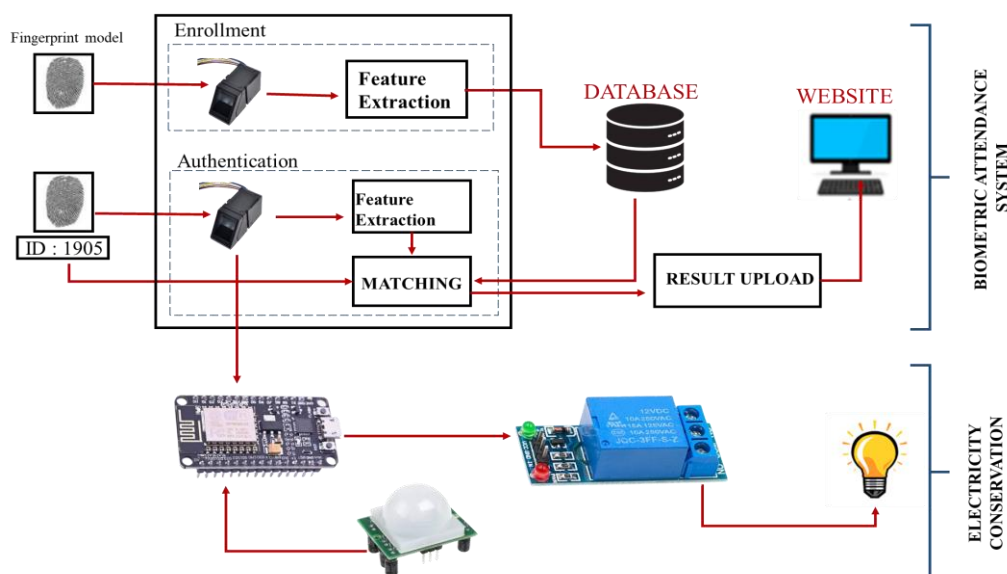


Fig.1. represents the complete architecture diagram of this project.

This involves two different modules namely,

A. CONSERVATION OF ELECTRICITY

B. FINGERPRINT-BASED BIOMETRIC ATTENDANCE SYSTEM

Getting focused on the first module 'Conservation of Electricity' is done using a PIR sensor. PIR sensors detect motion, usually used to determine whether a human has entered or left their range. Besides being small, inexpensive, and low-power, they are also easy to use and do not wear out. IR motion sensors are also known

as PIR, passive infrared sensors, or pyroelectric sensors. By utilizing all these advantages, students' presence in the classroom is identified and lights are turned on and off accordingly. The second module 'Fingerprint Based Biometric Attendance System' involves a website to register their fingerprint and get details of their logging in and off timing. After registration, the students enter the classroom by making attendance with their fingerprints. Their login time will be noted on the website. Soon after the class ends, students are asked

to authenticate themselves with their fingerprints to calculate their log-off timing.

V. ARCHITECTURAL FRAMEWORK

This paper proposes two functionalities that are integrated into the Internet of Things. As a result of both of these functionalities, a reduction in manual work is achieved, which in turn saves energy. An IoT-based classroom electricity-saving system that saves more electricity than manual switching off appliances in a classroom will

demonstrate the benefits of an IoT-based system in today's world, especially for saving electricity. As an added feature, a biometric attendance system has been integrated, which helps teachers manage the present and absent status of users with less effort. To implement this paper, we will be using a NodeMCU Microcontroller, PIR (Passive Infrared Sensor) and a Relay Control for conserving electricity, and Optical Fingerprint Sensor Module along with an OLED display for Biometric Attendance System.

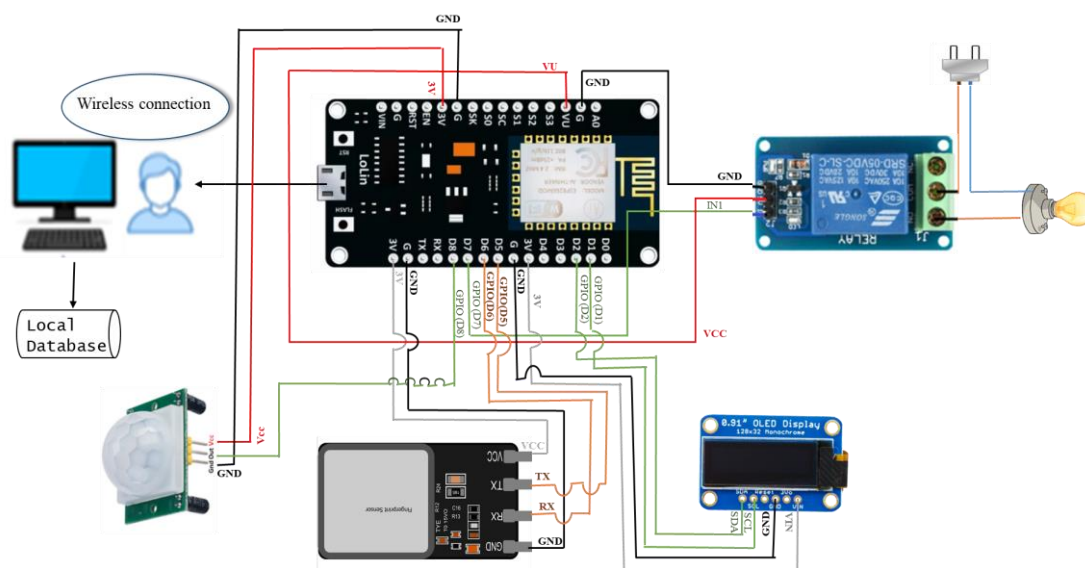


Fig.2. Circuit Diagram

Fig.2 apparently indicates the circuit diagram of this project where NodeMCU acts like a bridge for two features that are been discussed in detail in the following chapters.

Focusing on the explanation of the modules done in this project, this project is divided into two modules,

V.1. CONSERVATION OF ELECTRICITY

V.2. FINGERPRINT-BASED BIOMETRIC ATTENDANCE SYSTEM

Stepping toward the next part of the explanation,

V.1. CONSERVATION OF ELECTRICITY

1) Connections:

The pins (Output, Input, and Ground) of the PIR sensor and the pins (Output, Input, and Ground) of the Relay Module are connected to the NodeMCU ESP8266.

2) Implementation:

We have taken a classroom of size 6m by 6m, having 2 fluorescent tube lights. The next consideration was based on the Fresnel zone, thus the sensors were placed above the fan and the lamp so that the clearance is met, such that the sensors can detect every motion in the classroom to switch the fan or lamp automatically. The sensor will be able to detect body heat ranging from 0°C - 50

°C which is the average range comfortable enough for the system to detect the presence of users or an empty classroom.

After the data has been recorded by the PIR sensor, it will be sent to the microcontroller. The microcontroller has been programmed to do the following:

Table I: Procedure for Microcontroller

Steps	Instructions
Step: 1	Data is collected through the infrared radiation emitted by hot bodies.
Step: 2	An electrical signal is generated when the sensor detects infrared radiation. An internal PIR sensor has two halves, one of which is positive and the other negative.
Step: 3	Thus, one half detects a hot body's motion and the other half creates a signal.
Step: 4	Output signals are generated by the difference between the two signals.

Primarily, this sensor consists of Fresnel lenses which are bifurcated to detect the infrared radiation produced by the motion of a hot body over a wide range or specific area.

For the implementation of the design, the following software was used:

- i) Windows operating system (windows 10)
- ii) Arduino IDE (Integrated Development Environment).

The Pseudo Code for energy conservation using a PIR sensor has been mentioned in short. The concept mentioning pseudo code in this paper is to figure out some points like easy to understand even for non-programmers and can be quickly and easily converted into an actual programming language due to similarity to a programming language. It doesn't matter if

there are errors in the syntax-it is usually still obvious what is intended.

3) Hardware Specification:

i) Specification of NodeMCU

In addition to its ability to act as a standalone system, ESP32 can be used as a slave device to a host MCU, reducing communication stack overhead on the main application processor. Through its SPI / SDIO as well as I2C / UART interfaces, the ESP32 can interface with other systems for Wi-Fi and Bluetooth functionality.

There is 128 KB of RAM and 4MB of Flash memory on the NodeMCU for storing data and programs. The device's high processing power along with its Wi-Fi and Bluetooth capabilities make it ideal for Internet of Things projects.

TABLE II. Hardware specification of NodeMCU

DESCRIPTION	SPECIFICATION
Microcontroller	ESP-8266 32-bit
Node MCU Model	Clone LoLin
Node MCU Size	58mm x 32mm
Pin Spacing	1.1" (27.94mm)
Clock Speed	80 MHz
USB to Serial	CH340G
USB Connector	Micro USB
Operating Voltage	3.3V
Input Voltage	4.5V-10V
Flash Memory/ SRAM	4MB/64KB
Digital I/O Pins	11
Analog In Pins	1
ADC Range	0-3.3V
UART/ SPI/ I2C	1/1/1
Wi-Fi Built-In	802.11 b/g/n

b) Specification of PIR Sensor

TABLE III. Hardware specification of PIR sensor

DESCRIPTION	SPECIFICATION
Model	PIR HC-SR501
Operating Voltage(VDC)	4.5~ 20
Average Current Consumption(mA)	0.06
Distance Measuring Range(CM)	300 ~ 700
Output Type	(High/ Low-level Signal)3.3V TTL output

V.2) FINGERPRINT-BASED BIOMETRIC ATTENDANCE SYSTEM

There are many types of biometric systems. This research paper is aimed at implementing a system that is capable of identifying students in institutes and marking their attendance. As a result, fingerprint recognition is used to mark the

attendance of the students. This system provides flexibility in optimizing the attendance of the students, rather than identifying one by one the absentee's details manually.

i) Flow Chart:

Considering oneself as a new user, the user

has to register their fingerprint through the fingerprint sensor module and the registered data will be stored in the institution or an organization's database.

A new feature of this website extends the functionality of the fingerprint tracking system by allowing the administrator or supervisor to remove a user's fingerprint if he or she leaves the institution or leaves the campus.

Managing people's daily records is a difficult task for most organizations and maintaining their records is not an easy job. This biometric attendance system reduces the manual workload and effectively manages time. Based on the fingerprint stored in the institution's database, this track mainly involves extracting minutiae points from model fingerprint images and matching them with the stored fingerprints.

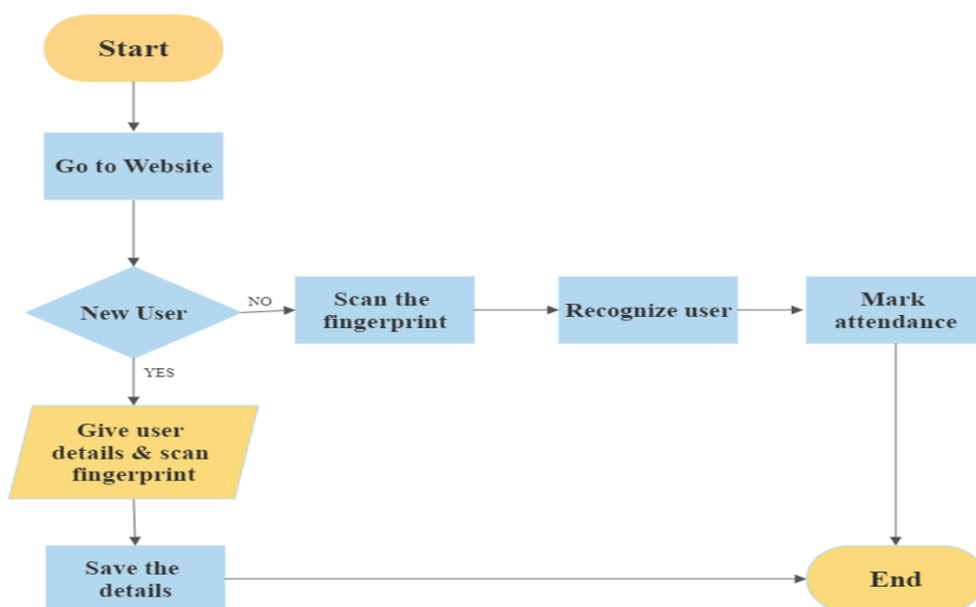


Fig.3. Flow chart of attendance monitoring website

ii) Connections:

The pins (Receiver, Transmitter, Voltage, Gnd) of the Optical Fingerprint sensor module along with the OLED display are connected to the NodeMCU ESP8266. The organic light-emitting diode (OLED), also called organic electroluminescent diodes (OLEDs), is a light-emitting device in which emissive electroluminescent layers are organic compounds that emit light when a current flows through them. It consists of an organic layer that is sandwiched between two electrodes, with at least one electrode being transparent. OLEDs are used to create digital displays on televisions, computer monitors, smartphones, and portable systems such as handheld game consoles. Developing white OLED devices

for use in solid-state lighting applications is a major area of research.

The fingerprint sensor is connected to the PC through Wi-Fi and the information is stored in Database for further retrieval and usage.

Implementation of the design was carried out using the following software:

- A) Windows operating system (windows 10)
- B) Arduino IDE.

The Hardware specifications are mentioned below,

iii) HARDWARE SPECIFICATION:

a) SPECIFICATION OF FINGERPRINT SENSOR MODULE:

TABLE IV. Hardware specification of a fingerprint sensor module

DESCRIPTION	SPECIFICATION
Model	AS608
Resolution	500dpi
Supply Voltage	3.3V
Peak Current	<60mA
Window area(mm)	15.3 x 18.2

4) Implementation:

Initially, users are asked to register for their fingerprint through the website. The fingerprint sensor and PC are connected via Wi-Fi and the sensor gets transmitted & received through NodeMCU. Databases are used for maintaining the user's attendance record.

Immediately after the registration and authentication process is complete, time in is recorded while the user enters the classroom by using fingerprint-based biometric attendance, and time out is recorded on exit. You can export all these user logs (Name, serial number, fingerprint

A. Energy Conservation System

ID, Time In, Time Out, and Date logs) in Excel.

VI. RESULTS & DISCUSSIONS

By implementing the energy conservation and biometric attendance system, we were able to achieve the objectives of this project that is to conserve energy and to save human time by turning manual work into automatic.

Here are the snapshots of this project module taken during the system execution. Each snapshot specifies different features that are implemented in this project.

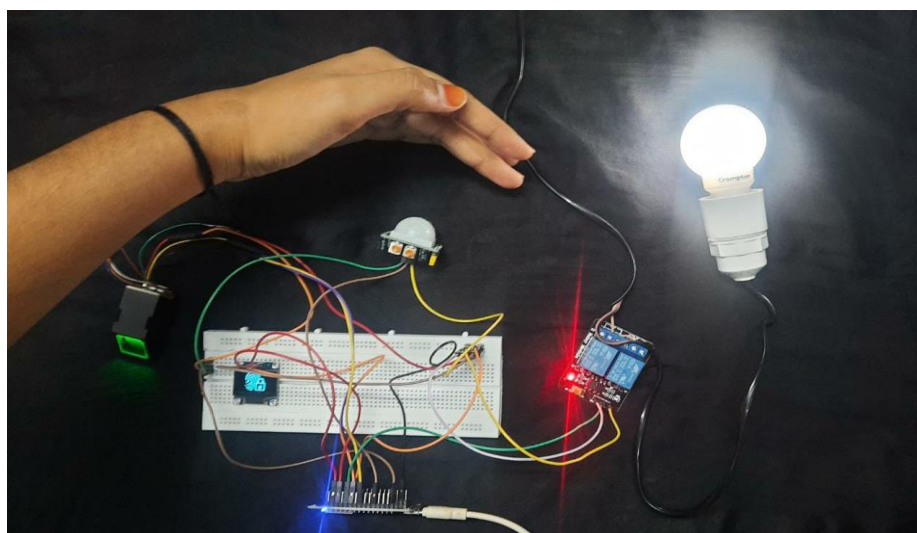


Fig.4. Implementation of energy conservation system

Based on the specified objective, energy conservation has been accomplished cost-effectively with the help of a PIR sensor as shown in Fig.4. This figure demonstrates energy conservation through motion

detection. When the user enters the room, the motion detection load is operated. So, the user need not consider turning on/off the appliances.

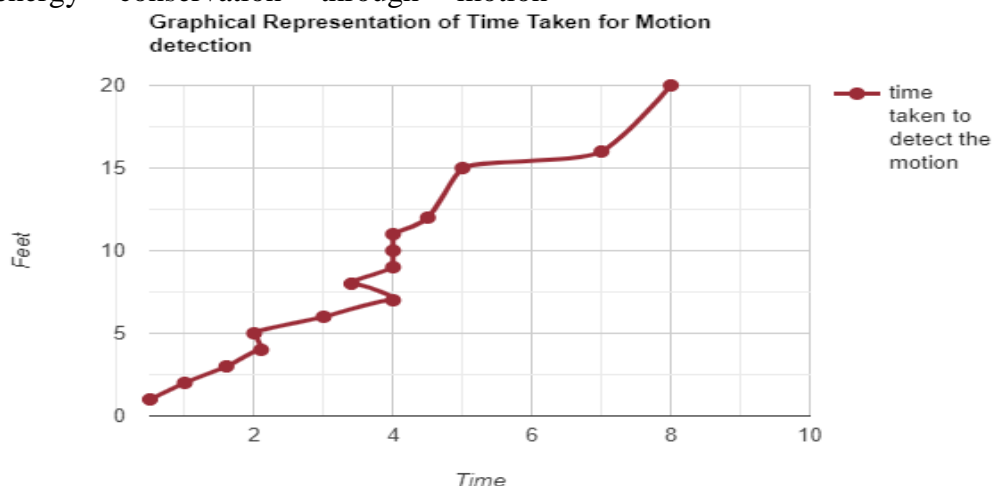


Fig.5. Graphical representation of Time Taken for Motion Detection

The linear representation of the graph shown in Fig.5 demonstrates the relation between time and distance (in feet). The PIR sensor used in this project covers a distance of 20 feet and the average time taken to cover this distance is 6 seconds.

A detailed description of the graph involves the x-axis which represents the time taken to detect and the y-axis which represents the number of feet covered by the PIR sensor. This graph does not produce an exact linear report but can be produced by sensitivity adjustments.

The sensitivity adjustment can be done by using the screw in the PIR sensor, turning them anti-clockwise up to which the desired sensitivity is being achieved.

B. Biometric Attendance System

Getting focused on the second functionality, the main goal of saving time has been fulfilled with the help of the registration website and AS608 Fingerprint Sensor Module.

The process proceeds in this manner, initially, the user is asked to register and authorized themselves with their fingerprint and with additional information like email ID and roll number.

Along with registration addition operations like updating and deletion can be done on the same website so that any changes in the existing user's details can be performed and any user dropping out from the institution or organization can be permanently deleted. Fig.6 illustrates the above-mentioned statement.

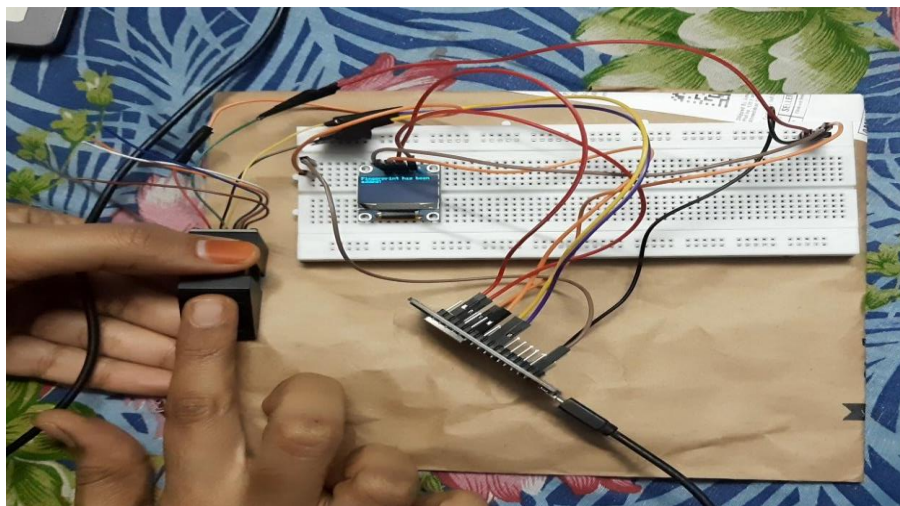


Fig.6. Registering your fingerprint for the first time through the website

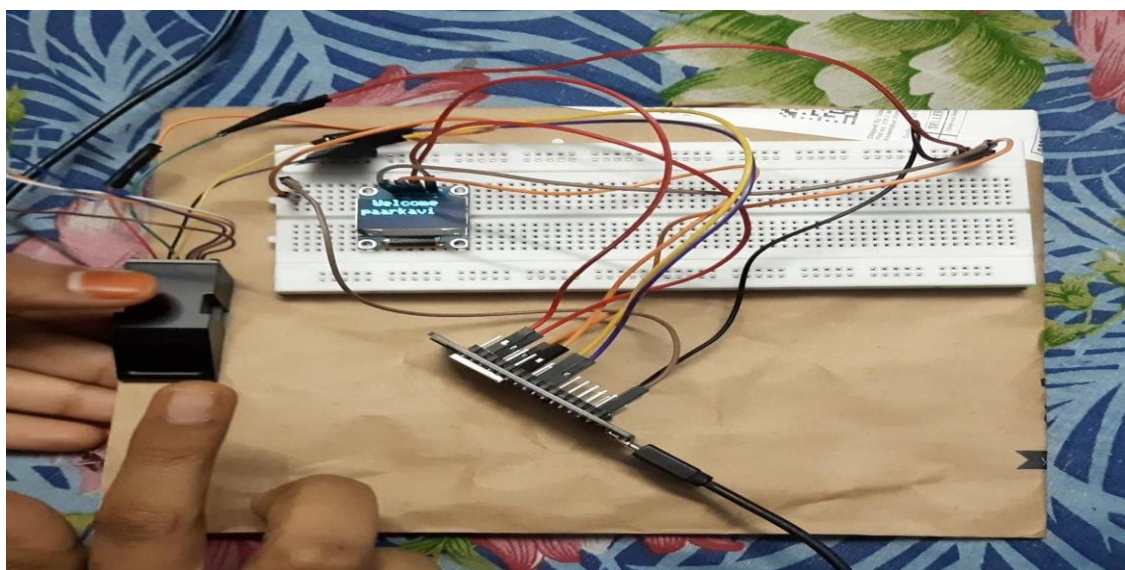


Fig.7. Welcome message displayed on the LED after it recognizes the user

Fig.7 manifests a welcome message for new users and gives them an identity. Once the user has been registered successfully each user gets an authorized fingerprint ID that helps the module to differentiate each user.

ID	Name	Serial Number	Fingerprint ID	Date log	Time In	Time Out
8	paarkavi	91	90	15-03-2023	22:49:52	22:49:59
7	Kirthana	564	87	15-03-2023	22:45:57	22:46:03
6	Aadhi	879	33	15-03-2023	22:45:40	22:45:46
5	paarkavi	95	95	15-03-2023	14:16:22	14:16:28
4	Kirthana	91	47	15-03-2023	14:12:06	14:12:12
3	varthia	900	10	15-03-2023	13:35:24	13:35:27
2	varthia	900	10	15-03-2023	13:33:05	13:35:27
1	varthia	900	10	15-03-2023	13:06:57	13:35:27

Fig.8.Attendance report downloaded as Excel

Once the attendance record has been completed, the one who handles the session can get all these records in the form of an Excel sheet which can be downloaded from the website. The snapshot of the downloaded Excel has been presented in Fig.8. And the Excel sheet that is generated through the website includes the fields like user name, fingerprint ID, roll number, date, log-in time, and logout time.

VII.FUTURE WORK

We have developed this system using a breadboard, which is a board for prototyping. In the upcoming future, we have planned to develop the system as a real-time working product using PCP (Primary Cross Connection Point). PCPs are control panels for all cables that go on to the data processor from the exchange. The main lines from the exchange terminate here. The PCP is responsible for controlling all cables leading to the DP.

Also, this system can be further enhanced by incorporating a sensor to measure room temperature and light intensity so that fans can be switched on if the temperature is high and lights can be turned on only when the surroundings are dark. As a result, we will be able to save even more energy than usual.

VIII. CONCLUSION

This paper presents an IoT-based energy conservation system that uses passive infrared radio sensors to turn off lights in classrooms when users aren't present and a

Biometric attendance system using Fingerprint sensors to maintain users' attendance reports. The electricity conservation system was placed in a range (6 feet surround) and connected to the light that covers that particular area. Biometric Attendance system reduces the workload of staff through automation. The cumulative of these systems comes with the advantage of saving energy, time, and cost.

REFERENCES

- [1] Cynthia Twumasi, Koffi Agbeblewu Dotche, Francois Sekyere, Energy saving system using a PIR sensor for classroom monitoring, IEEE, 2017
- [2] Talal H Noor, El-Sayed Atlam, Abdulqader M. Almars, Ayman Noor, Amer S.Malki, IoT Based Energy Conservation Smart Classroom System, Intelligent Automation and Soft Computing, Volume 35 Issue 3, 2023
- [3] M. A. Meor Said, M.H. Misran, M. A Othman, M M Ismail, Biometric Attendance, International Symposium on Technology

Management and Emerging Technologies (ISMET 2014), May 24, 2014

[4] Aswinth Raj, IoT-Based Biometric Attendance System using Arduino and Thingsboard, May 2019

[5] Yasodharan R, Bennaiah D, Hari Krishnan V, Karthick S, Prince Roy, IoT Based Classroom Automation Using Arduino, International Journal of Trend in Scientific Research and Development, Volume 2 Issue 2, February 2018

[6] Isanka Diddeniya, Niroshan Gunawardana, Kaveendra Maduwantha, Kaveenga Koswattage, Mahadurage Viduni Randima, Vasanthapriyan, IoT based Energy efficient smart classroom, International Journal of Multidisciplinary Engineering Science Studies, Volume 6 Issue 12, December 2020

[7] Mohd Wafi Nasrudin, Nur Asyikin Noordin, Iszaidy Ismail, Mohd Ilman Jais, Amir Nazren Abdul Rahim, Wan Azani Mustafa, Smart Classroom for Electricity saving with Integrated IoT system, Journal of Physics: Conference Series, Volume 2107, October 2021

[8] Tripti Jain, Urvashi Tomar, Umang Arora, Swati Jain, IoT-based Biometric Attendance System, International Journal of Electrical Engineering and Technology, Volume 11 Issue 2, May 2020

[9] D Sathiyaraj, Jeevanantham M, Dayalan S, Hariharan M, Suraj Punj, Classroom Automation Based IoT, Journal for Multidisciplinary Research Volume 11 Issue 4, 2021

[10] Shyamli u. Kamane, Akshay S. Bhoyar, Shubham V. Kusange, Swati M. Gajbe, Stuti S.Patil, Smart Classroom Automation System using Arduino and IoT, International Journal of Research and Analytical Reviews, Volume 7 Issue 1, March 2020

[11] Vishal Kolambkar, Tejas Patil, Sagar Anute, Prof. Rasika Shintre, Smart Classroom Automation Based on IoT, International Research Journal of Engineering and Technology Volume 7 Issue 3, March 2020

[12] S.A.I.P. Diddeniya, H.D.C.N. Gunawardana, K.Maduwantha, K.R.Koswattage, IoT Based Energy Efficient Smart Classroom, Journal of Multidisciplinary Engineering Science Studies, Volume 6 Issue 12, December 2020

[13] Kaustav Mani Pathak, Priyanka Jain, Swati Yadav, Veena Mittal, Prateek Jain, An IoT-based Mechanism for Automatic Classroom Electricity Saving, IEEE, October 2019

[14] Ganesh Kakade, Prathamesh Shivpuje, Sanket Awale, Shubham Rawale, IoT Based Classroom Automation System, International Research Journal of Engineering and Technology (IRJET), Volume 6 Issue 12, December 2019

[15] Sebastian Chennattu, Aditya Kelkar, Aaron Anthony, Sushma Nagdeote, Portable Biometric Attendance System using IoT, IEEE, November 2019

[16] Sri Madhu, Kavaya Kanagotagi, Devansh, IoT-based Automatic Attendance Management System, International Conference on Current Trends in Computer, Electrical, electronics and Communication (ICCTCEEC-2017)

[17] K C Arun, Mubashir Ali, Ayesha Siddique, Muhammad A Asim, Zaka Ullah, Energy Efficient Classroom Automation using IoT, June 2017

[18] Mohammad Kamrul Hasan, Musse Mohamud Ahmed, Bishwajeet Pandey, Hardik Gohel, Shayla Islam, Izzul Fitrie Khalid, IoT-Based Smart Electricity Monitoring Control System Using Usage Data, Wireless Communications and Mobile Computing, Volume 2021, October 2021

[19] Prabesh Paudel, Sangkyoon Kim, Soonyoung Park, A Context-Aware Architecture for Energy Saving in Smart Classroom Environments, IEEE International Conference On Consumer Electronics, 2019

[20] Fawaz Alassery ,A Smart Classroom of Wireless Sensor Networks for Students Time Attendance System, IEEE Integrated STEM Education Conference (ISEC),2019.



Accident Alert Along With Fatigue Detector

¹Mrs. K.Arunasakthi, ²M.Durga Vishalini, ³V.Priyanka, ⁴S.K.Rithiha, ⁵B.T.Venmathee

^{1,2,3,4,5}Department of Computer Science Engineering, Velammal College of Engineering and Technology, Madurai

aruna.sakthi10@gmail.com, durga19cse004@gmail.com, priyankavasudevan2002@gmail.com, 29.rithi@gmail.com,

matheethil@gmail.com

ABSTRACT

This paper describes for maintaining the car's safety and security through critical action. We are unable to look after our own while we operate in ignorance. This gadget has an eye blink sensor built in and also collision alert through GSM module and notifies to the respective person. This sensor's output is made with Arduino. A GSM modem is a mobile phone substitute without the screen, keypad, and speakers. The owner and the driver can both be alerted when a driver is acting in an unsafe manner. Consequently, the creation of an embedded sensor-based system is the main topic of this paper. Its goal is to help drivers prevent road collisions in order to preserve precious lives

Keywords – Collision alert, eyeblink sensor, Arduino, GSM.

I.INTRODUCTION

Vehicle accidents can cause serious injury or even fatalities, with a significant number of accidents occurring due to driver fatigue or distraction. To prevent such accidents, it is important to develop systems that can detect driver fatigue and alert the driver to take a break or adjust their driving behavior. A motor vehicle accident results in the deaths of 400 persons each day, or around 57 road accidents and 17 fatalities each hour (According to the International Research Journal of Modernization in Engineering Technology and Science). As a result In recent years, the advancement of technology has led to the development of intelligent transportation systems, which incorporate various sensors, communication technologies, and data analysis techniques to enhance the safety and efficiency of the transportation system.

One such system is the Accident Alert along with Fatigue Detector which tracks the behavior of the driver and looks for indicators of exhaustion using a variety of sensors, including an eyeblink sensor, GSM, GPS and an Arduino NANO. The system warns the driver with visual and audio alarms and suggests that the driver take a rest or modify their driving style when it detects a collision, regardless of the object's mobility or the driver's weariness. By drastically lowering the probability of accidents brought on by driver

drowsiness, this device can make both drivers and passengers safer on the road. The design, execution, and potential effects of this system on traffic safety will all be covered in this article.

II. RELATED WORKS

[1] System that uses a MEMS sensor to detect an accident and send the information as an input to the controller for processing. When a rollover is detected, the system would use a GPS module to determine the location and a GSM module to send a message. This paper presents a method that might be effective and simple to use, however it does not provide a switch or any kind of system to prevent a false alarm

[2] Vinit Agrawal proposes an android application-based solution that uses a smartphone to automatically detect and report an accident was proposed. An eCall implementation and accident detection system were integrated within an Android application that was connected to a USB port. The device's most useful characteristics are its GPS receiver. Even though a smartphone has a linear accelerometer with three axes, it was chosen as an application unit (AU) due to its hardware resources and software capabilities

[3] The Rajvardhan Rishi system is made up of an Arduino, an accelerometer, GPS, and GSM. During the incident, it notifies the closest hospital, police headquarters, and family primarily by sensing changes in the accelerometer. Using an Arduino and GPS module, the device transmits a Google Map link. Although this system functions well, it cannot detect the infrequent little accidents that result in no injuries.

[4] The technology in question utilizes a night vision camera to prevent and manage mishaps. When the automobile starts, this system watches the driver's face, which mostly aids in continual observation. It has two uses: the first is to read blinking and the second is to detect eye blinking. Until the driver is cognizant again and gets alert, speed is automatically lowered. However, if the driver has a medical condition or blinks at an abnormal rate despite not being tired, the system will provide a false alarm and fails to identify the impact and contact the necessary authorities.

[5] Mr S.Kailasam proposed a system when the automobile starts, this system watches the driver's face, which mostly aids in continual observation. It has two uses: the first is to read blinking and the second is to detect eye blinking. Until

the driver is cognizant again and gets alert, speed is automatically lowered

[6] Rally Vision grounded smart in- auto camera system for motorist yawning discovery detects the sleeping pattern of the motorist using live videotape capturing. Even though this paper is that if a person is speaking or keeping its mouth open for a longer period of time indeed also it'll find it as feeling drowsy.

[7].Armaghan Hussain's device has two major components that use IR sensors installed on eyeglasses to detect eye blinking. This technology recognizes and categorizes the eye blinking into normal blinking based on the reflected and absorbed IR radiation (NB). The system is made up of an Arduino, an accelerometer, GPS, and GSM. During the incident, it notifies the closest hospital, police headquarters, and family primarily by sensing changes in the accelerometer. Using an Arduino and GPS module, the device transmits a Google Map link Although this system functions well, it cannot detect the infrequent little accidents that result in no injuries. Consequently, in the event of minor mishaps, it will gradually lead to resource and time waste.

[8].Hoang Le paper presents reliable eye blink detection approach for Smart Glasses that use an eigen-eye approach in the first step of our technique to find closed eyes in specific video frames. Even though our prototype smart glasses have a poor power source and cannot support advanced imaging and computing capabilities, tests with them have revealed an accurate detection result.

III.EXISTING SOLUTION

In the existing system the system only has collision detection to notify road crash. The researchers in aims to design an smart vehicle system that can detect any abnormal condition or accident by sensing various parameters and the eye blink sensor placed within the vehicle even though there are few drawbacks which need to be taken into account such as, if the driver does not intervene in spite of the warning there is a possibility of collision, Depends on human responsiveness, Negligence can lead to accident and also, the system will issue a false warning and fail to recognize the impact and contact the appropriate authorities if the driver has a medical condition or blinks unusually quickly despite not being tired.

IV.PROPOSED SYSTEM

The system module includes: 1. Collision Alert: This system warns of collisions between vehicles that happen as a result of careless driving. 2. Accident Notifier: The eye blink sensor is positioned on top of the dashboard in front of the driver. During driving, the eye blinks normally because it monitors the time until the bell will indicate that he needs to wake up. The car has a smart rescue system that assists in sending the location of the accident site in the event of an accident. This system's primary goal is to lower the fatality rate by giving traffic accident victims prompt notification. Accidents are difficult

to totally prevent, but there are certain procedures that can be taken to stop them before they happen. One such method is the ability to swiftly identify risky circumstances and warn the driver. This project implements such a method by presenting an alert message on the screen. If a driver's irresponsibility causes an accident, this system also outlines the necessary actions to be taken in the aftermath. A GPS-equipped smart rescue system will send the accident's location to the main server quickly. This hybrid structure used by the suggested system aids in drowsiness and accident detection.

V.DESCRPTION:

Highway accidents are increasing in incidence these days as a result of both increased traffic and careless driving on the part of drivers. And in many cases, the family members are unable to receive information about the accident at the proper moment. This has the effect of delaying the assistance that the accident victim needs most. Our project, Vehicle Collision Alert Along With Driver's Fatigue Detector Using Eyeblink Sensor, is intended to address this issue and provide assistance to those involved in accidents while also potentially saving their lives by alerting the appropriate rescue personnel at the appropriate moment.

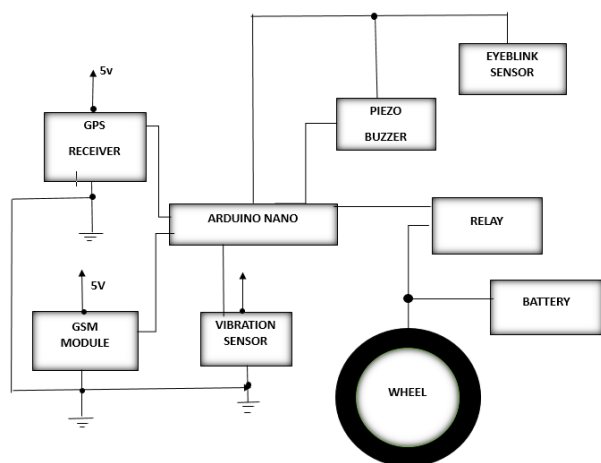
This gadget has an eye blink sensor built in and also collision alert regardless of the mobility of an object that gets in the path of the vehicle. Here we are using the vibration sensor that was installed in the vehicle by the collision detection unit. For instance, in the event of an accident, if the vehicle happens to be hit by another vehicle or an object, it may cause some vibration. In such situation, the vibration sensor will detect the signal and send the information to the Arduino Uno, which serves as the project's Central Processing Unit (CPU). After passing the message to the GSM modem as soon as the Arduino receives a signal from the vibration sensor, the GSM modem will begin operating.

When a crash scenario is recognized, the system diverts calls to the emergency number and sends alert notifications consisting a link that pins the location of the vehicle by using GPS module. A buzzer can also be used to trigger a beep to signal that an accident was detected. At the same time, the eye blink sensors recognize the blinking of the driver's eyes when the engine is started. The vehicle automatically stops when the value reaches the pre-set level after the eye blink sensor receives a signal from the transmission module; as a result, notification will be issued promptly to the emergency number. In this way, both the owner and the driver can be informed when the driver is engaged in an unsafe activity.

VI. SYSTEM DESIGN & IMPLEMENTATION

The components utilised in the proposed operation Fig(1) are Eye blink duration and frequency, Power supply, Buzzer,

LED ARDUINO (NANO), Relay Module, DC, and Eye blink (IR): connected to sleep detection and alert the driver. The major part is an ATmega328-based microcontroller (MC) called Arduino Uno, which handles all operations related to managing the embedded system circuit.



Fig(1) System Architecture

EYEBLINK SENSOR :

To detect eye blinks, a rather basic sensor called an eye blink sensor is employed in Fig(2). Simple infrared sensors are used to observe how long an individual's eyes blink in order to determine whether or not they are sleepy or fatigued. The accompanying data collected can then be processed by any logic necessary for the application.



Fig(2)Eyeblink Sensor

BUZZER:

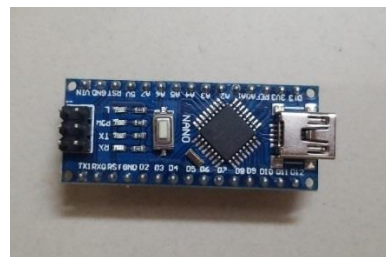
The buzzer used here in Fig(3) is piezo buzzer and the task allotted for this is to provide audio alert for the driver in case if driver's fatigue is detected.



Fig(3)Buzzer

ARDUINO NANO:

Analyse the data from the sensors and compare it with built-in maps to actually sense, control and perform the driving task using Fig(4).



Fig(4)Arduino

GPS :

GLOBAL POSITIONING SYSTEM Vehicles use Fig(5) for both navigation and tracking. The GPS technology detects the location of the car when an accident occurs and delivers the information to the specific person over GSM by calling or sending an SMS to alert them.



Fig(5)GPS Module

GSM :

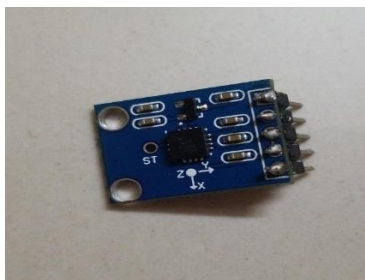
Global Mobile Communication System, By delivering a message, Fig(6) is employed as a medium for controlling and monitoring the transformer load from any location. By transmitting a communication through the GSM modem, GSM is utilised to cover and control the DC motor, Stepper motor, Temperature Detector, and Solid State Relay. Therefore, it is believed that mobile communication is generally successful and will be useful in artificial control, motor vehicles, and applications.



Fig(6)GSM module

VIBRATION SENSOR:

A high sensitivity non-directional vibration sensor, shown in Fig(7), may operate between 3.3V and 5V. The LM393 comparator is used by the sensor to identify the vibration. The circuit will briefly be cut off when there is movement or vibration. On the board, there are two LEDs: one for the power state and the other for the output of the sensor. Here, we powered the module with 5V..



Fig(7)Vibration sensor

LM256 CONVERTOR:

DC input ranges from 3 to 40 volts; the input voltage must be greater than the output voltage by 1.5 volts in order to boost. And the output, constantly variable DC 1.5V to 35V voltage, 3A of high-efficiency maximum output current.



Fig(8) LM256 Convertor

ARDUINO IDE:

Connects to the Arduino boards to interact and upload programmes to it.

In order to initialise the GSM module and test its response using AT commands, we have built a function called void initModule(String cmd, char *res, int t Fig(9).

```

4
5 @author: Rithin
6 ***
7
8 #include <AltSoftSerial.h>
9 #include <TinyGPS.h>
10 #include <Wire.h>
11 #include <math.h>
12 #include <SoftwareSerial.h>
13 #define Relay 18
14 #define buzzer A0
15
16 const String EMERGENCY_PHONE = "919944199201";
17 #define rxPin 2
18 #define txPin 3
19
20 SoftwareSerial sim800(rxPin, txPin);
21 AltSoftSerial neopgs;
22 TinyGPSPlus gps;
23 //gps(9,8)
24
25 String sms_status, sender_number, received_date, msg;
26 String latitude, longitude;
27 #define BUZZER 12
28 #define BUTTON 11
29 #define xPin A1
30 #define yPin A2
31 #define zPin A3
32
33 byte updateFlag;
34
35 static const int sensorPin = 10;
36 int SensorStatePrevious = LOW;
37
38 unsigned long minSensorDuration = 3000;

```

Fig(9)Data Source

After that, we initialised the GPS, GSM, and serial connectivity hardware and software in the void setup() function.

```

void setup()
{
  Serial1.begin(9600);
  Serial.begin(9600);
  lcd.begin(16,2);
  lcd.print("Accident Alert ");

```

```

  lcd.setCursor(0,1);
  lcd.print("  System  ");
  delay(2000);
  lcd.clear();
  ....
  ....

```

Methodology used:

This gadget has an eye blink sensor built in and also collision alert regardless of the mobility of an object that gets in the path of the vehicle. The collision detection alert system measures the distance between two vehicles and alert the drivers to prevent from collision. The sensors recognise the vibration during the crash and redirects a call to the emergency number with alert notification consisting a link that pins the location of the car. At the same time, the eye blink sensors recognise the blinking of the driver's eyes when the engine is started. The vehicle automatically stops when the value reaches the pre-set level after the eye blink sensor receives a signal from the transmission module; as a result, notification will be issued promptly to the emergency number. In this way, both the owner and the driver can be informed when the driver is engaged in an unsafe activity.

The Prototype of this Vehicle Collision Alert Along With Driver's Fatigue Detector using Eyeblink Sensor uses the following steps:

Sensor Installation: The vehicle's driver cabin has been fitted with eyeblink sensors. These sensors have the ability to recognise the eyeblink patterns of the driver, which can be utilized in determining their level of fatigue.

Data collection: Throughout the entire journey, the eyeblink sensors constantly record the driver's eyeblink patterns. The system gathers and processes the data in real-time.

Collision Detection: The system includes vibration detector for collision detection, which continuously monitor the area around the vehicle for any potential collision risks regardless of how handheld the object in the path of the vehicle.

Eyeblink Pattern Analysis: The amount of driver drowsiness is assessed using the eyeblink data that has been collected. The system compares patterns like the frequency and intensity of eyeblinks to predefined thresholds to evaluate the driver's level of fatigue using algorithms (such as data acquisition, preprocessing, and Fatigue Detection decision tree).

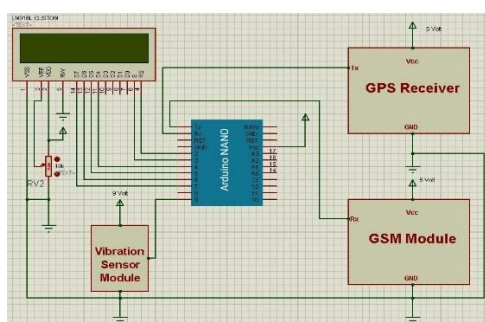
Alert Generation: The system generates a warning when it determines that the driver's level of fatigue has gone beyond a certain threshold or when it recognizes a potential collision hazard. The driver will be informed and remind to take proper action by peizo buzzer-based aural alarms.

Emergency Response: In the event of a possible collision, the system may also activate emergency response

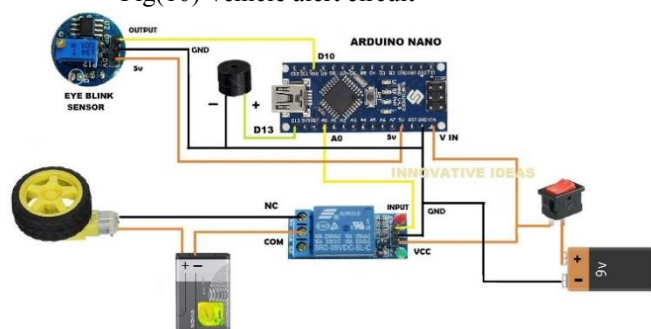
mechanisms, such as automatic braking that stops the car and sending a message to an emergency number that contains the location of the accident, in order to rescue the driver from danger.

System Integration: The system is co related with Vehicle Collision Alert Along With Driver's Fatigue Detector using Eyelink Sensor: And linked to other devices, such as GPS and GSM modules, to improve its utility and efficacy in spotting potential crash dangers and signs of drowsiness.

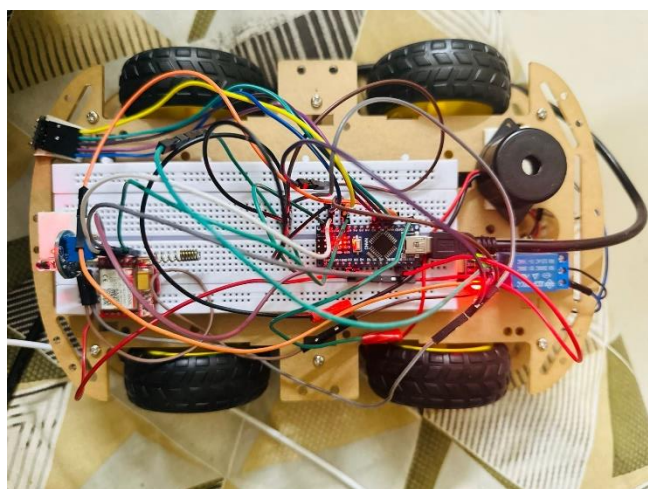
CIRCUIT DIAGRAM:



Fig(10) Vehicle alert circuit



Fig(11) Eyelink circuit

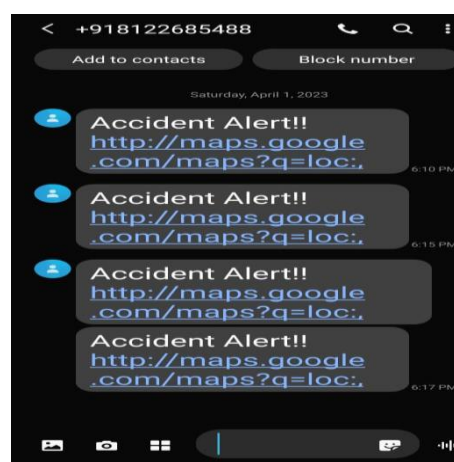


Fig(12)Final Prototype

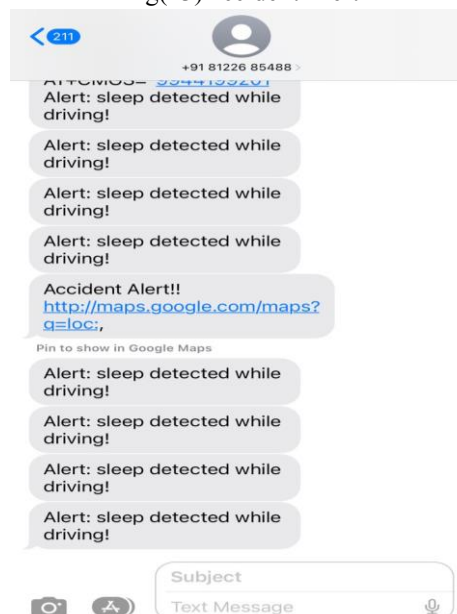
VII RESULT AND EVALUATION

The results and evaluations of the methods and techniques used for Vehicle Collision Alert Along With Driver's Fatigue Detector have been promising. Computer vision-based methods have been successful in alerting the driver, movement, and position.

The system sends a message Fig(13) via the GSM module after detecting an accident from the vehicle. Google Map will provide the precise accident location via SMS. Overall, the results and evaluations of the approaches and methods used for Vehicle Collision Alert Along with Driver's Fatigue Detector Using Eyelink Sensor have been promising and successful in alerting the driver, movement, and location Fig(14).



Fig(13)Accident Alert



Fig(14)Fatigue Alert

VIII CONCLUSION

Our conception automates exigency aid services and uses them to descry accidents. As a result, the system is

transferring SMS from the scene of the accident to the closest exigency aid service provider. The growing demand for buses has also led to more business traffic and motor accidents. This is due to the dearth of top exigency installations in our nation. a vehicle accident alert system that automatically sounds. This design is a system that can identify accidents in a lot lower time and transmit the essential data. Continued exploration and development in this area could lead to significant advancements in the lives of motorists

IX REFERENCES

- [1] [2016,P. Kaliuga Lakshmi, C.Thangamani]"An efficient vehicle accident detection using sensor technology"
- [2] [2017,Dnyanesh Dalvi, Vinit Agrawal, Sagar Bansod, Apurv Jadhav, Prof. Minal Shahakar] "Android Application for Automatic Accident Detection".
- [3][2008,Sharmila Gaikwad] "Mobile Agents in Heterogeneous Database Environment for Emergency Healthcare System", at ITNG 2008 5th International Conference on Information Technology- New Generations April 7-9, 2018, Las Vegas, Nevada, USA. Published in IEEE Computer society, ISBN:978- 0-7695-3099-4, PP.1220- 1221
- [4] [2020,Rajvardhan Rishi, Sofiya Yede, Keshav Kunal, Nutan V. Bansode] " Automatic Messaging System"for Vehicle Tracking and Accident Detection, Proceedings of the International Conference on Electronics and Sustainable Communication Systems,ICESC.
- [5] [2020,Mohanad ABDULHAMID] " Collision avoidance system using ultrasonic sensor " IEEE.
- [6] [2019,CharlesC.Liu, SimonG.Hosking, MichaelG.Lenné] "Predicting motorist doiness using vehicle measures" , International Journal of Engineering and Advanced Technology(IJEAT) ISSN 2249 – 8958.
- [7] [Hariri,S. Abtahi,S. Shirmohammadi andL. Martel ,2019],disadvantage of this paper is that if a person is speaking or keeping its mouth open for a longer period of time indeed also it'll find it as feeling drowsy.[7]
- [8]] [2019,Mr S.Kailasam, Mr Karthiga, Dr Kartheeban, R.M.Priyadarshani, K.Anithadevi] "Accident Alert System using face Recognition",IEEE.
- [9] [2020,Dr. K.Panimozhi,Shria Gupta, Sreya Chanda,Sushmitha R,Nagashree B R] "Eye-Blink Based Communication System for People with Motor Neuron Disease" International Journal of Computer Science and Mobile Computing ,ISSN 2320–088X.
- [10] [2018,Hoang Le ,Thanh Dang,Feng Liu] "Eye blink detection for smart glasses" IEEE International Symposium on Multimedia.
- [11] [2019,SIR MUHAMMAD IRFAN ,ARMAGHAN HUSSAIN KHAN,SYED ASKAR SHAH] "Real time eye blink detection system with IR sensor for driver dowsinesss" IEEE.



AUDIOFY – An AID for AUDITORY PROCESSING DISORDER (APD) in CHILDREN

¹Dr. R. Deepalakshmi Professor, ²Anitha Angeline X, ³Dharshanaa S,

⁴Harshitha S R, ⁵ Sushmitha G,

¹ rdl@vcet.ac.in, ² angelinepkt@gmail.com, ³ dharshanaa.s1114@gmail.com, ⁴ harshadeepthi1223@gmail.com, ⁵ sush11mitha@gmail.com

Department of Computer Science and Engineering, Velammal College of Engineering and Technology, Madurai, India.

Article History: Received: 12.05.2023

Revised: 25.05.2023

Accepted: 05.06.2023

Abstract

Auditory Processing Disorder (APD) is a neurological condition that affects the processing of auditory information by the brain. It primarily manifests in children and can significantly impact their ability to understand, interpret, and respond to auditory stimuli [1]. Approximately 2-7% of schoolaged children are considered to have Auditory Processing Disorder (APD) worldwide. The studies report that approximately 30-70% of children with APD exhibit reading and language-related difficulties, impacting their communication, academic performance, and overall quality of life [2]. Children with APD often pose unique challenges including understanding speech in noisy environments, processing verbal instructions, struggles with phonics, reading comprehension, poor auditory memory, and a tendency to misunderstand or misinterpret verbal information [5]. To address this issue, we developed an interactive website that offers a variety of memory games specifically designed to enhance auditory processing skills in children. Our website aimed to overcome Auditory Processing Disorder at the early stage [4]. The website incorporates evidence-based techniques and principles of auditory processing intervention. It features a range of captivating visuals, audio cues, and interactive elements to create an immersive and enjoyable learning experience [6]. The games are designed to gradually increase auditory processing which allows children to develop their auditory skills progressively.

Keywords: Auditory Processing Disorder (APD), Auditory Processing, Children, Memory, Sequencing, Website, Skills, Games, Verbal instructions, Learning.

1. INTRODUCTION

Auditory processing skills play a crucial role in children's overall cognitive and language development. Children with APD often experience difficulties in academic settings, with studies reporting that approximately 30- 70% of children with APD exhibit reading and language-related difficulties [7]. In fact, APD is a hearing disorder that causes the brain to have a hard time processing, remembering, and understanding words that have been spoken which can be significantly improved with proper training. For example, they may not recognize the difference between *cat*, *that*, and *bat*. The words *seventy* and *seventeen* may sound the same.

The main objective of our website is to support individuals with APD, empower them with the knowledge and resources needed to effectively address auditory processing difficulties. It is tailored to target different aspects of Auditory Processing, including Auditory Discrimination, Sequencing, Memory, and Auditory Attention [8]. Auditory discrimination is the capability to make a distinction between various sounds and differentiating verbal communication. Auditory sequencing refers to the ability to understand and process a series of auditory stimuli in the correct order which is essential for various cognitive and linguistic processes, including language comprehension, following directions, and problem-solving [9].

The application incorporates a set of exercises designed for the targeted deficits and offers a range of intervention strategies and resources to support children with APD [10]. These include evidence-based techniques for enhancing auditory discrimination and improving auditory memory which can include games that help users remember and recall sounds they have heard. Regular practice can gradually Strengthen auditory sequencing and boost auditory attention.

2. LITERATURE SURVEY

Ana-Marta Gabaldón-Pérez, María Dolón-Poza, Martina Eckert, Nuria Máximo-Bocanegra,

María-Luisa Martín-Ruiz, Iván Pau De La Cruz [1] presented Amalia's Planet, a game conceived for use in school environments, which allows a first assessment of a child through a series of events in relation to the execution of the tasks related to different aspects of auditory performance, which were evaluated for the subsequent optimization of its performance and the improvement of its usability.

Guzek, A.; Iwanicka-Pronicka, K. [2] The study aimed to examine the ability to discriminate sounds by children with and without APD, assessed through the FPT and phoneme discrimination test (PDT) administered to participants. Additionally, we are trying to determine the need to modify the APD diagnostic standards by the PDT test in the battery of regularly administrated APD diagnostic tests.

Morteza Farazi, Zahra Hosseini Dastgerdi & Bahare Khavarghazalani [3] This study aimed at presenting a comprehensive review of the literature to better explain the role of the auditory system and auditory processing disorder in stuttering. The evidence suggests that auditory processing deficits may be involved in stuttering.

Liu Panting, Zhu Huiqin, Chen Mingxia, Hong Qin, Chi Xia [4] This research aimed to provide evidence for the early identification and intervention of children at risk for auditory processing disorder (APD). Electrophysiological studies on children with suspected APDs were systematically reviewed to understand the different electrophysiological characteristics of children with suspected APDs.

C. N. Price and D. Moncrieff [5] The study reviewed relevant theories that guide the present understanding of attentional processes, discuss current electrophysiological evidence of attentional involvement in auditory processing across subcortical and cortical levels and propose areas for future study that will inform the development of more targeted and effective clinical interventions for individuals with speech-in-noise deficits.

Rouillon I, de Lamaze A, Ribot M, Collet G, de Bollardi re T, Elmir R, Parodi M, Achard S, Denoyelle F, Loundon N [6] The study is about the evaluation of a new battery of tests that involves speech, psychometric, phonemic, and ENT assessments to diagnose children with auditory processing disorder (APD). The article reports that 45% of the children suspected of APD were confirmed with the diagnosis and that dichotic testing and pattern recognition were the most effective tests. It also suggests that a multidisciplinary protocol can help identify other associated difficulties in children with APD.

Ahn JH, Oh SH, Jang H, Lee JB, Chung JW [7] The article is a study that investigated the impact of auditory processing disorder (APD) on the academic achievement of children aged 8–12 years. The article found that children with APD performed significantly worse than typically developing children on all academic tests, and similarly to children with dyslexia on reading and spelling tests. The article also found that children with APD had difficulties with phonological awareness, verbal working memory, and rapid naming, which are skills that are important for learning. The article concluded that APD can have a negative impact on academic achievement in children and that early identification and intervention are needed.

Choudhury, Manisha & Sanju, Himanshu [8] This paper provides an overview of the definition, etiology, diagnosis, and management of CAPD in children. It also discusses the challenges and controversies in this field, such as the lack of consensus on the criteria and methods for diagnosing CAPD, the overlap with other developmental disorders, and the limited evidence for the effectiveness of interventions. The study suggests some recommendations for the assessment and management of CAPD in children, such as using a multidisciplinary approach, involving parents and teachers, providing individualized intervention plans, and monitoring progress and outcomes.

Jain, Chandni & M B, Priya & Joshi, Kirti [9] The aim of the study was to investigate the auditory processing abilities in children with speech sound disorders and compare it with typically developing children. Results showed that there was a significant difference between both groups in all tests except for the masking level difference. The study revealed the correlation between temporal processing and syllable and phoneme oddity. There was also a high correlation between speech perception in noise and segmentation.

Nasiri, Nahid & Shirmohammadi, Shervin & Rashed, Ammar [10] This study is about Speech impediment affecting children with hearing difficulties and speech disorders that requires speech therapy and much practice to overcome. To motivate the children to practice more, serious games can be used because children are more inclined to play games. In this paper, we have designed and implemented a serious game in which children can learn to speak specific words that they are expected to know before the age of 7. This allows the child to practice long hours, compared to

clinical approaches under the supervision of a therapist, which are time-limited.

3. SYSTEM ARCHITECTURE

The system incorporates HTML, CSS, and Java Script for frontend Graphical User Interface (GUI) and used PHP My Sql for database connectivity to store user information(refer figure 1). The developed web application provides a personalized user experience through separate login for each user. The application allows the user to log in to the system to access the games that are specially designed with the purpose of training children who are suffering from Auditory Processing Disorder (APD).

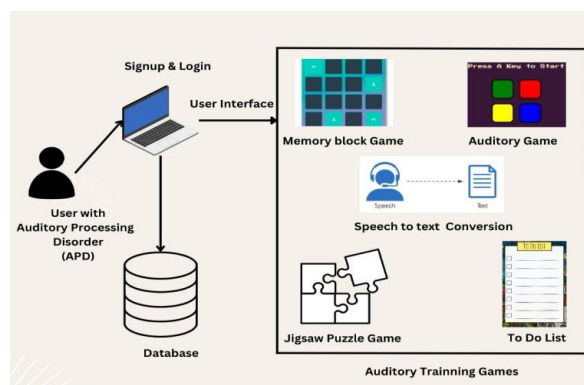


Figure 1 System Architecture

The user interface layer (i.e.) GUI provides the interface through which users interact with the application. The application layer consists of the core logic and functionality of the application(refer figure 2). The data layer handles the storage and retrieval of audio files, metadata, and user-related data using MySQL database connectivity. The infrastructure layer comprises the underlying servers, networking components, and security services that support the application's operation.

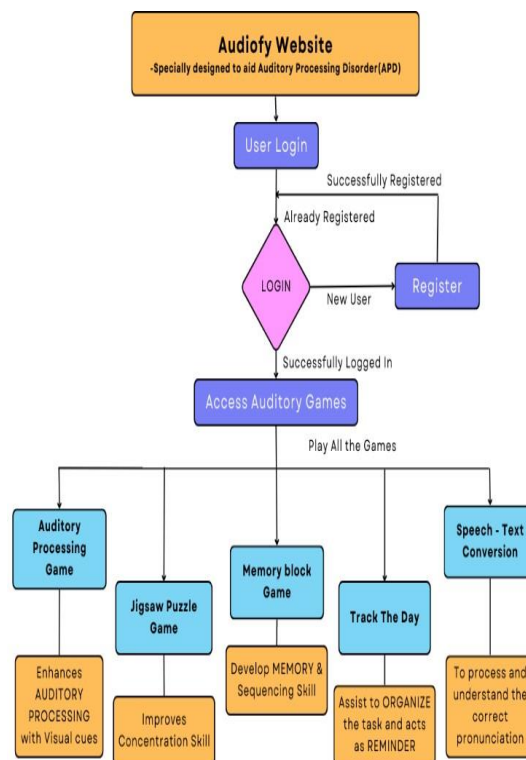


Figure 2 Flow of process

4. DESIGN AND IMPLEMENTATION

The Web Application facilitates a user-friendly interface to access the Auditory games which are designed to teach strong listening and cognitive skills through fun, interactive auditory training modules. These games provide targeted training for specific auditory processing skills, Memory, attention, and Concentration [4]. The benefits of the games are explained below.

We have come up with an effective and enjoyable tool for enhancing auditory skills. The auditory Training game (refer Figure 3) challenges children to remember a sequence of instructions and sounds [10]. Recalling the sounds and executing the commands in the correct order, strengthen their auditory processing skills. Playing a Jigsaw puzzle and Memory block games Figure 4 helps to increase brain functions such as attention level, concentration, intellectual skills, visual recognition, and

develop short-term memory [7]. Speech to Text system Figure 5 incorporates a multisensory approach by combining auditory stimuli with vocal cues or feedback [3] [9]. This integration of multiple senses helps children with APD better understand and process auditory information. Additionally, To-Do List

Figure 5 can assist children to organize tasks offering a clear and structured representation of tasks and responsibilities [6].

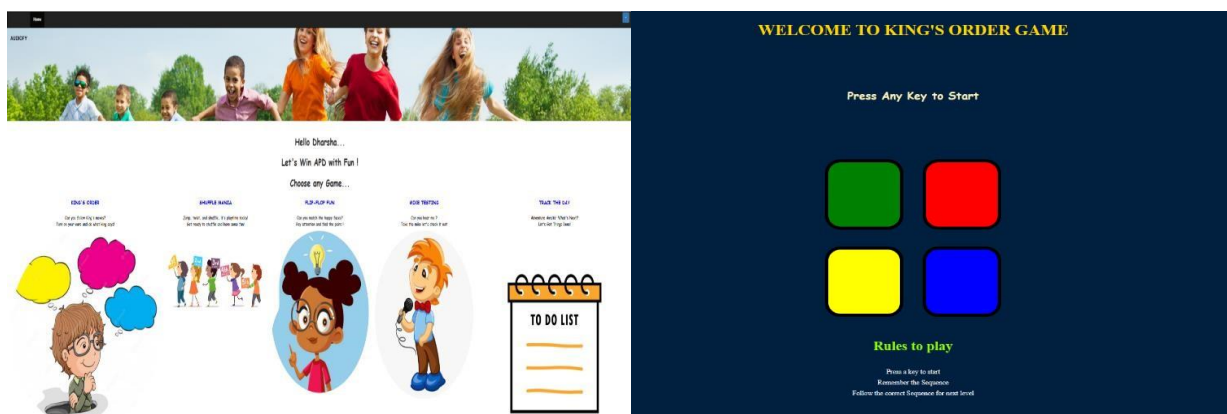


Figure 3. User Profile and Auditory Training Game



Figure 4. Jigsaw Puzzle Game & Memory Block Game

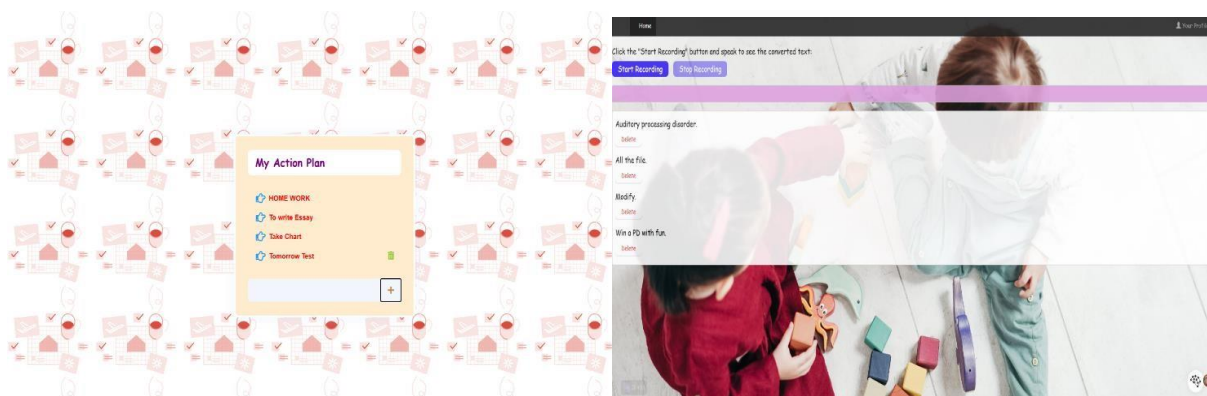


Figure 5 To-Do List Figure & Speech to Text Conversion

5. RESULT AND DISCUSSION

The vision and mission of the application is to overcome Auditory Processing Disorder in the early stage of detection [4]. It is exclusively designed for children with Auditory Processing Disorder (APD) in order to train and upgrade their Auditory processing and memory skills.

The specialized advantages of our proposed application include:

- i. Provide targeted training specifically focused on auditory processing skills such as auditory discrimination, auditory memory, and auditory sequencing.
- ii. Attractive and specially designed website easily kindles children who are reluctant to physical training [10].
- iii. Features Multimodal Learning [6] [9] with visual cues and respond to audio stimuli.
- iv. Repeated practice and regular engagement with the game can lead to significant improvements.
- v. The visual components can provide additional support and reinforcement, facilitating learning and comprehension.

6. CONCLUSION

This paper proposes and implements a responsive website with practically proven games [10] for children affected with Auditory Processing Disorder. Practicing these games on a regular basis can effectively elevate Auditory Processing skills and Memory [1]. This paper also highlights the comprehensive overview and impacts of APD on children. With appropriate strategies and interventions, children with APD can enhance their

communication, academic performance, and overall quality of life.

REFERENCES

- [1] Gabaldón-Pérez A, Dolón-Poza M, Eckert M, Máximo-Bocanegra N, Martín-Ruiz M, Pau De La Cruz I Serious Game for the Screening of Central Auditory Processing Disorder in School-Age Children: Development and Validation Study JMIR Serious Games (2023);11:e40284.
- [2] Guzek, A.; Iwanicka-Pronicka, K. Auditory Discrimination—A Missing Piece of Speech and Language Development: A Study on 6–9-Year-Old Children with Auditory Processing Disorder. Brain Sci. (2023), 13, 606.
- [3] Morteza Farazi, Zahra Hosseini Dastgerdi & Bahare Khavarghazalani (2022) What is the role of auditory processing in stuttering? A mini review of previous knowledge, Hearing, Balance and Communication.
- [4] Liu P, Zhu H, Chen M, Hong Q, Chi X. Electrophysiological Screening for Children With Suspected Auditory Processing Disorder: A Systematic Review. Front Neurol. (2021) Aug 23;12:692840. doi: 10.3389/fneur.2021.692840. PMID: 34497576; PMCID: PMC8419449
- [5] C. N. Price and D. Moncrieff, "Defining the Role of Attention in Hierarchical Auditory Processing," Audiology Research, vol. 11, no. 1, pp. 112–128, Mar(2021), doi: 10.3390/audiolres11010012.

- [6] Rouillon I, de Lamaze A, Ribot M, Collet G, de Bollardi re T, Elmir R, Parodi M, Achard S, Denoyelle F, Loundon N. Auditory processing disorder in children: the value of a multidisciplinary assessment. *Eur Arch Otorhinolaryngol.* (2021) Dec;278(12):4749-4756. doi 10.1007/s00405-02006601-8. Epub 2021 Jan 18. PMID: 33462745. 020-67033-2. PMID: 32572114; PMCID: PMC7308366.
- [7] Ahn JH, Oh SH, Jang H, Lee JB, Chung JW. Impact of hearing loss on the performance of auditory processing measured by questionnaires in Korean adolescents. *Sci Rep.* (2020) Jun 22;10(1):10118. doi 10.1038/s41598-
- [8] Choudhury, Manisha & Sanju, Himanshu. (2019). Central Auditory Processing Disorder (CAPD) in Schoolgoing Children. *SE. S15-S19.* 10.17140/OTLOJ-SE-1-104.
- [9] Jain, Chandni & M B, Priya & Joshi, Kirti. (2018). Auditory processing in children with speech sound disorders.
- [10] Nasiri, Nahid & Shirmohammadi, Shervin & Rashed, Ammar. (2017). A serious game for children with speech disorders and hearing problems. 1-7. 10.1109/SeGAH.2017.7939296.

BUILDING A ROBUST DATASET FOR INSCRIPTION CHARACTER RECOGNITION USING DEEP LEARNING

Dr.R.Deepalakshmi¹

Professor
Department of computer
science,
Velammal college of engineering and
technology, Madurai.
rdl@vcet.ac.in

M.B.Varun Adhityan², N.K.Srekaravarshan³,
V.K.Jeganath⁴, C.Pradeesha⁵

varunadhityanbaskar@gmail.com
, srekaravarshan@gmail.com,
jeganath2003@gmail.com,
pradeeshac994@gmail.com
Velammal college of engineering and
technology,
Madurai.

Abstract-- Even though inscription characters are a significant part of human history and culture, machine learning algorithms still struggle to recognize them. For the purpose of creating precise and dependable machine learning models for inscription character recognition, a high-quality dataset must be created. In this abstract, we provide an overview of the steps required in building a dataset for inscription characters, as well as the difficulties encountered during data collection and preprocessing. We explain the many methods for gathering inscription data, including digitization and photography, and offer suggestions for efficient data gathering. We also go over the many preprocessing methods that can be used to improve the dataset's quality, such as picture normalization, segmentation, and noise reduction. The creation of precise inscription character recognition models will be made possible by adhering to the best practices described in this abstract, and this will facilitate research in a variety of domains, such as linguistics, history, and archaeology.

Keywords—Dataset, Inscription, Machine Learning, Data Preprocessing

I. INTRODUCTION

The fascinating aspect of ancient Tamil culture has drawn the attention of scholars, historians, and enthusiasts all around the world. Tamil Nadu, a state in the south of India, has a lengthy history that goes back more than two thousand years. Tamil, one of the oldest and most sophisticated languages in the world, is spoken there and has a distinctive and complex writing system.

Tamil literature, art, and architecture from antiquity display the splendour and wealth of Tamil civilization. Tamil literature has a rich and diverse history which encompasses both secular and religious works. The ancient Tamil poems and songs that make up the Sangam literature, which is thought to have been written between the third century BCE and the third century CE, provides insights into the social, cultural, and political lives of the Tamil people.

The ancient temples of Tamil Nadu are among the best examples of Dravidian architecture, and Tamil art and architecture are also widely respected. The intricate carvings, towering gopurams (towers), and vast courtyards of these temples are well-known features. The bronze idols from the Chola era are among the most notable examples of the exquisite and detailed bronzes found in Tamil Nadu.

Tamil inscriptions are prehistoric texts that were inscribed using the Tamil script on rocks, metal plates, and other objects. They contain important details regarding the Tamil people's history, culture, language, and way of life. The Tamil people have lived in southern India for many centuries. One of the earliest and most important sources of knowledge about Tamil civilisation is thought to be Tamil inscriptions.

Tamil inscriptions have a long history that dates back to the third century BCE, when the language and script were originally created. The earliest inscriptions were discovered in the Tamil Nadu region, which was a centre of Tamil culture and learning. The inscriptions were primarily used to record royal edicts, land grants, and religious donations. They were frequently written in verse and were sometimes accompanied by illustrations and images. Tamil writing evolved over time to become more complex and sophisticated. They were used to document the

actions of rulers, the accomplishments of poets and academics, and the regular lives of people in society. The inscriptions were also employed to disseminate knowledge and learning, as well as to promote religious and cultural values.

Tamil inscriptions reached their pinnacle of complexity and sophistication during the mediaeval era. Large stone pillars that were placed in public areas like temples and markets were inscribed with them. These inscriptions were extremely elaborate, featuring dexterous calligraphy and exquisite designs, and they frequently came with in-depth depictions and images.

Tamil inscriptions are still a priceless source of knowledge about Tamil civilization. They offer insights into the Tamil people's social, cultural, and political lives, as well as their language, literature, and religious practises. Additionally, Tamil inscriptions have helped scholars in their understanding of the language's and script's historical development as well as the development of Tamil culture.

The wonder of datasets rests in the abundance of data and knowledge they contain. Individual data points or tiny data samples may not always show patterns, trends, or insights, but datasets can. Researchers and analysts can find hidden linkages, correlations, and causalities in massive datasets that can be used to guide decision-making, develop new products and services, or enhance current ones.

Datasets can also be used to train machine learning models, which are able to identify intricate data patterns and make predictions based on them. Large datasets can be used to train machine learning models to identify patterns and generate predictions that are more reliable and precise than those generated by people.

Moreover, datasets can assist researchers and analysts in testing theories, confirming or refuting hypotheses, and gaining fresh insights. Additionally, they can be used to compare performance and track advancement over time. Researchers and analysts can assess the efficacy of interventions, regulations, or other changes by comparing new data to previous databases.

The power of databases, in general, resides in their capacity to highlight information and insights that might otherwise go unnoticed. Researchers, analysts, and developers could improve decisions, create new technologies, and better the environment around us by using datasets to analyse data.

We are proposing to develop a system with a robust dataset and character recognition system to understand these inscriptions and learn more about our ancient history, civilization, and deeds carried out by our ancestors because technology provides solutions for any challenge we encounter.

II. LITERATURE REVIEW

The demand for high-quality Tamil language datasets is growing as more and more natural language processing (NLP) applications are created. In this review of the literature, we will look at the methodology employed, the many kinds of datasets that are available, and the applications that have been created utilising this dataset generation research in Tamil. Tamil native speakers manually annotating datasets is the way that is most frequently employed. In order to do this, a sizable corpus of text must be created and annotated with a variety of linguistic features, including part-of-speech tags, named entities, and sentiment labels. These annotated datasets can subsequently be used to train machine learning algorithms for a variety of NLP tasks. Another approach is to automatically create new datasets using already-existing resources like parallel corpora or machine translation tools.

[1] Giridharan.R,Vellingiriraj.E.K, and Dr.Balasubramanie have presented a method for character recognition and information retrieval of Brahmi,Vattezhuthu, and Grantha letters from temple epigraphy, as well as the conversion of these characters into digital form. They asserted that their method would address issues like maintaining language grammar and correcting the spellings.

[2]RajaKumar.s and Dr.V.subbaih Bharathi.s system tries to recognise and identify the characters used in Vatteluttu inscriptions from the 7th century, which are difficult to read due to age and damage. For historians and archaeologists who research the history and culture of the ancient Tamil people, this method can be helpful. This method is only focused on Tamil characters from the 7th century.

[3]Manigandan.T et al. have proposed a Tamil character recognition system based on OCR and NLP that focuses on Tamil characters from the 9th to 12th centuries. They pre-process and segment the inscription photos obtained from the Tamil Nadu Archaeological Department in their work. The colour photos were transformed to grayscale and binary images depending on threshold values during the segmentation process. For each letter, Scale Invariant Feature Transform (SIFT) methods have been used to extract image features such as the quantity of lines, curves, loops, and dots in order to precisely identify the character. Support Vector Machine (SVM) classifier will be used to classify and produce characters, and the patterns of the characters will be compared to those of well-known characters and predicted using the Trigram method. For further character identification and to improve the system's

ability to recognise the characters, each identified character will be given its matching Unicode value and updated in the image corpus. Thus, the major issues with reading the inscription images can be resolved by the proposed system. [4]Lalitha Giridhar, Aishwarya Dharani, and Velmathi Guruviah have presented a fresh approach to OCR that focuses on enhancing optical character recognition algorithms for the historic Tamil script, which was in use during the 7th and 12th centuries. While it is a difficult undertaking to thoroughly curate a useful data set for ancient Tamil characters, in this work a data set has been curated using cropped images of characters found on specific temple inscriptions, unique to this time period. A two-dimensional convolution neural network is created and used to train, classify, and recognise the historic Tamil characters after the image has been binarized using the Otsu thresholding method. The Pytesseract package in Python is used to connect the neural network to the Tesseract in order to create optical character recognition techniques. This effort also uses Google's text-to-speech voice engine as an extra feature to provide an audio output of the digitised text. Numerous samples of both contemporary and historic Tamil were gathered and processed. It is discovered that a combined efficiency (OCR and text to speech) of 77.7% may be reached for Tamil inscriptions analysed over the considered time span.

[5]Devi Priya R et al. introduced a self-adaptive Lion Optimisation Algorithm (LOA) that is used to optimise brightness and contrast in stone inscription images that have been pre-processed for noise removal, and then each character is separated by identifying contours. Transfer Learning (TL), a Deep Convolution Neural Network-based multi classification method, is used to recognise characters. When applied to images of stone inscriptions, the suggested hybrid model Self-Adaptive Lion Optimisation Algorithm with Transfer Learning (SLOA-TL) outperforms conventional methods in terms of accuracy and speed. The recognition of Tamil characters in stone inscriptions and the preservation of Tamil traditional knowledge are both accomplished by this method.

[6]Shalaka Deore Prasad and Albert Pravin has proposed a paper focusing on the analysis and fine-tuning of a cutting-edge Deep Convolutional Neural Network (DCNN) created for the classification of Devanagari Handwritten characters. They produced a brand-new Devanagari handwriting dataset that includes 5800 isolated images of 58 distinct character classes, including 12 vowels, 36 consonants, and 10 numbers. A two-stage VGG16 deep learning model was also used in conjunction with this database to recognise those characters using two cutting-edge adaptive gradient methods. To improve the overall effectiveness of the proposed Devanagari Handwritten Character Recognition System (DHCRS), a two-stage deep learning methodology was created. The initial model had a training loss of 0.18 and a testing accuracy of 94.84%. Additionally, the second fine-tuned model achieves cutting-edge performance on a very small dataset with a lot fewer trainable parameters and far less training time. Testing accuracy was 96.55% and training loss was 0.12 percent.

[7]Kavitha Subramani and Murugavalli Subramaniam have conducted a study that aims to separate out ancient Tamil palm leaf manuscripts related to the subject of medicine in order to develop a sizable amount of Tamil character datasets. In their investigation, the fictional characters are fed into expert systems as inputs in order to recognise context and content that are thought to be present in the chosen medical articles. Large numbers of the characters have been manually detected, and datasets are made using Gaussian distortion.

[8]Yong Haur Tay et al. described two offline handwriting recognition systems, the first employing standard discrete HMMs and the second a NN-HMM hybrid. Results on the IRONOFF-196, IRONOFF Cheque, and SRTP-Cheque databases are presented, showing the superiority of the hybrid recognizer. Finally, they showed how the hybrid recognizer can be automatically bootstrapped from the discrete HMM recognizer and how many training phases can considerably increase its recognition accuracy.

III. METHODOLOGY

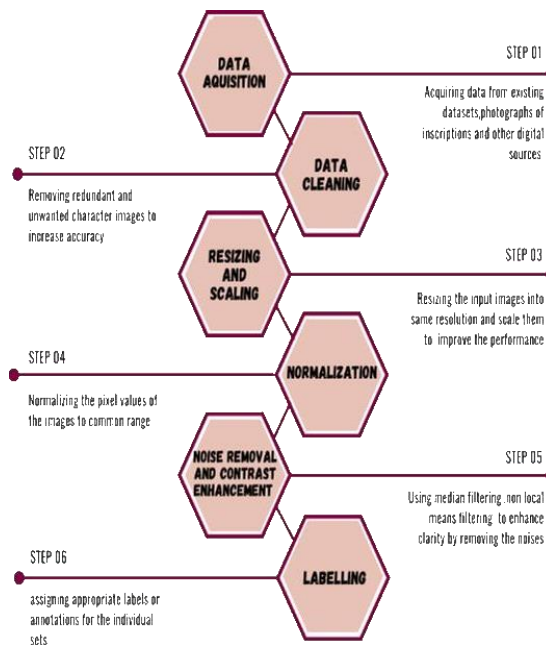


Fig. 1 Methodology for Creation of Image Dataset

IV. PURPOSE AND SCOPE OF THE DATASET

Our dataset's main objective is to provide as a source of data for Tamil character recognition systems. Given the vastly increased quantity of training set images, this dataset will be more effective than the current datasets.

V. PLANNING AND DESIGNING THE DATA COLLECTION METHODS:

A few sources and methods for the data gathering for the dataset include existing images of the inscriptions, accessible datasets, the collection of data images directly from the inscriptions by images, and organising a team to write multiple versions/copies of the characters.

VI. COLLECTION AND PREPROCESSING OF DATA:

Errors, missing numbers, outliers, and inconsistent data are frequently present in raw data. Data cleaning entails locating and addressing these problems. For greater accuracy, noise reduction and thresholding are applied to the data images.

A. Resizing and Scaling:

One of the major steps involved in pre-processing is image scaling. There are numerous benefits in using this strategy. A well-formed input data format must be taken into account in order to construct a successful data model and to make sure that all of the data inputs are the same size and ratio, resize. We must scale the images after making sure that all of the data inputs have been scaled. There are several suggested scaling techniques for the supplied image. In our work, the Lanczo Algorithm is built and used after extensive experimentation with numerous techniques.[9] The Lanczo interpolation algorithm preserves the edges in the scaled images since handwritten scripts have various dimensions and pixel counts. This is crucial for handwritten characters since they frequently feature delicate nuances and complicated strokes.



Fig. 2 Post result of Resizing and Scaling

B. Normalization:

Normalization is important when working with Inscription images that have varying pixel intensities, which can make it difficult to identify patterns, edges and feature of the characters. Normalization ensures that the pixel values of an image are within a specific range, which helps in representing the features of the image better. As the dataset will be fetched with enormous number of test images, captured under different lighting conditions can have varying pixel values, It will increase the effect of illumination. To reduce the effect of illumination and to visualize the outliers of the dataset, we used Z-Score algorithm is used.[10] Z-Score Algorithm allows data points to be standardized and compared against each other, regardless of their original scale. The main objective of this is to reduce the dimension of the original data image by normalizing the intensities.



Fig. 3 Post result of Normalization

C. Denoising:

Denoising an inscription image is a challenging task that requires special techniques to preserve the text while removing the noise and artifacts. Inscription images are often affected by noise due to various factors such as image capture conditions, scanner settings, and image processing algorithms. The presence of noise and artifacts can reduce the readability of the inscription and make it difficult to interpret. The efficient technique that is used in our dataset to denoise an inscription image is Fast Non-Local Means filtering. [10] It is a powerful technique that involves averaging the pixel values of the image within a window based on the similarity of their neighbourhoods. This technique is effective in removing noise while preserving the details and edges of the inscription. Mainly, it denoises the cracks and noised areas.



Fig. 4 Denoised image of normalized image

LABELING AND ANNOTATING THE DATA:

Labelling and annotating some forms of data, such as images or text, may be necessary. To enable supervised learning or other types of analysis, this entails giving the data relevant tags or labels. The dataset visuals are mapped to the actual words using Lableme. Here, we map the image folders for historical figures to the contemporary Tamil characters that correspond to them.

VII. SPLITTING AND DOCUMENTATION OF THE DATASET

A training set, a validation set, and a testing set were created from the dataset. Models are trained using training data, validated using validation data, and tested against testing data to determine the model's ultimate performance. After the dataset has been validated, we will produce a thorough documentation. Details including data sources, collection methods, variables, pre-processing stages, and other pertinent information are included in this documentation. This documentation is essential for comprehending, replicating, and sharing your study and dataset with others.

After dataset completion, we will post it in public spaces like GitHub, Kaggle, or the UCI Machine Learning Repository.

VIII. RESULT & DISCUSSION

This paper presents an efficient vattezhuthu dataset which will be useful for Tamil character recognition system that we are planning to develop in the near future. This dataset will be an improved version of the existing dataset and will provide more accuracy in the charter recognition system. the proposed dataset will contain 10000 images in the training set and 7000 images in the test set for providing an enhanced performance. M.A.Pragathi et al., have presented a solution for Tamil OCR that includes a database, algorithm and an application. Their dataset consists of 15,600 character images each of dimensions 224x224. Our proposed system for Tamil handwritten characters gives efficiency of 94.52%. Our dataset will be more efficient than the previously mentioned solution and will have the efficiency of 95.21%. After the deployment of our tamil character recognition system if the input data is not available in our dataset, then the image will be dynamically added into our dataset. Hence the accuracy of the dataset will also increase.

IX. CONCLUSION

In conclusion, the development of an Ancient Tamil Characters dataset is an essential step in protecting and upholding Tamil language. This dataset can be used for a variety of purposes, including machine learning-based recognition systems, digital archives, and historical research. The paper explains the pre-processing methods needed to improve the quality and legibility of the characters that are to be used for building the dataset. The paper also highlights the value of preserving these historic traits, which are a crucial component of Tamil's cultural identity. Researchers, historians, and linguists now have access to a comprehensive resource for researching and preserving the Tamil inscriptions. The creation of this dataset is a great illustration of the potential benefits that come from digitising and preserving the stone inscriptions. With the use of this dataset, we can learn more about the history of the Tamil language and its evolution, which will help us embrace Tamil Nadu's rich cultural heritage on a deeper level.

REFERENCES

- [1] Giridharan.R,Vellingiriraj.E.K,Dr. Balasubramanie.P, " *Identification of Tamil Ancient Characters and Information Retrieval from Temple Epigraphy Using Image Zoning*", International Conference on Recent Trends in Information Technology (2016), pp 1-5
- [2] RajaKumar.S, Dr.Subbiah Bharathi.V, "Eighth Century Tamil Consonants Recognition From Stone Inscriptions", International Conference on Recent Trends in Information Technology (2012),pp 40-43
- [3]Manigandan.T,Dr.Vidhya.V,Dr.Dhanalakshmi.V,Nirmal a.B,"Tamil Character Recognition from Ancient Epigraphical Inscription using OCR and NLP",International Conference on Energy,Communication, Data Analytics and Soft Computing (2017),pp 1008-1010
- [4] Lalitha Giridhar,Aishwarya Dharani,Velmathi Guruviah,"A Novel Approach to OCR using Image Recognition based Classification for Ancient Tamil Inscriptions in Temples",arXiv preprint arXiv:1907.04917(2019),pp 1-5
- [5] Devi Priya.R, Karthikeyan.S, Indra.J, Kirubashankar.S, Ajith Abraham, Lubna A. Gabralla,Sivaraj.R,

- Nandhagopal.SM,"Self-Adaptive Hybridized Lion Optimization Algorithm with Transfer Learning for Ancient Tamil Character Recognition in Stone Inscriptions",IEEE Access(2023), pp 1-13
- [6] Shalaka Prasad Deore,Albert Pravin,"Devanagari Handwritten Character Recognition using fine-tuned Deep Convolutional Neural Network on trivial dataset",Springer Nature(2020),pp 1-12
- [7]Kavitha Subramani,Murugavalli Subramaniam,"Creation of original Tamil character dataset through segregation of ancient palm leaf manuscripts in medicine",Expert Systems Volume 38,Issue 1(2020),pp 1-12
- [8] Yong Haur Tay,Pierre-Michel Lallican,Marzuki Khalid,Christian Viard-Gaudin,Stefan Knerr,"*An offline cursive handwritten word recognition system*",Proceedings of IEEE Region 10 International Conference on Electrical and Electronic Technology. TENCON (2001),pp 3-10
- [9] Pankaj S. Parsania,Dr. Paresh V. Virparia,"A Comparative Analysis of Image Interpolation Algorithms",International Journal of Advanced Research in Computer and Communication Engineering Vol. 5, Issue 1(2016),pp 29-34
- [10] Chris Cheadle, Marquis P. Vawter,William J. Freed, Kevin G. Becker,"Analysis of Microarray Data Using Z Score Transformation",Journal of Molecular Diagnostics, Vol. 5, No. 2(2003),pp 73-81
- [11] Yan-Li Liu, Jin Wang,Xi Chen,Yan-Wen Guo,Qun- Sheng Peng,"*A Robust and Fast Non-Local Means Algorithm for Image Denoising*",JOURNAL OF COMPUTER SCIENCE AND TECHNOLOGY 23(2) ,pp 270–279 (2008)
- [12] S.Gopal Krishna Patro,Kishore Kumar sahu,"Normalization: A Preprocessing Stage",arXiv:1503.06462 (2015),pp 1-3
- [13]Suganya Athisayamani, Dr.Robert Singh.A, Dr.Athithan.T,"Recognition of Ancient Tamil Palm Leaf Vowel Characters in Historical Documents using B-spline Curve Recognition",Third International Conference on Computing and Network Communications (CoCoNet'19),PP 1-8
- [14]Vijaya Lakshmi.TR , Panyam Narahari Sastry , Rajinikanth .TV,"A novel 3D approach to recognize Telugu palm leaf text", (ELSEVIER)Engineering science and technology,an international conference(2017),pp 143-150
- [15]M.A.Pragathi, K. Priyadarshini ,S. Saveetha ,A. Shavar Banu ,K. O. Mohammed Aarif ,"Handwritten Tamil Character Recognition Using Deep Learning ",International Conference on Vision Towards Emerging Trends in Communication and Networking (2019),pp 1-5
- [16]Shankar Mahadevan, Rahul Ponnusamy, Prasanna Kumar Kumaresan,Prabakaran Chandran, Ruba Priyadharshini, Sangeetha Sivanesan,Bharathi Raja Chakravarthi,"Thirumurai: A Large Dataset of Tamil Shaivite Poems and Classification of Tamil Pann",Proceedings of the 13th Conference on Language Resources and Evaluation (2022), pp 6556–6562
- [17]Rapeeporn Chamchong and Chun Che Fung,"A Framework for the Selection of Binarization Techniques on Palm Leaf Manuscripts Using Support Vector Machine",Hindawi Publishing Corporation Advances in Decision Sciences Volume 2015, Article ID 925935, pp 1-6, <http://dx.doi.org/10.1155/2015/925935>
- [18] O. Akbani, A.Gokrani, M. Quresh, Furqan M. Khan, Sadaf I. Behlim, Tahir Q. Syed ,"Character Recognition in Natural Scene Images",International Conference on Information and Communication Technologies(2015) pp1-4
- [19]AMIR YAVARIABDI , HUSEYIN KUSETOGULLARI , TURGAY CELIK,SHIVANI THUMMANAPALLY, SAKIB RIJWAN, AND JOHAN HALL ,"CARDIS: A Swedish Historical Handwritten Character and Word Dataset", IEEE Access ,Volume: 10(2022),pp 55338-55347
- [20]Khoi NGUYEN-TAN, Romain RAFFIN, Marc DANIEL and Cung LE ,"B-spline surface reconstruction by inverse subdivisions ", IEEE-RIVF International Conference on Computing and Communication Technologies(2009),pp 1-4
- [21]Mrs.G.Bhuvaneswari ,V. Subbiah Bharathi,"An Efficient Positional Algorithm for Recognition of Ancient Stone Inscription Characters ",Seventh International Conference on Advanced Computing(2015),pp 1-5
- [22]R.A.E. Coningham, F.R. Alicifrt, COM. Batt and D. Lucy ,"Passage to India? Anuradhapura and the Early Use of the Brahmi Script",Cambridge Archaeological Journal 6:1 (1996), pp. 73—97
- [23]Guang-Bin Huang, Qin-Yu Zhu, Chee-Kheong Siew," *Extreme learning machine: Theory and applications*", (ELSEVIER)Neurocomputing Volume 70, Issues 1–3(2006), Pp 489-501
- [24]Md Mahbubar Rahman,M. A. H. Akhand,M. M. Hafizur Rahman ,"Bangla Handwritten Character Recognition

- using Convolutional Neural Network", International Journal of Image, Graphics and Signal Processing (2015)
DOI: 10.5815/ijigsp.2015.08.05, pp 52-59
- [25] G. Janani, V. Vishalini, Dr .P. Mohan Kumar , " Recognition and Analysis of Tamil Inscriptions And Mapping Using Image Processing Techniques" ,2016 Second International Conference on Science Technology Engineering and Management, pp 181-184
- [25] Abdelrahman Abdallah, Mohamed Hamada and Daniyar Nurseitov , "Attention-Based Fully Gated CNN- BGRU for Russian Handwritten Text", arXiv:2008.05373 (2020), pp 1-21
- [26] Manoj Kumar Mahto ,Manoj Kumar Mahto ,R. K. Sharma , "Combined Horizontal and Vertical Projection Feature Extraction Technique for Gurmukhi Handwritten Character Recognition ",2015 International Conference on Advances in Computer Engineering and Applications ,pp 59-68
- [27] Dr.G.Bhuvaneswari, Dr.G.Manikandan
,"RECOGNITION OF ANCIENT STONE INSCRIPTION CHARACTERS USING HISTOGRAM OF ORIENTED GRADIENTS ", International Conference on Recent Trends in Computing, Communication and Networking Technologies (2019), pp 1-8
- [28] Somaya Al-ma'adee, Jihad Mohamad Aljaa, Abdelâali Hassaïne, "QUWI: *An Arabic and English Handwriting Dataset for Offline Writer Identification*", International Conference on Frontiers in Handwriting Recognition (2012), pp 1-8
- [29] LIANG XU , YUXI WANG, XIUXI LI, AND MING PAN , "Recognition of Handwritten Chinese Characters Based on Concept Learning", IEEE Access , Volume: 7 (2019), pp 102039 - 102053
- [30] Verónica Romeroa , Alicia Fornés, Nicolás Serrano, Joan Andreu Sánchez, Alejandro H. Toselli, Volkmar Frinken, Enrique Vidal, Josep Lladó's, "The ESPOSALLES Database: *An Ancient Marriage License Corpus for Offline Handwriting Recognition*", (ELSEVIER) Pattern Recognition Volume 46, Issue 6 (2013), Pages 1658-1669
- [32] N.Sridevi , "Combining Zernike Moments with Regional features for Classification of Handwritten Ancient Tamil Scripts using Extreme Learning Machine" , IEEE International Conference ON Emerging Trends in Computing, Communication and Nanotechnology (2013), PP 158-162, DOI:10.1109/ICE-CCN.2013.6528483
- [33] S. Thadchanamoorthy ,N. D. Kodikara; H. L. Premaretne ,Umapada Pal ,Fumitaka Kimura , "Tamil Handwritten City Name Database Development and Recognition for Postal Automation ", 12th International Conference on Document Analysis and Recognition (2013), pp 793_798
- [34] E.K.Vellingiriraj, Dr.M.Balamurugan, Dr.P.Balasubramanie, "Information Extraction and Text Mining of Ancient Vattezhuthu Characters in Historical Documents Using Image Zoning " ,2016 International Conference on Asian Language Processing (2016), pp 37-40.

Under water Image Enhancement and Classification

¹Manoj Pandian GV, ²Surendar M, ³Raja Pandi L, ⁴Bharath M,

B.E-CSE Final year, Velammal College of Engineering and Technology

⁵Dr.R.Deepalakshmi, B.E, M.E, Ph.D., Velammal College of Engineering and Technology,
rdl@vcet.ac.in

Abstract--Attenuation, uneven, colour distortion, and reduced contrast in submerged images all manage disputing to analyse and define optical information. Diverse forms and algorithms have existed proposed to enhance the character of underwater figures and extract valuable information from ruling class, making important progress in the field of submerged figure enhancement and categorization in current years. We supply a inclusive overview of ultimate current methods for undersea representation enhancement and categorization in this place paper. The challenges and characteristics of underwater images are first discussed, and then various enhancement techniques like colour correction, contrast enhancement, and dehazing are presented. In addition, various feature extraction and classification algorithms, such as object recognition, texture analysis, and deep learning for underwater image analysis, are examined in this paper. The paper concludes with a critical evaluation of the current methods and recommendations for future research.

Keywords—Underwater images, image enhancement, image classification, feature extraction, and deep learning.

I. INTRODUCTION

In recent years, there has been a growing emphasis on the study of underwater imaging, as it holds great significance in various fields such as marine biology, oceanography, naval surveillance, underwater inspection and exploration, and underwater robotics. However, the process of underwater imaging is particularly challenging due to the intricate and ever changing nature of the underwater environment. This complexity arises from factors like light attenuation, backscatter, and water turbidity, among others. These factors can significantly impact the quality of underwater images, making it difficult to accurately identify and classify underwater objects and features. To overcome these challenges, researchers have devised a range of techniques and algorithms that aim to enhance and classify underwater images, with the ultimate goal of improving their quality and facilitating the precise identification and classification of underwater objects and features. This paper will provide an overview of the current cutting-edge techniques employed in underwater image enhancement and classification, specifically focusing on the utilization of deep learning techniques.

II.UNDERWATER IMAGE ENHANCEMENT

The quality of underwater images is often subpar due to the limited amount of light available in the underwater environment. This can lead to issues such as low contrast, poor visibility, and color distortion. To address these challenges, various techniques have been developed for underwater image enhancement. The objective of these techniques is to improve the quality and clarity of underwater images.

One commonly employed technique for underwater image enhancement is image preprocessing. This involves the elimination of noise and artifacts from the image. Techniques such as filtering and deconvolution can be utilized to remove noise and blur, thereby enhancing the sharpness and clarity of the image.

Another frequently used technique for underwater image enhancement is colour correction. The goal of colour correction is to rectify colour distortion in underwater images caused by the absorption and scattering of light in water. Techniques such as white balancing and colour correction algorithms can be employed to adjust the colour temperature and colour balance of the image, thereby enhancing its overall appearance and visibility.

Furthermore, image fusion techniques can be employed to merge multiple images of the same scene captured from different viewpoints or at different times. This can enhance the overall quality and clarity of the image. These techniques are particularly valuable for underwater imaging, where images can be distorted due to the complex and dynamic nature of the underwater environment.

III. UNDERWATER IMAGE CLASSIFICATION

Underwater image classification involves the identification and classification of objects and features in underwater images, based on their visual characteristics and properties. This can be achieved using various machine learning techniques, such as supervised and unsupervised learning, deep learning, and convolutional neural networks (CNNs).

One of the most commonly used techniques for underwater image classification is supervised learning, which involves the use of labeled datasets to train a classifier to identify and classify objects in underwater images. This approach is highly effective for underwater image classification, particularly when combined with feature extraction techniques such as the bag-of-features approach.

Another commonly used technique for underwater image classification is unsupervised learning, which involves the use of unlabeled datasets to identify patterns and clusters in underwater images. This approach can be particularly useful for identifying new and previously unknown objects and features in underwater images.

Deep learning techniques, such as CNNs, have also been shown to be highly effective for underwater image classification, due to their ability to automatically learn and extract features from large datasets. These techniques have been used to classify a wide range of underwater objects and features, such as fish species, coral reefs, and ship wrecks.

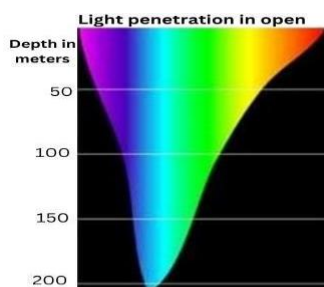


Fig 1

Figure: 1 Color penetration pattern It is obvious that because blue has the shortest apparent wavelength, it goes the farthest in the ocean and deep. This results in the bluehue dominating underwater photos, which has the unfavorable consequence of changing the original color of any underwater objects. The blurry photos also have an overwhelming amount of blue and minimal brightness, contrast, and other elements.

IV. LITERATURE SURVEY

A. *New underwater image dataset:*

Ashraf Shaleem Et.al[1] described the performance of selected models at different depths comparatively analyzed and got better-quality images than others at certain depths.

B. *Visual Perception:*

Md Jahidul Islam Et.al[2] suggest that the proposed model can learn to enhance underwater image quality from both paired and unpaired training saying visible guided underwater robot are suitable for real-time preprocessing in the autonomy pipeline.

C. *Classification on Data Augmentation:*

Yifeng Xu Et.al[3]described two augmentation methods that can improve classification probability by transforming raw data and increasing virtue data.

D. *Classification on Data Augmentation:*

According to Vimal Raj E.tal.[4], the classification of features in underwater optical images is challenging due to their low light intensity. To address this issue, the researchers have employed the SURF (Speeded-UP Robust Features) and SVM (Support Vector Machines) algorithms within bag of Features models. This approach aims to achieve the highest possible accuracy in feature classification.

E. *Benchmark Dataset and beyond:*

Chongyi Li Et.al[5]proposed an underwater image enhancement network Water-Net as a baseline for training CNNs and enhancement was done on Water-Net.

F. *Image processing technique:*

Arpit Wany Et.al[6]proposed to improve underwater images by using a technique to reduce medium scattering and absorption. It results in the sharpening of the image not being done to reduce noise issues.

V.PROBLEM STATEMENT

The Problem statement is identified and discussed below.

Enhancing and classifying underwater images poses a significant challenge due to the influence of environmental factors on the visual perception of underwater robots[7]. Underwater images often suffer from color distortion, low contrast, and lack of clarity[7]. To tackle these issues, researchers have put forth different image enhancement algorithms based on deep learning and image formation models[7][8][9].

In a recent study, Li et al. proposed the utilization of a deep neural network to classify and de-scatter underwater image data[9]. Their method employs a convolutional neural network to mitigate the scattering effect caused by the underwater environment and improve image quality[9]. Additionally, the authors employed a support vector machine classifier to categorize the enhanced images[9]. Experimental results demonstrated that their proposed method outperformed other state-of-the-art techniques in terms of image quality and classification accuracy[9].

Another approach to enhancing underwater images involves using particle swarm optimization to adjust the RGB values of the image[9]. AbuNaser et al. employed this method to enhance the illumination and true colors of underwater images[9]. Lu et al. proposed a weighted guided trigonometric filtering and artificial light correction approach to improve underwater images[9]. Their method incorporates a color correction algorithm to rectify color distortion and a guided filter to enhance image quality[9].

In conclusion, underwater image enhancement and classification is a significant research area that has garnered considerable attention in recent years. Researchers have proposed various algorithms based on deep learning, image formation models, and optimization techniques to address the challenges associated with underwater imaging. These methods have exhibited promising outcomes in enhancing image quality and classification accuracy of underwater images.

VI. METHODOLOGY

In the ever-evolving educational landscape, the adoption of Deep Learning (DL) algorithms has sparked a renaissance in understanding students' learning patterns. By amassing a captivating array of underwater fish images, a remarkable Convolutional Neural Network (CNN) algorithm is summoned to wield its prowess in discerning and identifying the diverse marine species that dwell beneath the waves.

A. *Data selection and loading:*

The data selection is the process of selecting the underwater fish species' digital image dataset. Recognizing the many undersea fish species is the focus of this study. The dataset contains information about the types of underwater images like, 'Corals', 'Crabs', 'Dolphin', 'Eel', 'Jelly Fish', 'Lobster', 'Nudibranchs', 'Octopus', 'Penguin', 'Puffers', 'Sea Rays', 'Sea Urchins', 'Seahorse', 'Seal', 'Sharks', 'Squid', 'Starfish', 'Turtle Tortoise', 'Whale'.

B. *Data preprocessing:*

Getting rescaled data from the dataset is the process of pre-processing image data. Data collection and picture dataset resizing. Rescale the size of the remote sensing scene dataset's pictures to 100. Collecting data: The variables in that categorical data are described as having a limited number of rescaled values. That array input and output variables are needed by the majority of deep learning techniques.

C. *Splitting Dataset Into Train And Test Data:*

The act of partitioning a set of available data into two distinct subsets, commonly done for the purpose of cross-validation, is referred to as data splitting. This involves the creation of a predictive model using one portion of the data, while the effectiveness of the model is evaluated using a separate portion. In the context of analyzing image processing models, a

critical step involves dividing the data into training and testing sets. Typically, the majority of the image data is allocated for training, while a smaller portion is reserved for testing, when the dataset is divided into these two subsets.

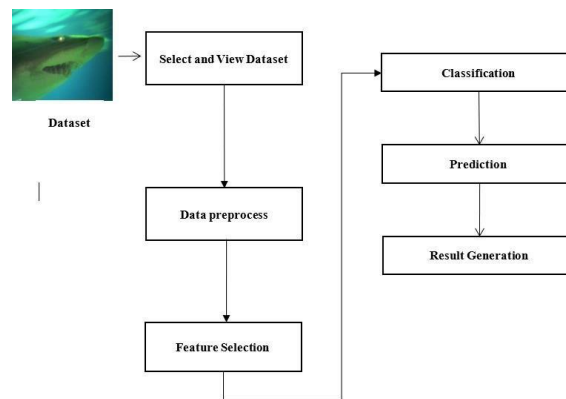


Fig 2: System Diagram

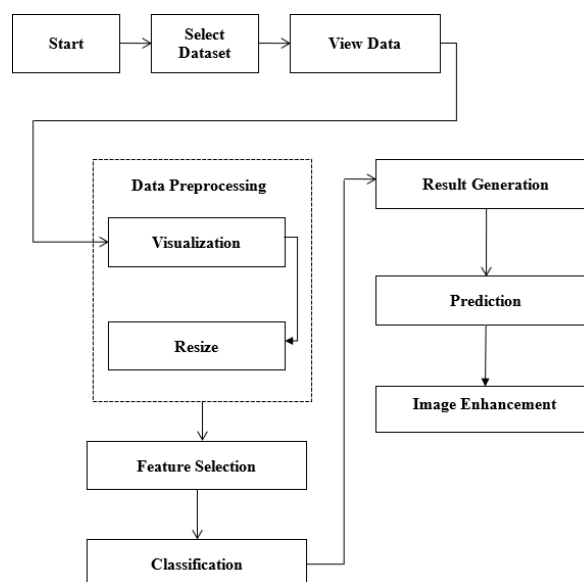


Fig 3: Flow Diagram

D. Classification:

The methodology for underwater classification using Convolutional Neural Networks (CNNs) involves several key steps. First, a diverse and representative dataset of underwater images is collected, containing various fish species, coral formations, and marine life. Data augmentation techniques may be applied to expand the dataset and enhance the model's generalization ability. The dataset is then split into training, validation, and testing sets. Next, a CNN architecture is designed, comprising multiple convolutional layers for feature extraction, pooling layers for dimensionality reduction, and fully connected layers for classification. The CNN model is trained on the training dataset using back propagation and optimization algorithms, aiming to minimize the classification error. Hyperparameter tuning and regularization methods are employed to prevent overfitting.

Transfer learning can also be considered, where pre-trained models on large-scale image datasets are fine-tuned for underwater classification. Once trained, the CNN model's performance is evaluated on the validation and testing datasets, using appropriate metrics such as accuracy, precision, recall, and F1 score. The final model is then deployed to classify underwater images, contributing to ecological research, conservation efforts, and better understanding of underwater ecosystems.

E. Prediction:

The approach involves utilizing a deep learning model to identify the type of undersea fish from the dataset. By optimizing the total prediction outcomes, this project will successfully forecast the data from the dataset.

- White Balance:

White balancing is a subject that has been discussed quite a bit, however, most of the replies I have read discuss automatic white balancing methods for a complete image without a clear distinction between what is white, grey, and black.

This strategy is characteristic of the Color Constancy adaption, which works similarly to how the human visual system does by looking for the lightest patch to serve as a white reference. Keep in mind that each channel in your RGB color space needs to be at its highest value for white to be visible in the image.

- Gamma Correction:

Gamma correction is a technique used to adjust the overall brightness of an image. When photos are not properly adjusted, they may appear either too dark or washed out. Additionally, accurate color reproduction also requires an understanding of gamma. Gamma correction is employed to enhance the contrast of images. In the typical scenario where $A = 1$, the inputs and outputs are typically non-negative real numbers, with A being a constant ranging from 0 to 1. Conversely, gamma compression involves encoding with a compressive power-law nonlinearity, where a gamma value of 1 is commonly referred to as an encoding gamma value, while a gamma value greater than 1 is known as a decoding gamma. On the other hand, gamma expansion refers to the utilization of an expansive power-law nonlinearity. The formula for gamma correction is $V_{out} = V_{in}^{\gamma}$.

- Histogram:

In underwater image classification, histogram equalization plays a pivotal role in enhancing image visibility and contrast. Underwater environments often suffer from poor lighting and water turbidity, resulting in images with limited visual information. By applying histogram equalization, the intensity levels of the underwater images are redistributed, leading to improved image quality and the revelation of hidden details. This preprocessing step effectively enhances the visibility of marine life, corals, and other underwater features, facilitating accurate classification. Histogram equalization proves to be instrumental in achieving higher classification accuracy, enabling a more comprehensive understanding of marine ecosystems and fostering advancements in underwater research and conservation efforts.



Fig 4: White Balance



Fig 5: Gamma correction

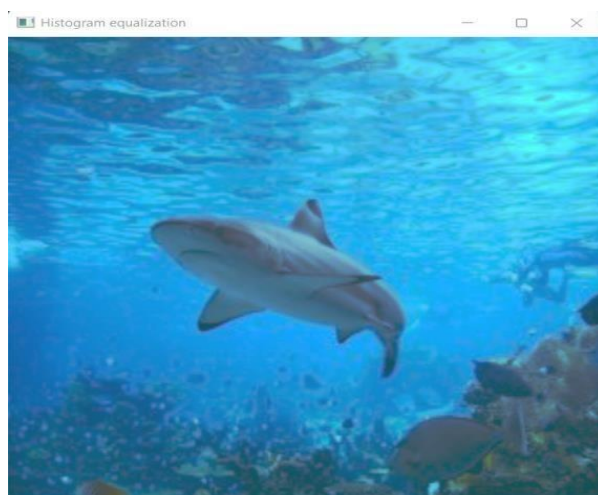


Fig 6: Histogram equalization

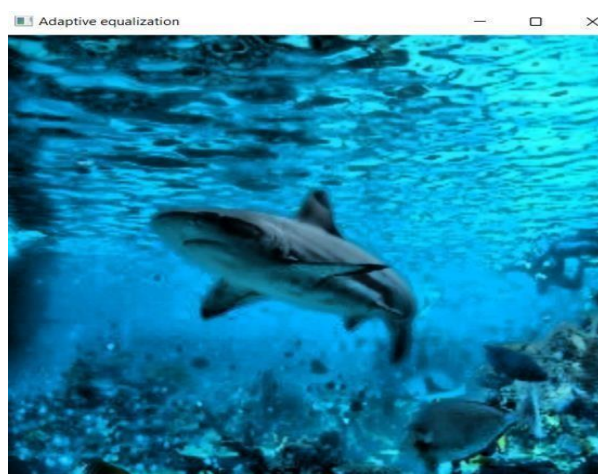


Fig 7: Adaptive Equalization

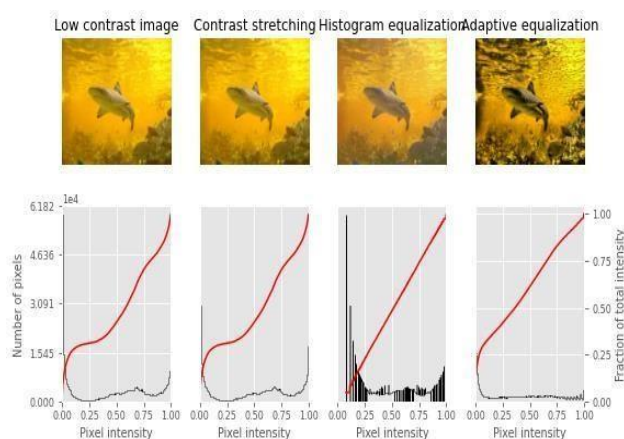


Fig 8: Enhanced Images

VII. RESULT & DISCUSSION

The main objective is to determine the accuracy of classifying pictures using clustered categories. A dataset consisting of 16,042 underwater photographs taken with a remotely

operated vehicle (ROV) in a shallow area was used. The photographs were divided into seven unrelated classes, including corals, crabs, dolphins, eels, jellyfish, lobsters, nudibranchs, octopuses, penguins, puffers, sea rays, sea urchins, seahorses, seals, sharks, squids, starfish, turtle tortoises, and whales. 80% of the dataset was used for training, while the remaining 20% was used for testing or validation. The analysis considered the top 33,280 strongest characteristics in each category, resulting in a total of 186,368 features. The default setting of 500 clusters was used. Two methods were used to extract patches: the region of interest and the grid methods. In this case, the grid method was used to recover all the features, and a histogram was created to show the frequency of occurrences. The confusion matrix showed that the majority of true positive values were correctly classified, resulting in an overall accuracy of 97.9%. Sample images can be seen in Fig 9, and the dataset is listed in Table 1.

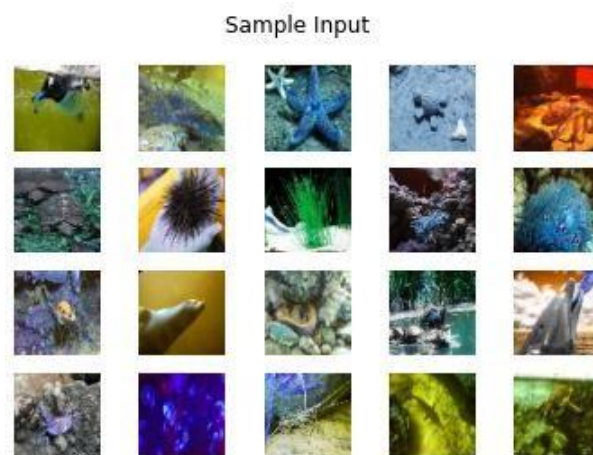


Fig 9: Sample Inputs

Data	IMAGES
Corals	500
Crabs	499
Dolphin	782
Eel	497
jelly fish	855
Lobster	499
Nudibranchs	500
Octopus	562
Penguin	482
Puffers	531
Sea Rays	517
Sea Urchins	579
Seahorse	4778
Seal	414
Sharks	590
Squid	483
Starfish	499
Turtle_Tortoise	1903
Whale	572
TOTAL	16042

Table 1: Dataset

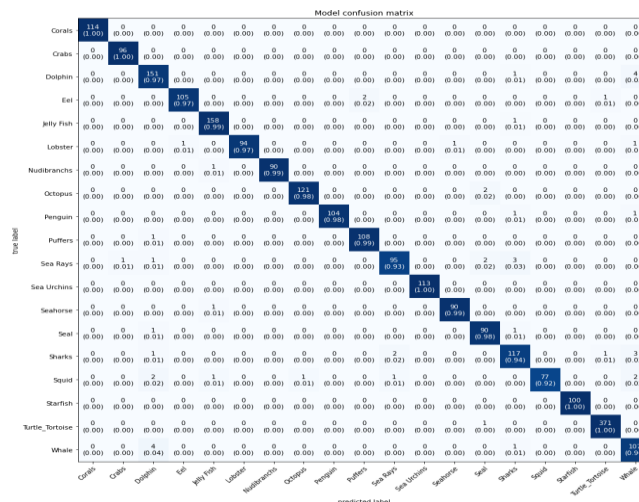


Fig 10: Confusion matrix

The model confusion matrix X as predicted label Y as a true label which gives merely 97.9 % accuracy the performance plot accuracy rises gradually and we can predict loss as rapidly are shown in the Fig 11 and classification on prediction found as shown as Fig 12.

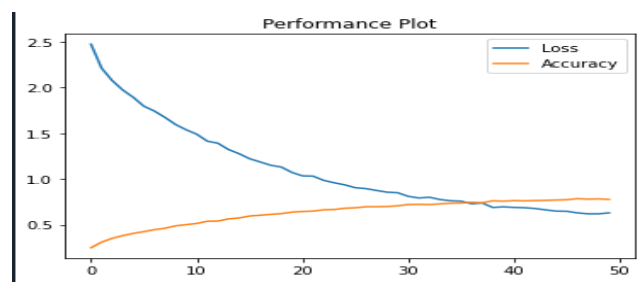


Fig 11: Performance Plot



Accuracy of the CNN is: 97.95657992362976 %

Fig 12: Output & Prediction

VII. CONCLUSION

In this study, a deep learning classifier is employed to analyze photographs of various underwater fish species. The pre-processing phase involves utilizing images of multiple underwater fish species as input data. These photos are resized and organized into an array. Subsequently, the dataset is divided into a training dataset and a testing dataset through the feature selection technique. All the photos are then downscaled and transformed into an array format. Finally, the classification approach is employed to classify the photos of underwater fish species. The deep learning method of Convolutional Neural Networks (CNN) is utilized to predict the outcome, employing metrics such as accuracy, precision, and recall f1-measure.

REFERENCE

- [1] Underwater Image Enhancement Methods Using A New Underwater Image Dataset Ashraf Shaleemet.at., (2023)
- [2] Md Jahidul Islam et.at., Fast Underwater Image Enhancement for Improved Visual Perception(2020).
- [3] Yifeng Xu et.at., Underwater Image Classification Using Deep CNN and Data Augmentation (2018)
- [4] M. Vimal Raj, et.at., "Underwater Image Classification using Machine Learning Technique" , International Symposium on Ocean Technology (SYMPOL), 2019
- [5] Chongyi Li et.at., Underwater Image Enhancement Benchmark Dataset and beyond(2019)
- [6] Arpit Wany et.at., Underwater Image Enhancement Using Image processing Techniques(2021)
- [7] An Experimental-Based Review of Image Enhancement and Image Restoration Methods for Underwater Imaging Yan Wang et.at., (2019)
- [8] Underwater Image Enhancement based on Deep Learning and Image Formation Model Xuele Chen, et.at., (2021)
- [9] Underwater image enhancement: a comprehensive review, recent trends, challenges and applications, Smitha Raveendran, (2021).
- [10] Swati Sonawane, et.al., Underwater image classification and enhancement.IJSDR, October 2022.
- [11] Devendar Marasakatla, et.at., Under Water Image Enhancement Using CNN ,ICAECIS, 2023
- [12] Anushka Yadav, et.al., Underwater image enhancement using convolutional neural network. IEEE 18 September 2021.
- [13] Shirin Shahana V, et.al., Underwater image enhancement and color correction a review. SEMANCTIC scholar, 2022.
- [14] S.-B. Gao, et.al., Underwater image enhancement using adaptive retinal mechanisms. IEEE, 28 November 2019.
- [15] [M. Han, et.al., A review on intelligence dehazing and color restoration for underwater images. IEEE, 23 January 2018.
- [16] Changli Li, et at, Color correction based on CFA and enhancement based on Retinex with dense pixels for underwater images. IEEE, 2020.
- [17] Zitong Kang, et at, Underwater image enhancement by maximum- likelihood based adaptive color correction and robust scattering removal.

- [18] R Prasath, et al, Application of Different Techniques for Underwater Image Processing- A Systematic Review. ICCEMS, 2020.
- [19] Yang Guan et.al., Fast underwater image enhancement based on a generative adversarial framework. IEEE, 2023.
- [20] Chengquan Zhang et.al "Underwater image enhancement based on an integrated color model." IET Computer Vision -2017

Under water Image Enhancement and Classification

¹Manoj Pandian GV, ²Surendar M, ³Raja Pandi L, ⁴Bharath M,

B.E-CSE Final year, Velammal College of Engineering and Technology

⁵Dr.R.Deepalakshmi, B.E, M.E, Ph.D., Velammal College of Engineering and Technology,
rdl@vcet.ac.in

Abstract--Attenuation, uneven, colour distortion, and reduced contrast in submerged images all manage disputing to analyse and define optical information. Diverse forms and algorithms have existed proposed to enhance the character of underwater figures and extract valuable information from ruling class, making important progress in the field of submerged figure enhancement and categorization in current years. We supply a inclusive overview of ultimate current methods for undersea representation enhancement and categorization in this place paper. The challenges and characteristics of underwater images are first discussed, and then various enhancement techniques like colour correction, contrast enhancement, and dehazing are presented. In addition, various feature extraction and classification algorithms, such as object recognition, texture analysis, and deep learning for underwater image analysis, are examined in this paper. The paper concludes with a critical evaluation of the current methods and recommendations for future research.

Keywords—Underwater images, image enhancement, image classification, feature extraction, and deep learning.

I. INTRODUCTION

In recent years, there has been a growing emphasis on the study of underwater imaging, as it holds great significance in various fields such as marine biology, oceanography, naval surveillance, underwater inspection and exploration, and underwater robotics. However, the process of underwater imaging is particularly challenging due to the intricate and ever changing nature of the underwater environment. This complexity arises from factors like light attenuation, backscatter, and water turbidity, among others. These factors can significantly impact the quality of underwater images, making it difficult to accurately identify and classify underwater objects and features. To overcome these challenges, researchers have devised a range of techniques and algorithms that aim to enhance and classify underwater images, with the ultimate goal of improving their quality and facilitating the precise identification and classification of underwater objects and features. This paper will provide an overview of the current cutting-edge techniques employed in underwater image enhancement and classification, specifically focusing on the utilization of deep learning techniques.

II.UNDERWATER IMAGE ENHANCEMENT

The quality of underwater images is often subpar due to the limited amount of light available in the underwater environment. This can lead to issues such as low contrast, poor visibility, and color distortion. To address these challenges, various techniques have been developed for underwater image enhancement. The objective of these techniques is to improve the quality and clarity of underwater images.

One commonly employed technique for underwater image enhancement is image preprocessing. This involves the elimination of noise and artifacts from the image. Techniques such as filtering and deconvolution can be utilized to remove noise and blur, thereby enhancing the sharpness and clarity of the image.

Another frequently used technique for underwater image enhancement is colour correction. The goal of colour correction is to rectify colour distortion in underwater images caused by the absorption and scattering of light in water. Techniques such as white balancing and colour correction algorithms can be employed to adjust the colour temperature and colour balance of the image, thereby enhancing its overall appearance and visibility.

Furthermore, image fusion techniques can be employed to merge multiple images of the same scene captured from different viewpoints or at different times. This can enhance the overall quality and clarity of the image. These techniques are particularly valuable for underwater imaging, where images can be distorted due to the complex and dynamic nature of the underwater environment.

III. UNDERWATER IMAGE CLASSIFICATION

Underwater image classification involves the identification and classification of objects and features in underwater images, based on their visual characteristics and properties. This can be achieved using various machine learning techniques, such as supervised and unsupervised learning, deep learning, and convolutional neural networks (CNNs).

One of the most commonly used techniques for underwater image classification is supervised learning, which involves the use of labeled datasets to train a classifier to identify and classify objects in underwater images. This approach is highly effective for underwater image classification, particularly when combined with feature extraction techniques such as the bag-of-features approach.

Another commonly used technique for underwater image classification is unsupervised learning, which involves the use of unlabeled datasets to identify patterns and clusters in underwater images. This approach can be particularly useful for identifying new and previously unknown objects and features in underwater images.

Deep learning techniques, such as CNNs, have also been shown to be highly effective for underwater image classification, due to their ability to automatically learn and extract features from large datasets. These techniques have been used to classify a wide range of underwater objects and features, such as fish species, coral reefs, and ship wrecks.

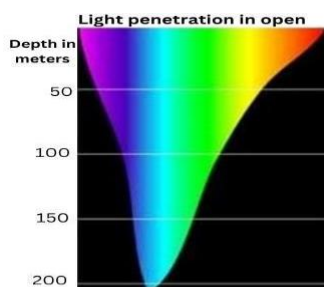


Fig 1

Figure: 1 Color penetration pattern It is obvious that because blue has the shortest apparent wavelength, it goes the farthest in the ocean and deep. This results in the bluehue dominating underwater photos, which has the unfavorable consequence of changing the original color of any underwater objects. The blurry photos also have an overwhelming amount of blue and minimal brightness, contrast, and other elements.

IV. LITERATURE SURVEY

A. *New underwater image dataset:*

Ashraf Shaleem Et.al[1] described the performance of selected models at different depths comparatively analyzed and got better-quality images than others at certain depths.

B. *Visual Perception:*

Md Jahidul Islam Et.al[2] suggest that the proposed model can learn to enhance underwater image quality from both paired and unpaired training saying visible guided underwater robot are suitable for real-time preprocessing in the autonomy pipeline.

C. *Classification on Data Augmentation:*

Yifeng Xu Et.al[3]described two augmentation methods that can improve classification probability by transforming raw data and increasing virtue data.

D. *Classification on Data Augmentation:*

According to Vimal Raj E.tal.[4], the classification of features in underwater optical images is challenging due to their low light intensity. To address this issue, the researchers have employed the SURF (Speeded-UP Robust Features) and SVM (Support Vector Machines) algorithms within bag of Features models. This approach aims to achieve the highest possible accuracy in feature classification.

E. *Benchmark Dataset and beyond:*

Chongyi Li Et.al[5]proposed an underwater image enhancement network Water-Net as a baseline for training CNNs and enhancement was done on Water-Net.

F. *Image processing technique:*

Arpit Wany Et.al[6]proposed to improve underwater images by using a technique to reduce medium scattering and absorption. It results in the sharpening of the image not being done to reduce noise issues.

V.PROBLEM STATEMENT

The Problem statement is identified and discussed below.

Enhancing and classifying underwater images poses a significant challenge due to the influence of environmental factors on the visual perception of underwater robots[7]. Underwater images often suffer from color distortion, low contrast, and lack of clarity[7]. To tackle these issues, researchers have put forth different image enhancement algorithms based on deep learning and image formation models[7][8][9].

In a recent study, Li et al. proposed the utilization of a deep neural network to classify and de-scatter underwater image data[9]. Their method employs a convolutional neural network to mitigate the scattering effect caused by the underwater environment and improve image quality[9]. Additionally, the authors employed a support vector machine classifier to categorize the enhanced images[9]. Experimental results demonstrated that their proposed method outperformed other state-of-the-art techniques in terms of image quality and classification accuracy[9].

Another approach to enhancing underwater images involves using particle swarm optimization to adjust the RGB values of the image[9]. AbuNaser et al. employed this method to enhance the illumination and true colors of underwater images[9]. Lu et al. proposed a weighted guided trigonometric filtering and artificial light correction approach to improve underwater images[9]. Their method incorporates a color correction algorithm to rectify color distortion and a guided filter to enhance image quality[9].

In conclusion, underwater image enhancement and classification is a significant research area that has garnered considerable attention in recent years. Researchers have proposed various algorithms based on deep learning, image formation models, and optimization techniques to address the challenges associated with underwater imaging. These methods have exhibited promising outcomes in enhancing image quality and classification accuracy of underwater images.

VI. METHODOLOGY

In the ever-evolving educational landscape, the adoption of Deep Learning (DL) algorithms has sparked a renaissance in understanding students' learning patterns. By amassing a captivating array of underwater fish images, a remarkable Convolutional Neural Network (CNN) algorithm is summoned to wield its prowess in discerning and identifying the diverse marine species that dwell beneath the waves.

A. *Data selection and loading:*

The data selection is the process of selecting the underwater fish species' digital image dataset. Recognizing the many undersea fish species is the focus of this study. The dataset contains information about the types of underwater images like, 'Corals', 'Crabs', 'Dolphin', 'Eel', 'Jelly Fish', 'Lobster', 'Nudibranchs', 'Octopus', 'Penguin', 'Puffers', 'Sea Rays', 'Sea Urchins', 'Seahorse', 'Seal', 'Sharks', 'Squid', 'Starfish', 'Turtle Tortoise', 'Whale'.

B. *Data preprocessing:*

Getting rescaled data from the dataset is the process of pre-processing image data. Data collection and picture dataset resizing. Rescale the size of the remote sensing scene dataset's pictures to 100. Collecting data: The variables in that categorical data are described as having a limited number of rescaled values. That array input and output variables are needed by the majority of deep learning techniques.

C. *Splitting Dataset Into Train And Test Data:*

The act of partitioning a set of available data into two distinct subsets, commonly done for the purpose of cross-validation, is referred to as data splitting. This involves the creation of a predictive model using one portion of the data, while the effectiveness of the model is evaluated using a separate portion. In the context of analyzing image processing models, a

critical step involves dividing the data into training and testing sets. Typically, the majority of the image data is allocated for training, while a smaller portion is reserved for testing, when the dataset is divided into these two subsets.

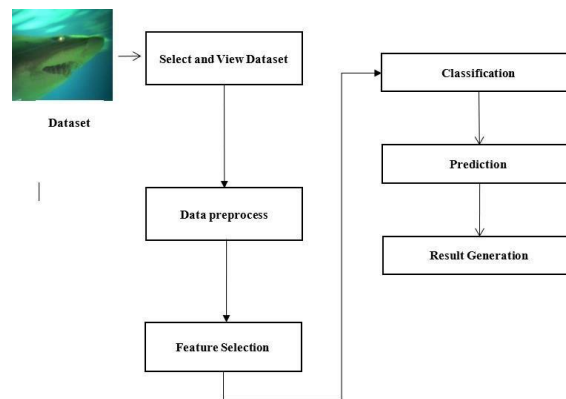


Fig 2: System Diagram

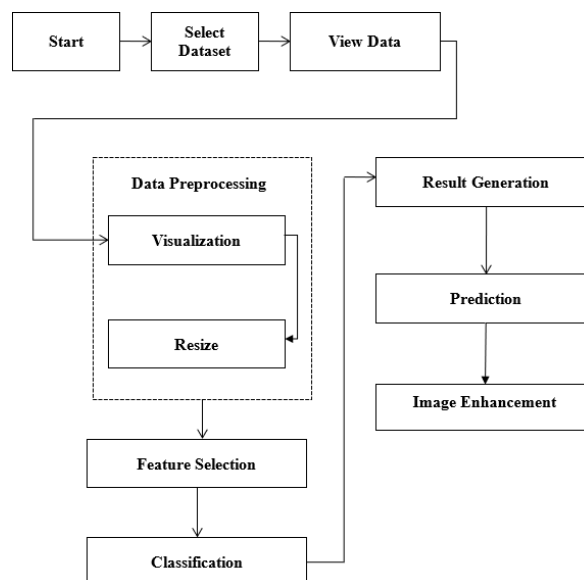


Fig 3: Flow Diagram

D. Classification:

The methodology for underwater classification using Convolutional Neural Networks (CNNs) involves several key steps. First, a diverse and representative dataset of underwater images is collected, containing various fish species, coral formations, and marine life. Data augmentation techniques may be applied to expand the dataset and enhance the model's generalization ability. The dataset is then split into training, validation, and testing sets. Next, a CNN architecture is designed, comprising multiple convolutional layers for feature extraction, pooling layers for dimensionality reduction, and fully connected layers for classification. The CNN model is trained on the training dataset using back propagation and optimization algorithms, aiming to minimize the classification error. Hyperparameter tuning and regularization methods are employed to prevent overfitting.

Transfer learning can also be considered, where pre-trained models on large-scale image datasets are fine-tuned for underwater classification. Once trained, the CNN model's performance is evaluated on the validation and testing datasets, using appropriate metrics such as accuracy, precision, recall, and F1 score. The final model is then deployed to classify underwater images, contributing to ecological research, conservation efforts, and better understanding of underwater ecosystems.

E. Prediction:

The approach involves utilizing a deep learning model to identify the type of undersea fish from the dataset. By optimizing the total prediction outcomes, this project will successfully forecast the data from the dataset.

- White Balance:

White balancing is a subject that has been discussed quite a bit, however, most of the replies I have read discuss automatic white balancing methods for a complete image without a clear distinction between what is white, grey, and black.

This strategy is characteristic of the Color Constancy adaption, which works similarly to how the human visual system does by looking for the lightest patch to serve as a white reference. Keep in mind that each channel in your RGB color space needs to be at its highest value for white to be visible in the image.

- Gamma Correction:

Gamma correction is a technique used to adjust the overall brightness of an image. When photos are not properly adjusted, they may appear either too dark or washed out. Additionally, accurate color reproduction also requires an understanding of gamma. Gamma correction is employed to enhance the contrast of images. In the typical scenario where $A = 1$, the inputs and outputs are typically non-negative real numbers, with A being a constant ranging from 0 to 1. Conversely, gamma compression involves encoding with a compressive power-law nonlinearity, where a gamma value of 1 is commonly referred to as an encoding gamma value, while a gamma value greater than 1 is known as a decoding gamma. On the other hand, gamma expansion refers to the utilization of an expansive power-law nonlinearity. The formula for gamma correction is $V_{out} = V_{in}^{\gamma}$.

- Histogram:

In underwater image classification, histogram equalization plays a pivotal role in enhancing image visibility and contrast. Underwater environments often suffer from poor lighting and water turbidity, resulting in images with limited visual information. By applying histogram equalization, the intensity levels of the underwater images are redistributed, leading to improved image quality and the revelation of hidden details. This preprocessing step effectively enhances the visibility of marine life, corals, and other underwater features, facilitating accurate classification. Histogram equalization proves to be instrumental in achieving higher classification accuracy, enabling a more comprehensive understanding of marine ecosystems and fostering advancements in underwater research and conservation efforts.



Fig 4: White Balance



Fig 5: Gamma correction

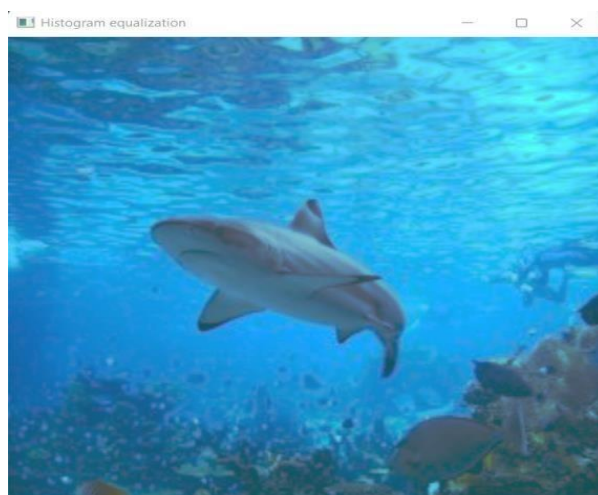


Fig 6: Histogram equalization

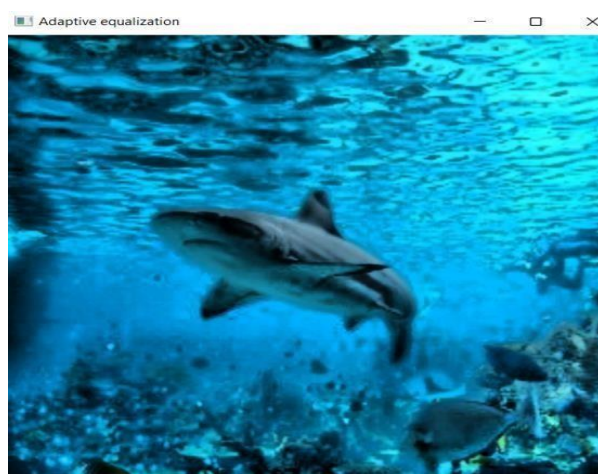


Fig 7: Adaptive Equalization

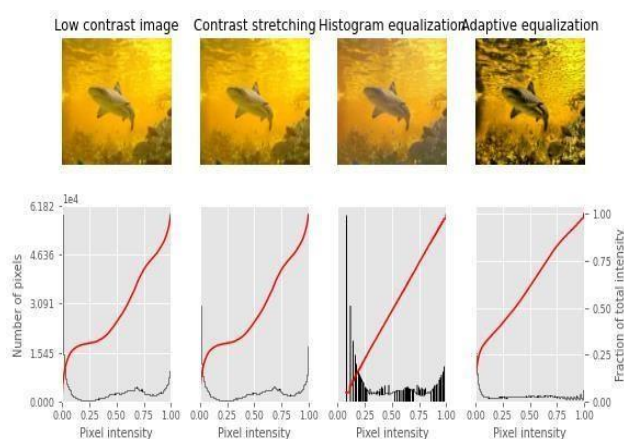


Fig 8: Enhanced Images

VII. RESULT & DISCUSSION

The main objective is to determine the accuracy of classifying pictures using clustered categories. A dataset consisting of 16,042 underwater photographs taken with a remotely

operated vehicle (ROV) in a shallow area was used. The photographs were divided into seven unrelated classes, including corals, crabs, dolphins, eels, jellyfish, lobsters, nudibranchs, octopuses, penguins, puffers, sea rays, sea urchins, seahorses, seals, sharks, squids, starfish, turtle tortoises, and whales. 80% of the dataset was used for training, while the remaining 20% was used for testing or validation. The analysis considered the top 33,280 strongest characteristics in each category, resulting in a total of 186,368 features. The default setting of 500 clusters was used. Two methods were used to extract patches: the region of interest and the grid methods. In this case, the grid method was used to recover all the features, and a histogram was created to show the frequency of occurrences. The confusion matrix showed that the majority of true positive values were correctly classified, resulting in an overall accuracy of 97.9%. Sample images can be seen in Fig 9, and the dataset is listed in Table 1.

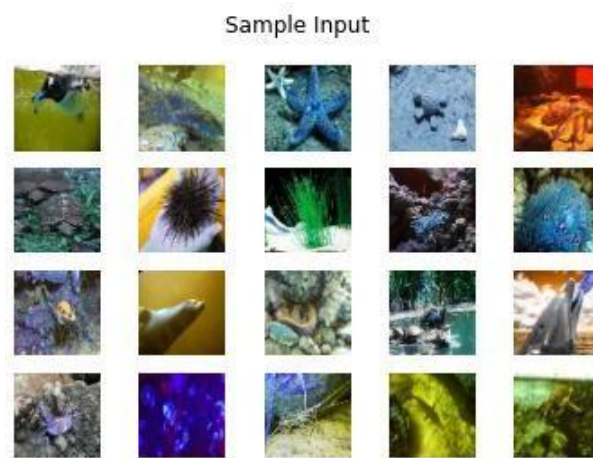
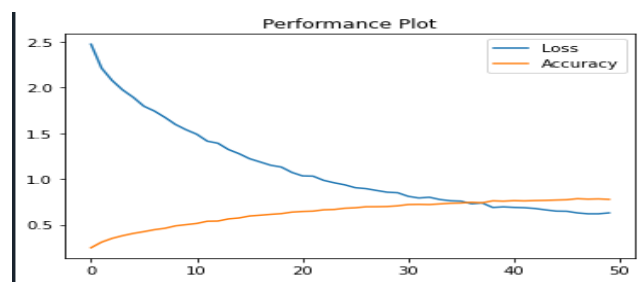


Fig 9: Sample Inputs

Data	IMAGES
Corals	500
Crabs	499
Dolphin	782
Eel	497
jelly fish	855
Lobster	499
Nudibranchs	500
Octopus	562
Penguin	482
Puffers	531
Sea Rays	517
Sea Urchins	579
Seahorse	4778
Seal	414
Sharks	590
Squid	483
Starfish	499
Turtle_Tortoise	1903
Whale	572
TOTAL	16042

	Catfish	Crabs	Dolphin	Eel	Jelly Fish	Lobster	Mudcranch	Octopus	Penguin	Puffers	Sea Rays	Sea Urchins	Seahorse	Seal	Sharks	Squid	Starfish	Turtle_Tortoise	Whale
Catfish	114 (0.97)	0 (0.00)	0 (0.00)	0 (0.00)	0 (0.00)	0 (0.00)	0 (0.00)	0 (0.00)	0 (0.00)	0 (0.00)	0 (0.00)	0 (0.00)	0 (0.00)	0 (0.00)	0 (0.00)	0 (0.00)	0 (0.00)	0 (0.00)	0 (0.00)
Crabs	0 (0.00)	150 (1.00)	0 (0.00)	0 (0.00)	0 (0.00)	0 (0.00)	0 (0.00)	0 (0.00)	0 (0.00)	0 (0.00)	0 (0.00)	0 (0.00)	0 (0.00)	0 (0.00)	0 (0.00)	0 (0.00)	0 (0.00)	0 (0.00)	0 (0.00)
Dolphin	0 (0.00)	0 (0.00)	151 (0.97)	0 (0.00)	0 (0.00)	0 (0.00)	0 (0.00)	0 (0.00)	0 (0.00)	0 (0.00)	0 (0.00)	0 (0.00)	0 (0.00)	0 (0.00)	0 (0.00)	0 (0.00)	0 (0.00)	0 (0.00)	4 (0.00)
Eel	0 (0.00)	0 (0.00)	0 (0.00)	150 (0.97)	0 (0.00)	0 (0.00)	0 (0.00)	0 (0.00)	0 (0.00)	0 (0.00)	0 (0.00)	0 (0.00)	0 (0.00)	0 (0.00)	0 (0.00)	0 (0.00)	0 (0.00)	0 (0.00)	0 (0.00)
Jelly Fish	0 (0.00)	0 (0.00)	0 (0.00)	0 (0.00)	150 (0.98)	0 (0.00)	0 (0.00)	0 (0.00)	0 (0.00)	0 (0.00)	0 (0.00)	0 (0.00)	0 (0.00)	0 (0.00)	0 (0.00)	0 (0.00)	0 (0.00)	0 (0.00)	0 (0.00)
Lobster	0 (0.00)	0 (0.00)	0 (0.00)	0 (0.00)	0 (0.00)	150 (0.97)	0 (0.00)	0 (0.00)	0 (0.00)	0 (0.00)	0 (0.00)	0 (0.00)	0 (0.00)	0 (0.00)	0 (0.00)	0 (0.00)	0 (0.00)	0 (0.00)	0 (0.00)
Mudcranch	0 (0.00)	0 (0.00)	0 (0.00)	0 (0.00)	0 (0.00)	0 (0.00)	151 (0.90)	0 (0.00)	0 (0.00)	0 (0.00)	0 (0.00)	0 (0.00)	0 (0.00)	0 (0.00)	0 (0.00)	0 (0.00)	0 (0.00)	0 (0.00)	0 (0.00)
Octopus	0 (0.00)	0 (0.00)	0 (0.00)	0 (0.00)	0 (0.00)	0 (0.00)	0 (0.00)	151 (0.98)	0 (0.00)	0 (0.00)	0 (0.00)	0 (0.00)	0 (0.00)	0 (0.00)	0 (0.00)	0 (0.00)	0 (0.00)	0 (0.00)	0 (0.00)
Penguin	0 (0.00)	0 (0.00)	0 (0.00)	0 (0.00)	0 (0.00)	0 (0.00)	0 (0.00)	0 (0.00)	154 (0.98)	0 (0.00)	0 (0.00)	0 (0.00)	0 (0.00)	0 (0.00)	0 (0.00)	0 (0.00)	0 (0.00)	0 (0.00)	1 (0.00)
Puffers	0 (0.00)	0 (0.00)	0 (0.00)	0 (0.00)	0 (0.00)	0 (0.00)	0 (0.00)	0 (0.00)	0 (0.00)	150 (0.98)	0 (0.00)	0 (0.00)	0 (0.00)	0 (0.00)	0 (0.00)	0 (0.00)	0 (0.00)	0 (0.00)	0 (0.00)
Sea Rays	0 (0.00)	1 (0.01)	0 (0.00)	0 (0.00)	0 (0.00)	0 (0.00)	0 (0.00)	0 (0.00)	0 (0.00)	0 (0.00)	96 (0.94)	0 (0.00)	0 (0.00)	2 (0.01)	3 (0.01)	0 (0.00)	0 (0.00)	0 (0.00)	0 (0.00)
Sea Urchins	0 (0.00)	0 (0.00)	0 (0.00)	0 (0.00)	0 (0.00)	0 (0.00)	0 (0.00)	0 (0.00)	0 (0.00)	0 (0.00)	0 (0.00)	117 (0.88)	0 (0.00)	0 (0.00)	0 (0.00)	0 (0.00)	0 (0.00)	0 (0.00)	0 (0.00)
Seahorse	0 (0.00)	0 (0.00)	0 (0.00)	0 (0.00)	0 (0.00)	0 (0.00)	0 (0.00)	0 (0.00)	0 (0.00)	0 (0.00)	0 (0.00)	0 (0.00)	90 (0.90)	0 (0.00)	0 (0.00)	0 (0.00)	0 (0.00)	0 (0.00)	0 (0.00)
Seal	0 (0.00)	0 (0.00)	0 (0.00)	0 (0.00)	0 (0.00)	0 (0.00)	0 (0.00)	0 (0.00)	0 (0.00)	0 (0.00)	0 (0.00)	0 (0.00)	0 (0.00)	150 (0.98)	0 (0.00)	0 (0.00)	0 (0.00)	0 (0.00)	0 (0.00)
Sharks	0 (0.00)	0 (0.00)	0 (0.00)	0 (0.00)	0 (0.00)	0 (0.00)	0 (0.00)	0 (0.00)	0 (0.00)	0 (0.00)	0 (0.00)	0 (0.00)	0 (0.00)	0 (0.00)	117 (0.94)	0 (0.00)	0 (0.00)	1 (0.01)	3 (0.01)
Squid	0 (0.00)	0 (0.00)	0 (0.00)	0 (0.00)	0 (0.00)	0 (0.00)	0 (0.00)	0 (0.00)	0 (0.00)	0 (0.00)	0 (0.00)	0 (0.00)	0 (0.00)	0 (0.00)	0 (0.00)	150 (0.95)	0 (0.00)	0 (0.00)	

The model confusion matrix X as predicted label Y as a true label which gives merely 97.9 % accuracy the performance plot accuracy rises gradually and we can predict loss as rapidly are shown in the Fig 11 and classification on prediction found as shown as Fig 12.



```
1/1 [=====] - 0s 16ms/step
Prediction : Sharks
Out[3]: <matplotlib.image.AxesImage at 0x25a01a61dc8>
```



Fig 12: Output & Prediction

VII. CONCLUSION

In this study, a deep learning classifier is employed to analyze photographs of various underwater fish species. The pre-processing phase involves utilizing images of multiple underwater fish species as input data. These photos are resized and organized into an array. Subsequently, the dataset is divided into a training dataset and a testing dataset through the feature selection technique. All the photos are then downscaled and transformed into an array format. Finally, the classification approach is employed to classify the photos of underwater fish species. The deep learning method of Convolutional Neural Networks (CNN) is utilized to predict the outcome, employing metrics such as accuracy, precision, and recall f1-measure.

REFERENCE

- [1] Underwater Image Enhancement Methods Using A New Underwater Image Dataset Ashraf Shaleemet.at., (2023)
- [2] Md Jahidul Islam et.at., Fast Underwater Image Enhancement for Improved Visual Perception(2020).
- [3] Yifeng Xu et.at., Underwater Image Classification Using Deep CNN and Data Augmentation (2018)
- [4] M. Vimal Raj, et.at., "Underwater Image Classification using Machine Learning Technique" , International Symposium on Ocean Technology (SYMPOL), 2019
- [5] Chongyi Li et.at., Underwater Image Enhancement Benchmark Dataset and beyond(2019)
- [6] Arpit Wany et.at., Underwater Image Enhancement Using Image processing Techniques(2021)
- [7] An Experimental-Based Review of Image Enhancement and Image Restoration Methods for Underwater Imaging Yan Wang et.at., (2019)
- [8] Underwater Image Enhancement based on Deep Learning and Image Formation Model Xuele Chen, et.at., (2021)
- [9] Underwater image enhancement: a comprehensive review, recent trends, challenges and applications, Smitha Raveendran, (2021).
- [10] Swati Sonawane, et.al., Underwater image classification and enhancement.IJSDR, October 2022.
- [11] Devendar Marasakatla, et.at., Under Water Image Enhancement Using CNN ,ICAECIS, 2023
- [12] Anushka Yadav, et.al., Underwater image enhancement using convolutional neural network. IEEE 18 September 2021.
- [13] Shirin Shahana V, et.al., Underwater image enhancement and color correction a review. SEMANCTIC scholar, 2022.
- [14] S.-B. Gao, et.al., Underwater image enhancement using adaptive retinal mechanisms. IEEE, 28 November 2019.
- [15] [M. Han, et.al., A review on intelligence dehazing and color restoration for underwater images. IEEE, 23 January 2018.
- [16] Changli Li, et at, Color correction based on CFA and enhancement based on Retinex with dense pixels for underwater images. IEEE, 2020.
- [17] Zitong Kang, et at, Underwater image enhancement by maximum- likelihood based adaptive color correction and robust scattering removal.

- [18] R Prasath, et al, Application of Different Techniques for Underwater Image Processing- A Systematic Review. ICCEMS, 2020.
- [19] Yang Guan et.al., Fast underwater image enhancement based on a generative adversarial framework. IEEE, 2023.
- [20] Chengquan Zhang et.al "Underwater image enhancement based on an integrated color model." IET Computer Vision -2017

Letter of Acceptance

TO

Mr. S. Murali, Mr. S. Shiva Rakesh, Mr. R.V.J. Dharwin, Mr. M. Gajendrapandi
Velammal College of Engineering and Technology

Herewith, the conference committee of the 2nd International Conference on Edge Computing and Applications ICECAA 2023 is pleased to inform you that the peer reviewed research paper **“Paper ID: ICECAA003”** entitled **“PhotoPlethysmoGraphy based Low-Cost Glucometer With Haemoglobin Measurement”** has been accepted for oral presentation as well as it will be recommended for inclusion in ICECAA Conference Proceedings.

ICECAA will be held on 19-21, July 2023 at Gnanamani College of Technology, Namakkal, India. ICECAA encourages only the active participation of highly qualified delegates to bring you various innovative research ideas.

We congratulate you on being successfully selected for the presentation of your research work in our esteemed conference.

Yours' Sincerely



Dr. G. Ranganathan
Conference Chair – ICECAA 2023





EFFICIENT DIAGNOSIS OF CERVICAL CANCER USING DEEP NEURAL NETWORK

Dr. S. Sasikala,

Associate Professor Department of Computer Science and Engineering
Velammal College of Engineering and Technology, Madurai, Tamil Nadu

Ms. N. Miruthula

Department of Computer Science and Engineering Velammal College of Engineering and
Technology Madurai, Tamil Nadu

Ms. A. Poornimadevi

Department of Computer Science and Engineering Velammal College of Engineering and
Technology, Madurai, Tamil Nadu

Ms. M. Suuky

Department of Computer Science and Engineering Velammal College of Engineering and
Technology, Madurai, Tamil Nadu

Ms. J. Subadhina

Department of computer Science and engineering Velammal College of Engineering and
Technology, Madurai, Tamil Nadu

Article History: Received: 12.05.2023

Revised: 25.05.2023

Accepted: 05.06.2023

Abstract

Women all around the world are affected by cervical cancer, which is a serious public health issue. Early detection and management can decrease the morbidity and mortality linked to this condition while increasing the likelihood of successful therapy. Hence, identifying women who are at risk of acquiring this condition requires the creation of accurate cervical cancer prediction algorithm. Accurate cervical cancer prediction models have been developed in recent years using Deep Learning (DL) techniques. This paper presents a simple novel method for identifying cervical cancer and shows the stage of the cancer whether lighter, moderate or severe. The Deep leaning algorithm Artificial Neural Network(ANN) is used to identify the stage of the cervical cancer.

Key words: Cervical cancer, Clustering, Human Papilloma Virus(HPV), Artificial Neural Network(ANN).

I INTRODUCTION

Women all around the world are affected by the major health issue of cervical cancer. With an estimated 570,000 new cases and 311,000 fatalities worldwide each year, cervical cancer is the fourth most frequent malignancy in women, according to the World Health Organization (WHO). Many women are still identified with cervical cancer in its advanced stages, when treatment options are few and survival rates are dismal, in spite of the existence of reliable screening techniques and vaccines. For early detection and treatment, reliable and timely prediction of cervical cancer risk is essential.

Cervical cancer has been linked to a number of risk factors, such as HPV infection, smoking, immunological deficiencies, and chronic use of oral contraceptives. While some women without

these risk factors may nevertheless be given a cervical cancer diagnosis, not all women with these risk factors will go on to get the illness. Hence, to identify women at high risk of cervical cancer, effective prediction models that combine numerous risk indicators must be developed. The severe stage of malignant cervix is seen in Figure.1. The ability to predict the risk of cervical cancer has recently showed promise thanks to developments in machine learning and data analysis approaches.

Deep Learning models analyze huge datasets that contain demographic, clinical, and genetic data to find patterns and associations that conventional statistical methods might miss. Deep learning algorithms can also gain knowledge from the past data and develop their predictions over time.

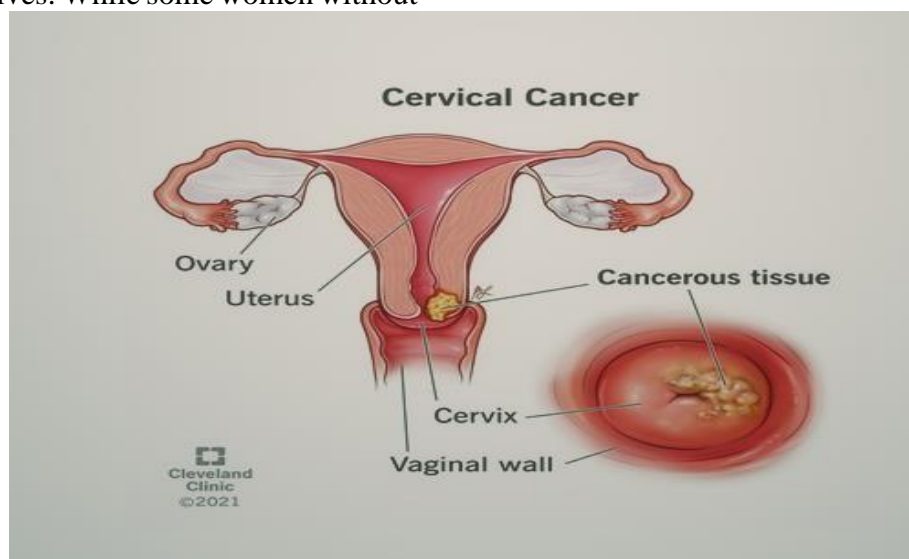


Figure.1 Cancerous Cervix

Proper risk assessment of cervical cancer can also guide women's individual screening and prevention plans. Women who are at high risk may benefit from more regular screenings or focused interventions, whereas women who are at low risk might just need screenings every few months or so. This strategy can lessen the impact of cervical cancer on women and society while making the best use of the scarce healthcare resources. The creation of reliable and precise risk prediction algorithms for

cervical cancer is a current field of research. These models are probably going to get better and better at forecasting the risk of cervical cancer as more data become accessible and deep learning techniques advance.

II RELATED WORKS

NINA YOUNESZADE et al. 2023 [2] discussed the architecture, opportunities, and Open Research Challenges in cervical

cancer diagnosis using Deep Learning methods. MD MAMUNUR RAHAMAN et al, 2020 [10] discussed the comprehensive study of deep learning approaches for the cervical cytology image analysis and discusses the datasets, evaluation metrics for segmentation and classification along with existing methodologies for the analysis of pap smear cells. PAN HUANG et al, 2020 [3] discussed a technique of cervical biopsy tissue image classification based on Least Absolute Shrinkage and Selection Operator (LASSO) and Ensemble Learning-Support Vector Machine (EL-SVM). This article discusses challenges with artificial classification of biopsy tissue images during diagnosis and offers solutions. SUXIANG YU et al, 2021 [6] discussed the method of four classification models CNN, SPP, Inception, CNN+SPP+inception for performance evaluation and the comparison is done, which concludes that fourth model is best. In this real time datasets are used.

FAHDI KANAVATI et al, 2022 [15] discussed the method to investigate the use of deep learning for the classification of whole-slide images of liquid-based cytology specimens into neoplastic and non-neoplastic. This model is used for screening process of cervical cancer. MERCY NYAMEWAA ASIEDU et al, 2019 [9] discussed a method for automatic feature extraction and classification for acetic acid and Lugol's iodine Cervi grams and methods for combining features/diagnosis of different contrast in Cervi grams for improved performance. DAN XUE et al, 2020 [12] discussed on classifying cervical histopathology pictures that are well, moderately, and badly differentiated using an Ensembled Transfer Learning (ETL) framework. FERNANDES KELWIN et al, 2018 [5] described a system for automated analysis of digital colposcopies and constructed a topology of issues and solutions, highlighting each

one's salient features, benefits, and drawbacks. highlighted the open issues in the field and published a database that acts as a standard framework for assessing such systems.

YUEXIANG LI et al, 2020 [1] discussed a method of a deep learning framework for the accurate identification of LSIL+ (including CIN and cervical cancer) using time-lapsed colposcopy images.

III EXISTING WORK

An essential step in the diagnosis of cervical cancer is a cervical biopsy. It is challenging to artificially classify biopsy images for diagnosis, and pathologists' clinical expertise is needed. Computerized biopsy tissue images of lesions that are identical to one another have low classification accuracy and can only determine if a cell is cancerous or not.

3.1. Existing Clinical Methodologies For Cervical Cancer Prediction

a) Pap Smear test

The pap smear test, which has been used for 60 years and has greatly lowered the death rate from cervical cancer, is shown in Figure. 2. Cells from the squamocolumnar terminal of the cervix are normally removed with a brush or spatula and spread onto glass slides for the test. Cytotechnologists examine the glass slides under a light microscope to identify whether the cell is malignant, enabling an early and effective course of therapy. The length of the screening operations varies from 5 to 10 minutes, depending on how difficult the cell orientation is. A cytotechnologist cannot evaluate more than 70 samples in a single day. This approach likewise needs constant, undivided attention to make sure no cancerous cells are overlooked.

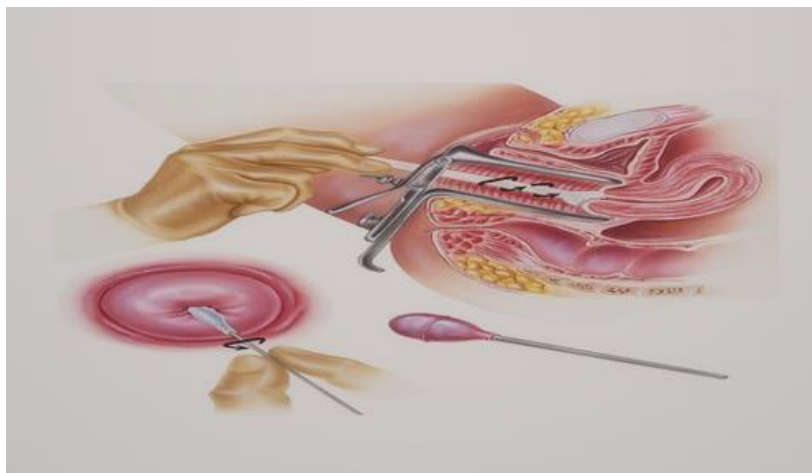


Figure.2 Pap Smear test

a) Diagnosis of colposcopy images using deep learning

abnormal and tells the stage of the cervical cancer

The use of DL approaches in medical image analysis, which is now the most popular and successful subset of machine learning algorithms, is not an exception in the analysis of cervical cytopathology images. In this sector, Artificial Neural Networks (ANNs) are frequently used as deep architectures and have had outstanding success with cell detection, segmentation, classification, and extraction of the region of interest (ROIs). To accurately classify the cells as normal or

IV PROPOSED WORK

The goal of this paper was to create a computer-aided cervical cancer diagnostic model that was incredibly accurate. The consistency and accuracy of cancer diagnosis are improved using Artificial Neural Network algorithm. In this, we forecast the cervical cancer progression stages as in figure 3.

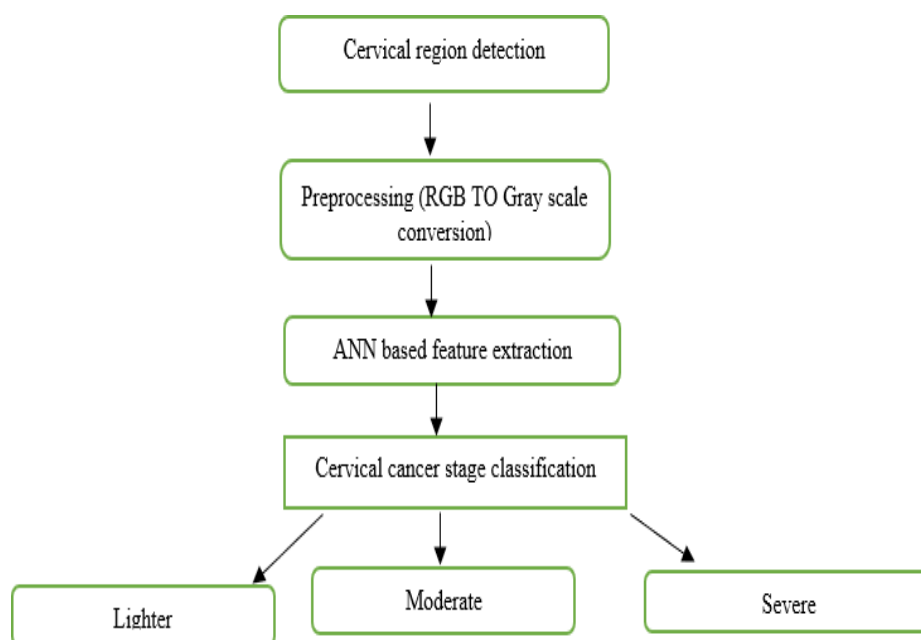


Figure.3 Flow diagram to detect the cervical cancer

4.1. RGB to grayscale conversion

RGB to grayscale conversion is a common image processing operation used to convert an RGB (Red, Green, Blue) image to a grayscale image which is shown in Figure.4 A grayscale image contains only one information channel, while an RGB image contains three information channels. There are several ways to perform RGB to grayscale conversion, but one of the most common is using the lightness method. The lightness method calculates a grayscale value for each pixel based on a weighted average of the three color channels. Weights are based on the perceived lightness of each color. where R, G, and B are the red, green, and blue color channels of the RGB image, respectively. The values for the coefficients 0.2126, 0.7152, and 0.0722 are derived from the perceived luminance of each color, based on the NTSC (National Television Standard Committee) standard for color television. To perform an RGB-to-grayscale conversion, iterate through each pixel in the RGB image and use the lightness method to compute the grayscale value for that pixel. The resulting grayscale image has only one channel of information, and each pixel represents the intensity or brightness of the corresponding pixel in the original RGB image (Figure 4).

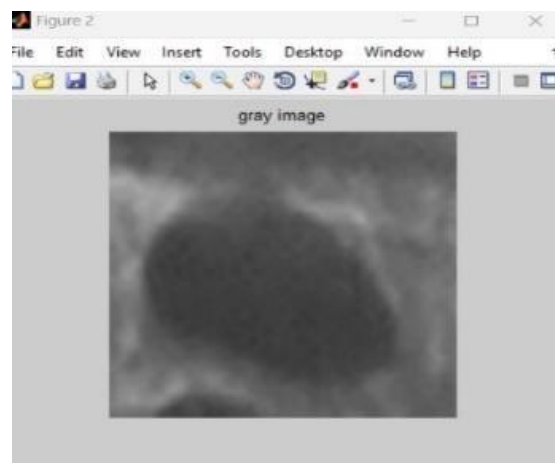
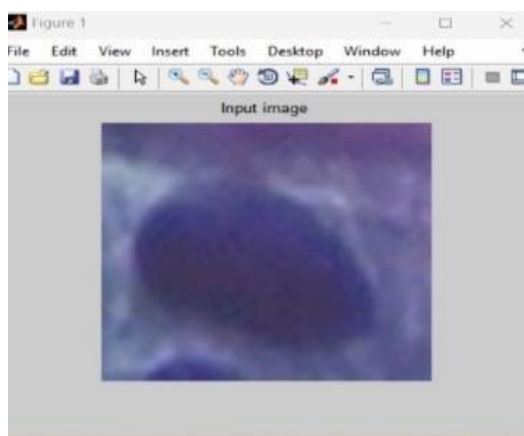


Figure.4 RGB to Grayscale conversion

4.2.Feature Selection

GLCM (Grey level co occurrence matrix) also known as grey level spatial ependence matrix feature is used for image analysis.They will extract the patches or portion of the image with thepixels that is pair of pixels after extract the image we put that image for training the algorithm like Artificial Neural Network(ANN).

In this paper we use following properties for image classification,

- 1.Contrast
- 2.Correlation
- 3.Energy
- 4.Homogeneity

4.3.K-Means Clustering

Supervised Deep learning method K-means clustering is used to arrange data points into clusters based on their similarity. K-means clustering can be used to find patterns or groups of cervical cancer patients who share similar traits or risk factors. It is a vector quantization technique that was first used in signal processing and is widely used in data mining for cluster analysis. K-means clustering seeks to divide n observations into k clusters, where each cluster serves as a prototype for the cluster and each observation belongs to the cluster with the nearest mean.We must first choose a set of features to be used for

clustering before we can apply k-means clustering to the data related to cervical cancer. After choosing our features, we can use k-means clustering to put the patients into groups based on how similar they are. When using k-means clustering, data points are iteratively assigned to the closest cluster centroid, which is then updated depending on the mean of the data points in each cluster. The algorithm must be executed after determining the k number of clusters. Nonetheless, k-means clustering can be a helpful technique for spotting trends or classifying patients according to shared traits. In this the input image is divided into three clusters which is shown in Figure.5.

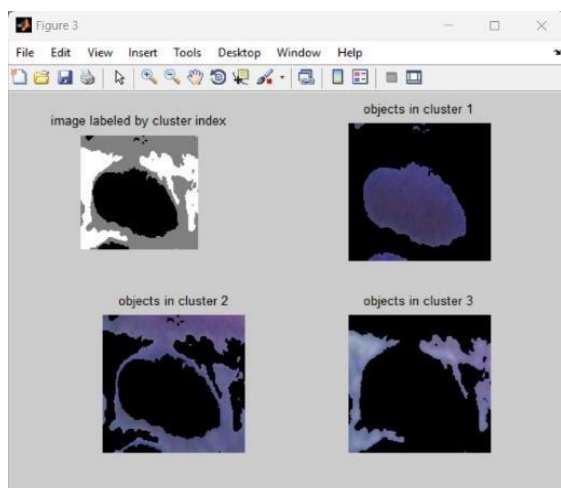


Figure.5 Clusters

4.4. Artificial Neural Network (ANN)

Machine learning algorithms known as artificial neural networks (ANNs) are frequently employed for categorization problems. The structure and operation of the organic brain network serve as the foundation for architecture (figure 6). The neurons of ANN are arranged in several layers, just like the neurons in the brain. A common type of neural network is the feed-forward neural network, which has three layers: an input layer for receiving outside data needed for pattern recognition, an output layer for providing the solution, and a hidden layer that acts as an intermediary layer between the other layers.

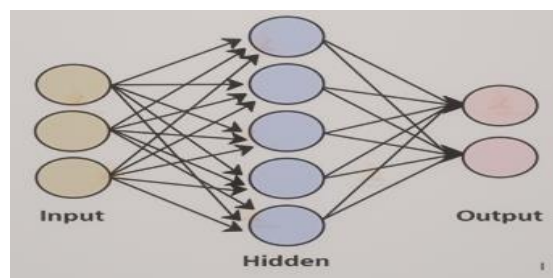


Figure 6. Architecture of ANN

4.4.1 Working and Training of ANN

The input layer is where the information is first fed. Following that, it is transferred to the hidden layers, where an interaction between these two layers first assigns weights to each input at random. The weight total, which is a combination of weights and bias, is then passed through the activation function once bias has been added to each input neuron. The duty for choosing which node to fire for feature extraction and final output calculation falls on the activation function. As a result, this entire process is referred to as forward propagation. Finally, after an output model is built to compare with the original output and the error is known, the backpropagation weights are updated to reduce the error, and this process continues for a specified number of epochs (iterations). increase. Finally, the model weights are updated and predictions are made. A dataset containing patient data and the related cervical cancer diagnosis would be required in order to train the ANN. It would be necessary to separate the dataset into training, validation, and testing sets. The training set would be utilized to fine-tune the ANN's weights, the validation set would be utilized to tweak the ANN's hyperparameters, and the testing set would be utilized to assess the ANN's performance on unlabeled data. The ANN can be used to predict if new patient data reveals the existence of cervical cancer once it has been trained. In this the first cluster image (figure 7). is taken and they are deeply analyzed and the stage of the cancer is predicted (figure 8- figure 11).

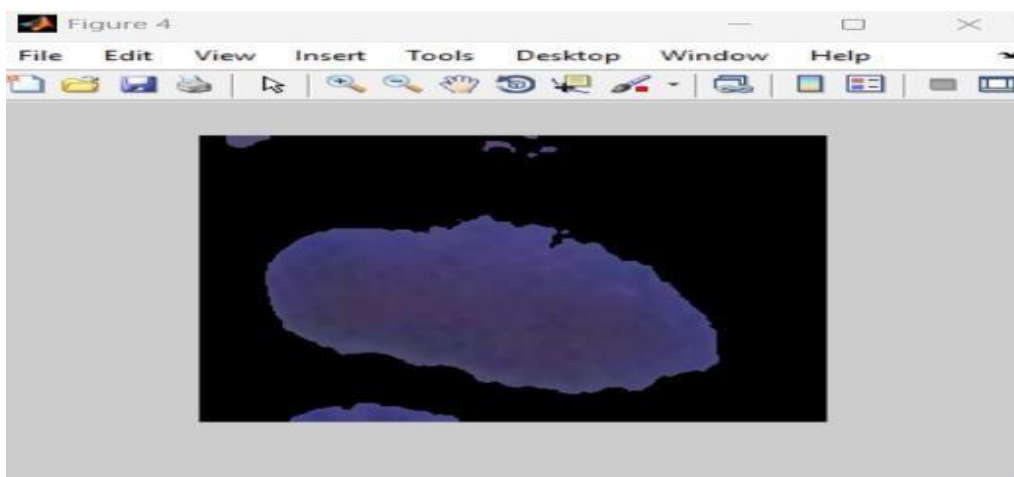


Figure 7. First cluster

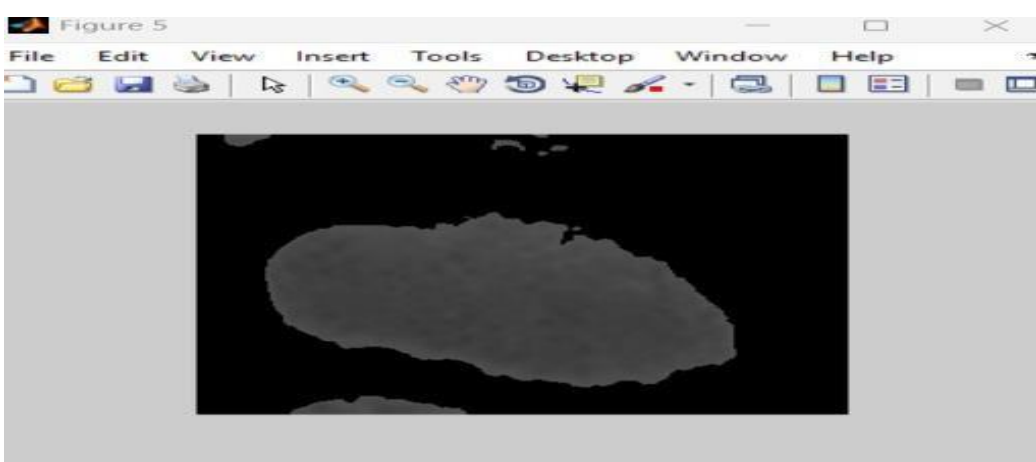


Figure 8. Analysing the feature and deeply classifying the cell

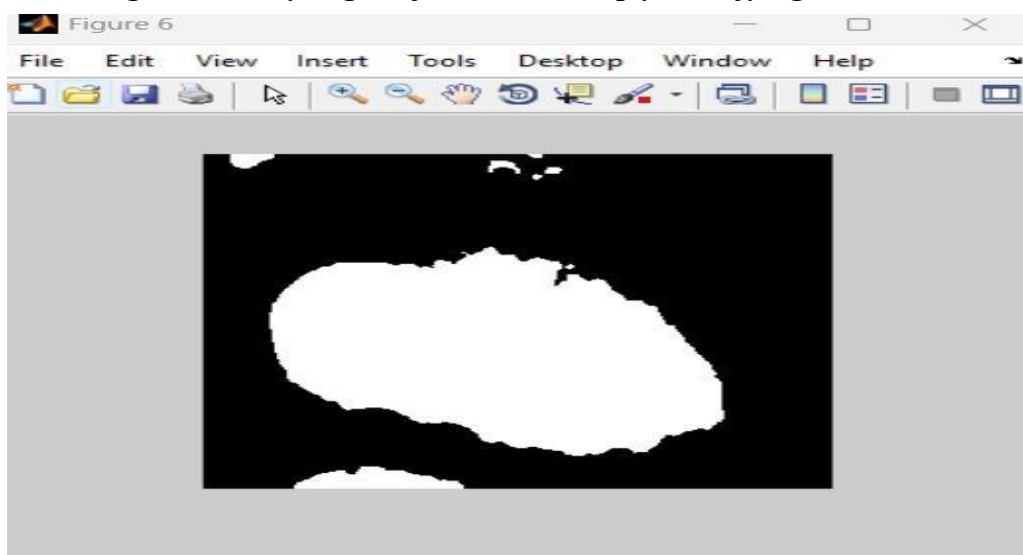


Figure 9. Gray Scale conversion

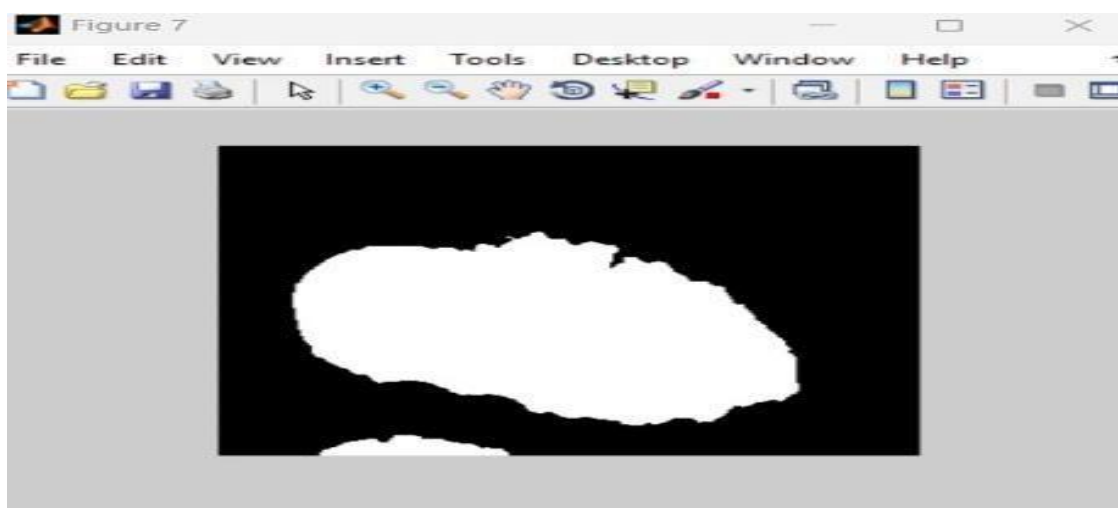


Figure 10. Noise Cancellation

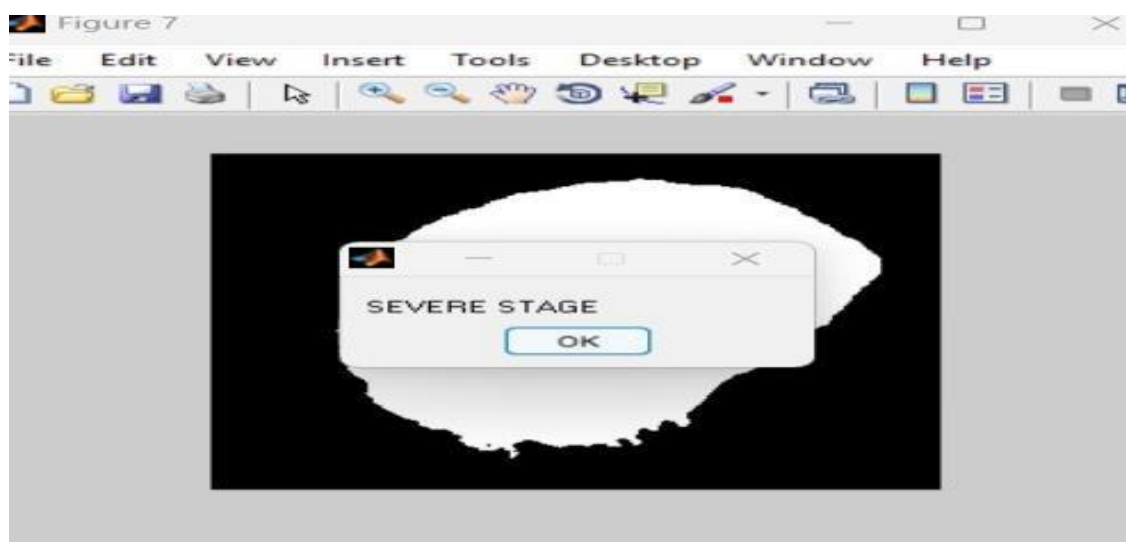


Figure.11 Identifying the stage of the cancer

V EVALUATION METRICS

We used the following criteria to assess the effectiveness of our model. The values of the properties are displayed in Table 1 using GLCM features.

Table 1 Values of the properties

S. No.	Properties	Value
1.	Dissimilarity	3.34865196078431e-02
2.	Homogeneity	9.85922181372549e-01
3.	Entropy	9.055881656303044e-01
4.	Standard Deviation	1.404392671575501e+01

5.	Mean	2.255688476562500e+01
----	------	-----------------------

VI EXPERIMENTAL AND ANALYSIS

We could give the cervical cancer image as the input, it deeply classify the image and tells the stage of the cancer and also provide the values of the properties in which they are classified.

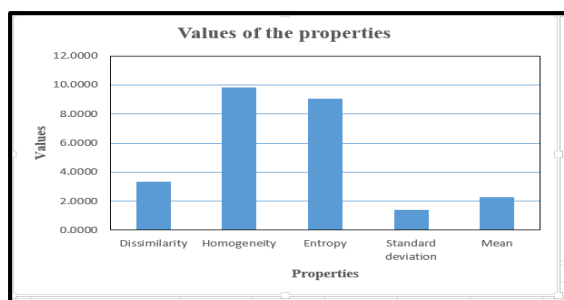


Figure.12 Value of Properties

In this the value of Entropy and Homogeneity is 9.0 and 9.8 respectively (as in figure 12). when the value of entropy and homogeneity is greater than 5 the code is effective and successfully identify the stage of the cancer.

VII. CONCLUSION AND FUTURE WORK

Here the Deep learning algorithm like Artificial Neural Network(ANN) is used for the cervical cancer detection and it's stage. From the Table 1 we knew that the values of Entropy and Homogeneity is greater than 5 i.e) 9.0 and 9.8 respectively , as we know in GLCM feature if the values of Entropy and Homogeneity is greater than 5, the code will be efficient. In future, We will use another Deep Learning algorithm like Convolutional Neural Network(CNN) and increase the values of the properties in future.

REFERENCES

- [1] YUEXIANG LI , JIAWEI CHEN , PENG XUE,Computer-Aided Cervical Cancer Diagnosis using Time-Lapsed Colposcopic Images, IEEE Transactions on Medical imaging, Vol. 39, pp.3403-3415,2020.
- [2] YOUNESZADE N , MARJANI M, Deep Learning in Cervical Cancer Diagnosis: Architecture, Opportunities, and Open Research Challenges , IEEE Access, Vol. 11(1),pp.6133- 6149,2023 .
- [3] HUANG P , ZHANG S , Classification of Cervical Biopsy Images Based on LASSO and EL-SVM, IEEE Access, Vol.8,pp. 24219-24228,2020.
- [4] PHATAK A S , Classification of Mr Images of Cervical Cancer Using SVM and ANN Engineering ,International Journal of Scientific Research,Vol.4,2015.
- [5] FERNANDES K, JAIME S CARDOSO ,Automated Methods for the Decision Support of Cervical Cancer Screening using Digital Colposcopies, IEEE Access , Vol.6, pp.33910-33927,2018.
- [6] SUXIANG YU, XINXING FENG, ,Automatic Classification of Cervical Cells using Deep Learning Method ,IEEE Access,Vol.9,pp. 46612 - 46625, 2021.
- [7] MABROUK K, ADWEB A, Cervical Cancer Diagnosis Using Very Deep Networks Over Different activation Functions, IEEE Access, Vol.9, pp. 46612-46625, 2021.
- [8] QAZI MUDASSAR ILYAS , MUNEER AHMAD , An Enhanced Ensemble Diagnosis of Cervical Cancer: A Pursuit of Machine Intelligence towards Sustainable Health, IEEE Access Vol.9 , pp. 12374-12388,2021.
- [9] MERCY NYAMEWAA ASIEDU , ANISH SIMHAL, Development of Algorithms for Automated Detection of Cervical Pre-Cancers With a Low-Cost, Point-of-Care,

- Pocket Colposcope, IEEE Transactions on Biomedical Engineering, Vol.66, pp.2306-2318, 2019.
- [10] MD MAMUNUR RAHAMAN, CHEN LI 1, A Survey for Cervical Cytopathology Image analysis Using Deep Learning, IEEE Access, Vol.8, pp. 61687-61710, 2020.
- [11] YAN-MIN LUO, TAO ZHANG, MDFI: Multi-CNN Decision Feature Integration for diagnosis of Cervical Precancerous Lesions, IEEE Access, Vol.8, pp. 29616 - 29626, 2020.
- [12] DAN XUE, XIAOMIN ZHOU, An Application of Transfer Learning and ensemble Learning Techniques for Cervical Histopathology Image Classification, IEEE Access, Vol.8, pp.104603-104618, 2020.
- [13] NESRINE BNOUNI, ISLEM REKIK, Cross-View Self-Similarity Using Shared dictionary Learning for Cervical Cancer Staging, IEEE Access, Vol. 7, pp.30079- 30088, 2019.
- [14] CHANDRAN V, SUMITHRA M G, Diagnosis of Cervical Cancer based on Ensemble Deep Learning network using Colposcopy Images, BioMed Research International, Vol.2021, pp.1-15, 2021.
- [15] KANAVATI F, HIROSE N, A Deep Learning Model for Cervical cancer Screening on Liquid-Based cytology Specimens in whole slide images, MDFI, pp.1-15, 2022.

A Machine Learning based Effectual Prediction Model for Breast Cancer Classification

¹Dr. S. Sasikala, Associate Professor, Department of CSE,
Velammal College of Engineering and Technology, Madurai, Tamil Nadu
²R.Nandhini, ³V Pooja, ⁴K.Priya dharshini, ⁵S.Maheswari,
Department of CSE,
Velammal College of Engineering and Technology, Madurai, Tamil Nadu

Abstract:

The second major cause of women's death is breast cancer (after lung cancer). Breast cancer cells usually form a tumour that can often be seen on an X-ray or felt like a lump. The cause of Breast Cancer includes changes and mutations in DNA. Breast cancer is a common type of cancer that affects women worldwide. However, if cancer is detected early and treated properly, it is possible to be cured of the condition. Early detection of breast cancer can dramatically improve the prognosis and chances of survival by allowing patients to receive timely clinical therapy. Furthermore, precise benign tumour classification can help patients avoid unneeded treatment. The goal of the research is to identify and classify Malignant and Benign patients and intending how to parameterize our classification techniques, achieving high accuracy. This paper uses the Supervised Machine Learning Algorithm - Random Forest to classify and identify Malignant and Benign Breast Cancer Wisconsin (Diagnostic) Data Set and validate the model using K-Fold Cross Validation Algorithm.

1. Introduction

Breast cancer is considered a multifactorial disease and the most common cancer in women worldwide with approximately 30% of all female cancers (i.e., 1.5 million women are diagnosed with breast cancer each year, and 500,000 women die from this disease in the world). [4] Over the past 30 years, this disease has increased, while the death rate has decreased. However, the reduction in mortality due to mammography screening is estimated at 20%, and improvement in cancer treatment is estimated at 60%.

[2] Diagnostic mammography can assess abnormal breast cancer tissue in patients with subtle and inconspicuous malignancy signs. Due to many images, this method cannot effectively be used in assessing suspected cancer areas. According to a report, approximately 50% of breast cancers were not detected in screenings of women with very dense breast tissue. However, about a quarter of women with breast cancer are diagnosed negatively within two years of screening. Therefore, the early and timely diagnosis of breast cancer is crucial.

[4] Artificial Intelligence (AI) has been growing considerably over the last ten years. Machine Learning (ML) is probably the most popular branch of AI to date. Most systems that use ML methods use them to perform predictive analysis. As a modelling approach, machine learning represents the process of extracting knowledge from data and discovering hidden relationships, widely used in healthcare in recent years to predict different diseases. The Random Forest algorithm was used in classifying breast tumours as either malignant or benign, it is a Supervised Machine Learning Algorithm that is used widely in Classification and Regression problems. It builds decision trees on different samples and takes their majority vote for classification and average in case of regression. One of the most important features of the Random Forest Algorithm is that it can handle the data set containing continuous variables, as in the case of regression, and categorical variables, as in the case of classification. It performs better for classification and regression tasks.

The prime objective is to implement the supervised learning algorithms of machine learning such as Random Forest and validation using K-Fold Cross Validation Algorithm. The models are to train the Breast cancer dataset using the machine learning approaches mentioned above. Early detection of breast cancer can dramatically increase the chances of survival rate.

2. Literature Survey

Table 1 depicts the detailed analysis on various existing methods with comparative study on their performance.

Table 1. Comparative Study on Existing Methods

Author	Dataset Used	Techniques Used	Tools Used	Result
Muktevi	Wisconsin breast cancer-Kaggle	SVM, Random Forest, KNN, LR, NB	Python	Random Forest had the best accuracy of all with 98.24%. RF had a mean absolute error of 0.01%
RamikRawal	Wisconsin - Kaggle	SVM, Logistic Regression, Random Forest, K-NN	JupyterNotebook-Python	SVM- 97.13% highest efficiency and accuracy
Gaurav Singh	UCI repository	K-NN, SVM, LR, NB	Python	K-NN- 99% SVM- 96% LR- 97% NB-95%
Min-Wei	UCI Repository, ACM SIGKDD Cup 2008	SVM classifiers, SVM ensembles	Weka	SVM ensembles perform slightly better than single SVM classifiers
Deepika	UCI repository	Naïve Bayes, MLP	Weka	Naïve Bayes had better accuracy
Ch. Shravya	UCI repository	SVM, K-NN, LR	Spyder Platform	SVM predicted the best accuracy of 92.78% followed by KNN-92.23%
Wang	Wisconsin Breast Cancer Database (1991), Wisconsin Diagnostic Breast Cancer (1995)	SVM, ANN, Adaboost, PCA	WEKA	8 PCs -92.6% correlation, 10 PCS- 95%.

3. Proposed Methodology

The research was conducted in 4 stages: [5] data collection, data pre-processing, model creation and model evaluation as given in figure.1.

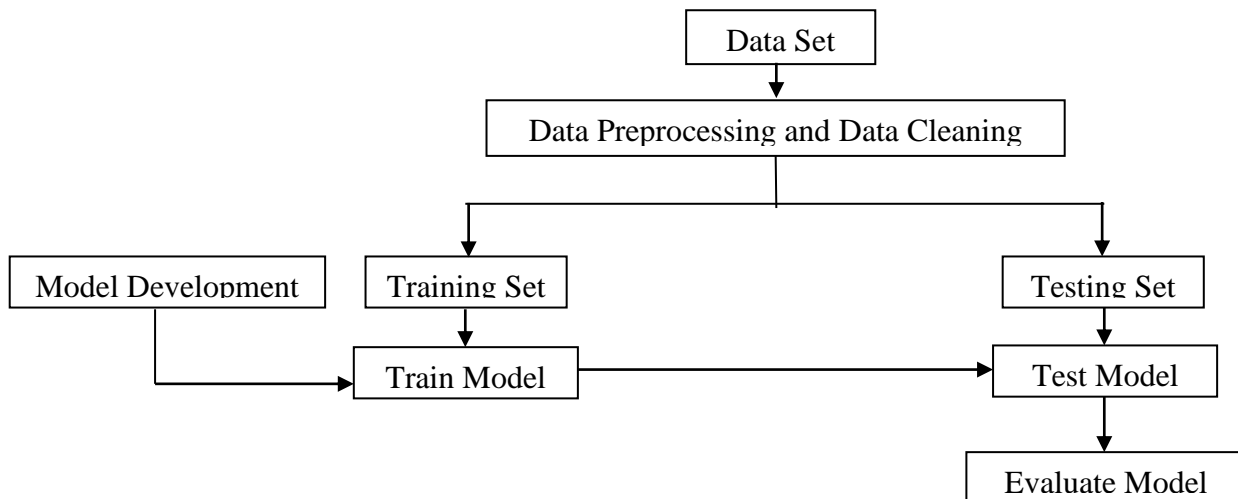


Figure 1: Phases of Proposed Methodology

3.1 Data Collection:

Features are computed from a digitized image of a breast mass's Fine Needle Aspirate (FNA). They describe the characteristics of the cell nuclei present in the image. In the 3-dimensional space is that described in: [K. P. Bennett and O. L. Mangasarian: "Robust Linear Programming Discrimination of Two Linearly Inseparable Sets", Optimization Methods and Software 1, 1992, 23-34].

Attribute Information:

- 1) ID number
- 2) Diagnosis(M = Malignant, B = Benign)
- 3) Ten real-valued features are computed for each cell nucleus:
 - a) radius (mean of distances from the centre to points on the perimeter)
 - b) texture (standard deviation of grey-scale values)
 - c) perimeter
 - d) area
 - e) smoothness (local variation in radius lengths)
 - f) compactness ($\text{perimeter}^2 / \text{area} - 1.0$)
 - g) concavity (severity of concave portions of the contour)
 - h) concave points (number of concave portions of the contour)
 - i) symmetry
 - j) fractal dimension ("coastline approximation" - 1)

All feature values are recorded with four significant digits.

Missing attribute values: none

Class distribution: 357 benign, 212 malignant as shown in the figure.2

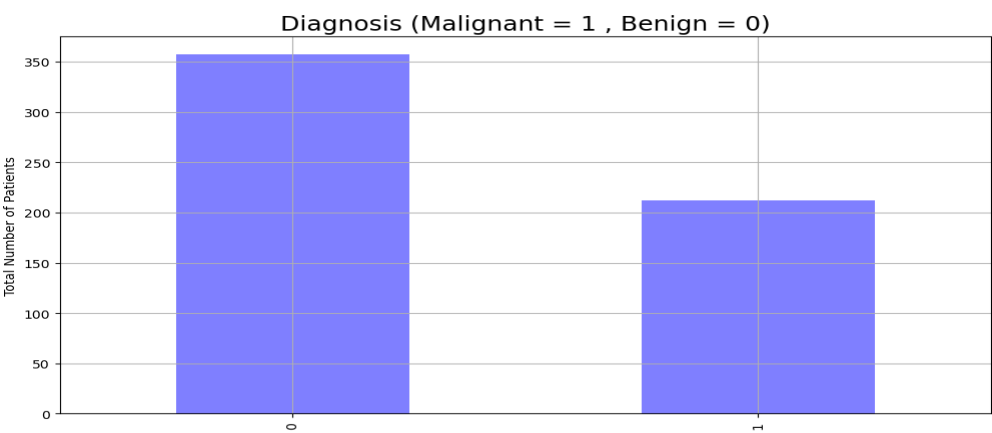


Figure 2: Number of patients with Malignant and Benign Tumours

a. Data Pre-Processing:

[6] The second step was associated with data pre-processing, [3] This dataset doesn't contain any NULL and missing values hence no need for cleaning and we simply remove the ID attribute in the dataset since we just try to diagnose if it is malignant or benign and binarizing the target variable as Malignant – 1, Benign – 0as shown in the figure.3.

0	id	569	non-null	int64
1	diagnosis	569	non-null	object
2	radius_mean	569	non-null	float64
3	texture_mean	569	non-null	float64
4	perimeter_mean	569	non-null	float64
5	area_mean	569	non-null	float64
6	smoothness_mean	569	non-null	float64
7	compactness_mean	569	non-null	float64
8	concavity_mean	569	non-null	float64
9	concave points_mean	569	non-null	float64
10	symmetry_mean	569	non-null	float64
11	fractal_dimension_mean	569	non-null	float64
12	radius_se	569	non-null	float64
13	texture_se	569	non-null	float64
14	perimeter_se	569	non-null	float64
15	area_se	569	non-null	float64
16	smoothness_se	569	non-null	float64
17	compactness_se	569	non-null	float64
18	concavity_se	569	non-null	float64
19	concave points_se	569	non-null	float64
20	symmetry_se	569	non-null	float64
21	fractal_dimension_se	569	non-null	float64
22	radius_worst	569	non-null	float64
23	texture_worst	569	non-null	float64
24	perimeter_worst	569	non-null	float64
25	area_worst	569	non-null	float64
26	smoothness_worst	569	non-null	float64
27	compactness_worst	569	non-null	float64
28	concavity_worst	569	non-null	float64
29	concave points_worst	569	non-null	float64
30	symmetry_worst	569	non-null	float64
31	fractal_dimension_worst	569	non-null	float64

Figure 3: Attributes Description

The statistical description on the dataset is revealed on the Figure 4 and Figure 5 under the preprocessing phase.

	diagnosis	radius_mean	texture_mean	perimeter_mean	area_mean	smoothness_mean	compactness_mean	concavity_mean	concave points_mean	symmetry_mean
count	569.000000	569.000000	569.000000	569.000000	569.000000	569.000000	569.000000	569.000000	569.000000	569.000000
mean	0.372583	14.127292	19.289649	91.969033	654.889104	0.096360	0.104341	0.088799	0.048919	0.104341
std	0.483918	3.524049	4.301036	24.298981	351.914129	0.014064	0.052813	0.079720	0.038803	0.038803
min	0.000000	6.981000	9.710000	43.790000	143.500000	0.052630	0.019380	0.000000	0.000000	0.019380
25%	0.000000	11.700000	16.170000	75.170000	420.300000	0.086370	0.064920	0.029560	0.020310	0.020310
50%	0.000000	13.370000	18.840000	86.240000	551.100000	0.095870	0.092630	0.061540	0.033500	0.033500
75%	1.000000	15.780000	21.800000	104.100000	782.700000	0.105300	0.130400	0.130700	0.074000	0.074000
max	1.000000	28.110000	39.280000	188.500000	2501.000000	0.163400	0.345400	0.426800	0.201200	0.345400

Figure 4: Statistical Analysis of Dataset

	diagnosis	radius_mean	texture_mean	perimeter_mean
0	1	17.99	10.38	
1	1	20.57	17.77	
2	1	19.69	21.25	
3	1	11.42	20.38	
4	1	20.29	14.34	
...	
564	1	21.56	22.39	
565	1	20.13	28.25	
566	1	16.60	28.08	
567	1	20.60	29.33	
568	0	7.76	24.54	

Figure 5: Pre-Processed Dataset

The Correlation between the variables is processed and their correlated analysis is provided in the Figure 6 -8.

data.corr()

	diagnosis	radius_mean	texture_mean	perimeter_mean	area_mean	smoothness_mean	compactness_mean	concavity_mean	conc points_m
diagnosis	1.000000	0.730029	0.415185	0.742636	0.708984	0.358560	0.596534	0.696360	0.776
radius_mean	0.730029	1.000000	0.323782	0.997855	0.987357	0.170581	0.506124	0.676764	0.822
texture_mean	0.415185	0.323782	1.000000	0.329533	0.321086	-0.023389	0.236702	0.302418	0.293
perimeter_mean	0.742636	0.997855	0.329533	1.000000	0.986507	0.207278	0.556936	0.716136	0.850
area_mean	0.708984	0.987357	0.321086	0.986507	1.000000	0.177028	0.498502	0.685983	0.823
smoothness_mean	0.358560	0.170581	-0.023389	0.207278	0.177028	1.000000	0.659123	0.521984	0.553
compactness_mean	0.596534	0.506124	0.236702	0.556936	0.498502	0.659123	1.000000	0.883121	0.831
concavity_mean	0.696360	0.676764	0.302418	0.716136	0.685983	0.521984	0.883121	1.000000	0.921
concave points_mean	0.776614	0.822529	0.293464	0.850977	0.823269	0.553695	0.831135	0.921391	1.000
symmetry_mean	0.330499	0.147741	0.071401	0.183027	0.151293	0.557775	0.602641	0.500667	0.462
fractal_dimension_mean	-0.012838	-0.311631	-0.076437	-0.261477	-0.283110	0.584792	0.565369	0.336783	0.166
radius_se	0.567134	0.679090	0.275869	0.691765	0.732562	0.301467	0.497473	0.631925	0.698
texture_se	-0.008303	-0.097317	0.386358	-0.086761	-0.066280	0.068406	0.046205	0.076218	0.021
perimeter_se	0.556141	0.674172	0.281673	0.693135	0.726628	0.296092	0.548905	0.660391	0.710
area_se	0.548236	0.735864	0.259845	0.744983	0.800086	0.246552	0.455653	0.617427	0.690
smoothness_se	-0.067016	-0.222600	0.006614	-0.202694	-0.166777	0.332375	0.135299	0.098564	0.027
compactness_se	0.292999	0.206000	0.191975	0.250744	0.212583	0.318943	0.738722	0.670279	0.490
concavity_se	0.253730	0.194204	0.143293	0.228082	0.207660	0.248396	0.570517	0.691270	0.439
concave points_se	0.408042	0.376169	0.163851	0.407217	0.372320	0.380676	0.642262	0.683260	0.615
symmetry_se	-0.006522	-0.104321	0.009127	-0.081629	-0.072497	0.200774	0.229977	0.178009	0.095
fractal_dimension_se	0.077972	-0.042641	0.054458	-0.005523	-0.019887	0.283607	0.507318	0.449301	0.257

Figure 6. Correlated Analysis on data variables

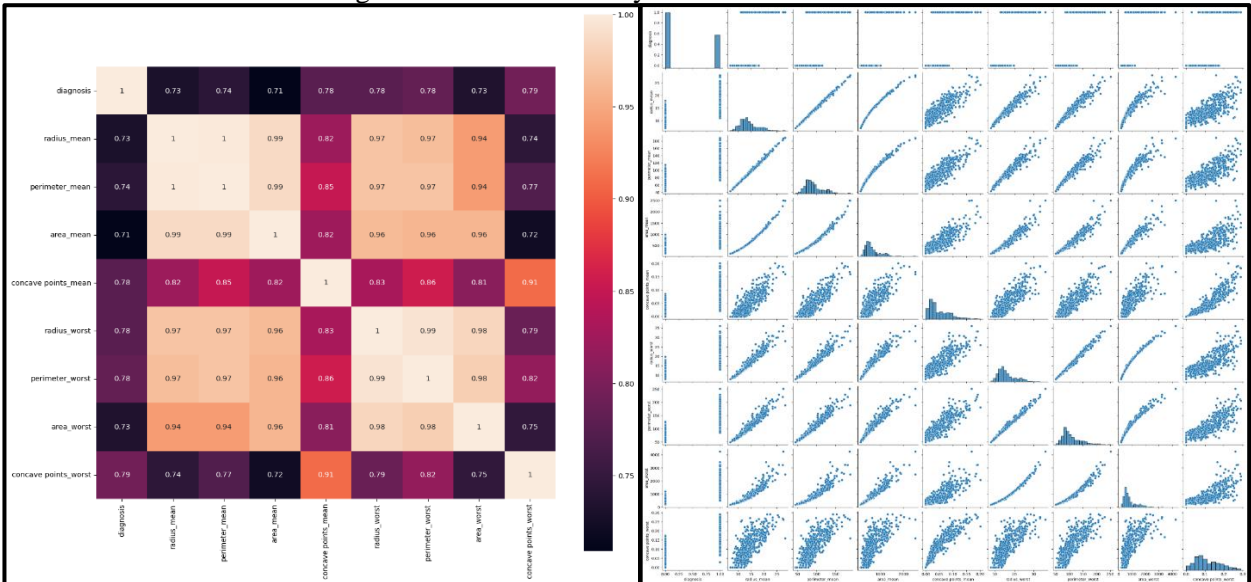


Figure 7: Correlation between the attributes in the dataset
Figure 8: Visual Representation of high correlation between the attributes

3.3 Model Creation and Evaluation
3.3.1 Logistics Regression:

Logistic regression estimates the probability of an event occurring, based on a given dataset of independent variables. Since the outcome is a probability, the dependent variable is bounded between 0 and 1 as its architecture is given in the figure9(a) & (b).In logistic regression, a logistics transformation is applied on the odd, the probability of success divided by the probability of failure. Logistic regression is also used to estimate the relationship between a dependent variable and one or more independent variables, but it is used to predict a categorical variable versus a continuous one. A categorical variable can be true or false, yes or no, 1 or 0, et cetera.

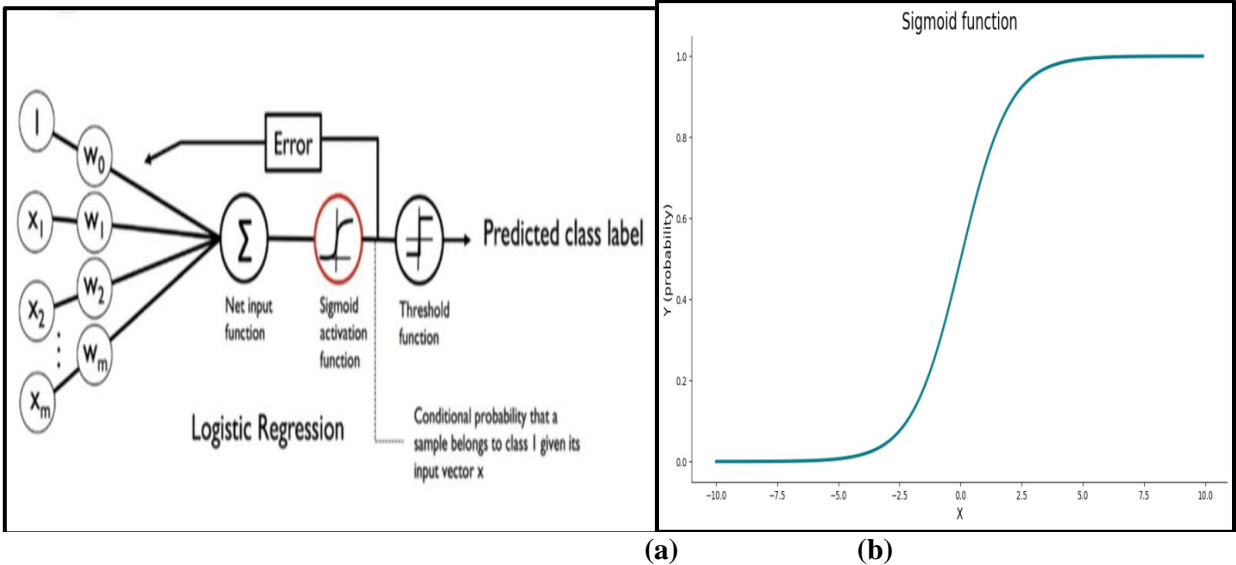


Figure 9(a) &(b). Logistics Regression Architecture with Sigmoid Function

3.4 Validation Algorithm K-Fold Cross-Validation Model

Cross-validation helps with the evaluation of machine learning models. This statistical method helps in comparing and selecting the model in applied machine learning. Understanding and implementing this predictive modelling problem is easy. This technique has a lower bias while estimating the skills of the model. The k-Fold cross-validation signifies the data set splits into a K number. It divides the dataset at the point where the testing set utilizes each fold. The steps to be followed under the K-Fold Cross- Validation is shown in figure 10.

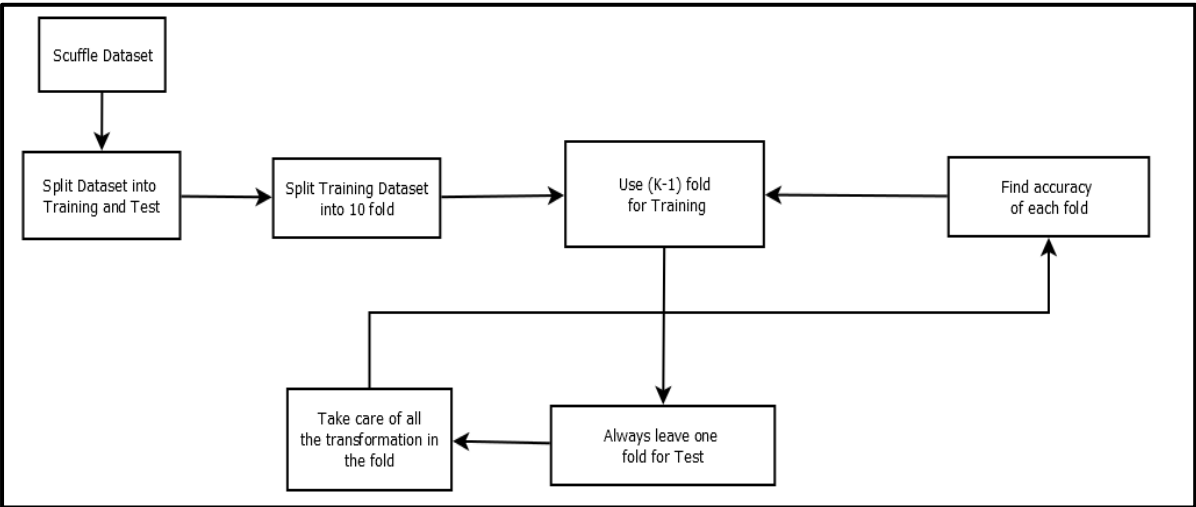


Figure10. K-Fold Cross-Validation

```

from sklearn.datasets import load_breast_cancer
from sklearn.model_selection import train_test_split

data = load_breast_cancer()
X = data.data
y = data.target

X_train, X_test, y_train, y_test = train_test_split(X, y, test_size=0.2, random_state=42)

model = LogisticRegression()
model.fit(X_train, y_train)
preds = model.predict(X_test)

from sklearn.metrics import accuracy_score, confusion_matrix

print(accuracy_score(y_test, preds))
print(confusion_matrix(y_test, preds))

0.9473684210526315
[[42  1]
 [ 5 66]]

```

```

In [53]: for train_idx, test_idx in kf.split(X):
X_train, y_train = X[train_idx], y[train_idx]
X_test, y_test = X[test_idx], y[test_idx]

model = LogisticRegression()
model.fit(X_train, y_train)
y_pred = model.predict(X_test)
score = accuracy_score(y_test, y_pred)
scores.append(score)
i += 1
print("N = " + str(i) + " :: Score = " + str(score))
average_score = sum(scores) / len(scores)
print(f"Average accuracy score: {average_score}")
print("The mean accuracy with 10-fold cross-validation is %s" % average_score)

N = 1 :: Score = 0.8541666666666666
N = 2 :: Score = 0.9166666666666666
N = 3 :: Score = 0.9583333333333334
N = 4 :: Score = 0.9166666666666666
N = 5 :: Score = 0.8541666666666666
N = 6 :: Score = 0.9787234042553191
N = 7 :: Score = 0.9361702127659575
N = 8 :: Score = 0.8936170212765957
N = 9 :: Score = 0.9574468085106383
N = 10 :: Score = 0.9574468085106383
N = 11 :: Score = 0.8297872340425532
N = 12 :: Score = 0.9574468085106383
Average accuracy score: 0.9175531914893619
The mean accuracy with 10-fold cross-validation is 91.76

```

Figure 11. Accuracy of Logistics Regression Model

On comparing the accuracy of logistics regression model obtained by confusion matrix and 10-fold cross validation, it seems to be 94.7 % for the confusion matrix and 91.75 % for the 10-fold cross -validation. On analysing these accuracy values, the best threshold for the accuracy 94.74% is 0.5. The threshold optimization is shown in figure 12. By K-Fold Validation we conclude the Logistics Regression gives an accuracy of 91.76%.

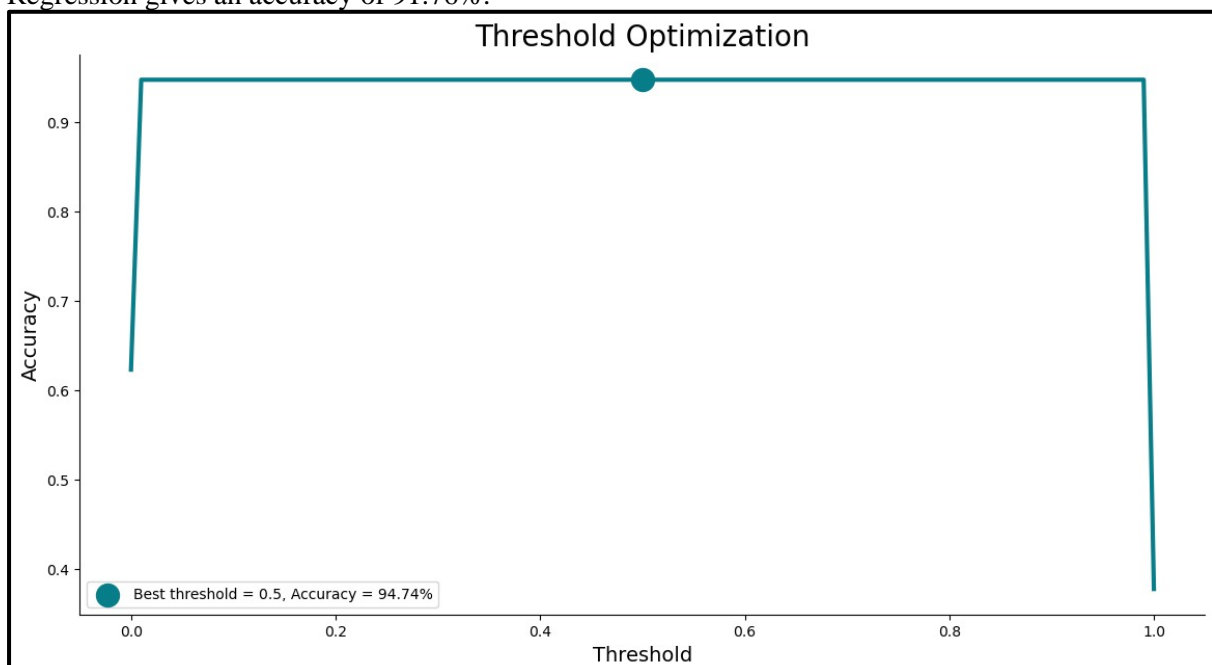


Figure 12: Threshold Optimization

3.3.2. K-Nearest Neighbour Algorithm:

K-Nearest Neighbor(K-NN) is one of the simplest Machine Learning algorithms based on Supervised Learning techniques. K-NN algorithm assumes the similarity between the new case/data and available cases and put the new case into the category that is most similar to the available categories. The k-NN algorithm stores all the available data and classifies a new data point based on

the similarity. This means when new data appears then it can be easily classified into a good suite category by using K-NN algorithm.K-NN algorithm can be used for Regression as well as for Classification problems. Figure 13 depicts the architecture of K-Nearest Neighbour.

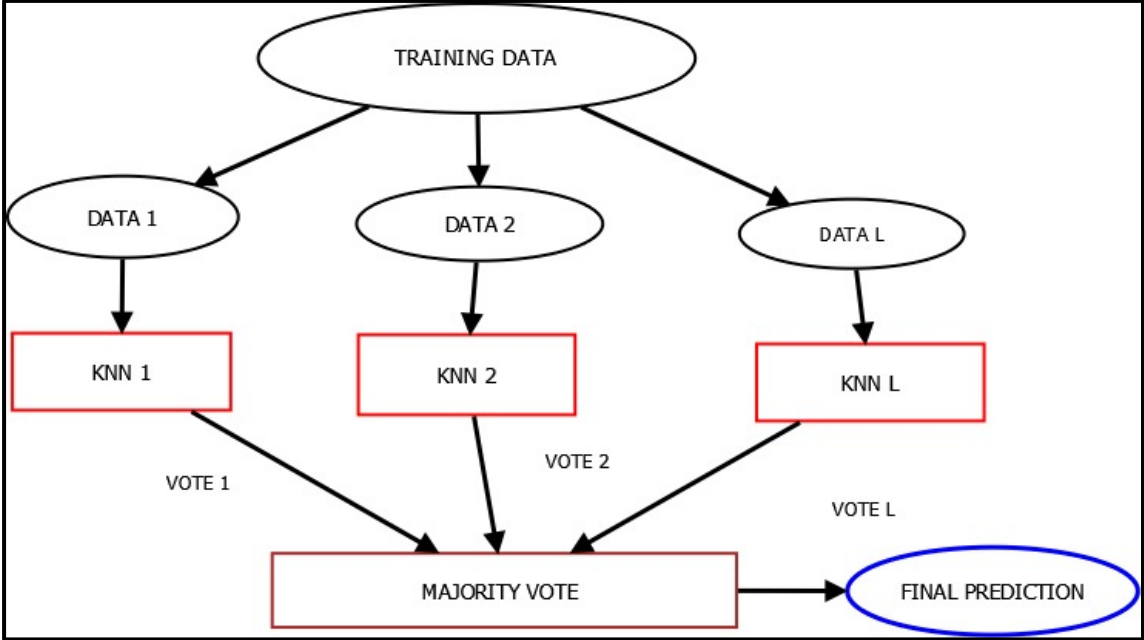


Figure 13: K-Nearest Neighbour Architecture

The results obtained by the K-Nearest Neighbour for the different K-values such as K=1,2,3.....,9 is shown in the figure 14. With these results, the highest accuracy obtained is 93.47 % and the maximum F-measure is 91.89% for k=1.

<pre>K_VALUE = K[f.index(max(f))]\nprint("\nMAXIMUM F MEASURE = ",max(f),"for K = ",K_VALUE)\n\nK = 1\nAccuracy : 0.9347869565217392\nPrecision : 0.9444395062277086\nRecall : 0.8947326870243472\nF-Measure : 0.9189143901147016\n\nK = 3\nAccuracy : 0.9130478260869566\nPrecision : 0.8947326870243472\nRecall : 0.8947326870243472\nF-Measure : 0.8947326870243472\n\nK = 5\nAccuracy : 0.9347869565217392\nPrecision : 0.9444395062277086\nRecall : 0.8947326870243472\nF-Measure : 0.9189143901147016</pre>	<pre>K = 9\nAccuracy : 0.9347869565217392\nPrecision : 0.9444395062277086\nRecall : 0.8947326870243472\nF-Measure : 0.9189143901147016\n\nK = 11\nAccuracy : 0.9347869565217392\nPrecision : 0.9444395062277086\nRecall : 0.8947326870243472\nF-Measure : 0.9189143901147016\n\nMAXIMUM F MEASURE = 0.9189143901147016 for K = 1\n\nfmeasure=knnAlgo(K_VALUE,X_train, y_train, X_test, y_test)\nfmeasure\n\nAccuracy : 0.9385982456140352\nPrecision : 0.8571411564706835\nRecall : 0.9729704163761276\nF-Measure : 0.9113903220743187\n0.9113903220743187</pre>
---	--

Figure 14:Accuracy of K-NN Model with K-Fold Validation

3.3.3 Support Vector Machine Algorithm:

Support Vector Machine(SVM) is a supervised machine learning algorithm used for both classification and regression. Though we say regression problems as well it's best suited for classification. The objective of the SVM algorithm is to find a hyperplane in an N-dimensional space that distinctly classifies the data points. The SVM kernel is a function that takes low-dimensional input space and transforms it into higher-dimensional space, it converts non-separable problems to separable problems. It is mostly useful in non-linear separation problems. Simply put the kernel, does some extremely complex data transformations and then finds out the process to separate the data based on the labels or outputs defined. Figure 15 shows the architecture of the Support Vector Machine.

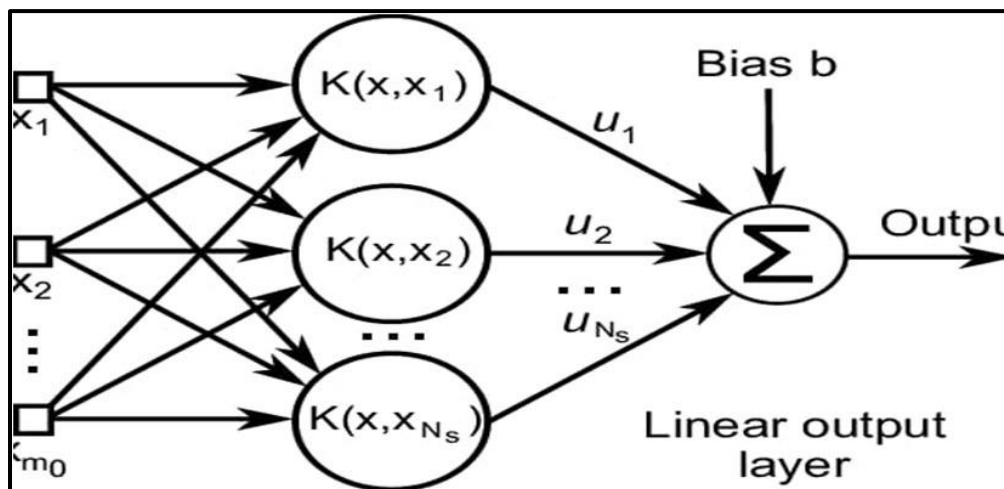


Figure 15: Support Vector Machine Architecture

The results obtained by the Support Vector Machine Architecture for the different K-values such as $K=1,2,3,\dots,9$ is shown in the figure 16. With these results for different k values, the highest accuracy obtained is 95 % for $k=9$.

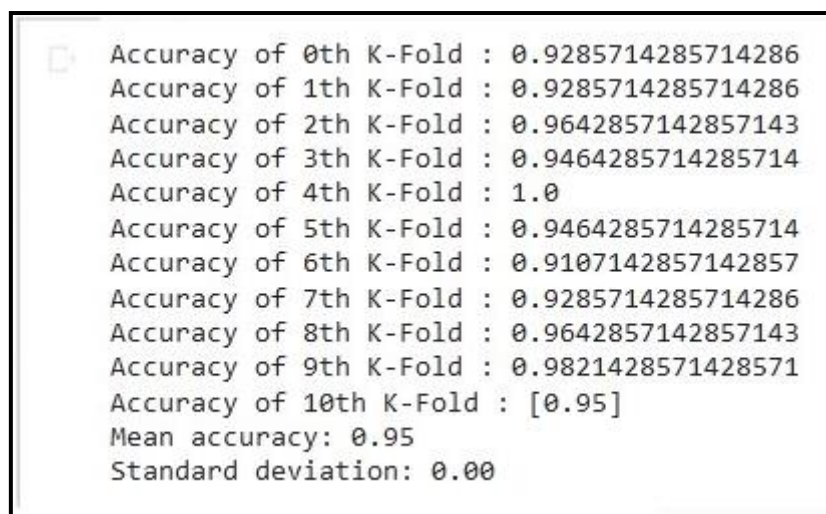


Figure 16: Accuracy of SVM Model with K-Fold Validation

3.3.4 Random Forest:

Random Forest is a popular machine learning algorithm that belongs to the supervised learning technique. It can be used for both Classification and Regression problems in ML. It is based on the concept of ensemble learning, which is a process of combining multiple classifiers to solve a complex problem and improve the performance of the model. Random Forest is a classifier that contains several decision trees on various subsets of the given dataset and takes the average to improve the predictive accuracy of that dataset. Instead of relying on one decision tree, the random forest takes the prediction from each tree and based on the majority votes of predictions, predicts the final output. Figure 17 shows the architecture of Random Forest.

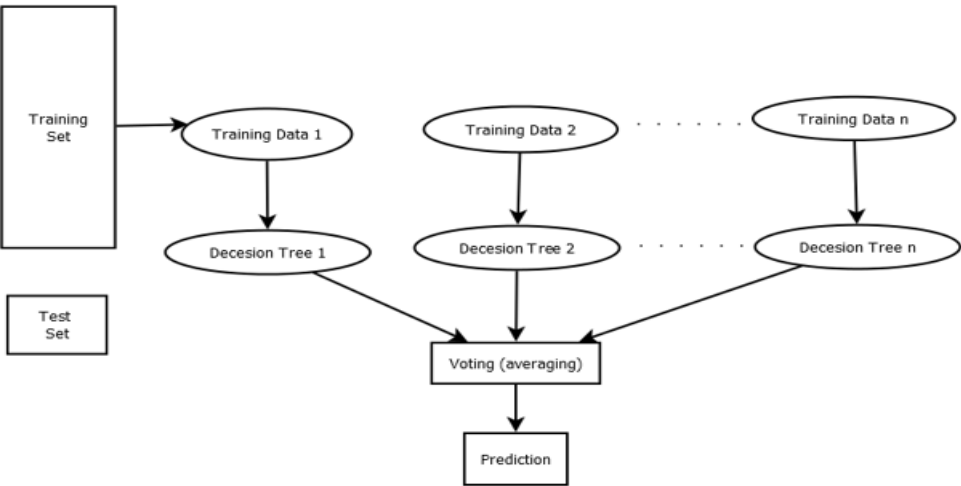


Figure17: Random Forest Architecture

The results obtained by the Random Forest is shown in the figure 18. With the results of different k values such as k=1,2,3,...,N, the highest accuracy obtained is 96.4 %. For k=1 and k=7.

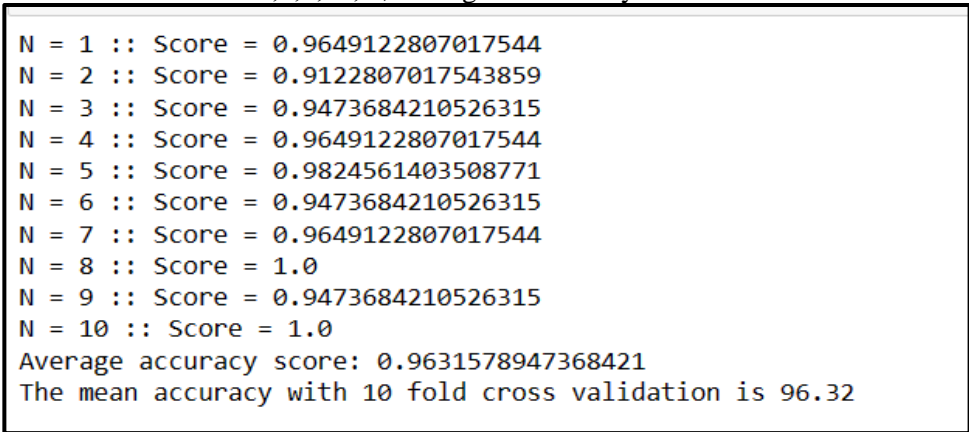


Figure 18:Accuracy of Random Forest

Finally on comparing the accuracies of Logistics Regression, K-Nearest Neighbour,Support Vector Machine and Random Forest, the highest accuracies is provided by the Random Forrest of 96.32% and followed by Support Vector Machine of 95%.The comparative analysis is shown in Table 2.

Table 2. Comparative Analysis of Various Models

S.No.	Models	Accuracy
-------	--------	----------

1.	Logistics Regression	91.76%
2.	K-Nearest Neighbour	91.13%
3.	Support Vector Machine	95%
4.	Random Forest	96.32%

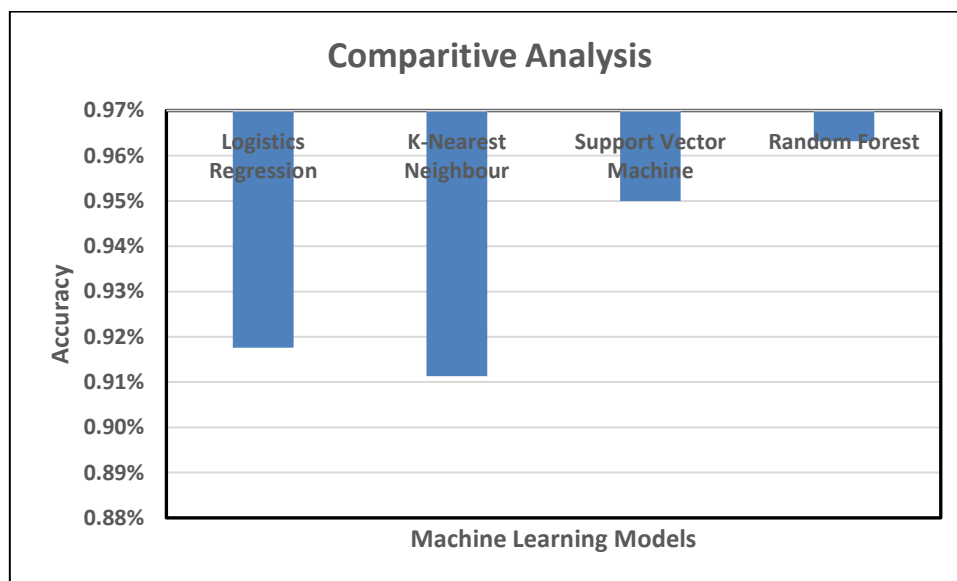


Figure 19. Comparative Analysis

Figure 19 shows Random Forest and Support Vector Machine gives the highest accuracy.

Conclusion

In this research, we proposed a comparative system for the prediction of breast cancer disease by classification of whether it is a Malignant or Benign tumour, we evaluate the performance of a Machine Learning Algorithm (Logistics Regression, K-Nearest Neighbour, Support Vector Machine, Random Forest), training and validating that algorithm using K-Fold Cross-Validation of 10 fold, we conclude that **Random Forest** was the best algorithm to predict whether the tumour is Benign or Malignant having an accuracy of **96.32%**.

References:

- [1] Habib Dhahri, Eslam Al Maghayreh, Awais Mahmood, Wail Elkilani, and Mohammed Faisal Nagi, "Automated Breast Cancer Diagnosis Based on Machine Learning Algorithms", 2019.
- [2] H. Gilbert Welch, Philip C. Prorok, A. James O'Malley, and Barnett S. Kramer, "Breast-Cancer Tumor Size, Overdiagnosis, and Mammography Screening Effectiveness", 2016.
- [3] Lucas Borges, "Analysis of the Wisconsin Breast Cancer Dataset and Machine Learning for Breast Cancer Detection", 2015.
- [4] Mohammed Amine Naji, Sanaa El Filali, Kawtar Aarika, EL Habib Benlahmar, Rachida Ait Abdelouhahid, Olivier Debauche, "Machine Learning Algorithms For Breast Cancer Prediction And Diagnosis", 2021.
- [5] Nayeem Showkat, Huma Parveen, "Data Collection", 2017.
- [6] Konstantinos Demertzis, "Data Preprocessing", 2019.
- [7] Moshe Sipper and Jason H. Moore, "Conservation machine learning: a case study of random forests", 2021.

- [8] Sanjay Yadav and Sanyam Shukla, “*Analysis of k-Fold Cross-Validation over Hold-Out Validation on Colossal Datasets for Quality Classification*”, 2016.
- [9] Payam Refaeilzadeh, Lei Tang and Huan Liu, “*Cross-Validation*”.
- [10] Krishna Battula, “*Research Of Machine Learning Algorithms Using K-Fold Cross Validation*”.
- [11] Meenu Bhagat and Brijesh Bakariya, “*Prediction of Heart Disease Through KNN, Random Forest, and Decision Tree Classifier Using K-Fold Cross-Validation*”, 2022.

Optimal control method for power system reactive power management considering real-time uncertainties

Preethi Vela Anandam¹ | Shunmugalatha Alagarsamy¹ |
Babulal Chittu Kuppasamy²

¹Department of Electrical and Electronics Engineering, Velammal College of Engineering and Technology, Madurai, India

²Department of Electrical and Electronics Engineering, Thiagarajar College of Engineering, Madurai, India

Correspondence

Preethi Vela Anandam, Department of Electrical and Electronics Engineering, Velammal College of Engineering and Technology, Viraganoor, Madurai 625009, Tamil Nadu, India.
Email: research.pree@gmail.com

Abstract

This article investigates multi-objective reactive power management while accounting for real-time generation and load uncertainties. The primary goal of this research is to investigate the effects of uncertainties on reactive power dispatch, while taking into account multiple objectives at the same time and keeping operational constraints in mind. The optimal reactive power dispatch (ORPD) problem is solved using an "indicator-based evolutionary technique" called "ISDE+," which considers two different goal functions: real power loss minimization and voltage deviation minimization. IEEE 30 and IEEE 57 bus test systems are taken into account in the simulation. ISDE+ generates a set of non-dominated optimal solutions, from which the best compromise solution is extracted using the "S" shaped fuzzy membership function. A hyper-volume indicator is used to evaluate the optimizer's performance. In addition, this work proposes a stochastic ORPD problem for tri-objective optimization with load demand and wind power uncertainty. The Weibull probability distribution function was used to model stochastic wind power using real-time wind speed data gathered from the National Institute of Wind Energy. Furthermore, to obtain a generalized wind speed set, a scenario-based reduction technique based on the Python programming language is developed. The outcomes of simulations in deterministic and stochastic instances were studied and compared using ISDE+, which outperforms other methods documented in the literature.

KEYWORDS

fuzzy decision-making, indicator-based evolutionary algorithm, optimal reactive power dispatch, Python programming language, renewable energy

1 | INTRODUCTION

Due to its significant impact on security, reliability, and economic issues, optimal reactive power dispatch (ORPD) plays a critical role in the operation and control of today's modernized power systems. It is also a critical component of a power energy management system. Reactive power control and management are required in the system to ensure that voltages on all system buses are maintained and network real power loss is kept to a minimum. Because most system loads are inductive, and components like transformers and transmission lines use reactive power, it is impossible to

Research Article

Design and Implementation of a New Fast and Efficient MPPT Controller under Different Solar Irradiance Conditions

K. Padmanaban¹, A. Shunmugalatha², and M. S. Kamalesh³

¹Department of Electrical and Electronics Engineering, Alagappa Chettiar Government College of Engineering and Technology, Karaikudi, 630003 Tamil Nadu, India

²Department of Electrical and Electronics Engineering, Velammal College of Engineering and Technology, Madurai, 625009 Tamil Nadu, India

³Department of Electrical and Electronics Engineering, Kongu Engineering College, Erode, 638060 Tamil Nadu, India

Correspondence should be addressed to K. Padmanaban; kpadmanaban@accet.edu.in

Received 16 May 2022; Revised 8 November 2022; Accepted 17 November 2022; Published 21 December 2022

Academic Editor: Regina De Fátima Peralta Muniz Moreira

Copyright © 2022 K. Padmanaban et al. This is an open access article distributed under the Creative Commons Attribution License, which permits unrestricted use, distribution, and reproduction in any medium, provided the original work is properly cited.

The power-voltage (P-V) characteristic curve of solar photovoltaic (PV) systems operating in partial shading conditions (PSC) is nonlinear and has multiple local maximum peak power (LMPP) points, rendering many of the maximum power point tracking (MPPT) algorithms ineffective at locating global maximum peak power (GMPP) points. This work proposes a novel slime mould algorithm- (SMA-) based MPPT controller to utilise maximum peak power (MPP) from solar PV systems during uniform irradiance conditions (UC) and nonuniform irradiance conditions (NUC). On the basis of the MPP they tracked, tracking time, and power efficiency, MPPT controller performance is assessed through MATLAB simulations and implemented experimentally with dSPACE MicroLabBox under various irradiance conditions. The effective performance of the proposed controller is validated and demonstrated in comparison to existing popular MPPT controllers.

1. Introduction

The need for increased power generation capacity today is unavoidable, and the majority of research are concentrating on renewable energy sources due to their infinite nature and little emissions [1]. Solar panels have the highest energy density of any energy source, making them the most cost-effective option today compared to thermal and vibration sources [2]. The main problem with using solar PV systems is the strong nonlinearity between power and voltage. Fluctuations in solar irradiation and temperature lower the PV array's overall maximum power delivery capacity [3]. MPPT is required to track the MPP of PV arrays in solar renewable energy systems (SRES) because solar PV systems are not a constant source of electric power [4]. PV arrays are made up of PV panels that are connected in series for high voltage and parallelly connected for high

current applications, respectively, to increase the PV array power. Blocking and bypassing diodes are important for efficient performance in solar PV systems. Backward discharge is avoided by blocking diodes. Bypass diodes minimize power loss caused by PSC and prevent hotspot heating [5]. The PSC occurs due to nonhomogeneous solar irradiation over the PV array due to a tree or building shading, dust, and bird droppings. Besides, PSC produces several peaks in P-V characteristics and power losses. To lessen power loss caused by PSC, numerous MPPT techniques have been developed and used [6].

The effectiveness of various MPPT approaches is analysed based on how accurately and instantaneously they track maximum power on different PSCs. Based on their tracking capabilities, the available MPPT methods are categorized into three types: classical MPPT controllers, intelligent MPPT controllers, and optimization MPPT

Research Article

Feature-Reduced Stability Analysis of Islanded Photovoltaic Microgrid Inverters

A. Om Prakash¹ and R. Narmatha Banu²

¹Department of EEE, Government Polytechnic College, Usilampatti, Madurai, India

²Department of EEE, Velammal College of Engineering and Technology, Madurai, India

Correspondence should be addressed to A. Om Prakash; aop@vcet.ac.in

Received 27 February 2022; Revised 4 October 2022; Accepted 20 October 2022; Published 21 November 2022

Academic Editor: Gianluca Coccia

Copyright © 2022 A. Om Prakash and R. Narmatha Banu. This is an open access article distributed under the Creative Commons Attribution License, which permits unrestricted use, distribution, and reproduction in any medium, provided the original work is properly cited.

A smart grid environment is prone to data explosion while controlling a microgrid system. Islanded Microgrid's stability analysis involves a large number of system state variables thus consuming more computational memory due to parallel connected inverter dynamics. Parallel inverters generate reference voltage and frequency using droop controllers, unlike grid-connected inverters where the primary grid provides the reference voltage and frequency. This paper develops feature-reduced stability analysis of the parallel inverters thus reducing the computational memory of its stability analysis. Principal component analysis being a feature extraction technique is applied to reduce the number of variables determining stability. MATLAB is used to develop the average model of a parallel inverter with an LCL filter and a three-phase AC load. Evaluation of the stability analysis using the state variable analysis with the virtual resistance method is simulated. Simulation validates stability analysis of the model with reduced state variables. An average model developed using MATLAB and PCA carried out using Python clearly indicated the validation of the dimensionality reduction in the stability analysis. The reduced number of variables is validated for a stable range of the parallel inverter droop controller. Both cases validated the dimensionality reduction in the stability analysis of parallel inverters.

1. Introduction

Renewable energy-based power generators connected to the distribution system are called distributed energy resources (DERs). DERs from different renewable sources form a microgrid. The microgrid, with its dynamic nature, needs stability analysis to understand the stability limits during disturbances in the system. Stability analysis uses state variables that impact the system's stability. Adopting smart technologies in the microgrid environment reckons exponential use of data since it involves localized power generation, independent power control, and dependency primarily on renewable sources. State variables are collected as data using smart devices. Microgrid facilitates the supply of remote end loads by grid-connected or islanded mode of operation. Grid-connected mode of operation uses decoupled control (direct axis/quadrature axis controller (DQ) and instantaneous real/reactive power (PQ)) for synchronizing

renewable energy to the main grid. Synchronization is maintaining the same voltage level and phase angle among parallel inverters using control techniques (Rodriguez-Cabero [1]). The higher penetration level of renewable energy in a power system promises microgrid's islanded mode of operation possible [2, 3]. Islanded mode of operation is a complex model involving many state variables for its stability analysis. Microgrid environments adopt soft computing techniques in the energy management system Leonori et al. [4] and load frequency controller (LFC) Gheisarnejad and Khooban [5]. Due to the absence of grid power in islanded mode, droop controllers employ autonomous operation to manage synchronism Firdaus and Mishra [6] and reactive power sharing problems (Zandi et al. [7]). Inverters supplied by renewable energy and connected to a common load are called parallel inverters. The islanded mode of Microgrid's operation uses a parallel inverter structure that synchronizes with a droop controller. Rasheduzzaman et al. [8] applied



Design and Analysis of LSANN-IPOMPPT with Zeta Converter in PV Systems for Fluctuating Atmospheric Circumstances

R. Divyasharon¹ · R. Narmatha Banu¹

Received: 20 March 2022 / Accepted: 22 August 2022
© King Fahd University of Petroleum & Minerals 2022

Abstract

Individual users are increasingly employing photovoltaic (PV) arrays on a commercial and small scale, and they are all attempting to obtain the maximum available power from the panels. The P-V characteristic of the PV module changes after every small-time duration because of the highly fluctuating atmospheric conditions. However, in such cases, it is indispensable to track the Maximum Power Point (MPP), and this becomes a strong nonlinear issue with a time-bounded solution. Therefore, this paper proposes a Logarithmic Seagull Artificial Neural Network-based Improved Perturb and Observe Maximum Power Point Tracking (LSANN-IPOMPPT) algorithm to acquire maximum power from the PV system. The temperature and irradiance are the input variables and the optimal current and voltages to trace the MPP are computed by using the LSANN method. Then, the IPOMPPT algorithm is built for the DC-DC converter, which functions as an interface connecting solar modules and the load for transferring maximum power. The DC-DC converter is tuned by an LSANN-IPOMPPT controller to exploit the solar array at a maximal power point. The tracking ability of the proposed LSANN-IPOMPPT is evaluated with current state-of-the-art approaches for differing irradiance and temperature levels. The simulation outcomes depicted that the implementation of LSANN-based IPOMPPT algorithm with a zeta converter exhibited a more efficient output power range than the existing methods.

Keywords PV panel · Maximum Power Point Tracking (MPPT) · Zeta DC-DC converter · Logarithmic Seagull in Artificial Neural Network-based Improved Perturb and Observe Maximum Power Point Tracking (LSANN-IPOMPPT)

Abbreviations

$J_{PV(cur)}, J_{PV(nom)}$	Current by incident light, photovoltaic current in nominal conditions
r_{SR}, r_{PR}	Series, shunt resistance
I, k_{BC}	Ideality factor, Boltzmann constant
$T_{imp}, T_{v(imp)}$	Module temperature, cell reference temperature
Q_E, w	Semiconductor bandgap energy, charge of an electron
$F_{irr}, F_{irr(nom)}$	Solar irradiance, nominal value of irradiance

J_{shc}, P_{opc}	Short circuit current, open-circuit voltage
$J_{shc(\kappa)}, J_{rev}$	Short circuit current per temperature factor κ , reverse saturation current
PW_{max}	Maximum power
$J_{Lind(1)}, J_{Lind(2)}$	Ripple current of inductors in Zeta converter
$P_{Vi}^{i/p}, P_{Vi}^{o/p}$	Input, output voltage of Zeta converter
$L_{ind(1)}, L_{ind(2)}$	Inductors of Zeta converter
$C_{cap}^{i/p}, C_{cap}^{o/p}$	Input, output capacitor of Zeta converter
$J_{cur}^{o/p}, P_{Ccap}^{o/p}$	Output current, output ripple voltage of Zeta converter
Stf, φ_D	Switching frequency, duty cycle of Zeta converter
$\Delta_{imp, irr}$	Temperature, irradiance of PV panel
$\Omega_{wt(n)}, \delta_{bias}, h_{AF}$	Assigned weight, bias values, activation function of neural network
J_{max}, P_{max}	Maximum current, maximum voltage

✉ R. Divyasharon
divyasharon@iecc.org

R. Narmatha Banu
r-n-banu@vcet.ac.in

¹ Department of EEE, Velammal College of Engineering and Technology, Madurai, Tamilnadu, India

Computer Vision-Based Cashew Nuts Grading System Using Machine Learning Methods*

A. Sivaranjani†

Department of CSE,
University College of Engineering Panruti (UCEP),
Tamilnadu 607106, India
siv.ranjani2000@gmail.com

S. Senthilrani

Department of EEE,
Velammal College of Engineering and Technology,
Madurai, Tamilnadu 625009, India
ssr@vcet.ac.in

Received 6 April 2022

Accepted 3 August 2022

Published 27 October 2022

In this paper, a computer vision-based cashew nut grading system has been designed and implemented for classifying different grades of cashew nuts using combined features and machine learning approaches. The important task in the cashew nut grading system is to classify the whole and split down cashew nuts. Since these cashew nuts look very similar from the top view, it is a challenging task to classify the whole cashew nut and split down cashew nuts. Hence, a single-view image of cashew nut has been captured by placing a camera with a distance of 17 cm (from the right side of the conveyor belt). The captured red, blue and green images are normalized and converted into hue, saturation and value color space. S channel from HSV image is used for segmentation process using Otsu threshold technique. The total numbers of features extracted are 275 and the features are texture (180), color (90), and shape (5). The constrained optimization-based feature selection method is used and 30 features are selected for further process. The Support Vector Machine (SVM) classifier is used for the classification, and the results obtained from different kernel functions are computed and compared. The 8-layer convolutional neural network (CNN) has been developed in this work for classification and to analyze the performance and accuracy. The accuracy of different machine learning classifiers like SVM 1-1, SVM 1-All and CNN model is also evaluated and compared. The overall accuracy obtained by SVM 1-All with kernel function radial basis for classification is 98.93%.

Keywords: Computer vision; image acquisition; features; SVM classifier; CNN; cashew nuts.

*This paper was recommended by Regional Editor Takuro Sato.

†Corresponding author.

Time Series-Based Photovoltaic Power Forecasting to Optimize Grid Stability

Parthasarathy Seshadri, Bagavat Perumaal T.S., Ashok Kumar B., Keerthana H., Kavimathi G. & Senthilrani S.

To cite this article: Parthasarathy Seshadri, Bagavat Perumaal T.S., Ashok Kumar B., Keerthana H., Kavimathi G. & Senthilrani S. (2022): Time Series-Based Photovoltaic Power Forecasting to Optimize Grid Stability, Electric Power Components and Systems, DOI: [10.1080/15325008.2022.2129871](https://doi.org/10.1080/15325008.2022.2129871)

To link to this article: <https://doi.org/10.1080/15325008.2022.2129871>



Published online: 02 Nov 2022.



Submit your article to this journal [↗](#)



View related articles [↗](#)



View Crossmark data [↗](#)

A Study on Various Medical Imaging Modalities and Image Fusion Methods



B. Ashok Kumar, A. Sivaranjani, S. Senthilrani, and A. Senthil Murugan

Abstract Multimodal medical image fusion is the effective assimilation of different imaging techniques for enhancing the capability to analyze, to guide therapy, treatment, or predict end results. The accuracy of the image obtained from various medical imaging modalities has a significant impact on successful diagnosis of a disease, as image fusion provides supplementary valuable information. Complete and accurate information cannot be acquired from single medical imaging modality. Predominantly, the modalities can be classified into anatomy and metabolism; the former one gives the structural information of the body parts, and the latter one gives the functional information of the cells in the organ. Hence, the integration of various modality images will provide supplementary valuable information. In medical field, multimodal image fusion has become the focusing area of research and development of medical field. This survey paper portrays the background of multimodal medical image process, different multimodal imaging modalities, and various state-of-art methods for multimodal fusion methods. This paper also discusses the importance, opportunities, challenges, and advantages of multimodal medical image processing.

Keywords Multimodal · Image fusion · Various modalities · X-ray · CT · PET · MRI · SPECT · Fusion methods

B. Ashok Kumar (✉)
Department of Electrical and Electronics Engineering, Thiagarajar College of Engineering,
Madurai, India
e-mail: ashokudt@tce.edu

A. Sivaranjani
Department of Computer Science and Engineering, University College of Engineering, Panruti,
India

S. Senthilrani
Department of Electrical and Electronics Engineering, Velammal College of Engineering and
Technology, Madurai, India
e-mail: ssr@vcet.ac.in

A. Senthil Murugan
Faculty of Information and Communication Engineering, Anna University, Chennai, India

© The Author(s), under exclusive license to Springer Nature Singapore Pte Ltd. 2023
M. Gupta et al. (eds.), *Artificial Intelligence on Medical Data*,
Lecture Notes in Computational Vision and Biomechanics 37,
https://doi.org/10.1007/978-981-19-0151-5_9

111





A CRITICAL SURVEY ON EFFICIENCY AND SECURITY OF INTERNET OF THINGS BASED INTELLIGENT TRANSPORT SYSTEM

K.Santha Sheela

939

Assistant Professor, CSE Department, Velammal college of engineering and technology Madurai-625009
santhasheela2022@gmail.com

Dr.A.Radhika

Associate professor,EEE, Velammal college of engineering and technology Madurai-625009
aradhika80@gmail.com

Corresponding author: santhasheela2022@gmail.com

ABSTRACT

With urbanization and increase in population and vehicle usage, transportation sector and people experience major challenges like traffic congestion, high accident rates, transportation delay, and air pollution. Nowadays, it has become a challenge to manage crowd and vehicular traffic in a way that is both efficient and safe in transportation. Traditional transport management system is ineffective in terms of time, cost, energy consumption, security, and quality of service (QoS). The Internet of Things (IoT) integration into transportation systems has helped alleviate such issues, while also facilitating the collection of useful commuting data that has led to the development of intelligent transport systems (ITS). Though ITS helps in reducing traffic congestion, accident rates, transportation delay, and air pollution, it is associated with certain challenges like cyber-security and energy efficiency issues. Hence, we presented a survey on recent techniques involved in enhancing energy efficiency and security of vehicular communication in IoT-based-ITS. Initially, architecture of ITS involving different layers, including data collection, sharing, and storage layers, is discussed. Then various applications and challenges in IoT-based-ITS are explained. Following this, recent approaches involved in mitigating the challenges encountered by IoT-based-ITS, are presented in this survey. Future trends to be incorporated in ITSs for alleviating efficient traffic control, monitoring, and management are also discussed.

Keywords: *Internet of Things (IoT), Intelligent Transport System (ITS), Traffic, Communication, Security, Efficiency.*

DOI Number: 10.48047/NQ.2022.20.20.NQ109094

NeuroQuantology2022;20(20): 939--949

I. INTRODUCTION

Transportation infrastructure has a significant role in a country's ability to compete globally, its economic health, and its level of productivity. Currently, transportation networks are crucial to almost every aspect of modern life. Forty percent of people, on average, are out and about for an hour or more every day, according to a recent survey. People's reliance on transportation networks has increased dramatically in recent years, posing new possibilities and problems for these networks.

Cities grow in size as their populations do, and with that come a corresponding growth in the total number of automobiles on the road. The contemporary city's daily routine and environment are both negatively impacted by the widespread traffic congestion that has emerged as a global issue in recent years. Transport-related difficulties include, but are not limited to, delays in departure times, excessive fuel use, and increased pollution levels. Developing and developed countries alike have challenges from the environmental



Blockchain-enabled electric vehicle charging

12

M. Jajini¹, N. Kamaraj², M. Santhiya³ and S. Chellam¹

¹Velammal College of Engineering and Technology, Madurai, Tamil Nadu, India,

²Thiagarajar College of Engineering, Madurai, Tamil Nadu, India, ³Department of Electrical and Instrumentation Engineering, Kongu Engineering College, Erode, Tamil Nadu, India

12.1 Introduction

Blockchain is the emerging technology in the fields of secured sharing of medical data, cross-border payments, logistics and food selling, etc. Simply put, it is a decentralized, shared network computing that demonstrates the overall origin of the digital item. Blockchain is trying to extend its features in numerous new industries, given its high potential. With its expertise proven in the supply chain, banking, digital authentication, investment management, and the arts and music sector, it is now expanding into the fast-growing market of EV. The foremost barrier to EV adoption is range anxiety. The majority concern is about power capacity running out on long road journeys. This is due to the fact that electric chargers are not readily available everywhere and, as a result, of the absence of charging infrastructure, potential consumers remain hesitant to switch to EVs. As already said before, blockchain is a peer-to-peer (P2P) technology that enables users to share their chargers when not in use. Moreover, in turn, charger owners will be benefited by getting paid for using the chargers. It also allows people and organizations to exchange, purchase, and transfer extra energy between their selves without the intrusion of a central authority or general public having control over how and when transactions can happen.

Experts think that by allowing P2P charging, this new blockchain enterprise will minimize drivers' range anxiety and boost the desirability of EVs in the future. This chapter shows the relationship between the broad field of machine learning (ML) and blockchain. Since ML is a venture of artificial intelligence (AI) where systems can analyze information processed from data, identify patterns, and make decisions with little or no human intervention, ML with Blockchain Fig. 12.1 can create a deadly combination if utilized properly. Both are more or less like the two sides of a coin if used together. While blockchain helps to store correct data that is unaltered and permanent, ML can utilize this data to analyze data patterns and give accurate predictions.

In blockchain's P2P network, mobile apps are used by users to access participating homeowners' locations to charge their EV. It always keeps track of the time taken by each vehicle to fully charged and the amount of energy consumed for the same. Further, a ledger account helps in the implementation of payment in digital

Blockchain-Based Systems for the Modern Energy Grid. DOI: <https://doi.org/10.1016/B978-0-323-91850-3.00008-1>

© 2023 Elsevier Inc. All rights reserved.

Velammal College of Engineering and Technology, Madurai.

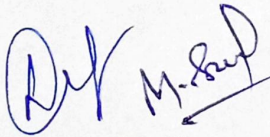
Department of Information Technology


Faculty Publication in Journals

Academic Year 2022-23

S.No	Title of the Paper	Name of the Author	Title of the Journal
1.	Performance Analysis With The Combination Of Visualization And Classification Techniques For Medical Chatbot	Dr.S.Kamalesh/ ASP	Eur. Chem. Bull ISBN: 2063-5346 May 2023 Doi:10.31838/ecb/2023.12.s3.262
2.	Review Based Opinion Classification Model For Medical Chatbot System Using Enhanced Cnn - BiLSTM Approach		Eur. Chem. Bull ISBN: 2063-5346 May 2023 Doi:10.31838/ecb/2023.12.s3.263
3.	Deep Learning Approach For Predicting Glaucoma Progression Using Electronic Health Records		Eur. Chem. Bull ISBN: 2063-5346 May 2023 Doi:10.31838/ecb/2023.12.si6.194
4.	Text to Image Translation using GAN with NLP and Computer Vision		Periodico di mineralogia ISBN: 0369-8963 August 2022 https://doi.org/10.37896/pd91.4/9141
5.	Hyperledger Based Farm Product Traceability Using Blockchain		Periodico di mineralogia ISBN: 0369-8963 August 2022 https://doi.org/10.37896/pd91.4/91492
6.	A Novel Approach to Detect Parkinsonism in Machine Learning	Mrs.P.Saraswathi/ AP-III	Eur. Chem. Bull pp.2063-5346 Volume - 12 , Special Issue-6, June, 2023 Doi:10.31838/ecb/2023.12.si6.329
7.	A Systematic Approach for Fallacious URL Detection in Machine Learning		Eur. Chem. Bull pp.2063-5346 Volume - 12 , Special Issue-6, June, 2023 Doi:10.31838/ecb/2023.12.si6.330
8.	Liver Infection Prediction Analysis using Machine learning to Evaluate Analytical Performance in Neural Networks	Mr.S.Jegadeesan	International Journal of Engineering and Technology Volume 71 Issue 3 377-384, March 2023 ISSN :2231-5381
9.	Reduction of Near-End and Far - End Crosstalk in Microwave and Millimetre Wave Band of Parallel Transmission Lines using Meander Shaped DMS	Mr.A.Gobinath / AP-III	Journal of Physics: Conference Series Doi: 10.1088/1742-6596/2466/1/012016

S.No	Title of the Paper	Name of the Author	Title of the Journal
10.	Artificial Neural Network Approach to Model Sidewall Metallization of Silicon-based Bistable Lateral RF MEMS Switch for Redundancy Applications	Dr.P.Uma Maheswari	Silicon, Springer Vol 14, August, 2022 doi: 10.1007/s12633-022-02070-2
11.	Computation of cloud in set statistics transferring	Mr.A.Srinivasan / AP-III	NeuroQuantology ISSN: 1303-5150 Volume 20 Issue 20 December 2022 doi: 10.48047/NQ.2022.20.20.NQ109151


Faculty In-Charge
Mrs.R.Nancy Deborah, AP
Ms.M.Soundarya, AP


HODAT
Dr.R.Kavitha, Professor



PERFORMANCE ANALYSIS WITH THE COMBINATION OF VISUALIZATION AND CLASSIFICATION TECHNIQUES FOR MEDICAL CHATBOT

S Kamalesh¹, Shajida M², Ganesh Kumar P³, Sakthiyadharshini N P⁴, Aswitha B⁵

Article History: Received: 29.01.2022

Revised: 19.03.2023

Accepted: 04.05.2023

Abstract:

Natural Language Processing (NLP) continues to play a strategic part in complaint discovery, medicine discovery during the current epidemic. This abstract provides an overview of performance analysis with Combination of visualization and Classification Technique of NLP for Medical Chatbot. Sentiment analysis is an important aspect of NLP that is used to determine the emotional tone behind a piece of text. This technique has been applied to various domains, including medical chatbots. In this we have compared the combination of Decision tree with Heatmap and Naïve Bayes with Word Cloud. The performance of the chatbot was evaluated using accuracy, and the results indicate that the combination of visualization and classification techniques significantly improves the chatbot's performance

Keywords: Sentimental analysis, NLP, medical chatbot, Decision tree, Heatmap, Naïve Bayes, Word Cloud.

¹Faculty, Department of Information Technology Velammal College of Engineering and Technology Madurai, Tamilnadu, India.

²IV yr Student, Department of Information Technology Velammal College of Engineering and Technology Madurai, Tamilnadu, India.

³Faculty, Department of Information Technology KLN College of Engineering Madurai, Tamilnadu, India.

⁴IV yr Student, Department of Information Technology Velammal College of Engineering and Technology Madurai, Tamilnadu, India.

⁵IV yr Student, Department of Information Technology Velammal College of Engineering and Technology Madurai, Tamilnadu, India.

Email: ¹skl@vcet.ac.in, ²sakthiyadharshiniprakash@gmail.com, ³ganesh_me@yahoo.com, ⁴sakthiyadharshiniprakash@gmail.com, ⁵shajidabatcha4@gmail.com

DOI: 10.31838/ecb/2023.12.s3.262



REVIEW BASED OPINION CLASSIFICATION MODEL FOR MEDICAL CHATBOT SYSTEM USING ENHANCED CNN-BILSTM APPROACH

S. Kamalesh¹, M. V. Praveen², S. Sujeet Krisna³, T. Raj Pranav⁴,
P Ganesh Kumar⁵

Article History: Received: 29.01.2022

Revised: 19.03.2023

Accepted: 04.05.2023

Abstract

Artificial intelligence (AI) and other automation technologies that can speak via chat with end users are used to replace or supplement human support agents in chatbots, which are conversational applications that help with customer care, engagement, and support. Chatbots are evolving into complicated software artefacts requiring a high level of proficiency across many technological fields. The software engineering difficulties of creating top-notch chatbots will be covered in this technical briefing. By utilizing the open-source chatbot creation platform, attendees will be able to design their own bots.

Keywords: Natural Language Processing, Artificial Intelligence, Machine Learning, Chatbot, Data, Training.

¹Faculty Department of Information Technology Velammal College of Engineering and Technology Madurai, Tamil Nadu, India.

²Faculty Department of Information Technology KLN College of Engineering Madurai, Tamil Nadu, India.

^{3,4,5}IV yr Student ,Department of Information Technology Velammal College of Engineering and Technology Madurai, Tamil Nadu, India.

DOI: 10.31838/ecb/2023.12.s3.263

1. Introduction

Platforms for instant messaging have become one of the most popular ways to communicate and



DEEP LEARNING APPROACH FOR PREDICTING GLAUCOMA PROGRESSION USING ELECTRONIC HEALTH RECORDS.

A. K. Gayathri¹, Dr. A. Muthukrishnan², Dr. S. Kamalesh³

Article History: Received: 02.03.2023

Revised: 16.04.2023

Accepted: 31.05.2023

Abstract:

The showing causations of blindness and equatorial unreality in the United States are primarily period-related eye conditions like age-related macular degener- ation, cataract, diabetic retinopathy, and glaucoma. Other common eye diseases in- clude amblyopia and hypermetropia. Correc- tive eyeglasses, contact lenses, refractive sur- gery, or lens implantation for diplopia are some of the most sought-after treatment op- tions for this eye complaint. Data booby-trap- ping ways can effectively prognosticate Ac- curacy, Precision, Recall, and F1_scorea. In this design, we use CNN and ANN to prog- nosticate the complaint.

Keywords: Corrective Eyeglasses, Cata-racts, Contact Lenses, Diabetic Retinopathy.

¹ PG Student, Department of IT, Velammal College of Engineering and Technology, Madurai.

² Associate Professor, Department of CSE, Vel Tech Rangarajan Dr.Sagunthala R&D Institute of Science and Technology, Chennai.

³ Associate professor, Department of IT, Velammal College of Engineering and Technology, Madurai

DOI: 10.31838/ecb/2023.12.si6.194

Text to Image Translation using GAN with NLP and Computer Vision

R. PERUMALRAJA, A.S. ARJUNKUMAR AND S. KAMALESH

*Velammal College of Engineering and Technology,
Madurai, Tamil Nadu, India.*

ABSTRACT

Generating high-quality images from text queries is a challenging problem in computer vision and has many practical applications. This paper proposes Stacked Generative Adversarial Networks (StackGAN) to generate 256 x 256 photo-realistic images conditioned on text descriptions. We resolve the hard problem into more manageable sub-problems through a sketch-refinement process. The Stage-I GAN gives the primitive shape and colors of the object based on the given text description, yielding Stage-I low-resolution images. The Stage-II GAN uses Stage-I results and text descriptions as inputs and generates high-resolution images with photo-realistic details. It can correct defects in Stage-I results and add compelling details to the refinement process. To improve the generated images' variety and regulate the conditional-GAN training, we introduce a novel Conditioning Augmentation technique. Various experiments and comparisons with state-of-the-art benchmark datasets demonstrate that the proposed method achieves significant improvements in generating photo-realistic images conditioned on text queries.

Keywords: *Generative Adversarial Networks, Image, Generation, Text, Translation, Deep CNN layers.*

INTRODUCTION

Generative Adversarial Networks are a powerful class of neural networks that are used for unsupervised learning. Ian J. Goodfellow developed and introduced the GAN in the year of 2014. GANs are naturally made up of a system of two competing neural network models which compete with each other and can examine, capture and copy the variations within a particular dataset. It has been noticed most mainstream neural nets can be easily fooled into misclassifying things by adding only a small amount of noise into the original data. Unexpectedly, the model after adding noise has higher confidence in the wrong prediction than when it was predicted correctly. The reason for such a dispute is that most machine learning models learn from a limited amount of data, which is a huge drawback, as it is prone to overfitting. Also, the mapping between the input and the output is almost linear. Even though it may seem that the boundaries of separation between the various classes are linear, in reality, they are composed of linearities and even a small change in a point in the feature space might lead to misclassification of data.

GANs are a clever way of training a generative model by framing the problem as a supervised learning problem with two sub-models: the generator model that we train to generate new examples, and the discriminator model that tries to classify examples as either real (from the domain) or fake (generated). The two models are trained together in a zero-sum game, adversarial, until the discriminator model is fooled about half the time, meaning the generator model is generating plausible examples. GANs are an exciting and rapidly changing field, delivering on the promise of generative models in their ability to generate realistic examples across a range of problem domains, most notably in image-to-image translation

Hyperledger Based Farm Product Traceability Using Blockchain

S. KAMALESH ¹, R. PERUMALRAJA ²
Department of Information Technology
Velammal College of Engineering and Technology
Madurai, India.

ABSTRACT

Consumers nowadays are very interested in food product quality and safety. It is challenging to track the provenance of data and maintain its traceability throughout the whole supply chain network without an integrated information system. For this purpose, Agriculture and Food (Agri-Food) force chains are developing complex systems which are responsible, in addition to track and store orders and deliveries, to guarantee translucency and traceability of the food product and metamorphosis process. Food force chains have a tremendous complexity which is regularly the cause of need for plumpness and traceability. In the proposed method, all the partners taking part within the agri supply chain (beginning from the agriculturists to the retail marketers) feed details like crop collected date, cleansing and packaging processes held in an permissioned blockchain network called as hyperledger fabric. The hyperledger fabric network requires all the nodes to be certified some time recently. Thus, it assures, only the trusted and certified partners can take part. By using the proposed model, the transparency of the product details are extended to the customers with Hyperledger Fabric.

Keywords — Supply chain, Food security, Blockchain, traceability system, Hyperledger, Docker, Traceability, Hyperledger Fabric

INTRODUCTION

Over usage of chemicals within the production process, use of uncertified chemicals and mechanisms for preservation and ripening processes, are the most important issues that impact on agricultural product's quality also as overall health of the consumers. Nowadays, consumer's concerns regarding food provenance and quality are extremely high, leading to the tendency to spend more cash on food products whose origin is certified. Existing systems lack transparency and consumers' trust because of the unavailability of a quick and trustworthy platform to retrieve information on the product's provenance. In our work we propose a whole model of a blockchain based agri-food supply chain traceability system and achieve transparency with Hyperledger Fabric. It's built on the Hyperledger Fabric platform where all data is stored on blockchain ledgers and are accessible throughout the complete supply chain from producer to consumer.

LITERATURE SURVEY

In the existing system the authors propose the use of a three- layered sharded armature that ensures trustability and vacuity of data for consumers and scalability with respect to sale prosecution outturn.[1] In the existing method, supply chain traceability, A dual storage structure of "database +



NANO STUDIES

Search for title, author, doi.

Search

ISSN 2063-5346



**European Chemical
Bulletin**

ISSN 2063-5346

Open Access E-Journal

DEVELOPMENT AND VALIDATION OF A
RELIABLE AND RAPID LC-MS/MS
METHOD FOR QUANTIFICATION OF
SIPONIMOD IN RAT PLASMA AND ITS

**A NOVEL APPROACH TO DETECT PARKINSONISM IN MACHINE
LEARNING**

PDF

Keywords:

Parkinsonism (Pd),
Machine Learning,
Lightgbm Algorithm.

P. Saraswathi, M. Prabha, A. K. Vidyabharathi, S.
Krishnaveni

» doi: 10.31838/ecb/2023.12.s16.329

Abstract

Parkinson's disease (PD) is a progressive neurodegenerative disorder that primarily affects the central nervous system. Symptoms of early Parkinson's disease include Tremors, Rigidity, Bradykinesia, and Postural instability. Although typically diagnosed in individuals over 60 years old, 5 to 10 percent of cases occur in those under 50. Early detection is critical for effective treatment, and machine learning algorithms can be utilized to process user input data alongside previously collected data to assess whether an individual is affected. The selection of an optimal classification algorithm for local datasets can be challenging.

Submit article



ELSEVIER

ORCID

Crossref

OPEN ACCESS



**European Chemical
Bulletin**

ISSN 2063-5346

Open Access E-Journal

DEVELOPMENT AND VALIDATION OF A
RELIABLE AND RAPID LC-MS/MS
METHOD FOR QUANTIFICATION OF
SIPONIMOD IN RAT PLASMA AND ITS

**A SYSTEMATIC APPROACH FOR FALLACIOUS URL DETECTION IN
MACHINE LEARNING**

PDF

Keywords:

Malicious Websites,
Lexical URL analysis,
Defacement, Benign
Malware and Phishing

P. Saraswathi, S. Harini, G. M. Premika, V. Shrinithi
» doi: 10.31838/ecb/2023.12.si6.330

Abstract

Innocent Internet users are paying the price for the increasing prevalence of fraudulent websites, which generate billions of dollars in illegal revenue. There is a need for intelligent technologies to recognise harmful websites as online criminal activity rises. It has been demonstrated that URL analysis is a useful method for identifying phishing, malware, benign and defacement. For URL categorization, previous studies have used lexical aspects, network traffic, hosting data, and other techniques. These methods necessitate time-consuming searches that cause real-time systems to experience severe delays. This paper represents a simple method for classifying dangerous

Submit article



ELSEVIER

ORCID

Crossref

OPEN ACCESS

Original Article

Liver Infection Prediction Analysis using Machine Learning to Evaluate Analytical Performance in Neural Networks by Optimization Techniques

P. Deivendran¹, S. Selvakanmani², S. Jegadeesan³, V. Vinoth Kumar⁴

¹Department of IT, Velammal Institute of Technology Panchetti, Chennai.

²Department of IT, R.M.K. Engineering College, Chennai.

³Department of IT, Velammal College of Engineering & Technology, Madurai.

⁴Department of IT, Velammal Institute of Technology, Panchetti, Chennai.

¹Corresponding Author : deivendran1973p@gmail.com

Received: 16 December 2022

Revised: 28 February 2023

Accepted: 12 March 2023

Published: 25 March 2023

Abstract - Liver infection is a common disease, which poses a great threat to human health, but there is still able to identify an optimal technique that can be used on large-level screening. This paper deals with ML algorithms using different data sets and predictive analyses. Therefore, machine ML can be utilized in different diseases for integrating a piece of pattern for visualization. This paper deals with various machine learning algorithms on different liver illness datasets to evaluate the analytical performance using different types of parameters and optimization techniques. The selected classification algorithms analyze the difference in results and find out the most excellent categorization models for liver disease. Machine learning optimization is the procedure of modifying hyperparameters in arrange to employ one of the optimization approaches to minimise the cost function. To set the hyperparameter, include a number of Phosphatase, Direct Billirubin, Protien, Albumin and Albumin Globulin. Since it describes the difference linking the predictable parameter's true importance and the model's prediction, it is crucial to minimise the cost function.

Keywords - Classification, Neural networks, Linear regression, Random forest, Naïve-Bayes.

1. Introduction

The liver is the biggest inner limb in our human deceased; it is behind in ribcage on the upper right half of the guts. A large portion of the liver's mass resides in the body's right half. The liver is a critical part of the assimilation and handling of nourishment. Liver cells produce bile, a greenish liquid that guides the processing from the breakdown of medications. There are there a category of diseases like Hepatitis A, B, and C. Most a human is eating or drinking something that is infected by fecal. It might not have some symptoms goes missing by themselves within a period of 6 months without any long-term harm. Hepatitis B is caused by defenseless gender or captivating drugs with communal gratuitous. The last solitary is the approach from impure blood that gets keen on the body. However, nonalcoholic fatty liver disease is when too much fat has built up inside the liver. The additional fact can cause irritation and cell injury in our liver. Acute liver collapse may occur. When one has an extended of liver disease, the liver quits functioning within a very tiny period. Cirrhosis is the swelling of scars in our liver and extra scars replacing the well parts of the liver. Most of the survey is

composed of medical ex-pediments in addition to the skin will be a suitable and the sum of the dataset to be used.

Even if liver tissue has been severely damaged, the early stages of liver disease are incredibly difficult to detect. According to several restorative professionals frequently overlook the analysis of the illness. Early detection is crucial and critical to protecting the patient because this could lead to improper medicine and treatment. The major goal of this learning is to enhance the correctness of result prediction and lower the cost of finding in medicinal engineering. As an effect, we classify patients with liver complaints by means of a variety of classification methods.

2. Literature Survey

Y Yugal Kuma & G. Sahoo published a document based on the unusual categorization technique that has been used in the northeast region of the dataset collected liver defects (2013) [10]. The outcome to facilitate the DT algorithm has improved, the accuracy is more than [1] (2017 Sontakke, Sumedh, et al.) 82.45% compare to further algorithms, and it gives an accuracy of 97.27%. P.M.Goel recommended a



Reduction of Near-End and Far - End Crosstalk in Microwave and Millimetre Wave Band of Parallel Transmission Lines using Meander Shaped DMS

A Gobinath^{1,3}, N Suresh Kumar^{2,3}, and P Rajeswari^{2,3}

¹Department of Information Technology

²Department of Electronics and Communication Engineering

³Velammal College of Engineering and Technology, Madurai

gopigopinath10@gmail.com

Abstract. This research proposes a unique design that makes use of a defective microstrip topology to decrease electromagnetic coupling between parallel high speed interconnects. The performance of this new microstrip construction with defects is evaluated using near-end crosstalk and far-end crosstalk. Serpentine shaped defected microstrip is introduced in one parallel of high speed interconnects and its performance is also compared the existing structure. In this research, the proposed defected microstrip structure (DMS) is simulated and compared with a conventional microstrip structure using Ansoft HFSS software which employs the Finite Element Method (FEM). Simulation results indicate that the DMS design effectively reduces crosstalk in comparison to the previous structure. It reduces more than 5dB near end crosstalk and more than 3dB far end crosstalk compared to conventional model.


1. Introduction

Nowadays, the demand for wireless devices are increasing rapidly since the growth of wireless communication and high speed data transmission increases simultaneously. These devices should have smaller in size and support high data rate. Therefore, it is necessary to accommodate more number of high speed interconnects with in a small feature size which lead to signal integrity problems. High speed interconnect is a conductive path between transmission end to receiving end which is used to carry the high speed signal. Generally, high speed interconnects are modeled as planar transmission lines like microstripline or stripline. Microstripline is generally preferred rather than stripline since low cost and ease of fabrication. In this research, the crosstalk is investigated by considering a duo of coupled microstrip transmission lines. Signal integrity is a measure of quality of signal at the receiver end. When the electrical signal on one transmission line is transferred to an adjacent line, it can cause a range of signal integrity issues. These signal integrity issues include crosstalk, electromagnetic emissions, propagation delay, impedance mismatch, and signal reflection. Crosstalk or coupling is a particularly significant signal integrity concern.

Several scholars have published studies and papers detailing various methods for reducing crosstalk between adjacent transmission lines in high-speed printed circuit boards. The methods presented in literatures are increasing the distance between two lines placing guard trace between two lines, inserting via guard fence, altering the geometry of the microstripline like serpentine and mitered bend lines. However these methods have their own pros and cons. In the literature, authors [1] through [17]

[Home](#) > [Silicon](#) > ArticleOriginal Paper | [Published: 27 August 2022](#)

Artificial Neural Network Approach to Model Sidewall Metallization of Silicon-based Bistable Lateral RF MEMS Switch for Redundancy Applications

[Joslin Percy](#) , [S. Kanthamani](#), [S. Sethuraman](#), [S. Mohamed Mansoor Roomi](#) & [P. Uma Maheswari](#)

[Silicon](#) **14**, 9175–9185 (2022)**136** Accesses | [Metrics](#)

Abstract

Radio Frequency Micro Electro Mechanical System (RF MEMS) switches are rapidly evolving due to the demand for low cost, high performance, and compact communication systems. An electrothermally actuated bistable lateral MEMS switch for redundancy applications has been already fabricated and tested for mechanical characteristics. In this paper to make this switch as a suitable candidate for RF applications, sidewall metallization using gold is proposed. Modelling of sidewall metallization in Bistable Lateral RF MEMS switch using Cascade Feedforward Scaled Conjugate Gradient (CFSCG) Artificial Neural Network approach is reported.



COMPUTATION OF CLOUD IN SET STATISTICS TRANSFERRING

S. Gokul Pran¹, S. Murugavalli², A. Srinivasan³, B. V. Sai Thrinath⁴ and B. Meghya Nayak⁵

¹Department of Computer Science and Engineering, Sree Vidyanikethan Engineering College, Tirupati, Andhra Pradesh, India

²Department of Artificial Intelligence, K. Ramakrishnan College of Technology, Trichy, Tamilnadu, India

³Department of Information Technology, Velammal College of Engineering and Technology, Madurai, Tamilnadu, India.

⁴Department of Electrical and Electronics Engineering, Sree Vidyanikethan Engineering College, Tirupati, Andhra Pradesh, India.

⁵Department of Electrical Engineering, Arvind Gavali College of Engineering, Satara. Maharashtra, India

1485

ABSTRACT:

Information participating in conveyed registering engages various individuals to energetically share the social affair data, which works on the productivity of work in needful conditions and is far and wide expected applications. In any case, how to confirm the Protection of statistics transferring inside a assembling and how to proficiently share the re-appropriated information in a collecting way are faced difficulties. Keep in mind that vital understanding conceptual meanings have assumed a vital part in protection and effective assembling details taking part in distributed computing. In this paper, by taking benefit of the similar adjusted deficient chunk plan (SADCP), we represent a clever chunk configuration based chief knowing conceptual meanings that upholds numerous spieces, that can deftly expand the amount of individuals in a cloud environment as per the construction of the chunk plan. In light of the proposed bunch information transferring type, we present general equations for creating the normal meeting chief M for numerous members. Identify that by profiting from the $(s, g+1, 1)$ -chunk plan, the computation intricacy of the proposal of convention straightly increments with the quantity of members and correspondence intricacy are extraordinarily decreased.

VITAL TERMS: chief understanding convention, similar adjusted deficient chunk plan (SADCP), information transferring, distributed computing.

DOI Number: 10.48047/NQ.2022.20.20.NQ109151

NeuroQuantology2022;20(20): 1485-1495

I.INTRODUCTION:

Dispersed processing and disseminated stockpiling have become hot focuses in continuous numerous years. Both are affecting the way we live and immensely further creating creation effective in few locales. At this point, due to the confined amassing sources and the need for supportive assessment, we like to hold all sorts of statistics in servers of the cloud, that is in like manner a respectable decision for the associations and relationship to prevent the above mentioned of passing on and staying aware of tools when information are set aside

locally. The server of cloud gives an free and comfortable limit stage for individual and affiliations; anyway, it also presents protection issues. For instance, a systems of cloud may be presented to attacks from the two malicious clients and cloud providers. In these circumstances, it is fundamental for ensure the protection of the set aside statistics in the cloud. In [1], [2], [3], a couple of plans were proposed to preserve the protection of the reexamined data. The previously mentioned contrives simply contemplated protection issues of a singular information owner. Regardless, in specific applications, different



3.4.3 Details of research papers per teacher in CARE Journals notified on UGC website during the year

Sl.No.	Name of the Author(s)	Department of the Author(s)	Title of the Paper	Name of the Journal	Month and Year of publication	ISSN	Link to the notification in UGC enlistment of the Journal
1	Dr. K. Kavitha	ECE	Design and Development of Parasitic Elements Loaded Quad band Frequency and Pattern Reconfigurable Antenna	International Journal of RF and Microwave Computer-Aided Engineering	01/05/2023	https://doi.org/10.1155/2023/4034241	
2	Dr. K. Kavitha	ECE	Leaf disease identification in South Asian Agriculture: a Deep Convolutional Neural Network Approach	Journal of Data Acquisition and Processing	01/06/2023	1004-9037	
3	Dr.P.Rajeswari	ECE	Reduction of Near-End and Far - End Crosstalk in Microwave and Millimetre Wave Band of Parallel Transmission Lines using Meander Shaped DMS	Journal of Physics	23/05/2023	DOI 10.1088/1742-6596/2466/1/012016	

4	Dr.P.Rajeswari	ECE	A Novel Branch line coupler with defected ground structure for bone density measurement Analysis	ARPN Journal	01/06/2023	1819-6608	
5	Dr.P.Karthikeyan	ECE	Steganalysis on Data embedded Medical image	Journal of Discrete Mathematical Sciences and Cryptography	15/07/1905	0972-0529	
6	Mr.G.Pradeep Kumar	ECE	Digital Reconstruction of underwater submerged objects using 3D photogrammetry techniques	Neuro Quantology	01/06/2022		
7	Mr.S.VijayGokul	ECE	SAR reduction techniques for WBAN and Mobile applications: A Survey	Frequenz	01/05/2023	https://doi.org/10.1515/freq-2022-0297	

Research Article

Design and Development of Parasitic Elements Loaded Quadband Frequency and Pattern Reconfigurable Antenna

K. Karthika¹ and K. Kavitha²

¹Department of Electronics and Communication Engineering, Kumaraguru College of Technology, Coimbatore, India

²Department of Electronics and Communication Engineering, Velammal College of Engineering and Technology, Madurai, India

Correspondence should be addressed to K. Karthika; karthika.svk@gmail.com

Received 23 March 2023; Revised 2 May 2023; Accepted 9 May 2023; Published 23 May 2023

Academic Editor: Xiao Ding

Copyright © 2023 K. Karthika and K. Kavitha. This is an open access article distributed under the Creative Commons Attribution License, which permits unrestricted use, distribution, and reproduction in any medium, provided the original work is properly cited.

Modern communication demands a low-profile, versatile antenna. In this paper, a low-profile antenna of size $38 \times 40 \times 0.787 \text{ mm}^3$ is proposed to reconfigure frequency and radiation pattern. The Rogers RT Duroid 5870 of dielectric constant 2.33 is used as a substrate. Frequency reconfiguration is achieved by connecting patches of different lengths corresponding to the resonant frequencies through three PIN diode switches. Switching on/off these three diodes results in frequency switching between four distinct frequency bands. The Yagi-Uda principle is utilized to alter the radiation pattern. Simple parasitic elements are loaded on either side of the radiating structure. Changing the electrical lengths of the parasitic elements using PIN diode switches facilitates pattern reconfiguration by making them behave as a reflector/director. The presented structure resonates at four distinct frequencies (5.3 GHz/3.82 GHz/2.77 GHz/2.2 GHz) with a maximum of three beam tilt angles for each resonating frequency. SMP1345-079LF PIN diode is used for switching operation. Biasing circuit has been designed to ensure RF and DC isolation. The proposed antenna offers acceptable radiation performance in all the switching states. The average measured gains are 2.43 dBi, 2.42 dBi, 3.5 dBi, and 3.29 dBi at 5.3 GHz, 3.82 GHz, 2.77 GHz, and 2.2 GHz, respectively. On an average, the proposed antenna exhibits the simulated efficiency of 81%. The proposed antenna is suitable for 5G communication as its bandwidth covers band 1, band 7, band 46, and band 77 of the 5G new radio (NR) standard. Fabrication and testing are done to validate the results.

1. Introduction

The integration of several applications into one device is necessary for contemporary wireless communication systems. To accomplish this, the system can either employ a single antenna with many functionalities or incorporate multiple antennas inside the device. The use of several antennas in a single system to support multiple applications is not a viable solution. Multiple antennas in a single system require more area to deploy, interfere with one another, have more installation costs, and have more complicated hardware platforms. Reconfigurable antennas are one of the potential methods for addressing the above-stated requirements [1]. The need for reconfigurable antennas is further driven by the demand for wireless communication systems that require antennas to adapt to changing operational

conditions. Reconfigurable antennas can provide frequency agility, beam steering, polarization control, multimode operation, and miniaturization, making them a critical component of modern wireless communication systems. Reconfiguration can be achieved through electrical switches/mechanical switches/optical switches/reconfigurable materials/structural alterations [2]. The majority of research on reconfigurable antennas concentrated on a single reconfiguration like either frequency or pattern or polarization.

Reconfigurable antennas can be designed to operate over a range of frequencies, allowing them to adapt to changing frequency bands in wireless communication systems. This can be particularly important in situations where frequency allocation is limited or when sharing of frequency bands is required. Spectrum can be effectively used with frequency reconfigurable antennas. A compact antenna that can switch frequencies

among thirty-six different states with a stable radiation pattern is presented in [3]. Six-pin diodes are loaded along the non-radiating edges of the patch. By connecting the ground plane and non-radiating edges of the patch with PIN diodes, the operating frequency can be altered. In [4], two PIN diodes are positioned in the feed line to switch between the wideband and triband modes of operation. [5] suggests an E-shaped antenna design reconfigure between six operating frequencies. The transmission line model theory is applied to compute the antenna's effective length. Two PIN diodes are employed to achieve frequency reconfiguration. Conformal antennas may be a preferable option for many practical applications. The conformal antenna's relevance in modern applications is enhanced by including reconfigurability. A flexible CPW-fed frequency agile antenna has been proposed in [6]. Switching on/off the PIN diode located in its structure changes its resonant length and offers reconfiguration between five distinct frequencies.

Pattern reconfiguration allows the antenna to direct the radiation pattern towards a specific location or direction. This can be particularly important in situations where there are multiple signal sources or when the antenna needs to track a moving target. By changing the radiation pattern, the antenna can avoid or reduce the interference caused by unwanted signal sources. Antennas loaded with parasitic elements follow the Yagi-Uda principle to realize pattern reconfiguration [7–10]. Four folded monopoles are positioned along the $+X$, $-X$, $+Y$, and $-Y$ directions, respectively. Then, the monopoles are connected to the main radiator positioned in the center via PIN diode switches. When any of the folded monopoles is connected to the main antenna, it behaves as a director, and the remaining three behave as a reflector. Using this way, the radiation pattern is deflected in four different directions [8]. Stubs loaded on the ground plane performs as a reflector or director to alter the radiation pattern par with the switching state [9]. In [11], pattern reconfiguration is accomplished by placing the switchable parasitic strip between the reflector and the monopole antenna. Pattern reconfiguration can also be accomplished through single to multiple excitations in an antenna design [12]. The radiation pattern can be continuously steered in different directions by mechanically rotating a semicircular metasurface disk over the circular patch antenna [13].

Incorporating hybrid reconfiguration capability in a single radiating structure satisfies the need for a contemporary communication system. Pattern and frequency reconfigurable antennas have a wide range of applications in wireless communication systems, radar systems, military and defense, medical imaging, and IoT applications. These antennas can provide better signal quality, coverage, and imaging resolution and adapt to changing operational conditions. In recent years, notable works have contributed towards compound reconfiguration like a combination of frequency, polarization, and pattern reconfiguration. Incorporation of pattern agility in frequency reconfigurable antennas improves the performance of wireless systems by reducing source noise, enhancing security, and conserving energy by directing the signal in the intended direction [14]. In 5G networks, there is a growing demand for pattern and frequency reconfigurable antennas (PFRA). These

antennas can provide directional radiation patterns that can be dynamically adjusted to suit the changing requirements of the network. Further, it can be designed to operate on multiple frequency bands, allowing them to switch between different frequency bands to avoid interference. Overall, designing a compact, highly efficient PFRA can offer a significant advantage in 5G networks by providing the flexibility, adaptability, and efficiency required to support the diverse range of applications and services that will be enabled by this technology. Several frequencies and pattern reconfigurable antennas are discussed in the literature. Most reconfigurable antennas use a rectangular patch as their basic structure. The impact of biasing lines in resonating frequency is inhibited by positioning them away from the antenna [15]. Four PIN diodes positioned along the two horizontal slits of a rectangular patch perform frequency reconfiguration and pattern reconfiguration [16].

The work presented in [17] utilizes four metallic strips of different lengths and four PIN diodes to perform pattern and frequency reconfiguration. Wideband operation in such antennas can be achieved by utilizing a symmetrical structure [18]. In [19], a modified rectangular patch with a single PIN diode is reported to perform frequency reconfiguration. Here, the stubs loaded on either side of the ground plane change the ground current and steer the beam direction based on the switching states. Parasitic patches and twelve PIN diodes are utilized to reconfigure the pattern and frequency presented in [20]. To perform pattern reconfiguration, a planar Yagi-Uda antenna on a coplanar structure is proposed in [21]. Two parasitic strips along with switches are loaded on the back side of the designed coplanar structure. Depending on the switching states, these parasitic strips either function as a reflector or a director. However, the majority of the reported compound reconfigurable antennas have relatively large sizes and utilize a greater number of actuators, complex biasing circuitry design, and limited operating bands.

Sub-6 GHz frequencies, which are typically in the frequency range between 600 MHz and 6 GHz, are used in 5G applications to provide large area coverage and high data rates. Band 1 (2.11–2.17 GHz), band 7 (2.62–2.69 GHz), band 46 (5.15–5.925 GHz), and band 77 (3.3–4.2 GHz) are some of the most widely used 5G new radio (NR) frequency bands. The proposed work is inspired and motivated by research challenges in the 5G network. This work focuses on the creation of a compact compound-reconfigurable antenna operating in the above-listed bands of 5G application. The following are the major contributions of this proposed work.

- (i) Design of a low-profile novel structure to reconfigure frequency and radiation pattern
- (ii) Design of biasing circuit to ensure RF and DC isolation
- (iii) Implementation of frequency reconfiguration by connecting patches of different lengths through PIN diode switches
- (iv) Pattern modification using the Yagi-Uda principle is available in the literature. In most of the works,

the pattern is changed by loading inverted L-shaped parasitic strips or dumbbell-shaped parasitic strips to the other side of the radiating element. In this work, simple parasitic strips are positioned along the radiating elements, and fewer diodes are utilized to realize pattern reconfiguration without altering the resonant frequency

The design evolution of the proposed antenna is presented in Section 2 of this research article. The findings of the simulation, measurement, and the proposed work's comparison with the existing state-of-the-art in literature are discussed in Section 3. The proposed work is concluded in Section 4.

2. Antenna Design

The proposed compound reconfigurable antenna printed on a substrate Rogers RT Duroid of dielectric constant 2.33 and thickness of 0.787 mm is depicted in Figure 1. The overall size of the presented microstrip-fed structure is $38 \times 40 \times 0.787 \text{ mm}^3$. The effective resonant lengths (L_{fr}) of the radiating elements are calculated using (1) and (2) [22].

$$L_{fr} = \frac{c}{4f_r \sqrt{\epsilon_{eff}}}, \quad (1)$$

$$\epsilon_{eff} = \frac{\epsilon_r + 1}{2} + \frac{\epsilon_r - 1}{2} \left(1 + 12 \left(\frac{w}{h} \right) \right)^{-0.5}, \quad (2)$$

where ϵ_{eff} denotes an effective dielectric constant, f_r represents resonating frequency, c indicates free space velocity, ϵ_r denotes the dielectric constant, and w and h indicate the width and thickness of the trace and the substrate, respectively.

For frequency reconfiguration, three radiating patches of different resonant lengths are designed and linked to the main radiator (P_1) through three PIN diode switches (D1, D2, and D3). Pattern reconfiguration is accomplished based on the Yagi-Uda principle. Parasitic elements are loaded on either side of the radiating elements. PIN diodes D4 and D5 are loaded along the respective parasitic elements to perform pattern reconfiguration. The proposed compound reconfigurable antenna's design evolution is shown in Figure 2.

2.1. Frequency Reconfiguration. The first step in the proposed structure's evolution is the design of the main radiator. The main radiator resonating at 5.2 GHz is achieved by modifying its effective resonant length through structural alteration. The calculated effective resonant length of the main radiating element (P_1) is optimized to 5.6 mm. Further, the partial ground plane's length (L_g) is varied and analyzed through parametric analysis as depicted in Figure 3. At $L_g = 8.2 \text{ mm}$, good impedance matching is observed for 5.2 GHz. The effective resonant length to have resonance at 3.8 GHz is calculated and optimized to 10.4 mm by connecting a patch (P_2) of length 3.1 mm to the main radiator (P_1) via PIN diode switch D1 (ON) (step 2 of Figure 2).

To provide proper biasing of the PIN diode, two RF choke inductors (to block the RF signal and pass the DC signal) and a DC block capacitor (to prevent the DC signal

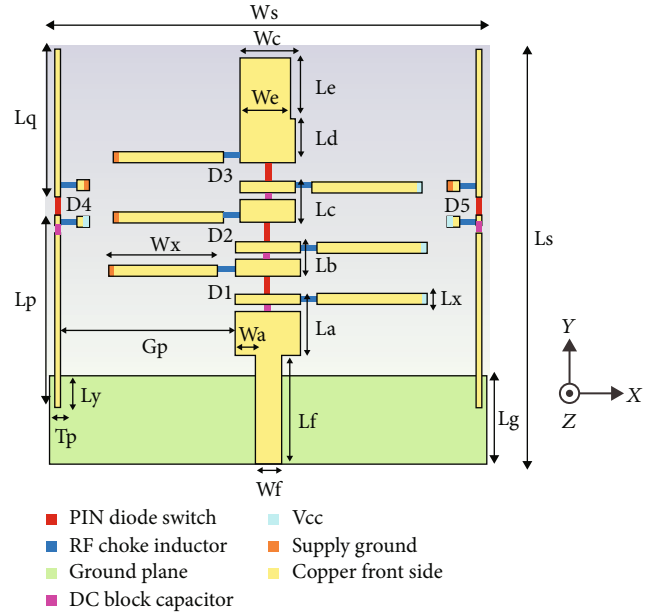


FIGURE 1: Proposed compound reconfigurable antenna - geometry (parameters: $L_s = 38 \text{ mm}$, $W_s = 40 \text{ mm}$, $L_g = 8.2 \text{ mm}$, $L_f = 10 \text{ mm}$, $W_f = 2.356 \text{ mm}$, $L_a = 5.6 \text{ mm}$, $L_b = 3.1 \text{ mm}$, $L_c = 3.85 \text{ mm}$, $L_d = 4 \text{ mm}$, $L_e = 5.5 \text{ mm}$, $W_a = 2 \text{ mm}$, $W_c = 5 \text{ mm}$, $W_e = 4.5 \text{ mm}$, $L_p = 16.6 \text{ mm}$, $L_q = 13.5 \text{ mm}$, $T_p = 0.5 \text{ mm}$, $L_x = 1 \text{ mm}$, $W_x = 10 \text{ mm}$, $G_p = 16 \text{ mm}$, $L_y = 2 \text{ mm}$, $h = 0.787 \text{ mm}$).

from interfering with the RF signal) are utilized. A slit has been made in the main radiator, and the capacitor is positioned along the slit rather than being given a separate space. To connect the RF choke inductors to the power supply, DC biasing lines/DC biasing patches have been designed and placed close to the radiating element as shown in step 3 of Figure 2. The dimensions of the DC biasing patch are chosen such that the performance of the antenna is not disrupted. Moreover, Figure 4 projects that the inclusion of biasing circuit for D1 does not have a significant impact on the proposed antenna's performance.

Switching on/off the diode D1 switches its operating frequency between 5.2 GHz and 3.8 GHz. In step 4, a patch (P_3) of a length of 3.85 mm is connected to the P_2 through D2. Switching on the diodes D1 and D2 increases the effective resonant length to 15.95 mm resulting in resonance at 2.9 GHz. To further achieve resonance at 2.1 GHz, a patch (P_4) of length 9.5 mm is connected to P_3 via D3 (on) (step 6 of Figure 2). However, the design offers dual resonance at 2.47 and 5.69 GHz. Hence, the shape of P_4 is modified to achieve the desired single resonance. Modified P_4 structure (step 7 of Figure 2) offers return loss below -10 dB at 2.17 GHz. The required biasing for D2 and D3 has been included, as specified in step 3, and it is shown in steps 5 and 8 of Figure 2.

2.2. Pattern Reconfiguration. The final step in the proposed design is aimed at pattern reconfiguration. Parasitic elements can be used for pattern reconfiguration by adjusting the length, distance, and orientation of the parasitic element relative to the main antenna element. This will change the phase and amplitude of the signal at different points in the

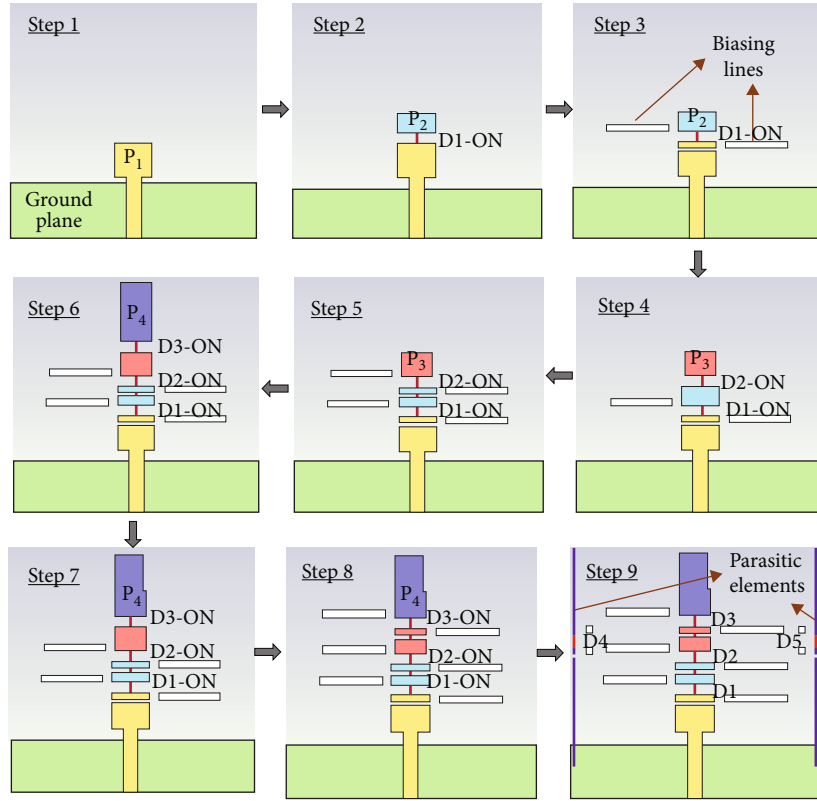


FIGURE 2: Proposed structure—design evolution.

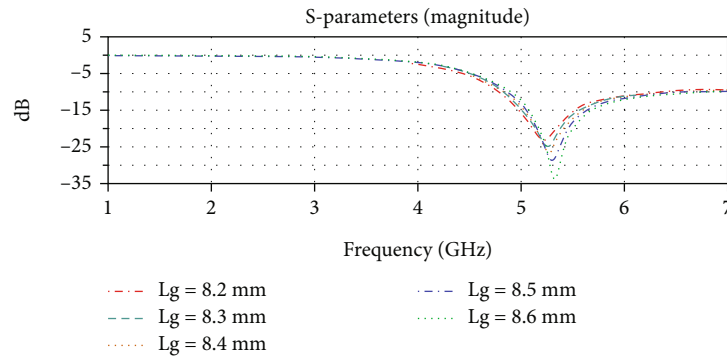
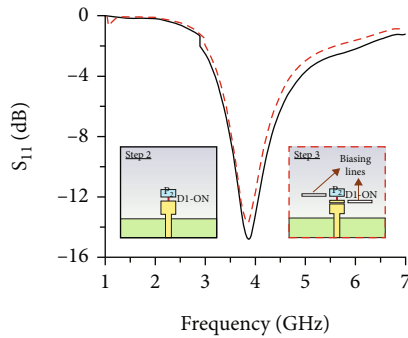
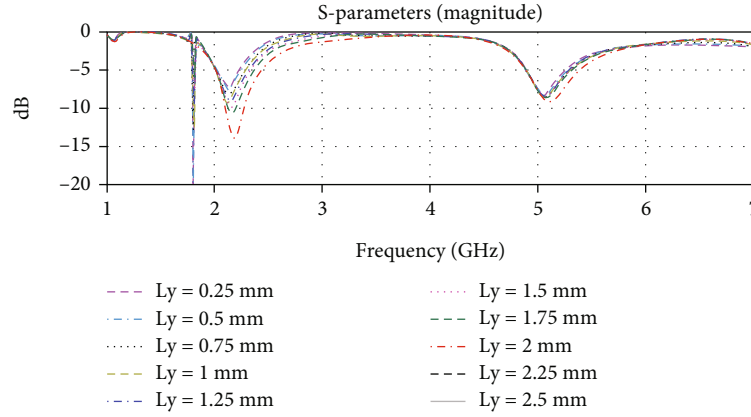
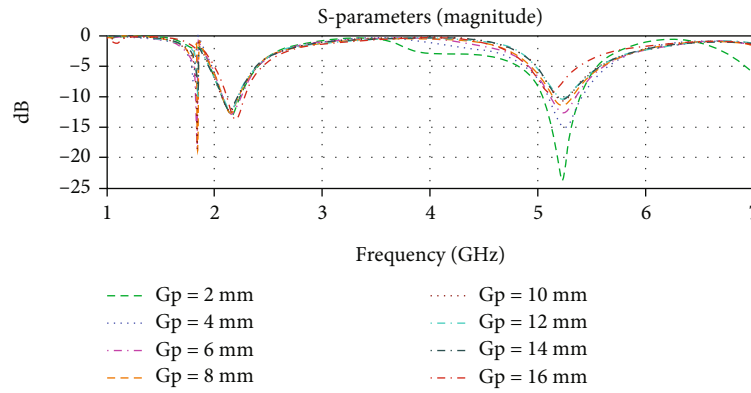
FIGURE 3: Parametric analysis—length of the ground plane (L_g).

FIGURE 4: Design evolution—return loss plot: step 2 (without biasing circuit) and step 3 (with the biasing circuit).

antenna, which will in turn change the radiation pattern. Two parallel parasitic elements of width 0.5 mm and length 31.8 mm are loaded to the sides of the designed antenna. These elements act as a reflector/director, and two PIN diode switches (D4 and D5) are positioned along the length of the two parasitic elements to facilitate pattern reconfiguration. Henceforth, the proposed structure can reconfigure frequency and pattern as well.

The radiation property is significantly impacted by the coupling length (L_y) between the parasitic element and the ground plane. The coupling length and the distance between the main radiator and parasitic elements (G_p) are obtained by performing a parametric sweep. Figures 5 and 6 present the parametric analysis of L_y and G_p , respectively. The

FIGURE 5: Parametric analysis of L_y .FIGURE 6: Parametric analysis—effect of varying the distance between the radiator and parasitic elements (G_p).

designed antenna is analyzed for $L_y = 0.25$ mm to 2.5 mm and $G_p = 2$ mm to 16 mm in case I-S4. The simulation reveals that the additional resonance is observed at 1.8 GHz in the simulated range excluding the value of $L_y = 2$ mm. At $L_y = 2$ mm, the additional resonance is nullified, and the resonance is observed at the intended resonating frequency of 2.17 GHz. At $G_p = 16$ mm, only the intended resonance is observed. Hence, the coupling length and the space between the radiating and parasitic elements are finalized as 2 mm and 16 mm, respectively.

To perform the switching operation, the SMP1345-079 LF PIN diode is used. It offers high-speed switching and is suitable for switch applications from 10 MHz to 6 GHz. The on state equivalent circuit of this diode is achieved by connecting $R = 1.5 \Omega$ in series with $L = 0.7$ nH. The off state equivalent circuit of this diode is achieved by connecting the parallel combination of $R = 1000 \Omega$ and $C = 0.18$ pF in series with $L = 0.7$ nH. Since the design involves PIN diodes for switching operation, a biasing circuit has been designed for proper excitation of the switches. The space for placement of PIN diode switches, capacitors, and inductors is decided as per data sheets.

3. Results and Discussion

The proposed antenna is analyzed for three cases. In case I, both D4 and D5 are in the OFF state. D4 is off and D5 is

on for case II. D4 is on, and D5 is off in case III. Each of the cases is analyzed for four switching states: switching state 1 (S1)—(D1-off, D2-off, and D3-off), switching state 2 (S2)—(D1-on, D2-off, and D3-off), switching state 3 (S3)—(D1-on, D2-on, and D3-off), and switching state 4 (S4)—(D1-on, D2-on, and D3-on). Frequency and pattern reconfigurability are observed through the comparative analysis of case II and case III concerning case I.

3.1. Case I: Frequency Reconfigurability Mode. In case I, the switching state 1 exhibits resonance at 5.2 GHz (4.71–5.84 GHz). Switching on D1 (case I-S2) connects P_1 and P_2 . This lengthens the current distribution and shifts the resonating frequency to 3.8 GHz (3.44–4.17 GHz). Case I-S3 mode increases the length further by turning ON D2. In this mode, the proposed antenna resonates at 2.9 GHz (2.61–3.13 GHz). In case I-S4 mode, resonance is observed at 2.17 GHz (2.08–2.27 GHz).

3.2. Cases II and III: Frequency and Pattern Reconfigurability Mode. Frequency and pattern reconfigurability are seen in cases II and III. The switching states S1, S2, S3, and S4 are analyzed for the abovementioned cases. The observed resonant frequencies for case II and case III's S1 are like the case I-S1 (5.2 GHz). In case I-S1, the main beam direction in the x - z plane is along -97° . Now, in case II-S1, switching off D4 makes the left parasitic element ($-x$ direction) behave as a

director, and switching on D5 makes the right parasitic element (+ x direction) behave as a reflector. As a result, the main lobe direction is changed to -164° ($-x$ direction). Whereas in case III-S1, switching on and off the D4 and D5 makes the left parasitic element ($-x$ direction) function as a reflector and the right parasitic element (+ x direction) as a director, respectively. This shifts the main lobe direction to $+164^\circ$ (+ x direction). Hence, the radiation pattern of the designed antenna is reconfigurable.

Similarly, frequency and pattern reconfiguration are observed for all the remaining switching states of case II and case III. In case II, the main lobe direction in the x - z plane ($\phi = 0^\circ$) is -90° at 3.8 GHz, -100° at 2.9 GHz, and 2.17 GHz. Whereas $+90^\circ$, $+100^\circ$, and $+100^\circ$ are observed for case III at 3.8 GHz, 2.9 GHz, and 2.17 GHz, respectively. This implies that the switching state of D4 and D5 switches the radiation pattern without altering the resonating frequencies of the radiating structure.

The proposed antenna is fabricated, and its measurement setup is depicted in Figure 7. The front and back views of the fabricated antenna are shown in Figures 7(a) and 7(b). The vector network analyzer (VNA) measurement setup for return loss measurement is seen in Figure 7(c). It is noted that the biasing lines are connected to the power supply for switching on/off the PIN diodes. Gain and pattern measurements are done using anechoic chamber measurement as depicted in Figure 7(d).

The measured results of all three cases are summarized in Figure 8 and are discussed as follows. Figure 9(a) presents an S_{11} comparison of the simulated and measured results for case I, whereas Figure 9(b) projects an S_{11} comparison of the simulated and measured results for case II and case III. Depending on the states of D1-D3, the design reconfigures to 5.3 GHz, 3.82 GHz, 2.77 GHz, and 2.2 GHz. When comparing the measured results with the simulation findings, slight variations in the resonant frequencies are observed due to the presence of biasing wires in the measurement setup. In case I, the bandwidths obtained at 5.3 GHz, 3.82 GHz, 2.77 GHz, and 2.2 GHz are 1225 MHz (5–6.225 GHz), 300 MHz (3.67–3.97 GHz), 900 MHz (2.625–3.525 GHz), and 335 MHz (2.09–2.425 GHz), respectively. In both case II and case III, 850 MHz (5–5.85 GHz), 425 MHz (3.675–4.1 GHz), 545 MHz (2.625–3.17 GHz), and 321 MHz (2.09–2.411 GHz) are the bandwidths obtained at 5.3 GHz, 3.82 GHz, 2.77 GHz, and 2.2 GHz, respectively. Figure 9(c) projects the average gain and efficiency of the proposed antenna. The average measured gain of 2.43 dBi, 2.42 dBi, 3.5 dBi, and 3.29 dBi is observed at 5.3 GHz, 3.82 GHz, 2.77 GHz, and 2.2 GHz, respectively. On average, a radiation efficiency of around 81% is obtained for the simulated antenna design. Further, the functionality of the proposed design is analyzed w.r.t their radiation pattern and surface current distribution.

In Figure 10, the simulated radiation pattern (black dotted line) in the x - z plane ($\phi = 0^\circ$) is compared with the measured radiation pattern (red solid line). The red solid arrow mark in all the switching cases indicates the main lobe's direction. The patterns in Figure 10 are used to identify the directionality and the direction of the main lobe

under different switching conditions. Changing the states of D4 and D5 reconfigures the radiation pattern from bidirectional to unidirectional at 5.3 GHz and omnidirectional to unidirectional at 3.82 GHz, 2.77 GHz, and 2.2 GHz. In case I-S1, the direction of the main lobe is -97° . It is tilted to -165° and $+165^\circ$ in case II-S1 and case III-S1, respectively. Henceforth, at 5.3 GHz, the beam steering angles are -68° and $+262^\circ$. In case I-S2, the main lobe direction is $+115^\circ$. This direction is changed to -93° and $+93^\circ$ in case II-S2 and case III-S2, respectively. The observed beam steering angles at 3.82 GHz are $+152^\circ$ and -22° .

The main lobe oriented towards $+180^\circ$ in case I-S3 has been shifted to -105° in case II-S3 and $+105^\circ$ in case III of S3. Hence, the beam steering angles of $\pm 75^\circ$ are obtained at 2.77 GHz. The same has been observed for switching state 4, and the corresponding beam steering angles at 2.2 GHz are $\pm 75^\circ$. In frequency and pattern reconfiguration, reconfiguring the frequency should not affect the radiation pattern and vice versa. It is observed that the beam steering angles at 2.77 GHz and 2.2 GHz remain the same. However, it differs at 5.3 GHz and 3.82 GHz. The presence of bias lines will have an impact on the antenna's radiation pattern. This will occur due to the coupling between bias lines and the radiating elements. To minimize this impact, the placement and orientation of bias lines are done carefully within the antenna structure. However, distortion in the pattern reduced realized gain, and shift in the resonant frequencies is seen in the measured results. Creating vias in the required biasing positions will make the bias lines move to the other side of the radiating elements. This technique can be used in future work to lessen the effects of bias lines.

Figure 11 illustrates the surface current distribution. According to the switching condition, a high surface current distribution is seen at the radiating structures. It is observed that the high current distribution in the main radiator and the feed line for all three cases in switching state 1 offers resonance at 5.2 GHz. In addition to that, during all the three cases, a high current density noted in the P_2 (during switching state 2), P_3 (during switching state 3), and P_4 (during switching state 4) contributed to resonance at 3.8 GHz, 2.9 GHz, and 2.17 GHz, respectively. Further, for all the switching states in case I, the current density is minimal in the parasitic elements.

The surface current on the reflector may be relatively low compared to other elements in the antenna. This is because the reflector's primary function is to reflect and redirect energy from the radiating element, rather than directly radiating energy itself. The director in the antenna is used to focus the energy on a particular direction. Hence, the surface current on the directors is typically higher than the surface current on the reflector or driven element. In case II, the high surface current is noted along the left parasitic element, and the low surface current is observed along the right parasitic element for all the switching states. Hence, the left parasitic element acts as a director and the right parasitic element acts as a reflector in all the switching states of case II, whereas the vice versa is observed for all the switching states in case III.

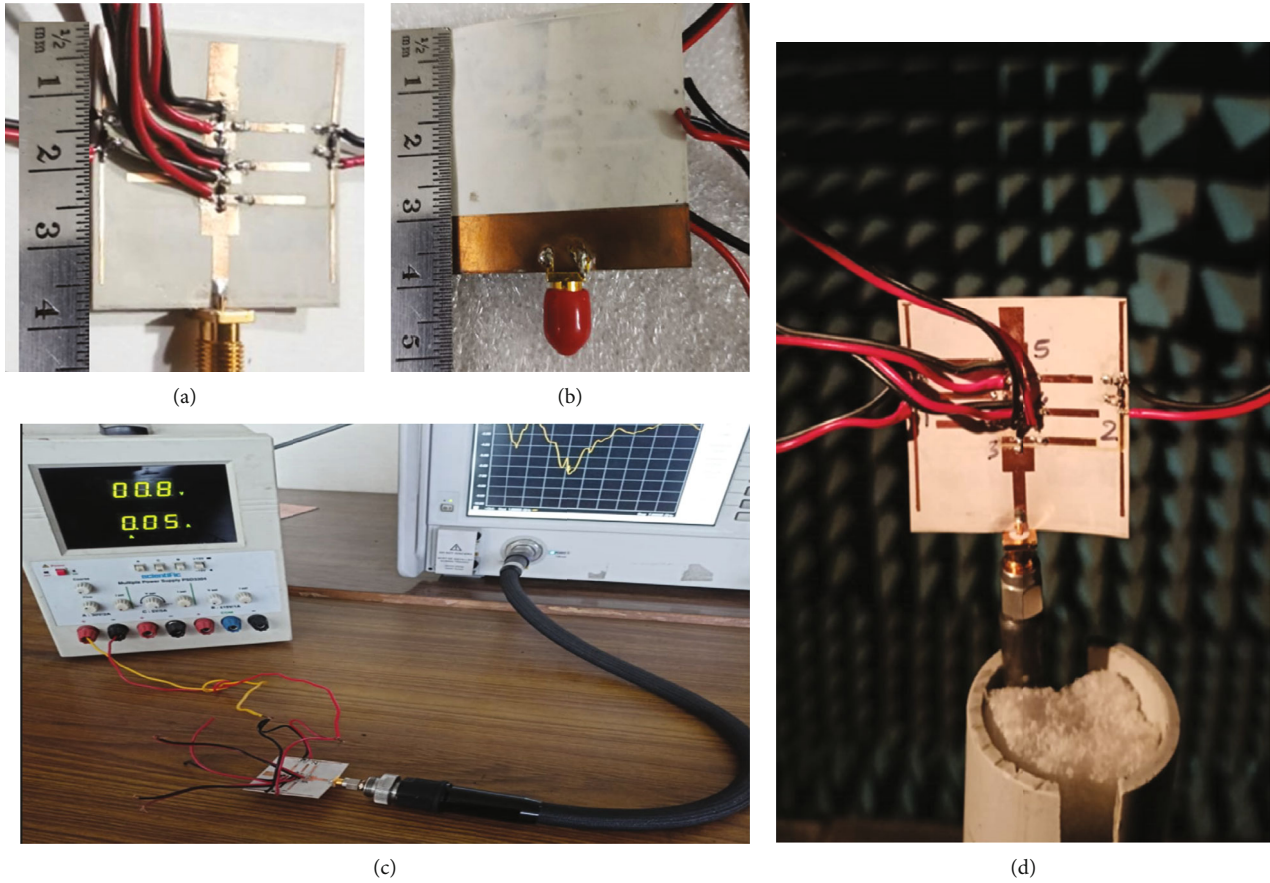


FIGURE 7: Measurement setup of fabricated antenna. (a) Top view, (b) rear view, (c) VNA testing, and (d) anechoic chamber measurement.

	Switching condition					Frequency (GHz)	S_{11} (dB)	Gain (dBi)	Bandwidth (MHz)	Main Lobe Direction ($\phi = 0^\circ$)	Beam Steering Angle
	D1	D2	D3	D4	D5						
Case I - S1	OFF	OFF	OFF	OFF	OFF	5.3	-15.56	2.24	1225	-97°	0°
Case I - S2	ON	OFF	OFF	OFF	OFF	3.82	-12.18	2.38	300	+115°	0°
Case I - S3	ON	ON	OFF	OFF	OFF	2.77	-19.38	3.72	900	+180°	0°
Case I - S4	ON	ON	ON	OFF	OFF	2.2	-12.11	3.19	335	+180°	0°
Case II - S1	OFF	OFF	OFF	OFF	ON	5.3	-15.8	2.58	850	-165°	-68°
Case III - S1	OFF	OFF	OFF	ON	OFF	5.3	-15.8	2.48	850	+165°	+262°
Case II - S2	ON	OFF	OFF	OFF	ON	3.82	-13.22	2.45	425	-93°	+152°
Case III - S2	ON	OFF	OFF	ON	OFF	3.82	-13.21	2.42	425	+93°	-22°
Case II - S3	ON	ON	OFF	OFF	ON	2.77	-19.09	3.35	545	-105°	+75°
Case III - S3	ON	ON	OFF	ON	OFF	2.77	-19.07	3.33	545	+105°	-75°
Case II - S4	ON	ON	ON	OFF	ON	2.2	-12.09	3.34	321	-105°	+75°
Case III - S4	ON	ON	ON	ON	OFF	2.2	-12.12	3.35	321	+105°	-75°

----- Switching conditions responsible for only frequency reconfiguration
----- Switching conditions responsible for only pattern reconfiguration

FIGURE 8: Measured results of proposed compound reconfigurable antenna.

The performance comparison summarized in Table 1 reveals that the presented work offers a low-profile, compact structure on comparing with [1, 16, 18, 20, 23, 24, 26–28]. The presented work requires fewer switches than [25, 28].

Using five switches, the suggested work operates at more operating bands than [1, 29]. This work has reduced design complexity by eliminating the separate layer for the biasing circuit as in [19, 20, 22].

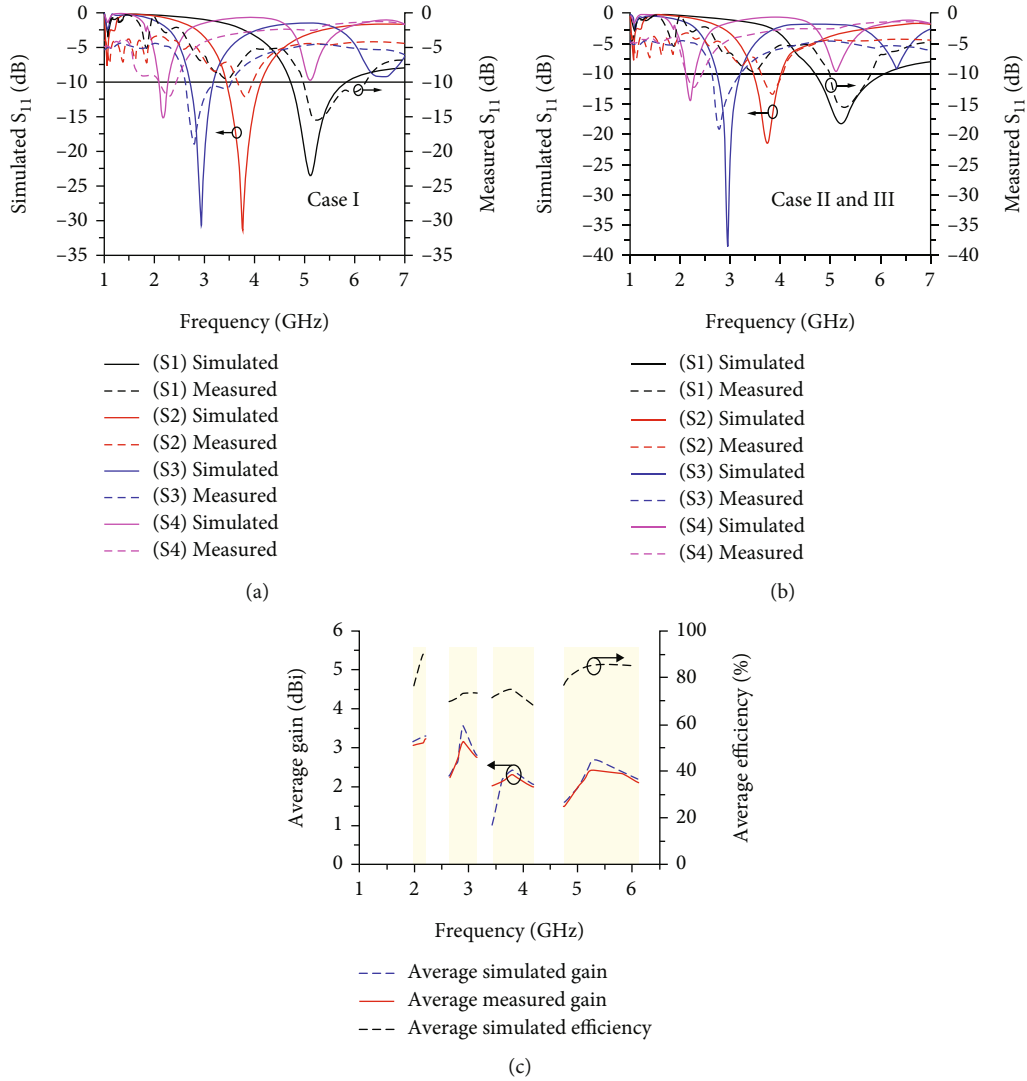
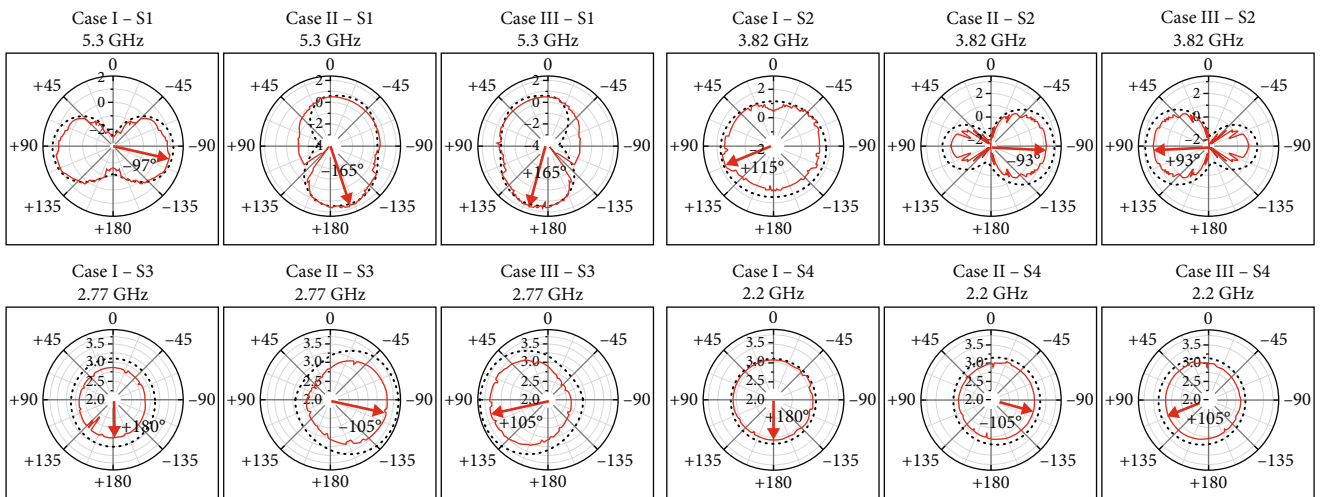


FIGURE 9: Results: (a) case I—return loss, (b) cases II and III—return loss, and (c) gain and efficiency.

FIGURE 10: Radiation pattern ($\phi = 0^\circ$) (x - z plane) (simulated result—black dotted line, measured result—red solid line).

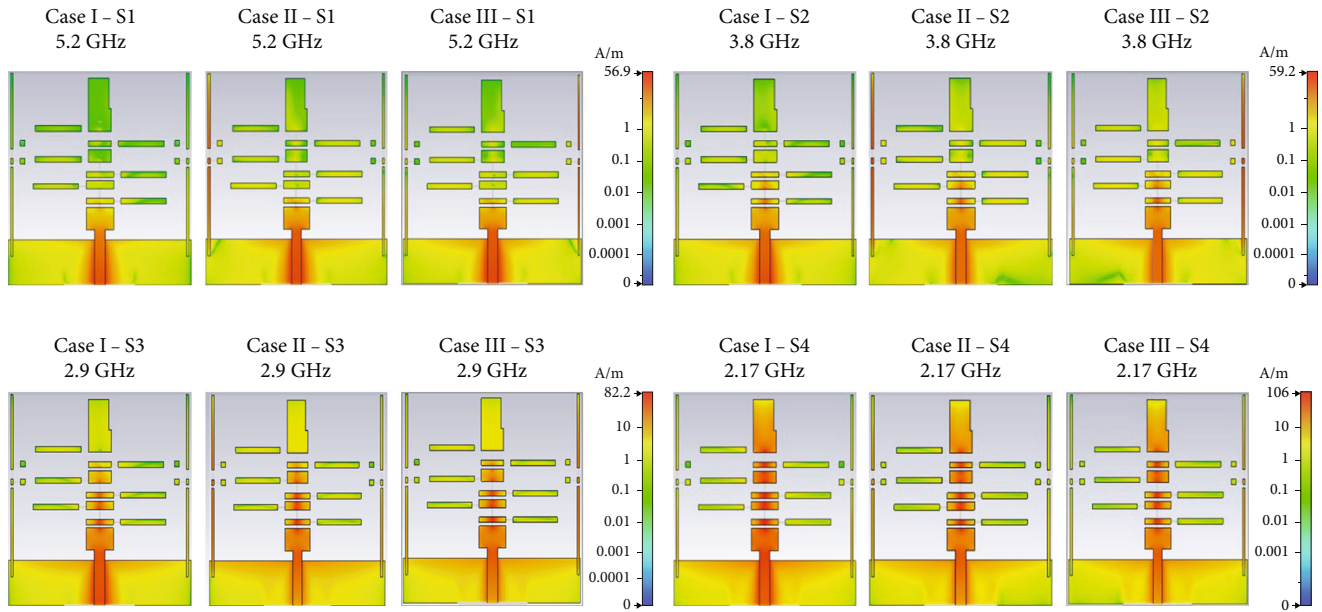


FIGURE 11: Simulated result—surface current distribution.

TABLE 1: Proposed work vs. existing frequency and pattern reconfigurable antennas.

Ref. no.	Dimension ($L \times W \times h$) (mm ³)	No. of switches/means of switching	Maximum number of beams	No. of frequency bands	Peak gain (dBi)
[1]	$47 \times 80 \times 1.5$	5/PIN	2	2	2.7/2.6
[16]	$50 \times 50 \times 1.6$	4/PIN	3	4	4/3.8/4.4/5
[18]	$40 \times 30 \times 1.6$	4/PIN	3	2	2.45/2.76
[20]	$46 \times 32 \times 1.6$	12/PIN	5	5	1.25/2.80/2.90/3.64/4.67
[23]	70×70	4/PIN	3	2	6.214/8.461
[24]	$50 \times 100 \times 1.6$	2/PIN	2	2	4.9/5.5
[25]	$42 \times 44 \times 0.127$	8/PIN	2	2	—
[26]	$66.4 \times 66.4 \times 1.5$	3/RF MEMS	2	4	—
[27]	$120 \times 120 \times 7.362$	-/PIN	3	2	8-9 dB/6-10.31 dB
[28]	$112 \times 52 \times 0.508$	18/NMOS transistors	8	2	3.8/8.3
[29]	—	8/PIN	4	2	5.63/5.55
This work	$38 \times 40 \times 0.787$	5/PIN	3	4	2.43/2.42/3.5/3.29

4. Conclusion

A compact antenna that can reconfigure quadband and radiation pattern is reported in this article. The proposed antenna can reconfigure to 5.3 GHz, 3.82 GHz, 2.77 GHz, and 2.2 GHz. At each operating frequency, the antenna can steer its main lobe into three different directions. In all the resonating frequencies, acceptable gains are realized. The presented design reduces structural complexity by utilizing fewer diodes and simple biasing circuits. The antenna performs well with an average efficiency of 85%, 75%, 73%, and 91% at 5.3 GHz, 3.82 GHz, 2.77 GHz, and 2.2 GHz, respectively. The proposed antenna covers band 1, band 7, band 46, and band 77 of the 5G new radio (NR) standard.

These bands are some of the most widely used 5G NR frequency bands. Hence, the proposed antenna is suitable for 5G applications in the sub-6 GHz frequency range.

Data Availability

The data used to support the findings of this study are included within the article.

Conflicts of Interest

The authors declare that they have no conflicts of interest.

Authors' Contributions

K. Karthika and K. Kavitha contributed to the conceptualization, methodology, results, and discussion.

References

- [1] P. K. Li, Z. H. Shao, Q. Wang, and Y. J. Cheng, "Frequency- and pattern-reconfigurable antenna for multistandard wireless applications," *IEEE Antennas and Wireless Propagation Letters*, vol. 14, pp. 333–336, 2015.
- [2] K. Karthika and K. Kavitha, "Reconfigurable antennas for advanced wireless communications: a review," *Wireless Personal Communications*, vol. 120, no. 4, pp. 2711–2771, 2021.
- [3] A. Boukarkar, X. Q. Lin, Y. Jiang, and X. F. Yang, "A compact frequency-reconfigurable 36-states patch antenna for wireless applications," *IEEE Antennas and Wireless Propagation Letters*, vol. 17, no. 7, pp. 1349–1353, 2018.
- [4] S. Sharma and C. C. Tripathi, "Wideband to concurrent tri-band frequency reconfigurable microstrip patch antenna for wireless communication," *International Journal of Microwave and Wireless Technologies*, vol. 9, no. 4, pp. 915–922, 2017.
- [5] S. Ullah, S. Ahmad, B. A. Khan, U. Ali, F. A. Tahir, and S. Bashir, "Design and analysis of a hexa-band frequency reconfigurable monopole antenna," *IETE Journal of Research*, vol. 64, no. 1, pp. 59–66, 2018.
- [6] A. Ahmad, F. Arshad, S. I. Naqvi, Y. Amin, H. Tenhunen, and J. Loo, "Flexible and compact spiral-shaped frequency reconfigurable antenna for wireless applications," *IETE Journal of Research*, vol. 66, no. 1, pp. 22–29, 2020.
- [7] Z. Shi, R. Zheng, J. Ding, and C. Guo, "A novel pattern-reconfigurable antenna using switched printed elements," *IEEE Antennas and Wireless Propagation Letters*, vol. 11, pp. 1100–1103, 2012.
- [8] G. Jin, M. Li, D. Liu, and G. Zeng, "A simple four-beam reconfigurable antenna based on monopole," *IEEE Access*, vol. 6, pp. 30309–30316, 2018.
- [9] T. Aboufoul, S. Member, C. Parini, X. Chen, S. Member, and A. Alomainy, "Pattern-reconfigurable planar circular ultra-wideband monopole antenna," *IEEE Transactions on Antennas and Propagation*, vol. 61, no. 10, pp. 4973–4980, 2013.
- [10] M. Jusoh, T. Aboufoul, T. Sabapathy, A. Alomainy, and M. R. Kamarudin, "Pattern-reconfigurable microstrip patch antenna with multidirectional beam for WiMAX application," *IEEE Antennas and Wireless Propagation Letters*, vol. 13, pp. 860–863, 2014.
- [11] Y. Juan, W. Che, W. Yang, and Z. N. Chen, "Compact pattern-reconfigurable monopole antenna using parasitic strips," *IEEE Antennas and Wireless Propagation Letters*, vol. 16, pp. 557–560, 2017.
- [12] B. Ashvanth, B. Partibane, M. G. N. Alsath, and R. Kalidoss, "Gain enhanced multipattern reconfigurable antenna for vehicular communications," *International Journal of RF and Microwave Computer-Aided Engineering*, vol. 30, no. 6, 2020.
- [13] M. S. Alam and A. Abbosh, "Planar pattern reconfigurable antenna with eight switchable beams for WiMax and WLAN applications," *IET Microwaves, Antennas and Propagation*, vol. 10, no. 10, pp. 1030–1035, 2016.
- [14] H. A. Majid, M. K. A. Rahim, M. R. Hamid, and M. F. Ismail, "Frequency and pattern reconfigurable slot antenna," *IEEE Transactions on Antennas and Propagation*, vol. 62, no. 10, pp. 5339–5343, 2014.
- [15] A. A. Palsokar and S. L. Lahudkar, "Frequency and pattern reconfigurable rectangular patch antenna using single PIN diode," *AEU-International Journal of Electronics and Communications*, vol. 125, article 153370, 2020.
- [16] Y. P. Selvam, M. Kanagasabai, M. G. N. Alsath et al., "A low-profile frequency- and pattern-reconfigurable antenna," *IEEE Antennas and Wireless Propagation Letters*, vol. 16, pp. 3047–3050, 2017.
- [17] P. Thanki and F. Raval, "Fork-shaped frequency and pattern reconfigurable antenna," *International Journal of Communication Systems*, vol. 33, no. 17, article e4613, 2020.
- [18] L. Han, C. Wang, W. Zhang, R. Ma, and Q. Zeng, "Design of frequency- and pattern-reconfigurable wideband slot antenna," *International Journal of Antennas and Propagation*, vol. 2018, Article ID 3678018, 7 pages, 2018.
- [19] A. Iqbal, A. Smida, N. Mallat et al., "Frequency and pattern reconfigurable antenna for emerging wireless communication systems," *Electronics*, vol. 8, no. 4, p. 407, 2019.
- [20] I. Ahmad, W. U. R. Khan, H. Dildar et al., "A pentaband compound reconfigurable antenna for 5G and multi-standard sub-6GHz wireless applications," *Electronics*, vol. 10, no. 20, p. 2526, 2021.
- [21] S. Raman, N. Timmons, and J. Morrison, "Gain enhanced pattern reconfigurable planar Yagi-Uda antenna on coplanar structure," *Electronics Letters*, vol. 49, no. 25, pp. 1593–1595, 2013.
- [22] I. Ahmad, H. Dildar, W. U. R. Khan et al., "Design and experimental analysis of multiband compound reconfigurable 5G antenna for Sub-6 GHz wireless applications," *Wireless Communications and Mobile Computing*, vol. 2021, Article ID 5588105, 14 pages, 2021.
- [23] R. Dewan, M. K. A. Rahim, M. R. Hamid, M. Himdi, H. A. Majid, and N. A. Samsuri, "HIS-EBG unit cells for pattern and frequency reconfigurable dual band array antenna," *Progress in Electromagnetics Research*, vol. 76, pp. 123–132, 2018.
- [24] M. S. Khan, A. Iftikhar, A. D. Capobianco, R. M. Shubair, and B. Ijaz, "Pattern and frequency reconfiguration of patch antenna using PIN diodes," *Microwave and Optical Technology Letters*, vol. 59, no. 9, pp. 2180–2185, 2017.
- [25] Z. Zhu, P. Wang, S. You, and P. Gao, "A flexible frequency and pattern reconfigurable antenna for wireless systems," *Progress in Electromagnetics Research*, vol. 76, pp. 63–70, 2018.
- [26] S. K. Patel, C. Argyropoulos, and Y. P. Kosta, "Pattern controlled and frequency tunable microstrip antenna loaded with multiple split ring resonators," *IET Microwaves, Antennas and Propagation*, vol. 12, no. 3, pp. 390–394, 2018.
- [27] A. X. Chen and X. Liu, "The high gain frequency-and radiation pattern-reconfigurable antenna based on meta-surface," in *Progress in electromagnetics research symposium-Fall (PIERS-FALL)*, pp. 565–569, Singapore, 2017.
- [28] M. K. Shereen, M. I. Khattak, and M. Al-Hasan, "A frequency and radiation pattern combo-reconfigurable novel antenna for 5G applications and beyond," *Electronics*, vol. 9, no. 9, p. 1372, 2020.
- [29] K. Saurav, D. Sarkar, and K. V. Srivastava, "A dual-band reconfigurable Yagi-Uda antenna with diverse radiation patterns," *Applied Physics A: Materials Science & Processing*, vol. 123, no. 7, pp. 1–8, 2017.

Deep Learning Framework for Identification of Leaf Diseases in Native Plants of Tamil Nadu Geographical Region

Dr. K. Kavitha,

Department of Electronics and Communication Engineering
Velammal College of Engineering and Technology

(Autonomous)

Madurai, India

email_id: kavi@vcet.ac.in

S. Naveena,

Department of Electronics and Communication Engineering
Velammal College of Engineering and Technology

(Autonomous)

Madurai, India

email_id: naveenasundaramurthi@gmail.com

Abstract—Plant pathogens are a prominent cause of reduced yields, resulting in decreased crop yields. Scientists are striving to develop a mechanism for identifying plant ailments in order to boost farm output. Deep learning algorithms have been developed for pathogen recognition and prediction in tomato plant leaves. Two different types of diseases impact both healthy and sick leaves. A Convolution Neural Network, which is effective for detection and prediction barrier, was used to forecast Septoria spot and bacterial spot. A dataset of 4930 images of healthy and damaged leaves from a plant community is used for the experiments. The model's performance is precisely evaluated, and the conclusion is accurate. The project makes use of Plant Village images of tomato, potato, and onion leaves. Four different classes can each be recognized by the suggested CNNs. In each instance, the trained model achieves accuracy of 100%, 98.3%, and 97.89%. The classification of leaf disease detection using simulation data shows the potential effectiveness of the proposed approach. The algorithm proposed can be applied to categories any additional species of native plant to Tamil Nadu. Self Help Groups (SHGs), which are found in each and every village in India, will be utilized to gather information on how farmers see themselves. The observations and ameliorate both will be communicated to the same SHGs. Because of its high success rate, the model is a good tool for counselling or early warning.

Keywords—Image processing, Convolution Neural Network, self Help Group, plant leaves, plant diseases.

I. INTRODUCTION

Images are the most widely used and practical method of communicating or sharing information. An image is said to represent a variety of phrases. Pictures provide unequivocal and unambiguous insights regarding object positioning, configurations, and interconnectedness. They represent information that we identify as items in geographical data. Because of our innate visual processing capabilities, humans are adept with extracting the information from such image data. Approximately 75% of the information that the human brain gets is in the form of visuals. To maintain rice plant productivity, it is essential to recognize indications of diseases in plants brought on by bacteria, nematodes, fungi, phytoplasma, and viruses[1-4]. The lack of plant pathologists in many regions of India, however, is really a serious issue. The vast plantation area presents additional difficulties due to logistical difficulties when

reaching these locations, making it challenging to obtain pathogen indication. In the Solanaceae family, potatoes are perennial herbaceous plants that are grown for their delectable tubers. A branching stem and alternately positioned leaflets of various sizes and structures define the potato plant. The leaves might be round or oblong and 10-30 cm (4-12 in) long and 5-15 cm (2-6 in) broad. The potato plant produces yellow-green fruit and white or blue blooms. Potato tubers are found in the top 25 cm of the soil, where they grow underground. Depending on the cultivar, the tubers may be red, yellow, or purple in color. Potato plants can grow to be more than 1 m (3.3 ft) tall and are planted as annuals with only one growth season. A Liliaceae herbaceous biennial prized for its delectable bulb is Allium cape. The pseudo stem of the plant is made up of tubular leaves that cross over their sheaths, and its base is a flattened disc. Each plant contains 3–8 erect or oblique leaves. The onion plant's tendrils resist clusters of pink or white flowers. Overlapping leaves that develop just above the plant's flattened stem are what make up the bulbs. The bulb has numerous layers, each of which corresponds to a leaf. They grow in clusters of 3-18 per plant and are normally oval in shape, but this can vary. A membrane that eventually transforms into a paper coat covers the bulb in order to protect it. Onion plants [2] grow to a height of 50 cm (20 in) and are harvested after one season. Onion cultivars include shallots, spring onions (sometimes called scallions), red and purple onions, and shallots.

II. PROPOSED METHODOLOGY

In order to identify plant leaf disease in real-time, this research uses the most recent deep learning technique[3], which is based on deep convolutional neural networks[4]. The dataset for plant leaf infection was developed to give a strong assurance of the suggested model's heuristic range, and the primary contributions of this study are outlined as follows. First, sick photos with uniform backgrounds for complex backgrounds are gathered both in the lab and in the field in order to increase the resilience of the CNN model[5]. Furthermore, to address the issue of inadequate malignant leaf images and avoid overfitting of the CNN-based model during the training process [6,] natural diseased images are processed to provide sufficient training images by data augmentation development. For the real-time detection of leaf disease, a deep convolutional neural network is used. The suggested deep-learning [7] based approach can

precisely recognise the distinguishing characteristics of the diseased tomato photos [8] and identify the five main leaf disease types. Simultaneously, the suggested technique can detect not only multiple diseases inside the same diseased image, but also the identical ailment in various shapes and sizes. Additionally, the suggested method is capable of handling all sick photos that were captured in actual field settings.

A. Dataset

Images from the Plant Village dataset, an available to the public collection containing approximately 895 images separated into seven kinds, were used to demonstrate the concept. The dataset contains images of native plant leaf diseases that can be detrimental to the crop. Two collections of damaged pictures were used in the suggested work: the bacterium spot and the septoria spot. A portion of Plant Village's library, which contains 4930 images of Native plants suffering from two diseases, was used as the database for the study. The dataset is separated into two parts: training and testing, with an 80:20 split. Each image that was downloaded was saved in the RGB colour space and in the uncompressed JPG file format.

B. Preprocessing

The acquired dataset only contained photos with minimum noise, noise removal was not required as a pre-processing step. To speed up the training process and make model training 36 computationally possible, the photos in the dataset were reduced to 60 resolutions. Standardizing the input or target variables has the effect of speeding up the training process. This is accomplished by improving the optimization problem's numerical condition. It's also double-checked that the various default settings used in start-up and termination are correct.

1) *Resize Image*: Image resizing is necessary when you need to increase or decrease the total number of pixels, whereas remapping can occur when you are correcting for rotating a picture. Resizing or distorting a picture from a one-pixel grid to another results in image interpolation. Resize a silhouette to enhance or massively reduce the pixel intensity, whereas remap it to compensate for lens distortion or rotate it., whereas you'll need to remap it if you're compensating for lens distortion or rotating it. The number of pixels in an image rises as you zoom in, allowing you to see more detail.

2) *Convert Image to Image Array*: Numeric Python is a widely used library for manipulating arrays. Because images are simply a collection of pixels with different color codes. An array can be converted to an image using NumPy. To edit and store arrays, we will use PIL, or Python Image Library, better known as Pillow, in addition to NumPy.

3) *Convert Image to Gray Scale*: A grayscale (or gray level) image is one in which the only colors used are grayscale. The reason that these images differ from any other type of color image is that each pixel requires less information. In actuality, a 'gray' color is one in which the red, green, and blue components are all of equal intensity in RGB space, requiring just a single intensity value for each pixel, as opposed to the three intensities required for a full-color picture. The grayscale intensity is frequently stored as an 8-bit integer, resulting in 256 different shades of grey ranging from black to white[21]. The

difference between successive grey levels is substantially better than the human eye's grey level resolving power if the levels are regularly spaced.

C. Feature Extraction

The CCM method [9] [10] is used to extract the feature set. It's a strategy for obtaining distinguishing features that represent a picture, considering both the texture and color of the image. There are three primary mathematical procedures in the CCM technique. First, the RGB color space leaf images are converted to HSI color space representation. After the process is done, each pixel map is used to generate a color co-occurrence matrix, resulting in three CCM matrices, one for each of the H, S, and I pixel maps. Furthermore, because it supports human color observation, HSI (Hue Saturation Intensity) space is a popular color space. Because the human sensory system is sensitive to electromagnetic waves with wavelengths spanning from 400 to 700 nanometers, they are referred to be visible light.

D. Image Segmentation

It is the technique of segmenting [11] [12] a digital image into several segments (pixel sets). The goal of segmentation is to make an image more intelligible and easier to examine by simplifying and/or changing its representation. Boundaries and objects (lines, curves, etc.) in images are often located via image segmentation. Image segmentation, to put it another way, is the process of giving a label to each pixel in an image so that pixels with the same label have similar visual properties. A set of segments that collectively encompass the full image, or a set of contours taken from the image, is the result of image segmentation (see edge detection). In terms of some characteristic or computed feature, such as color, intensity, or texture, each pixel in a region is comparable. When it comes to the same traits, adjacent regions differ greatly.

E. Classification & Detection of Diseases

In the end, classifiers are employed to train and test the datasets. Convolutional neural networks [13] [14] are a type of deep neural network that aids in disease diagnosis by assisting in the recognition, categorization, and size and color detection of leaves on the plant. These techniques are used to identify and classify leaf diseases. The block diagram of disease classification, as shown in Fig.1,

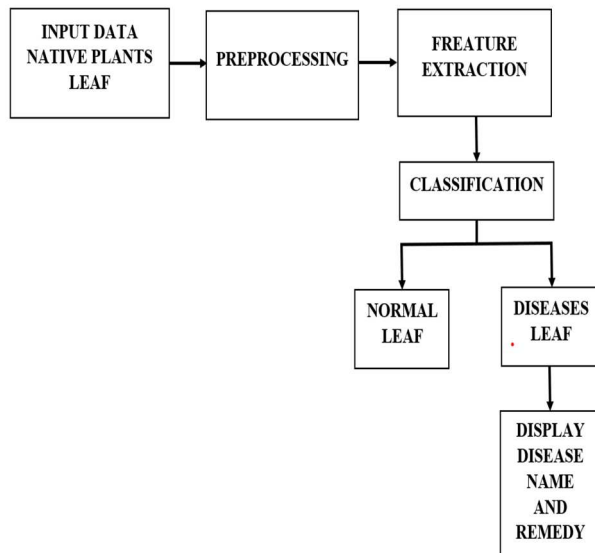


Figure 1. Block diagram of disease classification

F. Algorithm of Proposed System

We used Convolution Neural Network (CNNs) to extract features because our model takes raw photos as input. Numerous picture and video applications are possible using CNN. systems for recognizing, understanding, and recommending natural language CNNs and neural networks both fall under the category of AI. Networks are made up of interconnected neurons with programmable biases and weights. A signal is transmitted to each neuron. A weighted sum is created by combining several inputs, and it is then passed through an activation function tends to react towards the output's structure. For this, we're going to use CNN 2D. Two-dimensional convolutional layers convert a three-dimensional input, often an image having RGB image, into an output that is two-dimensional. They use a filter, commonly referred to as a convolution kernel, to scan the image, inspecting a small window of pixels at a time—for example, 33 or 55 pixels in size—and shifting the window until the entire image is scanned. Seven ReLU-activated convolutional layers make up our model. The Rectified Linear Unit (ReLU) is a form of activation function commonly employed in neural networks, particularly CNN. It is the identity function, $f(x) = x$, for all positive values of input 'x,' which zeros out for negative values.

1) *Convolutional Layer*: The activation maps of all filters are stacked along the depth dimension to produce the output level of the convolutional layer. Because the width and height of each filter are meant to be smaller than the input, each neuron inside this feature maps is only attached to a small local portion of the input volume. The layout of the animal visual cortex, where the receptive fields of the cells are narrow, motivates the local connectivity. Utilizing the input's spatial local correlation and the local connectivity of the convolutional layer, the network can train filters that react most strongly to a particular area of the input (a pixel in an input image is more connected to neighbouring pixels than to distant pixels). Additionally, since the activation map is produced by mixing the input and

filtering, filtration system parameters are shared by all local positions. The weight-sharing strategy reduces the amount of components necessary for effective expression, learning, and generalisation.

2) *A Rectified Linear Unit (ReLU) Layer*: In a neural network, the network node total weighted input is transformed into opcode activation, or output, for that input, by the activation function. The rectified linear activation function, or ReLU, is a piece - wise linear transformation that delivers the input directly if the input is positive; otherwise, it produces zero. It has evolved as the default activation function for many varieties of neural networks since a model using it trains more quickly and typically performs better.

3) *Pooling Layer*: The convolutional layer is abided by the pooling layer. The pooling layer is used to decrease the activation map, resulting in the production of medium-level features.

4) *Fully Connected layer*: Fully interconnected layers in a neural network are those that have all of their input connected to each activation block of the layer above them. Most common machine learning models have a final set of fully linked layers that combine the input gathered by earlier levels to produce the final output. It is the second-most time-consuming layer, behind the Convolution Layer. The Fully Connected Layer uses feedforward neural networks as its foundation. The Fully Connected Layers represent the bottom layers of the network. The final pooling or convolutional layer's output, which is flattened before being fed into the fully connected layer, serves as the input to this layer. a layer that is linked. In a neural network, completely linked layers are those from which all inputs originate. Each activation unit in the layer below is linked to the activation units in the layer above. The most common machine's final few learning model layers are fully connected layers that gather the data.

III. DESCRIPTION OF NATIVE PLANT LEAF DISEASES

A. Bacterial Spot

1) *Analysis of Bacterial Spot*: A leaf of a plant [15] with bacterial spots on it is fetched from the database and as shown in Fig.2. The image has undergone preprocessing and contrast enhancement. Bacterial Spot is the diagnosis, as can be seen in the diagram above. The image is run through 500 iterations with the algorithm choosing various clusters each time to assess the accuracy of our proposed methodology. The accuracy is then predicted, and the reported solution and result show a 97% accuracy rate.

2) *Prevention & Treatment of Bacterial Spot*: Use only certified disease-free seed and plant material. Avoid plantings of peppers or tomatoes from the previous year. It is possible to prevent over irrigation by using drip or furrow irrigation. The entire plant should be eliminated if it is diseased. In order to promote greater air circulation, plants should be trimmed. A copper fungicide application can help manage the bacterial infection. Fungicides can be applied in a home garden.



Figure 2. Bacterial spot

B. Late blight

1) *Analysis of Late Blight*: A blade of a plant with Late blight pathogen [16, 17], as shown in Fig. 3, is imported from the database. The picture has been preprocessed and juxtaposition. According to the accompanying graphic, the infection is referred as Late Blight. The image is processed through 500 iterations with the algorithm generating new patches each iteration to determine the accuracy of the approaches. To verify the accuracy of our methods, the image is run through 500 iterations, with the algorithm selecting various clusters each time, and the accuracy is predicted, with 73% accuracy and the presented solution.

2) *Prevention & Treatment of Late blight*: Maintain maximum aeration for the vegetation. Pick a spot for your garden where it will get morning sun. Plants should be spaced far apart, and watering from above should be avoided, especially later in the day. Disease-free seeds and plants can be purchased. In addition to 31 herbicides from the Nightshade family, untreated tomato and potato plants should also be removed since they could be fungus hosts. Potatoes purchased at a store shouldn't be composted. Highly infectious plants should be removed and removed and destroyed. If the infection is serious enough to require medication, pick one of the following fungicides: mancozeb, copper, or chlorothalonil (all three are excellent).

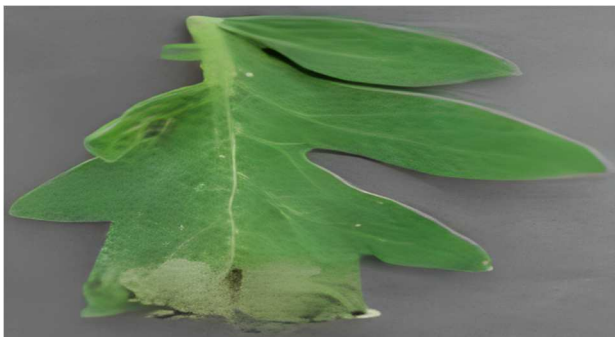


Figure 3. Late Blight

C. Early Blight

1) *Analysis of Early Blight*: Young plants[18] [19] [20], as shown in Fig.4, are rarely affected by early blight. The symptoms appear immediately on the oldest leaves of the plant. As the disease worsens, dark brown patches start to form on this older leaves, grow, and start to resemble angular shapes.

Because these lesions resemble targets, the condition is also known as the target spot.

2) *Prevention & Treatment of Early Blight*: Pathogen spores and mycelia can be found in diseased plant debris and soil, highly infectious rhizome, and germinating seeds symbiont crops and weeds. Spores are generated when temperatures range between 41 and 86 degrees Fahrenheit (5 and 30 degrees Celsius) and there are alternating periods of wetness and dryness. Following that, the wind, rain, and irrigation water spread these spores. They enter through wounds caused by mechanical damage or insect predation. Lesions appear approximately two to three days after the initial infection.



Figure 4. Early Blight

IV. RESULT AND DISCUSSION

In order to obtain classification performance and enhance model selection, assessment measures are crucial. The efficiency of the suggested approach has been assessed using confusion matrices, accuracy, precision, recall, and F1-score. A confusion matrix for classifying a native plant leaf disease is shown in Fig. with values for true positives (TP), false positives (FP), true negatives (TN), and false negatives (FN). If the classifier correctly predicts the class response in each case, it is considered a "success," and if not, it is considered a "error." The classifier's total performance is measured by its error rate, which is a percentage of all errors committed across all instances.

It is possible to extract statistical measures (Precision, Recall, and F-measure) from the confusion matrix for evaluating the effectiveness of classification algorithms, and these metrics are defined as follows: The proportion of occurrences that were successfully identified to all instances that were labelled is known as precision (P) or detection rate. It is the proportion of correctly predicted favorable outcomes in a given class. Using the following formula (1), the precision is computed.

$$\text{Precision}(P) = \frac{TP}{TP+FP} \quad (1)$$

Where TP represents the number of true positive predictions and FN represents the number of false negative predictions for the given class. TP + FP is the total number of test samples for the specific class. Recall (R) or sensitivity is the proportion of properly classified examples to the total number of examples in the class. A genuine positive is another name for it and it has the ability to measure the prediction model.

$$\text{Recall}(R) = \frac{TP}{TP+FN} \quad (2)$$

The number of true positives and false negative predictions for a given class is denoted by TP and FN, respectively. There are TP + FP test samples in total for this class. The F1 score, which aims to provide a single indicator of performance, is the harmonic mean of recall and precision. A skilled classifier can produce outstanding recall and precision numbers. Using the following formula (3), the F score is determined.

$$F1 = \frac{2 \times P \times R}{P + R} \quad (3)$$

The Accuracy can be defined as follow,

$$\text{Accuracy} = \frac{\text{Total Number of Correct Predictions}}{\text{Number of Input Samples}} \quad (4)$$

A. Accuracy and F score

The table I, II, and III represent the accuracy and f score of tomato, potato, and onion dataset.

TABLE I. ACCURACY AND SCORE OF TOMATO DATASET

Classes	Accuracy	Subhead
Bacterial spot	100.0	0.98
Septoria spot	96.1	0.94
Spotted wilt	98.7	0.96
Healthy leaf	96.48	0.90

TABLE II. ACCURACY AND F SCORE OF POTATO DATASET

Classes	Accuracy	Subhead
Bacterial wilt	100.0	0.98
Late blight	95.3	0.93
Early blight	97.36	0.95
Healthy leaf	97.6	0.96

TABLE III. ACCURACY AND F SCORE OF ONION DATASETS

Classes	Accuracy	Subhead
Black mold	98.0	0.97
Purple blotch	94.3	0.92
White rot (Sclerotia rot)	99.1	0.98
Healthy leaf	96.01	0.94

B. Testing

The proposed work test report, as shown in fig.5.



Figure 5. Testing

C. Deploying Model Flask

A web framework is Flask. This indicates that flask offers the technologies, libraries, and tooling necessary to enable you to create a web application. using a flask to upload an image, as shown in fig.6.

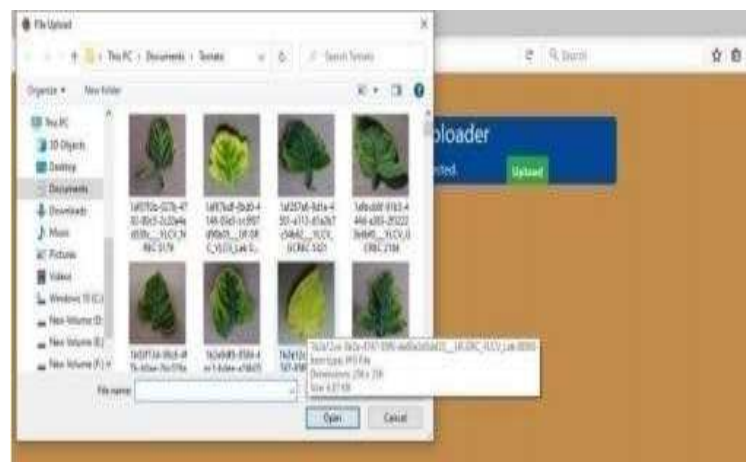


Figure 6. GUI for Sample Input Images

D. Final Output

Final output of the proposed method, as shown in fig.7,8,9.

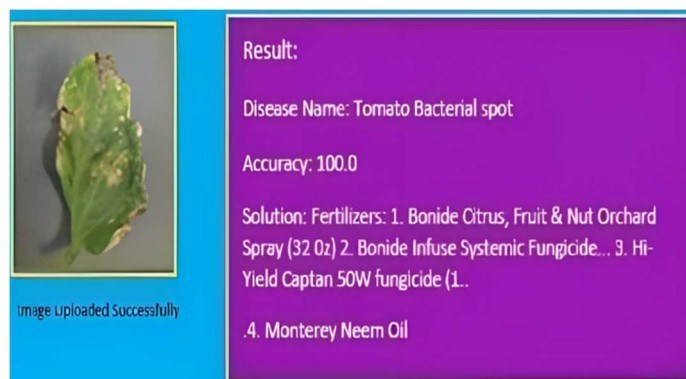


Figure 7. Tomato Output

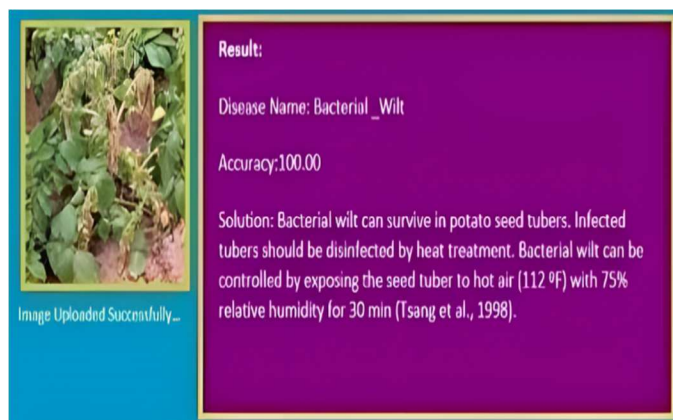


Figure 8. Potato Output

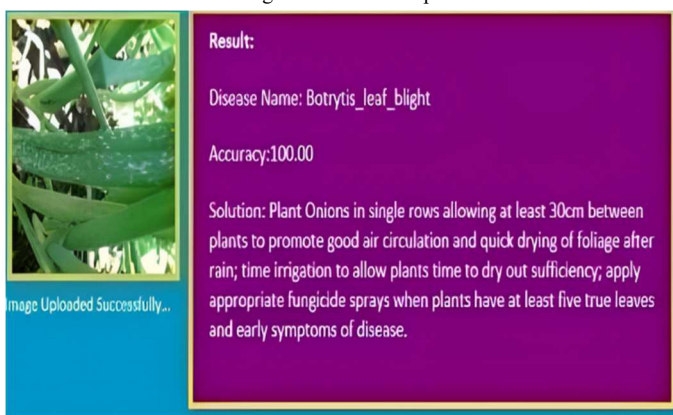


Figure 9. Onion Output

V. CONCLUSION

The main source of the nation's economic prosperity is agriculture. It is seen as an important aspect of society. As a result, the primary purpose of the planned endeavour is to reduce pesticide use in order to lower production costs and save the environment. By integrating data mining algorithms with image processing, it will be easy to detect whether a crop is infected or not, what type of infection it has, and what the remedy is for the same. There are numerous techniques for identifying and categorizing plant leaf diseases, including support vector machines, neural networks, and pattern recognition algorithms. It is easy to operate. The suggested study also explores various leaf disease signs and the fundamental idea of plant leaf disease detection.

REFERENCES

- [1] U. Suttapakti and A. Bupeng, "Potato Leaf Disease Classification Based on Distinct Color and Texture Feature Extraction," *2019 19th International Symposium on Communications and Information Technologies (ISCIT)*, 2019, pp. 82-85, doi: 10.1109/ISCIT.2019.8905128.
- [2] X. Wang, B. Xu, X. Liu and H. Ichinose, "Analysis of ultrastructures in Fe-encapsulating onion-like fullerenes," in *Microscopy*, vol. 55, no. 1, pp. 13-16, Jan. 2006, doi: 10.1093/jmicro/dfi003
- [3] J. Chen, J. Chen, D. Zhang, Y. Sun, Y.A. Nanehkaran, "Using deep transfer learning for image-based plant disease identification", *Computer, Electronics, and Agriculture*, 2020, vol. 173, doi: <https://doi.org/10.1016/j.compag.2020.105393>.
- [4] Dyrmann, Mads, Henrik Karstoft, and Henrik Skov Midtby. "Plant species classification using deep convolutional neural network." *Biosystems engineering*, 2016, vol. 151, pp: 72-80, doi: <https://doi.org/10.1016/j.biosystemseng.2016.08.024>.
- [5] J. Ma, K. Du, F. Zheng, L. Zhang, Z. Gong, and Z. Sun, "A recognition method for cucumber diseases using leaf symptom images based on deep convolutional neural network," *IEEE Access*, 2018, vol. 154, pp. 18-24, doi: <https://doi.org/10.1016/j.compag.2018.08.048>.
- [6] Li Ma, Xuiliang Guo, Shuke Zhao, Doud" Algorithm of Strawberry Disease Recognition Based on Deep Convolutional Neural Network", *International Journal of Engineering & Technology*, 2020. doi: <https://doi.org/10.1155/2021/6683255>.
- [7] G. Geetha Ramani and J. Arun Pandian, "Identification of plant leaf diseases using a nine-layer deep convolutional neural network", *IEEE Access*, 2019, vol. 76, pp. 323-338, doi: <https://doi.org/10.1016/j.compeleceng.2019.04.011>
- [8] E. Özbilge, M. K. Ulukök, Ö. Toygar and E. Ozbilge, "Tomato Disease Recognition Using a Compact Convolutional Neural Network," in *IEEE Access*, vol. 10, pp. 77213-77224, 2022, doi: 10.1109/ACCESS.2022.3192428.
- [9] Z. Zhang, M. Zhao and T. W. S. Chow, "Binary- and Multi-class Group Sparse Canonical Correlation Analysis for Feature Extraction and Classification," in *IEEE Transactions on Knowledge and Data Engineering*, vol. 25, no. 10, pp. 2192-2205, Oct. 2013, doi: 10.1109/TKDE.2012.217.
- [10] M. J. Mendenhall and E. Merenyi, "Relevance-Based Feature Extraction for Hyperspectral Images," in *IEEE Transactions on Neural Networks*, vol. 19, no. 4, pp. 658-672, April 2008, doi: 10.1109/TNN.2007.914156.
- [11] S. Minaee, Y. Boykov, F. Porikli, A. Plaza, N. Kehtarnavaz and D. Terzopoulos, "Image Segmentation Using Deep Learning: A Survey," in *IEEE Transactions on Pattern Analysis and Machine Intelligence*, vol. 44, no. 7, pp. 3523-3542, 1 July 2022, doi: 10.1109/TPAMI.2021.3059968.
- [12] A. Anaya-Isaza, L. Mera-Jiménez, J. M. Cabrera-Chavarro, L. Guachi-Guachi, D. Peluffo-Ordóñez and J. I. Rios-Patiño, "Comparison of Current Deep Convolutional Neural Networks for the Segmentation of Breast Masses in Mammograms," in *IEEE Access*, vol. 9, pp. 152206-152225, 2021, doi: 10.1109/ACCESS.2021.3127862.
- [13] S. Ren, K. He, R. Girshick and J. Sun, "Faster R-CNN: Towards Real-Time Object Detection with Region Proposal Networks," in *IEEE Transactions on Pattern Analysis and Machine Intelligence*, vol. 39, no. 6, pp. 1137-1149, 1 June 2017, doi: 10.1109/TPAMI.2016.2577031.
- [14] Mohanty, Sharada P., David P. Hughes, and Marcel Salathé. "Using deep learning for image-based plant disease detection." *Frontiers in plant science* 7, 2016, pp. 1419, doi: <https://doi.org/10.3389/fpls.2016.01419>.
- [15] S. S. Chouhan, A. Kaul, U. P. Singh and S. Jain, "Bacterial Foraging Optimization Based Radial Basis Function Neural Network (BRBFNN) for Identification and Classification of Plant Leaf Diseases: An Automatic Approach Towards Plant Pathology," in *IEEE Access*, vol. 6, pp. 8852-8863, 2018, doi: 10.1109/ACCESS.2018.2800685.
- [16] M. Islam, Anh Dinh, K. Wahid and P. Bhowmik, "Detection of potato diseases using image segmentation and multiclass support vector machine," *2017 IEEE 30th Canadian Conference on Electrical and Computer Engineering (CCECE)*, 2017, pp. 1-4, doi: 10.1109/CCECE.2017.7946594.
- [17] DONG, Suo-meng, and Shao-qun ZHOU. "Potato late blight caused by *Phytophthora infestans*: from molecular interactions to integrated management strategies." *Journal of Integrative Agriculture*, 2022, pp. 3456-3466, doi: <https://doi.org/10.1016/j.jia.2022.08.060>.
- [18] M. Kumar, A. Kumar and V. S. Palaparthi, "Soil Sensors-Based Prediction System for Plant Diseases Using Exploratory Data Analysis and Machine Learning," in *IEEE Sensors Journal*, vol. 21, no. 16, pp. 17455-17468, 15 Aug.15, 2021, doi: 10.1109/JSEN.2020.3046295.
- [19] K. Kavitha, S. Arivazhagan and N. Kayalvizhi, "Wavelet based spatial — Spectral hyperspectral image classification technique using Support Vector Machines," *Second International conference on Computing, Communication and Networking Technologies*, 2010, pp. 1-6, doi: 10.1109/ICCNT.2010.5591760.
- [20] Kavitha, K. and Arivazhagan. S, "Fuzzy inspired image classification algorithm for hyperspectral data using three-dimensional log-Gabor features", *Optik*, 2014, vol.125(20), pp.6236-6241, doi: <https://doi.org/10.1016/j.ijleo.2014.08.029>.

- [21] Poornam S, Francis Saviour Devaraj A, Image based Plant leaf disease detection using Deep learning, International journal of computer communication and informatics, volume-3,53-65,2021

PAPER • OPEN ACCESS

Reduction of Near-End and Far - End Crosstalk in Microwave and Millimetre Wave Band of Parallel Transmission Lines using Meander Shaped DMS

To cite this article: A Gobinath *et al* 2023 *J. Phys.: Conf. Ser.* **2466** 012016

View the [article online](#) for updates and enhancements.

You may also like

- [Ultra-low power anti-crosstalk collision avoidance light detection and ranging using chaotic pulse position modulation approach](#)
Jie Hao, , Ma-li Gong et al.
- [Crosstalk analysis and optimization in a compact microwave-microfluidic device towards simultaneous sensing and heating of individual droplets](#)
Weijia Cui, Zahra Abbasi and Carolyn L Ren
- [Mixed-mode RF reflectometry of quantum dots for reduction of crosstalk effects](#)
Masato Machida, Raisei Mizokuchi, Jun Yoneda et al.

Reduction of Near-End and Far - End Crosstalk in Microwave and Millimetre Wave Band of Parallel Transmission Lines using Meander Shaped DMS

A Gobinath^{1,3}, N Suresh Kumar^{2,3}, and P Rajeswari^{2,3}

¹Department of Information Technology

²Department of Electronics and Communication Engineering

³Velammal College of Engineering and Technology, Madurai

gopigopinath10@gmail.com

Abstract. This research proposes a unique design that makes use of a defective microstrip topology to decrease electromagnetic coupling between parallel high speed interconnects. The performance of this new microstrip construction with defects is evaluated using near-end crosstalk and far-end crosstalk. Serpentine shaped defected microstrip is introduced in one parallel of high speed interconnects and its performance is also compared the existing structure. In this research, the proposed defected microstrip structure (DMS) is simulated and compared with a conventional microstrip structure using Ansoft HFSS software which employs the Finite Element Method (FEM). Simulation results indicate that the DMS design effectively reduces crosstalk in comparison to the previous structure. It reduces more than 5dB near end crosstalk and more than 3dB far end crosstalk compared to conventional model.

1. Introduction

Nowadays, the demand for wireless devices are increasing rapidly since the growth of wireless communication and high speed data transmission increases simultaneously. These devices should have smaller in size and support high data rate. Therefore, it is necessary to accommodate more number of high speed interconnects with in a small feature size which lead to signal integrity problems. High speed interconnect is a conductive path between transmission end to receiving end which is used to carry the high speed signal. Generally, high speed interconnects are modeled as planar transmission lines like microstripline or stripline. Microstripline is generally preferred rather than stripline since low cost and ease of fabrication. In this research, the crosstalk is investigated by considering a duo of coupled microstrip transmission lines. Signal integrity is a measure of quality of signal at the receiver end. When the electrical signal on one transmission line is transferred to an adjacent line, it can cause a range of signal integrity issues. These signal integrity issues include crosstalk, electromagnetic emissions, propagation delay, impedance mismatch, and signal reflection. Crosstalk or coupling is a particularly significant signal integrity concern.

Several scholars have published studies and papers detailing various methods for reducing crosstalk between adjacent transmission lines in high-speed printed circuit boards. The methods presented in literatures are increasing the distance between two lines placing guard trace between two lines, inserting via guard fence, altering the geometry of the microstripline like serpentine and mitered bend lines. However these methods have their own pros and cons. In the literature, authors [1] through [17]



examined numerous methods for reducing crosstalk on printed circuit boards. This proposal presents a defective microstrip design to decrease crosstalk.

2. Defected Microstrip Structure

This research presents a novel approach to reduce crosstalk between high-speed interconnects through the use of a defected microstrip structure (DMS). The DMS is created by etching the microstrip in a specific shape that is tailored to the specific application at hand. The suggested DMS successfully lowers microwave emissions at particular frequencies and displays slow wave propagation characteristics. It offers higher effective inductance and electromagnetic interference noise immunity [1] [2]. When an etched microstrip is excited by a time varying electric field, the electromagnetic field will be concentrated around the conductor strip. A current distribution is disturbed by this structure. A DMS microstrip increases an electric length and also increases the effective inductance and capacitance [5].

Figure 1 shows a parallel microstrip line on a PCB in a non-uniform environment with the top metal layer exposed to air. The lines are parallel as they have the same width (W) throughout their length (L) and are separated by a distance S . The substrate dielectric constant is ϵ_r with height H . The thickness T mentioned in Figure 1 represents strip thickness. The transmission characteristics are very much important as the PCB is the support for the whole system. Control of the transmission lines' electrical properties is essential for high-speed systems, especially when taking into account the requirements of new high-speed applications. It depends on the physical dimensions of the interconnects.

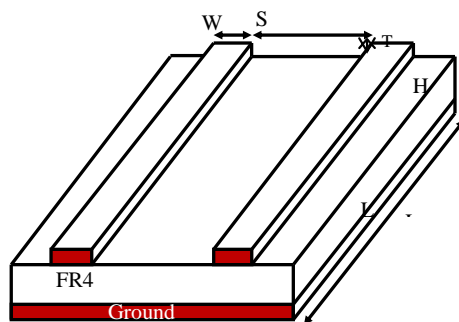


Figure 1 (a). Parallel Microstriplines

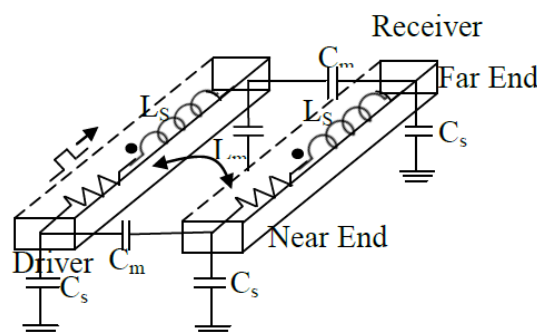


Figure 1(b). Equivalent circuit of Parallel Microstriplines

The level of far-end crosstalk is determined by the mutual capacitive and inductive interactions between long lines. The voltages at the near-end and far-end are determined by these mutual interactions. The capacitive coupling ratio (C_m/CT) is the ratio of mutual capacitance (C_m) to total capacitance (CT), which is the sum of mutual capacitance (C_m) and self-capacitance (C_s). [4].

The equations for the voltage caused by crosstalk at both ends of the affected line are as follows.

$$V_{ne}(t) = \frac{1}{4} \left(\frac{C_m}{C_t} + \frac{L_m}{L_s} \right) [V_s(t) - V_s(t - 2T_p)] \quad (1)$$

$$V_{fe}(t) = \frac{1}{2} \left(\frac{C_m}{C_t} - \frac{L_m}{L_s} \right) \frac{T_p \cdot dV_s(t - T_p)}{dt} \quad (2)$$

where V_s is the signal source's input voltage.

Electromagnetic coupling is typically represented by near-end crosstalk (NEXT) and far-end crosstalk (FEXT). Crosstalk on the affected line at the end closest to the source is called NEXT, while crosstalk on the affected line at the end farthest away from the source is called FEXT. Additionally, FEXT is proportional to the length of the connected microstrip interconnects. Both mutual inductive and capacitive coupling are proportional to both NEXT and FEXT.[6] [7]

The typical structure of a defective microstrip is shown in Figure 2. (DMS). The suggested DMS design is implemented on a 1.6mm thick and relative permittivity of 4.4, as illustrated in Figure 3. The suggested DMS structure, shown in Figure 4, is etched on parallel transmission lines, as shown in Figure 3.

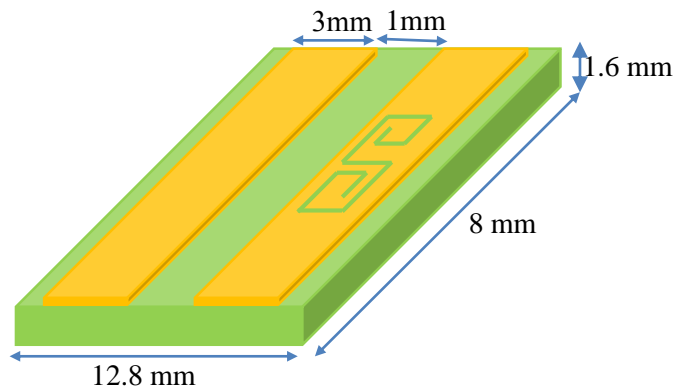


Figure 2. Conventional DMS on Parallel Transmission lines

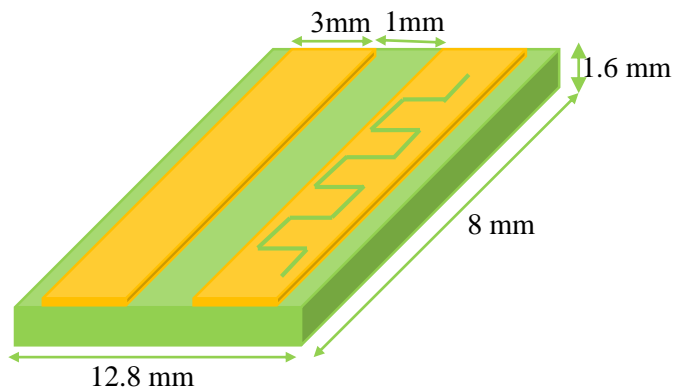


Figure 3. Proposed DMS on Parallel Transmission lines

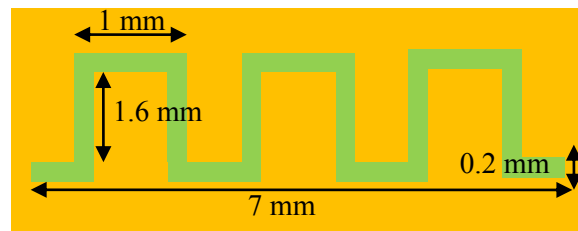


Figure 4. a Proposed DMS Structure

Voltages can be induced on an adjacent line (the victim) when a signal flows on a neighboring line (the aggressor). This is known as crosstalk and can occur if the signals from the two lines mix. Crosstalk is categorized into two types: Far-end crosstalk (FEXT) and near-end crosstalk (NEXT), which occur at the far and near ends of the victim line, respectively. Figure 1(b) shows a circuit of two transmission lines with distributed self-capacitance (C_s), self-inductance (L_s), mutual capacitance (C_m), and mutual inductance (L_m).

The proposed Meander DMS have 3-unit section, each unit section consists of two vertical segments and two horizontal segments, repeated along the length direction. The equivalent circuit model of the proposed structure is given in Figure 4 (b). The self-capacitance corresponds to the sum of Capacitance whereas self-inductance is the sum of Inductance. Compare with conventional structure Capacitive coupling is increased in the proposed structure due to the potential variation of the structure. It reduces the crosstalk as per the mathematical expressions (1) and (2).

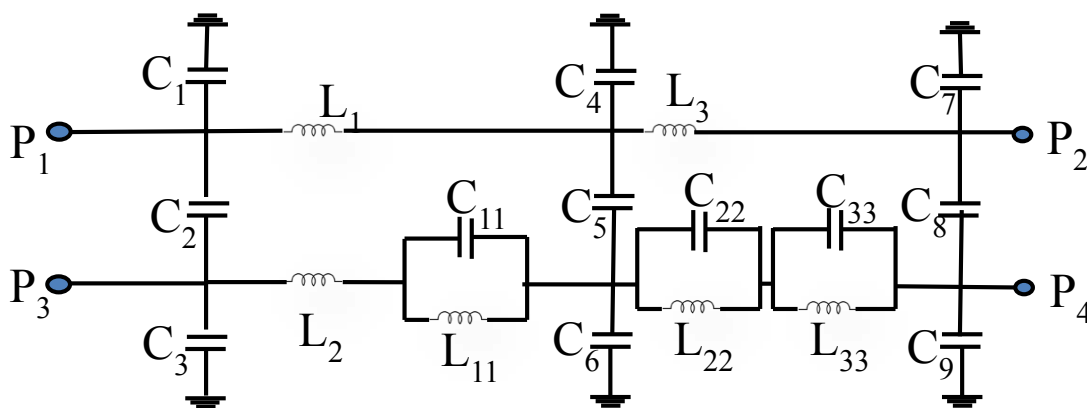


Figure 4. b A diagram showing the circuit model for the proposed meander DMS structure is presented

3. Results and Discussion

The performance of the proposed microstrip line interconnect architecture was analyzed using Ansoft HFSS across a frequency range of 0 to 12 GHz. The microstrip line had a length (L) of 8 mm and a width (W) of 3 mm. The two parallel lines were separated by 1mm, with dielectric constants of $\epsilon_r=4.6$ and a 1.6 mm thickness of printed circuit board substrate. The serpentine defective microstrip structure had a length of 4mm. The proposed microstrip interconnect with serpentine defective microstrip structure was modified to optimize performance. The structures shown in Figures 2 and 3 were modeled using the HFSS simulation program and their dimensions are also provided.

Utilizing scattering measures like S13 and S14, where S13 stands for near-end crosstalk and S14 for far-end crosstalk, the performance of the structures is assessed. When signal is applied at port1, the crosstalk induced voltage is measured at port 3 and port 4 which are in the adjacent transmission line with DMS structure.

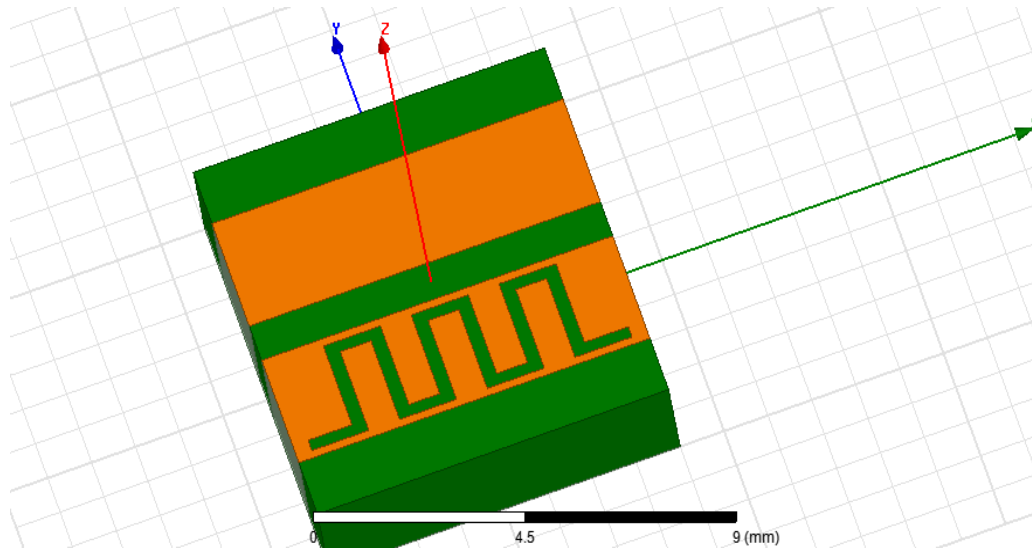


Figure 5. Simulated Structure of Proposed DMS

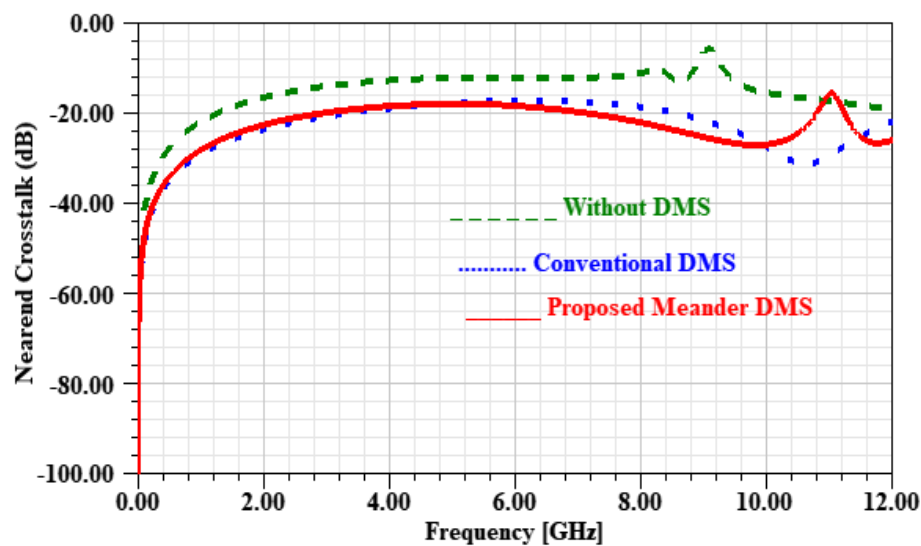


Figure 6. Comparison plot of Near end crosstalk for conventional and proposed DMS structure

Figure 6 represents Near end crosstalk (S13) versus frequency for the conventional and proposed structure. The results show that the proposed DMS structure reduced more than 5dB near end crosstalk compared to conventional DMS structure. And also it indicates that it performed well compared to without DMS structure. The figure 7 illustrates the comparison of far-end crosstalk for the conventional and suggested DMS structures.

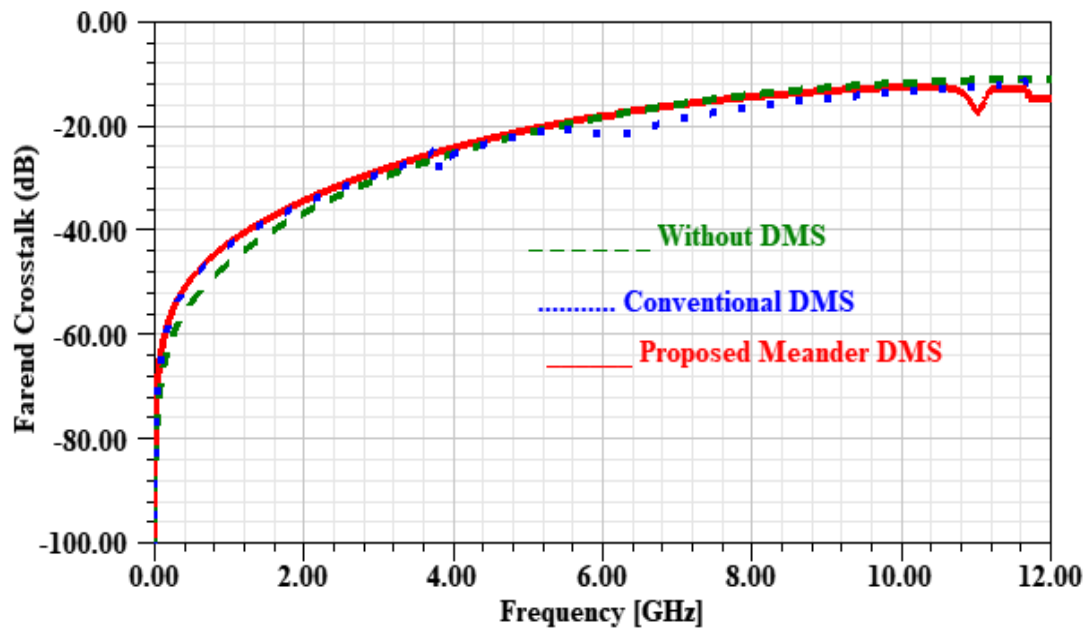


Figure 7. Comparison graph depicting the far-end crosstalk for both the conventional and proposed DMS structures

Table 1 provides a summary of the crosstalk reduction performance of the traditional and proposed DMS structures. It illustrates that the suggested DMS design is more effective in reducing crosstalk when compared to the conventional structure, with a reduction of more than 5 dB in NEXT and 3 dB in FEXT.

Table 1. Performance Comparison of conventional and proposed DMS structure.

Structure	S13 (dB)	S14 (dB)
Without DMS	-19.44	-10.95
Conventional	-21.85	-11.98
Proposed	-26.04	-14.82

4. Conclusion

This research introduces a new DMS design and evaluates its performance. The simulation of this structure is carried out using Ansoft HFSS software. Through an increase in capacitive coupling, the suggested DMS design successfully eliminates more than 3dB of FEXT and more than 5dB of NEXT. Reduced crosstalk is achieved with great efficiency by the suggested DMS structure.

References

- [1] R. Mallahzadeh, Ghaasemi, S. Akhlaghi Bayderkhani, 2010 Crosstalk Reduction Using Step Shaped Transmission Line *Progress In Electromagnetic Research* **12** 139-148.
- [2] F. D. Mbairi, W. P. Siebert and H. Hesselbom 2008 High-Frequency Transmission Lines Crosstalk Reduction Using Spacing Rules *IEEE Transactions on Components and Packaging*

- Technologies* **31** 601-610.
- [3] Y. Li, W. Li, Q. Ye, 2013 A reconfigurable triple notch band antenna integrated with defected microstrip structure band-stop filter for ultrawideband cognitive radio applications, *International Journal of Antennas and Propagation*.
 - [4] P.Rajeswari and S. Raju, 2016 Analytical and experimental study on suppression of electromagnetic interference on high speed printed circuit board for wireless communication systems *International Journal of Wireless Personal Communications, Springer, New York* **89**.
 - [5] P.Rajeswari and S. Raju, 2015 Comparative study of crosstalk reduction techniques in RF printed circuit board using FDTD method *International Journal of Antennas and Propagation, United States*.**2015**
 - [6] P.Rajeswari and S. Raju, 2012 Comparative study of crosstalk reduction techniques for parallel microstriplines *Lecture Notes on Computer Science* **108** 422-425.
 - [7] Rajeswari, P, Raju, S, Suresh Kumar, N & Gobinath, A 2016 Far end crosstalk reduction between parallel microstriplines using U shaped guard trace *ARPJN Journal of Engineering and Applied Sciences* **11** 3081-3085.
 - [8] Rajeswari, P, Raju, S, Divya Poornima, M, Sudharsana, R & Gobinath A, 2015 Signal integrity analysis of high speed interconnects in SATA connector *International Journal of Applied Engineering Research* **10**18007-18014.
 - [9] Rajeswari P Raju S Suresh Kumar, N Gobinath, A, 2015 Crosstalk reduction on coupled microstrip to three-line coupled microstrip transition using mitering configuration *International Journal of Applied Engineering Research* **10** 7923-7936.



A NOVEL BRANCH LINE COUPLER WITH DEFECTED GROUND STRUCTURE FOR BONE DENSITY MEASUREMENT ANALYSIS

P. Rajeswari¹, A. Gobinath¹, N. Suresh Kumar¹ and M. Anandan²

¹Velammal College of Engineering and Technology, Madurai, India

²Vel Tech Rangarajan Dr. Sagunthala R & D Institute of Science and Technology, India

E-Mail: agn@vcet.ac.in

ABSTRACT

Microwave Integrated Circuits play a vital role in the Medical field for sensing applications. Two hundred million people are affected globally by musculoskeletal diseases, a substantial healthcare burden and one of the most costly diseases. Our proposed design is dedicated to the Bone Density Measurement Analysis (BDAS) RF system. This paper investigates the development of a directional - Branch Line Coupler with Defected Ground Structure (DGS) to differentiate between transmitted and reflected signals in the split ring resonator (SRR) sensor for Bone Density Measurement Analysis using the HFSS V13 design tool. The Coupler operates within the range of 2 GHz - 3 GHz frequency band with a high directivity of 55 dB. The proposed design is compared with a conventional branch-line coupler, and S-Parameters are calculated. The design is optimized in HFSS to meet the required specifications.

Keywords: bone density, branch line coupler, S parameters, microstrip lines.

Manuscript Received 31 October 2022; Revised 29 July 2023; Published 13 August 2023

1. INTRODUCTION

The rapid development of microwave technology makes microwave devices and components more common compared to 10 years ago. Couplers are one of the critical devices which have applications in the design of microwave devices [1]. A directional coupler is generally a four-port device, often with a good load on the fourth port, but in practice, a load element is always permanently attached [2]. Of many microwave circuits, Branch Line Coupler is suitable for low-cost fabrication. They couple a defined amount of electromagnetic power in a transmission line to a port enabling the signal to be used in another circuit. They are commonly used for high return loss and power combinations in balanced amplifier circuits and mixers.

In the medical field, microwave-integrated circuits play an essential role in sensing applications. The design of a microwave-based sensor for the muscle analyzer system was proposed [3]. A microwave sensor is designed to monitor Intracranial Pressure (ICP) in a non-invasive method [4] and Osseointegration Analysis with proximity coupled Split Ring Resonator (SRR) [5].

This coupler has a tunable high directivity circuit to measure the reflected RF power [6]. A 3-dB coupler using microstrip to coplanar waveguide via hole transitions is proposed [7]. A high-directivity single and dual-band directional coupler operating at 2.35 GHz and 0.8/2.35 GHz are designed based on substrate-integrated coaxial line [8]. A multi-band directional coupler for front-end RF application with a low power loss of less than -21dB [9]. Miniaturized dual-band directional coupler with folded stubs operating at frequencies 0.9 and 2 GHz [10]. A multi resonant directional coupler in the range of 3 to 9 GHz with an open-circuit stub is proposed [11]. Directional couplers separate forward and reverse waves in a transmission system. A microstrip-fed split ring resonator antenna is designed for Osseo integration

analysis of skull implants [12]. The designed Coupler has a suitable impedance matching with the Split Ring Resonator (SRR) [13] sensor used in the Bone Density Measurement Analysis System (BDAS) [14] project. The designed Coupler reads the reflected signal from the SRR sensor.

2. CHARACTERISTICS OF BRANCH LINE COUPLER

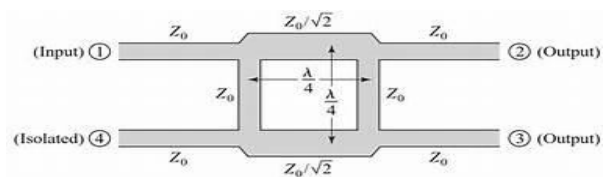


Figure-1. Geometry of typical branch line coupler.

The Basic Branch line coupler comprises four ports, as shown in Figure-1.

The first port is the input port. (Incident)

Port 2 is the output port (Transmitted)

Port 3 is the coupled port (Forward Coupled Port)

Port 4 is the isolated port. (Reverse Coupled Port)

Terms in brackets refer to alternative names for ports that may give little more explanation of coupler port. Typically the main line is the one between Port 1 and Port 2. The other ports are intended to carry a small portion of mainline power. Port 3 and Port 4 may even have small connectors to distinguish them from the mainline ports of Coupler.

Due to the high degree of symmetry, any port can be used as the input port, the other port on the same side will be the isolated port, and the output ports will be on the opposite side of the junction from the input port [15]. A Branch line Coupler is a 3 dB directional coupler with a



90° phase difference in the output of the through and coupled arms. The bandwidth of branch-line Coupler is limited to 10 - 20 %, which can be applied only for narrow band circuits [16]. It is composed of four-quarter wavelength transmission lines. The Characteristic Impedance of the shunt arm is 50 ohm. The characteristic impedance of the series arm is reduced by $1/\sqrt{2}$, i.e. 35.35 ohms. The characteristic impedance of the mainline and shunt branches of the branch line coupler can be computed using the given equations.

$$Z_{0s} = Z_0 |S_{21}| = Z_0 \sqrt{1 - |S_{31}|^2}$$

$$Z_{0p} = \frac{Z_{0s}}{|S_{31}|} = \frac{Z_{0s}}{\sqrt{1 - |S_{21}|^2}}$$

3. DESIGN OF CONVENTIONAL COUPLER

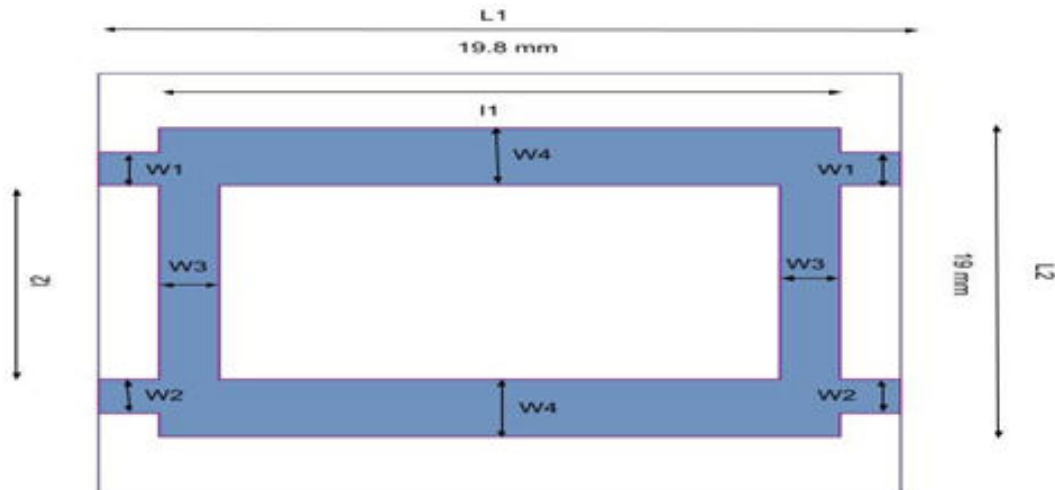


Figure-2. Geometry of conventional Coupler.

The Topology of the conventional Branch line coupler is shown in Figure-2. L1 is a series arm connecting Port 1 and Port 2. The arm connecting Port 3 and Port 4 is also a series arm. L2 is a shunt arm connecting Port 1 and Port 4. The arm connecting Port 2 and Port 3 is also a shunt arm. This branch line coupler design has symmetrical characteristics with L1=L2. The length and width of feeding lines, as well as shunt and series arm, is calculated using above mentioned design equations which are defined based on a theoretical study by R.K.Moniga *et al.* [17].

The design layout is shown in Figure-2, with dimensions shown in Table-1.

Table-1. Dimensions of the conventional coupler.

Symbol	W1 = W2=W3	W4	l1	l2
Value (mm)	1.5	2.1	16.8	13

The Total dimension of the Coupler is 19.8 x 13 mm². The length of the primary arm L1 is 19.8 mm. The length of the side arm is 19 mm. The width of the main arm is 2.1 mm. The width of the side arm is 1.5 mm. The substrate used for simulation is FR4 with a thickness of 1 mm, and copper cladding of 35 µm. The size of the Conventional Branch line coupler is enormous at lower frequencies. If dimensions of the branch line coupler are reduced, then bandwidth is also reduced. However, an increase in dimension causes the frequency to decrease, and the low width of the Branch line coupler causes an increase in permittivity. Hence to reduce these issues, FR4 substrate with the dielectric constant of 4.4 is used.

$$W = \left(\frac{e^H}{8} - \frac{1}{4e^H} \right)^{-1} \cdot h$$

$$L = \left(\frac{Z_0 \sqrt{2(\epsilon_r - 1)}}{119.9} \right) + \frac{1}{2} \left(\frac{\epsilon_r - 1}{\epsilon_r + 1} \right) \left(\ln \left(\frac{\pi}{2} \right) + \ln \left(\frac{4}{\pi} \right) \right)$$

$$\lambda_g = \frac{c}{f \sqrt{\epsilon_{eff}}}$$

$$\epsilon_{eff} = \frac{\epsilon_r + 1}{2} \left(1 - \frac{1}{2H} \left(\frac{\epsilon_r - 1}{\epsilon_r + 1} \right) \left(\ln \left(\frac{\pi}{2} \right) + \frac{1}{\epsilon_r} \ln \left(\frac{4}{\pi} \right) \right) \right)^{-2}$$

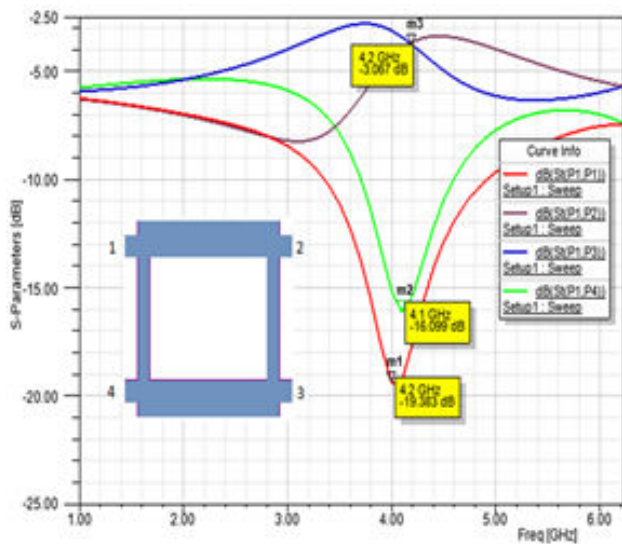


Figure-3. Simulated S-Parameters of conventional coupler.

Figure-3 depicts the simulated results of the conventional Coupler. There are four curves which are indicated in different colours. Each of the results is assessed in terms of

- Return loss (S_{11})
- Insertion loss (S_{21})
- Isolation (S_{41})
- Coupling factor (S_{31})

We can notice that the Reflection coefficient of Return loss S_{11} is -19.38 dB. The directivity coefficients S_{21} and S_{31} are in the range of best requirement results which are $-3 \text{ dB} \pm 1.5 \text{ dB}$, around -3.06 dB. Isolation S_{41} is -16.09 dB. Enhancements in these parameters are discussed in the proposed coupler section.

3.1 Phase error analysis

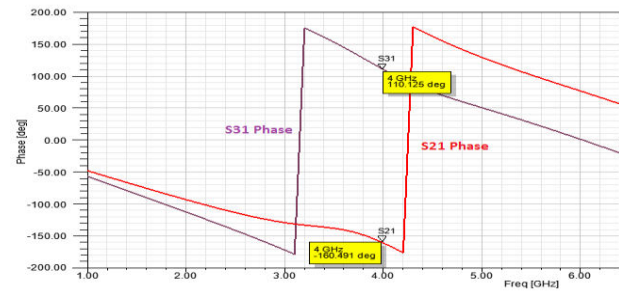


Figure-4. Phase Error Analysis.

The phase Error analysis is an essential measurement for Coupler when it is subjected to oscillations of microwave source. Figure-4 shows the phase error analysis. From Figure-4.4, we can notice sharp changes near the frequency of interest. Phase difference = 270.62 deg

4. PROPOSED DESIGN

It is seen that there is a physical discontinuity present at each port. It should be considered in evaluating the performance of the circuit. The key of the proposed design is substituting the quarter wavelength branch-line coupler with an equivalent section that exhibits desirable characteristics at the centre frequency.

The proposed design of the Branchline coupler is dedicated to applying in the RF System of the Bone Density Measurement Analysis. Figure-5 depicts the proposed branch-line coupler. The design comprises perfect Serpentine as shown in Figure-5(a) and etched on the ground plane as shown in Figure-5(b). Due to its simple structural design, DGS has been used in various microwave circuits to enhance the parameters, and increase coupling coefficient. Etched slots or defects in the ground plane of the microstrip circuit are referred to as Defected Ground Structure (DGS) [18]. It is incorporated in the Ground plane of the branch line coupler, which limits the current distribution and gives rise to increase capacitance. Inductance is one of the most exciting areas of research.

The occupied area of the proposed Coupler is $0.41 \lambda_g \times 0.21 \lambda_g$ (24 mm \times 12mm). The length of the main arm is 24mm, and the Sidearm length is 12mm.

The layout of the design's front view is shown in Figure-5 (a), with dimensions shown in Table-2.

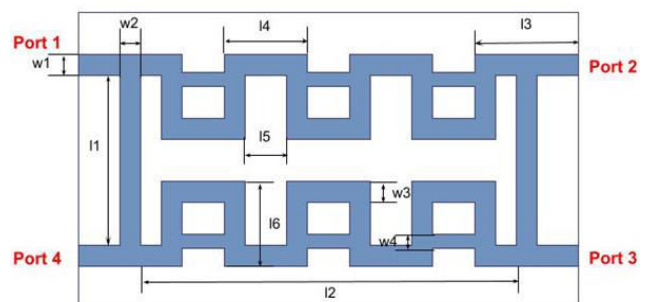


Figure-5. (a) Front view of proposed design.

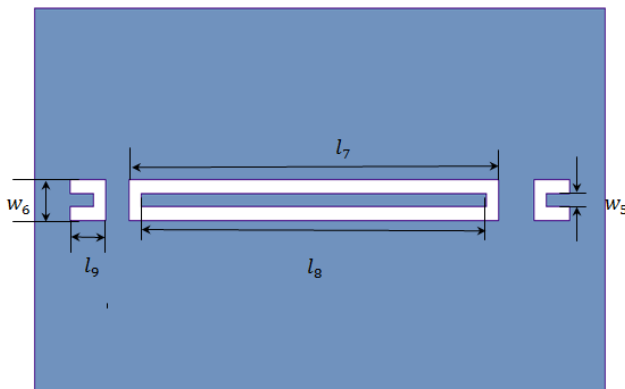
**Table-2.** Dimensions of the proposed coupler.

Symbol	$w_1 = w_2 = w_3$	w_4	l_1	l_2	l_3	$l_4 = l_6$	l_5
Value (mm)	1	0.65	10	18	5	4	2

The Total dimension of the Coupler is $24 \times 12\text{mm}^2$. The length of the primary arm L_1 is 10 mm. The length of the side arm is 18 mm. The width of the feeding lines, main arm and side arm is constant (1 mm).

This design comprises of inward serpentine structure in the main arm. The number of folds in this design is 5. The folded length is 4 mm Folds represent the simple strip displacement (two 90-degree bends). Stubs of width 0.65 mm are added in the central arm's odd folds (Fold 1, 3, 5). The stub is the length of the transmission line or waveguide. Several folds and stubs decide the shape factor and value of S_{11} , S_{21} . Several stubs improve the insertion loss, but the size also increases as many stubs increase. So the number of stubs should be chosen minimum, provided the insertion loss should be minimum and high selectivity.

The layout of the back view of the proposed design is shown below in Figure-5(b), with dimensions shown in Table-3.

**Figure-5.** (b) Back view of proposed design.**Table-3.** Dimensions of the back view of the proposed coupler.

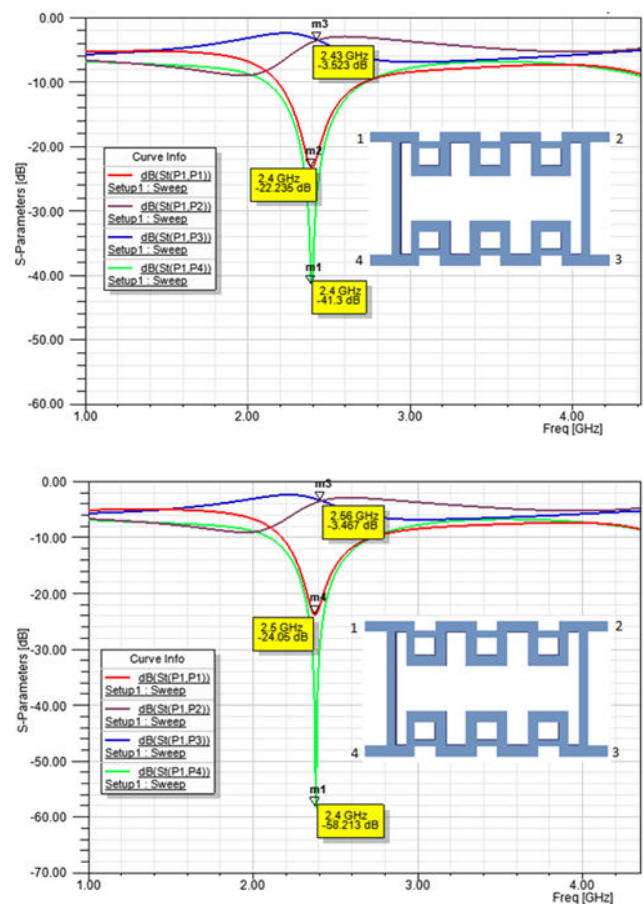
Symbol	w_5	w_6	l_7	l_8	l_9
Value (mm)	0.5	1.5	15.5	14.5	1.5

Pair of U-shaped DGS is etched along with a rectangular slot on the ground plane. U Shaped DGS can be seen as a transformation of the Conventional Dumbbell DGS.

5. SIMULATED RESULTS OF BRANCH LINE COUPLER WITH AND WITHOUT DGS

The designed Coupler is simulated in HFSS V13. The size of the Conventional Branch line coupler is huge at lower frequencies. If dimensions of the branch-line coupler are reduced, then bandwidth is also reduced. However, an increase in dimension causes the frequency

to decrease, and the low width of the Branchline coupler causes an increase in permittivity. Hence, an FR4 substrate with a dielectric constant of 4.4 is used to reduce these issues. The proposed Coupler operates at 2.5 GHz. The simulated S parameters of Branchline Coupler with and without DGS are shown in Figure-6(a) and Figure-6(b), respectively. Each result is assessed in terms of Return loss, Insertion loss, Isolation, and Coupling factor. From Fig (a), the reflection coefficient of return loss S_{11} is -22.235 dB. The directivity coefficient S_{21} is -3.523 dB. Coupling factor S_{31} is -3.523dB. Isolation loss S_{41} is -41.3 dB

**Figure-6.** Scattering parameter analysis of proposed branch line coupler with and without DGS.

The simulated S parameters from Figure-6. We can notice that directivity coefficient S_{21} and Coupling factor S_{31} are in the range of best requirement results which are $-3\text{ dB} \pm 1.5\text{dB}$.

- Reflection coefficient of Return loss S_{11} is -24.05dB.
- The directivity coefficient S_{21} is -3.467dB.



- Coupling factor S_{31} is -3.467dB.
- Isolation loss S_{41} is -58.213dB.

Comparing the results, it can be observed that Insertion loss and Coupling (S_{21} and S_{31}) are in the range of best requirement results which are $-3 \text{ dB} \pm 1.5 \text{ dB}$. However, Coupler with DGS shows better performance as Isolation reaches -58.213dB and Return loss reaches -24.05dB. Optimizations in the transmission line by modifying the length and width of the series arm and shunt arm are done to obtain the best Isolation value.

Comparing the Conventional Coupler and the Proposed Coupler, we notice an enhancement in all the parameters. A maximum Directivity of 55.035 dB has been measured, an improvement over Conventional Branch Line Coupler. This result is as expected as implementing branch line coupler with DGS increases the performance of Coupler.

5.1 Directivity

The performance of a coupler is computed using the Directivity factor. The directivity is a calculated parameter from the isolation and coupling factors. The performance of a directional Coupler is usually evaluated by its directivity between port 3 and port 4. Calculated Directivity [D] as 55.035

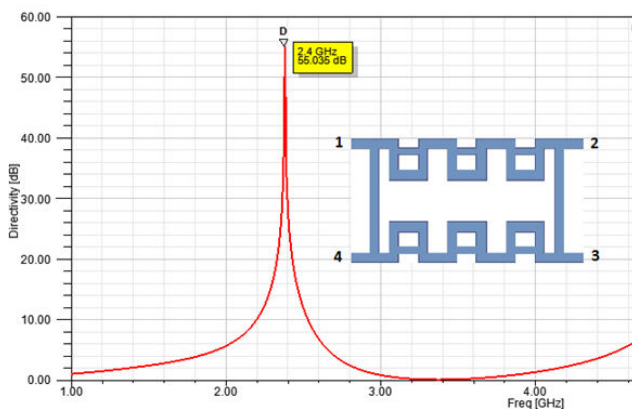


Figure-7. Directivity of proposed branch line coupler.

5.2 Phase Error Analysis

The phase Error analysis is an important measurement for Coupler from Figure-6.5 we can notice sharp changes near the frequency of interest. Phase difference = 274.2 deg

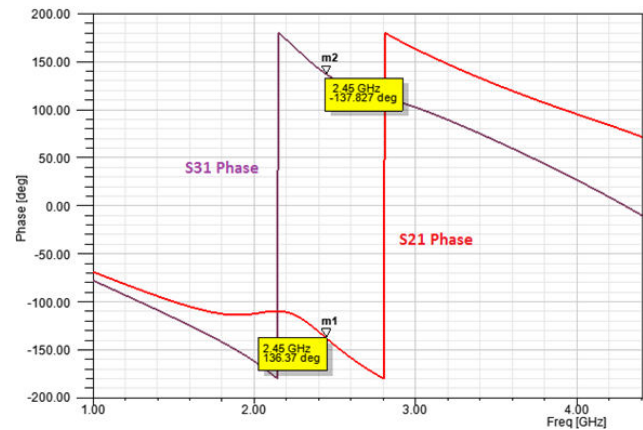


Figure-8. Phase difference of proposed branch line coupler.

Table-4. 13 Bandwidth summary of simulated results.

S-Parameter	Frequency (GHz)		Bandwidth (%)
S11	f_H	3	22.95
	f_L	1.88	
S21	f_H	3.4	19.88
	f_L	2.32	
S31	f_H	2.52	21.154
	f_L	1.64	
S41	f_H	3.22	27.52
	f_L	1.83	

6. APPLICATION OF PROPOSED BRANCH LINE COUPLER

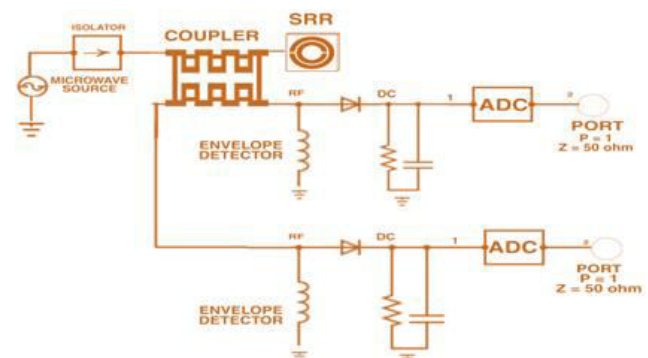


Figure-9. Application of proposed branch line coupler.



In this section, Radio Frequency (RF) system design using a directional coupler, envelope detector, Analog to digital converter, isolator, and signal source is depicted. Figure-10 shows a detailed schematic of the device block connection. The function of the microwave source is to produce an alternating voltage with a frequency defined by the analysis frequency. The device should be set up for reading the frequency characteristics from the split-ring resonator (SRR). The signal from the microwave source passes through an isolator implemented with low forward insertion loss and reverse isolation, which makes the signal travel in the forward direction only. The function of the directional Coupler places a very important role in this system design to read the reflected signal from the SRR.

7. CONCLUSIONS

A Branch line coupler operating at 2.5 GHz is designed and measured for sensing application. The proposed design is a symmetrical configuration of perfect Serpentine and Rectangular slot with U shaped Defected Ground Structure. The design is fabricated on FR4 substrate. The results are optimized as per the requirement. This work shows improvement over conventional branch line coupler and provides key parameters to tune Coupler. A maximum Directivity of 55.035 dB has been measured which is an improvement over Conventional Branch Line Coupler. The main goal of this work is to design a coupler that would be useful in measuring system of SRR of BDAS.

REFERENCES

- [1] K. Janis, I. Piekarz, K. Staszek, K. Wincza and S. Gruszczynski. 2018. Differentially Fed Directional Couplers with Coupled-Conductors of Unequal Widths. *IEEE Microw. Wirel. Components Lett.* 28(9): 759-761.
- [2] Mattsson V., Ackermans LLGC, Mandal B., Perez M.D., Vasseur M. A. M., Meaney P., Ten Bosch J. A., Blokhuis, T. J., Augustine R. 2021. MAS: Standalone Microwave Resonator to Assess Muscle Quality. *Sensors*, 21, 5485. <https://doi.org/10.3390/s21165485>
- [3] K. Krishnaswami. 2021. Microwave-Based Approach in Noninvasive Intracranial Pressure Monitoring (ICP). Dissertation.
- [4] S. Raman, R. Augustine and A. Rydberg. 2014. Noninvasive Osseointegration Analysis of Skull Implants with Proximity Coupled Split Ring Resonator Antenna. in *IEEE Transactions on Antennas and Propagation*, 62(11): 5431-5436, DOI: 10.1109/TAP.2014.2350522.
- [5] S. M. Sohn, A. Gopinath and J. T. Vaughan. 2016. A Compact, High Power Capable, and Tunable High Directivity Microstrip Coupler. in *IEEE Transactions on Microwave Theory and Techniques*, 64(10): 3217-3223, DOI: 10.1109/TMTT.2016.2602835.
- [6] Jui-Chieh Chiu, Jih-Ming Lin, Mau-Phon Houng and Yeong-Her Wang. 2006. A PCB-compatible 3-dB coupler using microstrip-to-CPW via-hole transitions. in *IEEE Microwave and Wireless Components Letters*, 16(6): 369-371, DOI: 10.1109/LMWC.2006.875592.
- [7] S. Jun-Yu *et al.* 2013. High-directivity single- and dual-band directional couplers based on substrate integrated coaxial line technology. 2013 IEEE MTT-S International Microwave Symposium Digest (MTT), pp. 1-4, DOI: 10.1109/MWSYM.2013.6697492.
- [8] D. Ji and J. Kim. 2018. A Multiband Directional Coupler Using SOI CMOS for RF Front-End Applications. in *IEEE Microwave and Wireless Components Letters*, 28(2): 126-128, DOI: 10.1109/LMWC.2017.2783196.
- [9] S. Singh, R. P. Yadav and A. Jain. 2019. Miniaturized Dual-Band Branch-line Coupler with Folded Stubs. 2019 IEEE 5th International Conference for Convergence in Technology (I2CT), pp. 1-4, DOI: 10.1109/I2CT45611.2019.9033531.
- [10] Santhanam, Suganthi. 2020. Design of Multiband Hybrid Coupler with Open Circuit Stub. *International Journal for Research in Applied Science and Engineering Technology*. 8. 1683-1689. 10.22214/ijraset.2020.5273.
- [11] S. Raman, R. Augustine and A. Rydberg. 2014. Osseointegration analysis of skull implants using microstrip fed split ring resonator antenna. 2014 XXXIth URSI General Assembly and Scientific Symposium (URSI GASS), pp. 1-4, DOI: 10.1109/URSIGASS.2014.6930083.
- [12] Mohd Shah S. R., Velander J., Mathur P., Perez M. D., Asan N. B., Kurup D. G., Blokhuis T. J., Augustine R. 2018. Split-Ring Resonator Sensor Penetration Depth Assessment Using In Vivo Microwave Reflectivity and Ultrasound Measurements for Lower Extremity Trauma Rehabilitation. *Sensors*, 18, 636. <https://doi.org/10.3390/s18020636>



- [13]BDAS. 2019. An embedded system for Bone Density measurement Analysis (BDAS) for the diagnosis and monitoring of the healing of fractures in the health care and home care environment. [Online] Available: <http://www.bdas.se/#>
- [14]Pozar D. M. 2005. Microwave engineering (3rd ed.). New York: Wiley.
- [15]Muhammad N. A., Rahim S. K. A., Jizat N. M. *et al.* 2012. Beam Forming Networks Using Reduced-Size Butler Matrix. *Wireless Pers Commun* 63, 765-784. <https://doi.org/10.1007/s11277-010-0164-8>
- [16]R. K. Mongia, I. J. Bahl, P. Bhartia, J. Hong, and A. H. O. U. S. E.
- [17]Boston | London. RF and Microwave Coupled-Line Circuits Second Edition.
- [18]Li Hong Weng, Yu-Chun Guo, Xiao-Wei Shi and Xiao-Qun Chen. 2008. An Overview on Defected Ground Structure. *Progress in Electromagnetics Research B*, Vol. 7, 173-189, 2008. doi:10.2528/PIERB08031401
- [19]<http://www.jpier.org/PIERB/pier.php?paper=08031401>



Print ISSN: 0972-0529 , Online ISSN: 2100-0009

Volume 26,2023 | Issue 3

[Journal Home page](#)

[View Journal Contents](#)

[This issue](#)

Enter keywords, authors, DOI, ORCID etc

This Journal



Advance search

[Aims & Scope of the Journal](#)

[Editorial Board](#)

[Submission Guidelines](#)

[Past Editors](#)

[Abstracted/Indexed](#)

[View Journal Contents](#)

[Publication Ethics](#)

[Subscriptions](#)

Research Article

Steganalysis on data embedded medical image

J. Stella*, P. Karthikeyan, S. J. Thomas Schwarz & S. J. John Rose

Pages 767-777 | Published online: 01/04/2023

<https://doi.org/10.47974/JDMSC-1753>

[Abstract](#)

[References](#)

[Download Pdf](#)

[Download C](#)

Keyword :

[Steganography](#)

[Steganalysis](#)

[Least significant](#)

Subject Classification :

[94A13](#)

S. J. John Rose

Department of IT
Xavier Institute of Engineering
Mumbai
India

0000-0001-8487-5370

johnrose@xavier.ac.in

38

Views

0

CrossRef
citations to
date

0

Altmetric

Abstract

Cybercrime around the world is increasing day by day abruptly. Stego attack is one of the popular methods of transferring the message secretly through the cover medium. Most of the sources are using this process for covert communication. The paper discusses the importance and analysis of data hiding theft and covert communication process through steganalysis where it talks about the "covered writing" in such a way that the mutation of an image is not discernible. The main motive of this paper is to attack and analyze the Digital Imaging and Communications in Medicine (DICOM) file format. The file format DICOM discussed in this research is mostly supported in the medical field. CT Scans and MRI Scans are widely used in hospitals to view the human body. The random pixels is chosen to hide the text on the DICOM formats and the performance is measured using different metrics. The proposed approach produces 100% recovery of the hidden text inside an image with maximum payload capacity.



Digital Reconstruction of Underwater Submerged Objects Using 3D Photogrammetry Techniques

Pradeep Kumar G¹, Sridevi B², Suveetha Dhanaselvam P³

Abstract

The proposed work has been conceived to achieve the exact measurement of objects underwater for archaeological study in the exploration of vanished cities like Poompuhar and Dwarka. The proposed work of Digital reconstruction is mainly used to identify the existing cultural behaviors, traditions, technologies and more. 3D photogrammetry is one of the fabulous techniques, which can be used for measuring any object by keeping a reference object with it. Modified SFM (Structure from Motion) is the algorithm used for generating 3D model of target object using dataset. Underwater imaging and processing are challenging tasks since the features of each image dataset get varies according to the physical properties of ocean water. The modified algorithm is tested in different underwater real time data set and could produce the satisfied result. Multiple snaps of the target object are taken across a 360-degree axis, by the in house ROV (Remotely Operated Vehicle) which was developed in our research lab. After image preprocessing and enhancement of dataset, 3D mapping of target object is generated. Using the reference object which is kept along with the target object, the target object can be measured easily in terms of length, width and volume. This proposed work helps the archaeologists for exploring the vanished traditional ancient cities.

7986

Key Words: 3D; ROV; SFM

DOI: 10.14704/ng.2022.20.6.NQ22794

NeuroQuantology 2022; 20(6): 7986 -7999

Introduction

The cities like Poompuhar and Dwarka are the most important and flourishing port cities which have attracted maritime traders from all over the world in olden days. Due to its fabulous architectural design and the narrations about culture and civilization, it has been the arena of attraction for the historians, archaeologists and other researchers from different fields since the beginning of the 20th century. Underwater archaeological explorations have revealed a large number of stone structures of semicircular, rectangular and square in shape and were randomly scattered over a vast area in the land region and offshore in proximity to present Poompuhar. From the literature it is inferred that some tectonic movements and 'kadalkol' (swallowing up of land by sea) might have

led to the submergence of Poompuhar. Despite several researchers and under water archaeological exploration, no comprehensive information is available to explain the history of Poompuhar. Of course, this would require a larger and more detailed inter disciplinary/inter-institutional collaborative study. However, to holistically understand all, the mandatory prerequisite is the location and spread of the dilapidated structures of Poompuhar. This could be achieved by capturing underwater photographs, digital processing of such photographs, identifying the structures, objects and their distributions.

All types of digital photographic data [1] [2] while using digital technique will have to undergo three stages which are pre-processing, enhancement and display the data extraction.

Corresponding author: Pradeep Kumar G

Address: ^{1,3}Velammal College of Engineering and Technology, Madurai, 625009, India. ²Velammal Institute of Technology, Chennai, 601204, India

Email:

prad.mypassion@gmail.com



In addition to underwater photography, underwater range scanning techniques are also used in underwater exploration, providing new

tools to represent the seafloor. These scans acquired by underwater vehicles usually result in an unstructured point cloud.



Figure 1: Underwater imaging of Terracotta

But on giving the common command for downward-looking or forward-looking configuration, these sensors recover a piecewise data linear approximation capable of approximating these 3D points using a height map. Apart from the invention of objects from the image in Fig. 1, it is also essential to determine the spatial change that has occurred in the past years. Hence we also focus on topography, which is the result of complex interactions between anthropogenic activities and natural processes. Analysis of short-term spatial change in this dynamic environment is decisive for sustainable coastal management. Traditional monitoring methods rely on survey transect approaches rather which are time consuming and require substantial manual processing.

The next segment of exploration [3][4] is to provide 3D modeling of the target area/object, using the available data. In order to implement this, 3D photogrammetry can be used to produce an exact measurement of the target area. From the literature[5][6], it is proved to be an efficient method to accomplish the temporal studies of coastal areas by means of post processing of images collected from unmanned vehicles. The unmanned system incorporates a full HD wide angle camera capable of capturing images suitable for post processing techniques such as developing a 3D orthomosaics model and for carrying out 3D photogrammetric measurements. The proposed work encompasses on the delivery of processed

image dataset as 3D printed object of the target area/object using a 3D printer.

2 Literature Survey

The underwater archaeological process becomes a bit challengeable where the features of dataset are not very clear and stable, hence each and every 2D image of the dataset of particular object gets varied due to water currents, minimal amount of light and general underwater noises. These disturbances varies for each ocean. Hence a particular algorithm for underwater image processing is not suitable for the all kinds of dataset. In the literature survey, different algorithms were studied and a method was derived which yielded almost the exact result.

Ricard Campos & Rafael Garcia et.al proposed Surface Reconstruction Method for In-Detail Underwater 3D Optical Mapping. Images acquired by underwater robots usually result in an unstructured point cloud, but given the common downward-looking or forward-looking configuration of these sensors with respect to the scene, the problem of recovering a piecewise linear representing the scene is normally solved by approximating these 3D points using a height map (2.5D). The method presented is robust to common defects in raw scanned data such as

7987

outliers and noise often present in extreme environments like underwater both for sonar and optical surveys. This property leads to wide application of any kind of range scanning technologies and we demonstrate its versatility using it on synthetic data, controlled laser-scans, and multi beam sonar surveys. Finally, and given the unbeatable level of detail those optical methods provide, we analyze the application of this method on optical datasets related to biology, geology and archaeology.

O.Willes et al.[7] proposed the Single and Multi-View Reconstruction by Learning from Silhouettes. It presented strategies and solutions to tackle the problems of very large underwater optical surveys (Giga mosaics), presenting contributions in the image preprocessing, enhancing, and blending steps, resulting in an improved visual quality in the final photomosaic. A comprehensive review of the existing methods is also presented and discussed. A photo mosaicking pipeline has been conceived to address the most relevant problems particular to underwater imaging. Nevertheless, the application field of the presented approach can be extended to the generation of conventional panoramas of terrestrial or aerial images.

Pierre Drap et al.[8] presented a Case Study in Underwater Photogrammetry and Object Modeling of Xlendi Wreck in Malta. Two major issues are discussed in this paper. The first concerns deep-sea surveys using photogrammetry from a submarine. Here the goal was to obtain a set of images that completely covered the selected site. Subsequently based on these images, a low-resolution 3D model is obtained in real-time, followed by a very high-resolution model produced back in the laboratory. The second issue involves the extraction of known artifacts present on the site. This aspect of the research is based on prior representation of the knowledge involved using systematic reasoning. Two parallel processes were developed to represent the photogrammetric process used for surveying as well as for identifying archaeological artifacts visible on the sea floor. Mapping involved the use of the CIDOC-CRM system (International Committee for Documentation(CIDOC)—Conceptual Reference Model) which is a system that has been previously utilized to in the heritage sector and is largely available to the established scientific community.

D.t. Rezende, S. A. Eslami, S. Mohamed, P. Battaglia, M. Jaderberg, and N. Heess [9] proposed the work of Unsupervised learning of 3D structure from

images. This work describes the model for learning the features of 2D images by comparing two or more different images and extracting a single cloud point. This model is best suitable when the features of the image dataset are highly accurate and clear.

M. Feng, S. Zulqarnain Gilani, Y. Wang, and A. Mian [10] proposed the 3D face reconstruction from light field images: A model-free approach. By dividing all pixels of a noisy image into edge region or non-edge region, the different strategies and parameters are adopted in the edge-based bilateral filter to balance the conservation of image features and the reduction of noise level. After the process, the mathematical modeling of 3D face reconstruction becomes quite easy with the process. This model can be helpful for the outdoor image dataset.

J. K. Pontes, C. Kong [11] proposed the Compact model representation for 3D reconstruction which has clearly explained the development of mathematical modelling for the underwater 3D reconstruction for different kinds of noisy images dataset. This model also includes the removal of noisy or unwanted pixels from the 3D surface, so that the target object is focused to retrieve the 3D model.

F. Alidoost, H. Arefi [12] proposed the Comparison of UAS-Based Photogrammetry Software for 3D Point Cloud Generation: A Survey over a historical site. This detailed study has clearly described the 3D cloud generation from the dataset taken by UAS systems. Most of the mathematical modelling supports the outdoor images dataset taken by drones and other unmanned aerial systems. The video is converted into frames and each frame will be considered for the process of 3D modelling. This model also supports the elimination of unwanted frames which leads to false cloud generation.

The underwater imaging is the critical task. So, it is important to eliminate the following parameters which affect the generation of the image dataset. In the outcome of survey of different papers, the proposed work of preprocessing technique for the 3D reconstruction has almost overcome all of the imaging barriers mentioned below.

2.1 Density

Water is 800 times denser than air and is capable of holding matter in suspension through which we have to take our underwater photographs. Hence, the density of ocean water might turn out to be a problem while capturing the images.

7988



2.2 Loss of Light

Water acts as a very efficient mirror and sponge, as it reflects back any light rays which hits the surface greater than the angle of 45 degrees. As you dive the light levels get progressively dimmer, in addition, the spectrum of light narrows as red light is diminished.

2.3 Loss of Color

What looks vibrant above water doesn't anymore when you are under the sea. The clean water has a strong cyan or blue/green cast and absorbs different colors at different rates. As a general rule, the result is that red is absorbed at approximately 15 feet, oranges at 30 feet, yellows at 60 feet and greens at 80 feet. This leaves the blue and black which doesn't have scope for color photography.

2.4 Loss of Contrast

The visibility under the water reduces the horizons. 100 foot Vis on land causes major aggravation but would be ideal for the underwater photographer. Not only does it limit your horizons it also reduces the contrast and this in turn affects the clarity of your shots. With black and white film the blacks are grey and the whites aren't clean whilst with color film the colors are muted.

2.5 Refraction

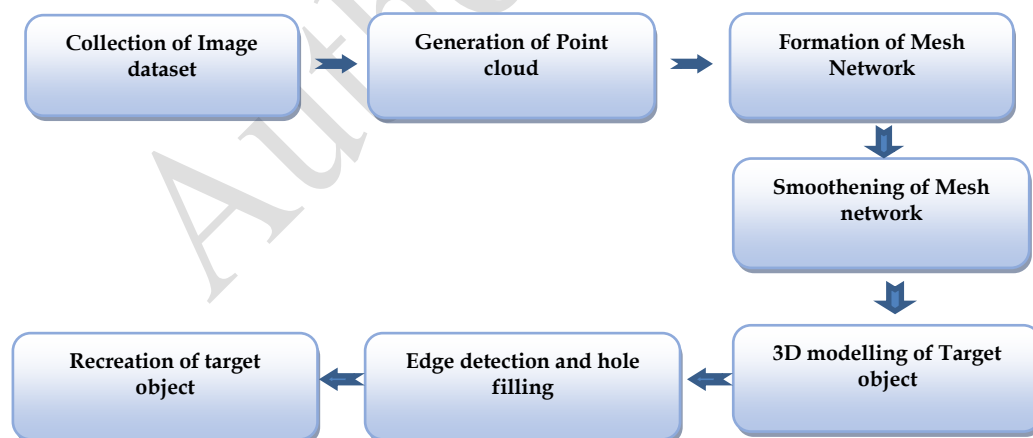
When light travels from air to water it slows down as it meets the denser medium. This is a kind of problem if all light rays could cross the dividing line at right angles.

2.6 Magnification

In addition, refraction causes a magnifying effect which makes objects appear to be 1/3rd larger and therefore nearer. Imaging is a technique in which the data from an image are digitized in order to create an enhanced image. Enhanced image and object/target detection is highly needed to aid in this research. After generation of Image dataset, the images will be enhanced before the process.

3 Proposed Work

The proposed work consists of several stages (Fig. 2) of 3D modelling process. The reconstruction [13] of semi structure of target object is implemented using the hole filling process. The work supports the underwater archaeologists in retrieving the real data of the target object, which is necessary to reveal the tradition, trade and culture hidden behind it. The work progress starts with the preprocessed underwater optical images.



7989

Figure 2: Process of 3D reconstruction

The industry readymade ROV (Remotely operated vehicle) is used for collecting the image dataset. The ROV is controlled and made

to move in a spiral pattern around the target object, for the collection of optical images. The bottom and top view of the target object is also

collected. Before the 3D modelling process, selective images are taken for preprocessing which includes enhancement, resizing and noise removal. This step helps out in extracting the features of images.

Point Cloud Generation:

Multiple images [14] of the target object are rendered from different viewpoints in 8 directions. The quality of the images depends on the camera specifications. The position of particular point is uniformly sampled on the sphere of radius. Using the VGG16 convolutional neural network, the vector of each image is extracted. By comparing the features of nearest object model which is obtained and stored in database, the similarity between the two vectors is measured by cosine distance which

can be defined as,

$$\text{Similarity}(a, b) = \frac{ab}{\|a\| \|b\|}$$

(1)

The voxel based approaches [15] is a sensitive process which is used to measure the distance between the two point sets. Where ω and τ are the point sets.

$$d_{cd} = \sum_{\omega \in S1} \min_{\tau \in S2} \|\omega - \tau\|_2^2 + \sum_{\omega \in S2} \min_{\tau \in S1} \|\omega - \tau\|_2^2$$

(2)

The picture (Fig. 3) is a broken part of a terracotta which is taken for the field test and the point cloud is generated as per the algorithm.

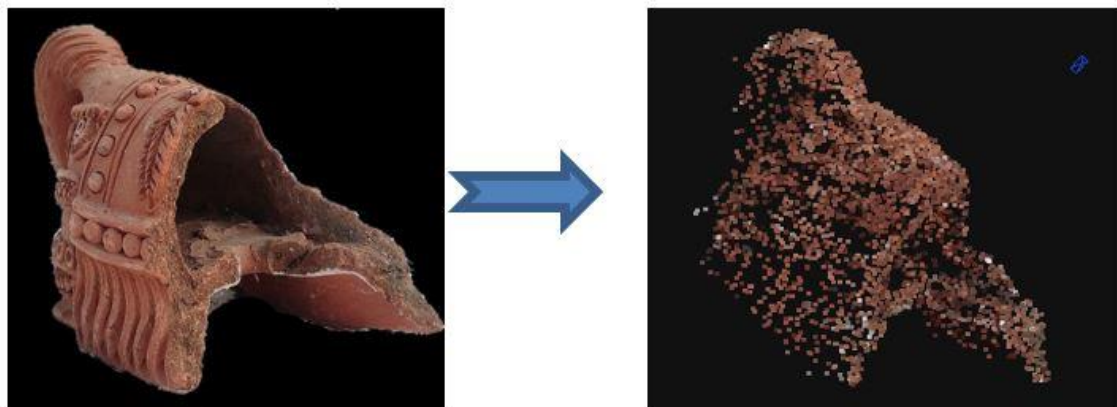


Figure 3: Cloud point generation

The mesh is a set of faces [16], vertices and edges defined as \hat{f} , \hat{v} , \hat{e} respectively,

$\hat{m} = \{\hat{v}, \hat{e}, \hat{f}\}$. Formation of mesh network is the next step of point cloud generation. The points which are generated by the algorithm are connected by an edge with the neighbor vertices and it forms the mesh network which produces the structure of 3D object. The edge prediction [17] of connection of vertexes depends on the previous vertices.

$$p(\epsilon) = \prod_{i=2}^n P(\vec{e}_i | \vartheta_1, \dots, \vartheta_i, \vec{e}_1, \dots, \vec{e}_{i-1})$$

(3)

In the above equation, ϑ and e are vertex and edge

for each point. The above relationship is used for finding the single edge connection between two vertices instead of going for multiple connections for the same vertices. The point cloud latent vector produces the exact structure of the object.

$$h_i = f_t(h_{i-1}, e_{i-1}, z)$$

(4)

The Fig. 4 shows the edge prediction is determined by the parameter θ_i , and this process continues till all the point cloud is connected with the other vertex.

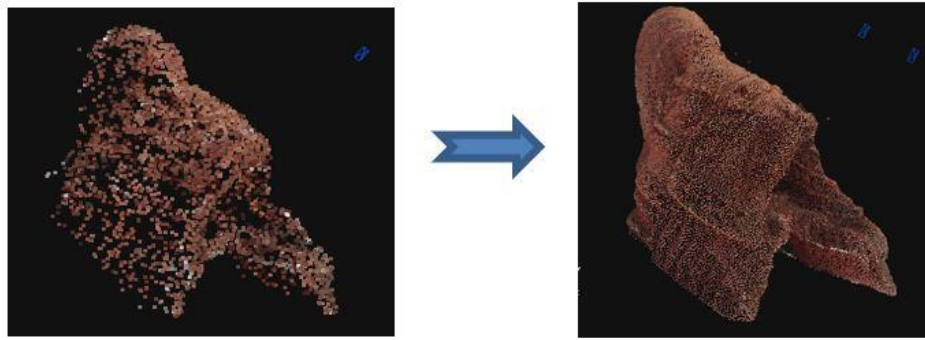


Figure 4: Generation of dense cloud point

Smoothing and 3D model generation:

Visual masking [18] is the opted process which smoothens the hard surface by decomposition of appropriate plane in the surface of 3D model. Before starting the decomposition process, modified filter is used to filter the different spatial frequencies which are measured in the plane. The filter can be represented as,

$$\mathcal{F} = A_i \left[e^{-x^2/\sigma_{x1i}^2} - B i e^{-x^2/\sigma_{x2i}^2} + C i e^{-x^2/\sigma_{x3i}^2} \right] e^{-y^2/\sigma_{y1i}^2}$$

Where x and y are spatial indexes or positions, A_i is the maximum gain and different scaling of Gaussian adopted to filter different spatial frequencies. The above equation states that decomposition process using the filter which is more suitable for this particular dataset. The smoothing process shown in Fig. 5 is an important step which gives the clear view of the structure of the target object.

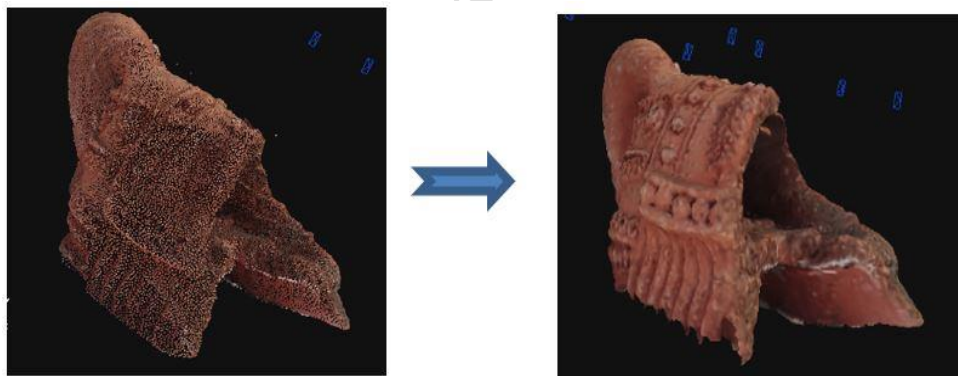


Figure 5: Formation of Mesh network

Hole Filling Process – The reconstruction:

The work comprises three major steps : i) Extracting the boundary and detecting the incomplete structure or hole ii) fixing the target region filled by appropriate pixel values using geometrical feature extraction iii) Decomposing the empty region into recovered region

Step1 : Consider the empty region E, in a three dimension object O and the extracted boundary points E_b using the nearest neighbor algorithm. Hence $E_n = O(E)$ is the extracted around the empty region.

Step 2: Extraction [18][19] of feature and decomposition of neighborhood region is the next

process. The Riemannian manifold (M, g) will be calculated at each point p. The parameter is calculated in each point,

$$d_s^2 = \sum_{\mu=1}^n \sum_{\vartheta=1}^n g_{\mu\vartheta} dx^\mu dx^\vartheta \quad (6)$$

Where dx^μ, dx^ϑ are the contravariant tangent vectors [20] [21] which defines the neighbor points E_n . For the non-uniform plane, the relationship between these two symbols can be related by the equation.

$$\Gamma_{\mu\nu}^\sigma = \frac{1}{2} \sum_{\rho=1}^3 g^{\sigma\rho} \left\{ \frac{\partial g_{\mu\vartheta}}{\partial x^\vartheta} + \frac{\partial g_{\rho\vartheta}}{\partial x^\mu} - \frac{\partial g_{\mu\vartheta}}{\partial x^\rho} \right\} \quad (7)$$

So the pair of those parameters mentioned is as follows,

$$O(E) \rightarrow \psi(M_i, g_i)$$

(8)

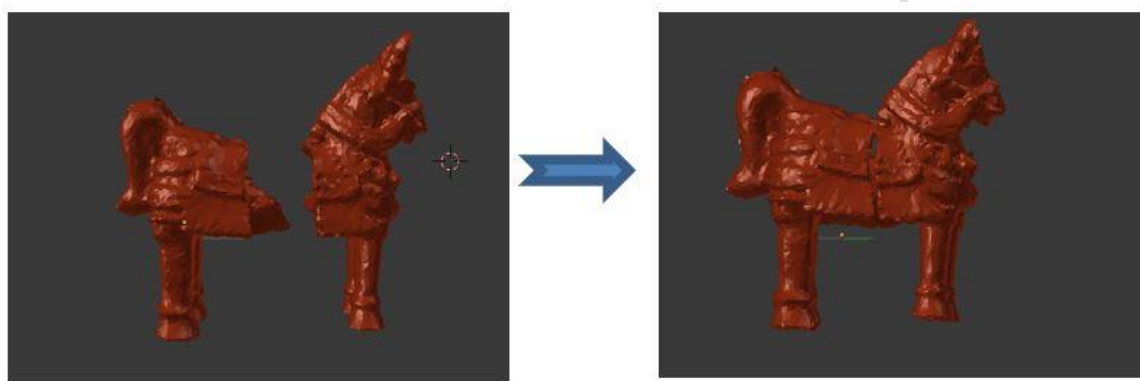
According to the neighborhood region, the framework chooses any form of shape to fill the empty region with consideration of two main parameters which we have discussed earlier and those can be related as,

$$E_n = \alpha(\Gamma, g) + \beta(\Gamma, g) + \gamma(\Gamma, g)$$

(9)

Pair of two parameters (Γ, g) considered for decomposition process and the α, β and γ are the constants.

Step 3: After choosing the shape of selected pixels, decomposition [22] [23] of pixels into the empty region is processed, so that the empty part of 3D modelling object is filled with the neighbor region pixels shown in Fig. 6



7992

Figure 6: Hole filling of 3D terracotta

4 Experimentation Results

Preprocessing of the images is the prime part before moving on to the reconstruction or 3D modelling

process. If the data is clear in the image, the generation of 3D modelling process may require less number of 2D images which are taken in a spiral pattern.



Figure 7: Preprocessing of a terracotta

The dataset is acquired from Rameshwaram Ocean and Poompuhar Ocean for the field test. The lighting was low under the Rameshwaram Ocean even though the vehicle was entailed with

underwater lighting. The preprocessing work was done based on an algorithm, written in python programming language. The above shown Fig. 7, is a sample preprocessing work of a terracotta which was taken under the ocean.

A pot was taken as another target object for the study and the results of enhancing 2D underwater

image was highly satisfactory for the next process of reconstruction. The exact preprocessing work is about extracting the features of the target object which is helpful for the 3D modelling. The enhanced image of the pot is shown in the Fig. 8 where maximum texture of the image was retrieved.

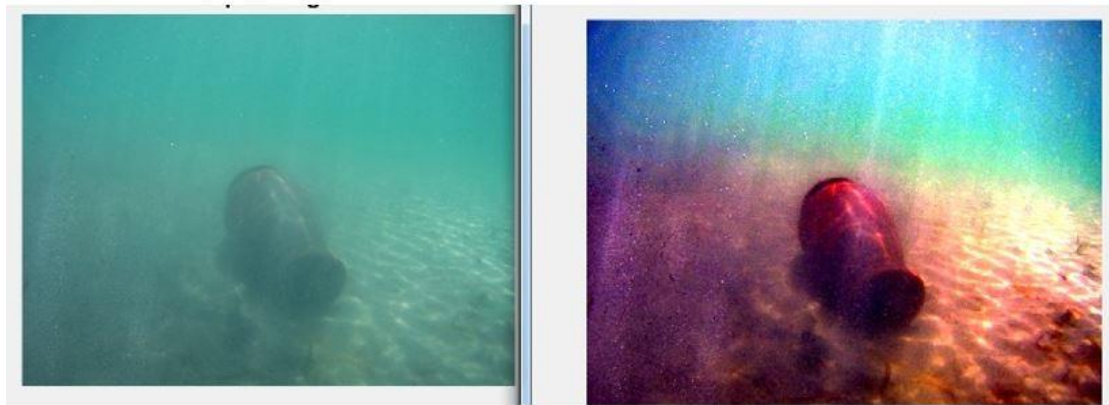


Figure 8: Enhanced image of an underwater pot

The reconstruction and 3D modelling of different objects have been taken for study and the results have come up with considerable accuracy. The aim of this project is to visualize the destroyed Poompuhar city in digital form that reveals the culture, tradition and trade during that period. Hence different image datasets is taken outdoor and underwater. The mathematical model supports especially for the underwater dataset. Generation of 3D model from the underwater image dataset is

quite critical since it has lots of noises. After preprocessing, the extraction of features from the target object is another challenging task. Extraction and preprocessing are the supporting process which helps in 3D reconstruction and modelling. Hence lot of study and process has made for the 3D model with the different image dataset. So, for the field study a few objects like terracotta, statue, brick and broken parts of terracotta were taken and the results are shown as follows,

7993

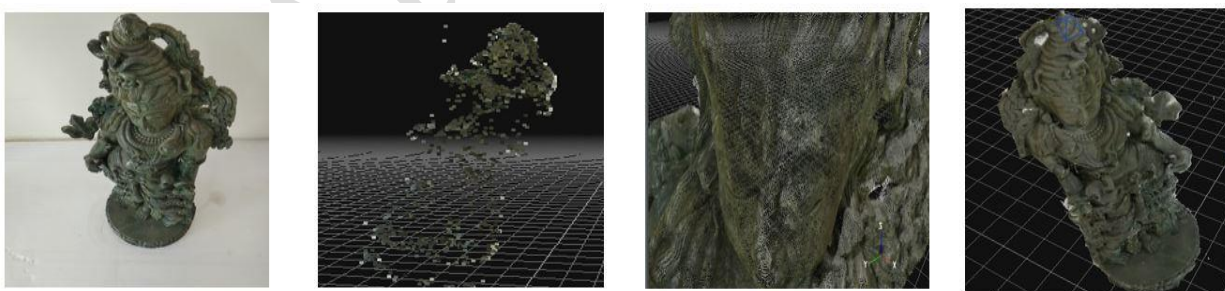


Figure 9: 3D Modelling of a metal statue

The above result (Fig. 9) is a metal statue taken in landform for the 3D modelling study. Almost 70 images were captured in the aspect ratio of 4:3, while moving the ROV in a spiral fashion. 40 images

of bottom view and 30 images of top view of the statue were captured. The python coding platform was utilized to construct the 3D structure of the metal statue. A few calibrations had been made by adding more images to get the exact 3D structure.

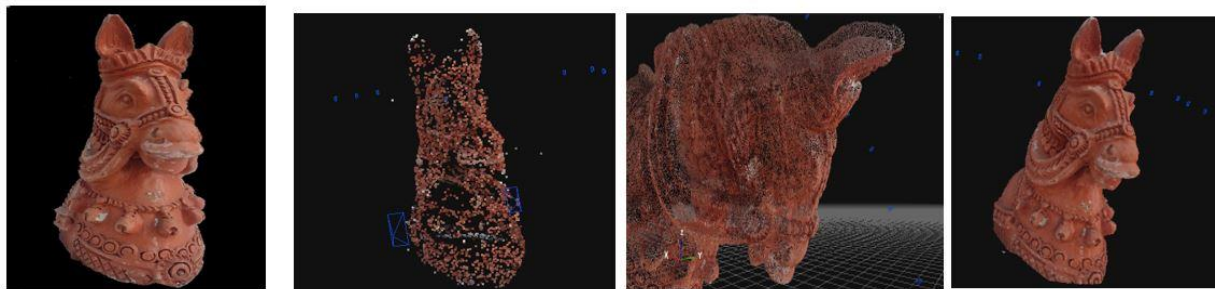


Figure 10: 3D modelling of a head of a terracotta horse

A terracotta horse (Fig. 10) was taken for field study. Initially, the complete structure of the terracotta was kept in the ocean and multiple images were captured using ROV. Later, the terracotta was broken into multiple pieces and the 3D modelling of each piece were considered. Only the head of the terracotta horse were considered

and 80 to 90 images of the same were captured. In case of clean water, the features can be extracted easily and it might require just 40 to 50 images for 3D model generation. In case of turbid water, we may need to take more 2D images, in order to retrieve the features of the target object.

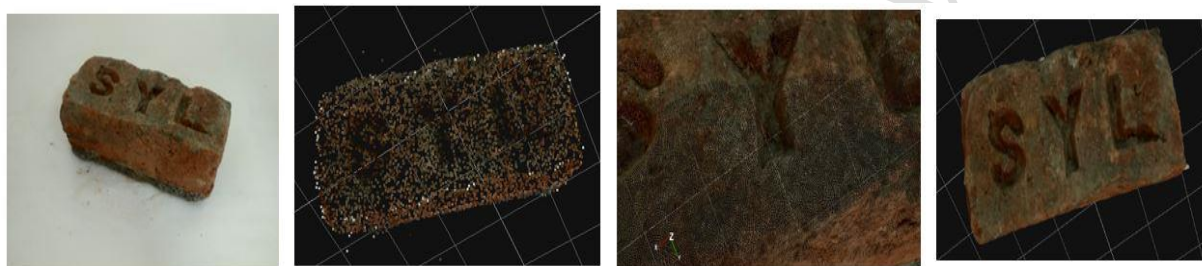


Figure 11: 3D modelling of a brick

A brick (Fig. 11) was taken for 3D modelling study, and 60 images were captured to produce accurate 3D structure of the brick. The amazing

detail of this study is that the text pattern engraved on the brick was also recovered during the 3D reconstruction process.

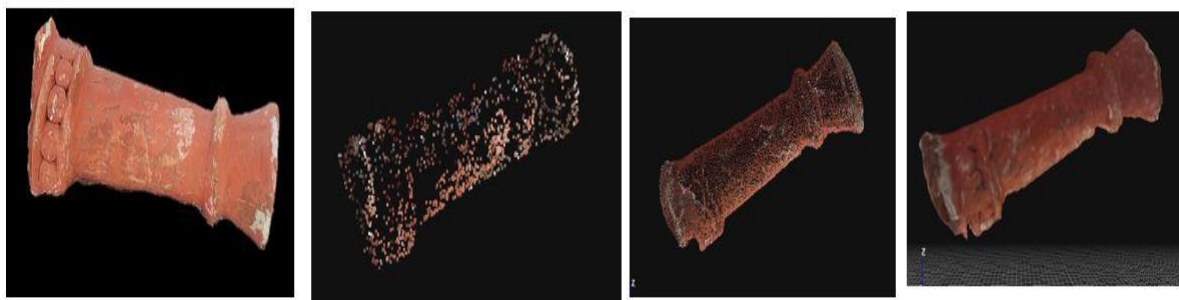


Figure 12: 3D modelling of a leg of a terracotta horse

During the reconstruction of the leg of the terracotta horse (Fig. 12), the features all over the leg were similar. Thereby only a few 2D images

were required for the feature matching process, making the process a lot easier.



Figure 13: 3D modelling of broken terracotta

The terracotta (Fig. 13) was broken into multiple pieces and the whole part was considered for the 3D modelling. The sand area in the image was removed during the 3D modelling process, by setting the threshold for feature extraction set. This calibration work was done by modifying the python algorithm.

For the reconstruction of object, the broken part of terracotta and the mug were taken for study. The

results produced the exact structure of the target object as shown in Fig. 14. The terracotta is considered as the prime object since the project work depends on the exploration of the tradition and culture of Poompuhar city. Hence terracotta is a suitable object which is very similar to the real time objects which are under Poompuhar Ocean.



Figure 14: Reconstruction of Terracotta

The reconstruction of mug (Fig. 15) is another approach to the reconstruction process. For this study, half portion of the mug was deployed in sand and the other half is visible. Since the feature mug around all the side is same, the replication of

mirrored object was joined together using modified reconstruction python algorithm. Almost the 90% of the total structure was recovered. The resulting 3D model was evaluated with the original structure and showed the highest accuracy level of 3D model of the mug.

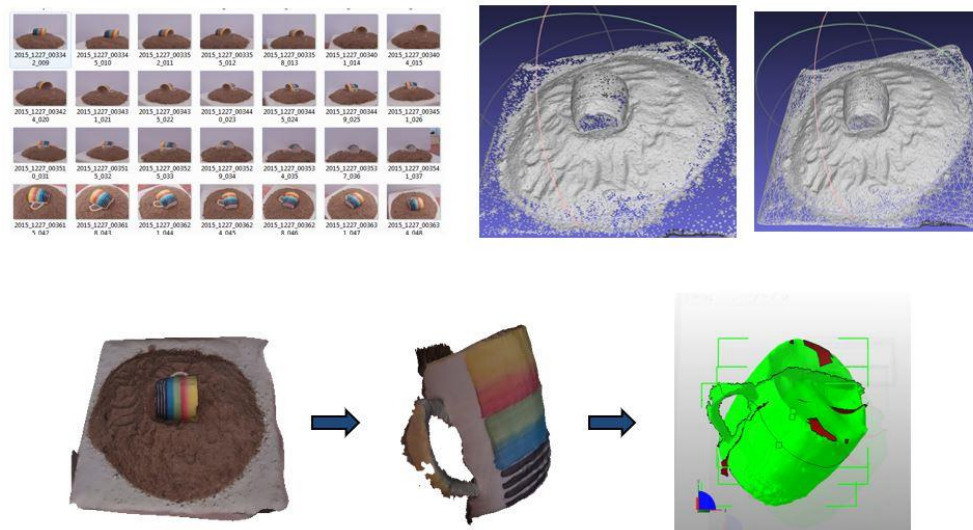


Figure 15: Reconstruction of Mug

In the proposed work, different steps of algorithm were carried out. Also the obtained results were more accurate as multiple field study was done.

The 3D model of the target object and the target object, which is a head of terracotta horse is considered. The 3D model of the target object is scaled down and was finally compared with the

target object based on the physical parameters to find the accuracy of our 3D reconstruction work. The physical parameters were measured using a 3D viewer software. The point-to-point measurement tool of the software, was used to simply locate and click the point on the surface of the model where we need the measurement. The measurement process is depicted in the following images:

7996

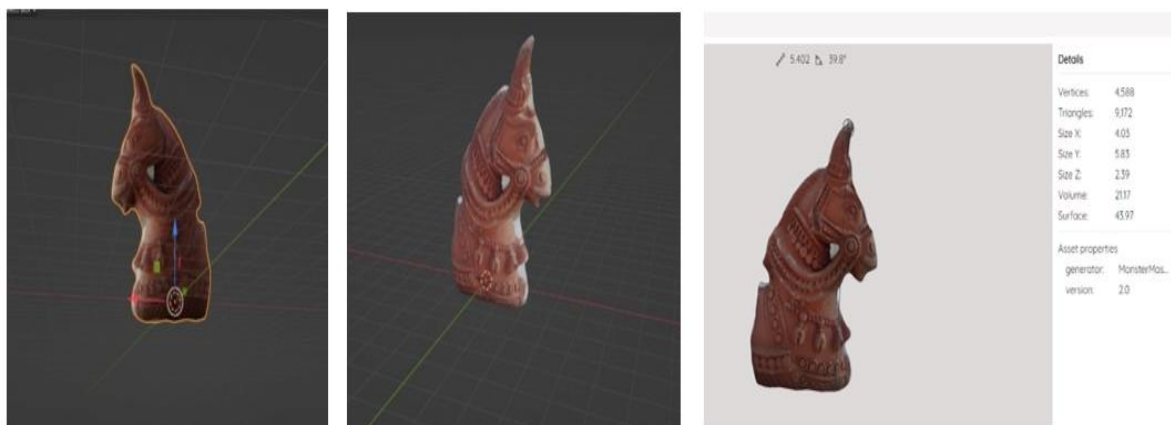


Figure 16: Measurement of Terracotta's Head

The 3D model of the terracotta horse was printed using a 3D printer and the images of the 3D printed model are as shown below. The resulting 3D printed model had almost similar structure and texture of

the terracotta horse which is notable in the first image. The results were remarkable due to the efficient hole filling process.



Figure 17: Comparison of Real object and 3D printed object

The hole filling process effectively helped in completing the surface of the 3D model with a realistic appearance, thereby improvising the structure of the model effectively. Due to the efficient pre-processing of the dataset and the hole filling processes, which were done during the

reconstruction phase of the 3D model the accuracy of our work was boosted to 95% approximately. The tabulation of the parameters used to compare the terracotta horse and the 3D model of it is depicted below:

Table 1: Comparison table of 3D model and target object

Parameters	3D Model	Target Object
Height of the terracotta	5.402 cm	48.2 cm
Circumference of the body	2.776 cm	24.2 cm
Height of a Horn	0.5 cm	5.2 cm
Circumference of the neck	2.311 cm	20.9 cm
width	3.1 cm	28.8 cm
Distance between the forehead and muzzle	2.63cm	23.6cm
Distance between neck and body	1.86 cm	16.7cm
Distance between the two horns	1.58cm	14.5cm
Vertices	4588	
Number of edges for sub-zone in the neck	664	
Total number of meshes	9172	

7997

5 Conclusion

The paper discusses the methods and algorithms to explore the submerged cities. The real time underwater images are captured in the vanished city, Poompuhar using ROV. The images are enhanced, broken submerged objects are reconstructed and their overall structure is modelled using novel efficient algorithms. The results projected showcases submerged objects, their 3D model and it also helps to find the timeline,

connecting the place with the past history. This work is also useful for archaeologists to study the trade and culture of the submerged cities.

Acknowledgement

The project has been funded by Department of Science and Technology (DST) for the project, "Image Pre-Processing, Enhancement, 2D Mosaicing and 3D Reconstruction Of Submerged Features / Objects For Digital Reconstruction Of

Poompuhar City Puhar-UW Photo” under the scheme Interdisciplinary Cyber Physical Systems (ICPS) and it’s gratefully acknowledged.

Funding Statement: Funded by ICPS, DST (Grant number:DST/ICPS/DIGITAL POOMPUHAR/2017) Principal Investigator: Dr.B.Sridevi, Professor & Head, ECE Department, Velammal Institute of Technology, Chennai. Co PI : Dr.P.Suveetha Dhanaselvam, Associate professor, ECE department, Velammal College of Engineering and Technology, Co PI: G.Pradeep Kumar, Assistant Professor, Velammal College of Engineering and Technology

Conflicts of Interest: The authors declare that they have no conflicts of interest to report regarding the present study.

References

- A. Irene, C. Filiberto, L. Andrea Lingua and N. Francesca, “Recent trends in cultural heritage 3D survey: The photogrammetric computer vision approach,” *Journal of Cultural Heritage*, vol. 32, no.27, pp. 257-266, 2018.
- A. Johnston, R. Garg, G. Carneiro, I. Reid and A. van den Hengel, “Scaling CNNs for high resolution volumetric reconstruction from a single image,” in *Proc. IEEE International Conference on Computer Vision workshop*, Venice, Italy, pp. 939-948, 2017.
- G. Yang, Y. Cui, S. Belongie and B. Hariharan, “Learning single view 3D reconstruction with limited pose supervision,” in *Proc. European Conference on Computer Vision*, Munich, Germany, pp. 99-105, 2018.
- X. Luan, Y. Xie, L. Ying and L. Wu, “Research and development of 3D modeling” *International Journal of Computer Science and Network Security*, vol. 8, no.1, pp. 49-53, 2008.
- X.F. Han, H. Laga and M. Bennamoun, “Image-based 3D object reconstruction: state-of-the-art and trends in the deep learning era,” *IEEE Transaction on Pattern Analysis and Machine Intelligence*, vol. 43, no.5, pp. 1578-1604, 2019.
- R. Campos, R. Garcia and P. Alliez, “A Surface reconstruction method for in-detail underwater 3D optical mapping,” *The International Journal of Robotics Research*, vol.1, no. 34, pp. 64-89, 2014.
- O. Wiles and A. Zisserman, “SilNet: Single-and Multi-view reconstruction by learning from Silhouettes,” in *Proc. The British Machine Vision Conference*, Honolulu, USA, pp. 1711-1726, 2017.
- P. Drap, D. Merad, B. Hijazi and L. Gaoua, “Underwater photogrammetry and object modeling: A case study of xlendi wreck in malta”, *Sensors and Techniques for 3D Object Modeling in Underwater Environments*, vol.15, no.12, pp. 30351-30384, 2015.
- D. T. Rezende, S. A. Eslami, S. Mohamed, P. Battaglia, M. Jaderberg et al., “Unsupervised learning of 3D structure from images,” in *Advances in Neural Information Processing Systems*, vol. 29, no. 311, pp. 4996-5004, 2016.
- M. Feng, S. Zulqarnain Gilani, Y. Wang and A. Mian, “3D face reconstruction from light field images: A model-free approach” in *European Conference on Computer Vision*, vol. 15, no. 193, pp. 501-518, 2018.
- J. K. Pontes, C. Kong, A. Eriksson, C. Fookes, S. Sridharan et al., “Compact model representation for 3D reconstruction,” in *Proc. International Conference on 3D Vision*, pp 88 – 96, 2017.
- F. Alidoost and H. Arefi, “Comparison of UAS-based photogrammetry software for 3D point cloud generation: a survey over a historical site,” *Remote Sensing and Spatial Information Sciences*, vol. 4, no.4, pp. 55-61, 2017
- C.-H. Lin, C. Kong and S. Lucey, “Learning efficient point cloud generation for dense 3D object reconstruction,” in *Proc. Conference on Artificial Intelligence*, vol. 1706, no. 237, pp. 1185-1196, 2018.
- A.M. Manferdini and F. Remondino, “Reality-based 3D modeling, segmentation and web-based visualization” in *Proc. Digital Heritage*, Cyprus, Berlin, New York, pp. 110-124, 2010.



- J.Y. Su , S.C Cheng , C.C Chang and J.M Chen, "Model-Based 3D pose estimation of a single RGB image using a deep viewpoint classification neural network," *Journal of Applied Sciences*, vol. 12, no. 9, pp. 2478-2491, 2019.
- X. Z. Xingyuan Sun, Jiajun Wu and Z. Zhang, "Pix3D: Dataset and methods for single-image 3D shape modeling," in *Proc. Computer Vision and Pattern Recognition*, Salt lake city, New York pp 2974 – 2983, 2018.
- S. Tulsiani, A. A. Efros and J. Malik, "Multi-view consistency as supervisory signal for learning shape and pose prediction," in *Proc. IEEE conference on Computer Vision and Pattern Recognition*, Salt lake city, New York, pp. 2897 – 2905, 2018.
- X. Han, Z. Li, H. Huang, E. Kalogerakis and Y. Yu, "High resolution shape completion using deep neural networks for global structure and local geometry inference," in *Proc. IEEE conference on Computer Vision and Pattern Recognition*, Honolulu, USA, pp. 85–93, 2017.
- M. Aernouts , B. Bellekens and M. Weyn, "MapFuse: Complete and realistic 3D modelling", *Hindawi*, *Journal of Robotics* ,vol. 2018, no. 4942034, pp. 1-13, 2018.
- F. Remondino and S. El-Hakim, "Image-Based 3D modelling: A Review," *The Photogrammetric Record* vol. 21, no. 115, pp. 269–291, 2006.
- S. Cho, S.G. Choi, D. Kim, K. Lee and C.B. Sohn, " How to generate image dataset based on 3D model and deep learning method" *International Journal of Engineering & Technology*, vol. 7 no. 3.34 , pp. 221-225, 2018.
- Y. Feng, Y. Feng, H. You, X. Zhao and Y. Gao, "MeshNet: Mesh neural network for 3D shape representation," in *Proc. AAAI conference on Artificial Intelligence*, Honolulu, USA, pp. 8279-8286, 2019.
- L. Li , F. Yang , H. Zhu , D. Li, Y. Li et al., "An improved RANSAC for 3D point cloud plane segmentation based on normal distribution transformation cells," *Remote Sensing*, vol. 9, no. 5 pp. 433-448, 2017.

SAR reduction techniques for WBAN and mobile applications

Vijay Gokul Selva Rajan , Kavitha Kaliappan und Suresh Kumar Natarajan

Aus der Zeitschrift **Frequenz**

<https://doi.org/10.1515/freq-2022-0297>

Abstract

In recent years there has been a substantial growth in the usage of wireless gadgets in various fields like mobile communication, health monitoring, warfare communications, etc. However, the performance of the antenna is evaluated by the parameters like gain, directivity and bandwidth, VSWR and is enhanced as a continuous process. But on the other side, Specific Absorption Rate (SAR) is a parameter that is likely to be watched out for the safety concern which should be as low as possible for any antenna to ensure the minimum risk to human health. Many researchers have contributed an enormous amount of work to the SAR reduction. From this perspective, this work proposes a brief survey on low SAR antennas. An optimal low SAR antenna needs a perfect lossless impedance matching over a lossy medium (human body) for the eradication of spurious surface waves. The deployment of SAR reduction strategies, outcomes of the design, and open-end research challenges with the relative results are addressed as a part of the survey. The core impulse of this work is to induct the antenna designers to get indulged in designing low SAR antenna with enhanced performance for several WBAN applications like health monitoring and many more.

Keywords: [artificial magnetic conductor](#); [defected ground plane](#); [electronic band gap](#); [meta structures](#); [SAR reduction](#)

Corresponding author: **Vijay Gokul Selva Rajan**, Department of Electronics and Communication Engineering, Velammal College of Engineering and Technology, Madurai, Tamil Nadu, India, E-mail: svgmdu@gmail.com

Author contribution: All the authors have accepted responsibility for the entire content of this submitted manuscript and approved submission.

Research funding: None declared.

Conflict of interest statement: The authors declare no conflicts of interest regarding this article.

References

- [1] R. Dasand and H. Yoo, "Application of a compact electromagnetic bandgap array in a phone case for suppression of mobile phone radiation exposure," *IEEE Trans. Microw. Theor. Tech.*, vol. 66, no. 5, pp. 2363–2372, 2018, <https://doi.org/10.1109/tmmt.2017.2786287> (<https://doi.org/10.1109/tmmt.2017.2786287>).
- [2] K.-H. Chan, R. Ikeuchi, and A. Hirata, "Effects of phase difference in dipole phased-array antenna above EBG substrates on SAR," *IEEE Antenn. Wireless Propag. Lett.*, vol. 12, pp. 579–582, 2013, <https://doi.org/10.1109/lawp.2013.2260717> (<https://doi.org/10.1109/lawp.2013.2260717>).
- [3] H. Li, A. Tsiaras, and B. K. Lau, "Analysis and estimation of MIMO-SAR for multi-antenna mobile handsets," *IEEE Trans. Antenn. Propag.*, vol. 65, no. 3, pp. 1522–1527, 2017, <https://doi.org/10.1109/tap.2016.2647708> (<https://doi.org/10.1109/tap.2016.2647708>).
- [4] K. S. Sultan, H. H. Abdullah, E. A. Abdallah, and E. A. Hashish, "Low SAR, miniaturized printed antenna for mobile, ISM, and WLAN services," *IEEE Antenn. Wireless Propag. Lett.*, vol. 12, pp. 1106–1109, 2013, <https://doi.org/10.1109/lawp.2013.2280955> (<https://doi.org/10.1109/lawp.2013.2280955>).
- [5] H. H. Zhang, G. G. Yu, Y. Liu, Y. X. Fang, G. Shi, and S. Wang, "Design of low-SAR mobile phone antenna: theory and applications," *IEEE Trans. Antenn. Propag.*, vol. 69, no. 2, pp. 698–707, 2021, <https://doi.org/10.1109/tap.2020.3016420> (<https://doi.org/10.1109/tap.2020.3016420>).
- [6] B. Lu, B. Pang, W. Hu, and W. Jiang, "Low-SAR antenna design and implementation for mobile phone applications," *IEEE Access*, vol. 9, pp. 96444–96452, 2021, <https://doi.org/10.1109/access.2021.3093720> (<https://doi.org/10.1109/access.2021.3093720>).
- [7] J. Bangand and J. Choi, "A SAR reduced mm-wave beam-steerable array antenna with dual-mode operation for fully metal-covered 5G cellular handsets," *IEEE Antenn. Wireless Propag. Lett.*, vol. 17, no. 6, pp. 1118–1122, 2018, <https://doi.org/10.1109/lawp.2018.2836196> (<https://doi.org/10.1109/lawp.2018.2836196>).
- [8] Z.-Q. Xu, Q.-Q. Zhou, Y.-L. Ban, and S. S. Ang, "Hepta-band coupled-fed loop antenna for LTE/WWAN unbroken metal-rimmed smart phone applications," *IEEE Antenn. Wireless Propag. Lett.*, vol. 17, no. 2, pp. 311–314, 2018, <https://doi.org/10.1109/lawp.2017.2787863> (<https://doi.org/10.1109/lawp.2017.2787863>).
- [9] D. Huang, Z. w. Du, and Y. Wang, "A quad-antenna system for 4G/5G/GPS metal frame mobile phones," *IEEE Antenn. Wireless Propag. Lett.*, vol. 18, no. 8, pp. 1586–1590, 2019, <https://doi.org/10.1109/lawp.2019.2924322> (<https://doi.org/10.1109/lawp.2019.2924322>).

- [10] Y. Liu, J. Zhang, A. Ren, H. Wang, and C.-Y.-D. Sim, "TCM-based hepta-band antenna with small clearance for metal-rimmed mobile phone applications," *IEEE Antenn. Wireless Propag. Lett.*, vol. 18, no. 4, pp. 717–721, 2019, <https://doi.org/10.1109/lawp.2019.2901808> (<https://doi.org/10.1109/lawp.2019.2901808>).
- [11] H. Wang, "Analysis of electromagnetic energy absorption in the human body for mobile terminals," *IEEE Open J. Antenn. Propag.*, vol. 1, no. 1, pp. 113–117, 2020, <https://doi.org/10.1109/ojap.2020.2982507> (<https://doi.org/10.1109/ojap.2020.2982507>).
- [12] J. Khan, D. Ali Sehrai, and U. Ali, "Design of dual band 5G antenna array with SAR analysis for future mobile handsets," *J. Electr. Eng. Technol.*, vol. 14, no. 2, pp. 809–816, 2019, <https://doi.org/10.1007/s42835-018-00059-9> (<https://doi.org/10.1007/s42835-018-00059-9>).
- [13] H. Ben Hamadi, S. Ghnimi, L. Latrach, P. Benech, and A. Gharsallah, "New design of multi-band PIFA antenna with reduced SAR for mobile and wireless applications," *Wireless Pers. Commun.*, vol. 115, no. 2, pp. 1211–1226, 2020, <https://doi.org/10.1007/s11277-020-07619-1> (<https://doi.org/10.1007/s11277-020-07619-1>).
- [14] N. Nasser, D. Serhal, R. Barake, M. Rammal, and P. Vaudon, "A novel low SAR water-based mobile handset antenna," *Analog Integr. Circuits Signal Process.*, vol. 96, no. 2, pp. 353–361, 2018, <https://doi.org/10.1007/s10470-018-1130-8> (<https://doi.org/10.1007/s10470-018-1130-8>).
- [15] T. Ramachandran, M. R. I. Faruque, E. Ahamed, and S. Abdullah, "Specific absorption rate reduction of multi split square ring metamaterial for L- and S-band application," *Results Phys.*, vol. 15, p. 102668, 2019, <https://doi.org/10.1016/j.rinp.2019.102668> (<https://doi.org/10.1016/j.rinp.2019.102668>).
- [16] A. A. Al-Ghamdi, O. A. Al-Hartomy, F. R. Al-Solamy, N. T. Dishovskyc, N. T. Atanasov, and G. L. Atanasova, "Enhancing antenna performance and SAR reduction by a conductive composite loaded with carbon-silica hybrid filler," *AEU - Int. J. Electron. Commun.*, vol. 72, pp. 184–191, 2017, <https://doi.org/10.1016/j.aeue.2016.12.013> (<https://doi.org/10.1016/j.aeue.2016.12.013>).
- [17] A. M. Tamim, M. R. I. Faruque, M. U. Khandaker, M. T. Islam, and D. A. Bradley, "Electromagnetic radiation reduction using novel metamaterial for cellular applications," *Radiat. Phys. Chem.*, vol. 178, p. 108976, 2021, <https://doi.org/10.1016/j.radphyschem.2020.108976> (<https://doi.org/10.1016/j.radphyschem.2020.108976>).
- [18] A. M. Ali, M. A. Al Ghamdi, M. M. Iqbal, S. Khalid, H. Aldabbas, and S. Saeed, "Next generation UWB antennas gadgets for human health care using SAR," *EURASIP J. Wirel. Commun. Netw.*, vol. 2021, no. 1, 2021, <https://doi.org/10.1186/s13638-021-01906-6> (<https://doi.org/10.1186/s13638-021-01906-6>).

PubMed (<https://pubmed.ncbi.nlm.nih.gov/33613666/>)

PubMed Central (<https://www.ncbi.nlm.nih.gov/pmc/articles/PMC7885984/>)

- [19] B. P. Nadh, B. T. P. Madhav, and M. Siva Kumar, "Design and analysis of dual band implantable DGS antenna for medical applications," *EURASIP J. Wirel. Commun. Netw.*, vol. 2021, p. 33, 2021.
- [20] V. Karthik and T. Rama Rao, "Investigations on SAR and thermal effects of a body wearable microstrip antenna," *Wireless Pers. Commun.*, vol. 96, no. 3, pp. 3385–3401, 2017, <https://doi.org/10.1007/s11277-017-4059-9> (<https://doi.org/10.1007/s11277-017-4059-9>).
- [21] C.-L. Tsai, K.-W. Chen, and C.-L. Yang, "Implantable wideband low-SAR antenna with C-shaped coupled ground," *IEEE Antenn. Wireless Propag. Lett.*, vol. 14, pp. 1594–1597, 2015, <https://doi.org/10.1109/lawp.2015.2413839> (<https://doi.org/10.1109/lawp.2015.2413839>).
- [22] T. Mary Neebha, M. Nesusudha, and D. K. Janapala, "A stable miniaturised AMC loaded flexible monopole antenna for ingestible applications," *Comput. Biol. Med.*, vol. 116, p. 103578, 2020, <https://doi.org/10.1016/j.compbiomed.2019.103578> (<https://doi.org/10.1016/j.compbiomed.2019.103578>).
- PubMed** (<https://pubmed.ncbi.nlm.nih.gov/31999556/>)
- [23] B. Yin, J. Gu, X. Feng, B. Wang, Y. Yu, and W. Ruan, "A low SAR value wearable antenna for wireless body area network based on AMC structure," *Prog. Electromagn. Res.*, vol. 95, pp. 119–129, 2019, <https://doi.org/10.2528/pierc19040103> (<https://doi.org/10.2528/pierc19040103>).
- [24] Al-Adhami, A. and Ercelebi, E., "A flexible metamaterial based printed antenna for wearable biomedical applications," *Sensors*, vol. 21, no. 23, pp. 1–18, 2021. <https://doi.org/10.3390/s21237960> (<https://doi.org/10.3390/s21237960>).
- PubMed** (<https://pubmed.ncbi.nlm.nih.gov/34883966/>)
- PubMed Central** (<https://www.ncbi.nlm.nih.gov/pmc/articles/PMC8659625/>)
- [25] M. El Atrash, M. A. Abdalla, and H. M. Elhennawy, "A wearable dual-band low profile high gain low SAR antenna AMC-backed for WBAN applications," *IEEE Trans. Antenn. Propag.*, vol. 67, no. 10, pp. 6378–6388, 2019, <https://doi.org/10.1109/tap.2019.2923058> (<https://doi.org/10.1109/tap.2019.2923058>).
- [26] M. Wang, Z. Yang, J. Wu, et al., "Investigation of SAR reduction using flexible antenna with metamaterial structure in wireless body area network," *IEEE Trans. Antenn. Propag.*, vol. 66, no. 6, pp. 3076–3086, 2018, <https://doi.org/10.1109/tap.2018.2820733> (<https://doi.org/10.1109/tap.2018.2820733>).
- [27] H. Yalduz, T. E. Tabaru, V. T. Kilic, and M. Turkmen, "Design and analysis of low profile and low SAR full-textile UWB wearable antenna with metamaterial for WBAN applications," *AEU - Int. J. Electron. Commun.*, vol. 126, p. 153465, 2020, <https://doi.org/10.1016/j.aeue.2020.153465> (<https://doi.org/10.1016/j.aeue.2020.153465>).
- [28] U. Ali, S. Ullah, J. Khan, et al., "Design and SAR analysis of wearable antenna on various parts of human body, using conventional and artificial ground planes," *J. Electr. Eng. Technol.*, vol. 12, no. 1, pp. 317–328, 2017, <https://doi.org/10.5370/jeeet.2017.12.1.317>

(<https://doi.org/10.5370/jeet.2017.12.1.317>) .

- [29] M. El Atrash, O. F. Abdalgalil, I. S. Mahmoud, M. A. Abdalla, and S. R. Zahran, "Wearable high gain low SAR antenna loaded with backed all-textile EBG for WBAN applications," *IET Microw. Antenn. Propag.*, vol. 14, no. 8, pp. 791–799, 2020, <https://doi.org/10.1049/iet-map.2019.1089> (<https://doi.org/10.1049/iet-map.2019.1089>) .
- [30] N. Ramanpreet, M. Rattan, and S. S. Gill, "Compact and low profile planar antenna with novel metastructure for wearable MBAN devices," *Wireless Pers. Commun.*, vol. 118, no. 4, pp. 3335–3347, 2021, <https://doi.org/10.1007/s11277-021-08182-z> (<https://doi.org/10.1007/s11277-021-08182-z>) .
- [31] M. Munde, A. Nandgaonkar, and S. Deosarkar, "Low specific absorption rate antenna using electromagnetic band gap structure for long term evolution band 3 application," *Prog. Electromagn. Res.*, vol. 80, pp. 23–34, 2019, <https://doi.org/10.2528/pierm18102103> (<https://doi.org/10.2528/pierm18102103>) .
- [32] M. El Atrash, M. A. Abdalla, and H. M. Elhennawy, "Gain enhancement of a compact thin flexible reflector-based asymmetric meander line antenna with low SAR," *IET Microw. Antenn. Propag.*, vol. 13, no. 6, pp. 827–832, 2019, <https://doi.org/10.1049/iet-map.2018.5397> (<https://doi.org/10.1049/iet-map.2018.5397>) .
- [33] Z. H. Jiang, D. E. Brocker, P. E. Sieber, and D. H. Werner, "A compact, low-profile metasurface-enabled antenna for wearable medical body-area network devices," *IEEE Trans. Antenn. Propag.*, vol. 62, no. 8, pp. 4021–4030, 2014, <https://doi.org/10.1109/tap.2014.2327650> (<https://doi.org/10.1109/tap.2014.2327650>) .
- [34] Rubesh Kumar, T. and Madhavan, M., "Hybrid fabric wearable antenna design and evaluation for high speed 5G applications," *Wireless Pers. Commun.*, vol. 127, no. 2, pp. 1517–1528, 2021. <https://doi.org/10.1007/s11277-021-08702-x> (<https://doi.org/10.1007/s11277-021-08702-x>) .
- [35] A. Shah and P. Patel, "E-textile slot antenna with spurious mode suppression and low SAR for medical wearable applications," *J. Electromagn. Waves Appl.*, vol. 35, no. 16, pp. 2224–2238, 2021, <https://doi.org/10.1080/09205071.2021.1934905> (<https://doi.org/10.1080/09205071.2021.1934905>) .
- [36] B. Sugumaran, R. B. subramanian, and S. K. Palaniswamy, "Reduced specific absorption rate compact flexible monopole antenna system for smart wearable wireless communications," *Eng. Sci. Technol. Int. J.*, vol. 24, no. 3, pp. 682–693, 2021, <https://doi.org/10.1016/j.jestch.2020.12.012> (<https://doi.org/10.1016/j.jestch.2020.12.012>) .
- [37] S. Rajebi, C. Ghobadi, J. Nourinia, and E. Mostafapour, "SAR enhancement of slot microstrip antenna by using silicon layer in hyperthermia applications," *Wireless Pers. Commun.*, vol. 111, no. 3, pp. 1761–1774, 2020, <https://doi.org/10.1007/s11277-019-06955-1> (<https://doi.org/10.1007/s11277-019-06955-1>) .

- [38] Tu. T. Le and T.-Y. Yun, "Wearable dual-band high-gain low-SAR antenna for off-body communication," *IEEE Antenn. Wireless Propag. Lett.*, vol. 20, no. 7, pp. 1175–1179, 2021, <https://doi.org/10.1109/lawp.2021.3074641> (<https://doi.org/10.1109/lawp.2021.3074641>).
- [39] A. Amsaveni, M. Bharathi, and J. N. Swaminathan, "Design and performance analysis of low SAR hexagonal slot antenna using cotton substrate," *Microsyst. Technol.*, vol. 25, no. 6, pp. 2273–2278, 2019, <https://doi.org/10.1007/s00542-018-4109-6> (<https://doi.org/10.1007/s00542-018-4109-6>).
- [40] J. Trajkovikj and A. K. Skrivervik, "Diminishing SAR for wearable UHF antennas," *IEEE Antenn. Wireless Propag. Lett.*, no. 14, pp. 1530–1533, 2015, <https://doi.org/10.1109/lawp.2014.2374423> (<https://doi.org/10.1109/lawp.2014.2374423>).
- [41] K. Badhan and J. Singh, "Analysis of different performance parameters of body wearable antenna—a review," *Adv. Wireless Mobile Commun.*, vol. 10, no. 5, pp. 735–745, 2017.
- [42] K. N. Paracha, S. K. A. Rahim, P. J. Soh, and M. Khalily, "Wearable antennas: a review of materials, structures, and innovative features for autonomous communication and sensing," *IEEE Access*, vol. 7, pp. 56694–56712, 2019, <https://doi.org/10.1109/access.2019.2909146> (<https://doi.org/10.1109/access.2019.2909146>).
- [43] A. Nazeri, A. Abdolali, and M. Mehdi, "An extremely safe low-SAR antenna with study of its electromagnetic biological effects on human head," *Wireless Pers. Commun.*, vol. 109, no. 2, pp. 1449–1462, 2019, <https://doi.org/10.1007/s11277-019-06621-6> (<https://doi.org/10.1007/s11277-019-06621-6>).
- [44] H. N. Awl, Y. I. Abdulkarim, L. Deng, et al., "Bandwidth improvement in bow-tie microstrip antennas: the effect of substrate type and design dimensions," *Appl. Sci.*, vol. 10, no. 2, 2020, <https://doi.org/10.3390/app10020504> (<https://doi.org/10.3390/app10020504>).
- [45] S. Bhattacharjee, M. Mitra, and S. R. B. Chaudhuri, "An effective SAR reduction technique of a compact meander line antenna for wearable applications," *Prog. Electromagn. Res.*, vol. 55, pp. 143–152, 2017, <https://doi.org/10.2528/pierm16121501> (<https://doi.org/10.2528/pierm16121501>).

Supplementary Material

This article contains supplementary material (<https://doi.org/10.1515/freq-2022-0297> (<https://doi.org/10.1515/freq-2022-0297>)).

Received: 2022-12-21

Accepted: 2023-04-21

Published Online: 2023-05-29

Published in Print: 2023-12-15

© 2023 Walter de Gruyter GmbH, Berlin/Boston

— or —

PDF **30,00 €**

Aus der Zeitschrift



Frequenz
Band 77 Heft 11-12

Artikel in diesem Heft

Frontmatter

REVIEW ARTICLE

SAR reduction techniques for WBAN and mobile applications

RESEARCH ARTICLES

Defected ground structure based compact UWB dielectric resonator antennas with enhanced bandwidth

Performance analysis of a flexible wearable antenna with low SAR for biomedical application

Compact hybrid EBG microstrip antenna for wearable applications

Compact eight-shaped ISM-I band wearable antenna for wireless body area network applications

A high-gain dual-beam folded transmit-reflect-array antenna based on phase-shifting surface

High isolation frequency-reconfigurable UWB-MIMO antenna with on-demand WiMAX band elimination

Performance analysis of mmWave/sub-terahertz communication link for 5G and B5G mobile networks

Heruntergeladen am 16.11.2023 von

[https://www.degruyter.com/document/doi/10.1515/freq-2022-0297/html?](https://www.degruyter.com/document/doi/10.1515/freq-2022-0297/html?lang=de)
lang=de